Study of Cyclophilin A Function in Models of Amyotrophic Lateral Sclerosis

Thesis

UNRESTRICTED

ELIANA LAURANZANO

Master's degree in Medical Biotechnologies and Molecular Medicine

Personal Identifier: A4162993

Study of Cyclophilin A function in models of Amyotrophic Lateral Sclerosis

---

Registered degree:

Doctor of Philosophy at The Open University, UK

Life and Biomolecular Sciences

Affiliated Research Centre:

"Mario Negri" Institute for Pharmacological Research

Submitted: 28th September 2012

Date of Submission: 27 September 2012

Date of Award: 7 February 2013

ABSTRACT

Amyotrophic lateral sclerosis (ALS) is an incurable neurodegenerative disease targeting preferentially motor neurons. Cyclophilin A (CypA) was identified as a hallmark of disease in mutant SOD1 (mSOD1) animal models of familial ALS (fALS) at a presymptomatic stage, and in sporadic (sALS) patients (Massignan 2007; Nardo 2011). Moreover, CypA was enriched in the spinal cord aggregates of mSOD1 mice and sALS patients (Basso 2009). CypA is an ubiquitous protein with multiple functions relevant to the CNS, where it is abundantly expressed.

Insights into CypA function in ALS were provided via a proteomic analysis of its interacting proteins, that functionally associated CypA with different proteins networks. In particular, it extensively binds proteins regulating RNA metabolism, including several hnRNPs and TDP-43, a major disease protein in ALS. TDP-43 and CypA interact in the nucleus, in an RNA-dependent way. CypA has a key role in the stabilization of TDP-43/hnRNP A2/B1 interaction, and TDP-43-mediated HDAC6 expression regulation, properties impaired in TDP-43 ALS-mutants, possibly because of a loss-of-interaction with CypA. CypA interacts also with mSOD1, suggesting a gain-of-interaction specifically linked to fALS. Mice expressing mSOD1 and lacking CypA show increased levels of insoluble mSOD1 and hyperphosphorylated TDP-43 in the spinal cord at the onset.

This thesis work shows that CypA has a protective role in ALS: as a chaperone (for mSOD1) and in maintenance of multi-protein (TDP-43/hnRNPs) complex stability. Regardless the cause of the disease, mSOD1 or alterations in TDP-43, the interaction with CypA is impaired and it is co-sequestered in proteinaceous aggregates, altering its protective activities. The net effect is the formation of pathological inclusions that may lead to a compromised RNA metabolism. CypA being a key interacting partner of both mSOD1 and TDP-43 can represent the "missing link" of these two patho-mechanisms in ALS and an interesting target for therapeutic interventions.

ACKNOWLEDGEMENTS

At the end of my PhD, it is a pleasant task to express my gratitude to all those who contributed in many ways to make this thesis possible and an unforgettable experience for me. I am very grateful to my director of studies Dr. Valentina Bonetto for the scientific support and guidance during my PhD studies, and to my supervisor Dr. Andrew Grierson for his advices and his availability during these years. I'm also grateful to Dr. Mario Salmona, Dr. Roberto Chiesa and Dr. Caterina Bendotti for all stimulating scientific discussions we had during these years. A special thank goes to Dr. Tania Massignan for her patience and fundamental advices she gave me when I started my research experience at the Mario Negri Institute, and to Dr. Emiliano Biasini for his enthusiasm in Science, his insightful comments and hard questions. My sincere thank goes to Riccardo Stucchi for the numerous stimulating discussions and feedback, his patience and hard work in helping me with experiments. My gratitude also goes to all the present and past components of the Translational Proteomics laboratory, and in particular to Dr. Silvia Pozzi, Laura Pasetto, Dr. Giovanni Nardo and Dr. Manuela Basso for their constructive criticism and extensive discussions on my work, for the long days spent in the lab, for the fun we had together and for their friendship. Besides my labmates, I would like to thank all the collaborators, collegues, summer students and friends of the Mario Negri Institute, in particular all the past and present components of the Neurobiology of Prions, Pharmacodynamics and Pharmacokinetics and Molecular Neurobiology labs. I also would like to aknowledge the Mario Negri Institute for Pharmacological Research and the director Prof. Silvio Garattini for providing necessary infrastructure, motivation and immense knowledge. I express my gratitude to the Telethon Foundation and AriSLA for funding my research. I expand my thanks to Franca, Enrica, Maria Teresa, Caterina and Marlien who shared with me all the good and bad days in these four years during my stay at the "ResiDance" in Milan, for their friendship and our "ape" time.

I take this opportunity to warmly thank my Family: Giuseppe this work is dedicated to you. This thesis is the end (finally!) of a long journey: the road we have travelled together. Thanks for your invaluable help and confidence in me, and for reminding me life's true priorities. My heartful thanks go to my mother Alessandra, my father Francesco and my sister Sonia for their love, generous care and support in the inevitable ups and downs in my research and everyday life. Huge thanks to my cousins and my friends, my aunts & uncles, and all my relatives spread all over the world, for their support, encouragement, understanding and precious friendship. Last but not least, thanks to Muma (!) for creating a pleasant homely feeling.

INDEX

LIST OF FIGURES

INTRODUCTION

MATERIALS AND METHODS

RESULTS

CONCLUSION

LIST OF ABBREVIATIONS

2DE	2-dimensional electrophoresis
2D-DIGE	2-dimensional differential in gel electrophoresis
3'-UTR	3-prime untranslated region
aa	amino acid
AD	Alzheimer's disease
AIF	apoptosis inducing factor
ALS	amyotrophic lateral sclerosis
ALS2	alsin
AMPA	α-amino-3-hydroxy-5-methyl-4-isoxazole propionic acid
ANG	angiogenin
AR	autosomal recessive
Arg (R)	arginine
ATXN2	ataxin 2
BDNF	brain-derived neurotrophic factor
C9ORF72	chromosome 9 open reading frame 72
cDNA	complementary DNA
CHMP2B	charged multivescicular body protein 2B
CLD	cyclophilin-like domain
Cn	calcineurin
CNS	central nervous system
CsA	cyclosporin A
CSF	cerebrospinal fluid
CypA	cyclophilin A
Cyps	cyclophilins
DAO	D-amino acid oxidase

DCTN1	Dynactin
DMSO	Dimethyl sulfoxide
ER	endoplasmic reticulum
ERAD	ER-associated protein degradation
EWSR1	Ewing sarcoma breakpoint region 1
FIG4	polyphosphoinositide phosphatase
FKBPs	FK506 binding proteins
FTD	frontotemporal dementia
FTLD-U	frontotemporal lobar degeneration with ubiquitin-positive inclusions
FUS/TLS	fused in sarcoma/translated in liposarcoma
Gln (Q)	glutamine
Gly (G)	glycine
GWAS	genome wide association study
HD	Huntington's disease
HDAC	histone deacetylase
HEK293	human embryonic kidney 293
His (H)	histidine
HIV	human immunodeficiency virus
hnRNP	heterogeneous nuclear ribonucleoprotein
HSPs	heat shock proteins
IBMPFD	inclusion body myopathy associated with Paget's disease of bone and FTD
IF	immunofluorescence
IP	immunoprecipitation
IR	immunoreactivity
Itk	interleukin-2 tyrosine kinase
LMN	lower motor neuron
Lys (K)	lysine

MALDI-TOF	matrix assisted laser desorption ionization-time of flight
MAPT	Microtubule-associated protein tau
miRNA	microRNA
MMPs	metalloproteinases
MN	motor neuron
MRI	magnetic resonance imaging
mRNA	messenger RNA
MS	mass spectrometry
MTT	3-(4,5-Dimethylthiazol-2-yl)-2,5-diphenyltetrazolium bromide
NEFH	neurofilament heavy polipeptide
NES	nuclear export sequence
NF-AT	nuclear factor of activated T cells
NLS	nuclear localisation signal
NMDA	N-methyl-D-aspartate
NTg	non-transgenic
OPTN	optineurin
PBMC	peripheral blood mononuclear cells
PCR	polymerase chain reaction
PD	Parkinson's disease
PFN1	Profilin 1
Phe (F)	phenylalanine
POAG	primary open angle glaucoma and ataxia
PPIase	peptydil-prolyl *cis-trans* isomerase
Pro (P)	proline
PRPH	Peripherin
PTM	post-translational modification
Prx	peroxiredoxin

RNP	ribonucleoprotein
RNS	reactive nitrogen species
ROS	reactive oxygen species
RRM	RNA recognition motif
RT	room temperature
SDS-PAGE	SDS-polyacrylamide gel electrophoresis
Ser (S)	serine
SETX	senataxin
SIGMAR1	sigma non-opioid receptor 1
siRNA	small interfering RNA
SOD1	copper/zinc superoxide dismutase
SpC	spinal cord
SPG11	spataxin
SQSTM1	p62/sequestosome 1
TAF15	TATA-binding protein-associated factor 15
TDP-43	TAR DNA binding protein-43
TIF	Triton X-100 insoluble fraction
Trp (W)	tryptophane
Tyr (Y)	tyrosine
UBIs	ubiquitinated inclusions
UBQLN2	ubiquilin 2
UMN	upper motor neuron
UPR	unfolded protein response
VAPB	VAMP/synaptobrevin-associated membrane protein B
VCP	valosin-containing protein/p97
WB	Western blotting
WT	wild-type

I. INTRODUCTION

Many neurogenetic disorders are caused by the mutation of ubiquitously expressed genes. Amyotrophic lateral sclerosis is one such disorder.

1. Amyotrophic Lateral Sclerosis

Amyotrophic lateral sclerosis (ALS) is an adult-onset fatal neurodegenerative disorder characterised by progressive muscular paralysis reflecting degeneration of motor neurons (MNs) in the primary motor cortex (upper motor neurons, UMN), motor nuclei in the brainstem and anterior horn cells of the spinal cord (lower motor neurons, LMN). In particular, ALS refers to one specific form of MN disease, in which there are both UMN and LMN signs. "Amyotrophy" refers to the atrophy of muscle fibres, which are denervated as their corresponding anterior horn cells degenerate, leading to weakness of affected muscles and visible fasciculations. "Lateral Sclerosis" refers to hardening of the anterior and lateral corticospinal tracts as MNs in these areas degenerate and are replaced by gliosis (Rowland 2001).

Clinical, pathological and genetic advances indicate heterogeneity in phenotype, pathological substrate and genetic predisposition, suggesting that ALS should be considered a syndrome rather than a single disease entity (Deng 2010; Beleza-Meireles 2009; Beghi 2011). Although the clinical presentation and progression of ALS vary considerably, the course is inexorably progressive, and patients die within three to five years after presentation, usually from respiratory failure, due to denervation of the diaphragm and respiratory muscles.

Although ALS is the most common disorder of MNs, it is considered a rare disease. The majority of ALS cases are sporadic (sporadic ALS or sALS), although 5-10% of cases show a Mendelian pattern of inheritance (familial ALS or fALS) (Byrne 2011). Sporadic and familial forms share similar pathological hallmarks. SALS is a complex disease, in which genetic and environmental factors combine to increase the risk of developing the condition (Deng 2010). Despite extensive efforts to understand the molecular mechanisms causing this disease, nowadays ALS still lacks an effective therapy, and the single drug approved for use in patients, riluzole, only slightly prolongs survival.

1.1 Clinical presentation

The features of ALS were first clearly described as a clinicopathological entity by the French neurobiologist and physician Jean Martin Charcot (Charcot 1869; Charcot 1874). However, before that Bell, Aran, Duchenne, and Cruveilher made important observations that contributed to the understanding of the clinical and pathological syndrome (Tyler 1991; Aran 1850; Duchenne de Boulogne 1851; Cruveilhier 1853; Goetz 2000; Rowland 2001).

1.1.1 Main clinical features

Disease phenotype is often classified by the site of onset. Approximately two thirds (65%) of patients with typical ALS have a spinal form of the disease (classical 'Charcot ALS'). They present with symptoms related to focal muscle weakness where the symptoms may start either distally or proximally in the upper limbs and lower limbs. Rarely, patients may notice focal muscle wasting before onset of weakness, and some patients may present with a spastic paraparesis. Patients may have noticed fasciculations (as involuntary muscle twitching) or cramps preceding the onset of weakness or wasting for some months (or years), but rarely are these the presenting symptoms. Although it is usually asymmetrical at onset, the other limbs develop weakness and wasting sooner or later, and most patients go on to develop bulbar symptoms and eventually respiratory symptoms (although not necessarily in that sequence). Gradually, spasticity may develop in the weakened atrophic limbs, affecting manual dexterity and gait. During late stages of the disease patients may develop 'flexor spasms', which are involuntary spasms occurring due to excess activation of the flexor arc in a spastic limb. Occasionally encountered symptoms include bladder dysfunction, sensory symptoms, cognitive symptoms and multi-system involvement (e.g. dementia, parkinsonism).

30% of patients present with bulbar onset ALS, usually in the form of dysarthria of speech and dysphagia. Limb symptoms can develop almost simultaneously with bulbar symptoms or within 1–2 years. Almost all patients with bulbar symptoms develop sialorrhoea (excessive drooling) due to

difficulty swallowing saliva and mild UMN type bilateral facial weakness which affects the lower part of the face. 'Pseudobulbar' symptoms such as emotional lability and excessive yawning are seen in a significant number of cases.

About 5% of cases with ALS present with respiratory weakness without significant limb or bulbar symptoms (De Carvalho 1996; Chen 1996). These patients present with symptoms of type 2 respiratory failure or nocturnal hypoventilation such as dyspnoea, orthopnoea, disturbed sleep, morning headaches, excessive day time somnolence, anorexia, decreased concentration and irritability or mood changes (Polkey 1999).

Examination early in the course of limb onset disease usually reveals focal muscle atrophy especially involving the muscles of the hands, forearms or shoulders in the upper limbs, and proximal thigh or distal foot muscle in the lower limbs. Fasciculations are usually visible in more than one muscle group. Spasticity is evident in the upper limbs by increased tone and a supinator 'catch', and in the lower limbs with a patellar 'catch' and clonus together with hypertonia. Tendon reflexes are pathologically brisk in a symmetrical manner, including finger jerks in the upper limbs and positive crossed adductor reflex in the lower limbs. Abnormal spread of tendon reflexes beyond the stimulated muscle group may be evident. In patients with bulbar dysfunction, dysarthria may arise from either LMN pathology or pseudobulbar palsy from UMN disorder, leading to slow slurred speech or a nasal quality. On examining the cranial nerves, the jaw jerk may be brisk, especially in bulbar-onset disease. An UMN type facial weakness affects the lower half of the face causing difficulty with lip seal and blowing cheeks, but often varying degrees of UMN and LMN facial weakness coexist. The gag reflex is preserved and is often brisk while the soft palate may be weak. Patients develop fasciculations and wasting of the tongue, and tongue movements are slowed due to spasticity. The rest of the cranial nerves remain intact, although in late stages of the disease patients may very rarely develop a supranuclear gaze palsy (Okuda 1992; Kobayashi 1999).

As disease progresses, patients develop the characteristic picture of the combination of UMN and LMN signs coexisting within the same central nervous system (CNS) region, affecting the bulbar, cervical, thoracic and lumbar territories. Patients who are kept alive by tracheostomy assisted ventilation are found to eventually develop a profound state of motor paralysis termed the 'totally locked-in state' (TLS), where there is paralysis of all voluntary muscles and varying degrees of oculomotor impairment (Hayashi 1989; Sasaki 1992).

ALS probably begins a long time before its clinical manifestation, since a large number of MNs are lost before any clinical signs develop (Côté 1993; Kennel 1996). Unfortunately, at the moment no neuropathological, neurophysiological nor biochemical markers are yet available to identify a patient as potentially susceptible for ALS prior to symptom onset (Swash 2000).

1.1.2 Cognitive and behavioural impairment

Recent findings revealed that the selectivity of ALS for the motor system is not absolute. In fact, patients with ALS may exhibit a range of cognitive abnormalities ranging from impaired frontal executive dysfunction in 20-40% of patients, to overt frontotemporal lobar degeneration (FTLD) in up to 15% of cases (Leigh 2003; Phukan 2007 and 2012; Strong 2008 and 2009; Raaphorst 2010; Elamin 2011). FTLD is characterised by personality change, irritability, poor insight and pervasive deficits on frontal executive tests (Phukan 2007; Strong 2009), while executive dysfunction is associated with impaired judgement and impulsivity, and is a strong negative prognostic indicator (Elamin 2011; Phukan 2011). Behavioural impairment in the absence of cognitive abnormalities can also occur (Strong 2009; Raaphorst 2010), and both cognitive and behavioural dysfunction may precede or follow the onset of motor symptoms. However in the majority of cases, the rate of cognitive decline is very slow as compared to the devastating motor deterioration. Neuropathological and neuroimaging studies have indicated that this subset of patients with ALS-dementia may represent part of a spectrum between patients with pure FTLD and ALS (Ince 1998; Phukan 2007).

1.2 Histopathological features

In order to acquire a better understanding of the aetiology and the pathogenesis of ALS MN death, the pathologists are usually dependent on autopsy samples from ALS patients at a terminal phase of the disease, thus they can supply only little information about previous clinical stages. The pathological hallmarks of ALS are the degeneration and loss of MNs with astrocytic gliosis and the presence of intraneuronal inclusions in degenerating neurons and glia. UMN pathology in ALS is indicated by depopulation of the Betz cells in the motor cortex (Brodmann area 4), variable astrocytic gliosis affecting both the grey matter and underlying subcortical white matter of the motor cortex, and axonal loss within the descending pyramidal motor pathway associated with myelin pallor and gliosis of the corticospinal tracts (Wharton 2003; Ince 2007). LMN pathology primarily affects the ventral horn MNs of the spinal cord (SpC) and brainstem. There is relative sparing of the motor nucleus of Onufrowicz in the S2 spinal segment and the cranial nerve oculomotor nuclei (Kato 2003; Iwata 1978). The number of LMNs can be reduced by up to 50% at autopsy (Ince 2000) but there is considerable variation both between cases and between different spinal levels within cases (Ince 2007). The remaining neurones are atrophic and contain intraneuronal inclusions such as:

→ **Ubiquitinated inclusions (UBIs) or ubiquitin-immunoreactive (Ub-IR)**

According to their morphology, UBIs can be divided into more compact spherical bodies, also defined as Lewy body-like inclusions, or skein-like inclusions which have a filamentous profile. The former are found also in other disorders, like Parkinson's disease (PD) (Jellinger 2008), whereas the latter can be considered a specific hallmark of ALS. In patients, UBIs are frequently found in the LMN of the SpC and brainstem and are localized both in normal appearing MNs and in some shrunken cells. They are almost universal in ALS and its variants (95% of cases) (Leigh 1991 and 1988; Lowe 1988; Ince 2003). Protein constituents of these inclusions have been partially characterised. Recently, the TAR DNA binding protein 43 (TDP-43) has been identified as the major component of these UBIs (Neumann 2006; Tan 2007; Arai

2006) and, as in the case of TDP-43, several of the proteins encoded by genes mutated in a small subset of ALS, such as superoxide dismutase 1 (SOD1), fused in sarcoma (FUS), optineurin (OPTN), ubiquilin 2 (UBQLN2), neurofilament heavy polipeptide (NEFH), valosin-containing protein (VCP), C9orf72 and p62 are prominent components of such inclusions (Deng 2010; Mackenzie 2007; Shibata 1996; Keller 2012).

→ **Bunina bodies**

Bunina bodies are small, eosinophilic, intracytoplasmatic inclusions localized in the soma or dendrites of MNs but not in their axoplasm. Although not all ALS patients necessarily have Bunina bodies, they are currently considered a specific histopathological hallmark of ALS (Bunina 1962; Piao 2003), since they are rarely described in other conditions. At the ultrastructural analysis, they appear like electrondense, amorphous material containing tubular and vesicular structures; they can also contain filaments and other cellular micro-organelles (Kato 2003). They stain positive for cystatin C, a protein inhibitor of lysosomal cysteine proteases, but they are usually negative for ubiquitin, and do not contain TDP-43 (Okamoto 2008).

→ **Hyaline conglomerate inclusions (HCIs)**

HCIs are argyrophilic inclusions seen in SpC MNs that stain for phosphorylated and non phosphorylated neurofilaments that can be in association with other cytoplasmic proteins and organelles (Schochet 1969; Leigh 1989; Sasaki 1991). They are associated mainly with fALS and rarely seen in sALS cases. However these inclusions do not seem very specific for ALS pathology, in fact they have also been described in other neurodegenerative diseases and are found in normal individuals too (Leigh 1989).

Moreover, both UMNs and LMNs of ALS patients might show signs of fragmentation of the Golgi apparatus (Mourelatos 1994; Fujita 2005) and morphological alterations of mitochondria (Hirano 1984; Swerdlow 1998).

Contrary to early belief that ALS was a disease exclusive to the motor system, there is now significant evidence to suggest that ALS is in fact a multisystem disorder. Extra motor pathology is found in regions such as the frontotemporal cortex, hippocampus, thalamus (Brownell 1970), substantia nigra (Al-Sarraj 2002), spinocerebellar pathways (Swash 1986), dorsal columns (Lawyer 1953) and peripheral sensory nerves (Dyck 1975; Bradley 1983).

1.3 Epidemiology and aetiology

ALS is one of the most common neuromuscular diseases worldwide, and people of all races and ethnic backgrounds are affected. ALS affects worldwide 1.5-2.7 (average incidence 1.89) per 100.000 individual/year and has a prevalence which ranges from 2.7 to 7.4 (average prevalence 5.2) per 100.000 (Worms 2001; Silani 2011). The frequency of ALS is reduced in populations of non-European or mixed ethnicity and genetic admixture might be protective (Cronin 2007; Zaldivar 2009). The incidence of ALS in Europe is 2-3 people per 100.000 of the general population, and the overall lifetime risk of developing the condition is 1:400 (Johnston 2006; Alonso 2009; Cronin 2007). In populations of European extraction, ALS is more common in men than in women by a ratio of 1.2-1.5:1.7. This disparity is largely attributable to the increased frequency of spinal-onset ALS in men (Kuzuhara 2011). Explanations for this male excess have been also attributed to possible protective hormonal factors in women, increased likelihood of males being exposed to putative risk factors and under ascertainment of elderly women in some population registers (Armon 2003; Nelson 2000).

In contrast to other neurodegenerative diseases, such as PD and Alzheimer's disease (AD), the risk of developing ALS peaks between the ages of 50 and 75 years, and declines thereafter (Logroscino

2010; Chiò 2009; O'Toole 2008). This feature suggests that ALS is not a disease of aging, but rather a disease for which age is one of numerous risk factors.

A particularly high frequency of ALS cases that often present with parkinsonism and dementia was first described in 1945 in the Chamorro tribe who live on the Pacific island of Guam (Steele 2005). A similarly high frequency of ALS has been reported in two separate areas in the Kii peninsula of Honshu island, Japan (Kuzuhara 2005). The frequency of ALS in Guam has declined rapidly over the past five decades, although elevated rates of PD and dementia persist (Steele 2005), as do increased rates of ALS in parts of Japan (Kuzuhara 2011). A high content of cyanotoxins has been reported in the diet of the indigenous population in Guam. However, detailed epidemiological and toxicological studies do not support the hypothesis that these forms of ALS result from cyanotoxic effects, and no environmental toxin has been conclusively identified (Steele 2008). The pathobiology underlying these disease clusters remains unclear.

Sporadic forms of ALS likely result from complex interplay between genetic predisposition and environmental exposures. In fact, although a number of genes have been identified as causative of fALS, genetic studies have also been performed in sALS, finding candidate genes which confer susceptibility to sALS (see ALS genetics section). Environmental factors that confer an increased risk of developing ALS outside of Guam and the Kii peninsula have also been difficult to identify (Sutedja 2009) and currently no robust evidence or conclusive proof exists for any environmental factor as a causative or risk factor for sALS. Clustering of ALS has been identified in certain occupations, possibly including individuals deployed in military service (Kasarskis 2009; Horner 2008) and professional soccer activity, although not in other athletes (Chiò 2005 and 2009). In particular, given the high excess of deaths for ALS among soccer players during the last decade, several hypothesis have been formulated including also chronic misuse of drugs (most often anti-inflammatory) and doping, dietary supplement, pesticides used on the playgrounds, head and SpC trauma or microtrauma history (Al-Chalabi 2005). Other environmental factors that have been associated with ALS include smoking (Armon, 2009; Alonso 2010) and exposure to pesticides, lead, organic toxins, and electromagnetic radiation (Sutedja 2009).

In the last years also persistent viral infection has been considered a possible cause of sALS (Rowland 2001). Selective vulnerability of MNs to certain viruses, such as Polio virus, some entero- and retroviruses, has been described; in particular, retroviral infections may cause MN damage and ALS-like syndromes in both laboratory animals and humans. Epidemiological and experimental data suggest a pathogenetic link between HIV infection and ALS. Patients with HIV-associated ALS syndrome displayed significant reversal of neurological symptoms after antiretroviral therapy. However, although evidence exists that correlate viral infections to some forms of ALS, as of yet no causal relationship has been proved.

The theory of an autoimmune cause of ALS is controversial. Activated microglia and T-cells have been found in the SpC of patients with ALS who have IgG antibodies against both MNs and voltage-gated calcium channels (Appel 1999; Pullen 2000). However, immunotherapy has not been effective in patients with ALS: corticosteroids, plasmapheresis, intravenous immune globulin, cyclophosphamide, and whole-body radiation have all failed.

1.4 ALS genetics

The genetic landscape in ALS is changing rapidly. The principle that ALS is rarely familial (Charcot 1881) has persisted until 1990s, when several genes have been found associated with both fALS and sALS. In a similar way, for several years, only one gene was known to have a role in ALS pathogenesis, SOD1. However, in the very last few years there has been considerable success in finding ALS genes, together with rapid advances in the relationship of the genetic subtypes with pathological subtypes and clinical phenotype.

Similarly to other neurodegenerative diseases, like AD, PD or prion disease, ALS occurs predominantly in a sporadic manner (sALS), although several fALS mutations have been identified as causative in rare sporadic cases of disease. Recently, considerable evidence of a further genetic contribution to all ALS types has been generated, pointing out the lack of clear distinction between hereditable and apparently sporadic ALS (Al-Chalabi 2012). Indeed, many cases

designated as sALS actually represent fALS with reduced disease penetrance. In addition, the fALS label does not exclude the possibility that environmental, endogenous or epigenetic factors contribute to the disease. Thus, large effect of Mendelian genes can account for 75% of inherited forms and about 14% of those with no obvious familial history, even if the underlying causes remain largely unknown (Andersen 2011). Moreover, it is increasingly clarified that ALS is not only a monogenic, but often a digenic or polygenic disease with variable penetrance. In addition, mutations in the genes unequivocally linked to an ALS phenotype predominantly cause disease with high penetrance and a lower mean age of onset than sALS (and will be easily recognized as fALS), but may, in some rare individuals, give rise to other neurodegenerative syndromes, sometimes in combination with ALS, thus underlying their pleiotropic character (Al-Chalabi 2012).

1.4.1 Genetic causes

ALS is a genetically heterogeneous disorder, with several causative genes and mapped loci (**Table 1**). To date, seventeen loci with established ALS causation have been reported (OMIM®, Online Mendelian Inheritance in Man® at NCBI) and at least nine other loci have been mapped and pend confirmation. Most of these are identified via genetic linkage analysis in affected families and display an autosomal dominant inheritance pattern with some autosomal recessive pedigrees reported. The genes associated with ALS show no common biological denominator, but can be divided into six main categories: oxidative stress (SOD1), mRNA processing (FUS, TARDBP, ANG, SETX, TAF15, ELP3, ATXN2 and C9ORF72), endosomal vesicle trafficking (ALS2, VAPB, FIG4 and OPTN), ubiquitination and protein degradation (VCP, UBQLN2, SQSTM1 and UNC13A), axonal transport (DCTN1, CHMP2B, SPG11, PFN1 and NEFH), and other functions (SIGMAR1).

GENETIC SUBTYPE	GENE	PROTEIN	LOCUS	ONSET	INHERITANCE	INITIAL REPORT
ALS1	SOD1	Cu/Zn superoxide dismutase	21q22.1	Adult	AD, AR, *de novo*	Rosen et al., 1993
ALS2	ALS2	Alsin	2q33.2	Juvenile	AR	Hadano et al., 2001
ALS3	unknown	unknown	18q21	Adult	AD	Hand et al., 2002
ALS4	SETX	Senataxin	9q34	Juvenile	AD	Chen et al., 2004
ALS5	SPG11	Spatacsin	15q21.1	Juvenile	AR	Orlacchio et al., 2010
ALS6	FUS	Fused in sarcoma	16p11.2	Adult	AD, AR, *de novo*	Vance et al., 2009 Kwiatkowski et al., 2009
ALS7	unknown	unknown	20p13	Adult	AD	Sapp et al., 2003
ALS8	VAPB	VAMP-associated protein B	20q13.3	Adult	AD	Nishimura et al., 2004
ALS9	ANG	Angiogenin	14q11.2	Adult	AD	Chen et al., 2010
ALS10	TARDBP	TAR-DNA binding protein (TDP-43)	1p36.2	Adult	AD and AR	Gitcho et al., 2008 Sreedharan et al., 2008 Kabashi et al., 2008
ALS11	FIG4	Polyphosphoinositide phosphatase	6q21	Adult	AD	Chow et al., 2009
ALS12	OPTN	Optineurin	10p13	Adult	AD and AR	Van Es et al., 2009
ALS13	ATXN2	Ataxin 2	12q24.1	Adult	AD	Elden et al., 2010
ALS14	VCP	valosin-containing protein	9p13	Adult	AD	Johnson et al., 2010
ALS15	UBQLN2	Ubiquilin 2	Xp11.21	Adult	X-linked	Deng et al., 2011
ALS16	SIGMAR1	Sigma non-opioid receptor 1	9p13.3	Juvenile	AD	Al-Saif et al., 2011
ALS17	CHMP2B	Charged Multivesicular Body Protein 2B	3p12.1	Adult	AD	Parkinson et al., 2006
ALS-FTD	C9ORF72	Chromosome 9 open reading frame 72	9p21.2	Adult	AD	DeJesus-Hernandez et al., 2011 Renton et al., 2011
ND	TAF15	TATA box binding protein -associated factor	17q11.1-q11.2	Adult	AD and AR	Ticozzi et al., 2003
ND	DCTN1	Dynactin	2p13	Adult	-	Münch et al., 2004
ND	DAO	D-amino acid oxidase	12q24	Adult	AD	Mitchell et al., 2010
ND	NEFH	Neurofilament heavy polypeptide	22q12.1-q13.1	Adult	AD	Figlewics et al., 1994 Vecchio et al., 1996 Rooke et al., 1996 Tomkins et al., 1998 Al-Chalabi et al., 1999
ND	PRPH	Peripherin	12q12	-	-	Gro-Louis et al., 2004 Leung et al., 2004
ND	PFN1	Profilin 1	17p13.2	Adult	AD	Wu et al., 2012
ND	SQSTM1	Sequestosome 1 / p62	5q35	Adult	-, *de novo*	Fecto et al., 2011 Rubino et al., 2012
ALS-FTD-P	MAPT	Microtubule-associated protein tau	17q21	Adult	AD	Siddique and Hentati, 1995 Hosler et al., 2000 Wilhelmsen et al., 2004

Table 1 Established and selected ALS-associated genes as of September 2012.

Abbreviations: AD, autosomal dominant; AR, autosomal recessive; FTD, frontotemporal dementia; ND, not determined; P, parkinsonism.

→ ALS1 – Cu/Zn superoxide dismutase (SOD1)

In 1993, the first ALS gene was identified as SOD1, coding for the copper/zinc superoxide dismutase (Rosen 1993). It scavanges the superoxide ion, a free radical that is formed during mitochondrial respiration, by catalyzing the reaction: $4O_2^- + 2H^+ \rightarrow H_2O_2 + O_2$ (McCord 1969).

SOD1 is a ubiquitously expressed homodimeric protein and it is found mainly in the cytoplasm, where it represents ~1% of all cytoplasmic proteins, but it has also been detected in the intermembrane space in mitochondria, and in the nucleus. SOD1 has been the most heavily researched protein in ALS following linkage of the SOD1 gene to ALS. In different populations, 12-23% of patients diagnosed with fALS and 2-7% of sALS patients carry a SOD1 mutation. There are now 166 recorded mutations in its 153 evolutionarily conserved amino acids (**Figure 1**). Most ALS-causing SOD1 mutations are missense, with nonsense and deletion mutations being much rarer. Eight silent and nine intronic mutations have also been reported, presumed to be non-pathogenic (Andersen 2011). All mutations are associated with autosomal dominant fALS, except for D90A and D96N, which can cause both dominant and recessive ALS (Andersen 1995; Robberecht 1996; Orrell 2000). The most frequent SOD1 mutation is A4V. Penetrance, clinical manifestations, age of onset, disease progression and survival vary greatly among specific mutations. Although FTD can occur in individuals with SOD1 mutation, this is not a common finding (Wicks 2009). Neuropathologically, ALS patients with SOD1 mutation show loss of anterior horn neurons in the cord but, while there is immunopositivity for ubiquitin and p62 in the form of skeins or rounded inclusions, there is usually negativity for TDP-43 (Mackenzie 2007; Tan 2007).

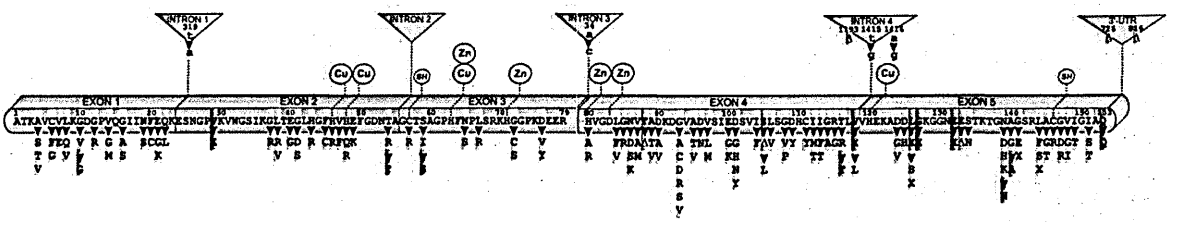

Figure 1 Mutations identified in SOD1 in sporadic and familial ALS cases.

Schematic diagram (modified from Turner 2008) of human SOD1 primary sequence with exons, introns, metal binding domains (Cu, Zn), intramolecular disulfide bond (SH). Mutation legend: grey, missense; purple, insertion; red, deletion; blue/green, silent; Δ, inframe deletion; X, truncation. SOD1 mutations are updated at the http://alsod.iop.kcl.ac.uk/als website.

How it is that almost any mutation in the protein sequence can apparently result in subsequent MN death through what seems to be a common mechanism is unclear. Initially it was hypothesised that mutations would impair the enzymatic activity of the protein, thus resulting in increased cellular levels of reactive oxygen species, oxidative stress, and neuronal death (Deng 1993). However, subsequent studies revealed that some mutants retain full catalytic activity. Additional evidence against a loss-of-function hypothesis came from animal models: knock out of endogenous SOD1 in mice does not lead to spontaneous MN disease (Reaume 1996), while transgenic mice (Gurney 1994) and rats (Nagai 2001) overexpressing human SOD1 carrying the mutations found in human ALS patients do. Also, the expression of mutant SOD1 alleles in cell culture models induces neuron death (Pasinelli 1998). Both *in vivo* and *in vitro* studies strongly suggest that reduced catalytic SOD1 activity does not account for the observed pathology. Currently, it is believed that mutated SOD1 either loses some protective property, such as the ability to reach the nucleus to scavenge DNA-damaging free radicals (Sau 2007) or, more likely, it acquires a general toxic gain-of-function, such as propensity to aggregate. Indeed, several studies showed that mutant SOD1 is prone to misfolding and forms cytoplasmic aggregates. In turn, aggregates may lead to cell death by sequestering other cytoplasmic proteins essential for neuronal survival, by clogging the ubiquitin/proteasome system, by depleting chaperones, or by disrupting mitochondria, the cytoskeleton and/or axonal transport (reviewed in Pasinelli 2006; Boillée 2006). To date, there is no conclusive explanation of how mutations in the SOD1 gene cause ALS.

→ **ALS2 – Alsin (ALS2)**

Autosomal recessive mutations in the ALS2 gene have been linked to young or infantile onset MN degeneration with slow progression (Hadano 2001; Yang 2001), resembling ALS or primary lateral sclerosis or juvenile-onset ascending hereditary spastic paraparesis (Devon 2003; Eymard-Pierre 2002; Lesca 2003). To date, at least 19 different mutations in the 34 exons of the ALS2 gene have been described. Except for two recently identified missense mutations, all other mutations in the

ALS2 gene lead to a premature stop codon and likely result in protein instability and loss-of-function of the encoded protein alsin (Yamanaka 2003). However, mice lacking alsin surprisingly did not recapitulate the symptoms of MN disease, but showed only subtle deficits in motor performance, probably because of potential compensatory mechanisms within the mouse genome (Cai 2005; Hadano 2006; Yamanaka 2006).

Alsin is ubiquitously expressed and is abundant in neurons, where it is localized to the cytosolic portion of the endosomal membrane. Alsin acts as a guanine nucleotide exchange factor for the small GTPase Rab5 *in vitro* (Otomo 2003; Topp 2004), suggesting a possible involvement in vescicular trafficking, cytoskeletal organization and endosomal dynamics. In addition, alsin can interact with the small Rho GTPase Rac1 (Otomo 2003; Topp 2004; Tudor 2005), mediating actin dynamics related to neuritic outgrowth. However, the physiological function of alsin is still unclear.

→ **ALS3**

In a large European family in which at least 20 members had autosomal dominant, adult-onset ALS, a genome-wide search established linkage to chromosome 18q21 (Hand 2002). This locus was associated to ALS3 and it was the first adult-onset reported since ALS1.

→ **ALS4 – Senataxin (SETX)**

Nine missense mutations have been described in the senataxin gene (SETX) in unrelated families with a rare, childhood- or adolescent-onset, slowly progressive form of ALS (Chen 2004). Homozygous or compound heterozygous SETX mutations, mostly leading to a premature termination of the protein product, have been also identified in patients with ataxia-ocular apraxia-2 (Moreira 2004).

Senataxin is a ubiquitously expressed DNA/RNA helicase, possibly involved in repairing DNA double-strand breaks following oxidative stress (Suraweera 2007). Moreover, it binds RNA polymerase II and other proteins involved in mRNA transcription and processing, suggesting that it is involved in transcriptional regulation (Suraweera 2009). These observations suggest that mutations in SETX may cause neuronal degeneration through dysfunction of the helicase activity or other steps in RNA processing.

→ **ALS5 – Spataxin (SPG11)**

Twelve homozygous or compound heterozygous mutations have been identified in the SPG11 gene in 10 unrelated pedigrees (Orlacchio 2010). ALS5 is an autosomal-recessive, juvenile-onset MN disease characterised by distal muscle atrophy and weakness associated with pyramidal signs and involvement of bulbar muscles. The majority of the identified variants are frameshift mutations or nonsense substitutions. Homozygous mutations in the same gene have been previously been described in patients with autosomal recessive hereditary spastic paraplegia with thin corpus callosum (ARHSP-TCC) (Stevanin 2007) and have been recently identified in early-onset L-dopa-responsive parkinsonism with pyramidal signs (Paisán-Ruiz 2010). However, none of the ALS5 patients displayed features suggestive of a concomitant ARHSP-TCC.

SPG11 is composed of 40 exons and encodes for the 2443-residue long protein spatacsin. The protein contains four putative transmembrane domains, suggesting that it may be a receptor or a transporter, a leucine zipper and a coiled-coil domain. The physiological role of spatacsin is still unknown, although it is reputed to be involved in axonal transport (Salinas 2008) and it is important for proper development of the axons of spinal MNs (Martin 2012).

→ **ALS6 – Fused in sarcoma/Translocated in liposarcoma (FUS/TLS)**

Mutations in the FUS/TLS gene have been recently identified as the primary cause of fALS linked to chromosome 16 (Kwiatkowski 2009; Vance 2009). Mutations in FUS/TLS occur in 4-5% of fALS

cases (approximately 0,4% of all ALS). The clinical picture in patients with FUS/TLS mutations is LMN dominant and, often, upper limb onset, but otherwise they are indistinguishable from sALS. Although ALS is the commonest phenotype observed, ALS-FTD or FTD alone also occurs. Originally, FUS was found to have a role as a sarcoma gene, with translocation or fusion gene rearrangement involved in myxoid liposarcoma and low-grade fibromyxoid sarcoma pathogenesis. The FUS/TLS gene encodes a 526 amino acids (aa) protein that belongs to the family of multifunctional DNA/RNA binding proteins. It contains an N-terminal Gln-Gly-Ser-Tyr rich domain (QGSY region) followed by a glycine-rich domain, an RNA recognition motif (RRM), an Arg-Gly-Gly (RGG) repeat-rich domain, zinc finger domains and highly conserved extreme C-terminus that encodes for a non-classical nuclear localisation signal (NLS) that is recognized by transportin-1 (**Figure 2B**).

FUS is almost ubiquitously expressed, it shows nuclear and cytoplasmic localisation (Andersson 2008) and continuously shuttles between the two compartments (Zinszner 1997). It is implicated in numerous cellular processes including: cell proliferation, DNA repair, transcription regulation, and RNA and microRNA (miRNA) processing, although its precise function is poorly characterised. FUS can also be involved in neuronal plasticity and in maintenance of dendritic activity by transporting messenger RNA (mRNA) to dendritic spines for local translation (Fujii 2005a and 2005b).

The majority of ALS linked missense mutations are clustered in the extreme C-terminal portion of the protein, with several of them leading to disruption of NLS, which impairs trasportin-1-mediated nuclear import (Dormann 2010), and disrupt the interaction with other FET proteins (EWS and TAF15). Disruption of nuclear import by ALS-causing mutations may explain why FUS is redistributed to the cytoplasm and incorporated into stress granules. Indeed, FUS seems to behave similarly to TDP-43 in that it is nuclear in the normal state but found to be cytosolic in ALS cases, although FUS pathology is rarer than TDP-43 pathology in post-mortem examination (Kwiatkowski 2009; Lagier-Tourenne 2009; Neumann 2009; Vance 2009).

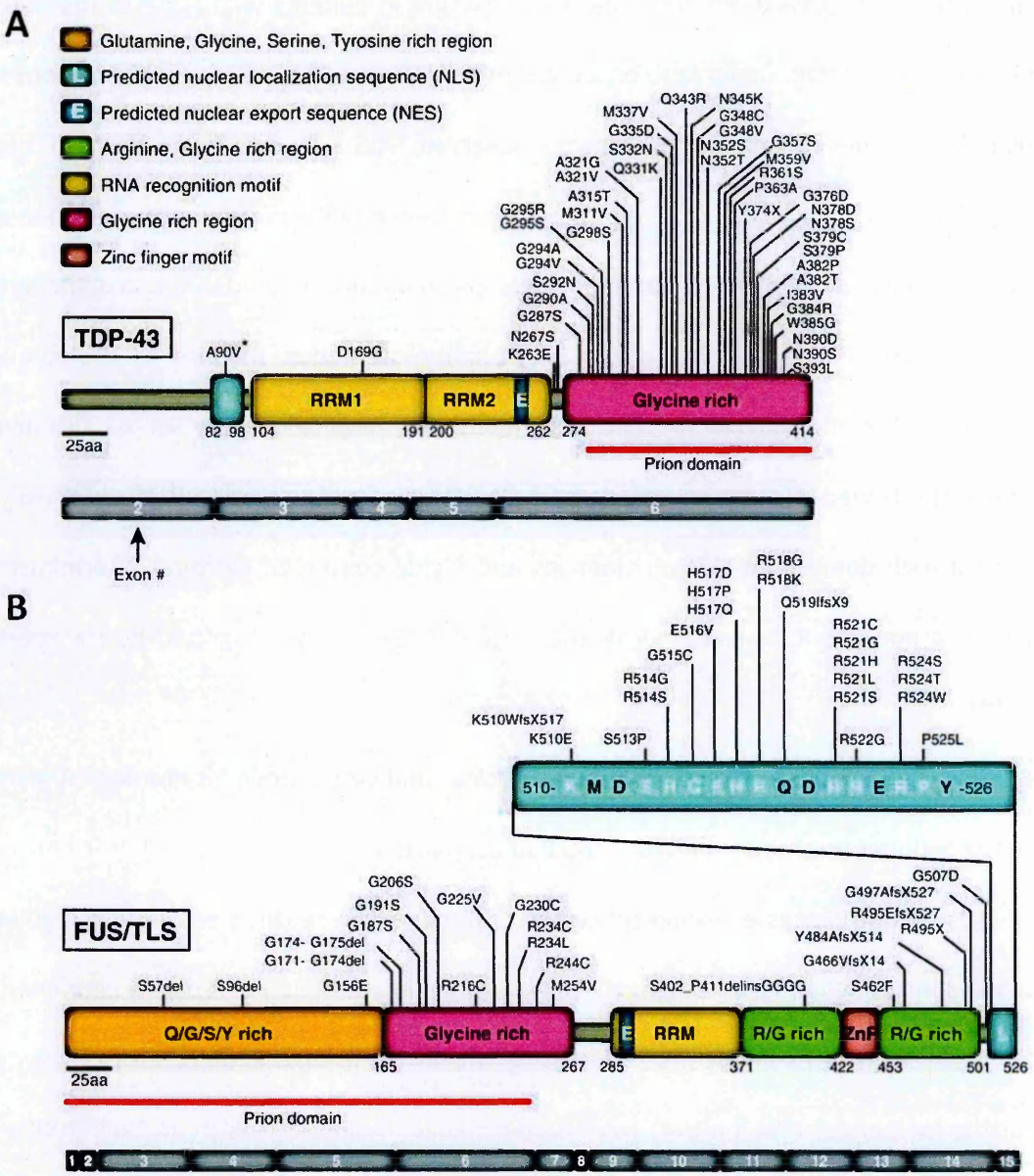

Figure 2 Mutations identified in TDP-43 and FUS/TLS in ALS cases and in rare FTLD patients.

(**A**) Forty-four mutations have been identified in TDP-43 in sALS and fALS patients and in rare FTLD patients, with most lying in the C-terminal glycine-rich region. The putative prion domain comprises amino acids from 277 to 414. (**B**) Forty-six mutations have been identified in FUS/TLS in sALS and fALS cases and in rare FTLD patients. Most mutations are clustered in the last 17 aa and in the glycine-rich region and the putative prion domain comprises aa 1–239. * TDP-43 variant (A90V) reported in a FTLD/ALS patient. Adapted from Da Cruz 2011.

FUS immunohistochemistry shows normal staining of FUS in the nuclei of many neurons and glial cells, but aggregates of FUS in the cytoplasm of LMNs, as well as in dystrophic neurites (Kwiatkowski 2009; Vance 2009). However, some of the nuclear staining is preserved in neurons with FUS inclusions, indicating that the protein is not fully sequestered in pathological conditions

(Rademakers 2010; Aizawa 2000). FUS positive cytoplasmic and nuclear inclusions have also been identified in several subtypes of FTLD cases, neuronal intermediate filament inclusion disease, basophilic inclusion body disease and atypical FTLD (Neumann 2009), and are collectively named FTLD-FUS, althought, in contrast to ALS-FUS, they are not associated with FUS gene mutations (Mackenzie 2010). Ubiquitin and p62 positive cytoplasmic inclusions in the anterior horn of the SpC are rare (Mackenzie 2010), contrary to FTLD-FUS inclusions (Lee 2006), and TDP-43 positive inclusions are notably absent (Kwiatkowski 2009; Vance 2009). Interestingly, EWS, TAF15 and transportin-1 have been reported to co-localise with FUS within cytoplasmic inclusions in FUS-FTLD but not in ALS-FUS, thus distinguishing the two pathologies and implicating different disease mechanisms (Neumann 2011; Brelstaff 2011; Davidson 2012; Troakes 2012).

→ **ALS7**

In the same genetic analysis where ALS6 locus was identified, a novel ALS locus was discovered in another family on chromosome 20p13 and termed ALS7 (Sapp 2003).

→ **ALS8 – VAMP-associated protein B (VAPB)**

Mutations in the VAMP/synaptobrevin-associated membrane protein B (VAPB) gene was correlated with late-onset, autosomal dominant, slowly progressive MN degeneration with ALS and ALS-FTD. Missense mutations were observed in several large Brasilian (Nishimura 2004 and 2005; Landers 2008) and German pedigrees (Funke 2010), also in association with C9orf72 mutations (van Blitterswijk 2012).

The VAPB gene encodes a ubiquitously expressed homodimer, which belongs to a family of intracellular vesicle-associated/membrane-bound proteins. It associates with microtubules and is presumed to regulate vesicle trafficking (Nishimura 2004; Kanekura 2006). In particular, VAPB has been shown to act during transport through the endoplasmic reticulum (ER), Golgi apparatus and secretion. The ALS-mutant P56S-VAPB dramatically disrupts the sub-cellular distribution of VAPB

and induces the formation of intracellular protein aggregates (Nishimura 2004). In addition, P56S-VAPB contributes to nuclear envelope defects (Tran 2012) and perturbs anterograde mitochondrial axonal transport by disrupting calcium homeostasis and affecting the Miro1/kinesin-1 interaction with tubulin (Mórotz 2012). Moreover, VAPB is physiologically involved in the unfolded protein response (UPR), suggesting that ALS mutations may contribute to the MN degeneration also by impairment of the proteasome activity (Moumen 2011).

→ **ALS9 - Angiogenin (ANG)**

Although heterozygous missense mutations in the coding region of ANG have been reported in both fALS and sALS patients, in association with functional loss of protein function, later studies also demonstrated ANG mutations in control subjects (Greenway 2004 and 2006; van Es 2009 and 2011; Fernandez-Santiago 2009; Gellera 2008; Conforti 2008). Furthermore, ANG variants were detected in ALS families with incomplete penetrance or in association with mutations in TARDBP or FUS (van Blitterswijk 2012). Patients showed typical ALS, and one presented ALS-parkinsonism and later developed FTD (van Es 2009). In addition, a large international collaborative study showed that ANG mutations are a risk factor for ALS, as well as for PD (van Es 2011). These features indicate an oligogenic disease model of ALS and suggest that multiple genetic factors influence phenotypic characteristics (van Blitterswijk 2012)

Angiogenin is a 14 kDa ribonuclease and its angiogenic activity is related to its ability in regulating tRNA transcription, ribosome biogenesis, protein translation and cell proliferation (Moroianu 1994; Smith 2006). The majority of the mutations described are predicted to disrupt angiogenin secretion, ribonucleolytic activity and/or nuclear translocation, ultimately resulting in angiogenesis impairment (Wu 2007; Sebastia 2009). Thus, a deficiency in angiogenin function may result in insufficient transcription in MNs which require robust ribosome biogenesis due to the demand of long-distance axonal transport. ANG mutations have also been shown to affect neurite extension/pathfinding and survival of MNs (Subramanian 2007 and 2008).

→ **ALS10 - TDP-43 (TARDBP)**

The discovery that neuronal cytoplasmic UBIs in patients with ALS or FTD contain TDP-43 (Neumann 2006), prompted the analysis of TARDBP, the gene that encodes this protein, in ALS families. Since 2008 (Gitcho 2008; Sreedharan 2008; Kabashi 2008), 44 heterozygous mutations have been described in individuals with sALS and fALS, nearly all affecting the C-terminus (**Figure 2A**), and all but one are missense (Chio 2011), the exception being Tyr374X (Daoud 2009). TARDBP mutations account for 4-6% of fALS cases, and 0.5-2% cases of diagnosed sALS (Andersen 2011). Although ALS is the commonest phenotype, FTD, either in other individuals of the same family or in those with ALS, has also been reported, usually manifesting as behavioral changes, but also with semantic dementia. Although disease progression is more rapid than usual, the phenotype is indistinguishable from sALS. Also neuropathological features are similar to those of sALS, with neuronal loss, gliosis and Bunina bodies in the anterior horn of the SpC, and pallor of the corticospinal tracts. In unaffected neurons TDP-43 localises in the cell nucleus, while it is absent from the nuclei of neurons with UBIs, suggesting a nucleo-cytoplasmic redistribution of the protein. Immunohistochemically, there are TDP-43 positive cytoplasmic inclusions in UMNs and LMNs, but also in other regions of the CNS including frontal and temporal cortex (Van Deerlin 2008; Yokoseki 2008). These observations lead to intense speculations on the pathogenic role of TDP-43 in ALS: toxicity might be caused by aggregating TDP-43 being sequestered away from its normal function or, conversely, TDP-43 aggregates might have a toxic gain-of-function independent of the protein's physiological cellular activities (Lagier-Tourenne 2010; Strong 2010; Ticozzi 2010; van Blitterswijk 2010).

TDP-43 is a 414 aa multifunctional DNA/RNA binding protein belonging to the heterogeneous nuclear ribonucleoprotein (hnRNP) family. The function of TDP-43 in the nervous system is uncertain. TDP-43 was originally identified as having roles in human immmunodeficiency virus (HIV) infection and cystic fibrosis (Ou 1995; Buratti 2001). TDP-43 and FUS have striking structural and functional similarities, implicating alterations in RNA processing as central in ALS (see Pathogenic hypothesis section).

→ **ALS11 – Polyphosphoinositide phosphatase (FIG4)**

Mutations in FIG4 have been recently identified in both sALS and fALS patients, suggesting that this gene is another cause of this disease (Chow 2009). Mutations in FIG4 are also responsible for a variant of Charcot Marie Tooth disease, a peripheral-nerve disorder (Chow 2007). FIG4 is a phosphoinositide 5-phosphatase that regulates the cellular levels of phosphatidylinositol 3,5-bisphosphate, a lipid involved in signalling processes and retrograde trafficking of endosomal vescicles to the trans-Golgi network (Rutherford 2006).

→ **ALS12 – Optineurin (OPTN)**

Recently, mutations in OPTN, a gene already known to be mutated in primary open angle glaucoma and ataxia (POAG), were found to cause ALS (Maruyama 2010). Most of the individuals with OPTN mutations showed a relatively slow progression and long disease duration, although the clinical phenotypes were not homogeneous. The mechanisms through which dominant and recessive mutations cause ALS are likely to differ, as are the mechanisms through which different mutations result in ALS or POAG phenotypes. OPTN mutations abolished the inhibition of activation of nuclear factor kappa B (Maruyama 2010). Effects on localisation of the optineurin protein and nuclear factor κB signaling probably account for differences in phenotypic expression. Intracytoplasmic neuronal inclusions, positive for optineurin were observed in SpC tissue of patients with OPTN mutation, as were skein-like inclusions (Maruyama 2010). TDP-43 or SOD1-positive inclusions of sALS or SOD1-fALS patients were also noticeably immunolabeled by anti-optineurin antibodies. However, further studies have produced differing results regarding the presence of optineurin-positive inclusions in ALS and other neurodegenerative conditions (Hortobagyi 2011; Osawa 2011).

→ **ALS13 – Ataxin 2 (ATXN2)**

CAG-trinucleotide repeat expansion in the ATXN2 gene to 34 or more repeats is associated to spinocerebellar ataxia type 2 (SCA2). Very recently, an intermediate length expansion (27-33 repeats) on one allele in ATXN2 gene has been linked to sALS and fALS cases, with fewer than 27 repeats having no clinical phenotype (Elden 2010; Lee 2011; Daoud 2011; Van Damme 2011; Ross 2011; Gispert 2012; Chen 2011; Van Langenhove 2011). The frequency of this genetic alteration is about 4.7% in familial cases. ALS13 shows an earlier onset and mislocalisation of TDP-43 from nucleus to cytoplasm (Elden 2010). This association raises the possibility that ALS and ataxia may also form a spectrum of disease in the same way as ALS and FTD (Al-Chalabi 2012), and this is further supported by the finding of ataxia in some patients with SOD1 or SETX mutations (Andersen 1996; Hirano 2011; Yasser 2010).

→ **ALS14 – Valosin-containing protein (VCP)**

Mutations in the VCP gene, already linked to the genetic disease inclusion body myopathy associated with Paget's disease of bone and FTD (IBMPFD) (Watts 2004), were found also to be associated with features of ALS in some patients (Kimonis 2008). Furthermore, VCP mutations have been linked to 1-2% of isolated familial cases, which are associated with ubiquitin-positive TDP-43 deposition (Johnson 2010). Affected individuals presented with ALS disease in adulthood with a classic ALS phenotype, and none had evidence of Paget disease. In another family, two patients had ALS-FTD, and a third had Paget disease followed by ALS, suggesting an overlap with IBMPFD. Very recently, mutations in VCP have been found also in isolated sALS patients (Dejesus-Hernandez 2011; Abramzon 2012) and in individuals diagnosed with PD (Chan 2012; Spina 2012) or AD (Kaleem 2007; Mehta 2012). The findings indicate an expanded and variable phenotypic spectrum for VCP mutations.

VCP is an ubiquitous and highly abundant protein that accounts for more than 1% of protein in the cell cytosol and is known to have various chaperone-like activities. It is essential in cells where

it is involved in a wide variety of functions: nuclear envelope reconstruction, post-mitotic Golgi reassembly, ER-associated degradation (ERAD) pathway during the "quality control process" and apoptosis (Halawani 2006). It is an ATPase characterised by the presence of the N-terminal domain involved in ubiquitin binding (Ogura 2001; Dai 2001). Indeed, VCP is essential for the turnover of aggregation-prone proteins associated with neurodegenerative diseases, in a fine-tuned balance with HDAC6. In particular, while VCP promotes proteasomal degradation of aggregating proteins and ubiquitin turnover, HDAC6 favours the accumulation of ubiquitinated protein aggregates and inclusion body formation (Boyault 2006). Interestingly, histopathological studies revealed positive staining for VCP in neuronal nuclear inclusions in Huntington's disease (HD), and in intraneuronal UBIs in ALS with dementia, ballooned neurons in Creutzfeldt-Jakob disease, dystrophic neuritis of senile plaques in AD, and Lewy bodies in PD (Hirabayashi 2001; Mizuno 2003). In addition VCP was found aggregated and nitrated in the SpC of symptomatic G93A-SOD1 mice (Basso 2009). Furthermore, VCP physically interacts with the E3-ubiquitin ligase Dorfin, functionally regulating recognition and ubiquitylation of ALS-mutant SOD1 to enhance its degradation (Niwa 2002), and the two proteins are colocalised in the ubiquitylated inclusions in the affected neurons of ALS and PD (Ishigaki 2004). Thus, mutations in VCP together with its localisation in UBIs in various neurodegenerative disordes, provide evidence directly implicating defects in the ubiquitination/protein degradation pathway in MN degeneration.

→ **ALS15 – Ubiquilin 2 (UBQLN2)**

A five-generation family showing X-linked dominant transmission of ALS has shown linkage and cosegregation of a mutation in the UBQLN2 gene (Deng 2011). In the same study, five different proline substitutions in the PXX repeat domain of UBQLN2 were identified as causative of ALS in five unrelated families. The age of onset ranged from 16 to 71 years, with males having a significantly younger age of onset than female, presumably because they are hemizygous for the mutation, while females are heterozygous. Some patients manifested both ALS and FTD. Pathologic analysis of SpC autopsy samples revealed axonal loss in the corticospinal tract, loss of

anterior horn cells, and astrocytosis. Ubiquilin-2-positive skein-like inclusions from ALS15 patients were immunoreactive also for ubiquitin, p62, TDP-43, FUS, and optineurin, but not SOD1. The brain of patients with UBQLN2 mutations with ALS-FTD, showed ubiquilin-2 inclusions in the hippocampus, small inclusions in the neuropil, and large inclusion in some pyramidal neurons. This type of hippocampal pathology had not previously been observed in any other neurodegenerative disorder, indicating that ubiquilin-2 is widely involved in ALS-related dementia. Prominent ubiquilin-2 pathology was observed also in ALS-FTD, sALS and fALS cases without UBQLN2, suggesting a common final pathway for all ALS (Andersen 2011).

Ubiquilin-2 is one of the four members of the ubiquitin-like protein family. Ubiquilins are characterised by the presence of an N-terminal ubiquitin-like domain, that binds to subunits in the proteasome, and a C-terminal ubiquitin-associated domain, that binds to the polyubiquitin chains that are typically conjugated onto proteins marked for degradation by the proteasome. Ubiquilin-2 has a unique repeat region containing 12 PXX tandem repeats. Mutations in ubiquilin-2 may change the ubiquitin modification on substrates, influence recognition by p62 and reduce the clearance of ubiquitinated misfolded proteins (Chen 2012), suggesting that defects in the protein degradation pathway are a shared pathogenic mechanism in ALS.

→ **ALS16 – Sigma non-opioid receptor 1 (SIGMAR1)**

The homozygous E102Q substitution in a highly conserved residue of the SIGMAR1 gene was identified in affected members of a consanguineous Saudi Arabian family with juvenile ALS (Al-Saif 2011). Patients had a very early age of onset (1-2 years) of lower limb spasticity and weakness, with slow progression, without bulbar or respiratory or cognition involvement.

In addition, a heterozygous transversion (672*51G-T) in the 3-prime untranslated region (3'-UTR) of the SIGMAR1 gene was identified in affected members of an Australian family with FTD and/or MND (Luty 2010). This mutation alters SIGMAR1 transcript stability and increases protein expression, resulting in pathogenic alterations of TDP-43 and FUS.

SIGMAR1 encodes a ER chaperone that binds a wide variety of ligands, including neurosteroids, psychostimulants, and dextrobenzomorphans. It is ubiquitously expressed and enriched in MNs. *In vitro*, the mutant protein forms detergent-resistant complexes and decreases the viability of MNs.

→ **ALS17 – Charged Multivescicular Body protein 2B (CHMP2B)**

Heterozygous mutations in the CHMP2B gene were identified in 1% of patients with ALS (Parkinson 2006; Cox 2010). A different heterozygous mutation was identified in an unrelated man with FTD-ALS. All had symptoms of predominant LMN degeneration without UMN involvement. Neuropathologic examination showed no evidence of corticospinal involvement on conventional stains, consistent with the lack of UMN clinical signs. Severe loss of MNs at all levels of the SpC, and surviving neurons had UB-/p62-/TDP-43-positive inclusion bodies. Skein-like inclusion bodies and Bunina bodies were notably absent in these patients. Previously, CHMPB2 gene association (Brown 1995; Gydesen 2002) and heterozygous mutations were reported in unrelated patients with FTD (Skibinski 2005; Momeni 2006; Van der Zee 2008).

CHMP2B is a member of ESCRT-III (endosomal sorting complex required for transport III), which is required for formation of the multivesicular body, a late endosomal structure involved in lysosome-mediated degradation of endocitosed proteins and in autophagy. It is widely expressed in all neuronal populations, especially in the hippocampus, frontal and temporal lobes, and cerebellum and not in astrocytes or oligodendrocytes (Skibinski 2005). Mutations of CHMP2B may contribute to MN injury through dysfunction of the autophagic clearance of cellular proteins, and the formation of UBIs (Cox 2010).

→ **ALS-FTD - C9ORF72**

The existence of a common genetic aetiology between ALS and FTD was proposed with the finding of ALS and FTD in multiple generations in a large Swedish family (Gunnarson 1991). Every affected

patient had a parent with either ALS or FTD, and no individual had both conditions, suggesting that a common genetic factor could cause either conditions. Linkage analysis in this and in similar pedigrees, pointed to a major locus on 9p21.2 for fALS, fALS-FTD, fALS with parkinsonism, and also sALS in some populations (Morita 2006; Vance 2006; Pearson 2011; Laaksovirta 2010; Boxer 2011; Rollinson 2011), suggesting a possible single founder for this form of disease (Mok 2011). Recently, the causative gene defect has been reported as a massive hexanucleotide-repeat expansion, (GGGGCC)n, in the intron between noncoding exons 1a and 1b of the uncharacterised gene chromosome 9 open reading frame 72 (*C9ORF72*) (Dejesus-Hernandez 2011; Renton 2011; Gijselinck 2012). Normal individuals have, at most, 23 repeats, whereas individuals with ALS or FTD can have up to 1600 repeats. This repeat expansion was present in up to 62% of the cases with both fALS and FTD, 46% of the cases with fALS, and 21% of the cases with sALS. Therefore, it is currently the most important genetic risk factor for ALS, and it is not a common cause of AD or PD (Zhengrui 2012). Patients with the mutation presented with typical motor features of ALS, although subjects with the *C9ORF72* mutation had more frequent bulbar onset (Stewart 2012). Dementia was significantly more common in ALS patients and families with the *C9ORF72* mutation and was usually early-onset FTD. There was striking clinical heterogeneity among the members of individual families with the mutation. The associated neuropathology was a combination of ALS with TDP-43-positive inclusions and FTLD-TDP. In addition, a consistent and specific feature of cases with the *C9ORF72* mutation was the presence of UB-/p62-positive, TDP-43-negative inclusions in a variety of neuroanatomical regions, such as the cerebellar cortex. Speculatively, the dynamics of such a hexanucleotide-repeat expansion may explain the variability in phenotypes and disease penetrance in these families, and the association to the 9p21 locus of many cases with apparently sporadic disease.

In addition, *C9ORF72* repeat expansions were found in combination with TARDBP, or SOD1, or FUS mutations in affected individuals within fALS families (van Blitterswijk 2012). The presence of a second mutation supports the hypothesis of an oligogenic aetiology of ALS, implying that additional genetic factors contribute to ALS pathogenesis in some *C9ORF72* families. Moreover,

this also suggests that genetic modifiers exist that determine why some individuals with *C9ORF72* repeat expansion develop ALS, whereas others develop FTD or a combination of ALS and FTD. Furthermore, *C9ORF72* large repeat expansions were present in <1% of families apparently affected with AD (Majounie 2012).

In normal individuals, at least three alternatively spliced *C9ORF72* transcripts (variants 1-3) are expressed in most tissues, including brain, with predominantly a cytoplasmic and synaptic localisation (Dejesus-Hernandez 2011). The mutation results in the loss of one alternatively spliced *C9ORF72* transcript, leading to a significant overall reduction in *C9ORF72* transcripts encoding *C9ORF72* isoform a, thus suggesting a possible loss-of-function mechanism. In addition, the formation of toxic nuclear RNA foci in post-mortem cerebral cortex and SpC tissue of *C9ORF72* expanded repeat carriers, suggested also a possible gain-of-function mechanism. Indeed, RNA foci, a common feature of non-coding repeat expansion disorders, are composed of the repeated nucleotides that sequester RNA-binding proteins, leading to dysregulation of alternative mRNA splicing (Todd 2010; Miller 2000; Sofola 2007; Timchenko 1996; White 2010). Thus, these observations add evidence to RNA misprocessing as a potential pathogenic mechanism in both ALS and FTD.

→ **Other ALS-associated genes**

Susceptibility to ALS has been associated with mutations in other genes, including:

- **TAF15 and EWSR1**

The TATA-binding protein-associated factor 15 (TAF15) is a member of the FET protein family, that includes also FUS and EWSR1. In 2011, six changes in TAF15 gene were identified in a cohort of 263 familial cases (Ticozzi 2011). Immunohistochemical analysis of FET proteins, showed differentiation in FUS-pathology between ALS and FTD. In particular, while ALS-FUS showed only accumulation of FUS, inclusions in FTLD-FUS revealed co-accumulation of all members of the FET protein family, suggesting a more complex disturbance of transportin-mediated nuclear import of

proteins in FTLD-FUS compared to ALS-FUS (Neumann 2011). Recently, two studies (Couthouis 2011 and 2012) have confirmed additional TAF15 missense polymorphisms in sALS patients and found three in the Ewing sarcoma breakpoint region 1 (EWSR1) gene, suggesting that all three genes of the FET family are involved in fALS, sALS or FTD, and promote discrete proteinopathies and phenotypes.

- **Dynactin (DCTN1)**

The DCTN1 gene encodes for the p150 subunit of the dynein/dynactin transport complex. A dominantly transmitted missense mutation (G59S) was identified (Puls 2003) that caused an adult onset, slowly progressive atypical MN disorder with vocal cord paresis, and weakness of facial and hand muscles. Subsequently, three additional heterozygous missense mutations have been found in sporadic and familial patients with classic ALS (Munch 2004). Interestingly, heterozygous mutations in DCTN1 have also been identified in Perry syndrome, a rapidly progressive, autosomal dominant atypical parkinsonism characterised by weight loss, depression, nocturnal hypoventilation, and the presence in the extrapyramidal system of TDP-43 immunoreactive inclusions indistinguishable from those found in ALS (Farrer 2009).

Dynactin is a component of the dynein complex, the molecular motor that plays critical role in intracellular and axonal transport. This complex is required for fast retrograde transport of vesicles, organelles, RNAs and proteins along microtubules. The G59S mutation appears to affect the binding of the dynactin-dynein motor complex to microtubules (Puls 2003). Impaired dynein/dynactin function can explain several pathological features observed in ALS patients and is shown to induce MN disease in mice overexpressing dynamitin, characterised by defects in vesicular transport in cell bodies of MNs, axonal swelling and axo-terminal degeneration and autophagic cell death (LaMonte 2002).

- **D-amino acid oxidase (DAO)**

A unique mutation (R199W) in the D-amino acid oxidase (DAO) gene was associated with classical adult onset fALS in a three generational kindred (Mitchell 2010). DAO is an enzyme controlling the levels of D-serine, a coagonist at the glycine site of the NMDA glutamate receptor. Increased levels of D-serine and its producing enzyme, serine racemase, have been found in the SpC of ALS patients and G93A-SOD1 mice (Sasabe 2007). It has been proposed that DAO mutations, in ALS patients, participate to the buildup of D-serine in the CNS, thus contributing to excitotoxicity.

- **Neurofilament heavy polypeptide (NEFH)**

Six deletions within the C-terminal lysine-serine-proline (KSP) phosphorylation domain of the NEFH gene, encoding for the neurofilament heavy subunit, have been found in several sALS patients and in a pedigree with autosomal dominant fALS (Figlewicz 1994; Tomkins 1998; Al-Chalabi 1999). However, another study on 117 unrelated fALS cases did not identify any mutation in the KSP region of NEFH (Rooke 1996). The possible explanations are that such genetic variation only causes low penetrance disease, so fALS would rarely result, or that associations in apparently sALS are false positives. Nevertheless, neurofilaments are interesting potential candidate genes in ALS pathogenesis, not only because of their restriction to neurons, but also because neurofilamentous inclusions are found in degenerating LMNs in ALS.

- **Peripherin (PRPH)**

A homozygous missense mutation and a heterozygous frameshift deletion in the PRPH gene, encoding for peripherin, have been identified in sALS patients (Gros-Louis 2004; Leung 2004). Immunohistochemical analysis of their SpC showed the presence of aggregates containing peripherin within surviving MNs.

Peripherin is a neuronal intermediate filament protein primarily expressed in autonomic nerves and in peripheral sensory neurons. It is involved in axonal outgrowth, and commonly detected

within UBIs in MNs of ALS patients (He 2004). Mice overexpressing wild-type peripherin develop over time a selective degeneration of spinal ventral roots and motor axons, as well as intermediate filament inclusions within MNs (Beaulieu 1999).

- **Profilin 1 (PFN1)**

Different mutations within the PFN1 gene have been recently reported to cause ALS in two large families (Wu 2012). Further analysis identified that mutations in the PFN1 gene can account for 1–2% of fALS. Cells expressing PFN1 mutants contain UBIs that in many cases contain TDP-43.

PFN1 is crucial for the conversion of monomeric (G)-actin to filamentous (F)-actin. PFN1 mutants display decreased bound actin levels and can inhibit axon outgrowth. Furthermore, primary MNs expressing mutant PFN1 display smaller growth cones with a reduced F/G-actin ratio. These observations further document that cytoskeletal defects have a major role in MN diseases and disruption of cytoskeletal pathway contribute importantly to ALS pathogenesis.

- **p62/sequestosome 1 (SQSTM1)**

Several mutations in the SQSTM1 gene, which encodes the p62 protein, were described in independent cohorts of patients with either FTLD, fALS or sALS, with an overall frequency around 3% (Fecto 2011; Rubino 2012). Previous histopathologic studies have shown that p62 is present in protein aggregates in neurodegenerative disorders such as AD, PD, HD and Pick disease, multisystem atrophy and ALS (Nakaso 2004; Babu 2005; Kuusisto 2001; Zatloukal 2002). In particular, p62 colocalises with UBIs in ALS patients with CHMP2B or C9orf72 mutations or other forms of ALS, and in the G93A-SOD1 mouse model of fALS, suggesting a common pathogenic mechanism (Nakano 2004; Parkinson 2006; Mizuno 2006; Gal 2007; Al-Sarraj 2011). Furthermore, p62 colocalizes with TDP-43-/UBQLN2-positive cytoplasmic UBIs in patients with FTLD-MND (Hiji 2008), and with FUS-/TDP-43-positive UBIs in patients with sALS, non-SOD1 fALS, and ALS with dementia (Deng 2010).

p62 is a multifunctional protein with an important dual role in protein degradation via the proteasome (Seibenhener 2004), and as a link between protein aggregation and autophagy (Bjørkøy 2006) via its interaction with LC3/Atg8 (Pankiv 2007). SQSTM1 mutations may confer a toxic gain-of-function through novel protein interactions and deregulation of cell signaling pathways or may also lead to protein misfolding and aggregation. Indeed autophagy is a critical pathway for degrading misfolded and/or damaged proteins, including mutant SOD1, that can be recognized by p62 in a ubiquitin-independent fashion and targeted for autophagy (Gal 2009), as well as TDP-43. Indeed, overexpression of p62 reduces TDP-43 aggregation in an autophagy- and proteasome-dependent manner (Brady 2011). Furthermore, substrate recognition by p62 is not limited to misfolded protein aggregates, but also includes organelles, such as mitochondria (Kim 2008). These observations provide evidence of autophagy dysregulation as a possible pathogenic process in ALS.

- **Microtubule-associated protein tau (MAPT)**

Tau is a member of the microtubule-associated protein family, which binds to tubulin and has the principal function of stabilizing microtubules and promoting their assembly. In addition, tau is likely to regulate motor protein-mediated transport of vesicles and organelles along the microtubules by modulating their stability (Sato-Harada 1996; Ebneth 1998). In FTD with parkinsonism, mutation of the tau gene affects the alternative splicing of exon 10, resulting in an excess of four repeat tau isoforms; this may cause a reduced binding of tau to microtubules in axons. No case of pure ALS has been associated with tau mutations (Siddique 1995; Hosler 2000; Wilhelmsen 2004; Ogaki 2012).

Reports on novel ALS related mutations constantly extend the list of genes that might be implicated in the disease although most of them are still awaiting for the conclusive studies that prove the associations emerged from genetic screenings. Testing for mutations in the established monogenic ALS genes has now become part of the clinical investigation of ALS, although only a

small group of patients carry such a mutation. The revised diagnostic ALS criteria now couple the finding of progressive LMN lesions with a pathogenic mutation as sufficient grounds to establish a diagnosis of ALS, thus expediting the diagnostic process. As a general rule, only patients with a diagnosis of fALS are tested, but as more is learnt about the genetics of sALS this may change. At present, DNA testing is recommended only for mutations in SOD1, TARDBP and FUS.

1.4.2 Genetic susceptibility

In addition to the genes now claimed as being causative in ALS, several candidate genes have been proposed to increase the risk of ALS based on hypotheses of ALS causation, genome-wide association (GWA) or exome capture sequencing studies (**Table 2**). Mutations in these genes may occasionally give rise to an ALS phenotype or a mixed phenotype. Although the results are still controversial and preliminary, studying these genes may give further insight into the possible pathogenetic mechanisms involved in ALS.

GENE	PROTEIN	VARIATION	INITIAL REPORTS
ELP3	Elongation Protein 3	Microsatellite	Simpson 2009
UNC13A	Munc13-1	SNP	Van Es 2009 Shatunov 2010
DPP6	Dipeptidyl-peptidase 6	SNP	Van Es 2008 Cronin 2008
VEGF	Vascular endothelial growth factor	SNP, haplotype	Lambrechts 2003
SMN	Survival motor neuron	Copy number variation	Corcia 2002 Veldink 2005
PON1	Paraoxonase	SNP	Slowik 2006
HFE	Hemochromatosis	SNP	Wang 2004 Yen 2004
KIFAP3	Kinesin-Associated Protein 3	SNP	Landers 2009
APOE	Apolipoprotein E	Haplotype	Li 2004 Zetterberg 2008
APEX1	Apurinic endonuclease	SNP	Hayward 1999

Table 2 Selected genes putatively associated with ALS as of September 2012.

Abbreviations: SNP, single-nucleotide polymorphism.

- **Elongation Protein 3 (ELP3)** codes for an RNA processing protein. GWAS associated ELP3 gene with ALS in populations from the UK, Belgium and the USA (Simpson 2009). Mutations of the same gene were identified as the cause of neurodegeneration in a fly model.

- **UNC13A** is a diacylglycerol and phorbol ester receptor that regulates the release of neurotransmitters such as glutamate at neuromuscular synapses. Rodent UNC13A is a presynaptic protein with an essential role in synaptic vesicle priming (Rossner 2004). A GWAS revealed significant association for the SNP rs12608932 located at 19p13.3 that maps to a haplotype block within the boundaries of UNC13A, with ALS (Van Es 2009). Meta-analysis of the GWAS data with existing studies on the ALSGene website confirms that this is an extremely strong association (Lill 2011). Furthermore, in cohorts of sALS patients with Italian, Dutch, Belgian, or Swedish descent, UNC13A was confirmed as a modifier of prognosis, thus providing a new potential therapeutic target aimed at slowing disease progression (Chiò 2012; Diekstra 2012).

- **Dipeptidyl-peptidase 6 (DPP6)**, a component of type A neuronal transmembrane potassium channels, was found associated with ALS in two GWAS of sALS datasets from Ireland, the US and The Netherlands and different populations of European ancestry (van Es 2008; Cronin 2006) but was not replicated in subsequent studies on Italian, Polish, French, Canadian, Chinese patients (Chiò 2009; Fogh 2011; Daoud 2010; Li 2009).

- **Vascular endothelial growth factor (VEGF)** has been identified as a candidate gene on the basis of a transgenic mouse model that showed progressive MN degeneration as a consequence of deletion of the hypoxia response element in the promoter of VEGF (Oosthuyse 2001). A number of studies initially associated specific haplotypes of the VEGF promoter with increased risk of developing ALS (Lambrechts 2003), however recent reports failed to confirm any association between polymorphisms in the VEGF promoter and sALS

thus ruling out a causative role in the pathology (Lambrechts 2009; Gros-Louis 2003; Chen 2006).

- **Survival motor neuron 1 and 2 (SMN1, SMN2)** are neuron-specific proteins involved in RNA processing. Deletions or mutations of SMN1 cause child-onset spinal muscular atrophy, whereas variations in SMN2 copy number affect disease severity. A study conducted on 600 sALS cases found that altered copy number of SMN1 occurred more frequently in cases than in controls. It has been suggested that disruptions to the genomic organization of the SMN region may result in lower total SMN protein levels, thus increasing susceptibility of ALS (Corcia 2002 and 2006; Veldink 2001 and 2005).

- **Paraoxonase (PON)** enzymes (PON1, PON2 and PON3) are a major detoxifying system for organophosphorous compounds and are also involved in protecting cells against oxidative damage. Several studies have suggested an association between common haplotypes in the PON cluster and sALS susceptibility (Saeed 2006; Slowik 2006; Cronin 2007; Morahan 2007; Landers 2008; Valdmanis 2008), although published GWAS and a metanalysis of the literature failed to replicate these results (Wills 2009; Ricci 2011; Chen 2012; van Blitterswijk 2012). A recent study, identified eight mutations in the PON cluster in 12 patients, of which nine were fALS and three sALS. All were heterozygous missense or splice site mutations, with the exception of a single homozygous mutation in PON2, identified in an autosomal recessive pedigree (Ticozzi 2010). Since, however, the segregation of the mutations with the disease could not be proven, nor functional data are available, further studies will be needed to validate the role of PON mutations in ALS pathogenesis.

- **Hemochromatosis (HFE)** is involved in iron metabolism and was selected as a candidate gene for sequencing because iron promotes oxidative stress, and abnormally high iron levels have been found in ALS SpC. There have been several independent replications of association in

populations from the UK, Ireland, Italy, Netherlands, USA and China (Goodall 2005; Sutedja 2007; Wang 2004; Yen 2004), but a recent study could not replicate these findings (Praline 2012).

- **Kinesin-Associated Protein 3 (KIFAP3)** is an ubiquitously expressed protein that associates with kinesin to mediate anterograde transport of vesicles along microtubules. A GWAS conducted on sALS cases from the U.S. and Europe revealed a significant association between two variants that lead to reduced expression of KIFAP3 gene, and a 14 month survival advantage. This suggests that decreased expression of KIFAP3 is associated with an increase in survival in sALS (Landers 2009). However this association was not replicated in a subsequent study (Traynor 2010).

- **Apolipoprotein E (APOE)** epsilon4 gene variant is a risk factor for AD. While no major influence of APOE on disease risk was detected in sALS and fALS patients, a gene dose-dependent effect has been associated with the age at which ALS manifests (Li 2004; Zetterberg 2008). Recently, a GWAS in the French population provided evidence for a contribution of the ε4 allele in the occurrence of bulbar-onset ALS amongst men, suggesting that men are normally protected by androgens against bulbar onset and that the ε4 allele inhibits this protection, perhaps by interfering with the androgen pathway (Praline 2011).

- **Apurinic endonuclease gene (APEX1)** was initially selected on the basis of its protective role against oxidative stress. A variant of this gene showed moderate association with ALS (Hayward 1999) although it was not confirmed in the Italian population (Coppedè 2010).

- **Epha4** is a receptor in the ephrin axonal repellent system and has been recently identified as a modifier of ALS in animal models and humans (Van Hoecke 2012). In particular, in sALS patients, Epha4 expression inversely correlates with disease onset and survival, and loss-of-function mutations are associated with long survival. In addition, genetic as well as

pharmacological inhibition of Epha4 signaling rescues mutant SOD1 phenotype and axonopathy induced by expression of TDP-43 or knockdown of SMN1 in zebrafish and increases survival in mouse and rat models of ALS.

Lack of overlap among these studies underlie the heterogeneous nature of this disease and highlights the necessity to analyse ALS associated SNPs in a very large population of patients and controls. Moreover genetic variants in sALS cases are not sure causes of disease whereas their meaning rely on susceptibility to a major risk of the disease which is generally linked and related to restricted and different population cohorts.

Nevertheless, the information provided by genetic studies toward the understanding of the pathogenesis of both fALS and sALS has been invaluable. It has led over the years to the identification of novel cellular pathways involved in MN degeneration, has provided potential therapeutic targets, and made possible the engineering of animal models of ALS. Undoubtedly, the discovery of novel ALS associated genes, will dramatically further our knowledge of ALS pathogenesis.

1.5 Pathogenic hypotheses

The pathogenic mechanisms underlying neurodegeneration in ALS are multifactorial and operate through inter-related molecular and genetic pathways (**Figure 3**). Specifically, putative mechanisms of toxicity targeting MNs in ALS might result from a complex interplay between oxidative stress, excitotoxicity, mitochondrial dysfunction, combined with accumulation of protein aggregates, and alterations of axonal transport and RNA processing. Convergence of multiple pathways is likely to mediate disease onset and progression, and this partially reflects the failure of most single therapeutic approaches in patients (Peviani 2010).

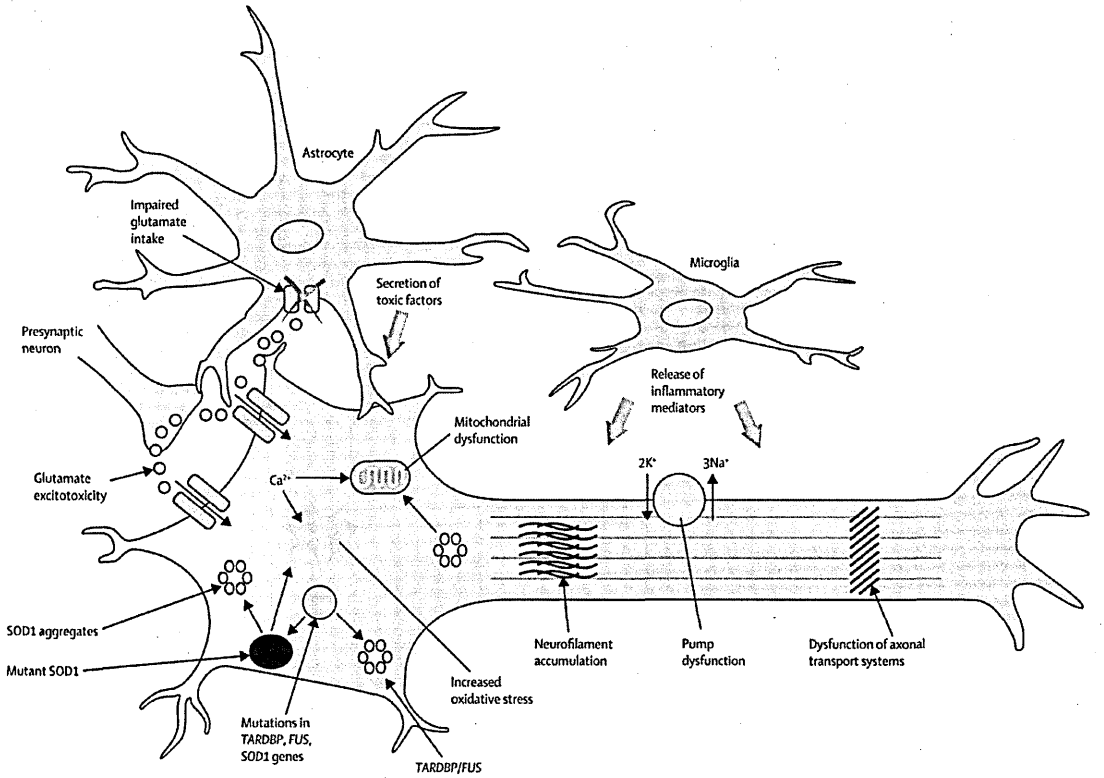

Figure 3 Main pathogenic mechanisms in ALS.

They include glutamate-mediated excitotoxicity, protein misaggregation (SOD1, TDP-43 and FUS), oxidative stress, mitochondrial dysfunction, impaired axonal transport and impaired RNA processing. All these alterations can ultimately lead to neuronal death and to a loss of neuromuscular connectivity and muscle atrophy. Activation of microglia results in secretion of proinflammatory cytokines, resulting in further toxicity. Adapted from Kiernan 2012.

Most current knowledge on the mechanisms leading to the degeneration of MNs in ALS has come from the study of fALS cases, in which mutations in single genes have been identified. Indeed, since the clinical and pathological profiles of sALS and fALS are similar, it can be predicted that evidence emerging from studies on ALS-causing gene mutations may apply also to sALS. However, since the discovery of SOD1 mutations as causative genetic factor for fALS, several hypotheses have been formulated on the possible molecular players involved in the neurodegeneration, and the pathways leading to neuronal death appear to be complex even in this defined genetic subgroup. In addition, one biochemical difference appears to be the absence of pathologic TDP-43 (a hallmark of affected neurons in sALS and FTD) in fALS cases due to SOD1 mutation (Mackenzie 2007). Nevertheless this observation remains controversial since there are contrastating results on human cases and mutant SOD1 mice (Robertson 2007; Turner 2008; Shan 2009).

1.5.1 Oxidative stress

Early evidence suggesting a role for oxidative damage in ALS came from the identification of markers of oxidative stress in the cortex and SpC of patients with sALS and fALS and in transgenic mouse models of the disease (Bowling 1993; Beal 1997; Ferrante 1997; Andrus 1998). In cerebrospinal fluid (CSF) samples from ALS patients, increased levels of oxidative stress markers have been reported too (Smith 1998; Simpson 2004; Ihara 2005; Siciliano 2007). Oxidative stress and accumulation of reactive oxygen species (ROS) is known to cause cell death. The increase of oxidative damage with age fits with middle- or advanced-age onset of ALS, although the age related disease pattern suggests that ALS occurs within a succeptible group within the population rather than being a disease of aging (Logroscino 2010).

ROS and reactive nitrogen species (RNS) are molecular entities that can react with cellular components, causing detrimental effects on their function. Reactive species include both free radicals (species capable of independent existence containing one or more unpaired electrons) and other molecular species listed in **Table 3**. The majority of ROS derive from the incomplete metabolic reduction of oxygen to water during the oxidative phosphorylation of the mitochondrial respiratory chain, where superoxide radical anion ($O_2\bullet^-$) is formed. The mitochondrion is the major site of ROS production. All these species can cause oxidative damage to proteins, lipids, RNA and DNA, as documented in postmortem tissue from sALS and SOD1-related fALS cases, as well as in mutant SOD1 (mSOD1) murine and cellular models, already in the early presymptomatic disease stages (Shaw 1995; Shibata 2001; Fitzmaurice 1996; Chang 2008). Such damage can alter protein conformations and disrupt enzyme active sites, change the properties of cellular membranes by oxidation of unsaturated fatty acids, and introduce mutations into DNA. Interestingly, the SOD1 protein itself seems to be particularly susceptible to oxidative post-translational modification (Andrus 1998). In addition, recently developed cellular models of ALS-mutant TDP-43 indicate that the presence of this mutant protein also induces oxidative stress in MN cell lines (Duan 2010).

Reactive species	
Free radicals	Non radicals
Superoxide, $O_2\bullet^-$	Hydrogen peroxide, H_2O_2
Hydroxyl, OH•	Peroxynitrite, $ONOO^-$
Carbonate, $CO_3\bullet^-$	Peroxynitrous acid, ONOOH
Peroxyl, $RO_2\bullet$	Nitrous Acid, HNO_2

Table 3 Most common reactive species.

They include ROS and RNS, radicals and not radicals species. All of them are oxidizing agents.

As mutations in a major anti-oxidant enzyme, SOD1 gene, account for 20% of fALS cases, there is significant interest in this mechanism. Indeed, it has been hypothesised that mutated SOD1 (mSOD1) may acquire a toxic function and become a source of oxidative stress. Mutations in this anti-oxidant enzyme may alter its folding, impairing either the structural and the catalytic sites, thus leading SOD1 to catalyse aberrant oxidative reaction, altering subsequently the structure and the functionality of other essential proteins (Cleveland 2001). A number of chemical models have been proposed to explain mechanisms which can trigger oxidative stress in mSOD1:

- Peroxidase hypothesis (**Figure 4B**): the reduced form of mSOD1 (Cu^{1+}-bound state) can accept hydrogen peroxide as a substrate thus producing the extraordinary reactive hydroxyl radical, OH•, leading to a cascade of peroxidation (Wiedau-Pazos 1996).

- Peroxynitrite hypothesis (**Figure 4C**): mSOD1 may accept abnormal substrates such as peroxynitrite ($ONOO^-$) (formed by the spontaneous combination of superoxide and nitric oxide), thus causing aberrant nitration of tyrosine residues on different proteins (Beckman 1993).

- Backward catalysis (**Figure 4D**): mSOD1 protein fails to bind zinc properly, thus destabilizing the structure of the enzyme, and allowing a rapid reduction of Cu^{2+} to Cu^{1+}. In its reduced state mSOD1 catalyses the conversion of oxygen into superoxide (backward catalysis), rather than dismutation. The superoxide produced would then combine in the enzymatic active site with freely diffusing nitric oxide, thereby producing peroxynitrite ($ONOO^-$), which can promote intracellular damage, including protein nitration (Estevez 1999).

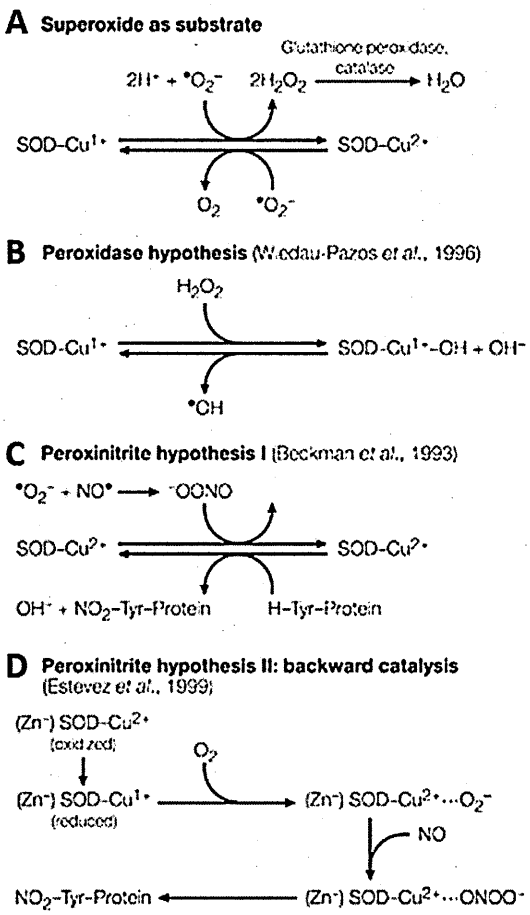

Figure 4 SOD1 chemistry.

WT-SOD1 enzyme uses superoxide ion as a substrate, producing H_2O_2 and molecular oxygen (O_2) as products (**A**). fALS linked SOD1 mutants may acquire aberrant chemical reactivity. leading to production of highly reactive hydroxyl radicals (**B**) or to abnormal nitration of other proteins (**C-D**). Adapted from Cleveland 2001.

However, the concept that mSOD1 provokes aberrant oxyradical reactions still remains quite controversial and recent evidence suggests that mSOD1 may cause oxidative stress by mechanisms beyond its catalytic activity. In particular, mSOD1 in microglia increases NADPH oxidase (NOX)-mediated superoxide production (Harraz 2008). Nevertheless, the manipulation of wild-type SOD1 levels in mSOD1 mice (Jaarsma 2000; Deng 2006), has provided some evidence that heightened oxygen-mediated toxicity is unlikely to be the main player in the degeneration of MNs. Thus, oxidative stress might link and potentially exacerbate other proposed pathogenic mechanisms such as excitotoxicity, mitochondrial impairment, protein aggregation, ER-stress, axonal transport defects and alterations in signaling from astrocytes and microglia (Rao 2004; Duffy 2011; Wood 2003; Kanekura 2009; Blackburn 2009; Sargsyan 2005). In addition, although

antioxidant therapies were the most effective class of drug at improving survival in mSOD1 mice, they have not yet shown benefit in patients (Benatar 2007; Orrell 2007).

1.5.2 Mitochondrial dysfunction

Mitochondria are cellular fueling pumps implicated in many neurodegenerative disorders (Boillee 2006). Morphological and biochemical mitochondrial abnormalities, such as swelling and vacuolization, have been reported in both sALS and fALS patients, animal and cellular model of the disease. In particular, postmortem and biopsy samples from SpC, nerves and muscles show abnormalities in mitochondrial structure, number, localisation (Wiedemann 1998; Siklos 1996), electron transfer chain complexes and DNA (Vielhaber 2000). In addition, mitochondrial mutations have been described in ALS patients (Dhaliwal 2000; Ro 2003). Nonetheless *in vitro* and *in vivo* studies of ALS-mSOD1 models evidenced the presence of mitochondrial pathology in addition to a reduced chain activity and therefore a decrease in ATP synthesis and disruption of energy metabolism, impaired calcium buffering, mitochondria depolarization and worsening of these defects with disease progression (Kong 1998; Higgins 2003; Bendotti 2001; Sasaki 2004; Rizzardini 2006; Jung 2002; Damiano 2006; Menzies 2002).

Moreover, several studies have shown that mSOD1 can directly damage these organelles (**Figure 5**). In fact, a fraction of both wild-type and mSOD1 is localized in the mitochondrial outer membrane, intermembrane space and matrix (Higgins 2002; Pasinelli 2004; Vijayvergiya 2005). SOD1 localisation to mitochondria occurs only in affected tissues, and preferentially for mSOD1 (Liu 2004). Furthermore, mSOD1 strongly triggers cell death when targeted to mitochondria and, when interacting with these organelles, it is able to form protein aggregates and to cause cytochrome c (CytC) release (Takeuchi 2002). The mislocalisation in mitochondria of mutant forms of the protein may account for the toxic gain-of-function of the enzyme through a number of mechanisms, such as abnormal interaction with mitochondrial proteins, like Bcl-2 (Pasinelli 2004), rendering them unavailable for anti-apoptotic functions. Alternatively, SOD1 accumulating and

aggregating in the outer mitochondrial membrane can clog the protein importation machinery, thus resulting in severe dysfunction (Liu 2004).

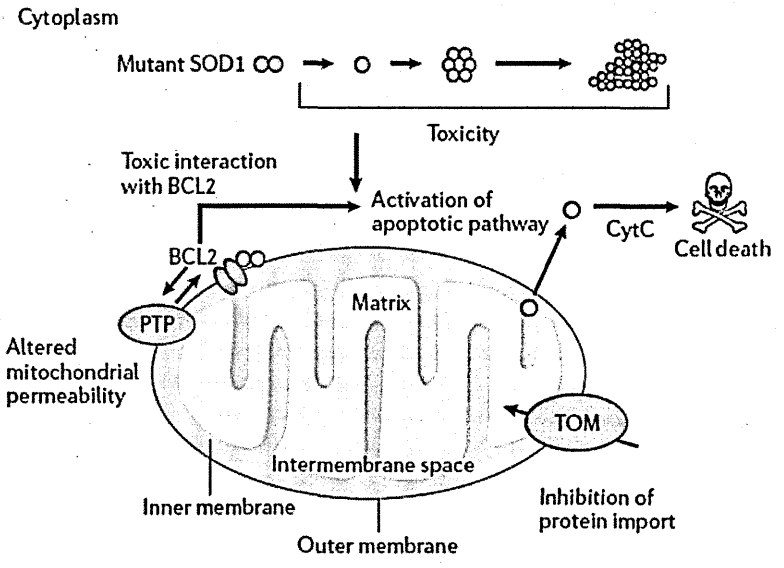

Figure 5 The mitochondrion as a target of mSOD1 toxicity.

SOD1 is not just a cytoplasmic protein but it has recently been observed in mitochondrion in different sub-compartments. mSOD1 can form insoluble aggregates that could directly damage the mitochondrion, thus leading to the release of the CytC, and caspase activation. There is an inhibition of the translocator outer membrane (TOM) complex, preventing mitochondrial protein import and an aberrant interaction with Bcl-2, important in the apoptotic prevention. Adapted from Pasinelli 2006.

These organelles are especially critical to MNs, as these cells must meet extraordinary energetic demands. However, mitochondrial dysfunction in ALS does not seem to be restricted only to MNs as it is also present in other tissue, particularly the skeletal muscle. Interestingly, the lifespan of transgenic mSOD1 mice is increased by a highly energetic diet compensating both the metabolic defect and the MN function. Nevertheless, it is still unknown whether mitochondria can contribute directly to pathogenesis or are only innocent bystanders, and whether mitochondrial abnormalities and dysfunction can both result from or cause oxidative toxicity.

1.5.3 Excitotoxicity

Glutamate is the main excitatory neurotransmitter in the CNS and, in normal synaptic transmission it is released, after depolarization, in the synaptic space and there can bind to specific glutamate postsynaptic receptors. To prevent the aberrant activation of glutamate receptors, glial cells and neurons express glutamate transporters (EAATs) that facilitate the removal of glutamate from the synaptic cleft. Excitotoxicity refers to a neuronal injury caused by prolonged and excessive excitation, typically by glutamate-induced stimulation of the postsynaptic glutamate receptors such as cell surface NMDA (N-methyl-D-aspartate) and AMPA (α-amino-3-hydroxy-5-methyl-4-isoxazole propionic acid) receptors. Glutamate's toxicity is thought to result in massive calcium influxes in the cytoplasm that are potentially detrimental through calcium-activated processes and molecules, leading to increased nitric oxide and free radicals formation, and triggering programmed cell death.

Glutamate-mediated neurotoxicity was first proposed as a mechanism when increased levels of glutamate were discovered in the CSF of a subset of ALS patients (Rothstein 1990). This elevation has been attributed to a significant reduction in the expression and activity of the astroglial glutamate clearing transporter EAAT2, observed in the cortex and SpC in most cases (~65%) of sALS and in transgenic ALS mice (Rothstein 1995; Trotti 1999; Howland 2002), thus evidencing that neuronal degeneration is not a cell-autonomous process. It is still not clear how EAAT2 disruption occurs (given the absence of evidence for mutations, altered expression or splicing in ALS patients), and whether this is a cause or a consequence of neuronal loss (Foran 2009).

In addition, *in vitro* studies have demonstrated that MNs are particularly sensitive to glutamate excitotoxicity mediated through AMPA receptors (Carriedo 1996) (**Figure 6**). In particular, a defect in the RNA editing of the AMPA GluR2 subunit, or a lack of this receptor subunit, have been shown to be involved in the selective vulnerability of MNs in ALS by conferring calcium permeability to AMPA-gated channels (Kawahara 2004). Indeed MNs display a diminished capacity in respect to other types of neurons, to buffer calcium (Alexianu 1994). These increased

Ca^{2+} levels are evidenced also by the appearance of calcium-containing deposits in the LMNs of sALS patients and G93A-SOD1 mice (Siklos 1996 and 1998). Treatments with AMPA receptor antagonists slow disease progression and increase survival of mSOD1 mice, suggesting that AMPA receptors may represent promising targets for therapies (Van Damme 2003; Tortarolo 2006).

In addition, a recently identified ALS-linked gene encodes D-amino acid oxidase (DAO), the enzyme responsible for the oxidative deamination of D-amino acids, one of which (D-serine) is an activator and co-agonist of NMDA receptors (Mitchell 2010). Thus, mutations in DAO could potentially contribute to MN excitotoxicity.

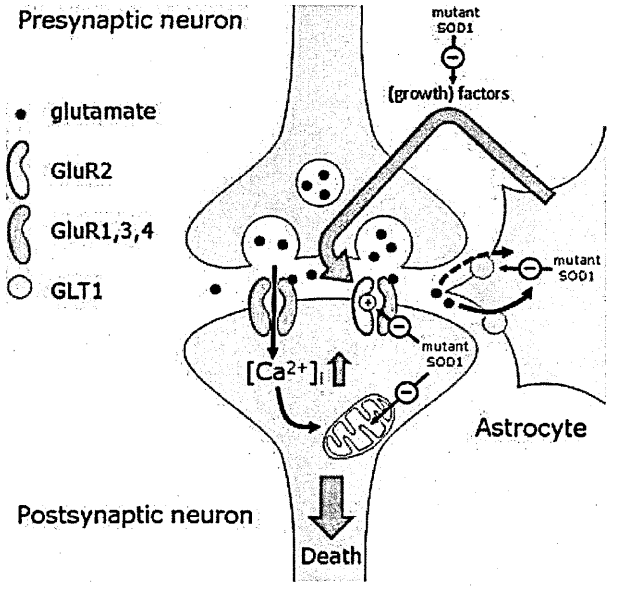

Figure 6 Schematic overview of excitotoxic MN death.

Glutamate released from the presynaptic neuron stimulates AMPA receptors on the postsynaptic neuron. MNs express a large number of Ca^{2+}permeable receptors lacking the GluR2 subunit. As a consequence, glutamatergic stimulation increases the intracellular Ca^{2+} concentration and because of the low Ca^{2+}-buffering capacity of MNs part of this Ca^{2+} could be uptaken by the mitochondria. The presence of mSOD1 in neurons as well as in astrocytes interferes at different levels with this process. Consequently, the balance is shifted from normal glutamatergic communication to excitotoxic MN death. Adapted from Grosskreutz 2010.

Increased glutamate clearance has been considered a possible therapeutic approach. Indeed, Riluzole which is the only drug currently approved for the treatment of ALS patients, is believed to antagonize glutamate-mediated excitotoxicity, although its precise mechanism of action is rather

controversial. Overall, abnormal glutamate metabolism and loss of glutamate transporters in ALS patients, along with proved MN susceptibility to glutamate toxicity and clinical efficacy of anti-glutamate agents support the role of glutamate excitotoxicity in ALS, although clear evidence that it is a primary disease mechanism is lacking.

1.5.4 Impaired axonal transport

MNs are highly polarized cells and have extensive dendritic arbors and axonal processes that may reach up to one metre in length in humans, and rely on active efficient intracellular transport systems to convey newly made materials to even the farthest reaching nerve endings (which includes synaptic structures at the neuromuscular junction) and needed nutrients back to the cell body. These systems consist of anterograde (slow and fast) and retrograde transport systems, and rely on "molecular motors": the kinesin and the dynein-dynactin complexes for anterograde and retrograde transport, respectively (**Figure 7**).

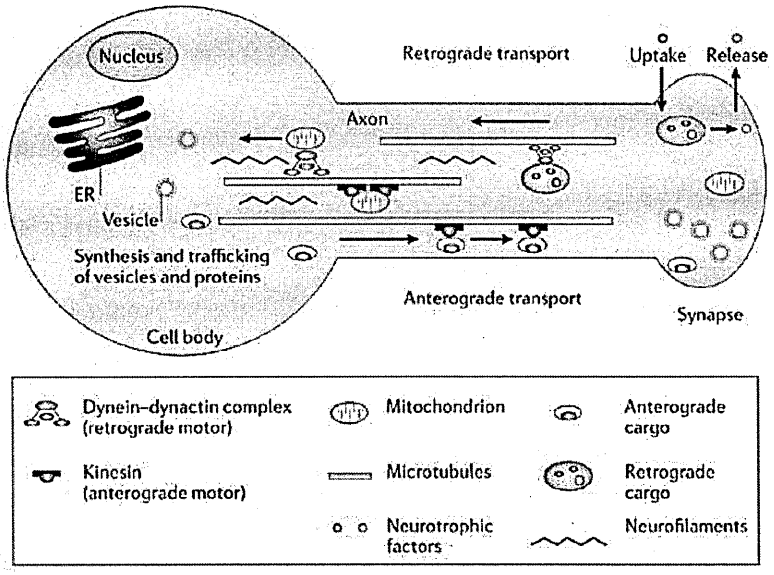

Figure 7 Schematic overview of axonal transport.

The motors for anterograde and retrograde fast axonal transport are the kinesins and dynactin complex proteins, respectively; microtubules provide the tracks for these motors. Vesicles for transport are sorted and loaded onto transport motors both in the cell body and the distal nerve terminal. The former are transported not only into the axon but also into dendrites. Those in the distal nerve terminal permit uptake and axosomatic movement of substances such as trophic proteins. Adapted from Pasinelli 2006.

The reduced activity of axonal transport of the cytoskeleton is one of the earliest pathological events seen both in patients (Sasaki 1996) and in mSOD1 mice (Zhang 1997; Williamson 1999). The SOD1 mouse model shows evidence of axonal degeneration and slowed anterograde and retrograde transport of several cargoes (Borchelt 1998; Murakami 2001; De Vos 2008). Recently, a possible molecular mechanism for axonal transport impairment in ALS pathology was provided by mSOD1 proteins interaction with both the anterograde motor protein kinesin-2 complex via KAP3 (kinesin-associated protein 3) and the retrograde motor protein complex dynein-dynactin (Zhang 2007; Strom 2008). As previously reported, also organelles, such as mitochondria, are transported by the kinesin and dynein motor complexes. Recent *in vitro* studies have shown that mSOD1 can alter mitochondrial transport in both anterograde (De Vos 2007) and retrograde directions (Magrané 2009), thus resulting in inefficient delivery or removal of distal mitochondria, with fewer mitochondria in axons and nerve terminals. This could in turn cause the defective transport of other cargoes, because of the energy requirement of axonal transport.

Moreover, abnormal accumulation of neurofilaments in the cell body and proximal axons of MNs has been described in both sALS and fALS patients (Hirano 1984; Carpenter 1968). Neurofilaments are the most abundant cytoskeletal proteins in MNs and play a key role in defining and maintaining the structure of the axon; their disruption can induce these proteins to form inclusions that can damage MNs, producing symptoms bearing many similarities to ALS. Peripherin and α-internexin are two intermediate filament proteins that colocalize with neurofilaments and are found in axonal inclusions in ALS patients (Corbo 1992); their overexpression in transgenic mice causes MN degeneration (Robertson 2003). A further evidence that disruption of axonal transport could have a role in the pathogenesis of ALS come from the genetic: variants or mutations in the genes encoding the MAPT, NEFH, PRPH, DCTN1 and PFN1 have been recently described in ALS patients (see ALS genetics section). In addition, mutations in the kinesin genes are known to cause other neurodegenerative motor diseases such as hereditary spastic paraplegia and type 2A Charcot-Marie-Tooth disease (Reid 2002; Zhao 2001).

1.5.5 Protein misfolding and aggregation

Abnormal protein aggregates are a common feature of the vast majority of neurological diseases. These lesions, in the form of extra- and intra-cellular inclusions containing ubiquitin, are a hallmark of both sALS and fALS (see Histopathological Features section), suggesting a shared pathogenic link. However, the role of protein aggregation in ALS pathogenesis is unclear: they might cause cellular toxicity, be only by-products of the neurodegeneration process or even a mean of cell protection by sequestering toxic proteins (Cleveland 1999; Tran 1999).

→ SOD1 aggregates

The hypothesis of toxicity from protein aggregation in ALS initially arose from the discovery of intracellular inclusions in MNs and astrocytes in mouse models and patients with mSOD1 (Watanabe 2001; Kato 1999). Insoluble SOD1-containing aggregates appear before or coincident with onset of disease symptoms and increase in abundance with disease progression, suggesting that SOD1 aggregation may be an early event in disease pathogenesis (Johnston 2000; Wang 2002). Aggregates can be composed of different proteins such as SOD1, ubiquitin, dorfin, neurofilaments, peripherin; additionally, chaperones and proteasome subunits may also be sequestered (Watanabe 2001; Strong 2005; Basso 2009).

The oligomerisation hypothesis has been proposed as an alternative mechanism to the oxidative damage hypothesis (see Oxidative stress section **1.5.1**), to explain the toxicity acquired by mSOD1 in ALS. Mutant proteins are likely to cause disease through a toxic gain-of-function, possibly an increase in the propensity of the protein to misfold and aggregate because of conformational instability. SOD1 conformational stability seems to be tightly linked to Cu^{2+} and Zn^{2+} ion coordination, which drives the formation of an intramolecular disulfide bond; metallation and disulfide bond promote the homodimerisation of SOD1 subunits (Arnesano 2004). Indeed, *in vitro* studies have shown that in contrast to stable, dimeric wild-type SOD1, mutant proteins are more prone to oligomerize over time and to form SOD1-rich fibrils (similar to some forms of β-amyloid protein) (Ray 2004; Matsumoto 2006), suggesting that the conversion of soluble SOD1 into

amyloid fibrils may play an important role in the aetiology of fALS. Generally, the mutations can determine both local perturbations of the secondary, tertiary or quaternary structure, diminishing the metal coordination or altering the net charge (Shaw 2007). In addition, SOD1 aggregation might also be promoted by ROS: the active site Cu^{2+} ion can react with hydrogen peroxide, leading to enzyme inactivation (Valentine 2002) and therefore promoting the population of metal free (thus destabilised) SOD1 states. The common result is a destabilization of the enzyme causing non-native interactions with itself or other proteins, thus altering their normal function and leading to high-molecular weight species that ultimately aggregate.

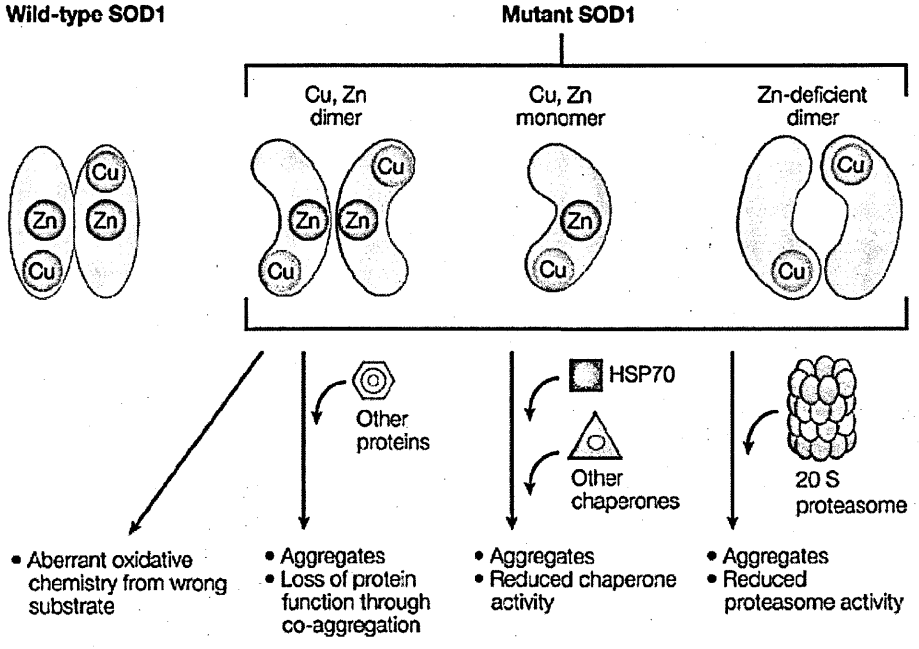

Figure 8 Models for SOD1-mediated toxicity.

SOD1-mediated toxicity linked to altered conformation and aggregation of mSOD1 subunits. Adapted from Cleveland 2001.

Various hypotheses have been proposed regarding the cytotoxicity of SOD1 aggregates (**Figure 8**), including the disruption of axonal transport (Stokin 2005), the aberrant binding of apoptosis regulators (Pasinelli 2004; Tomik 2005) and chaperones proteins, such as heat shock proteins (HSPs), that are crucial for the correct folding of many other important cellular proteins (Shinder 2001; Okado-Matsumoto 2001). Indeed, the overall chaperone activity is modestly diminished in SpC of G93A-SOD1 mice, suggesting that insufficient levels of chaperones can be partially

responsible for the accumulation of insoluble aggregates (Bruening 1999). In addition, treatments with arimoclomol, which increases HSPs expression, extend lifespan of ALS transgenic mice (Kieran 2004). Nevertheless, recent studies proposed that aggregation occurs despite HSPs expression (Krishnan 2008) which anyway contribute in protecting MNs (Patel 2005).

Aggregated SOD1 has also been linked to perturbations in mitochondrial function and calcium homeostasis (Hervias 2006; Sumi 2006), and progressive failure of the proteasome system to eliminate ubiquitinated aggregates (Cleveland 2001; Cheroni 2005 and 2009; Kabashi 2008). Consistent with the latter hypotesis, aggregates in mSOD1 mice are intensely immunoreactive to antibodies for ubiquitin (Stieber 2000; Watanabe 2001), whose role is to label and target misfolded and inactive proteins to the proteasome machinery. Thus, proteasome activity could be inhibited by SOD1 and this pathologic starting event could trigger the accumulation of aberrantly folded forms of SOD1 and other proteins (Cleveland 2001). Finally, unfolded protein response, which follows a severe ER-stress, may contribute to protein misfolding and aggregation. Indeed, two ER chaperones recognized as markers of ER stress, GRP78 and protein disulfide isomerase (PDI), are up-regulated in G93A-SOD1 mice MNs, in sALS patients and in fALS cases linked to SOD1 and TDP-43 (Tobisawa 2003; Zetterstrom 2011; Atkin 2006 and 2008; Honjo 2011). Misfolded SOD1 can specifically aggregate in the ER-Golgi compartments, thus impairing also the Golgi apparatus that has been detected fragmented in MNs of sALS and fALS patients (Okamoto 2010).

→ TDP-43 inclusions

TDP-43 misaccumulation was observed in all variants of ALS, with rare reports in ALS-mSOD1 cases (Mackenzie 2007; Robertson 2007; Tan 2007; Okamoto 2011; Sumi 2009). Besides ALS and FTLD-U, TDP-43 cytoplasmic accumulation and loss of nuclear localisation in affected neurons are now reported in a number of neurodegenerative conditions, including a fraction of AD, PD and HD patients (reviewed in Lagier-Tourenne 2010). In most ALS cases, the cytoplasmic accumulation of TDP-43 was seen mainly in neurons and glia of the primary motor cortex, brainstem motor nuclei and SpC (Mackenzie 2007). ALS patients MNs, showing a normal TDP-43 staining, have a normal

Golgi apparatus profile, whereas Golgi fragmentation is detectable in neurons with cytoplasmatic TDP-43 inclusions, thus suggesting that aggregation of TDP-43 in the cytoplasm can be linked to impairment in the secretory pathway mediated by the Golgi (Okamoto 2010).

The C-terminal domain of this protein is crucial for spontaneous aggregation and several mutations, within this domain, increase the number of TDP-43 aggregates, thus promoting toxicity (Johnson 2009). The observation that ALS-linked mutations increase the stability of TDP-43 protein (Guo 2011; Johnson 2009; Ling 2010) supports the view that protein aggregation may initiate the pathogenic cascade in ALS.

Moreover, pathological TDP-43 is hyperphosphorylated and cleaved to generate C-terminal fragments of approximately 25kDa (Neumann 2006; Arai 2006) (**Figure 9**). The phosphorylation of full length TDP-43 results in a product of 45kDa that was observed in FTLD-U and ALS brains. Although the pathological significance of TDP-43 phosphorylation is not yet known, it has been proposed that this modification might promote TDP-43 aggregation. I*n vitro* studies have demonstrated that phosphorylation of recombinant TDP-43 leads to an increase in the level of TDP-43 oligomers (Hasegawa 2008). Additionally, abundant filaments, immunopositive for S409/S410 phosphorylation-specific TDP-43 antibody, have been observed by electron microscopy (Hasegawa 2008). Although phosphorylation may enhance TDP-43 oligomerization, it may not actually be necessary for aggregation to occur: recent findings have suggested that phosphorylation occurs late in the conversion of soluble to insoluble TDP-43, thus indicating that it is not an essential prerequisite for TDP-43 aggregation (Dormann 2009) and that is not required for C-terminal cleavage (Zhang 2009).

TDP-43 truncation is supposed to be region specific; in fact an enrichment in C-terminal fragments was observed in TDP-43 inclusions in the hippocampus and cortex of FTLD-U and ALS cases, while lesions in MNs consist primarily of full-length TDP-43 (Igaz 2008). Several *in vitro* studies have shown that C-terminal fragments of TDP-43 are more likely than full-length TDP-43 to form insoluble cytoplasmic aggregates that become phosphorylated, ubiquitinated and toxic to cells (Igaz 2009; Nonaka 2009; Arai 2010). It has been also demonstrated that the expression of C-

terminal TDP-43 fragments in cultured cells leads to an aberrant sequestration of the endogenous full-length protein, depleting it from the nucleus (Nonaka 2009), while another study showed retention of normal nuclear expression, thus suggesting a pure toxic effect of cleavage products (Zhang 2009). In addition, C-terminal fragments may also affect TDP-43 function aberrantly interacting with hnRNP A/B proteins, and thus perturbing the equilibrium of available hnRNPs inside the cell. Indeed, TDP-43 is able to bind hnRNPs A/B through its C-terminal domain (Buratti 2005) and, like TDP-43, hnRNPs are involved in RNA processing and, in physiological condition they are able to continuously shuttle between the cytoplasm and the nucleus. However hnRNPs have not been found in TDP-43 positive inclusions (Neumann 2007). Moreover, the cleavage of TDP-43 itself results in loss of TDP-43 function, given that truncations products lack key functional domains (Buratti 2001).

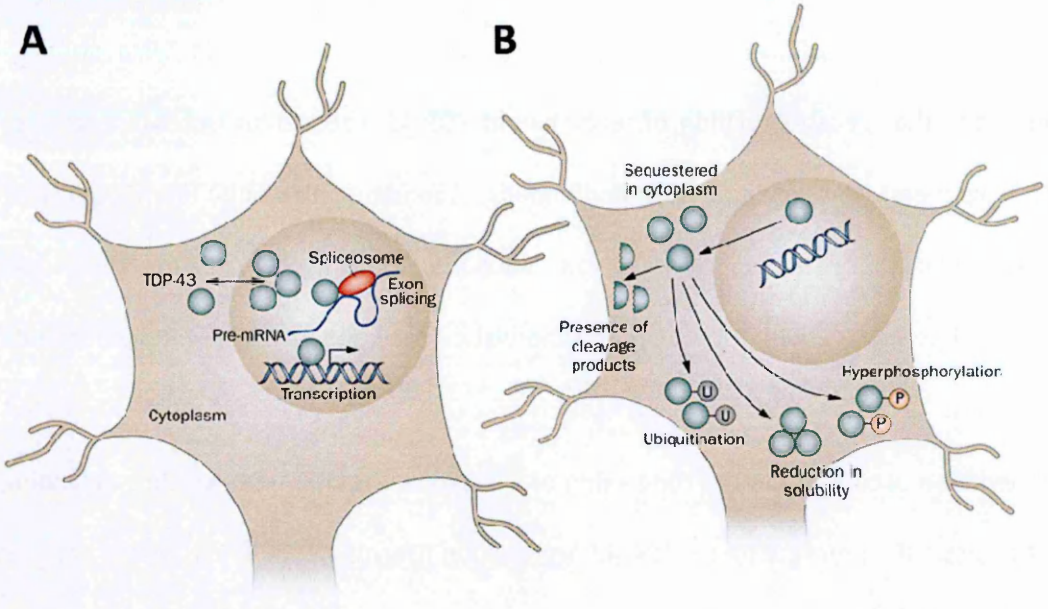

Figure 9 Physiological and pathological TDP-43.

(**A**) Under physiological conditions, TDP-43 primarily resides in the nucleus, although the protein has the capacity to shuttle between the nucleus and the cytoplasm. TDP-43 has roles in regulating transcription, splicing, and mRNA stabilization. (**B**) In pathological conditions, TDP-43 is cleared from the nuclear compartment and accumulates in the cytoplasm. Pathological TDP-43 has been demonstrated to be hyperphosphorylated and/or ubiquitinated and also C-terminal cleaved. TDP-43 is also more prone to aggregation. Adapted from Chen-Plotkin 2010.

The expression of mutant TDP-43 in cultured cells results in increased formation of C-terminal fragments, with even more aggregation and toxic effects than the wild-type protein (Kabashi 2010; Nonaka 2009; Arai 2010; Barmada 2010). *In vivo* studies [conducted in fruit fly (*Drosophila melanogaster*), mice and rats] have shown that overexpression of wild-type human TDP-43 can cause the abnormal formation of TDP-43 cytoplasmic inclusions, with the associated neurodegeneration and motor dysfunction (Li 2010; Wils 2010; Tatom 2009). Whereas results from transgenic animal models overexpressing mutant forms of human TDP-43 are rather inconsistent and difficult to interpret, indicating that the pathogenic mechanism in TDP-43 proteinopathy is still unresolved.

→ FUS/TLS inclusions

As for TDP-43 proteinopathies, also FUS cytoplasmic inclusions have been detected in a growing number of neurodegenerative disorders (Doi 2010; Woulfe 2010). Analyses of the brains and SpCs of ALS patients with FUS mutations have revealed normal staining of FUS in the nuclei of many neurons and glial cells, while it is partially cleared from those nuclei in neurons that contain cytoplasmic aggregation (Neumann 2009; Tateishi 2009; Kwiatkowski 2009; Vance 2009). *In vitro* expression of C-terminal FUS mutations has revealed variable increases in cytoplasmic concentrations of FUS that are compatible with the disruption of its nuclear localisation signal and impaired transportin-mediated nuclear import (Dormann 2010), suggesting that an altered nuclear import of FUS can represent a crucial event in disease pathogenesis.

In contrast with TDP-43 proteinopathies, FUS lacks most of the post-translational modifications (such as hyperphosphorylation, ubiquitination and cleavage) that have been reported for TDP-43. Thus, if common mechanisms underlie toxicity mediated by TDP-43 and FUS, this divergence in the biochemical properties of the proteins may suggest that these alterations are not key contributors to pathogenesis (Da Cruz 2011).

→ p62 inclusions

The presence of p62 in ubiquitin-positive inclusions in many different neurodegenerative diseases, including ALS-FTD, further provides evidence for a potential common mechanism in these disorders, namely, proteins misfolding and impaired proteasomal digestion and autophagy. In addition, mutations in VCP, ubiquilin 2, and p62 (see ALS genetics section), further contribute to alter or impair proteasomal digestion and different steps of the autophagic process, leading to accelerated neurotoxicity, as the catabolic mechanisms of proteasomal degradation and lysosomal-mediated autophagy are hoverwhelmed, and undigested misfolded proteins wreak havoc in the cell (Appel 2012).

Nevertheless, it is not yet clear which one among these events is the cause and which one is the consequence of ALS: it can be proposed that a vicious circle where aggregation and impairment of protein folding and degradation are both present and involved in the pathology.

1.5.6 Impaired RNA processing

Reports from nearly 10 years ago first showed aberrant exon and intron splicing of astroglial glutamate transporter EAAT2 as the cause of abnormal RNA metabolism in sALS (Lin 1998). During the last decade, the discovery of alterations in TDP-43, FUS and C9orf72 firmly established ALS as a disease of impaired RNA processing. Nevertheless, the role of RNA metabolism in ALS is further underscored by disease-causing mutations in ANG, SETX, TAF15 and ELP3, encoding for proteins involved in RNA processing, as well as by the recognition of intermediate length polyglutamine expansions in ATXN2, a RNA binding protein, as a risk factor for ALS (see ALS genetics section).
TDP-43 and FUS, are both abnormally aggregated and mislocalised in ALS and FTLD. They display structural similarities and participate in multiple levels of mRNA processing, such as transcription, splicing, transport and translation (Buratti 2008; Janknecht 2005) (**Figure 10**). With the exception

of a mutation located in a RRM, all TDP-43 mutations identified are located in the C-terminal domain of the protein, which is important for interactions with members of the hnRNP family of splicing regulators (Buratti 2005; D'Ambrogio 2009; Kabashi 2008; Lagier-Tourenne 2009). Recent technologies coupled with high-throughput sequencing have improved the ability in identifying RNA targets. Thus, over 6000 TDP-43 RNA targets have been identified, including transcripts of genes relevant to neurodegeneration, such as FUS, VCP, TARDBP, progranulin and choline acetyltransferase, transcripts encoding proteins involved in RNA metabolism, synaptic function and CNS development (Sephton 2011; Polymenidou 2011; Tollervey 2011), suggesting that disrupting the function of a single RNA-binding protein can affect at the same time many alternative spliced transcripts (Licatalosi 2008). Moreover, multiple RNA targets of TDP-43 are deregulated in ALS, when TDP-43 is mutated or depleted, suggesting that a nuclear loss-of-function is likely to contribute to the pathophysiology of ALS (Xiao 2011).

TDP-43 was initially proposed to repress transcription by binding to the TAR DNA sequence of HIV-1 (Ou 1995) and to mouse SP-10 gene promoter (Abhyankar 2007). FUS can influence the general transcriptional machinery associating with RNA polymerase II and TFIID complex (Bertolotti 1996; Yang 2000). In response to DNA damage it can also be recruited by noncoding RNAs transcribed in the 5' regulatory region of the gene encoding cyclin D1, leading to the repression of cyclin D1 transcription (Wang 2008).

Beyond transcription, these two proteins have also a role in splicing regulation. They associate with other splicing factors and their depletion or overexpression affects the splicing pattern of specific targets (Buratti 2005; Freibaum 2010). In particular, TDP-43 regulates tha alternative splicing of the cystic fibrosis transmembrane regulator (CFTR) (Buratti 2001), and promotes the inclusion of SMN exon 7 (Bose 2008). Abnormal expression of peripherin splice variants (Xiao 2008), mRNA-editing errors of the GluR2 AMPA receptor subunit (Kawhara 2004) and other splicing alterations (Rabin 2010) have been reported in sALS patients.

Although TDP-43 and FUS are mainly nuclear proteins, they are also present in the cytosol, where their binding onto RNA 3'UTRs has been linked with other aspects of RNA metabolism, like

stabilization, transport, translation or degradation. Indeed, TDP-43 binding sites were identified on the 3'UTR of several genes involved in ALS pathogenesis including FUS, the glutamate transporter EAAT2 and the light chain of neurofilament (NFL) (Polymenidou 2011). In particular, TDP-43 stabilises NFL mRNA, whose levels are decreased in degenerating spinal MNs in ALS (Strong 2007). Moreover, in neurons TDP-43 and FUS are found in RNA-transporting granules which translocate to dendritic spines following different neuronal stimuli (Fujii 2005; Wang 2008; Belly 2005; Elvira 2006). TDP-43 depletion reduces dendritic branching and synaptic formation in drosophila neurons (Lu 2009; Feiguin 2009); while cultured neurons from FUS-/- mice show abnormal spine morphology (Fujii 2005). Collectively, these works suggest that both proteins could play a role in the modulation of synaptic plasticity by influencing mRNA stabilization, transport and local translation in neuronal cells, and as a consequence of the mislocalisation and aggregation could thereby contribute to MN injury. In agreement with this hypothesis, other studies have shown that TDP-43 and FUS are components of cytoplasmic RNA stress granules, cytoplasmic foci containing mRNA and ribonucleoprotein (RNP) complexes in which the translation is stalled under stress conditions (Colombrita 2009; Moisse 2009; Nishimoto 2010). Hence it is plausible that the physiologic TDP-43- or FUS-containing stress granules may transform into pathogenic inclusions during neurodegeneration. Therefore, sequestration of specific cellular RNAs within cytoplasmic TDP-43 and FUS inclusions may deplete the cell of essential RNA components, contributing to pathogenesis, and possibly explaining the observation that TDP-43 and FUS binding to RNA is linked to their cytotoxicity independently of their propensity to aggregate (Elden 2010; Sun 2011; Voigt 2010). Indeed, an interesting possibility is that aggregation might cause TDP-43 to bind RNA more avidly; alternatively, or in addition, RNA might stabilize or divert TDP-43 to adopt specific misfolded forms that are highly toxic (King 2012).

The high expression level of microRNAs (miRNAs) and the exclusive expression of certain miRNAs in the CNS highlights their biological importance at all stages of neural development as well as in differentiated neurons. In particular, miRNA activity is essential for long-term survival of postmitotic spinal MNs and for the bidirectional signaling between MNs and skeletal muscle fibers

at neuromuscular synapses. Several miRNAs potentially implicated in skeletal muscle and neuromuscular junction regeneration were de-regulated in ALS brains and specific miRNAs disease-related changes were detected at an earlier stage of sALS (Williams 2009; Russell 2012; De Felice 2012). TDP-43 and FUS may also be involved in these pathways, since they participate in miRNA biogenesis through association with the Drosha complex (Buratti 2008). In addition, TDP-43 is also involved in the next steps of miRNA maturation, via interactions with argonaute 2 and DDX17 (Freibaum 2010). Indeed, TDP-43 binds miRNA let-7b and miR-663 and, following TDP-43 knockdown, their levels were deregulated (Buratti 2010).

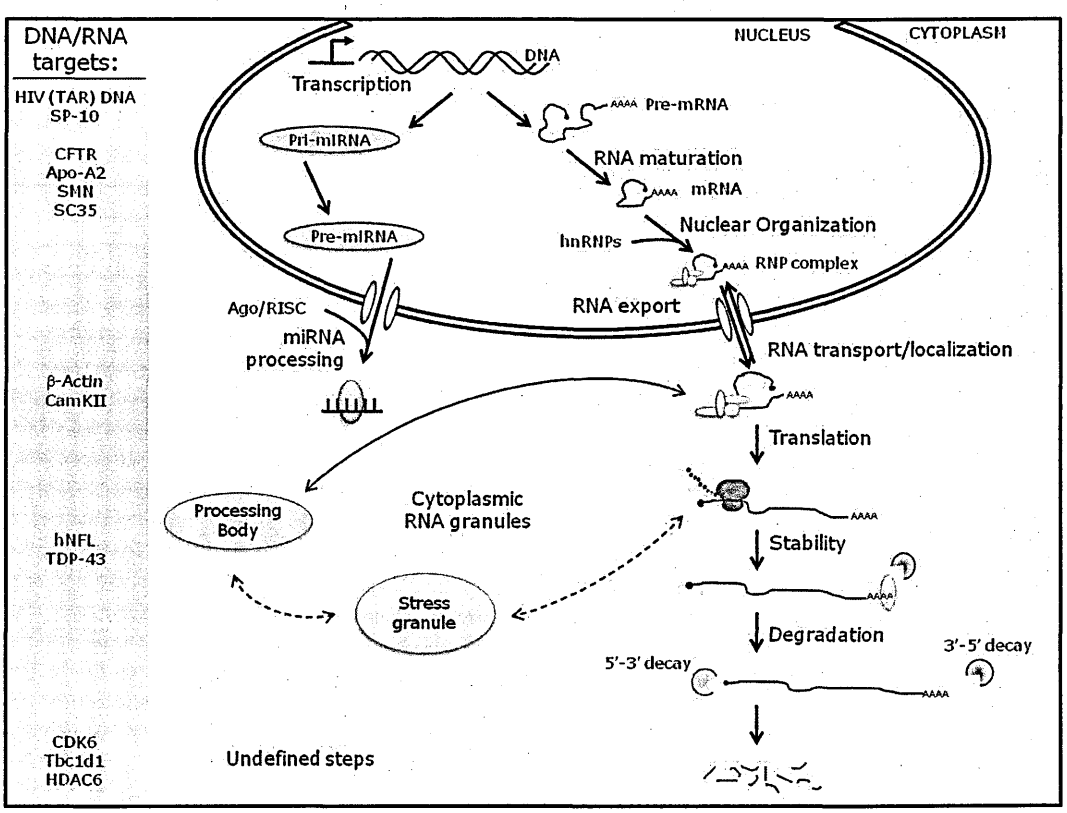

Figure 10 Proposed roles of TDP-43.

Major steps in RNA processing and relative DNA/RNA targets. Modifed from Fiesel 2011.

Another mechanism of RNA toxicity in ALS and FTLD is caused by pathological $(G_4C_2)_{30\text{-}1600}$ hexanucleotide repeat expansions in nontranslated regions of the *C9ORF72* gene. As established in other neurological diseases, especially myotonic dystrophy types 1 and 2 or Fragile X-associated tremor ataxia syndrome (FXTAS), pathogenicity is initiated at the RNA level through two possible pathways. (i) Consistent with a loss-of-function mechanism and supported by the 50% reduction

in C9orf72 transcript levels in patients with expansions, repeats prevent the expression of the normal protein (haploinsufficiency of *C9ORF72*). (ii) In addition, expanded RNA forms pathogenic nuclear RNA foci that trap specific RNA-binding proteins with affinity for the expanded RNA, resulting in their depletion and loss-of-function (protein sequestration mechanism) (DeJesus-Hernandez 2011). hnRNP A2/B1 is a potentially interesting RNA-binding protein in this context, since it interacts with the C/G-rich repeats that form RNA foci in another neurodegenerative condition (FXTAS) (Sofola 2007) and is also a direct interactor of TDP-43 (Buratti 2005). Thus, these observations could possibly explain the presence of TDP-43-based pathology in expanded repeats carriers and add evidence to RNA misprocessing as a common pathogenic mechanism in ALS and FTD.

The RNA-based mechanisms described are extensively coupled with protein misfolding and aggregation, suggesting that these defects are inevitably interconnected in neurodegenerative processes. Moreover, both contribute to neurogegeneration broadly, thus, regardless which one is the primary or secondary event, they represent key steps in the pathological cascade, further supporting the hypothesis (Dormann 2011) of a "multiple hit" pathogenesis of ALS.

1.5.7 Insufficient neurotrophic/growth factors signaling

Neurons development and maintenance is dependent on crucial trophic factors supply. Decreased levels of neutrophic factors (e.g. CTNF, BDNF, GDNF and IGF-1) have been observed in ALS patients post-mortem and in *in vitro* models (Anand 1995; Elliott 1996; Oppenheim 1996). A neuroprotective role for trophic factors is supported by studies in animal models of ALS demonstrating delayed disease onset and progression (Wang 2007; Storkebaum 2005; Azzouz 2004; Kaspar 2003). Nevertheless, human trials have failed so far to follow up on that success (Borasio 1998; Lai 1997).

In addition, mutations in VEGF have been reported as causative of MND in mice and, in some populations, mutations in VEGF and angiogenin are indicated as risk factors in sALS (see ALS genetics section). These angiogenic factors are thought to influence MNs via direct neurotrophic effect and via their action to maintain blood flow to these highly metabolically active cells. The reduced vascular perfusion that occurs with age, the increased incidence of ALS in males who are more likely to develop vascular disease compared to premenopausal females, and smoking as risk factor for ALS, provide circumstantial evidence that supports this mechanism.

1.5.8 Contribution of non-neuronal cells and neuroinflammation

A growing body of evidence suggests a non-cell-autonomous mechanism in ALS pathogenesis as well as in MN protection. Indeed, the restricted expression of mSOD1 only in MNs or in other cellular populations led to the conclusion that in ALS multiple cell types are differentially implicated in the selective degeneration of MNs. Thus, defective non-neuronal cells in the local microenvironment are required to fully recapitulate disease symptomatology in murine models, whereas functional non-neuronal cells could play a protective role in halting disease propagation. Likewise, therapeutic manipulation within neurons alone only prevents degeneration while surrounding cells, notably astrocytes and microglia, appears capable of modifying disease progression.

Glial cells, that normally support the neuronal function, outnumber MNs in the brain by five to ten times. When the function of the brain is imbalanced, glial cells move from a resting state to an activated state, and can either preserve neurons from damage or contribute to their degeneration. In normal conditions astrocytes provide nutrients for neurons, and also ensure the efficient and correct cell-cell interactions. Microglial cells instead perform a pivotal role in the CNS as the chief mediator of immune function. The role of both cell types in ALS development is not yet very well understood. Overall, it is likely that glial cells do not trigger the neurodegeneration

and have little effect on the early disease phase, but have a striking impact on later disease progression. Prevailing hypotheses for astrocyte contribution include direct or indirect contributions to glutamate-induced excitotoxicity, impaired metabolic support, alterations in gliotransmission, or direct release of diffusible neurotoxic factors, such as proinflammatory cytokines and chemokines.

Although ALS is not primarily a disorder of autoimmunity or immune dysregulation, there is considerable evidence that inflammatory processes and non-neuronal cells may play a part in ALS pathogenesis. Indeed, microglial and dendritic cell activation and infiltrating lymphocytes were observed in the SpC of ALS patients and mSOD1 mice (Troost 1989 and 1990; Kawamata 1992; Henkel 2004; Hall 1998; Appel 2010), suggesting the involvement of the innate and adaptive immune responses. These activated non-neuronal cells produce some key inflammation meditors such as interleukins, COX-2, TNFα and MCP-1, and evidence of upregulation is found in CSF or SpC specimens of ALS patients or *in vitro* models (Almer 2001; Robertson 2001; Sekizawa 1998; Wilms 2003). Recently, denervation was demonstrated to occur prior to inflammation in mSOD1 mice, suggesting that peripheral nerve inflammation is probably not the cause of denervation, but rather a response to the neurodegenerative process (Kano 2012). Indeed, microglial activation occurs at presymptomatic stage in mSOD1 mouse model and is sustained throughout the course of the disease. Activated microglia release mediators that cause astrocytes to downregulate the production of neurotrophic factors and, in turn, secrete additional inflammatory moleculs that further activate microglia, closing thus a vicious circle. A similar inflammatory response is preceded by evidence of a "dying back phenomenon" which includes motor axon degeneration and alterations of the neuromuscular junction (Fischer 2004). These and other observations further suggest that neuroinflammation may indeed contribute to the pathoprogression of MN degeneration (Beers 2011). Immunomodulatory therapies have been envisaged for ALS; clinical trials of neuroprotective agents, including stem cells and non-neuronal cells directed approaches are ongoing.

1.6 Experimental models of ALS

Major breakthroughs in the field of ALS research derived from the identification of mutations in genes as a cause of ALS, that allowed the development of experimental models of the disease. In particular, the expression of mutant forms of the relative proteins in laboratory animals and cells is widely used to study the pathology and its progression, and to test potential therapeutic approaches. *In vivo* models are particularly useful to investigate complex cellular processes at different stages of the disease, whereas *in vitro* models are useful tools for the study of the molecular mechanisms underlying neurotoxicity. These models are clearly not precise replicas of the human condition, but the key issue in working with them is that cellular and biochemical pathways are largely conserved.

1.6.1 In vitro models

In vitro cell cultures are the most widely used system developed to study individual cell types under stress conditions. Several *in vitro* models have been developed to investigate the cellular processes involved in the pathogenesis of ALS. The main advantage offered by *in vitro* systems is the possibility to dissect specific molecular pathways in defined cell populations. In addition, although these experimental models have intrinsic drawbacks, thanks to their relative ease of manipulation they have often been regarded as the starting point for testing pharmacologic treatments, or for studying the toxic effects induced by expression of mutant genes linked with ALS.

In vitro models currently used in ALS research comprise both transgenic and wild-type neuronal-like, MN-enriched, astrocyte and microglial cultures, as well as ALS patients derived lymphocytes and fibroblasts. MN cultures, including either primary fetal neuronal or glial cell cultures (Spalloni 2004; Tortarolo 2004; Gingras 2007) or co-cultures systems (Ferri 2004; Bilsland 2008) have been used to study non-cell autonomous mechanisms of ALS pathogenesis and identify neuroprotective

pathways (Bendotti 2004). As an alternative approach organotypic cultures of SpC sections from postnatal rodents have been produced (Drachman 2000). Recently, neuronal cultures are obtained from both embryonic cells and induced pluripotent stem cells (iPS), with the advantage of creating patient specific lines that carry human ALS linked mutations (Marchetto 2010; Mitne-Neto 2011; Haidet-Phillips 2011). Usually, to study specific features of ALS, MN-like hybridoma cell line, such as NSC-34 or SH-SY5Y, or other immortalized cell lines are employed. In particular, immortalized cell lines transiently or stably expressing wild-type and mutant ALS-related genes have been created, as for SOD1 and TDP-43, or are in development (Gomes 2008; Ferri 2006, Colombrita 2009, Duan 2010; Babetto 2005; Raimondi 2006; Liu 2009).

1.6.2 In vivo models

Animal models are an invaluable experimental paradigm to examine the multiple aspects of the pathogenesis of a neurodegenerative disease, particularly when many cellular systems are involved, as in ALS. A great advantage of such models is the possibility to investigate the earliest cellular and molecular events that initiate the neuropathological process, and to monitor the mechanisms that influence disease progression at each clinical stage, from onset to death. Transgenic rodents have also provided the benchmark preclinical tool for evaluation of potential therapeutic pharmacological agents and diagnostic markers.

Murine models are the most widely used i*n vivo* model for studies on ALS/MND (reviewed by Peviani 2010), and can be subdivided into:

- spontaneous mutants, derived from natural mutations occurring in genes that lead to impairment of the motor system, including *PNM* (Martin 2002), *Wasted* (Newbery 2005) and *Wobbler* (Schmitt-John 2005) mice;
- N-ethyl-N-nitrosurea (ENU)-induced mutants, obtained by the induction of point mutations in the genome through exposure to the alkylating agent ENU (Hafezparast 2003; Puls 2003);

- targeted mutants, transgenic animals expressing mutated genes linked to ALS or knock-out mice.

In particular, identification of ALS-causative genes allowed genetic modeling of ALS in rodents as well as in easy-to-manipulate organisms including Drosophila, C. elegans and zebrafish. Indeed, fALS gene knock-in mice recapitulate most of clinical symptoms and histopathological marks encountered in patients (Turner 2008; Wergorzewska 2009). Nevertheless, it must be kept in mind that identical mutations result in surprisingly divergent phenotypes in different strains and no model perfectly mimics the human disease. Available genetic animal models comprise murine and rat strains bearing wild-type or mutated human gene, or gene knock-outs for SOD1, TDP-43, ALS2, ADAR2, Dynactin, FUS, VCP, while some other are being developed ahead with the discovery of novel ALS genetic determinants. Transgenic animals show clinical signs associated with MN disease, or some features of MN impairments without reducing life span.

The most widely used animal model of ALS is represented by transgenic mice expressing the human SOD1 gene with mutations found in patients. Indeed, mSOD1 transgenic mice have become widely accepted and, over the last 15 years, an almost exclusive animal model of ALS. At present, transgenic expression of 12 human SOD1 mutations driven by the endogenous promoter is disease-causative and uniformly lethal in mice and rats, despite consistent variation in transgene copy number, protein level, dismutase activity and neuropathology between different mutants (Turner 2008). In addition, the background effect of the gender or the mouse strain on the age of onset, disease duration and several pathological features, suggest the existence of strong modifying genetic factors (Alexander 2004; Heiman-Patterson 2005). Nevertheless, these animals develop a phenotype that closely resembles ALS, with an adult onset progressive motor paralysis, muscle wasting and reduced lifespan. Pathological changes mainly consist of depletion of MNs in the SpC, gliosis, axonal swelling and presence of UBIs in surviving MNs, and muscular atrophy. In contrast, mice overexpressing or knock-out for wild-type SOD1 do not develop ALS-like phenotype.

mSOD1 model proved to be useful to identify non-neuronal cell targets of SOD1 toxicity, misregulated neurotrophic and cell death pathways, and to survey other genetic interactors that can modify the disease. Indeed, around 100 genetic cross-breeding experiments with transgenic mSOD1 mice have been performed to verify molecular mechanisms proposed to drive ALS pathogenesis *in vivo* (glutamate-induced excitotoxicity, axonal transport blockade, mitochondrial dysfunction, neuroinflammation, protein misfolding and apoptosis).

In particular, the mouse model most extensively used in ALS is a line expressing human SOD1 with the Gly93Ala substitution. Despite the relative rarity of this mutation, it has been studied intensely as it was the first mutation to be modeled in mice (Gurney 1994), and due to the ready availability of the G93A-SOD1 mouse. Established in 1994, the G93A-SOD1 mouse model is internationally accepted as a robust model for ALS research. Transgenic mice carrying 23 copies of the human gene are considered the standard model of ALS in therapeutic studies (Bendotti 2004). The model develops a motor system disease prevalently affecting LMNs. Clinical onset of symptoms is generally established when mice present tremors and impairment of motor tasks, concomitant with hindlimbs paresis. MNs loss is present already before symptoms onset and further increase with the progression of the disease. The earliest pathological sign in these mice is the vacuolization of large neurons in the anterior horns of the SpC (Bendotti 2001), as a consequence of rough-ER dilatation and degenerating mitochondria. Starting with symptoms onset, astrocytosis and microglial activation are detected. With disease progression, also forelimbs are affected, and an increase in SpC protein inclusions, ubiquitin-proteasome impairment, ER-stress, gliosis and degenerated MNs are detected. Mice die about one month after symptoms onset (Bendotti 2004; Turner 2008).

While several studies have reported promising results in SOD1 rodent models prolonging survival of the animals and preventing MNs loss, the therapeutic relevance of animal models remains questionable, as most preclinical trials failed to translate into effective therapies for ALS patients. Recently, it has been suggested that the results of most trials performed so far in mSOD1 mouse are likely to reflect some variables intrinsic to the model, such as genetic background and vast

phenotypic variability, as well as those associated with preclinical studies management, rather than actual drug effects. Thus, attempts to standardize preclinical testing in animal models have been made and findings from promising therapies in transgenic mSOD1 mice now await successful translation in patients.

1.7 Biomarkers of ALS

The National Institutes of Health has defined a biomarker as "an objective measurement that acts as an indicator of normal biological processes, pathogenic processes or pharmacological responses to therapeutic intervention" (Biomarkers Definitions Working Group 2001).

1.7.1 Significance of biomarkers in ALS

Limited understanding of ALS pathogenesis along with a lack of diagnostic and prognostic tools impair efficient detection and treatment of the disease. In fact, the mean diagnostic delay from the appearance of the first symptoms to a correct diagnosis of ALS has been reported to be between 8 and 15 months. Advanced progression of the disease at the time of diagnosis is detrimental to the management of the disease, because it limits the possibilities for effective therapeutic intervention and clinical trials. For this reason, the establishment of early diagnostic biomarkers might be clinically very useful to identify and screen individuals at risk of developing ALS before symptoms onset. Biomarkers would also enable an earlier and correct diagnosis by distinguishing patients with ALS from those with other neurological diseases, as well as discriminate between ALS subtypes. In addition, biomarkers that correlate with disease progression could serve as surrogate end points markers to facilitate the screening for effective therapeutic strategies by monitoring drug efficacy and toxicity. Indeed, this would facilitate go-no-go decisions during clinical trials, increasing safety and efficacy, and overall speeding drug development. Current efforts are underway with both large consortia and individual groups being involved in biomarkers identification.

A consensus has been found for the development of magnetic resonance imaging (MRI) markers, "dry markers" (Turner 2011); major candidates are decreased fractional anisotropy within the corticospinal tract and the posterior body of the corpus callosum (Unrath 2011). Furthermore, a number of biochemical markers, "wet biomarkers", not only for the diagnosis, but also for the longitudinal assessment of ALS have been suggested. However, they have not been validated between internationally active laboratories and probed in large cohorts of patients.

Most of the current research efforts are focused on the discovery of protein biomarkers in biofluids and tissue samples. Disease specific material (spinal cord, brain stem, motor cortex) is not available for diagnostics or monitoring in ALS. Thus, tissue-based biomarker analysis for ALS is limited to muscle biopsy in living patients and postmortem CNS and muscle tissue samples, that are representative of advanced and end stages of the disease. Major candidate samples for wet biomarker development include blood plasma (Mitchell 2010), peripheral blood mononuclear cells (PBMCs) (Nardo 2011), CSF (Ryberg 2010; Jesse 2011) and skin biopsies (Weis 2011). Advantages of the use of blood and CSF as surrogate tissues for biomarker discovery regard their availability for routine sampling during all stages of disease and well optimized standard operating procedures for sample acquisition, processing, and storage. CSF contains proteins released from different neuronal and non neuronal cell types while blood samples provide also information on systemic events. Moreover, an important benefit for current and future proteomic studies is the existence of consistent knowledge on their proteome. Urine and saliva represent alternative sources of protein, or more likely, peptide biomarkers, that are readily available through non-invasive collection.

1.7.2 Biologic markers of ALS

Technologies that can quantify changes in protein levels or identify abnormal post-translational modifications (PTMs) of proteins have enabled detailed searches for protein-based biomarkers for ALS. Indeed, several recent studies have identified individual proteins and/or protein panels from

blood samples and CSF that represent putative ALS biomarkers. At the same time, these protein biomarkers, demonstrating the presence of anomalies in various pathways implicated in ALS, can also provide new insights into the pathogenesis of the disease and can support the identification of new targets for drug treatment.

The first blood based study has lead to the discovery of aminoaciduria in some patients with disrupted calcium metabolism and neuromuscular symptoms (Patten 1978). More recent findings have revealed higher concentrations of tyrosine in the serum, and glutamate (excitotoxicity hypothesis) in the plasma, as well as decreased concentrations of large neutral amino acids (Camu 1993; Ilzecka 2003). An increased concentration of excitatory aa, notably glutamate and aspartate, has also been observed in the CSF of patients with ALS (Rothstein 1990), as well as increased neurofilaments concentration (Rosengren 1996).

On the basis of the presence of oxidative stress and inflammation as important pathogenic effectors in ALS, an increase in 4-hydroxy-2,3-nonenal and monocyte chemoattractant protein 1-α levels have been detected in serum of ALS patients (Simpson 2004; Baron 2005). Moreover, altered levels of multiple inflammatory cytokines (IL-2, IL-6, IL-10, IL-15 and GM-CSF) and individual chemokines (MCP-1 and IL-8) have been detected in the CSF and in blood (IL-8, CCL11, CCL24 and CCL26) of ALS patients (Mitchell 2009; Kuhle 2009).

Altered concentration of growth factors, such as plasma-transforming growth factor-beta 1 in plasma (Ilzecka 2002), VEGF, FGF2, HGF, GDNF and PEDF in CSF (Moreau 2006; Johansson 2003; Kern 2001; Grundstrom 2000; Kuncl 2002), IGF-1 in both fluids (Hosback 2007), angiogenin in serum (Cronin 2006) were also observed.

In the last few years, the use of mass-spectrometry-based proteomics has greatly increased the yield of candidate biomarkers for ALS. In particular, cystatin C and transthyretin have been identified as candidate biomarkers for ALS in different studies in CSF and blood samples, in association with the neuroendocrine protein 7B2, the neurosecretory protein VGF or fetuin-A in CSF (Ranganathan 2005; Pasinetti 2006; Ryberg 2010; Brettschneider 2010). In addition, a

longitudinal study on CSF samples identified cystatin C as a prognostic indicator of disease progression (Wilson 2010). Interestingly, one protein, galectin-3, emerged as a candidate biomarker for ALS, as it was highly enriched in G93A-SOD1 tissues, as well as in human ALS SpC and CSF (Zhou 2010).

Recently, two-dimensional differential in gel electrophoresis (2D-DIGE), a robust fluorescence-based quantitative system, with subsequent MALDI-TOF/TOF mass spectrometry, was used to identify protein alterations in PBMC from patients with ALS (Nardo 2011). A panel of 14 protein biomarkers was validated and the following combinations of proteins may be useful in clinic:

- CLIC1, actin^{NT} and hnRNP A2/B1, to support diagnosis with 98% discriminatory power;
- ERP57, to discriminate between patients with high and low disease severity with 89% discriminatory power;
- ERP57, TDP-43 and CypA, to determine disease progression (confirmed in an independent set of sporadic patients in a pilot longitudinal study);
- CypA and IRAK4, to significantly distinguish ALS from other neurological disorders with 91% discriminatory power;
- CypA, GSTO1, FUBP1, CLIC1 and actin^{NT}, to link pathogenic events between human and animal models. Indeed, these are translational biomarkers, since showed similar changes in PBMC of sALS patients and G93A-SOD1 rats, and were also altered in the SpC of G93A-SOD1 rodents before disease onset.

It is difficult to know whether the proteomic changes reported in ALS are a consequence or a cause of its complex pathology. Moreover, many of these proteins are not unique for the disease. Thus, further investigations are required to validate these initial findings and pursue the role of these proteins in a clinical context as diagnostic or surrogate markers of the disease.

1.7.3 TDP-43 as a biomarker in ALS

TDP-43 can be considered a biochemical marker of ALS and FTLD. Following its identification as the main component of UBIs (Neumann 2006; Arai 2006), several human tissues have been analysed for TDP-43 levels or the presence of aggregates, in order to evaluate the possibility of using TDP-43 as a biomarker to detect disease onset and progression. The presence of abnormal TDP-43 levels or modifications has been detected in CSF (Kasai 2009; Noto 2011; Steinacker 2008), blood plasma (Foulds 2008; Kuiperij 2010), circulating lymphomonocytes (De Marco 2011; Nardo 2011), skin biopsies (Suzuki 2010) and skeletal muscle (Soraru 2010) from sALS patients. The most promising sources of TDP-43 material to be used for biomarker studies include PBMCs and CSF (Buratti 2012).

Interestingly, TDP-43 levels in the CSF are increased only in ALS patients and not in patients with other neurodegenerative or inflammatory diseases such as PD, multiple sclerosis, or Guillain-Barré syndrome, thus indicating a specificity for this pathology (Noto 2010). Moreover, lower CSF TDP-43 levels are associated with shorter survival time, thus suggesting that among ALS patients, lower levels of TDP-43 in the CSF may reflect its accumulation in cortical and spinal MNs and thereby are associated with a worst prognosis.

1.7.4 Cyclophilin A is a candidate biomarker for ALS

The protein cyclophilin A (CypA) recently emerged as a lead biomarker candidate for ALS from the proteomic analysis of PBMC of sALS patients conducted in our laboratory (Nardo 2011). In particular, increased levels of CypA were first identified in a small group of patients (n=11) compared with healthy controls, and then verified on a relatively large cohort of patients (n=60). Multivariate logistic regression analyses showed that CypA was able to differentiate two levels of disease severity and, more importantly, to distinguish ALS from other neurological disorders. In the same study, a well-characterised and relevant model of ALS, the G93A-SOD1 rat, was analysed

and CypA showed an interesting correlation with sALS patients. Indeed, CypA was up-regulated in the rat model PBMC, as observed for patients and, more interestingly, its up-regulation was detectable also in SpC ventral horns, where the population of MNs is enriched. In both cases CypA altered levels were detectable already at pre-symptomatic stages of the disease.

Moreover, CypA is a secreted protein that could potentially be measured in human biofluids. Indeed CypA was also analysed in CSF of sALS patients where it was increasingly concentrated in comparison with healthy controls and with multiple sclerosis patients (unpublished results from the lab).

In addition, alterations in CypA had been previously reported by our lab in two proteomic studies conducted in the G93A-SOD1 mouse model. In particular, extracts from the lumbar SpC of pre-symptomatic G93A-SOD1 mice were analysed to identify the cellular pathways specifically altered in the tissue mainly affected by the disease. Fifteen proteins differentially expressed were identified, including mitochondrial proteins, molecular chaperones, proteins involved in oxidative stress and in protein degradation pathways (Massignan 2007). Among them, a specific alteration of CypA isoform pattern was observed: an up-regulation of the phosphorylated-acidic isoform and a down-regulation of the N-terminal acetylated-basic isoform. Thus, CypA PTMs are altered in an animal model of ALS, as well as in PBMCs from sALS patients (unpublished results from the lab). Another proteomic study performed in our laboratory, identified the proteins enriched in the triton-insoluble fraction, as a model of protein aggregates, in the SpC of WT-SOD1 and G93A-SOD1 mice at different stages of the disease (Basso 2009). In mSOD1 mice SpC, CypA was found aggregated already at early-symptomatic stage and was highly enriched in aggregates at end stages of the disease. Interestingly, CypA was present also in the insoluble fraction of the SpC of sALS patients.

CypA should be thus further investigated for its potential as a marker for differentiating ALS from disease mimics, for monitoring disease progression and response to therapies in patients and ALS animal models. Furthermore, since CypA alterations were found both in periphery and in affected

tissue of mouse and human ALS, it should be further studied also as a putative key modulator of the disease, in order to unravel its possible involvement in ALS pathogenesis and progression.

2. Cyclophilin A

CypA is an ubiquitous and highly expressed protein that can be involved in several pathways. However, the specific roles it plays in the CNS and in neuronal cells, where it is abundantly expressed, have not been defined yet.

In 1984, Fischer and his coworkers isolated the first prolyl isomerase from porcine kidney, as an enzyme able to accelerate the proline-limited folding reactions of many proteins *in vitro*. A surprising result emerged when the porcine prolyl isomerase was sequenced. It was found to be identical to CypA, the cytosolic binding protein for the immunosuppressive drug CsA. In fact, this protein was discovered twice in 1984: by virtue of its tight binding with CsA, and by its catalytic activity as a PPIase. CypA is the most abundant among the cyclophilins and is widely distributed in almost all tissues in prokaryotes and eukaryotes.

2.1 The cyclophilins family

Cyclophilins (Cyps) form a large family of proteins with two main recognised features: the peptidyl-prolyl *cis-trans* isomerase (PPIase) (Fischer 1984) and the immunosuppressive activity (Handschumacher 1984). Cyps are highly conserved proteins since have been documented in every Domain of life including Archaea, Bacteria and Eukaryotes. In humans, Cyps are found in most tissues with remarkable heterogeneity in distribution, and are mainly expressed in brain and kidney (Koletsky 1986). Their presence has been documented in most cellular compartments, including the mitochondria, ER, Golgi, nucleus and cytoplasm (Galat 2003; Wang 2005), which implies their importance in cellular functions. Nine major Cyps have been identified: CypA, CypB, CypC, CypD, CypE, Cyp20, Cyp40, CypH and CypNK. All Cyps share a common domain of approximately 140-180 residues, the cyclophilin-like domain (CLD) (**Figure 11**), surrounded by a localisation domain, which is unique to each family member and determins the subcellular compartmentalization and the functional specialisation (Galat 2003; Marks 1996; Arevalo-Rodriguez 2004). Little is known on the genomic structure of cyclophilins genes, which are not linked each other in the genome.

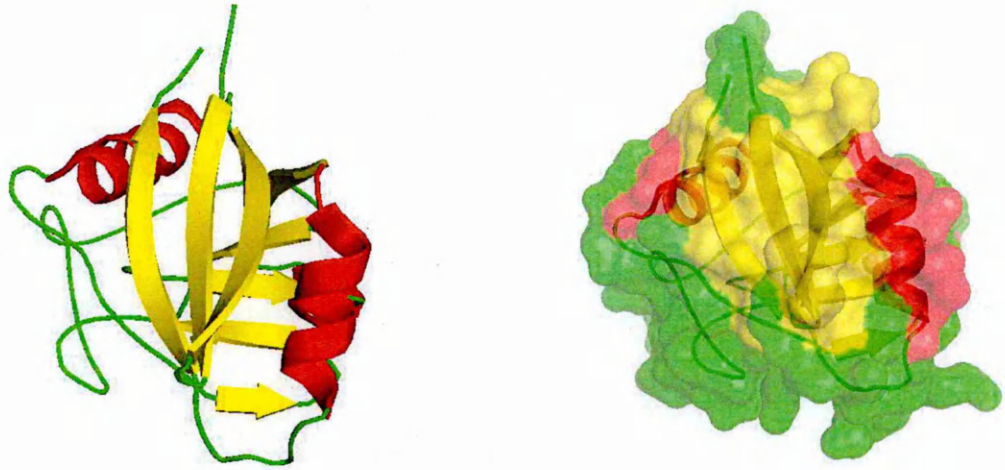

Figure 11 Representations of the molecular structure of cyclophilins.

The eight β-strands which form the characteristic cyclophilin β-barrel are shown in yellow; while the two α-helices flanking the barrel are shown in red.

→ CypA, the archetypal cyclophilin, is encoded by the PPIA gene on chromosome 7p13, is composed of 165 residues encoding a 18kDa protein, which contains only the CLD. It is mainly located in the cytoplasm, although it is found also in the nucleus or it can be released by several cellular types. It is found in all tissue of mammals where it represents the 0.1-0.4% of the total proteins in the cell (Galat 2003).

→ CypB is a ubiquitous protein composed of 208 aa encoded on the chromosome 15q21-q22 (Galat 2003). The overall structure of CypB resembles that of CypA with two extensions at the N- and C-terminals (Mikol 1994). The N-terminal fragment contains an ER signal sequence, thus CypB main localisation is in this organelle and participates in protein secretory pathway (Galat 2003; Wang 2005).

→ CypC is a 212 aa protein encoded on chromosome 5, which gives rise to a 22kDa protein (Galat 2003). CypC has a structure similar to that of CypA, differing mainly in the conformation of three surface loop regions (Ke 1993), and like CypB is found in the ER.

→ CypD is encoded on chromosome 10q22-q23 and is a 40kDa protein encoded by 370 aa (Galat 2003). CypD has a signal sequence for mitochondria (Andreeva 1999; Galat 2003; Wang 2005).

→ CypE is encoded on chromosome 1p32 and is a 33kDa protein made of 301 residues (Galat 2003). CypE shows an N-terminal RNA-binding domain, which localises it in the nucleus (Mi 1996).

→ Cyp40, is encoded in chromosome 4q31.3 and is a 40kDa protein made by 301 residues (Galat 2003). This protein is mainly cytosolic and consists of a CLD with a domain similar to tetraticopeptide (TPR) repeats which is implicated in protein-protein interaction (Ratajczak 2003).

→ CypNK is the largest cyclophilin and was first identified from natural killer cells. It is composed of 1403 amino acids, encodes a 157kDa protein, and its gene is on chromosome 3p23-p21 (Galat 2003). This cyclophilin contains a large, hydrophilic and positively-charged C-terminal and is localised in cytoplasm of natural killer cells.

2.1.1 Cyps peptiyl-prolyl cis-trans isomerase activity

Although protein folding is a spontaneous process, many proteins *in vivo* require assistance by two kinds of protein factors: foldase, such as PPIase, and protein disulfide isomerase (PDI), that catalyse the formation and exchange of disulfide bonds, as well as molecular chaperones.

The structural conservation throughout evolution as well as the PPIase activity of all cyclophilins highlights the importance of this enzymatic reaction. Peptide bonds have a partial double bond character and can exist in two distinct isomeric forms: *cis* and *trans*. Ribosomes synthesise peptide bonds with a *trans* isomeric form, corresponding to a lower energy-state, since side chains are 180° opposite each other and sterically favoured. For all aa residues the *trans* conformation is more energetically favourable than the *cis* one. Unlike other peptide bonds, those preceding proline (Pro) (peptydil-prolyl bonds) often occur in the *cis* conformation, and in oligopeptides, *cis-trans* isomerisations about these bonds are intrinsically slow processes with high activation energies (~90kJ mol^{-1}). Prolyl isomerisations might retard *in vitro* folding and also *de novo* protein folding in the cell.

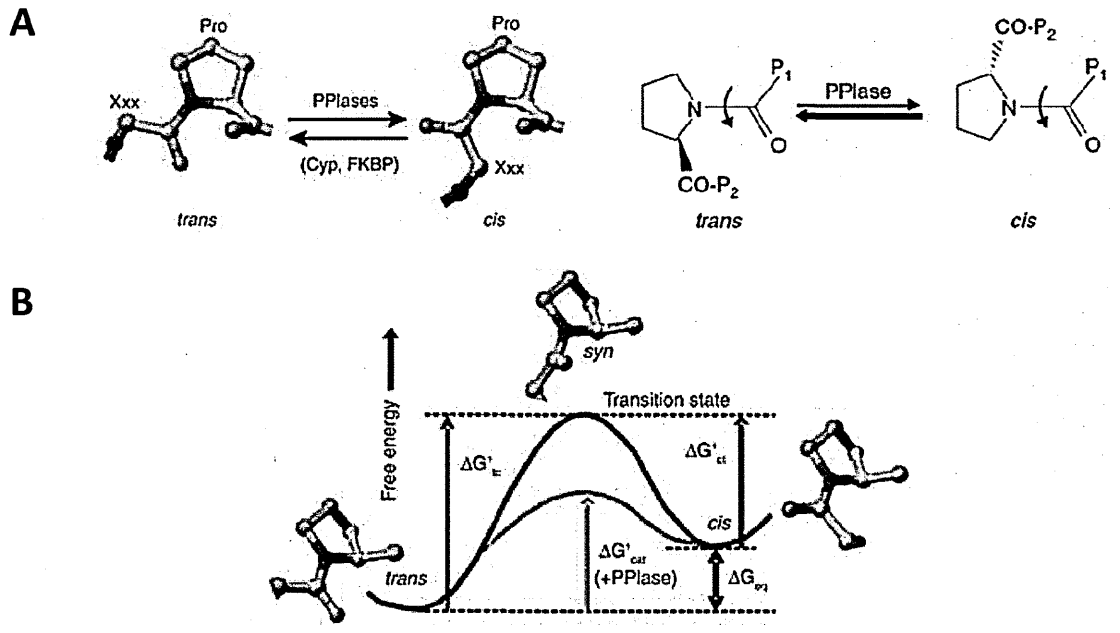

Figure 12 Peptidyl-prolyl *cis-trans* isomerase activity of cyclophilins.

(**A**) Schematic illustration of the *trans* and the *cis* isomers of the petide bond between proline and another aa. The interconversion between the two forms is catalyzed by cyclophilins or other PPIases.

(**B**) Energy diagram for prolyl *cis-trans* isomerisation. Modified from Lu 2007.

Since the conversion of proteins from *cis* to *trans* at Xaa-Pro bonds is often a rate-limiting step in protein folding and activity (Baneyx 2004), Cyps can accelerate protein folding *in vitro* (Schmid 1995) catalysing this intrinsically slow conversion (**Figure 12**). Indeed, Cyps act stabilising the *cis-trans* transition state, thus accelerating isomerisation, a process important both in *de novo* protein folding and refolding processes, but also during the assembly of multidomain proteins (Gothel 1999). For example, blocking the *cis-trans* isomerase activity of Cyps cause a delay in the maturation of collagen (Steinmann 1991; Kruse 1995). Moreover, a number of studies detected the presence of Cyps in the nucleus, including CypG, CypE, PPIL1, CypH, PPIL2 and PPIL3a/b, where they can interact directly with splicing factors (Horowitz 2002), be part of the spliceosomal complexes (Jurica 2003; Chen 2007), or bind the C-terminal domain of the RNA polymerase II (Bourquin 1997). The involvement of Cyps in these processes seems to be an ancient and universal trait due to their presence in the splicing and transcriptional machinery in a multitude of taxa. Given the constitutive and ubiquitous nature of RNA processing, the presence of Cyps in the

splicing machinery may be significant in modulating spliceosomal activity (Mesa 2008). Indeed Cyps have been demonstrated to catalyse a number of transport and foldase reactions that possibly assist in the assembly/disassembly dynamics of the spliceosome as well as in its coupling to the transcription machinery. In addition, it is possible that the capacity of Cyps to alter folding may provide accessibility and a mechanism for activating/inactivating spliceosomal proteins.

In addition to PPIase activity, Cyps exhibit also chaperone activity *in vitro* (Freskgård 1992). A chaperone binds to unfolded states and prevents the polypeptide chain from making illicit associations with other unfolded proteins or being trapped in misfolded conformations. While multidomain Cyps have been shown to conduct the chaperone activity in domains different from the catalytic one, small single-domain Cyps, such as CypA, present both isomerase and chaperone activities in the active site (Moparthi 2010). Nevertheless, Cyps role *in vivo* is not clear, and they can have two possible functions, which are not mutually exclusive. First, Cyps may participate in protein folding (Schiene 2000), with only an incremental effect, thus arguing against their essential role in protein maturation. Indeed, all deletions of cyclophilin genes in yeast produce strains that are viable, as is the mutant that lacks all the cyclophilins (Dolinski 1997). Secondly, PPIases can bind at hydrophobic patches on their target proteins without necessarily isomerising a peptidyl-prolyl bond, thereby preventing misfolding (Baker 1994; Ferreira 1996; Arié 2001) and/or modulating activity of the target protein (Braaten 1997; Streblow 1998; Shen 1998; Crenshaw 1998; Wu 2000). Moreover, PPIase enzymes could be also involved in repairing damaged proteins due to environmental stresses including thermal stress, UV irradiation, changes in the pH of the cell environment, and treatment with oxidants (Parsell 1993).

2.1.2 Cyps immunosuppressant activity

Cyps show an immunosuppressant activity by binding to the potent immunosuppressant agent Cyclosporin A (CsA), and for this reason they are also called immunophilins. CsA is a hydrophobic cyclic undecapeptide produced by the fungus *Tolypocladium inflatum* (Borel 1989). Beginning in the 1980s, CsA was used as an immunosuppressive drug and is now employed for prophylaxis and

treatment of allograft rejection following organ or tissue transplants. Actually, CypA was firstly recognised as the main target of CsA (Handschumacher 1984). Subsequently further Cyps were characterised and several members of the cyclophilin family were shown to have varying degrees of affinity for the drug CsA. The inhibitor constant, K_i is the binding affinity of an inhibitor to its enzyme and is an indication of how potent an inhibitor is, thus it represents the concentration required to produce half maximum inhibition: lower K_i means lower inhibitor concentration to use to obtain the result. K_i values of CsA inhibitory activity have been determined for CypA (2.9nM), CypD (6.7nM), CypC (7.7nM) and CypB (8.4nM) (Daum 2009). Therefore, CsA binds and inhibits with more efficiency CypA, with an IC_{50} (the concentration of CsA that induces 50% of inhibition) of 25nM, whereas CypB, the least efficient cyclophilin, shows and IC_{50} of 84nM (Mikol 1994).

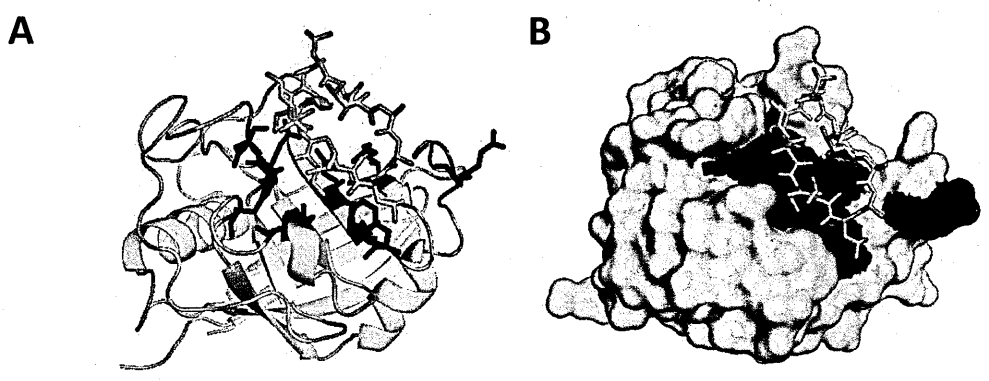

Figure 13 Cyclophilin A and cyclosporin A complex.

(**A**) Ribbon diagrams of CypA/CsA. The CypA residues directly involved in the binding with CsA are shown as blue sticks, while CsA is shown in red stick representation. (**B**) Predicted surface of CypA in complex with CsA.

The immunophilin super family is classified into three major subfamilies, including the CsA binding proteins (Cyps) (Pemberton 2006), FK506 binding proteins (FKBPs) (Ho 1996) and parvulins (Fujiyama 2002). The functional role of CypA and of the other immunophilins in immunosuppression does not involve their PPIase activity or the catalysis of a protein folding reaction. Rather, these proteins are recruited by CsA and FK506 for association in tight complexes. In mammals CsA-cyclophilin complex, but neither the drug itself nor the protein alone, is able to bind calcineurin and inhibit its phosphatase activity *in vitro* and *in vivo* (Fruman 1992). In fact,

calcineurin is a calcium-calmodulin-activated serine/threonine phosphatase, and its inhibition blocks the translocation of the nuclear factor of activated T cells (NF-AT) from the cytosol to the nucleus, thus stopping the transcription of genes encoding cytokines such as interleukin-2 (Liu 1991; O'Keefe 1992). Ideed, under physiologic conditions NF-AT is transported to the nucleus upon dephosphorylation and there binds to the enhancer of the interleukin-2 gene promoting its expression. X-ray structure analyses of human cyclophilin-CsA complex have shown that the residues involved in the binding with CsA are approximately those composing the hydrophobic active site of the enzyme (**Figure 13**).

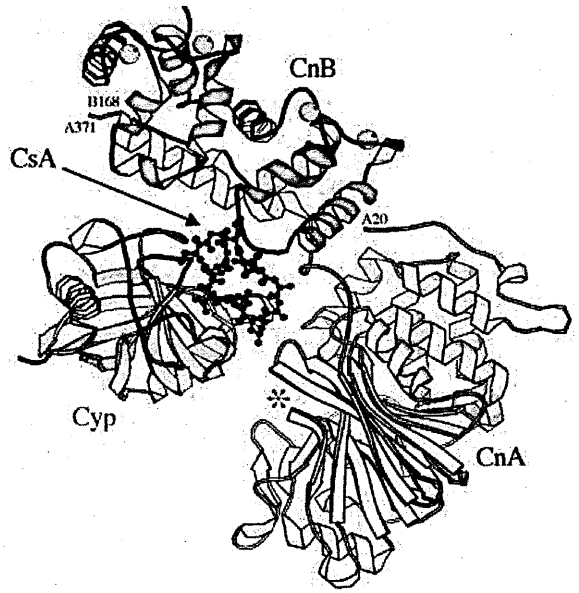

Figure 14 Ribbon diagram of CypA/CsA/Cn ternary complex.

The crystal structure of this super complex has recently been determined to a resolution of 2,8Å. CsA is shown in ball-and-stick representation. CnA is in yellow; CnB is in red; CypA is in green; Ca^{2+} ions are cyan balls. Modified from Jin 2002.

The CsA/CypA complex binds with a high affinity to the ternary complex formed with calcineurin A (CnA), calcineurin B (CnB) and calmodulin (Cd1) (**Figure 14**). The binding of CsA-CypA complex to calcineurin increases the complex stability; this is possible because upon CsA binding to CypA the charges and hydrophobic surfaces of the drug-protein become more congruent with the binding site on calcineurin (Hornbogen 1992).

2.2 CypA structural features

X-ray and NMR studies have revealed that human CypA is characterised by the presence of eight anti-parallel β-strands that together form a right-handed β-barrel, with an α-helix at either ends (Richardson 1981; Sawyer 1987) and another short α-helix located between residues 119-122. These structured regions of the protein are connected by loops. One of these loops (Lys118-His126) and four β-strands make up the binding site for CsA (Kallen 1991; Ke 1991) (**Figure 15**). The interior cavity of the barrel in CypA is highly hydrophobic, indeed the compact core of the protein is formed by seven aromatic and other hydrophobic residues.

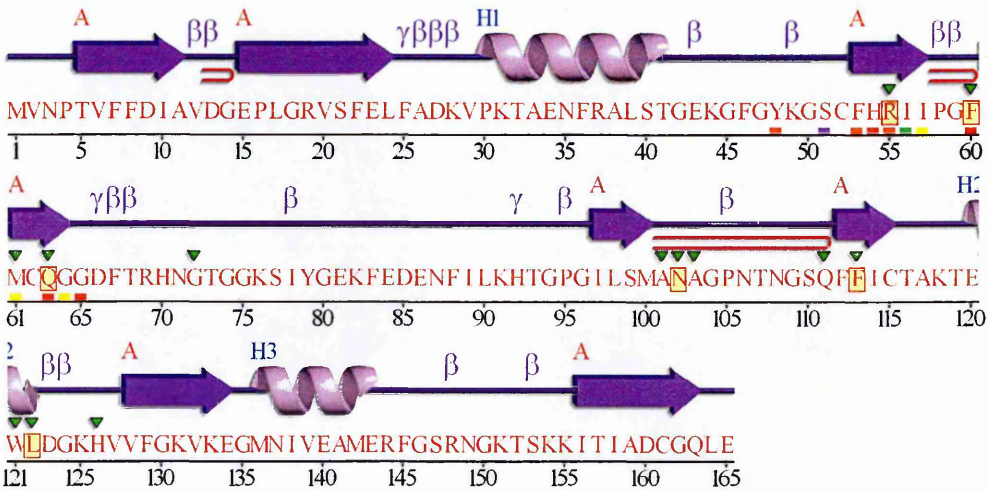

Figure 15 Aa sequence of human CypA with elements of secondary structure.

The crucial catalytic residues involved in the PPIase activity are shown in the boxes. The green triangles indicate the residues interacting with CsA. Low ▬▬▬▬▬▬▬▬High conservation (source: PDB; Protein Data Bank)

The active site of the human CypA is localized to the outer surface and is formed by the residues R55, F60, M61, Q63, A101, F113, W121, L122 and H126 (Ke 1994; Zhao 1997; Howard 2003) (**Figure 16**). Analyses of the aligned sequences of the human CLDs have revealed that aa crucial for PPIase activity and the aa composing the aromatic/hydrophobic network are the most well conserved in all 19 sequences of the human CLDs. In particular, the equivalent sequence positions occupied by Arg55 in CypA are highly conserved in the sequences of the human CLDs (Ke 2004). Indeed, Arg55 (in human CypA) is extremely conserved in all cyclophilins because it plays a crucial

role in PPIase catalysis. The active site of the wild-type enzyme is structurally very stable and puts Arg55 in a favourable position to perform its catalytic role in the transition state. Arg55 guanidinium group facilitates catalysis by anchoring the substrate proline oxygen and stabilizing sp^3 hybridization of the proline nitrogen in the transition state (Howard 2003). The substitution of the Arg55 with an alanine residue causes a 1000-fold reduction in the catalytic efficiency (Zydowsky 1992). Moreover, also F60A and H126Q substitutions retain less than 1% of the wild-type catalytic efficiency, thus indicating a key role also for these residues in PPIase catalysis (Zydowsky 1992).

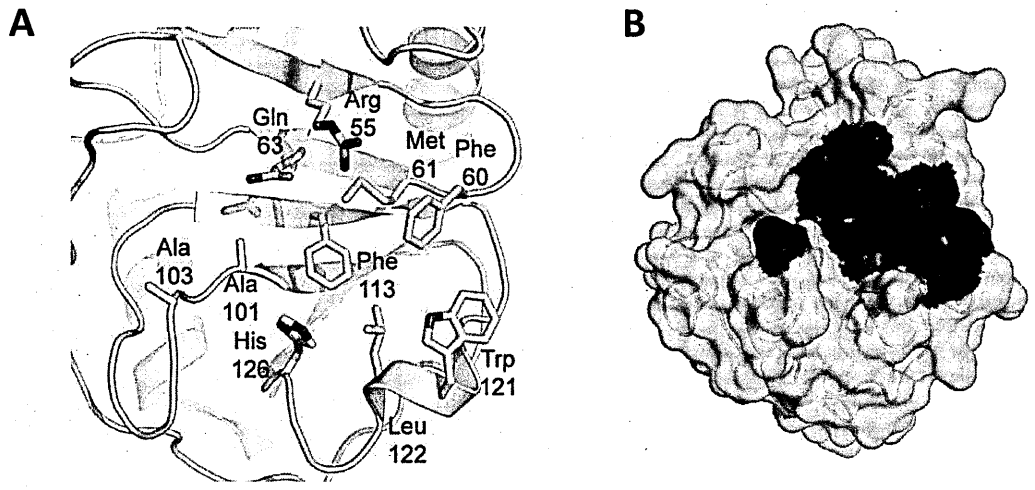

Figure 16 Human CypA active site.

(A) Residues composing the active site of CypA. **(B)** Surface representation of CypA with residues involved in PPIase activity highlighted in blue.

2.3 CypA localisation

CypA is widely distributed in all tissues, but it is found with the highest concentration in the CNS where it is located primarily in neurons (Göldner 1996). Despite its abundance in the CNS, its primary functions in this compartment remain largely undefined. Nevertheless, CypA seems to be implicated in neuronal differentiation (Hovland 1999; Nahreini 2001; Chiu 2003; Song 2004; Urano 2006) and in adult cortical plasticity and reorganisation following retinal injury (Arckens 2003).

In the cell, CypA is mainly localised in the cytoplasm, but it can be found also in the nucleus (Krummerei 1995), despite the absence of a classic nuclear localisation signal. Indeed, CypA contains a M9-like motif which is necessary for transportin 1, an importin protein, recognition to mediate protein nuclear import (Pan 2008). In addition, CypA can also be secreted from a huge variety of cell types, in response to different stimuli (Seko 2004; Sherry 1992, Suzuki 2006; Jin 2000). CypA release is mediated by vescicle transport and plasma membrane binding, processes mediated by actin remodelling, RhoGTPase activity and phosphorylation of myosin II light chain (Suzuki 2006). Moreover, CypA has been found in human urine (Pisitkun 2004), plasma (Endrich 1998), synovial fluids of patients with rheumatoid arthritis (Billich 1997) and in rat cortical primary cultures exosomes (Faure 2006). CypA is believed to play several important roles both inside the cell and in the extracellular space. However none of these functions is essential for viability since transgenic mice lacking both copies of CypA gene (CypA-/-) suffer no obvious decrease in life span (Colgan 2004).

2.4 CypA intracellular functions

CypA has a dual folding role: it can act as an acceleration factor in protein folding thanks to its well characterised ability to catalyse the *cis-trans* isomerisation of peptidyl-prolyl bonds (Kern 1995), and as a chaperone, increasing the yield of native protein during the folding reaction (Freskgård 1992).

2.4.1 CypA isomerase activity

CypA-catalysed prolyl isomerisation can have a profound impact on many key proteins in diverse cellular processing, including cell growth, stress responses, cell signalling, immune response, viral infection, cytokinesis. Unlike covalent modification or global unfolding, proline isomerisation is an intrinsic conformational exchange process that has the potential to direct ligand recognition and to control protein activity within the confines of the native state (Andreotti 2003). Indeed, of the naturally occurring aa, proline is unique and appears to fulfil multiple roles in the context of

native, folded proteins. In some proteins, proline isomerisation may confer conformer-specific properties to a native protein fold by modulating the features of a protein surface. Alternatively, a conformational heterogeneous proline residue may cause minimal structural perturbations, but could instead serve as a recognition site for PPIase. The *cis* and *trans* isomers of many proteins have distinct functions, and their conversions by PPIases can function as a new general class of protein regulatory switches. Indeed, the *cis* and *trans* isomers provide stable local motifs that differ dramatically in structure, thereby providing a mechanism for selecting distinct pools of binding partners, even in the context of otherwise unstructured regions of proteins. Therefore, *cis-trans* isomerisation is a molecular switch that can be used in an enzyme-regulated manner to help control the timing of biological events such as isomer-specific protein-protein interactions, as well as the amplitude and duration of a cellular process (Lu 2007).

NMR and X-ray studies have shown CypA in complex with the HIV-1 capsid protein (Gamble 1996; Campos-Olivas 1999) and with the interleukin-2 tyrosine kinase (Itk) (Brazin 2002; Andreotti 2003). In these cases a similar equilibrium of the *cis-trans* isomerisation state ratio of the substrates has been observed, that is altered when they are in complex with CypA, suggesting that an increase in the *cis* conformation of the bound substrate may be a general mechanism for CypA to mediate the control of the protein function.

The HIV-1 capsid protein forms the conical core structure at the center of the mature virion and can bind with high affinity human CypA, thereby packaging it into the virion. Through this interaction CypA is able to promote both the formation and the infectivity of human immunodeficiency virus (Luban 1993; Bosco 2002; Braaten 1996 and 2001; Sokolskaja 2004). The N-terminal portion of HIV-1 capsid protein binds efficiently human CypA's active site (Howard 2003; Gamble 1996; Campos-Olivas 1999) (**Figure 17**); in particular, CypA binds to an exposed proline-rich loop in the HIV-1 capsid protein A (CA) domain of HIV-1 Gag envelope protein that has been demonstrated to have 44,4% identity with the sequence of another CypA interactor, that is CD147 (Yurchenko 2002). This indicates that microorganisms can also use prolyl *cis-trans* isomerisation as a regulatory mechanism to gain entry into host cells. The binding site for CypA,

Gly89–Pro90 in capsid, exists in the *cis* and *trans* forms and CypA can catalyse Gly89–Pro90 isomerisation, thus suggesting a role in maturation or disassembly of viruses. Indeed, conditions that disrupt CA-CypA interaction, such as mutational inactivation of the CypA binding site or inhibition by CsA, inhibit replication of most HIV-1 strains, and HIV-1 replication is attenuated in a human T-cell line that lacks CypA (Braaten 1996). In this case, the Cyp-CA interaction seems to block the recognition of the HIV-1 virion by the host cell restriction factor Ref1, an intrinsic antiviral cellular protection mechanism (Howard 2003; Towers 2003). CypA was also shown to enahance HCV RNA replication stimulating the RNA binding ability of the NS5A protein, modulating the conformation of the RNA binding motif by *cis-trans* isomerisation (Foster 2011).

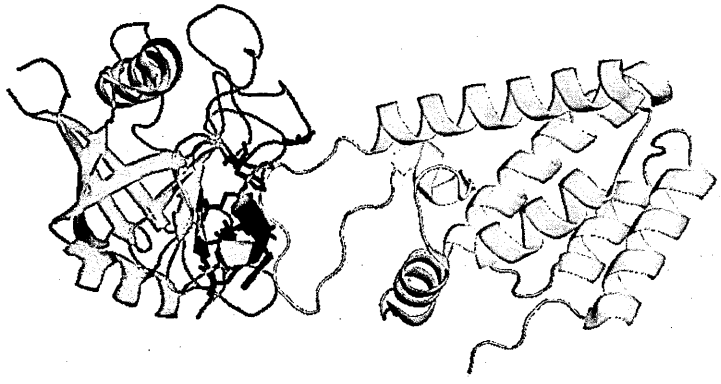

Figure 17 CypA/HIV-1 capsid complex.

X-ray structure of the N-terminal portion of the HIV-1 capsid (yellow) interacting with the PPIase cavity of CypA (green). The CypA residues involved in the catalytic actvity are shown in blue. A loop of the capsid protein (that contains 4 prolines) can undergo the *cis-trans* isomerisation and the following conformational switch (Howard 2003).

In addition, CypA may also have an important role in the immune response through the interaction with the tyrosine kinase Itk, a non-receptor protein that participates in the intracellular signaling events leading to Th2 cell activation. NMR structural studies combined with mutational analysis have shown that CypA can bind to the Itk SH2 domain which is generally in a *cis* conformation, and catalyse the *cis-trans* isomerisation of the Asn286/Pro-287 imide bond (**Figure 18**). The *cis* conformer of Itk is likely an inactive form of the enzyme and CypA acts as a

repressor, thus maintaining its inactivated form. CypA PPIase activity, via interaction with Itk and proline-dependent conformational switch, can thus regulate substrate recognition and mediate regulatory interactions in $CD4^+$ T-cell activation (Brazin 2002; Colgan 2004; Andreotti 2003).

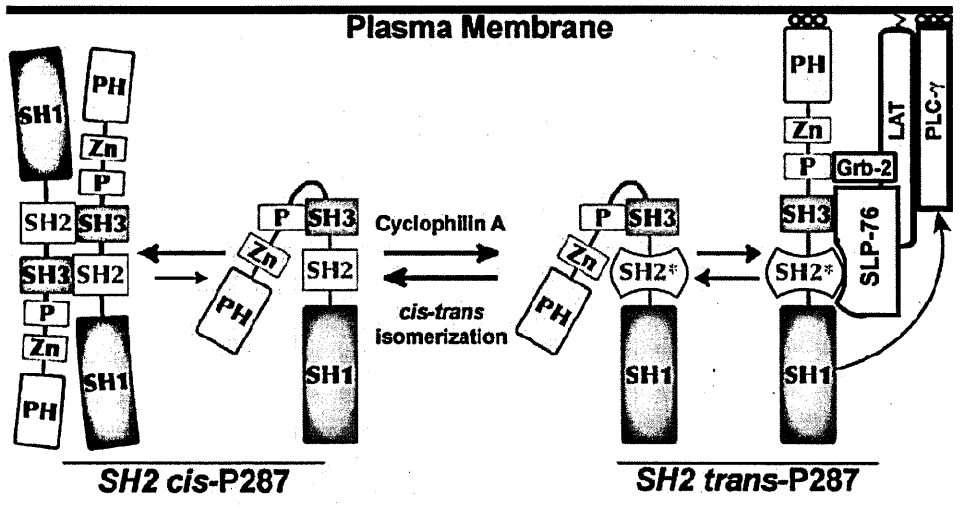

Figure 18 Model of Itk regulation by CypA.

The imide bond preceding Pro287 in the Itk SH2 domain spontaneously interconverts between *cis* and *trans* conformers. The self-associated, dimeric form of Itk predominates for the *cis* imide bond containing conformer (left), while the *trans* imide bond within the SH2 domain (denoted SH2*) favours interactions with signaling partners, such as Slp-76 (right). Interconversion between the two conformations of Itk likely occurs via the monomeric form of the enzyme (center). Itk catalytic activity is inhibited by the PPIase activity of CypA. Adapted from Colgan 2004.

The importance of CypA PPIase activity in cell signalling has also been documented. Crk is a member of an adaptor protein family that has several SH2 and SH3 domains. NMR studies have revealed that *cis-trans* isomerisation of the prolyl bond at position Gly237-Pro238 (located between two of the SH3 domains) is very slow and that PPIase binding to the SH3 domain facilitates an opening of the "gate," where the isomerisation rate is increased and the adaptor forms an "open," less restricted active conformation, that is catalysed by CypA (**Figure 19**) (Sarkar 2007).

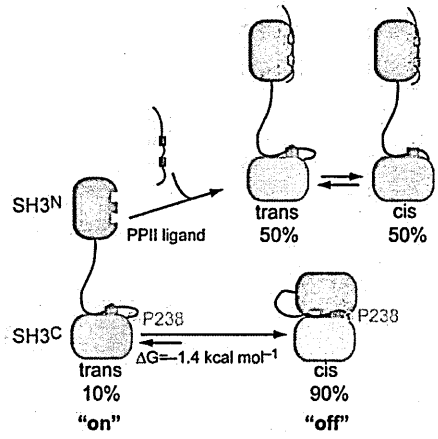

Figure 19 Model of the equilibrium of conformational states of Crk.

The intramolecular inhibitory $SH3^N/SH3^C$ interaction is stabilised by the *cis* conformer of the Gly237-Pro238 prolyl bond, whereas the *trans* conformer favours an uninhibited state. Activation occurs by PPII ligand binding to a low population of uninhibited states wherein $SH3^N$ binding site is accessible, thereby shifting the equilibrium towards the $SH3^N$-PPII ligand bound state. Pro238 acts as a molecular switch that has the intrinsic capacity to regulate the autoinhibition of Crk. Adapted from Sarkar 2007.

CypA constitutively associates with prolactin receptor (PRLr) and Janus kinase 2 (Jak2) (Syed 2003) (**Figure 20**), resulting in enhanced Jak2 and Stat5 activity. In particular, CypA directly acts on PRLr through Pro-334, mediating a conformational change within the PRLr/Jak2 complex. Thus, CypA is required for effective PRLr-induced signaling, a mechanism particularly relevant in the progression of human breast cancer (Zheng 2008).

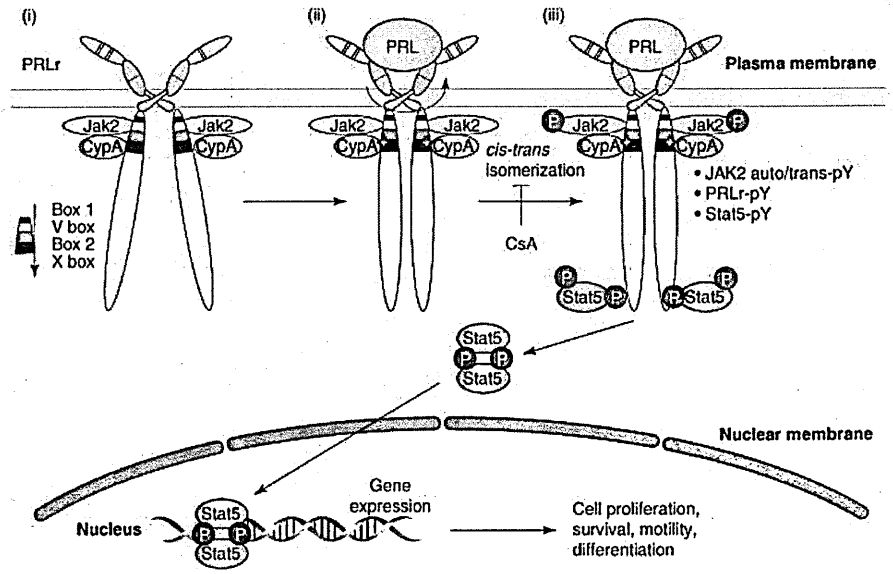

Figure 20 Regulation of the PRLr/Jak2 complex by CypA.

(i) CypA is constitutively associated with PRLr and Jak2 during unstimulated conditions. (ii) Upon binding of PRL to PRLr, CypA positively regulates Jak2 activity by exerting its isomerase activity, (iii) presumably through its switching function of a *cis-trans* peptidyl prolyl isomerase. Ablation of CypA PPI activity by cyclosporine A (CsA) and other approaches inhibits PRL signaling and might be a novel therapeutic strategy in the treatment of human breast cancer. The red arrow in (ii) denotes cis-trans interconversion of proline 334 in the X-box motif of the PRLr; the red circle containing P indicates phosphorylation of JAK2 kinase, PRLr, and signal transducer and activator of transcription 5a (Stat5a). Adapted from Clevanger 2009.

These findings suggest that prolyl isomerisation is emerging as a complementary regulatory mechanism to control signalling networks.

2.4.2 CypA chaperone activity

CypA posseses a chaperone function independent of its PPIase activity. CypA is indeed a natural "protein-philin" (Greek *philin*= friend) that interacts with proteins to guide their proper folding and assembly (Barik 2006). In particular, CypA transiently interacts with the early folding intermediates of its protein substrates and can function as a hydrophobic collector basket for misfolding-prone regions and can, at later stages, protect the protein from misfolding, thereby preventing incorrect interactions leading to aggregation.

A list of protein containing a consensus peptide for CypA binding has been identified in 2005 (Piotukh 2005), however until now very few substrates of its chaperone activity have been clearly identified. The effects shown by CypA on creatine kinase (Yang 1997; OU 2001), carbonic anhydrase II (Freskgård 1992), citrate synthase (Moparthi 2010), and stefin B (Smajlović 2009) refolding indicate that CypA could act as a chaperone *in vitro*. CypA chaperone activity in living cells was firstly demonstrated on procollagen I triple-helix, whose correct folding was accelerated by CypA and delayed by CsA treatment (Steinmann 1991).

Interestingly, CypA chaperone activity has been directly associated with ALS. In particular, the death-inducing effect of mutant V148G-SOD1 overexpression in PC12 neuronal cells was potentiated by CsA treatment, and overexpression of wild-type CypA, but not the PPIase-deficient

mutant R55A, restored cell survival rate in mSOD1 neurons. This effect was correlated with an overall decreased cellular PPIase activity, indicating that mSOD1-induced death was mediated by an increase in misfolded proteins and that CypA can have a protective intracellular activity (Lee 1999). These data also suggest that the chaperone activity of CypA can restore the balance inside the cell and a surplus of CypA can be useful for the maintenance of protein homeostasis.

2.4.3 CypA and oxidative stress

CypA is a protein generally up-regulated after oxidative stress. Since CypA behaves as a molecular chaperone for proteins, its higher expression is thought to contribute to the correct folding of misfolded proteins that can accumulate due to oxidative stress, thus displaying a strong cytoprotective effect (Lee 1999; Hu 2000; Matsumoto 2005).

CypA mRNA levels are elevated in cortical neuronal culture after exposure to ischemic insult (Boulos 2007) and in rat brain microvessels after traumatic brain injury *in vivo* (Redell 2007). CypA is up-regulated in cortical neurons pre-conditioned with cycloheximide, which targets protein synthesis, heat stress or MK801, an NMDA membrane receptor blocker, and thus less sensitive to further ischemic stress, suggesting that CypA can be involved in neuroprotective pathways against ischemic injury (Meloni 2005). Moreover, cortical neuronal cultures pre-conditioned with erythropoietin (EPO), a potent neuroprotective factor against hypoxia-induced oxidative stress (Liu 2005), show increased levels of intracellular CypA, which is thus implicated in protective effect induced by EPO (Meloni 2006). Furthermore, hypoxia has been demonstrated to stimulate the production of CypA mRNA and protein also in cancer cells (Choi 2007). In addition, CypA overexpression increases the growth rates of human embryonic brain cells (Nahreini 2001), protects neurons from oxidative stress (induced by cumene hydroperoxide) and *in vitro* ischemia (induced by oxygen glucose deprivation) (Boulos 2007). Whereas the down-regulation of CypA levels decreases the viability of cardiomyocyte cultures treated with t-butylhydroperoxide (Doyle 1999). Moreover, CsA is neurotoxic for both cortical and hippocampal neurons (McDonald 1996; Kaminska 2001), and is able to mediate the generation of ROS by inhibiting PPIase activity in

cultured myoblasts (Hong 2002). According to these evidences, a neuroprotective role for CypA could be hypothesised.

Other studies have highlighted CypA capability to bind to peroxiredoxins (Prx) activating their peroxidase activity (Lee 2001). CypA supports antioxidant activity of PrxII and PrxVI, both against thiol and ascorbate. Specifically two cysteine of CypA, Cys115 and Cys161, are involved in the activation and in the reduction of Prx. CypA is also able to bind the antioxidant enzyme gluthatione-S-transferase (Piotukh 2005). Furthermore, CypA was shown to be part of a cytosolic heat-shock protein-immunophilin chaperone complex (Uittenbogaard 1998), and to bind the heat shock protein Hsp90 (Nadeau 1993). Moreover, CypA is able to bind the antioxidant protein Aop1 in T-cells and to increase its protection activity on glutamine synthetase from oxidative inactivation, in a CsA-independent way (Jäschke 1998). Also the expression of the yeast homologous of CypA, Cpr1 has been shown to be activated by stress conditions, indicating that Cpr1 may participate in protecting the cell against cellular stresses (Arevalo-Rodriguez 2004). The overexpression of Cpr1 also drastically increases cell viability in the presence of stress inducers, both in yeast and E.coli, illustrating the importance of Cpr1 as a molecular chaperone and as rescue protein, in the presence of adverse conditions (Kim 2010a, 2010b).

2.4.4 CypA and apoptosis

As previously mentioned CypA can localise also in the nucleus. Apoptosis is generally related to DNA fragmentation and several works have demonstrated an active function of CypA in DNA degradation (Montague 1994). CypA displays sequence and structural similarities with NUC18, a 18kDa nuclease isolated from apoptotic rat thymocytes (Gaido 1991). CypA is able to degrade single-stranded, double-stranded and supercoiled DNA in a Ca^{2+}/Mg^{2+} dependent way, and independently of CsA inactivation. Thus CypA also possesses a nuclease activity independently from its PPIAse function (Montague 1997), that is similar to the activity of apoptotic endonucleases. Moreover, CypA was found in the nucleus of macrophages, where it exhibited a zinc-dependent DNA binding activity and PPIase activity only in the absence of zinc ions.

A pro-apoptotic activity of CypA is also supported by several reports demonstrating CypA interaction with the apoptosis inducing factor (AIF) (Candé 2004). AIF is a flavoprotein with NADH oxidase activity, normally contained in the mitochondrial intermembrane space (Susin 1999). Under pathological conditions, AIF translocates from the mitochondria to the cytosol and then to the nucleus (Daugas 2000), where it undergoes electrostatic interactions with the DNA and tethers CypA to chromatin (Ye 2002). The AIF/CypA complex then causes DNA degradation, and the two proteins together have a higher DNase activity than each protein alone (Candé 2004). In dying neurons, the lethal translocation of AIF to the nucleus requires the interaction with CypA, suggesting a model in which two proteins that normally reside in separate cytoplasmic compartments acquire novel properties when moving together to the nucleus (Zhu 2007). Interestingly, AIF is abundant in MNs and reactive astrocytes in the SpC of G93A-SOD1 transgenic mice, where its expression is increased with disease progression (Oh 2006). Moreover, in the symptomatic mSOD1 mice AIF translocates from mitochondria to the nucleus of degenerating MNs, thus suggesting that AIF may play a role in MN death in an ALS mouse model (Oh 2006). In addition, in sALS patients both MNs and astrocytes show co-localisation with AIF, and biochemical analyses indicate nuclear translocation of AIF in the degenerating MNs in the SpC of ALS patients compared to healthy controls (Shibata 2009). Interestingly, CypA was demonstrated to co-localise with AIF in MNs of lumbar SpC, both by biochemical and immohistochemical assays (Tanaka 2010). Moreover, AIF and CypA cooperate in inducing apoptosis since (i) cells lacking CypA are relatively resistant to AIF-induced cell death, (ii) in WT-CypA cells AIF silencing reduces apoptosis events and (iii) transfection with mutant forms of AIF that are unable to bind CypA abolishes apoptosis (Cande 2004). In the same way, disruption of CypA yeast orthologue Cpr1 abrogates cell death induced by AIF overexpression (Wissing 2004). The pro-apoptotic activity of CypA mediated by AIF has also been reported *in vivo*: after an hypoxia-ischemia insult, CypA knock-out mice showed a reduced brain infarct volume and neuronal loss (Zhu 2007). This protective effect is explained by a reduced nuclear translocation of AIF in the neurons of CypA knock-out mice located in the damaged area. Interestingly, also CypA translocation to nuclei is reduced in AIF-

deficient mice (Zhu 2007). Therefore, these data suggest that CypA and AIF translocation and activity need the presence of both factors and strengthen the hypothesis of the involvement of CypA in apoptosis and possibly in ALS.

CypA can also be involved in excitotoxicity-mediated apoptosis due to an increased calcium influx in the cell mediated by glutamate receptors (Capano 2002). Indeed, CsA can suppress glutamate toxicity in hippocampal neurons (Uchino 1995) and cortical neurons (Nieminen et al. 1996). Thus, although CypD can be involved in this protection mechanism, given that CypA is the main intracellular ligand for CsA, CypA has been proposed to play a role in the excitotoxin-induced apoptosis (Capano 2002). Silencing CypA in rat neuronal cells treated with glutamate and NO has the same reducing effect on caspase-8, -9, -6 and -3 activation as CsA, suggesting that CypA-caspase activation is mediated by CypA PPIase activity (Capano 2002). In this context, an involvement of CypA-calreticulin interaction has also been hypothesised (Reddy 1999), suggesting that it may inhibit calcium fluxes required for apoptosis, even if no demonstration is yet available. Notably, stable heterodimers composed of CypA and cytochrome c (CytC) were described in brain tissue and in the cytoplasm of apoptotic cells *in vitro* (Bonfils 2010). CypA was shown to inhibit CytC-dependent procaspase-3 activation in a cell-free system, suggesting that an anti-apoptotic effect of CypA may be due to the ability of CypA to bind free cytoplasmic CytC. The regulation of caspase-3 mediated by CypA is still unclear.

Concluding, it is still difficult to understand whether CypA is an anti- or pro-apoptotic factor, since the results obtained are still controversial.

2.4.5 CypA and the subcellular localisation of proteins

A role for CypA has also been hypothesised in promoting the functional expression of membrane proteins. Indeed, CsA treatment, inhibiting both CypA PPIase and chaperone activities, resulted in impaired cell-surface externalisation of the homo-oligomeric acetylcholine receptor containing

the α7 subunit (Helekar 1994), the homo-oligomeric 5-hydroxytryptamine type 3 receptor (Helekar 1997), the Kir2.1 potassium channel (Chen 1998), the insulin receptor (Shiraishi 2000) and the creatinine transporter (Tran 2000). In particular, the specific involvement of CypA PPIase activity in the maturation of the homo-oligomeric receptors containing nicotinic acetylcholine subunit α7 has been demonstrated (Helekar 1994), since overexpression of WT-CypA, but not the PPIase-deficient mutant R55A, reversed the effect of CsA. Furthermore, the cell surface expression level of the creatine transporter was reduced by CsA treatment in muscle cells, without significantly altering its total expression level, but with a concomitant decrease in creatine uptake (Tran 2000). Therefore, the resulting creatine-depletion in the muscle could adversely affect the energy metabolism, which in turn might lead to muscle myopathy, that is a clinically relevant muscle disorder developed on chronic CsA therapeutic treatment. In addition, CypA is also involved in the functional expression of the Na^+-Ca^{2+} exchanger (NCX1), a major Ca^{2+} regulating protein (Elbaz 2010). Indeed, CypA knockdown reduced NCX1 surface expression, transport activity, and Na^+-dependent Ca^{2+} fluxes, but did not change the total amount of NCX1 expression, thus suggesting a post-translational modulation effect of CypA, not mediated by its PPIase activity. CypA is also a regulator of SERCA2b in human platelets (Rosado 2010), where it can act as Ca^{2+} modulator (Elvers 2012).

Furthermore, a role for CypA has been hypothesised in nuclear transport of cellular factors. In fact, in addition to AIF, CypA cytoplasm-nuclear transport activity has been reported also for the zinc-finger-containing protein Zpr1p (Ansari 2002) and the spliceosomal RNA-binding protein hnRNP A2/B1 (Pan 2008). In particular, in *S. cerevisiae* the nuclear export of Zpr1p was defective in CypA-lacking cells, and rescue of this defect was correlated with PPIase activity (Ansari 2002). Moreover, CypA was observed in complex with CXCR4, the cognate receptor of the stromal cell-derived factor 1 (SDF-1)/CXCL12, in endosomal compartments (Pan 2008), and CXCL12 stimulation of CXCR4 induced phosphorylation and nuclear translocation of CypA in a transportin-1-dependent manner. Furthermore, in response to CXCR4 activation CypA formed a complex hnRNP A2, which underwent nuclear export, thus suggesting a regulatory role of CypA in the trafficking of

hnRNP A2. Interestingly, hnRNP A2 is one of the best characterised interactor of TDP-43, it is among the most abundant nuclear protein, and it shuttles rapidly between the nucleus and the cytoplasm playing important roles in all steps of mRNA metabolism. In addition, CypA played a role in CXCL12-induced activation and nuclear translocation of ERK1/2, and in chemotactic cell migration toward CXCL12 gradients, suggesting a possible involvement of CypA in chemotaxis. These findings highlight the importance of this poorly explored function of CypA, whose relevance could be linked to ALS patho-mechanisms involving TDP-43.

Possibly CypA can exert these effects through maintenance of a normal actin structure. The regulation of actin polymerisation requires *de novo* nucleation of actin filaments, which relies on the activation of the Arp2/3 complex by N-WASP (Suetsugu 2001). CypA can bind N-WASP, and its PPIase activity is required to protect degradation of N-WASP, thus stabilising its complex formation with Arp2/3, and in turn favouring the nucleation/initiation of F-actin polymerisation (Calhoun 2009). In addition, CypA knockdown or CsA treatment resulted in an altered actin cytoskeleton in U2O2 cells (a human osteosarcoma cell line) (Calhoun 2009), Jurkat cells (a T-cell line), peripheral blood lymphocytes (isolated from CsA-treated patients) (Hasková 1994), chick cardiomyocytes (Kołcz 1999). Moreover, like actin, CypA was found to be a prominent component of slow axonal transport in chicken sciatic nerve, and to be localised in neuritis at points of branching, occasional swellings and growth cones (Yuan 1997). These findings raised the possibility that CypA could co-operate with Hsc70 in maintaining the native folding of actin and associated proteins during transit in axons, and assembly and disassembly in growth cones. Thus, CypA PPIase and chaperone activities may be further important in relation to neurons. Furthermore, CypA was shown to colocalise with microtubules and to exist in the form of a heterocomplex containing tubulin and dynein *in vitro* (Galignana 2004a). CypA associated to dynein indirectly, by binding to dynamitin in a PPIase-dependent manner (Galignana 2004b). These data suggest that CypA may perform a general function related to the binding, and possibly recognition, of cargo for retrograde movement system as a CypA/dynamitin/dynein/microtubule complex (**Figure 21**).

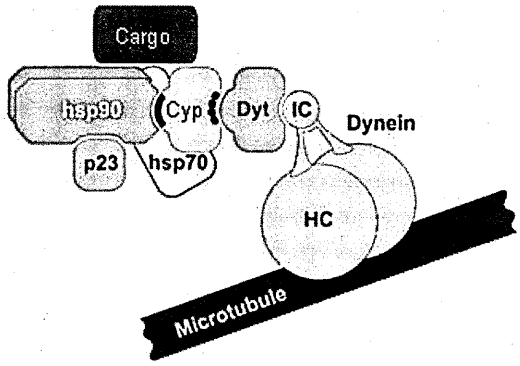

Figure 21 Model of CypA/dynamitin/dynein/microtubule heterocomplex.

Dynein is a large multi-subunit complex composed of two heavy chains (HC) that have the processive motor activity, three intermediate chains (IC), and some light chains (not shown). Cyclophilins (Cyp), such as CypA, link the client protein (cargo) bound to hsp90, to the dynamitin (Dyt) component of the dynein heterocomplex for retrograde movement along microtubules. Modified from Galigniana 2004.

In addition, although CypA has been traditionally considered a cytoplasmic protein, CypA nuclear localisation has been reported in several studies, also associating it with possible nuclear functions. In yeast cells, CypA interacted with and modulated the activity of two histone deacetylase (HDAC) complexes, Sin-Rpd3 and Set3C, which both control meiosis (Arévalo-Rodríguez 2000 and 2005), possibly suggesting that CypA can affect gene expression by interacting with HDAC. Moreover, an epigenetic function of CypA was demonstrated in p19 cells, where CypA protected the paternal allele of *Peg3* from DNA methylation and inactive histone modification (Lu 2006). Furthermore, CypA and YY1, a zinc finger transcriptional factor, interacted to mediate transcriptional activation, and CsA disrupted this complex (Yang 1995). CsA also blocked the nuclear transport of cytoplasmic transcription factors, primarily NFAT, thereby inhibiting the activation of cytokine transcription (Flanagan 1991; Emmel 1989; Jain 1993; McCaffrey 1993). CsA also inhibited transcription mediated by AP-3, Oct-1 and NF-κB (Frantz 1994), further suggesting a possible association with CypA. In a model of neuronal differentiation, the nuclear translocation of CypA, the appearance of hypophosphorylated retinoblastoma (RB) and the enhancement of RB/CypA complex formation correlated with retinoic acid induced neuronal differentiation (Chiu 2003). The evidence of enriched CypA and colocalisation of RB with

CypA in the nucleus of primary adult sensory neurons substantiated the important event of RB-mediated neuronal differentiation of p19 EC cells.

In summary, the hydrophobic cavity of CypA and the surrounding residues could be associated to various exposed loops of different proteins or receptors, but which physiological effects all those interactions may have and how their possible disruption (for example by using CsA) could alter some cellular processes still remain unclear.

2.5 CypA extracellular functions

CypA is released under inflammatory stimuli by macrophages/monocytes (Sherry 1992; Kim 2005; Yuan 2010), leukocytes (Xu 1992), astrocytes (Lafon-Cazal 2003) and under oxidative stress by vasculature smooth muscle cells (Jin 2000; Suzuki 2006), mouse fibroblasts (Jin 2000), myocytes (Seko 2004), endothelial cells (Jin 2004; Kim 2004), platelets under coagulating conditions (Coppinger 2004), and neurons (Boulos 2007). Extracellular CypA shows a proinflammatory cytokine-like behaviour, a chemoattractant effect and has been implicated in oxidative-stress induced cellular death. The extracellular functions of CypA are mediated by the interaction with its ubiquitous Ig-like receptor, CD147 (EMMPRIN) (Yurchenko 2002). Secreted CypA binds and activates the cell surface of its receptor CD147, leading to the phosporylation of ERK1/2 and Akt (Boulos 2007; Yurchenko 2002). Evidence was provided for a protective effect of CypA on neurons from oxidative stress and *in vitro* ischemia through CD147 activation of the ERK1/2 pathways. In addition, CypA interaction with CD147 increases the expression of the anti-apoptotic protein Bcl-2 (Seko 2004). Moreover, CypA/CD147 signaling stimulates the phosphorylation of c-jun NH2-terminal kinase (JNK), p38 kinase and Ikb (Jin 2004; Seko 2004; Yurchenko 2002). CypA can also promote the production and secretion of other pro-inflammatory cytokines, like TNFα, IL-8, MCP1, IL-1β (Jin 2004; Kim 2004; Kim 2005). From a biological point of view the CypA/CD147 mediated signaling seems to induce cell migration, proliferation and differentiation. Indeed, through the interaction with CD147, CypA can also trigger intracellular pathways involving metalloproteinases (MMPs) activation (Seizer 2010; Yang 2008; Wang 2010; Yuan 2010).

Interestingly, and suggesting a potential role of CypA signalling in ALS pathogenesis, activation of MMP-2 and MMP-9 has been observed in ALS patients and animal models (Fang 2009 and 2010; Lim 1996; Niebroj-Dobosz 2010), and knocking-out MMP9 gene in G93A-SOD1 mice results in extending the life span of these animals (Kiaei 2007). Recently, elevated levels of CD147 have been observed in ALS patient serum (Iłżecka 2011) and increasing levels of CD147 mRNA have been reported in G93A-SOD1 lumbar SpC (Yoshihara 2002). Regulating the interaction between CypA and its receptor, has been considered as an attractive pharmacological target in a variety of acute and chronic inflammatory disease models (Yurchenko 2010), and should be considered as a therapeutic option also in ALS.

In addition, the analyses of CypA knockout mice in other disease context suggest interesting functions of CypA in pathogenetic mechanisms possibly relevant for ALS. Indeed, CypA knockout mice displayed a reduced injury and marked attenuation of ROS production, MMPs activation and MCP-1 secretion following aortic aneurism (Satoh 2009), effects linked to a lack of interaction with CD147. Moreover, CypA was suggested as a key target for treating APOE-mediated neurovascular injury and the resulting neuronal dysfunction and degeneration, such as AD, since the APOE increased blood brain barrier susceptibility to injury was mediated by CypA activation of nuclear factor κB-MMP9 pathway in pericytes (Bell 2012). Furthermore, CypA was investigated as an inflammatory factor promoting atherosclerosis, and a reduction of extracellular CypA was demonstrated to promote eNOS down-regulation and a marked decrease of TNF-induced apoptosis (Nigro 2011).

Moreover, a catalytic role for CypA has also been hypothesised in CD147 mediated signalling. Indeed, the PPIase-deficient mutant R55A-CypA shows only little activity compared to WT-CypA (Yang 2007), suggesting that the interaction is mediated through CypA active site. NMR studies demonstrated that CypA binds and catalyses the isomerisation of a single site within CD147: Pro211, a residue predicted to lie just outside the extracellular membrane. CD147 Pro211 exists in an inherent *cis-trans* equilibrium in the absence of CypA; when CypA is present, it can mediate the catalysis of this site, leading to an higher rate of prolyl-bond interconversion and to an higher *cis*

content (Schlegel 2009) (**Figure 22**). CypA mediated CD147 isomerisation on the outside of the cell may result in a conformational rearrangement of the receptor inside the cell, that is responsible of the following signal transduction. These data demonstrate that CypA can regulate the *cis-trans* "conformational switch" of its protein substrates both inside and outside the cells.

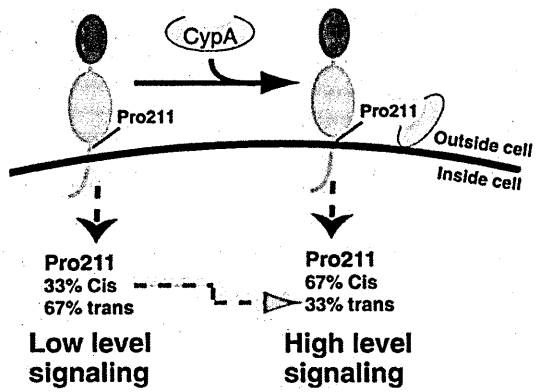

Figure 22 CypA mediated isomerisation of CD147 receptor.
CypA can alter the inherent *cis-trans* equilibrium of CD147 Pro211 through its PPIase activity. Adapted from Schlegel 2009.

Although CD147 is the only known cellular protein receptor for extracellular CypA, possibly other cell surface receptors exist. Indeed, CypA was also found to associate with CD99, a surface glycoprotein with essential roles in inflammation and immune responses, mediating and affecting CD99 signaling pathways (Kim 2004). Therefore, CypA could exert possibly multiple functions binding different molecular targets, with a mechanism dependent on the cell type, as well as on the type and duration of the triggering event.

In addition, CypA has been suggested as a marker of cell death, since it is released from necroptotic cells as a result of early membrane permeabilisation (Christofferson 2010). Furthermore, the presence of increased levels of secreted CypA was described in human serum in the nanomolar range (Endrich 1998), in several inflammatory diseases, such as rheumatoid arthritis (Jin 2000 and 2004; Tegeder 1997), in HIV infection (Billich 1997; Endrich 1998) and by

progressive solid tumors (Arora 2005; Huang 2006). Whether CypA is protective or detrimental when secreted is still debated.

2.6 CypA post-translational modifications

CypA displays multiple cellular localisations, inside and outside the cell, and has important roles in many key cellular processes, nevertheless the molecular mechanisms underlying its pleiotropic activities are still a matter of study. It is likely that the different functions played by CypA might be modulated by its high propensity to undergo co- and post-translational modifications (PTMs) (**Table 4**). Indeed, PTMs have been demonstrated to be crucial in regulating the functions of many eukaryotic proteins.

2.6.1 Phosphorylation

Phosphorylation is a reversible PTM occurring in cytoplasm to folded proteins well after their synthesis and it is mediated by protein kinases using ATP as the phosphoryl donor, whereas the phosphoryl group is removed by specific phosphatases. Protein phosphorylation is an important regulatory mechanism in both prokaryotic and eukaryotic organisms. It usually occurs at serine, threonine, and tyrosine residues in eukaryotic proteins and results in a conformational change in the structure of many enzymes and receptors, causing their activation or inactivation. Indeed, the addition of a phosphate (PO_4^{2-}) to a polar R group of an amino acid can turn a hydrophobic portion of a protein into a polar and extremely hydrophilic region.

CypA has been demonstrated to be phosphorylated on Ser21 in mouse brain, and on Thr157 in hepatocarcinoma cells (Gevaert 2005; Vosseller 2005). In particular, phSer21 has been found to influence neuronal protein maturation and folding. Moreover, one study indicates that the C-terminal domain of CXCR4 receptor can mediate CypA phosphorylation and this modification may stimulate the nuclear translocation of CypA (Pan 2008). However, the precise effect of phosphorylation in the molecular dynamics of CypA is not well understood; furthermore it is still

unknown which are the kinase and phosphatase regulating CypA phosphorylation or which is the trigger for this PTM.

Position	Amino acid	Post-translational modification	Reference
1	Met	Partial N-terminal methionine removal	Chevalier 2012
2	Val	Partial N-terminal acetylation	Massignan 2007; Chevalier 2012
21	Ser	Phosphorylation	Vosseler 2005
9	Asp	Methylation at acidic groups	Chevalier 2012
13	Asp	Methylation at acidic groups	Chevalier 2012
15	Glu	Methylation at acidic groups	Chevalier 2012
21	Ser	Phosphorylation	Gavaert 2005
23	Glu	Methylation at acidic groups	Chevalier 2012
28	Lys	Acetylation	Choudhary 2009
28	Lys	Ubiquitination	Meierhofer 2008
31	Lys	Acetylation	Chevalier 2012
44	Lys	Acetylation	Choudhary 2009; Chevalier 2012
48	Tyr	Phosphorylation	Gavaert 2005
49	Lys	Acetylation	Choudhary 2009
52	Cys	Glutathionylation	Ghezzi 2006
55	Arg	ADP-ribosylation	Dinovo 2006
62	Cys	Glutathionylation	Ghezzi 2006
62	Cys	S-nitrosylation	Wu 2011
69	Arg	ADP-rybosylation	DiNovo 2006
76	Lys	Acetylation	Choudhary 2009
77	Ser	Phosphorylation	Gavaert 2005
82	Lys	Acetylation	Choudhary 2009; Chevalier 2012
84	Glu	Methylation at acidic groups	Chevalier 2012
85	Asp	Methylation at acidic groups	Chevalier 2012
86	Glu	Methylation at acidic groups	Chevalier 2012
93	Thr	Phosphorylation	Gavaert 2005
110	Ser	Phosphorylation	Gavaert 2005
115	Cys	S-nitrosylation	Camerini 2007
125	Lys	Acetylation	Choudhary 2009; Kim 2006
131	Lys	Acetylation	Choudhary 2009
134	Glu	Methylation at acidic groups	Chevalier 2012
140	Glu	Methylation at acidic groups	Chevalier 2012
143	Glu	Methylation at acidic groups	Chevalier 2012
157	Thr	Phosphorylation	Gavaert 2005
161	Cys	S-nitrosylation	Wu 2011

Table 4 Human CypA co- and post-translational modifications.

2.6.2 S-glutathionylation

S-glutathionylation is an important PTM occurring under normal conditions as well as during oxidative stress. This modification is selective, occurring only on cysteine residues positioned in specific context on the surface of target proteins. S-glutathionylation is the formation of a disulfide bond between Cys in a protein and Cys in the tripeptide glutathione (GSH). Glutathione is the most abundant non-protein thiol in cells and, as a major antioxidant, it is maintained in a reduced (GSH) state. In the presence of reactive oxygen and nitrogen species, GSH donates a reducing equivalent and becomes highly reactive. It can partner with another molecule of reactive glutathione, forming glutathione disulfide (GSSG). Alternatively, it can react with the sulfhydryl group of cysteines on proteins. Glutathionylation of proteins is a reversible process since glutaredoxins can reduce proteins. This process in cells is useful to maintain the correct redox state (GSH/GSSG) and to regulate protein functions (Creighton 1996; Casagrande 2002).

CypA contains four Cys, and none of them is stably involved in disulfide bridges, thus are all potential sites of glutathionylation. CypA glutathionylation has been observed *in vivo* (Fratelli 2002 and 2003). In particular, Cys52 and Cys62 are targets of glutathionylation in T-lymphocytes (Ghezzi 2006). The glutathionylation of these two Cys residues results in a decrease of the α-helix content of the protein, increasing the portion of the unstructured protein (Ghezzi 2006). Moreover, Cys52 is close to Arg55, the main aa involved in PPIase activity, whereas both Cys52 and Cys62 are close to Phe60 and Arg55 that are part of the CsA-CypA binding domain. Therefore, this modification could alter CypA function by altering its structure. In particular, *in vitro* glutathionylated CypA showed a significantly lower CsA-dependent inhibitory effect on calcineurin phosphatase activity (unpublished data from the lab).

2.6.3 Acetylation

Acetylation describes a reaction that introduces an acetyl functional group, whereas deacetylation is the removal of the acetyl group. In living cells, acetylation occurs as a co-translational and post-translational modification of proteins.

Acetylation of the ε-amine of specific lysine residues in proteins is a dynamic modification that plays a key role in regulating transcription and other DNA dependent nuclear processes, but it is also involved in subcellular localisation and protein stability. This PTM was initially discovered on histones (Vidali 1968) as part of gene regulation. However, also non-histone proteins, such as p53, are lysine-acetylated (Gu 1997). Regulatory enzymes, such as acetyl-CoA-dependent histone acetyltransferases (HATs) and zinc-dependent histone deacetylase (HDACs), catalyze these reactions (**Figure 23**). Despite the fact that Lys acetylation can affect a wide range of proteins and can possibly contribute to the regulation of several nuclear and cytoplasmic functions (Lammers 2010) the role of this PTM in different cellular proteins remains to be established. Interestingly, lysine-acetylation and its regulatory enzymes are also intimately linked to aging and several major pathological states such as cancer, neurodegenerative disorders, and cardiovascular diseases (Blander 2004; Carrozza 2003; McKinsey 2004).

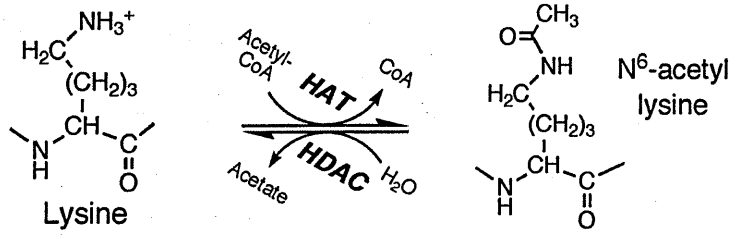

Figure 23 Lysine can be acetylated by HATs and de-acetylated by HDACs.

Several acetylated lysines have been identified using large proteomic approaches *in vitro* (Choudhary 2009). One recent study has highlighted the specific role of Lys125 acetylation on CypA dynamics (Lammers 2010). Acetylation on this residue does not seem to substantially rearrange the active site, however it markedly affects its surface electrostatics: Lys125 provides the strongest patch of positive charge in the active site (**Figure 24**) and its charge is largely neutralized by the acetyl group. This charge change mediated by the acetyl group reduces the affinity of CypA for CsA 20-fold and decreases CypA-catalysed *cis-trans* isomerisation. Moreover, acetylated-Lys125 CypA-CsA complex mediates a two-fold decrease in calcineurin inhibition (Lammers 2010).

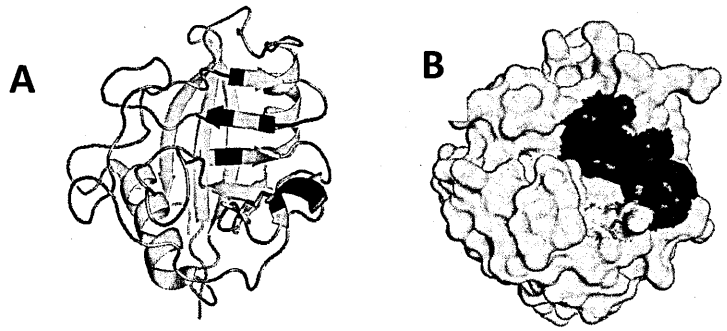

Figure 24 CypA Lys125.

Lys125 is shown in red whereas the residues of the active site are shown in blue. Lys125 residue is located in a loop surrounding the active site and acetylation in this position alter the active site charge. (**A**) Ribbon representation of CypA. (**B**) Electrostatic surface potential of CypA.

Acetylation of the N-terminal α-amine of proteins is a widespread co-translational modification in eukaryotes; 80-90% of human proteins are modified in this manner. This modification is performed by N-α-acetyltransferases enzymes. Despite being a conserved and widespread modification, little is known about the biological role of N-α-terminal acetylation. CypA is acetylated on the N-terminal α-amine of the Val2 residue (Massignan 2007), following methionine cleavage. The intriguing feature is that only a portion of CypA proteins are acetylated at their N-terminus, whereas the other remains unmodified, thus suggesting a possible functional role for N-terminal acetylation in this protein. In particular, CypA was found to be more N-terminally acetylated in Th1 than in Th2 T-cells leading to the assumption that this modification can be involved in T-cell functions (Rautajoki 2004). In the context of ALS, CypA has been found partially N-terminal acetylated in the SpC of pre-symptomatic G93A-SOD1 mice (Massignan 2007). However, it has not been established yet whether it has a role in MN degeneration.

2.6.4 ADP-rybosylation

ADP-rybosylation is mediated by ADP-rybosil transferases which cleave the cofactor NAD^+ and transfer the ADP-rybosyl moiety to proteins. This modification is reversible since the poly(ADP-

rybose) glycohydrolase can remove the ADP-rybosyl group. It occurs preferentially in the nucleus and can affect Arg, Asn, Lys, His and Glu (Creighton 1996).

Human CypA can be subjected to ADP-ribosylation on Arg55 and 69 by the opportunistic pathogen *Pseudomonas aeruginosa*, thus leading to moderate decrease in PPIase activity (≈20%) and affecting the ability to bind calcineurin (DiNovo 2006).

2.6.5 S-nitrosylation

Nitrosylation is a reversible modification mediated by transnitrosylase enzyme. This modification occurs at Cys and a nitric oxide (NO) is attached to the sulfhydryl group in a covalent manner, providing a mechanism for redox-based physiological regulation. The NO can be also detached from proteins by specific denitrosylases enzymes. S-nitrosylation occurs physiologically in cell, determining protein function and structure (Derakhshan 2007), and it obviously increases in oxidative stress conditions where NO is highly abundant.

CypA has been found to be S-nitrosylated at Cys62, Cys115 and Cys161 (Wu 2011; Camerini 2007). Although the role of CypA S-nitrosylation is unknown, it is possible to hypothesise that CypA serves as a NO scavenger during nitrative stress.

2.6.6 Ubiquitination

Ubiquitination is a reversible modification which attaches an ubiquitin molecule to a Lys (Huang 2010). This physiological modification is used by the cell to deliver proteins through the proteasome system in order to degrade them. CypA is ubiquitinated at Lys28 (Meierhofer 2008), which is a residue that can be acetylated too, suggesting that acetylation on this position could be important in regulating the successive ubiquitination. Indeed, it is possible that ubiquitination is blocked by the presence of the acetyl group on this residue, thereby preventing protein

proteasomal degradation. This mechanism was first described for p53 (Ito 2002; Tang 2008) and later for others human proteins.

CypA has been described with a lot of potential PTMs. Nevertheless, still little is known about their biological significance. Thus, a deeper characterization is required to better understand CypA functionality. Moreover, CypA PTMs have been described to be especially important in ALS pathology, where a variation in CypA isoform pattern was found in lumbar SpC of G93A-SOD1 mice at the pre-symptomatic stage (Massignan 2007). Therefore, studying CypA PTMs could give insights into ALS patho-mechanisms.

II. AIMS OF THE THESIS

HYPOTHESIS OF THE STUDY

ALS is a neurodegenerative disorder characterised by the accumulation of aggregated proteins. Either in sporadic patients and in mSOD1 animal models of ALS, CypA is up-regulated early in the pathology (Massignan 2007; Nardo 2011), and is enriched in SpC aggregates at symptomatic and end stages of the disease (Basso 2009). CypA is widely expressed in many tissues, but it is found in the highest concentration in the CNS and is located primarily in neurons and MNs (Goldner 1996). Nevertheless, the specific role that CypA plays in ALS and in neurons and MNs has not been defined yet. Indeed, although the primary intracellular function of CypA is the PPIase activity (Fischer 1989), as a chaperone protein CypA may be involved in the pathogenesis of ALS, since protein misfolding and aggregation are hallmarks of human ALS and animal models of the disease (Cheroni 2005; Basso 2009).

The hypothesis of this study is that progressive neurodegeneration in ALS, either caused by mutant SOD1 or alterations in TDP-43, could be mediated by impaired association with a common chaperone protein, CypA. Therefore, CypA can have a protective role in ALS through its intracellular activities in neurons and MNs, that are particularly vulnerable to the detrimental effects of misfolded and/or aggregated proteins.

AIMS OF THE STUDY

→ To provide insights into CypA intracellular functions that could be relevant in ALS.

→ To unravel if CypA is involved in ALS pathogenesis and whether it influences the neurodegenerative process.

The specific issues pursued during the study are:

→ Development of a cellular model system of fALS to investigate how CypA could exert its functions and possible effects in the disease.

→ Identification of CypA cytosolic and nuclear interactors *in vitro*, validation of the most interesting binding partners *in vivo*, and functional analysis of these protein complexes for their relevance in the disease.

→ Functional characterization of CypA PTM associated to its localisation and activity on specific substrates, in normal and pathological conditions.

III. MATERIALS AND METHODS

1. CELLULAR CULTURES

Experiments performed in this work were done on HEK293 cells (ATCC CRL-1573). The 293 cell line was derived by transformation of primary cultures of human embryonic kidney cells with sheared adenovirus (Ad)5 DNA (Graham 1977). HEK293 cells were kindly provided by Dr. David Harris (Boston University, School of Medicine).

HEK293 cells were plated in Dulbecco's modified Eagle's medium (DMEM) (Invitrogen) containing 10% fetal bovine serum (Invitrogen), 2mM L-glutamine (Invitrogen), 1% non-essential amino acids (VWR International PBI) and a 1:100 dilution penicillin/streptomycin (Invitrogen). Cells were maintained at 37°C in a humidified atmosphere at 95% air and 5% CO_2.

1.1 Stable clones generation

Wild-type human SOD1 (WT-SOD1) or human SOD1 carrying a single base mutation that produces a protein with alanine instead of glycine in position 93 (G93A-SOD1) were stably expressed in HEK293 cells. Plasmids encoding WT- or G93A-SOD1 were generated in the laboratory of Dr. Caterina Bendotti at the "Mario Negri" Institute for Pharmacological Research (Tortarolo 2004).

HEK293 cells were transfected with pcDNA3.1(+)-Hygro or -G418 expression plasmids using Lipofectamine™ 2000 (Invitrogen), according to the manufacturer's instructions. One day after transfection cells were passaged at high dilution into fresh growth medium. HEK293 cells stably expressing the constructs were selected with 200µg/ml Hygromycin (Sigma) or 1200µg/ml G418 (Invitrogen) for 15-20 days, then individual clones were isolated and maintained using 100µg/ml Hygromycin or 800µg/ml G418. Isolated resistant clones were tested for human SOD1 expression by Western blotting (WB) using an anti-SOD1 antibody (Millipore).

1.2 Plasmid DNA transfection

The day before transfection, an appropriate number of HEK293 cells was plated into a 24-well plate in 500µl of serum-containing growth medium without antibiotics, so that cells would have

been 80-90% confluent at the time of transfection. Cells were incubated at 37°C in a 5% CO_2 incubator overnight.

The following day, for each transfection sample, complexes were prepared as follow:

- 0.8µg plasmid DNA were diluted in 50µl Opti-MEM® I Reduced Serum Medium (Invitrogen);
- 1.8µl Lipofectamine™ 2000 (Invitrogen) were diluted in 50µl Opti-MEM®.

After 5min of incubation at room temperature (RT), the diluted DNA was combined with diluted Lipofectamine™ 2000 (total volume = 100µl) and they were incubated at RT for 20min to allow DNA-lipid complexes to form. 100µl of complexes were added directly to each well containing cells and medium. Cells were incubated at 37°C in a CO_2 incubator for 24-48 hours prior to testing for transgene expression. Medium was changed after 4-6 hours.

Alternatively, FuGENE® HD Transfection Reagent (Promega) was used, with a FuGENE®:DNA ratio of 2.5:1.0. The day of transfection, for each sample, a 0.020µg/µl plasmid solution was prepared as follow:

- 0.5µg plasmid DNA were diluted in 25µl Opti-MEM®;
- 1.4µl FuGENE® HD reagent was added and mixed carefully.

After 5-10min of incubation at RT, 25µl of complexes were added to each well, and mixed. Cells were incubated at 37°C in a CO_2 incubator for 24-48 hours prior to testing for transgene expression.

Transfection conditions, such as plasmid DNA concentration, cell confluency, the DNA:lipid ratio and the duration of the transfection were optimized in this cellular model. Transgene expression was detected monitoring the protein level by direct WB analysis.

1.3 Silencing

RNA interference (RNAi) is the sequence-specific gene silencing induced by small interfering RNAs (siRNAs), double-stranded RNA molecules, 21 nucleotides in length. RNAi was used as a tool to manipulate gene expression.

In this cell line and for each siRNA molecule tested, optimum transfection and silencing efficiencies were achieved by adjusting: cell density at the time of transfection, amount and type of lipid reagent, siRNA concentration and length of exposure of cells to lipid-siRNA complexes. Calibration of knockdown efficiency was done with 5/10/20/30/50/80/100nM siRNA for 24/48/72/96h using WB analysis. On the basis of calibration, 10nM siRNA for CypA and 5nM siRNA for TDP-43 were used. siRNA molecules used are listed in **Table 5**.

siRNA	Company	target seq	target	GENE
SI04145925	Qiagen	AGCCAGGTACTTGGTGCTACA	3'-UTR	PPIA
SI04193469	Qiagen	AAGGGATACCCTTCCCACTAA	3'-UTR	PPIA
SI04240824	Qiagen	CACTAAGGACTTGGTTTCTCA	3'-UTR	PPIA
SI04351718	Qiagen	CTGGGTGATACCATTCAATGT	3'-UTR	PPIA
D-004979-17-0005	Thermo Scientific	UCCUAGAGGUGGCGGAUUU	3'-UTR	PPIA
4616	Applied Biosystems	5'-AGGAUUUGGUUAUAAGGGUTT-3'	EXON	PPIA
s310	Ambion	5'-GGGUGAUACCAUUCAAUGUtt-3'	3'-UTR	PPIA
s311	Ambion	5'-GCAGUUAGAUGUCAGGACAtt-3'	3'-UTR	PPIA
s312	Ambion	5'-CCACCUUAACAGACCUCUAtt-3'	3'-UTR	PPIA
s57823	Ambion	5'-AGCAGAAAAUUUUCGUGCUtt-3'	EXON 2	PPIA
4616	Applied Biosystems	5'-ACCCUUAUAACCAAAUCCUTT-3'	scramble	none
12935-300	Invitrogen	medium GC duplex content	scramble	none
SI00739501	Qiagen	5'-CACACTACAATTGATATCAAA-3'	3'-UTR	TARDBP

Table 5 siRNA duplex molecules used in this study.

The day before transfection, 24-well plates were inoculated with an appropriate number of cells in serum-containing medium (without antibiotics) such that they would be 50-70% confluent the following day. Cells were plated between 0.1 and 4.0 x 10^5 cells in 0.5ml of medium and incubated at 37° C in a 5% CO_2 incubator overnight.

Fifteen to sixty minutes prior to transfection, medium was aspirated from the wells and 250µl of fresh growth medium (without antibiotics) were added to each well. For each well to be transfected, 25µl of serum-free medium containing 0.75µl of siLentFect Lipid Reagent (BioRad) were prepared and 25µl of OptiMEM medium were supplemented with CypA or TDP-43 siRNA. As

a negative control for these experiments, a scrambled siRNA of approximately the same length and the same GC% content, and possessing a sequence not targeting any known vertebrate transcript, was used. The diluted siRNA was added to the diluted siLentFect and mixed. When RNAi molecules were co-transfected with plasmid DNA, 0.6μg of DNA were added to the lipid-siRNA complexes. This mixture was incubated at RT for 20min to allow lipid-siRNA complexes to form. After this incubation time complexes were added directly to cells in serum-containing medium. The plate was rocked back and forth to mix and incubated at 37°C in a CO2 incubator. Twenty-four hours after transfection the media was substituted with fresh growth medium for an additional 24-48 hours. Gene silencing was monitored at the protein level 24-72hours after transfection.

1.4 Cell survival

MTT [3-(4,5-Dimethylthiazol-2-yl)-2,5-diphenyltetrazolium bromide] is a colourimetric assay system used to assess cell viability as a function of redox potential. MTT assay is based on the ability of a mitochondrial dehydrogenase enzyme from viable cells to convert the water-soluble tetrazolium rings of the pale yellow MTT and form insoluble purple formazan crystals which are largely impermeable to cell membranes, thus resulting in their accumulation within healthy and metabolically active cells. The formazan is then solubilized by the addition of DMSO (Dimethyl sulfoxide) and its concentration is determined by optical density.

Cells were seeded in 24- or 48-well plates one day before treatment. Depending on the experiment performed, 1 to 3 days after treatment culture medium was removed and cells were incubated with a solution: 0.32 mg/ml MTT resuspended in LOCKE's buffer (NaCl 154 mM, KCl 5.6 mM, $MgCl_2$ 1 mM, $CaCl_2$ 2.3 mM, HEPES 8.6 mM, Glucose 5.6 mM). Cells were incubated at 37°C for at least 30min. The crystals were solubilized by the addiction of DMSO for 30min at RT. The concentration was quantified by spectrophotometric means (excitation OD-575nm was measured in Infinite® 200 multimode plate reader, Tecan). Data ($n \geq 6$ replicates) were expressed as percentage of absorbance compared to non-treated control cells.

2. ANIMAL MODELS

All animal tissues used in this study were collected by Dr. Silvia Pozzi and Laura Pasetto in our laboratory or by the laboratory of Dr. Caterina Bendotti (Molecular Neurobiology Lab., Mario Negri Institute, Milan). All animal models considered in the study were housed under standard conditions (temperature of 21 ± 1°C, relative humidity of 55 ± 10% and 12h light/dark schedule), 3-4 per cage, food and water supplied *ad libitum*. Procedures involving animals and their care were conducted in conformity with Institutional guidelines that are in compliance with national (D.L. No. 116, Suppl. 40, Feb. 18, 1992 Circolare No. 8, G.U., 14 luglio 1994) and international laws and policies (EEC Council Directive 86/609. OJ L 358,1, Dec.12, 1987; NIH Guide for Care and use of Laboratory Animals, U.S. National Research Council, 1996). Before every analysis, animals were deeply anesthetized with 20µl/g of Equitensin (1% pentobarbital, 4% chloral hydrate, 2% $MgSO_47H_2O$, 40% propilenglicole, 10% ethanol) by intra-peritoneal injection and killed by decapitation.

2.1 G93A-SOD1 mouse model

G93A-SOD1 mice on a C57BL/6JOlaHsd (C57) or 129S2/SvHsd (129Sv) genetic background and corresponding non-transgenic littermates were used in this study. Both mouse lines derive from the originally obtained from Jackson Laboratories (B6SJL-TgNSOD-1-SOD1-G93A-1Gur) line, which expresses about 20 copies of mutant human SOD1 with a Gly93Ala substitution. Animals were maintained on a C57BL/6OlaHsd or 129S2/SvHsd background (more than 30 or 10 breeding, respectively) at Harlan Italy S.R.L. (Bresso, Milano, Italy). G93ASOD1^{G93A} transgenic mice were identified with PCR on DNA tail biopsies. These two strains showed a different disease onset and progression and different survival length.

2.1.1 *SOD1^{G93A} C57 mice*

A hSOD1^{G93A} C57BL/6JOlaHsd mouse line was maintained heterozygote for the transgene by repeated backcrossing of heterozygote G93A-SOD1 male mice with non-transgenic females C57BL/6 JOlaHsd. Heterozygote mice G93A-SOD1 developed first signs of neuromuscular junction loss and denervation at 8 weeks of age while symptoms are clearly visible at 16 weeks of age when 40% of MNs are lost. From 16 to 20 weeks of age mice progressively worsen presenting reduction in the extension reflex of the hind limbs, when mice are raised by the tail, and muscular weakness, revealed by the increasing difficulty in staying on the rotating bar. Complete paralysis of hind limb appeared at 20 weeks of age when over the 60% of motor neurons were lost (Peviani 2010).

2.1.2 *G93A-SOD1 129sv mice*

The hSOD1^{G93A} 129S2/SvHsd mouse line was obtained in the laboratory of Dr. Bendotti by repeated backcrossing of SOD1^{G93A} C57BL/6JOlaHsd male mice with 129S2/SvHsd female mice, leading to heterozygote transgenic mice on the homogeneous 129Sv background. Mice showed a faster and more severe pathology compared to the G93A-SOD1 C57 transgenic line. They generally developed first signs of neuropathology at the MN level around 4 weeks of age, while the first symptoms of muscular dysfunction appeared around 14 weeks of age, with progressive reduction in the extension reflex of the hind limbs. At about 15 weeks of age mice showed a progressive muscular weakness, revealed by the increasing difficulty in staying on the rotating bar. At 18 weeks of age animals presented hind limbs complete paralysis and could not recover if laid on one side (Pizzasegola 2009).

2.2 CypA knockout mice

To study the function of CypA *in vivo*, CypA wild-type (CypA+/+), heterozygous (CypA+/-) or knockout (CypA-/-) mice were analysed and compared to non-transgenic littermates. CypA knockout mice were identified with PCR on DNA tail biopsies.

CypA knockout mice 129S6/SvEvTac $Ppia^{tm1Lubn}/Ppia^{tm1Lbn}$ mice (Ppia is the gene for CypA) were obtained from Charles River Laboratories (France) and maintained on 129S6/SvEvTac background. CypA knockout mice were generated (Colgan 2000) in the laboratory of Dr J. Luban (Department of Microbiology and Department of Medicine, Columbia University College of Physicians and Surgeons, New York City, USA) and further characterised in the same laboratory (Colgan 2004 and 2005). Homologous recombination between a targeting vector containing the neomycin resistance (neo^r) gene controlled by the mPpia promoter and the endogenous allele results in the replacement of all but the last 60bp of CypA-coding sequences with a neomycin-resistance gene cassette (Colgan 2000). Genotype distribution from CypA+/- x CypA+/- backcrosses did not follow Mendel laws. Jackson Laboratories predicted a 25% to 15% reduction in CypA-/- frequency.

2.3 G93A-SOD1/CypA knockout double transgenic mice

To observe the involvement of CypA on ALS disease onset and progression, G93A-SOD1/CypA wild-type (CypA+/+), heterozygous (CypA+/-) or knockout (CypA-/-) were analysed and compared to non-transgenic littermates. G93A-SOD1/CypA knockout mice were identified with PCR on DNA tail biopsies. The experimental groups were derived from breeding $SOD1^{G93A}$ 129S2/SvHsd mice with 129S6/SvEvTac $Ppia^{tm1Lubn}/Ppia^{tm1Lbn}$ mice. First, G93A-SOD1 male mice wild-type for the CypA gene were backcrossed with female mice CypA+/- or CypA-/-. From this backcrossing male and female mice NTg or G93A-SOD1 carrying the wild-type gene for CypA or heterozygous for the deletion were obtained. The aim was to obtain the greatest number of male mice G93A-SOD1/CypA+/- and female mice NTg/CypA+/-. These animals were considered as the F1 progeny.

Male mice G93A-SOD1/CypA+/- F1 and female mice NTg/CypA+/- F1 were backcrossed obtaining all the genotypes used in the study. The progeny is defined as F2, and both male and female mice were used for further analyses.

2.4 Neuronal spinal primary cultures

Preparation of mouse astrocyte-neurons co-cultures was performed by Dr. Massimo Tortarolo and his co-workers in the laboratory of Dr. Caterina Bendotti, Molecular Neurobiology Laboratory, Mario Negri Institute, Milan.

Primary spinal neurons were prepared from 14 to 15 day old mouse embryos. SpC were isolated by dissection and the meninges were removed. SpC were then mechanically dissociated using a fire-polished glass Pasteur pipette in phosphate-buffered saline (Ca^{2+} and Mg^{2+}-free PBS 1X, Invitrogen) supplemented with 33mM glucose. The cell suspension was layered onto a 4% BSA cushion, centrifuged at 1000rpm for 10min, and cells from the pellet were resuspended in culture medium composed of Neurobasal medium (Invitrogen) supplemented with 10% inactivated horse serum, 16.5mM glucose,0.5mM L-glutamine, 10ng/ml BDNF, 5µM β-mercaptoethanol, 100µg/mL streptomycin and 60µg/mL penicillin, 5µg/ml gentamicine, 25µM L-glutamic acid and 2% B27 (all from Sigma). Cells were plated (one SpC/8 wells) in each well of 48-well Nunc multiwell plates that had been previously coated with a confluent monolayer of astrocytes, to support neuronal health and survival. Cells were cultured at 37°C in a humidified atmosphere of 95% air and 5% CO_2 and used after 5-6 days *in vitro*. A mixture of hormones and salts composed of 25µg/mL insulin, 100µg/mL transferrin, 60µM putrescine, 20nM progesterone and 30nM sodium selenate (all from Sigma) was added to the culture medium. Cells were fixed for immunocytochemistry experiments. Medium was removed, cells were washed with PBS 1X and 4% paraformaldehyde (Merk) solution in PBS 1X was added for 30 min. After three washes in PBS 1X slides were stored a 4°C.

3. SAMPLE PREPARATION

3.1 Cell pellet preparation

Confluent cells were scraped from the flask (well) in an adequate volume of ice-cold collection buffer (10mM Tris-HCl pH 7.4; 250mM sucrose) keeping the plate on ice, and the suspension was centrifuged at 1000rpm for 5min at 4°C in a 5702/R centrifuge, rotor A-4-38 (Eppendorf). The pellet was resuspended in 1ml of ice-cold collection buffer and put in a 1,5ml tube. This solution was then centrifuged at 3200rpm for 3,5min at 4°C in a 5424/R microcentrifuge, rotor FA-45-24-11 (Eppendorf). The cell pellet obtained was further processed or quickly stored at -20°C until use.

3.2 Total protein extraction

By gentle pipetting the cell pellet was resuspended in ice-cold lysis buffer (10mM Tris-HCl pH 7.5; 0.5% Zwittergent; 0.5% sodium deoxycholate; protease inhibitors cocktail [Roche; 1 tablet/10ml]). To disrupt the DNA complexes the sample was passed for approximately 10 passages through a 26-gauge needle of a 1,5ml syringe. The sample was further incubated with Benzonase Nuclease™ (375U for 500ul buffer) (Novagen) for 15 min at RT while shaking, then kept on ice.

3.3 Animal tissue protein extraction

Mouse SpC or brain tissues were stored at -80°C. When necessary the lumbar tract of the spinal cord was cut on a cryostat into ventral and dorsal horn sections. Samples were homogenized in 50mM Tris-HCl, pH 7.5; 2% (w/v) CHAPS (3-[(3-Cholamidopropyl) dimethylammonio]-1-propane sulfonate, Sigma); 37.5U benzonase (Merck, Darmstadt, Germany), supplemented with Protease Inhibitors (Sigma) using a potter in ice. Homogenates were centrifuged at 13000rpm and 4°C for 15min and supernatant proteins were stored at -20°C until quantification.

3.4 Subcellular fractionation

HEK293 cells expressing wild-type and mSOD1 were harvested and washed in ice-cold PBS1X. Cell pellets were resuspended in RIPA-A buffer (0.3% Triton-X-100; 50mM Tris-HCl pH 7.4; 1mM EDTA; protease inhibitors cocktail [Roche; 1 tablet/10ml]) and incubated at 4°C for 30-60 min with slow tilt rotation. Cell extracts were centrifuged to pellet nuclei at 12000g and 4°C for 10min. The supernatant, that is the cytoplasmic fraction, was saved, while the nuclei pellet was washed with RIPA-A buffer and centrifuged at 12000g and 4°C for 10min. Supernatant was discarded and the nuclei pellet was resuspended in RIPA-B buffer (1% Triton X-100; 1% SDS; 50mM Tris-HCl pH 7.4; 500mM NaCl; 1mM EDTA; protease inhibitors cocktail [Roche; 1 tablet/10ml]). DNA complexes contained in this fraction were disrupted using an insulin syringe and further incubating with Benzonase Nuclease for 15 min at RT.

In order to validate each subcellular fractionation experiment, the immunoreactivity for actin was used as a specific cytosolic marker to exclude cytoplasmatic contamination of the nuclei preparation, whereas lamin A/C (an intermediate filament protein, component of the nuclear envelope) and stat1 (a transcription factor) were used as nuclear markers.

3.5 Aggregated proteins extraction

Extraction of detergent-insoluble proteins was performed on the lumbar tract of the SpC splitted into dorsal and ventral horn sections. Only the MNs enriched fraction was considered for this analysis. Detergent concentration was optimized in this experimental setting.

Tissues were manually homogenized using a potter in ice in 10 volumes (w/v) of ice-cold homogenization buffer 1 (15mM Tris-HCl pH 7.6; 1mM DTT; 0.25M sucrose; 1mM $MgCl_2$; 0.25M Na_3VO_4; 25mM NaF; 2mM NaPP; 1mM EGTA; 2.5mM EDTA; 5µM MG132; protease inhibitors cocktail [Roche; 1 tablet/10ml]). Samples were centrifuged at 10000rpm and 4°C for 15min. Supernatant (S1) was collected in a new tube. The pellet was resuspended in 100µl ice-cold buffer 2 (15mM Tris-HCl pH 7.6; 1mM DTT; 0.25M sucrose; 1mM $MgCl_2$; 0.25M Na_3VO_4; 25mM NaF; 2mM NaPP; 1mM EGTA; 2.5mM EDTA; 5µM MG132; 2% Triton X-100; 150mM KCl; protease

inhibitors cocktail [Roche; 1 tablet/10ml]). Samples were sonicated for three times for 10sec and shaken for 1hour at 4°C. Samples were centrifuged at 10000rpm and 4°C for 15min, obtaining the triton-resistant pellet. Supernatant (S2) was collected in a new tube. The pellet was washed for three times in 150µl ice-cold buffer 1 and centrifuged at 10000rpm and 4°C for 10min. The pellet was resuspended in 50µl UTC buffer (7M urea; 2M thiourea; 4% CHAPS) and sonicated for 10sec in ice. Samples were centrifuged at RT and 1000rpm for 10min and the supernatant was saved as the TIF (Triton X-100-insoluble fraction). Proteins from the TIF were quantified using the Bradford assay. One third of the volume of S1 and S2 were pooled to obtain the soluble fraction. Proteins from the soluble fraction were quantified using the BCA assay. Samples were frozen at -80°C until further analyses.

3.6 Protein quantification

3.6.1 BCA assay

Proteins extracted from animal tissues or cultured cells were quantified using the bicinchoninic acid assay (Protein assay Reagent Kit BCA, Pierce Biotechnology, Rockford, Illinois). This is a colourimetric method based on the biuretic reaction, i.e. the reduction of Cu^{2+} to Cu^{1+} by proteins. 25µl of cellular lysate diluted 1:10, 1:20, 1:40 in H_2O were pipetted into a 96-wells microplate in duplicate. A fresh set of protein standards was prepared by serially diluting bovine serum albumin (BSA) stock solution (2mg/ml). 200µl of reaction mix, prepared by mixing 50 parts of BCA reagent A with 1 part of BCA reagent B, was subsequently added to each well and incubated for 30min at 37°C in the dark. The absorbance of the solution was read at 575nm wavelength using Infinite® 200 multimode reader (Tecan).

3.6.2 Bradford assay

Quantification of protein samples extracted from the Triton X-100-insoluble fraction (TIF) or from the IP fraction was performed with a modified Bradford method (Bio-Rad Protein Assay). The

assay is based on the observation that the absorbance maximum for an acidic solution of Coomassie brilliant blue G-250 shifts from 465nm to 595nm when binding to protein occurs. Both hydrophobic and ionic interactions stabilize the anionic form of the dye, causing a visible colour change. The dye reagent reacts primarily with arginine residues and less with histidine, lysine, tyrosine, tryptophan and phenylalanine residues.

10µl of cellular lysate diluted 1:5, 1:10, 1:20 in H_2O were pipetted into a 96-wells microplate in duplicate. A fresh set of protein standards was prepared by serially diluting BSA stock solution (2mg/ml). 200µl of reaction mix, prepared by mixing 1 part of Bradford solution with 4 parts of H_2O, was added to each well and incubated for 10min at RT in the dark. The absorbance of the solution was read at 595nm wavelength using Infinite® 200 multimode reader (Tecan).

4. PROTEIN IMMUNOPRECIPITATION (IP)

Magnetic beads with coupled sheep polyclonal antibodies anti-Mouse IgG (Dynabeads® M280 sheep a-rabbit) or anti-Rabbit IgG (Dynabeads® M280 sheep a-mouse; Invitrogen) and a magnet (Dynal®; Invitrogen) were used to perform co-immunoprecipitation experiments. All the procedure, including starting sample preparation and dilution, washing buffers composition, primary antibody and dynabeads (DB) concentration, antibody cross-linking and IP complexes elution, were optimized for WB or 2-DE and MS analyses.

4.1 IP for 1-DE analysis

Cells were collected and lysed as previously described using ice-cold IP buffer (50mM Tris-HCl pH 7.4; 2% CHAPS; protease inhibitors cocktail [Roche; 1 tablet/10ml]). Alternatively, when IP was performed in the cytosolic and nuclear fractions, the nuclei pellet was directly resuspended in ice-cold IP buffer. When confirmatory experiments were performed on animal tissues, samples were homogenized as previously described using ice-cold IP buffer. Protein concentration was

determined by the BCA protein assay (Pierce). Protein extracts equivalent to 500µg of proteins were diluted to 0.5µg/µl using IP buffer and this corresponds to the INPUT fraction.

DB were washed with 0.1% BSA (Ig-free, Sigma) in PBS1X to remove preservatives. Approximately 0.1-1 µg Ig/10^7 beads were incubated at 4°C for at least 2hours with the primary antibody (AbI). DB were washed with 0.1% BSA in PBS1X to remove the excess of AbI unbound to the secondary antibody (AbII) coupled to the DB. The immunoglobulin chains were chemically cross-linked by 30min incubation with 20mM dimethyl pimelimidate dihydrochloride (Sigma) in 0,2M triethanolamine pH 8.2. The reaction was stopped by 15min incubation with 50mM Tris-HCl pH 7.5. DB cross-linked to the AbI were washed with 0.1% BSA in PBS1X and resuspended in 0.5% BSA in PBS1X. In the meantime protein lysates were pre-cleared by incubation at 4°C for at least 2hours with the same amount of magnetic beads alone, in order to reduce aspecific binding.

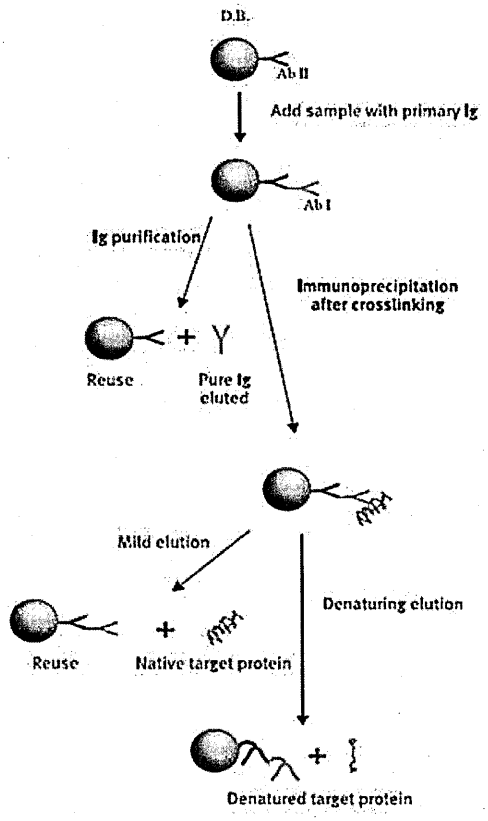

Figure 25 Schematic representation of the immunoprecipitation procedure used in this study.
The sheep anti-rabbit or anti-mouse Ig covalently bound to the surface of the beads recognized defined antigens through a rabbit or mouse specific primary antibody. The target molecule and its interactors were eluted off the beads simply boiling the sample and denaturing it using Laemmli sample buffer.

After beads removal, the cleared lysate was collected and incubated overnight at 4°C with Abl coupled to DB. The complexes of immunoprecipitated proteins (IP fraction) were separated from the supernatant (collected as the OUTPUT fraction) and washed with 50mM Tris-HCl pH 7.2 + 0.3% CHAPS + 0.1% BSA and with 50mM Tris-HCl pH 7.2 + 0.3% CHAPS. The immunoprecipitated proteins were separated from the beads and eluted using Laemmli sample buffer (without DTT). Proteins from the OUTPUT fraction were quantified using the BCA assay. Protein samples from the IP fraction were boiled for 10min and briefly spun. Samples were frozen at -20°C until further analyses. Samples from the IP, as well as the INPUT and OUTPUT fractions were subjected to SDS-PAGE separation and WB analyses to examine for specific immunoreactivity.

4.2 IP for 2-DE analysis

Samples were lysed as previously described and IP was performed starting from 4.5mg of proteins and a quantitatively proportional amount of Abl and DB. After IP, proteins from the IP fraction were eluted in 50mM Tris-HCl pH 6.8 + 2% SDS + 100mM DTT and quantified using the Bradford assay. Proteins were precipitated in methanol/chloroform and resuspended in Destreak™ Rehydration Solution (GE Healthcare) added with 0,5% (v/v) IPG buffer (non linear ampholine pI 3-10; GE Healthcare). The solution was shacked for 2hours at RT and spun. Samples were loaded by in-gel rehydration on immobilized pH gradient (IPG) 3-10 non-linear 7cm strips and run in a IPG-phor apparatus (GE Healthcare). Strips were then re-equilibrated in NuPAGE LDS sample buffer (Invitrogen) and incubated with DTT and IAA for 15 min. Single gel strips were mounted on 10% or 12% polyacrylamide pre-cast gels (Invitrogen) and second dimension was run. Gels were fixed and stained with Sypro® Ruby protein gel stain (Invitrogen) for MS analyses or transferred to PVDF membranes for WB studies.

5. SDS-POLYACRYLAMIDE GEL ELECTROPHORESIS (SDS-PAGE)

Equal amounts of proteins, prepared as previously described, were diluted in Laemmli sample buffer (2% SDS; 10% glycerol; 0.002% bromophenol blue; 100mM Tris-HCl pH 6.8; 100mM DTT) and denatured by heating for 10min at 95°C and briefly spun in a microcentrifuge. Samples were loaded in wells at the top of 12% SDS-PAGE (sodium dodecyl sulphate-polyacrylamide) gels , made up of a stacking gel (4% polyacrylamide; SDS; Tris-HCl pH 6,8; ammonium persulfate; TEMED) and a running gel (12% polyacrylamide; SDS; Tris-HCl pH 8,8; ammonium persulfate; TEMED). Proteins moved into the gel when the electric field was applied: 15mA in the stacking gel to allow a correct alignment of the proteins; then proteins were run at 30mA for approximately 1hour in the running gel. The electrophoretic separation was performed in a Mini-PROTEAN® electrophoresis cell (Biorad) in running buffer (3g/L Tris; 0,1% SDS; 14,44g/L glycine).

6. SLOT/DOT BLOTTING

For dot/slot-blot analyses, aliquots of 2-5µg of proteins for each sample were diluted in equal volumes of TBS1X (20mM Tris-HCl pH 7.4; 150mM NaCl) and loaded in duplicate on 0.45µm nitrocellulose Trans-Blot Transfer Medium membrane (BioRad), by vacuum deposition on the Bio-Dot SF blotting apparatus (BioRad). Membranes were immunoblotted and immunoreactivity was normalized to the actual amount of proteins loaded on the membrane, as detected after ATX Ponceau S red (Fluka BioChemika) staining.

7. TWO DIMENSIONAL GEL ELECTROPHORESIS (2DE)

Proteins from cell lysates were prepared for 2DE analysis: 50-75µg of total proteins were precipitated using an excess volume of cold methanol. After an incubation of at least 4h at -80°C, protein samples were centrifuged at 13000rpm and 4°C for 30min. The protein pellet was

resuspended in Destreak™ Rehydration Solution (GE Healthcare) added with 0,5% (v/v) IPG buffer (non linear ampholine pI 3-10; GE Healthcare). Each sample was incubated at 22°C for 1h mixing, centrifuged at 13000rpm for 2min and loaded on IPG strip. Proteins were first separated by electrophoresis according to charge. Isoelectrofocousing (IEF) was carried out using gel strips forming an immobilized non-linear pH gradient from 3 to 10 (Immobiline™ DryStrip, pH 3-10 NL, 7 cm; GE Healthcare). IPG strips were positioned into a holder, covered with oil, and run into an IPG-phor apparatus (GE Healthcare). Strips were rehydrated for 10h at 30V, IEF was performed at 20°C with current limited to 50mA per strip (0.5h at 200V, 0.5h at 500V, 0.5h at 2000V, 1,5h of a linear gradient to 3500V, 2h at 3500V, 2,5h of a linear gradient to 8000V followed by 8000V for 4h, and forever at 30V). Proteins were then separated according to size. Prior to the second dimension, the gel strips were equilibrated for 15min in NuPage LDS Buffer (Invitrogen) containing 1% DTT (Sigma) and washed with mqH_2O; IPG strips were alkylated for 15min in the same buffer containing 2.5% iodoacetamide (Sigma) and washed again. For SDS-PAGE separation, equilibrated IPG strips were mounted on the top of a pre-cast 10% or 12% Bis-Tris-acrylamide gel (Invitrogen) and sealed with a 0.5% agarose solution. After agarose solidification, electrophoresis was performed at 200V for 1hour at RT using MOPS (Biorad) as running buffer. Up to six gels were run in parallel and for each condition analysed, 2D-gels were made in triplicate from independent protein extractions.

Gels for 2D-WB were transferred on PVDF membranes (Millipore), while gels for protein identification by MS were fixed overnight in 50% methanol and 7% acetic acid, visualised with Sypro Ruby Gel Staining (Invitrogen) and scanned with Molecular Imager FX Laser Scanner (excitation, 532 nm; BioRad).

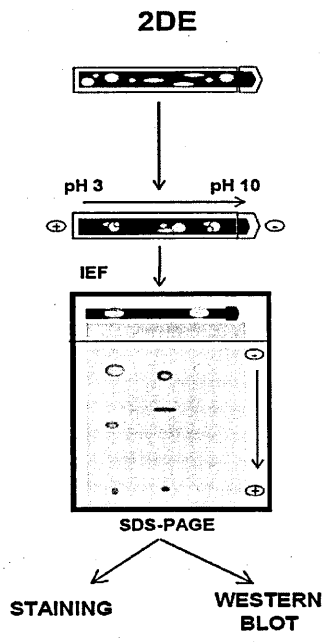

Figure 26 General 2DE workflow.

Proteins are first separated by their isoelectric point in the first dimension (IEF). The strip with the gel is then laid horizontally on a second gel in which the proteins are separated by SDS-PAGE. Thus, horizontal separation reflects differences in pI, while vertical separation reflects differences in molecular weight.

8. Gel/membrane staining

8.1 Sypro Ruby Staining

Sypro Ruby staining is a sensitive method to detect proteins in SDS-PAGE and 2-DE gels or membranes which does not interfere with MS protein identification (Nishihara 2002).

After electrophoresis, gels were fixed in 50% methanol and 7% acetic acid for 1h at room temperature, incubated with Sypro Ruby Gel Stain (Bio-Rad Laboratories) overnight and washed with 10% methanol and 7% acetic acid for 30min.

PVDF membranes for 2DE-WB were air-dried, fixed in 10% methanol and 7% acetic acid for 15min, washed in deionized water, stained with Sypro Ruby Blot Stain (Bio-Rad Laboratories) for 15min and washed in deionized water.

Total proteins, in gels or transferred onto membranes, were visualised by scanning using the Molecular Imager FX Laser Scanner (excitation, 532nm; Bio-Rad Laboratories), with the same parameters for all the gels/membranes in the analysis.

8.2 Red Ponceau S staining

Ponceau staining is a reversible negative stain for the detection of the positively charged amino groups of proteins. It also binds non-covalently to non-polar regions in the protein. Membranes were incubated for 10min with Ponceau S (Sigma), briefly washed with deionized water and images were acquired with Epson Expression 1680 Pro scanner (Epson, Suwa, Japan).

9. WESTERN BLOTTING

Proteins separated by electrophoresis on polyacrylamide gels were transferred to a polyvinylidene fluoride membrane (PVDF Immobilion FL; Millipore) previously activated in methanol for 30sec, applying a constant current of 250mA to a Mini Trans-blot® (Biorad) apparatus for 2h or alternatively overnight at 85mA in transfer buffer (5,52g/L CAPS pH 11; 10% MeOH). To check for protein loading and transfer, membranes were incubated with ATX Ponceau S red staining solution and scanned for later analysis.

Membranes with separated proteins were rinsed in TBST (20mM Tris-HCl pH7.5; 150mM NaCl; 0,1% Tween 20) to remove Ponceau-S stain and were blocked for 60min at RT in a 3% BSA (Sigma) or 5% non-fat dry milk-based solution diluted in TBST before incubation with primary antibody. Membranes were probed for 1h at RT or overnight at 4°C with a primary antibody, according to the manufacturer's protocol, followed by incubation for 60min at RT with a peroxidase-conjugated secondary antibody diluted 1:5000. Each antibody was diluted in blocking solution and after incubation membranes were washed in TBST to remove unbound antibody. When anti-mouse or anti-rabbit or anti-goat peroxidase-conjugated secondary antibodies (Santa Cruz Biotechnology) were used, blots were developed with Immobilon Western Chemiluminescent HRP

Substrate (Millipore) on the Chemi-Doc XRS System (BioRad). This system uses horse radish peroxidase (HRP)-conjugated secondary antibodies for luminol-based detection. The oxidation of luminol by the HRP is then detected by exposure to Chemi-Doc XRS System (Biorad) at a wavelength of 428nm. When Qdot800 or Qdot655 goat anti-mouse or anti-rabbit IgG-conjugated secondary antibodies (Molecular Probes, Invitrogen) were used, blots were scanned with Molecular Imager FX Laser Scanner (BioRad). WB signals and the corresponding red ponceau stained blots were digitalized and densitometry was determined using the Progenesis PG240 Software (Non Linear Dynamics Ltd). For a correct quantification, the measured immunoreactivity was normalized on the total amount of proteins loaded on the gel (detected with Ponceau staining).

Primary antibodies were obtained from the following companies: polyclonal rabbit anti-**SOD1** (1:2000; Upstate), monoclonal mouse anti-**Nitro tyrosine** (1:1000; Hycult Biotechnology), polyclonal rabbit anti-**Nitro actin** (1:7500), polyclonal rabbit anti-**Cyclophilin A** (1:2500; Upstate), monoclonal mouse anti-**Myc tag** (1:1000; OriGene), polyclonal goat anti-**Actin** (1:2000; Santa Cruz Biotechnology), monoclonal mouse anti-**STAT1 p84/p91** (1:200; Santa Cruz Biotechnology), monoclonal mouse anti **Lamin A+C** (1:500; Chemicon); monoclonal mouse anti-**Cyclophilin A** (1:2000; Abcam); polyclonal rabbit anti-**TDP43** (1:4000; kindly provided by Baralle Francisco, ICGEB, Trieste); polyclonal rabbit anti-**TDP43** (1:2500; Protein Tech); polyclonal rabbit anti-**Myc tag** (1:30000; Bethyl laboratories); monoclonal mouse anti-**Flag tag** (1:10000; Sigma); monoclonal rabbit anti-**Flag tag** (1:2000; Sigma); monoclonal mouse anti-**hnRNP A2/B1** (1:2000; Abnova); monoclonal mouse anti-**TDP43** (1:1000; Abnova); monoclonal mouse anti-**phS409/410 TDP43** (1:2000; Cosmo Bio Co.,Ltd.); monoclonal anti-**Ubiquitin** (1:800; DAKO); polyclonal rabbit anti-**HDAC6** (1:500; Santa Cruz); monoclonal mouse anti-**Tubulin** (1:1000; Sigma); monoclonal mouse anti-**Acetyl-tubulin** (1:35000; Sigma); polyclonal rabbit anti-**HSP90** (1:1000); monoclonal mouse anti-**HSC70** (1:1000; Santa Cruz); monoclonal mouse anti-**DNP** (1:15000; Sigma); polyclonal rabbit anti-**PDI** (1:1000; StressMarq Biosciences Inc.).

10. IDENTIFICATION OF PROTEINS BY MASS SPECTROMETRY

The protein spots of interest were located and excised from 2D-gels with the EXQuest spot cutter (Bio-Rad). Spots were de-stained for 2h in a solution containing 25mM ammonium bicarbonate + 40% ethanol, and then washed with a sequentially increasing percentage of acetonitrile (0-50-100%). Protein spots were processed manually or in a protein digestor, DigestPRO MS (Intavis). Proteins were in gel-digested overnight at 37°C with 10ng/µl of modified trypsin from bovine pancreas (Roche) in 25mM ammonium bicarbonate + 10% acetonitrile.

Peptide mass fingerprinting and MS/MS analysis were done on a 4800 MALDI-TOF/TOF mass spectrometer (Applied Biosystem, Carlsbad, CA, USA) using α-cyano-4-hydroxycinnamic acid (Bruker Daltons, Billerica, MA, USA) matrix. Stock solution of matrix was prepared as saturated solution in 50% acetonitrile and 0.1% trifluoracetic acid (Sigma) and diluted 1:1 with the same solution before mixing with the samples. Tryptic digested peptides were desalted and concentrated using ZipTip® pipette tips with C18 resin and 0.2µl bed volume (Millipore) and MALDI target deposition were carried out on an automated protein digestor DigestPro (Intavis AG, Koeln, Germany). Tryptic digests were mixed with matrix solution 2:1 to be deposited on the target. The mass spectra were internally calibrated with trypsin autolysis fragments.

The five most abundant precursor ions, of the exclusion mass list (ions from human keratin and trypsin), were selected for MS/MS analysis. The combined MS and MS/MS data were submitted by the GPS Explorer v.3.6 software (Applied Biosystems) to the MASCOT database search engine (Version 2.1, Matrix Science, http://www.matrixscience.com) and searched with the following parameters: Swissprot 56.5 database over all *Homo sapiens* protein sequences deposited, no fixed modifications, as possible modifications carboamidomethylation of cysteine and oxidation of methionine, one missed trypsin cleavage, a mass tolerance of ±0.1Da for the peptide mass values and of ±0.3Da for the MS/MS fragment ion mass values. Swiss-Prot is a high quality protein database with non-redundant and non-identical sequences allowing specific matches for an

MS/MS search. A protein was regarded as identified if the MASCOT protein score, based on combined MS and MS/MS data, was above the 5% significance threshold for the database (Pappin 1993), probability-based MOWSE scores greater than 51 were considered significant ($p<0.05$).

11. IMMUNOFLUORESCENCE

11.1 Primary cell cultures

Primary cells plated in 48-wells plate, as described in section **2.4**, were fixed in 4% paraformaldehyde for 30 min and washed with PBS 1X, incubated 1h in blocking solution (10% NGS (Vector) + 0.2% Triton X-100 (Fluka) in PBS 1X) at RT, followed by overnight incubation at 4°C with primary antibodies (monoclonal anti-CypA, Abcam, 1:500; polyclonal anti-TDP-43, Protein Tech, 1:300; monoclonal anti-Smi-32, Covance, Princeton, NJ, USA, 1:3000) diluted in blocking solution. After washing with PBS 1X, cells were incubated for 1h at RT with the appropriate secondary antibody conjugated to a fluorophore, generally Alexa Fluor®594 or 488 anti-mouse or rabbit (Invitrogen), prepared in blocking solution. The secondary antibody used for Smi-32 was an anti-mouse biotinylated antibody (Vector) diluted 1:500 in blocking solution for 1h at RT, followed by Tyramide signal amplification using the TSA™ system (Perkin-Elmer) as described in section **11.1.1**. Alternatively Alexa Fluor®647 anti-mouse (Invitrogen) diluted 1:500 in blocking solution was used for 1h at RT. Three washes in PBS 1X ended the protocol.

To visualise nuclei after the immunocytochemical procedure, wells were incubated for 10min at RT with DAPI (Sigma; 20 mg/mL) diluted 1:500 in PBS 1X or Hoechst (pentahydrate (bis-benzimide); Invitrogen; 10 mg/mL) diluted 1:1000 in PBS 1X, then washed in PBS 1X. Slides were finally blocked with Fluorsave (Millipore).

11.1.1 Tyramide signal amplification

After biotinylated secondary antibody, samples were incubated for 150min in Blocking Reagent (Perkin Elmer proprietary formulation) and 30min in Streptavidin conjugated to horseradish peroxidase diluted 1:300 in blocking reagent. They were then washed in TNT (0.04% Tween in 0.1M Tris/HCl pH 7.6) and finally, the reaction was developed by incubation for 8min in Tyramide (Perkin Elmer proprietary formulation) diluted 1:500 in Amplification Diluent (0.003% H_2O_2 in 0.1M Borate pH 8.5). Samples were then washed in PBS 1X.

11.2 Immortalized cell cultures

HEK293 cells were plated on round glass coverslips in 24 or 48-well plates and grown to 50% confluence. Cells were washed with PBS1X and fixed with 4% paraformaldehyde for 1hour at RT. After washing with PBS1X, cells were permeabilized, to ensure free access of the antibody to its antigen, and blocked for non-specific binding using a blocking-permebilization solution (10% normal goat serum + 0.2% Triton-X-100 in PBS1X). Cells were incubated overnight at 4°C with primary antibody: polyclonal rabbit anti-CypA (1:500; Upstate); monoclonal mouse anti-CypA (1:500; Abcam); polyclonal rabbit anti-TDP43 (1:500; kindly provided by Baralle Francisco, ICGEB, Trieste); polyclonal mouse anti-TDP43 (1:250; Abnova); rabbit anti-Myc (1:2000; Bethyl laboratories); monoclonal mouse anti-Myc (1:200; Origene); monoclonal rabbit anti-FLAG (1:250; Sigma); monoclonal mouse anti-FLAG (1:2000; Sigma); monoclonal mouse anti-hnRNP A2/B1 (1:200; Abnova); monoclonal mouse anti Smi-32 (1:3000; Covance). Cells were washed in PBS1X and incubated with fluorochrome-conjugated secondary antibodies (Alexa Fluor®; Invitrogen) diluted 1:500 in blocking solution for 1hour at RT. Finally, cells were washed 3 times with PBS1X and counterstained with DAPI (Sigma; 20 mg/mL) or Hoechst (Invitrogen; 10 mg/mL) diluted 1:1000 in PBS 1X for 10min.

Coverslips were mounted on the slides using Gel/Mount (Biomedia) and allowed to dry. Appropriate negative controls without the primary antibodies were performed. None of the immunofluorescence reactions revealed unspecific fluorescent signal in the negative controls.

Confocal microscopy was performed on a Olympus FluoView™ FV1000 microscope, equipped with 3 laser lines: Ar-Kr (488 nm), He-Ne red (646 nm), and He-Ne green (532 nm) (Olympus, Tokyo, Japan) and a UV diode. The lens used for the analysis were the 20X and the 40X. Three-dimensional images were acquired over a 6-10µm z-axis with a 0.3µm step size and processed using Volocity® software (PerkinElmer Inc., USA).

12. SITE-DIRECTED MUTAGENESIS

To produce single aa substitutions in the wild-type sequence a site-directed mutagenesis approach was used. In particular, a overlap PCR approach was used that employs oligonucleotides containing the desired altered portion of the gene's nucleotide sequence as primers in a first round of PCR. The products of the first round are then used as primers for a second round of PCR, whose product corresponds to the cDNA coding for the mutant protein. The sequence obtained is then inserted into an expression vector so that the redesigned protein can be produced in cells.

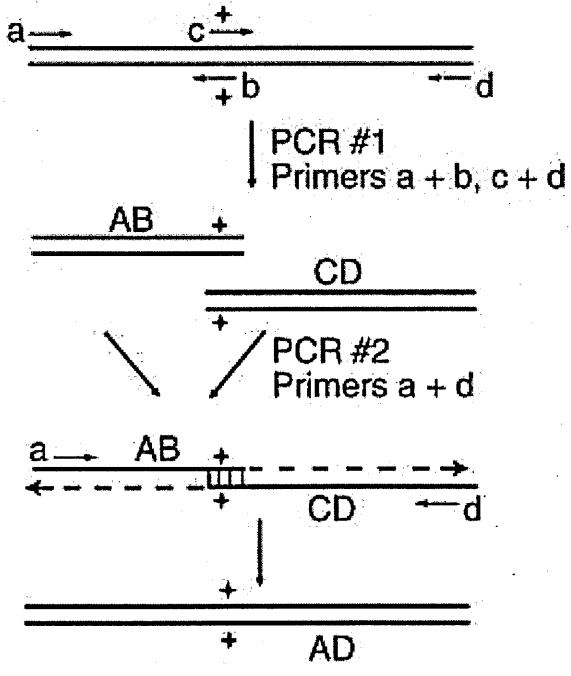

Figure 27 Schematic representation of the overlap PCR technique.

This site-directed mutagenesis approach has been used to obtain the cDNAs coding for CypA and TDP-43 mutants. (a) and (d) are the external primers while (b) and (c) are the internal "mutagenic" primers carrying inside their sequence the mutation we want to generate.

As shown in **Figure 27**, the first PCR products (AB and CD) were obtained combining the external sense primer with the respective internal antisense primer, and vice versa. Once obtained these PCR fragments, they were used as new primers in the second PCR, and a single fragment (AD) was generated. This was then inserted in the vector of interest.

12.1 Cyclophilin A mutagenesis

The cDNA encoding human wild-type CypA was cloned into the sites Sgf I and Mlu I of the pCMV6-AC-Myc vector (Origene), so that the construct carries wild-type human CypA with a Myc-Tag epitope at its C-terminus. This pCMV6-AC-CypA-Myc vector was purchased from Origene (**Figure 28**) and was used in site-directed mutagenesis experiments and to transiently transfect cells.

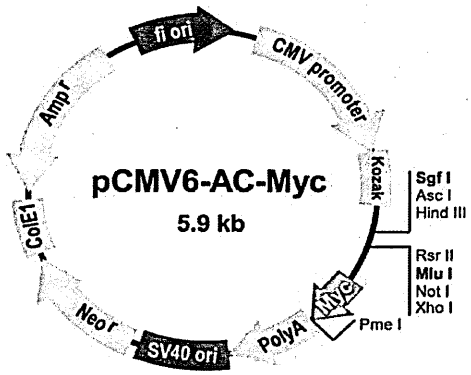

Figure 28 Schematic representation of pCMV6-AC-Myc (Origene) plasmid.
The construct was cloned with the cDNA for Homo Sapiens Peptidyl-prolyl Isomerase A (PPIA), corresponding to the protein Cyclophilin A, into restriction sites Sgf I and Mlu I. This vector encodes for wild-type CypA fused with the Myc-tag at the C-terminus.

The PPIase-deficient mutant of CypA was generated mutagenizing the arginine in position 55 into an alanine(Arg-55-Ala or R55A) (Zydowsky 1992), corresponding to the substitution: AGA → GCA. CypA is known to be post-translationally modified: in particular Lysine 125 was reported to be acetylated in mammals (Kim 2006). To study the influence of this PTM on CypA functions, lysine in position 125 was mutated into a glutamine (Lys-125-Gln or K125Q) or an arginine (Lys-125-Arg or K125R), corresponding respectively to the substitutions AAG → CAG and AAG → AGG. These

mutant forms of CypA were characterised by non-modifiable amino acids in this crucial position, with glutamine and arginine mimicking a stably acetylated or not-acetylated form of the protein.

To insert specific mutations in wild-type cDNA, different overlap PCRs were performed. For each overlap PCR two *ad hoc* mutagenic oligonucleotidic sequences were synthesized while the oligonucleotides used as external primers were the same.

The following criteria were followed to design the primers:

- the length of the annealing region to the cDNA was chosen to have a melting temperature (T_m) of approximately 55°C;
- the primers were designed to have one or more G/C at their 3' end, since it favours the correct annealing of the primers with the target;
- the internal primers were characterised by a melting temperature (T_m) similar to the external primers, since in the first step of the overlap PCR they should anneal with the target at approximately the same temperature.

The external primers used for CypA overlap PCR were:
5'-TCAACGGGACTTTCCAAAATGTCG-3' (sense primer) (a)
5'-TATTAGGACAAGGCTGGTGGGCAC-3' (antisense primer) (d)

The internal primers used to generate the R55A-CypA sequence were:
5'-TTTCACGCAATTATTCCAGGGTTTATG-3' (sense primer) (c)
5'-TGGAATAATTGCGTGAAAGCAGGAAC-3' (antisense primer) (b)

The internal primers used to generate the K125Q-CypA sequence were:
5'-GATGGCCAGCATGTGGTGTTTGGC-3' (sense primer) (c)
5'- CACATGCTGGCCATCCAACCACTC-3' (antisense primer) (b)

The internal primers used to generate the K125R-CypA sequence were:
5'-GATGGCAGGCATGTGGTGTTTGGC-3' (sense primer) (c)
5'- CACATGCCTGCCATCCAACCACTC-3' (antisense primer) (b)

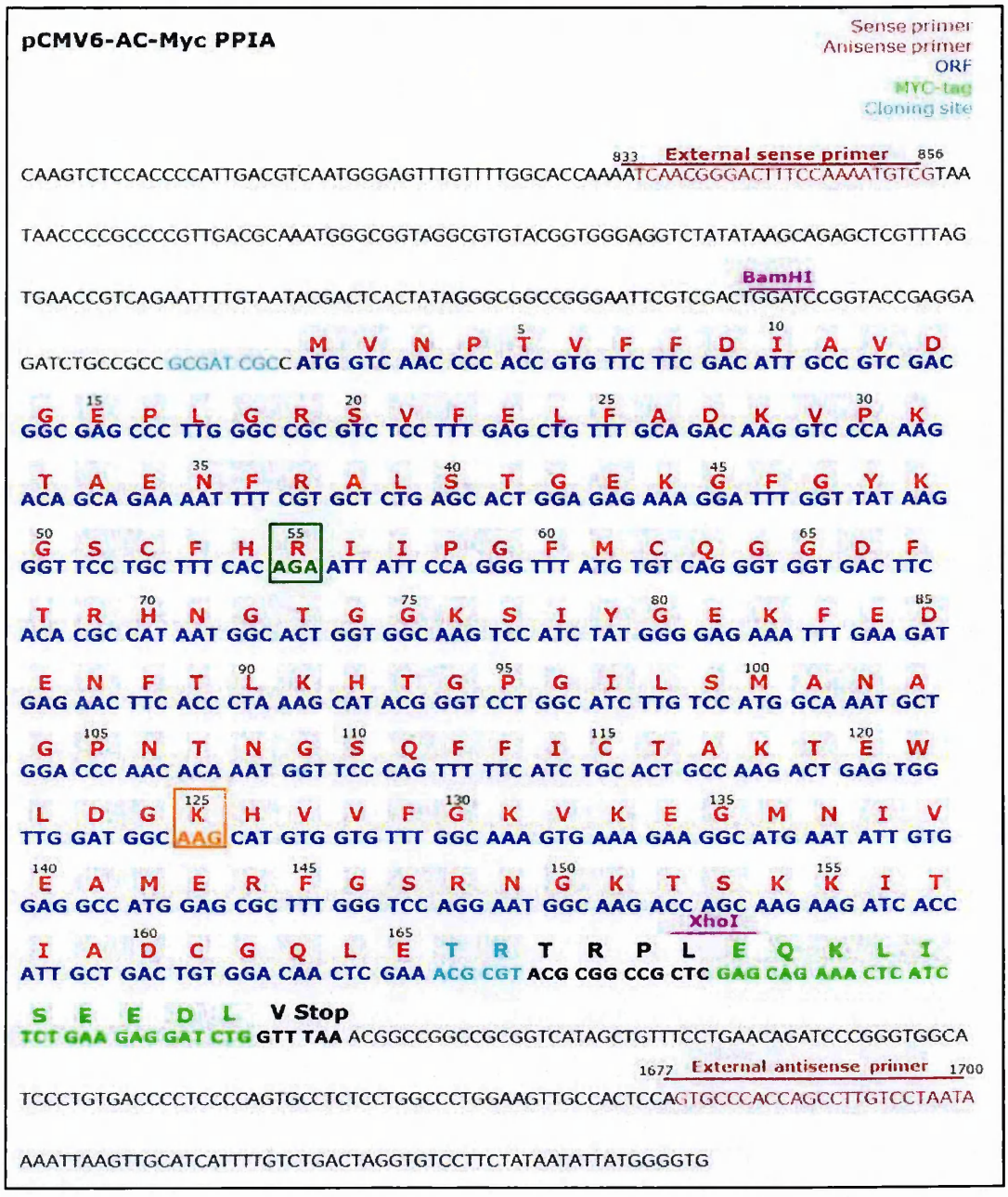

Figure 29 Schematic representation of human CypA cDNA sequence.

The ORF is in blue and it is inserted into the sites SgfI and MluI (cloning sites are in light blue) of the commercial plasmid pCMV6-Ac-Myc (Origene). Amino acids corresponding to each codon are in red, the sequence corresponding to the Myc-tag is in light green. Codons that have been mutagenized in this study are shown in green (AGA; arginine 55) and orange (AAG; lysine 125). The external primers used for the overlap PCR match with the red sequences bordering the cDNA of interest (FW: 833-856; RV:1677-1700). Restriction sites recognized by BamHI and XhoI, which correspond to the restriction enzymes used to digest the generated fragments, are highlighted in pink.

The first PCR (PCR #1) was performed using a thermal cycler (PTC-100; Mj Research) for 25 cycles at 95°C for 15sec, 50°C for 30sec, and 68°C for 60sec. 100ng of template (pCMV6-AC-CypA-Myc plasmid) were added to 50µl of reaction mixture containing 10% Accuprime™ Pfx reaction mix

(Promega), 0,3µM of each primer and 1U of Pfx DNA polymerase (Promega) possessing a proofreading 3' to 5' exonuclease activity. The calculated length of the amplified fragments was 379bp (AB) and 525bp (CD) for R55A-CypA; 307bp (AB) and 577bp (CD) for K125Q-CypA and for K125R-CypA.

A second PCR (PCR #2) was then performed for 5 cycles at 95°C for 15sec, 50°C for 60sec, and 68°C for 60sec. The PCR #1 products (AB and CD) (1µl of each fragment) were added to 50µl of reaction mixture containing 10% Accuprime™ Pfx reaction mix (Promega) and 1U of Pfx DNA polymerase (Promega). At the end of the first 5 cycles a mixture of external primers (0,6µM) was added and other 25 cycles of PCR were executed (95°C for 15sec, 50°C for 60sec, and 68°C for 60sec). The calculated length of the amplified fragments was 869bp (AD) for all the mutants. At the end of each PCR, as check over the experimental procedure, the obtained products were loaded on 1% low-melting agarose gels and the purity of the band was verified. In some cases, in order to further purify the correct PCR product, the Wizard® SV Gel and PCR Clean-up System (Promega) was used according to the procedures suggested by the manufacturer.

The purified PCR products were digested with an excess of BamHI (0,5µl; 20000U/ml) (New England Biolabs) and with an excess of XhoI (0,5µl; 20000U/ml) (New England Biolabs) for 6h at 37°C. Digested samples were separated onto a 1% low-melting agarose gel and purified using the Wizard mini-columns (Promega). 5µg of pCMV6-AC-CypA-Myc plasmid were digested with an excess of the same restriction enzymes used for the fragments: BamHI (1,5µl; 20000U/ml) and XhoI (1,5µl; 20000U/ml) for 6h at 37°C. The linearized plasmid was then dephosphorylated by further 15min incubation with 1U of TSAP (Thermosensitive Alkaline Phosphatase, Promega). The enzyme was then heat inactivated at 74°C for 15min. At the end linearized-dephosphorylated plasmid was isolated from 1% low-melting agarose gel with the Wizard mini-columns (Promega). For the ligation reaction 100ng of linearized-dephosphorylated pCMV6-AC-CypA-Myc vector DNA (≈6Kb) and 16,6ng of each insert DNA (550bp; R55A, K125Q, K125R) were incubated with 6U of bacteriophage T4 DNA ligase (Promega) in 2X rapid ligation buffer and nuclease free water (Ligafast™ Rapid DNA Ligation System). The reaction was performed for 5min at RT.

10ng and 25ng of the ligation mixture were used to transform 50µl of MAX efficiency DH5α competent cells (Invitrogen) according to the protocol suggested by the kit. As negative control 10ng of linearized-dephosphorylated pCMV6-AC-CypA-Myc vector DNA (not ligated with the insert) were added to the bacteria. Each transformation mixture was then spread on Luria Broth agar (Sigma) plates with 100µg/ml ampicillin (Roche) and grown at 37°C overnight. 4 colonies selected for ampicillin resistance were isolated from each plate using a sterile pipette tip and were used to inoculate 4ml of Luria Broth (Sigma) containing 100µg/ml ampicillin. After 10 hours bacteria from 2ml of culture were harvested by centrifugation at 10000g for 5min in a microcentrifuge. After pouring off the supernatant, plasmid DNA was isolated from cell pellet using the Wizard Plus SV Minipreps DNA Purification System (Promega). 1/10 of the total DNA sample (100 µl) was digested with 0,3µl of the same restriction enzymes used before (BamHI and XhoI) in a final volume of 10µl for 6h at 37°C, to release insert DNA from the plasmid. To screen for the presence of the insert, 5µl of digestion product were loaded in 1% agarose gel. The colonies were chosen based on the presence of the insert and the absence of abnormal products of digestion after restriction analysis. To confirm the presence of the mutation, cDNAs were sequenced by Primm srl (Milan, Italy) using 500ng of plasmid and 1µM of primers mix. The primers used for the sequencing were the following: 5'-GGACTTTCCAAAATGTCG-3' (sense) and 5'-ATTAGGACAAGGCTGGTGGG-3' (antisense) spanning respectively nucleotides 838-856 and 1680-1699 of the pCMV6-AC-CypA-Myc plasmid.

One third of the starting liquid culture corresponding to the correct construct, was transferred to -80°C for long-term storage in a solution containing 15% sterile glycerol, while two thirds of the same bacterial culture were used to inoculate 250ml of fresh selective LB medium and grown overnight at 37°C with vigorous shaking. Plasmid DNA was then purified from the bacterial culture using a NucleoBond® Xtra Maxi Plus kit (Machery-Nagel) according to the protocol suggested by the manufacturer. Plasmid DNA was resuspended in ultrapure water and Nanodrop® ND1000 spectrophotometer (Thermo Scientific) was used to quantify the amount of DNA and evaluate the

presence of contaminants. The vectors obtained were then used to transfect HEK293 cells, in order to check for the exogenous proteins expression.

12.2 TDP-43 mutagenesis

The cDNA coding for human wild-type TDP-43 cloned between the HindIII and BamHI sites of pFLAG-CMV2 (Sigma) was kindly provided from Prof. Baralle F (ICGEB, Trieste) (Ayala 2008). This construct, carrying Flag-tagged N-terminal TDP-43, was used for transfection and site-directed mutagenesis experiments. To investigate the mechanism by which TDP-43 mutations lead to neurodegeneration in ALS, the constructs containing the A315T or R361S or Y374X mutations were generated. The procedure applied was the same previously described for CypA mutagenesis.

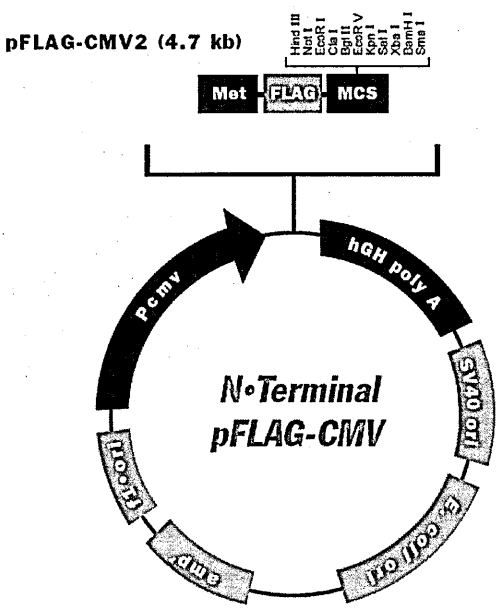

Figure 30 Schematic representation of the pFLAG-CMV2 (Sigma) plasmid.
This vector, carrying the cDNA coding for wild-type TDP-43 fused with the Flag-tag at the N-terminus, was used for transfection and site-directed mutagenesis experiments.

The external primers used for overlap PCR were:

5'- GTAATAACCCCGCCCCGTTGACG-3' (sense primer) (a)

5'- GGAGATTGCAGTGAGCCAAGATTGTGCC-3' (antisense primer) (d)

The internal primers used to generate the A315T-TDP-43 sequence were:

5'- ACTTTGGTACGTTCAGCATTAATCCAGC-3' (sense primer) (c)

5'-ATGCTGAACGTACCAAAGTTCATCCCACC-3' (antisense primer) (b)

The internal primers used to generate the Y374X-TDP-43 sequence were:

5'- ATAACTCTTAAAGTGGCTCTAATTCTGG-3' (sense primer) (c)

5'-GAGCCACTTTAAGAGTTATTTCCAGAACC-3' (antisense primer) (b)

The internal primers used to generate the R361S-TDP-43 sequence were:

5'-ACATGCAGAGCGAGCCAAACCAGGCCTTCG-3' (sense primer) (c)

5'-TTTGGCTCGCTCTGCATGTTGCCTTGG-3' (antisense primer) (b)

IV. RESULTS

1. HEK293 WT and G93A cell lines

ALS is a neurodegenerative disease that can be inherited directly in approximately 10% of affected families (Siddique 1996). SOD1, the gene coding for the enzyme copper-zinc superoxide dismutase, was first linked to ALS and known mutations in its sequence account for about 20% of fALS cases (Rosen 1993). To investigate the molecular mechanisms activated in ALS pathogenesis we decided to generate an *in vitro* model of the disease by the expression of mutant SOD1. For this purpose, the Human Embryonic Kidney 293 (HEK293) cell line was chosen for its ease of handling as well as the wealth of available tools and information (Graham 1977).

1.1 In vitro ALS model generation

HEK293 cells were stably transfected with the empty vector (VEC) or the vector containing wild-type (WT-hSOD1) or mutant (G93A-hSOD1) human SOD1. For each cell line individual clones were isolated, grown and tested for the expression of hSOD1 protein by Western blotting (WB) or dot/slot blotting (**Figure 1.1A-B**). Single clones over-expressing comparable levels of WT or G93A-SOD1 were selected for this study. In particular, their immunoreactivity was two times higher than the endogenous protein in VEC cells, as measured by densitometry analysis through the Progenesis PG240® (Nonlinear Dynamics, Ltd.) software (**Figure 1.1C**).

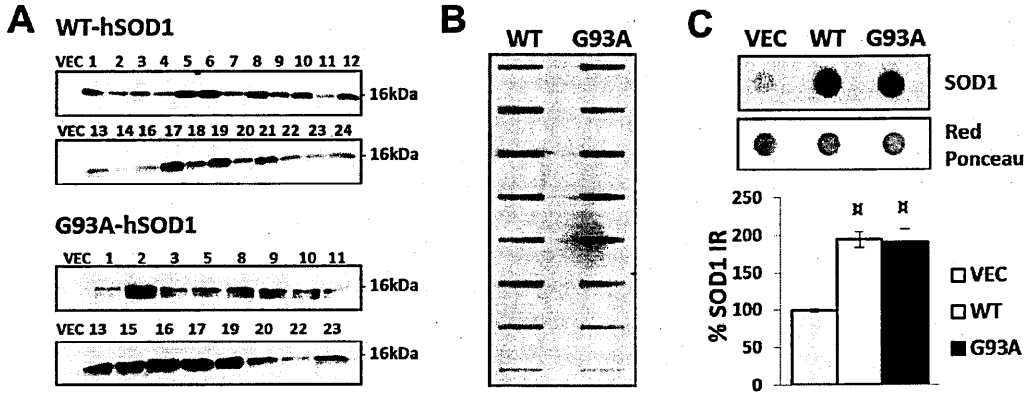

Figure 1.1 Western blot, slot blot and dot blot analyses for SOD1.

(**A**) The expression of hSOD1 after stable transfection of HEK293 cells with empty vector (VEC), wild-type (WT) or mutant (G93A)-hSOD1 was first tested by WB for SOD1 to select individual clones with

similar protein levels. (**B**) These were then tested by slot blotting for SOD1 and further selected. (**C**) Representative dot blot for SOD1 on selected cellular clones and corresponding histogram obtained by spot densities quantification normalized on the actual amount of protein loaded, as measured by Red Ponceau staining. Data (mean ± S.E., n≥3) are expressed as percentages of immunoreactivity (IR) of control cells (VEC). Symbols indicate that samples are significantly different (¤=p≤0.001 VEC vs WT or G93A), as assessed by Student's t-test.

1.2 *In vitro* ALS model characterization

1.2.1 Cell viability evaluation

In order to characterise this *in vitro* model of fALS, the effect of the mutant protein on cell viability was evaluated using the MTT (3-(4,5-dimethylthiazol-2-yl)-2,5-diphenyltetrazolium bromide) assay (see Materials and Methods section 1.4). The simple overexpression of WT-SOD1 did not affect the survival of HEK293 cells compared to the VEC cell line. Indeed a significant toxic effect of the mutant protein (G93A) on cell survival was observed already under basal conditions (UNT) (**Figure 1.2**). Cell-vulnerability was then investigated after serum withdrawal (STARV), in order to exacerbate the death-inducing effect of the mutant protein. In fact, serum withdrawal induces oxidative stress, with the generation of free radical species in the cell. All cell lines were susceptible to serum deprivation stress with an increased effect on G93A-hSOD1 expressing cells compared to both WT and VEC cells.

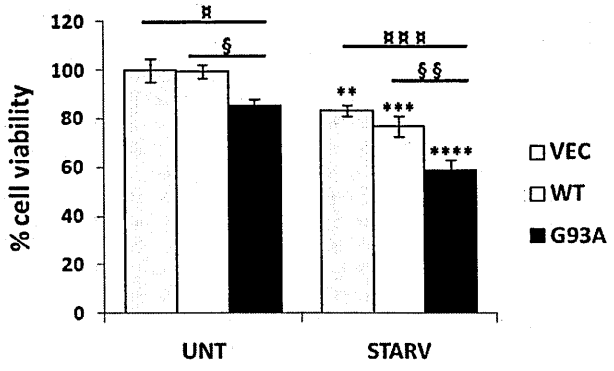

Figure 1.2 Effect of SOD1 overexpression on cell viability.

Histograms represent the effect of the empty vector (grey), WT-SOD1 (white) or G93A-SOD1 (black) overexpression on HEK293 cell survival, evaluated in basal condition (UNT) or after serum

withdrawal (STARV). The conversion of MTT to formazan was used as an index of cell viability. Data (mean ± S.E., n≥4 for each sample) are expressed as percentages of control cells (UNT VEC). Symbols indicate that samples are significantly different (*=p≤0.05 UNT vs. STARV; ¤=p≤0.05 VEC vs. WT or G93A; §= p≤0.05 WT vs. G93A), as assessed by two-way ANOVA test followed by Bonferroni multiple comparisons post-test.

1.2.2 Markers of nitrative stress

To further characterise the *in vitro* model, we next considered molecular markers that have been previously associated with ALS in *in vitro* and *in vivo* animal models and in patients. First, markers of nitrative and oxidative stress were evaluated, since they are characteristic signs of a pathological process. Increased levels of free and protein-bound 3-nitrotyrosine (3-NT) in the central nervous system (CNS) are considered a marker of oxidative stress for different neurodegenerative diseases (Pacher 2007), and increased levels of free 3-NT have been found in the cerebrospinal fluid (CSF) and serum of patients with ALS and in the CNS of fALS mice (Abe 1997; Beal 1997; Bruijn 1997; Ferrante 1997). Recently, in our lab, some 3-NT-modified proteins have been identified in the spinal cord of fALS mice (Casoni 2005; Basso 2009) and in peripheral blood mononuclear cells (PBMC) from sALS patients and a rat model of ALS (Nardo 2009 and 2011). Immunostaining for 3-NT was performed in our *in vitro* model (**Figure 1.3A**), revealing a substantially increased level of protein nitration in mutant cells if compared to WT cells, already under basal conditions (UNT). No significant difference in 3-NT levels was detected after serum withdrawal.

Moreover, an antibody developed in-house was used to evaluate the level of a NT-linked protein: actin^{NT}. The anti-actin^{NT} antibody recognizes a band at 42kDa, which is the expected molecular weight for actin^{NT}, but also other bands at higher molecular weight (MW), that are probably polymerized actin forms. The high MW species were essentially detected only in PBMC lysates from sALS patients, making the antibody especially useful to distinguish ALS patients from controls (Nardo 2011). The immunoreactivity pattern of this antibody against lysates from WT and G93A-SOD1 over-expressing cells was analysed (**Figure 1.3B**). Under basal conditions, in WT and

mutant cells a staining pattern similar to control and ALS patients respectively was observed. Quantitative analysis of the WB revealed a statistically significant difference between WT and mutant cells. In both cell lines there was a significant further increase after serum withdrawal, and it was still possible to appreciate a statistically significant difference between WT and G93A-SOD1 over-expressing cells. Collectively, these data are indicative of the presence of nitrative and oxidative stress in this *in vitro* fALS model. This is in line with the observation that mutant SOD1 has an increased ability to catalyse aberrant oxidative reactions, including protein nitration (Beckman 1993; Estévez 1999).

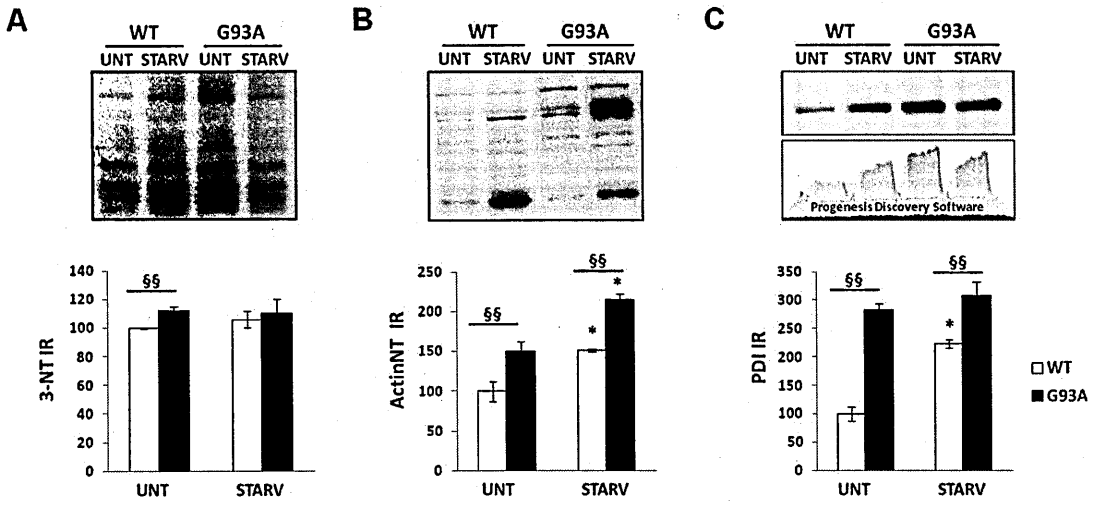

Figure 1.3 Markers of nitrative and ER-stress in WT- and G93A-SOD1 HEK293 cells.

Representative WB for (**A**) total 3-nitrotyrosine (3-NT), (**B**) nitrated actin (actin^{NT}) and (**C**) Protein-Disulfide Isomerase (PDI) from WT-SOD1 and G93A-SOD1 cells, under basal conditions (UNT) or after serum withdrawal (STARV). 15µg of total protein lysates were loaded, run on SDS-PAGE gels, transferred on PVDF membrane, stained with Red Ponceau as loading control, incubated with primary and secondary antibodies and detected by chemiluminescence. Histograms represent the quantification of total immunoreactivity normalized to the actual amount of protein loaded. Data (mean ± S.E., n≥3) are expressed as percentages of control cells (UNT WT). Symbols indicate that samples are significantly different (*=p≤0.05 UNT vs. STARV; §= p≤0.05 WT vs. G93A), as assessed by Student's t-test.

1.2.3 Markers of ER-stress

Subsequently, the expression level of the Protein-Disulfide Isomerase (PDI) was considered. PDI is an endoplasmic reticulum (ER) chaperone that catalyzes the formation and rearrangement of

intra- and inter-molecule disulfide bonds. An increase in its levels is a typical cellular response to ER-stress that triggers the unfolded protein response, leading eventually to cell death (Kim 2008). Studies in SpC tissues (Atkin 2008) and PBMC of sALS patients (Nardo 2011) showed that PDI was up-regulated with the disease. Its alteration is considered a hallmark of disease also in animal models and motor-neuron-like cellular models of fALS (Atkin 2006; Massignan 2007). Interestingly, quantitative analysis of PDI WB showed a significant up-regulation in mutant cells if compared with WT cells, already under basal conditions (**Figure 1.3C**). Increased amounts of PDI were also observed in both cell lines after serum deprivation.

In summary, the protein profile changes detected demonstrated that G93A-SOD1 stably expressed in HEK293 cells is toxic and confers these cells important characteristic features of fALS, such as nitrative, oxidative and ER-stress, that makes these cells a valid *in vitro* model to analyse the molecular events induced by SOD1 mutation.

1.3 Cyclophilin A analysis

CypA has been validated as a translational early biomarker of ALS in PBMC (Nardo 2011). In particular, CypA expression was increased in sALS patients compared to healthy controls, and was altered in a G93A-hSOD1 rat model of ALS before disease onset. CypA also contributed to discriminate between patients with high- and low-severity disease, and to distinguish ALS from other neurological disorders. Furthermore, CypA was demonstrated to be accumulated in the detergent-insoluble fraction isolated from spinal cord tissue of sALS patients (Basso 2009). Therefore, the biochemical properties of CypA were investigated in selected HEK293 SOD1-overexpressing clones.

1.3.1 CypA expression level

First, CypA total level was evaluated in cell lysates from WT and mSOD1 expressing cells by WB and slot blotting, and the ratio between CypA immunoreactivity and Red Ponceau signals was

quantified. The result from this analysis did not reveal any statistically significant difference (**Figure 1.4**). This result is in agreement with the one obtained in the spinal cord of the G93A-SOD1 mouse model at an early presymptomatic stage of the disease, where the expression level, as detected by standard WB, did not change in respect to WT animals (Massignan 2007). However, when cells were serum-deprived, CypA protein level was increased in both cell lines, with a statistically significant difference between mutant and WT cells.

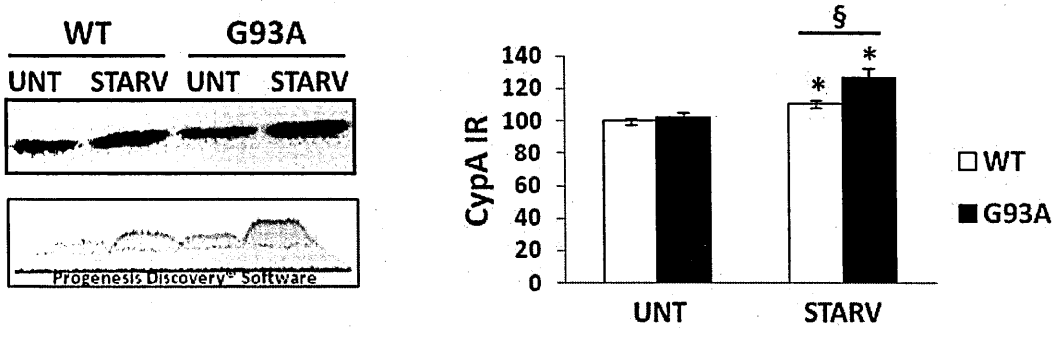

Figure 1.4 CypA expression level in WT- and G93A-SOD1 HEK293 cells.

Representative WB and 3D rendering for CypA from WT-SOD1 and G93A-SOD1 cells, under basal conditions or after serum withdrawal. 15µg of total protein lysates were loaded, run on SDS-PAGE gels, transferred on PVDF membrane, stained with Red Ponceau as loading control, blotted for CypA and detected by chemiluminescence. The histogram represents quantification of total immunoreactivity normalized to the actual amount of protein loaded. Data (mean ± S.E., n≥3) are expressed as percentages of control cells (UNT WT). Symbols indicate that samples are significantly different (*=p≤0.05 UNT vs. STARV; §= p≤0.05 WT vs. G93A), as assessed by Student's t-test.

1.3.2 CypA isoform pattern

Next, our attention was focused on the analysis of CypA behaviour by two-dimensional gel electrophoresis (2DE)-WB. From previous studies in our laboratory CypA was already demonstrated to be post-translationally modified, indeed four CypA positive isoforms could be detected by WB and MS in mouse spinal cord tissue (Massignan 2007). Protein extracts from WT and mutant HEK293 cells were separated on 2DE-gels and blotted. The membranes were probed with anti-CypA antibody and CypA appeared as a train of at least four spots at the same MW in the isoelectric point (pI) range 6.5-7.5 (**Figure 1.5**). Immunoreactivity for all CypA isoforms was

measured and a variation in its isoform pattern was detected under basal conditions. In particular, isoform four almost disappeared in mutant cells with a shift towards the acidic forms of the protein, mainly isoform three, which is the N-terminally acetylated one. A similar isoform pattern change, a shift toward acidic pI, has been observed also in sporadic ALS patients (unpublished data from the laboratory) and in fALS mice (Massignan 2007).

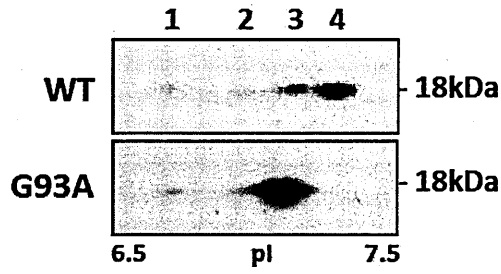

Figure 1.5 CypA isoform pattern in WT- and G93A-SOD1 HEK293 cells.

2DE blot for CypA from WT-SOD1 and G93A-SOD1 cells under basal conditions. 75µg of total protein lysates were separated by IEF, run on SDS-PAGE gels, transferred to PVDF membranes, stained with Sypro® Ruby Protein Blot stain as loading control, blotted for CypA and detected by chemiluminescence. The 2DE-WB was repeated several times with consistent results and representative images are shown here.

Mutant SOD1 expression produced an altered pattern of CypA isoforms, pointing out a variation in the post-translational modifications (PTM) profile, under basal conditions. PTM are likely to be key-features for protein versatility. Since CypA can have different activities in different cellular compartments, it is fundamental to associate CypA functions, localisation and interactors with specific PTM.

1.3.3 CypA subcellular distribution

To have insights into CypA subcellular distribution, a protocol for the biochemical fractionation of HEK293 cells was set up. In particular, the cytoplasmic and the nuclear fractions were isolated from HEK293 cells stably expressing WT- or G93A-SOD1, as described in the Materials and Methods section. WB analyses for lamin A+C (nuclear envelope markers) and actin (a cytoplasmic

marker) were performed in order to assess if the fractionation between the nuclear and the cytosolic compartments was effective (**Figure 1.6**).

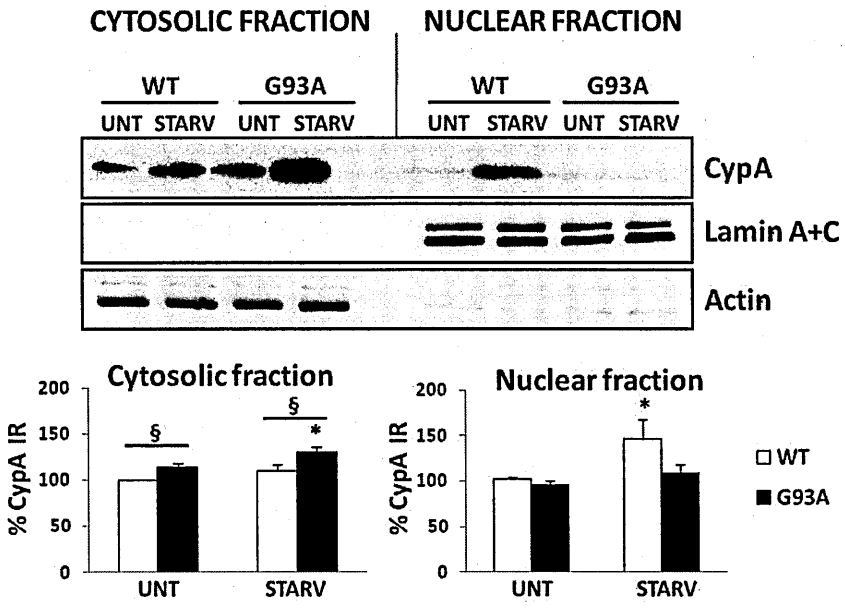

Figure 1.6 CypA subcellular distribution in WT- and G93A-SOD1 HEK293 cells.

Representative WB for CypA, lamin A+C and actin from WT- and G93A-SOD1 cells, in basal condition or after serum withdrawal. 15µg of cytosolic and corresponding nuclear protein fractions were loaded, run on SDS-PAGE gels, transferred to PVDF membranes, stained with Red Ponceau as a loading control, blotted and detected by chemiluminescence. Histograms represent the quantification of total immunoreactivity normalized to the actual amount of protein loaded. Data (mean ± S.E., n≥3) are expressed as percentages of control cells (UNT WT) in the respective fraction. Symbols indicate that samples are significantly different (*=p≤0.05 UNT vs. STARV; §= p≤0.05 WT vs. G93A), as assessed by Student's t-test.

CypA subcellular localisation was evaluated in WT and mutant cells under basal conditions and after serum withdrawal, replicating the conditions used to assess cell viability and CypA total expression level. In the cytosolic fraction the level of CypA was higher in mutant cells than in WT cells. This difference was exacerbated after starvation. In the nuclear fraction no differences were detectable between WT and mutant cells when untreated. However, after starvation CypA had a completely different behaviour: in WT cells the CypA expression level was increased greatly, while no significant alteration was observed in mutant cells. These results indicate that WT cells react to

a toxic stimulus by up-regulating CypA in the cytosol and especially in the nucleus. This feature is lost in mutant cells, where there is an increase only in CypA cytosolic levels.

To investigate further the alterations in CypA distribution, immunofluorescence (IF) staining for CypA was performed by confocal microscopy. In particular, images from HEK293 cells stably expressing WT or mutant SOD1 were acquired; DAPI staining was used to visualise the nuclei (**Figure 1.7**). In WT-SOD1 expressing cells CypA was widely distributed in the cell and its localisation in the nuclei was clear. Mutant cells showed a diffuse signal for CypA that seemed shifted from the nuclei towards the cytosol with a spot-like staining (as shown in the inset). After starvation it was possible to observe an overall increased staining for CypA in WT cells (mainly in the nuclei), which became higher in G93A cells (data not shown). The protein distribution observed by IF was in agreement with the results previously obtained by WB and biochemical fractionation.

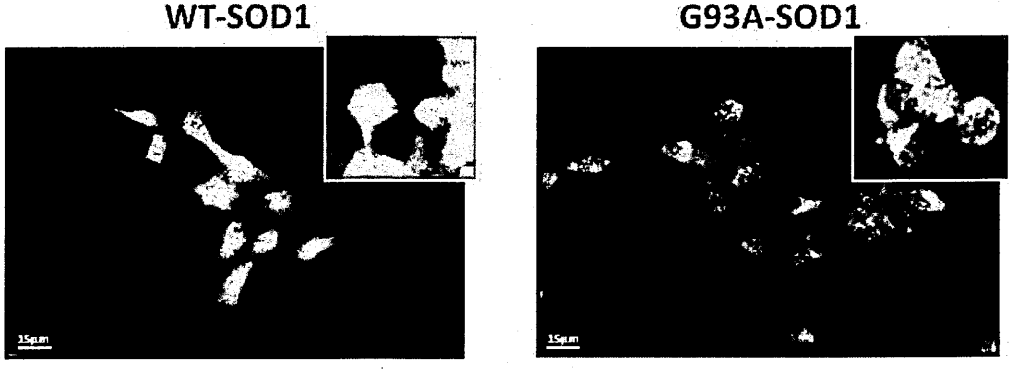

Figure 1.7 CypA immunofluorescence confocal analysis in WT- and G93A-SOD1 HEK293 cells.

WT- and G93A-SOD1 cells were stained for CypA using Alexa®488 (green) (bar: 15µm). Nuclei were counter-stained with DAPI (blue). Insets show images at higher magnification. Immunofluorescence images shown represent consistent results obtained in multiple replicates.

Collectively, these data demonstrated that in this *in vitro* model G93A-hSOD1 overexpression, even though not evidently altering CypA total level, was sufficient to alter the CypA isoform pattern, mirroring the trend observed in sALS patients and fALS murine models (Nardo,

unpublished data from the lab; Massignan 2007), and this should be directly correlated to the shift observed in its subcellular localisation and possibly PTM profile.

1.4 Cyclophilin A lysine-acetylation

CypA displays a complex pattern of maturation and PTM. Starting from the results obtained by 2DE-WB analysis of CypA in WT and mutant cells, a deeper investigation of CypA PTM was performed, and in particular lysine-acetylation was explored in the *in vitro* model. In fact, this PTM has been described in human CypA and eight potential N6-acetyllysine sites were proposed on amino acids 28, 31, 44, 49, 76, 82, 125, 131 (Kim 2006; Choudhary 2009; Chevalier 2012).

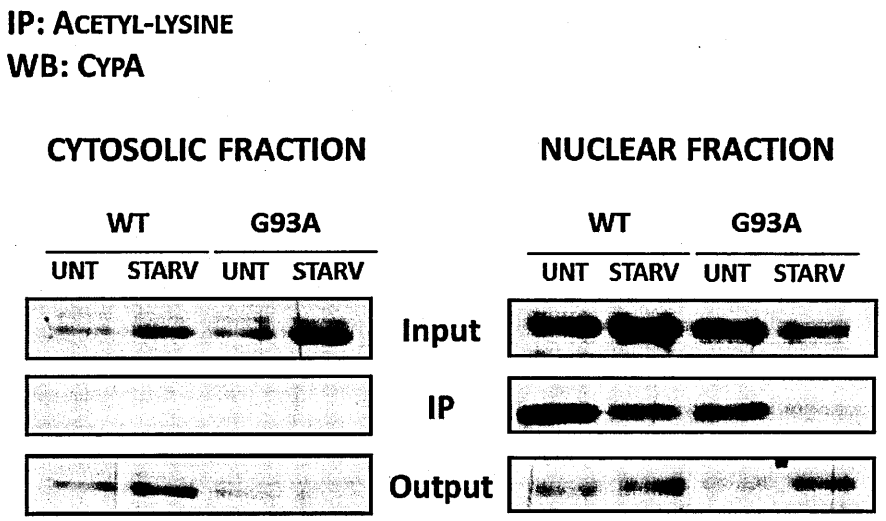

Figure 1.8 CypA is lysine-acetylated in the nucleus and its regulation is associated with stress response.

Equal amounts of proteins (500µg) were independently co-precipitated with the anti-Acetyl-lysine antibody from the cytosolic and the corresponding nuclear fractions of HEK293 cells stably expressing WT- or G93A-SOD1 under basal conditions or after serum withdrawal. Aliquots of the cytosolic and nuclear lysates (INPUT), of the immunoprecipitates (IP), of the proteins from the remaining fraction (OUTPUT) were loaded together, subjected to SDS-PAGE, transferred to PVDF membranes, stained with Red Ponceau as loading control, blotted for CypA and revealed through chemiluminescence. Representative WB are shown.

WT and mutant cells were collected under basal conditions or after serum withdrawal and the cytosol/nuclei extraction was performed as previously described. An antibody raised against a mixture of chemically acetylated antigens was used to specifically immunoprecipitate (IP) acetylated lysine (AcK)-containing proteins. CypA was detected by subsequent immunoblot analysis (**Figure 1.8**). The trend observed in the input fraction was the same reported previously in biochemical fractionation experiments. This experiment was replicated with a clear result: CypA was co-IP with the anti-AcK antibody only in the nuclear and not in the cytosolic fraction. Furthermore, from this experiment it was possible to infer that not all the nuclear protein was acetylated at lysine. In fact, an up-regulation of CypA expression in the nuclei after starvation, as observed in the input fraction, did not correspond to an increase of the protein in the IP fraction, that is lysine-acetylated CypA. Indeed a reduction in CypA lysine-acetylation was shown after starvation, both in WT and mutant cells.

These data demonstrate that CypA is acetylated at lysine exclusively in the nucleus with an altered pattern in mutant cells and in stress conditions, suggesting that the fine regulation of CypA lysine-acetylation and de-acetylation could play a role in the stress response.

1.5 Cyclophilin A knockdown

In order to directly observe the effects of the loss of CypA function in WT and mutant cells RNA interference technology has been used. CypA silencing experiments were performed in HEK293 cells delivering specific $siRNA^{CypA}$ or, as a negative control for knockdown, a scrambled siRNA that did not lead to the degradation of any aspecific cellular message. Several siRNA molecules targeting different regions on CypA locus, both coding and untranslated regions, were transiently transfected using a cationic lipid-mediated transfection system. RNA silencing experimental conditions were optimized to obtain a reduction in CypA protein expression of up to 95% (**Figure 1.9A**). In all experiments performed, CypA knockdown was always verified analysing the protein expression level by Western or dot blotting (**Figure 1.9B**).

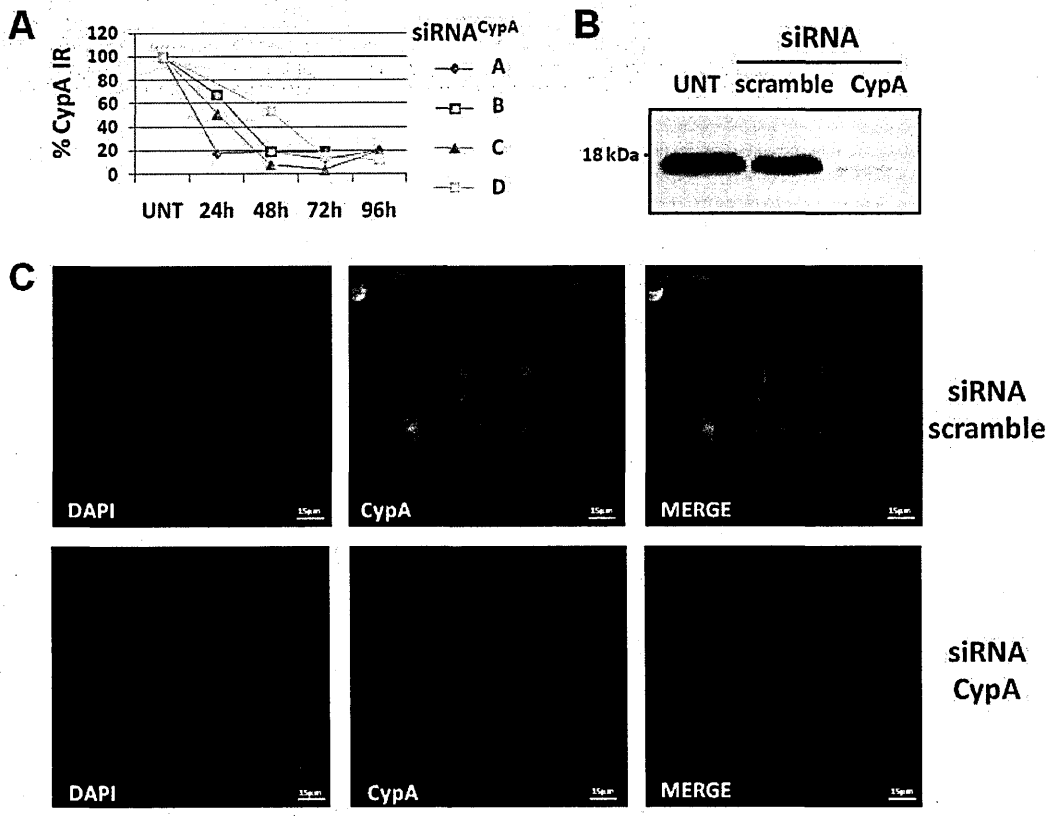

Figure 1.9 CypA knockdown in HEK293 cells.

HEK293 cells were untreated, or transfected with $siRNA^{scramble}$ or $siRNA^{CypA}$. (**A**) The graph represents the quantification of CypA expression level by slot blotting, normalized to the amount of protein loaded as detected by Red Ponceau staining, using different $siRNA^{CypA}$ at different time points. (**B**) Representative WB for CypA in cells treated with the selected $siRNA^{CypA}$. (**C**) Representative immunofluorescence images of HEK293 cells stained for CypA (red) after silencing (bar: 15μm). Nuclei were stained with DAPI (blue).

To further confirm CypA silencing, immunofluorescence (IF) staining for CypA was performed and cells were counter-stained with DAPI to visualise the nuclei. In scrambled siRNA transfected cells the protein was homogenously expressed, both in the nuclei and in the cytosol, with a marked staining also in cellular protrusions (**Figure 1.9C**). In cells treated with $siRNA^{CypA}$ the extent of CypA silencing was clear also by IF, confirming the results obtained by WB.

1.6 Myc-tagged CypA overexpression

To further investigate CypA function, a plasmid carrying the human CypA coding sequence was purchased from OriGene and sequenced to confirm the sequence. In order to specifically detect

the exogenous protein and to distinguish the transfected protein from endogenous CypA, the sequence was fused with a Myc-tag epitope at the C-terminal end. Transfection was optimized to obtain the highest expression level in cells.

1.6.1 Myc-CypA expression level

To verify the correct expression of the exogenous Myc-tagged CypA protein, HEK293 cells were transiently transfected with either an empty vector or with the vector expressing Myc-CypA. Cells were lysed and the expression of both endogenous and exogenous CypA was tested by WB analyses, using an antibody against CypA or alternatively an antibody against the Myc-tag (**Figure 1.10A1-2**). The tagged protein was clearly detectable only in Myc-CypA transfected cells, and not in cells transfected with the empty vector and could be easily distinguished also using the anti-CypA antibody. A good expression level of the transfected protein was measured (comparable to endogenous CypA) thus indicating that HEK293 were efficiently transfected and effectively expressed the exogenous protein. The Myc-tag adds 18 aas to the original protein, which explains the increased molecular weight. In fact, the observed MW coincided with the predicted MW, computed through the proteomic server Expasy (www.expasy.org) at the Swiss Institute of Bioinformatics.

1.6.2 Myc-CypA isoform pattern

Once verified Myc-CypA expression, it was checked if the exogenous protein could undergo the same post-translational modifications as the endogenous CypA protein when transiently transfected in HEK293 cells. To do that, cell lysates were subjected to 2DE separation, followed by WB for CypA or the Myc-tag. Using the anti-Myc-tag antibody, four protein spots were clearly detected. When a polyclonal antibody against CypA was used, eight major spots were distinguished and corresponded to four isoforms of the endogenous protein and, four isoforms at

higher MW, of the exogenous tagged protein, positive for both CypA and Myc-tag antibodies (**Figure 1.10B1-2**).

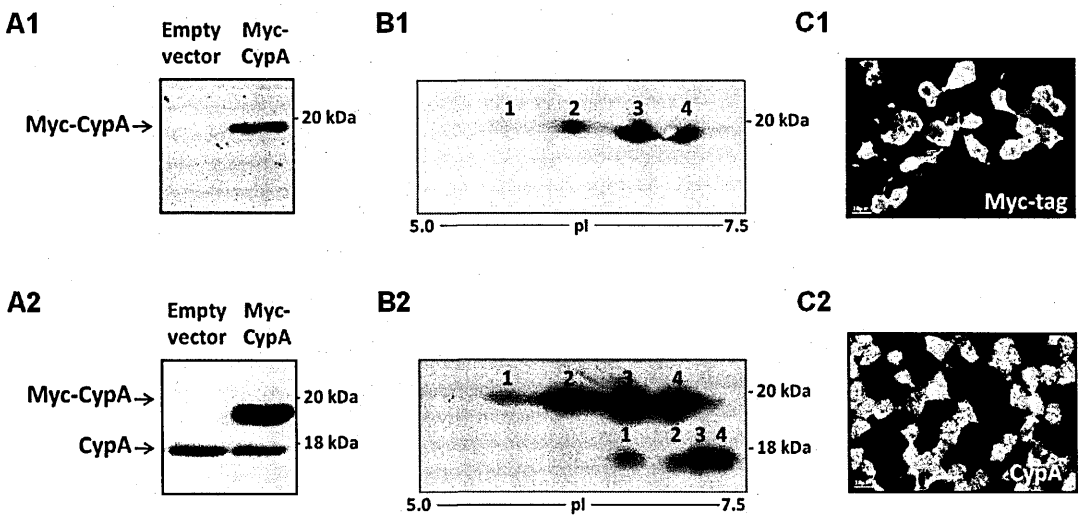

Figure 1.10 Myc-CypA expression in HEK293 cells.

HEK293 cells were transiently transfected with the empty vector or the vector cloned with Myc-CypA. (**A**) 15 µg of total protein lysates were loaded, run on 12% SDS-PAGE gels, transferred to a PVDF membrane, stained with Red Ponceau as loading control, analysed by WB using the anti-Myc-tag (**1**) or the anti-CypA (**2**) antibodies and detected by chemiluminescence. (**B**) 75µg of total protein lysates from Myc-CypA transfected cells were separated by IEF, run on 12% SDS-PAGE gel, transferred on a PVDF membrane, stained with Sypro Ruby Blot® stain as loading control, analyzed by WB using the anti-Myc-tag (**1**) or the anti-CypA (**2**) antibodies and detected by chemiluminescence. Representative 2DE blots are shown. (**C**) Representative immunofluorescence images of HEK293 cells stained for Myc-tag (**1**) or CypA (**2**) after Myc-CypA transfection (bar: 10µm). Nuclei were stained with DAPI (blue). Experiments were repeated several times with consistent results and representative images were chosen for display.

The isoform patterns observed were similar for endogenous CypA and Myc-CypA, suggesting that they were prone to be post-translationally modified in a similar way. Apart from the molecular weight, the only difference between the two proteins was the isoelectric point (pI): the endogenous unmodified CypA has a predicted pI of 7.68, whereas the computed pI of Myc-CypA was 6.90, as evidenced by a shift in the gel towards a more acidic pI. So, the values calculated through the Expasy proteomic server perfectly fitted with the experimental observations. By

comparison with data previously obtained in the laboratory (Massignan 2007), it was possible to deduce that isoforms one and three were the N-terminally acetylated ones, while isoforms two and four were the non N-terminally acetylated ones. The shift towards more acidic pI of isoforms one and two can be due to the presence of a combination of post-translational modifications (PTMs), such as phosphorylation, Lys-acetylation and methylation (Chevalier 2012).

1.6.3 Myc-CypA localisation

The expression of the exogenous tagged protein was also verified by immunofluorescence using confocal microscopy. HEK293 cells transfected with the empty vector were used as controls. CypA immunostaining in these cells revealed a homogeneous localisation of the endogenous protein, as previously shown, while, as expected, no signal was detectable using the Myc-tag antibody. HEK293 cells transfected with the Myc-CypA vector were clearly recognizable with both stains. In particular using the CypA antibody, overexpressing cells were distinguishable from non-transfected cells because of a more intense immunostaining, whereas using the Myc-tag antibody, only cells overexpressing CypA were selectively stained (**Figure 1.10C1-2**). Moreover, the Myc-tag staining revealed that the exogenous protein retained the same cellular localisation of the endogenous one and showed a good expression of the plasmid, denoting a transfection efficiency greater than 50%.

1.6.4 Cell viability evaluation after CypA overexpression

In order to determine whether overexpression of CypA in this *in vitro* model of ALS could have a protective or a toxic effect, cell viability was assessed by MTT assay in three independent experiments. An increase in CypA protein level had no statistically significant effects on cell survival rate (**Figure 1.11**).

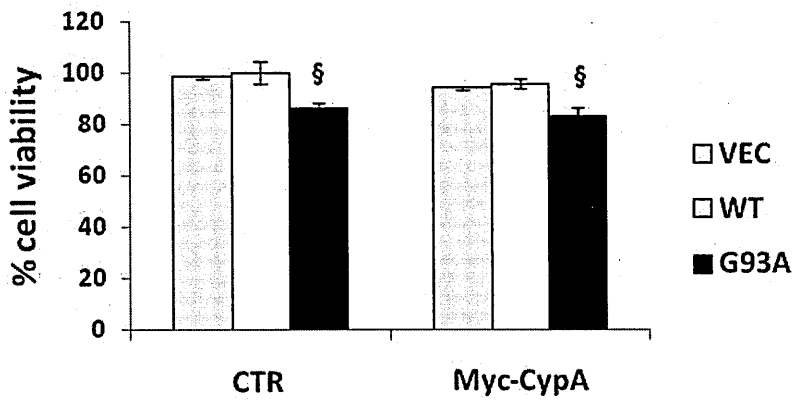

Figure 1.11 Effect of CypA overexpression on cell viability.

Histograms represent the effect of Myc-CypA overexpression in HEK293 cells stably expressing VEC (grey), WT-SOD1 (white) or G93A-SOD1 (black) on viability, compared to cells transfected with the empty vector (CTR). The conversion of MTT to formazan was used as an index of cell survival. Data (mean ± S.E., n≥4 for each sample) are expressed as percentages of control cells (WT CTR). Symbols indicate that samples are significantly different (§= p≤0.05 WT vs G93A), as assessed by two-way ANOVA test followed by Bonferroni multiple comparisons post-test.

2. Identification of Cyclophilin A interacting proteins

A possible involvement of CypA in ALS pathogenesis has been hypothesised. Nevertheless its role and possible effects in the disease have remained elusive. Recently, different aspects of CypA biological functions have emerged, suggesting that it is involved in multiple signalling events of eukaryotic cells. CypA either possesses enzymatic peptidyl-prolyl isomerase activity, which is essential to protein folding *in vivo* (Schiene 2000), or it might form stoichiometric complexes with target proteins without necessarily isomerizing a peptidyl-prolyl bond, thereby preventing misfolding and/or modulating activity of the target protein (Braaten 1997; Streblow 1998; Brazin 2002). We decided to investigate the CypA interactome because the identification of novel interactions can be the key to provide further insights into the (patho)physiologically relevant molecular functions of this protein in ALS.

2.1 CypA interactome in HEK293 cells

A proteomic-based strategy was employed to investigate the CypA interactome network. Novel potential interactors were first identified through mass spectrometry and then the most interesting results were validated through WB. The experimental approach is outlined in **Figure 2.1** and it foresaw the separation of CypA interactors from wild-type and mutant SOD1 stably expressing cells. Proteins from whole cell lysates were first solubilised by a weak detergent-based buffer, in order to maintain non-covalent interactions within intact protein complexes. The complexes of CypA-interacting proteins were enriched by co-immunoprecipitation (IP) using anti-CypA antibodies, separated by isoelectrofocusing (IEF) and then by SDS-PAGE. Protein spots were located on 2DE-gels stained with Sypro® Ruby Protein Gel Stain (Invitrogen), excised by a spot cutter, incubated with trypsin in a protein digestor and analysed by MALDI-TOF/TOF mass spectrometry (further details are discussed in Materials and Methods section). Benzonase® Nuclease, an endonuclease that attacks and degrades all forms of DNA and RNA (single stranded,

double stranded, linear and circular), was included in all reaction mixtures to exclude the possibility of protein interactions mediated by protein-RNA/DNA-protein interaction through possibly contaminating RNA/DNA.

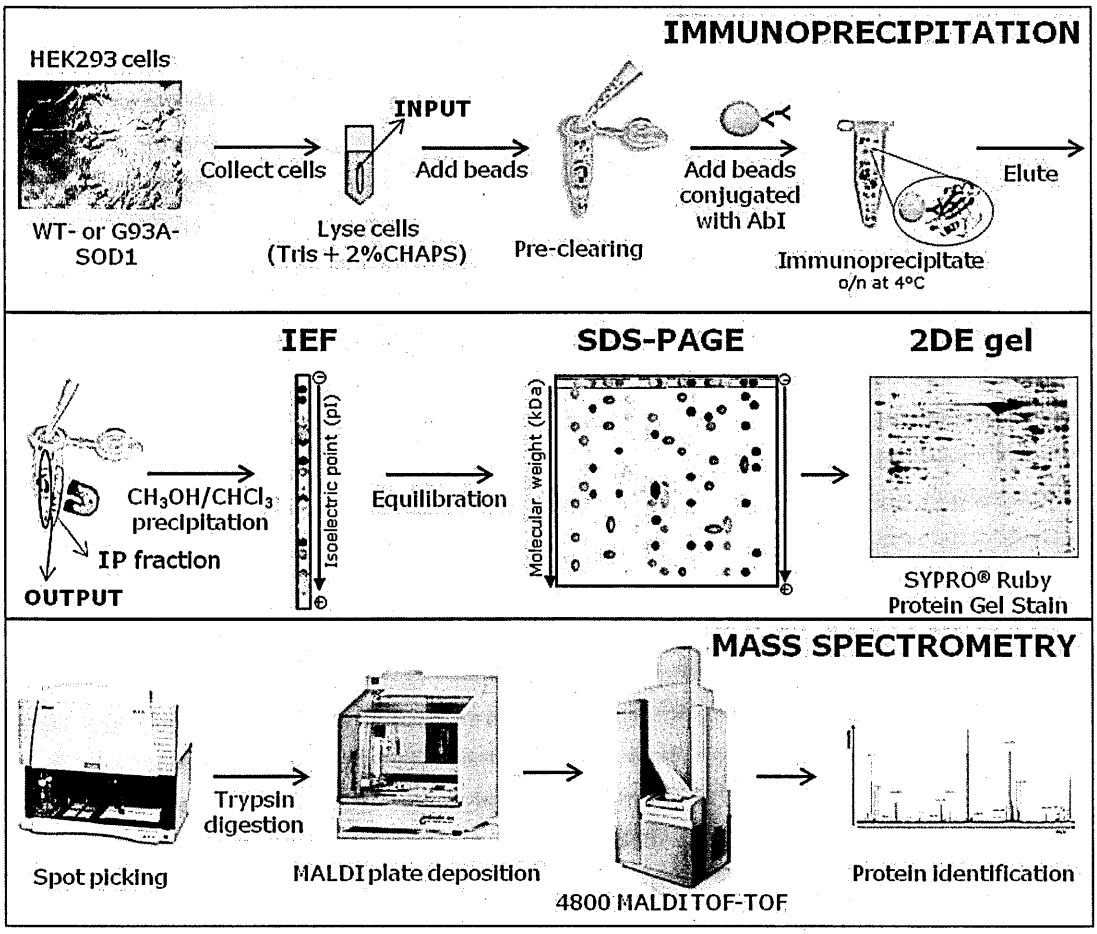

Figure 2.1 Analytical workflow used to identify CypA interactors.

The experimental procedure included: collecting samples from cultures of HEK293 cells expressing WT- or G93A-SOD1, preparing 4.5mg of protein extracts for each experimental condition per replicate, performing sample pre-clearing using uncoated magnetic beads, cross-linking anti-CypA antibody (AbI) to the secondary antibody-conjugated magnetic beads, immunoprecipitating the complexes of CypA-interacting proteins, eluting the immunoprecipitate fraction from the magnetic beads, preparing the sample for 2DE analysis by methanol/chloroform precipitation and solubilization, separating the proteins by IEF and SDS-PAGE, staining the gels with Sypro Ruby, scanning the gels and identifying protein spots, picking the spots of interest, digesting proteins with trypsin, preparing samples for mass spectrometry, performing peptide mass fingerprinting and MS/MS analysis to identify potential interactors.

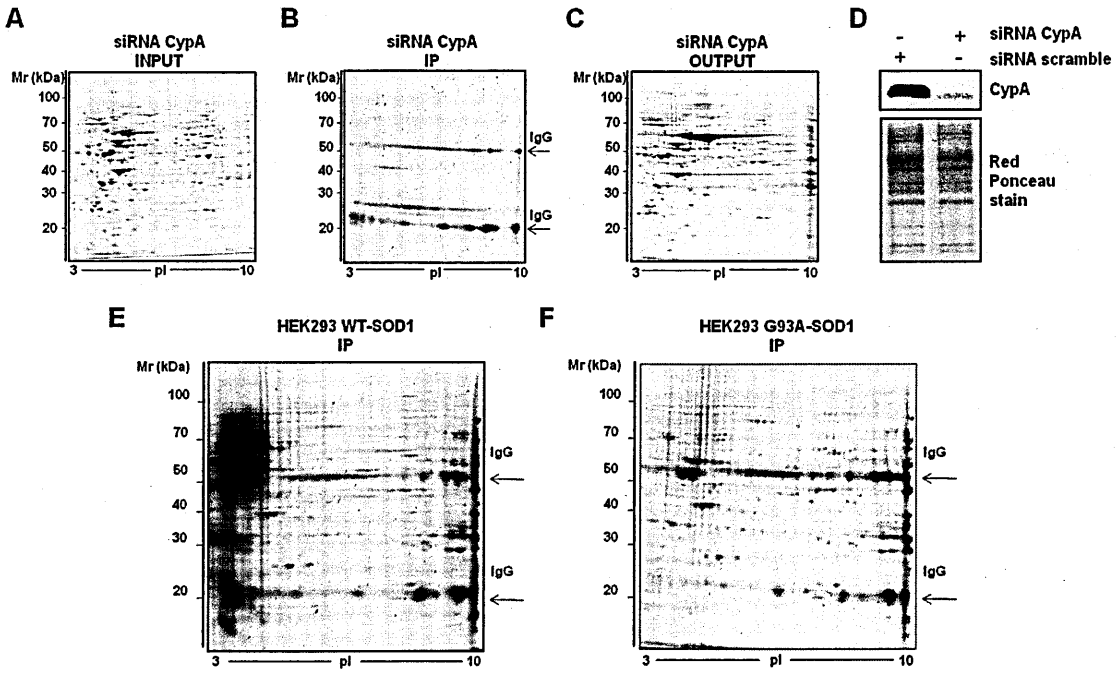

Figure 2.2 2DE maps of CypA interactome in HEK293 cells.

Representative preparative 2DE gels of CypA co-immunoprecipitated proteins from WT- or G93A-SOD1 expressing HEK293 cells transfected with a scrambled siRNA or a specific siRNA against CypA sequence. (**A-C**) After CypA knockdown, 4.5mg of proteins were used to immunoprecipitate CypA and the IP fraction (**B**) was separated by 2DE in parallel with the corresponding INPUT (**A**) and OUTPUT (**C**) fractions. (**D**) At the same time 15µg of proteins from cells silenced with 10nM of a scrambled sequence or a CypA-specific siRNA underwent SDS-PAGE and WB for CypA (small box) to verify protein down-regulation and Red Ponceau staining as a loading control (lower panel). (**E-F**) 4.5mg of proteins from HEK293 cells stably expressing WT (**E**) or mutant hSOD1 (**F**) were immunoprecipitated for CypA and underwent two-dimensional gel electrophoresis. Proteins in 2DE-gels were stained with Sypro® Ruby Protein Gel Stain (Invitrogen). Proteins are distributed vertically according to their molecular weight and horizontally according to their pI.

As a negative control for this experimental procedure, co-IP experiments followed by 2DE separation, were also performed in cells depleted of CypA by RNA interference (**Figure 2.2A-D**). CypA knockdown has been performed delivering a specific small interfering RNA (siRNA) molecule, as previously described. The comparison between the co-IP fractions isolated from cells expressing CypA or silenced for CypA provided a powerful tool to discern specific CypA-binding partners. Furthermore, only proteins co-purified in independent IP experiments using two different antibodies for CypA, one polyclonal and one monoclonal, were considered as specific CypA interactors, and corresponding spots were selected for MS analysis.

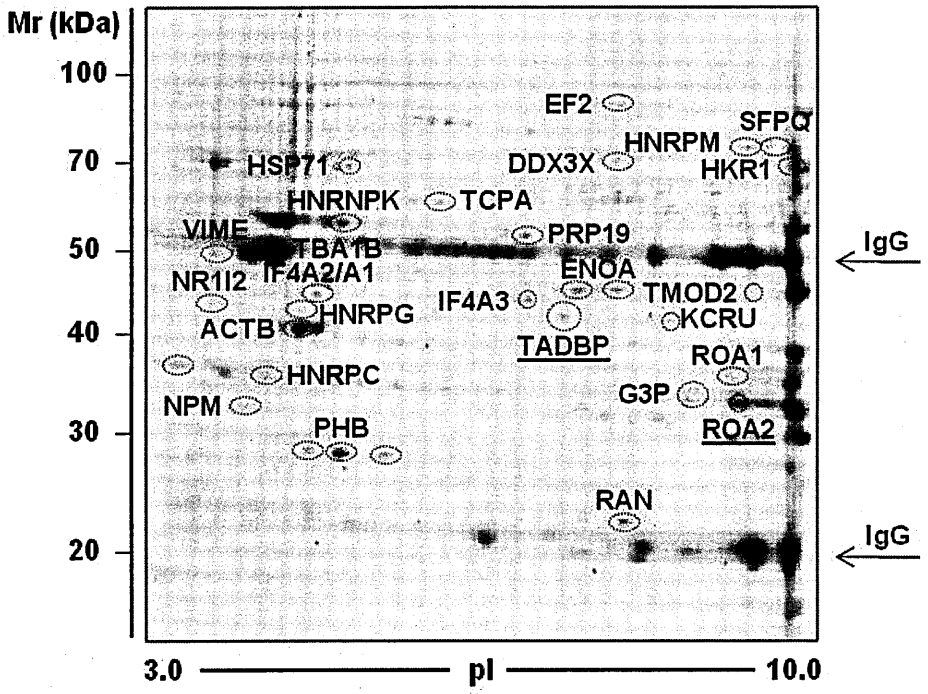

Figure 2.3 CypA interactome in HEK293 cells.

2DE map of CypA interacting proteins showing spots identified by MALDI-TOF/TOF. Proteins in the gel were stained with Sypro Ruby Protein Gel Stain (Invitrogen). Proteins are distributed vertically according to their molecular weight and horizontally according to their pI.

In **Figure 2.2** a representative experiment is shown with 2DE-gels of CypA co-IP fractions isolated from total protein homogenates of HEK293 cells expressing wild-type (**Figure 2.2E**) or mutant SOD1 (**Figure 2.2F**) or cells previously silenced for CypA (**Figure 2.2B**) as negative control. This procedure seems really specific since in the negative control sample only IgG were present. This means that when CypA was silenced, the antibody against CypA was not co-immunoprecipitating any aspecific protein complex, and that the spots observed in the other two gels are specific CypA-binding partners. 28 proteins, found in association with CypA, were identified by mass spectrometry in both WT and mutant cells (**Table 2.1**).

Spot	Entry	AC	Mr_{calc}	pI_{calc}	Mr_{obs}	pI_{obs}	Score[c]	Coverage (%)[b]	Peptide count	Matched/ unmatched[a]	Best ion score	Peptide sequence
DNA/RNA binding proteins												
1	ROA1	P09651	38.7	9.21	34.2	9.27	66	21	7	7/38	15	R.SSGPYGGGGQYFAKPR.N
2	ROA2	P22626	37.4	8.97	37	8.9	555	47	13	13/8	114	R.GGGGNFGPGPGSNFR.G
3	HNRPC	P07910	33.6	4.95	34	4.9	222	14	4	4/10	83	R.MIAGQVLDINLAAEPK.V
4	HNRPG	P38159	42.3	10.06	43	5.3	105	28	11	11/15	16	R.RGPPPPPR.S
5	HNRPK	P61978	50.9	5.39	51	5.4	287	33	14	14/18	83	R.TDYNASVSVPDSSGPER.I
6	HNRPM	P52272	77.5	8.84	77	8.84	77	41	28	28/110	-	-
7	TADBP	Q13148	44.7	5.85	44.7	6.5	78	4	1	1/16	71	R.FGGNPGGFGNQGGFGNSR.G
8	IF4A3	P38919	46.8	6.30	46.8	6.3	97	13	5	5/13	64	R.GIYAYGFEKPSAIQQR.A
9	IF4A2	Q14240	46.4	5.33	46	5.3	92	6	3	3/10	72	R.GIYAYGFEKPSAIQQR.A
10	IF4A1	P60842	46.1	5.32	46	5.3	92	6	3	3/10	72	R.GIYAYGFEKPSAIQQR.A
11	DDX3X	O00571	73.2	6.73	73.2	6.8	117	18	13	13/17	31	R.VGNLGLATSFFNER.N
12	PRP19	Q9UMS4	55.1	6.14	55.1	6.1	90	24	7	7/17	30	K.TVPEELVKPEELSK.Y
13	SFPQ	P23246	76.1	9.4	76	9.4	73	31	24	24/72	-	-
14	HKR1	P10072	75.1	9.44	75.1	9.44	69	44	25	25/157	-	-
15	NR1I2	O75469	49.7	8.70	45	5.5	59	31	13	13/84	-	-
16	NPM	P06748	32.5	4.64	32.5	4.6	95	14	4	4/18	70	R.MTDQEAIQDLWQWR.K
Protein biosynthesis												
17	EF2	P13639	95.3	6.41	95.3	6.8	127	11	8	8/9	65	K.AYLPVNESFGFTADLR.S
Protein folding and degradation												
18	TCPA	P17987	60.3	5.80	60.3	5.8	108	13	6	6/13	66	R.AFHNEAQVNPER.K
19	HSP71	P08107	70.0	5.48	70	5.5	660	41	22	22/14	88	K.DAGVIAGLNVLR.I
Trafficking												
20	RAN	P62826	24.42	7.01	24	7.0	65	10	3	3/17	44	K.NLQYYDISAK.S
Cytoskeleton-associated proteins												
21	ACTB	P60709	41.71	5.29	41.8	5.3	458	37	11	11/15	116	K.SYELPDGQVITIGNER.F
22	TBA1B	P68363	50.1	4.94	50	4.9	384	46	13	13/24	96	R.AVFVDLEPTVIDEVR.T
23	VIME	P08670	53.6	5.06	53.6	5.06	60	27	10	10/42	-	-
24	TMOD2	Q9NZR1	39.5	5.21	40	8.9	61	37	13	13/96	-	-
Energy metabolism												
25	ENOA	P06733	47.14	7.01	47.1	7.0	375	29	9	9/5	147	R.AAVPSGASTGIYEALELR.D
26	G3P	P04406	36.03	8.57	37	8.6	76	4	1	1/14	69	K.LISWYDNEFGYSNR.V
27	KCRU	P12532	47.01	8.6	44.5	8.5	87	12	4	4/11	56	R.LYPPSAEYPDLR.K
Others												
28	PHB	P35232	29.8	5.57	29.8	5.4	628	39	8	8/11	190	K.AAELIANSLATAGDGLIELR.K

Table 2.1 CypA interacting proteins identified by MALDI-TOF/TOF mass spectrometry.

List of CypA interactors classified by the proteins' main function. Identified proteins correspond to spots shown in **Figure 2.3**. *AC,* accession numbers from swissprot database; *calc,* calculated; *obs,* observed. [a]Matched/unmatched, the number of peaks that match/unmatch to the theoretical peptide mass fingerprinting. [b]Sequence coverage as the number of amino acids spanned by the assigned peptides divided by the sequence length. [c]Protein score based on combined MS and MS/MS spectra from MALDI-TOF/TOF analysis using MASCOT search engine (Matrix Science). The proteins that had a statistically significant ($P < 0.05$) protein score (>51), were considered successfully identified.

Notably, although CypA is predominantly a cytosolic protein, the CypA interactome revealed interaction with both nuclear and cytoplasmic proteins (**Table 2.2**). In order to understand whether CypA co-purified proteins, belonging to these two cellular components, differed also

with respect to their functions, the Gene Ontology (GO) database was searched for functional classification. Analysis of the biological processes-GO terms, revealed that CypA interacting proteins largely cluster into functionally distinct protein networks (**Figure 2.3**). Remarkably, CypA has extensive interactions with proteins that associate with DNA/RNA and a set of proteins involved in multiple steps of RNA metabolism (**Figure 2.4**). These results are consistent with the observation that CypA is a cellular component of both the nucleus and the cytoplasm, and provide an important perspective about how CypA could be involved in different biological pathways, likely suggesting a possible functional role in these processes too.

Gene name	Protein name	Biological function	Cellular component
HNRNPA1	Heterogeneous nuclear ribonucleoprotein A1	mRNA processing, splicing, transport	Cytoplasm, Nucleus
HNRNPA2B1	Heterogeneous nuclear ribonucleoproteins A2/B1	mRNA processing, splicing	Cytoplasm, Nucleus
HNRNPC	Heterogeneous nuclear ribonucleoproteins C1/C2	mRNA processing, splicing	Nucleus
HNRPG	Heterogeneous nuclear ribonucleoprotein G	mRNA processing, splicing, transcription	Nucleus
hnRNP K	Heterogeneous nuclear ribonucleoprotein K	mRNA processing, splicing	Cytoplasm, Nucleus
HNRNPM	Heterogeneous nuclear ribonucleoprotein M	mRNA processing, splicing	Nucleus
TARDBP	TAR DNA-binding protein 43	mRNA processing, splicing, transcription	Nucleus
EIF4A3	Eukaryotic initiation factor 4A-III	mRNA processing, splicing, transport	Cytoplasm, Nucleus
EIF4A2	Eukaryotic initiation factor 4A-II	Protein biosynthesis	Cytoplasm
EIF4A1	Eukaryotic initiation factor 4A-I	Protein biosynthesis	Cytoplasm
DDX3X	ATP-dependent RNA helicase DDX3X	mRNA processing, splicing	Cytoplasm, Nucleus
PRPF19	Pre-mRNA processing factor 19	mRNA processing, splicing, DNA repair	Cytoplasm, Nucleus
SFPQ	Splicing factor, proline- and glutamine-rich	mRNA processing, splicing, DNA repair	Cytoplasm, Nucleus
HKR1	Krueppel-related zinc finger protein 1	Transcription, Transcription regulation	Nucleus
PXR	Nuclear receptor subfamily 1 group I member 2	Transcription, Transcription regulation	Nucleus
NPM1	Nucleophosmin	Ribosome assembly, DNA repair, protein transport	Cytoplasm, Nucleus
EEF2	Elongation factor 2	Protein biosynthesis	Cytoplasm
TCP1	T-complex protein 1 subunit alpha	Protein folding	Cytoplasm
HSPA1A	Heat shock 70 kDa protein 1A/1B	Protein folding	Cytoplasm
RAN	GTP-binding nuclear protein Ran	Protein transport	Cytoplasm
ACTB	Actin, cytoplasmic 1	Cytoskeleton	Cytoplasm
TUBA1B	Tubulin alpha-1B chain	Cytoskeleton	Cytoplasm
VIM	Vimentin	Cytoskeleton	Cytoplasm
TMOD2	Tropomodulin-2	Cytoskeleton	Cytoplasm
ENO1	Alpha-enolase	Glycolysis	Cytoplasm
GAPDH	Glyceraldehyde-3-phosphate dehydrogenase	Glycolysis	Cytoplasm
CKMT1A	Creatine kinase U-type, mitochondrial	Creatine metabolic process	Mitochondrion
PHB	Prohibitin	DNA synthesis, transcription	Mitochondrion, Nucleus

Table 2.2 CypA interactome functional classification.

List of CypA interactors with corresponding name retrieved from UniProt Knowledgebase (UniProtKB) database (http://www.uniprot.org/), and functional classification using Gene Ontology terms.

Among the identified CypA interacting proteins, there are several members of the heterogeneous nuclear ribonucleoprotein (hnRNP) family. HnRNPs are abundant nuclear proteins that shuttle between the nucleus and the cytosol and, organized in large complexes, have key roles in RNA processing, transport, localisation, translation and stability (Dreyfuss 2002).

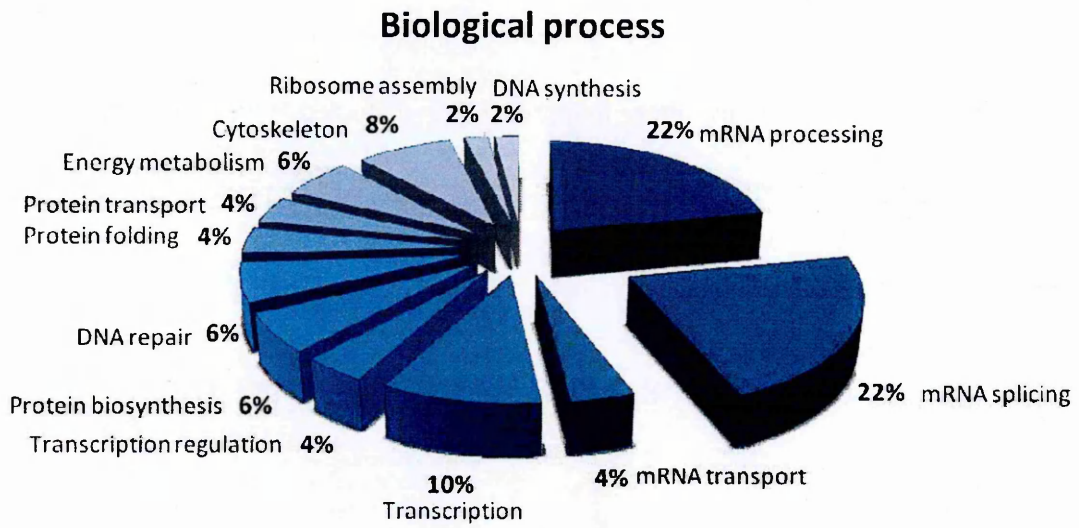

Figure 2.4 Functional blocks of CypA-interacting proteins.

The pie-chart representation is indicative of the impact of a single functional class on the total functions classified. Percentages on slices are calculated as number of proteins associated to a particular block, normalized to all the proteins associated with functional blocks, set as 100.

2.2 Verification of CypA interacting proteins

In order to validate the observations made by mass spectrometry analyses, a subset of CypA interacting proteins was verified by co-immunoprecipitation followed by WB.

Among all CypA novel interactors, the 43kDa transactivation response element (TAR)-DNA-binding protein (TDP-43) (**Figure 2.5A**) was of exceptional interest, as it has recently emerged as a key player in ALS pathology and has been associated with other neurodegenerative diseases (Geser 2009a). TDP-43 is a RNA/DNA binding protein and it structurally resembles a typical hnRNP. TDP-43 has been identified as the major component of neuronal ubiquitinated inclusions (Neumann

2006) in sALS and SOD1-negative fALS patients, and is considered the most striking pathological hallmark of ALS. Furthermore, mutations in the TARDBP gene were found both in sporadic and familial ALS patients (Kabashi 2008; Sreedharan 2008), mainly in the C-terminal region that is the site of interaction with other proteins, and among them also members of the hnRNP A/B family (Buratti 2005). TDP-43 is involved in multiple steps of the RNA lifecycle including transcription, splicing, transport, translation, stability, degradation and miRNA processing (reviewed in Fiesel 2011). Nevertheless, its precise role in ALS pathogenesis has not been deciphered yet. Thus, this interaction was further validated by different approaches and studied in different systems for its possible significance in ALS pathogenesis.

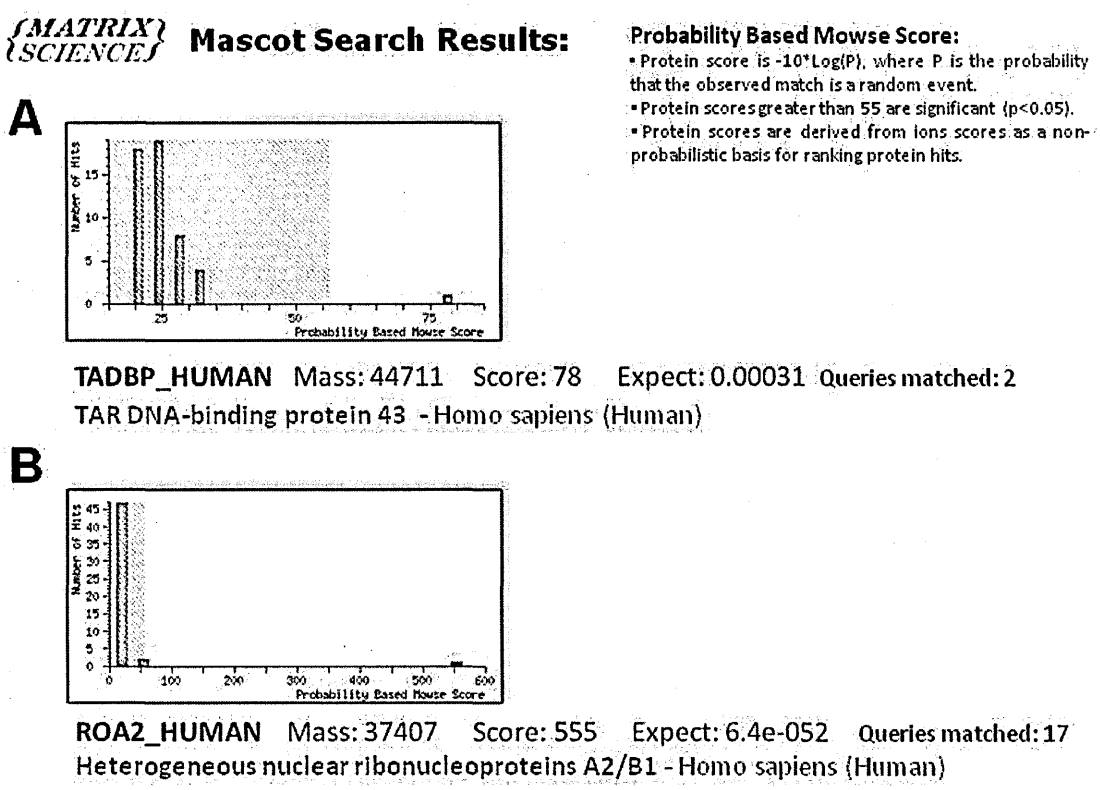

Figure 2.5 Mascot Search Result for TDP-43 and hnRNP A2/B1 identifications.

(**A**) TDP-43 (TADBP_HUMAN) and (**B**) hnRNP A2/B1 (ROA2_HUMAN) have been positively identified by a significant Mascot Score in the Mascot database search software. The Mascot Score is a statistical score for how well the experimental data match the database sequence (www.matrixscience.com).

2.2.1 In vitro interaction validation using endogenous proteins

First, candidate CypA-interacting proteins were investigated *in vitro* to confirm the interactions. Thus, endogenously expressed proteins were immunoprecipitated from HEK293 cells overexpressing WT- or G93A-SOD1.

2.2.1.1 CypA interacts with TDP-43

An antibody anti-CypA was used to co-IP and an antibody anti-TDP-43 was used to evaluate its presence in CypA IP fraction (**Figure 2.6A**). The interaction between CypA and TDP-43 was confirmed, both in wild-type and in mutant SOD1 expressing cells. The association of CypA with TDP-43 was specific, as determined by several positive and negative controls. In particular, different starting IP solutions were used as experimental controls in the co-IP assay. The starting IP mix contained respectively: [Buffer] the magnetic beads conjugated to a secondary antibody (AbII), with neither the cellular lysate nor a primary antibody (AbI); [AbI] the magnetic beads conjugated to the AbII and pre-incubated with anti-CypA AbI, without cellular lysate; [Lysate] the magnetic beads conjugated to the AbII were incubated with the cellular lysate without AbI. In the first control [Buffer], only the heavy and light chains of the Immunoglobulins (Ig) of the AbII were detected in the IP fraction. In the second control [AbI], a stronger signal was observed in the IP fraction, corresponding to the Ig of the AbI and AbII. In both cases there was only a faint signal in the post-IP fractions corresponding to residual BSA contained in the washing buffers used in several steps of the co-IP procedure. In the third control [Lysate], the band pattern in the IP fraction overlapped to the first one, where only the IgG of the AbII were present, while in the post-IP fraction TDP-43 was detected as in the input and output fractions, because in the absence of the AbI no cellular proteins were co-IP and TDP-43 was completely recovered in the remaining fraction.

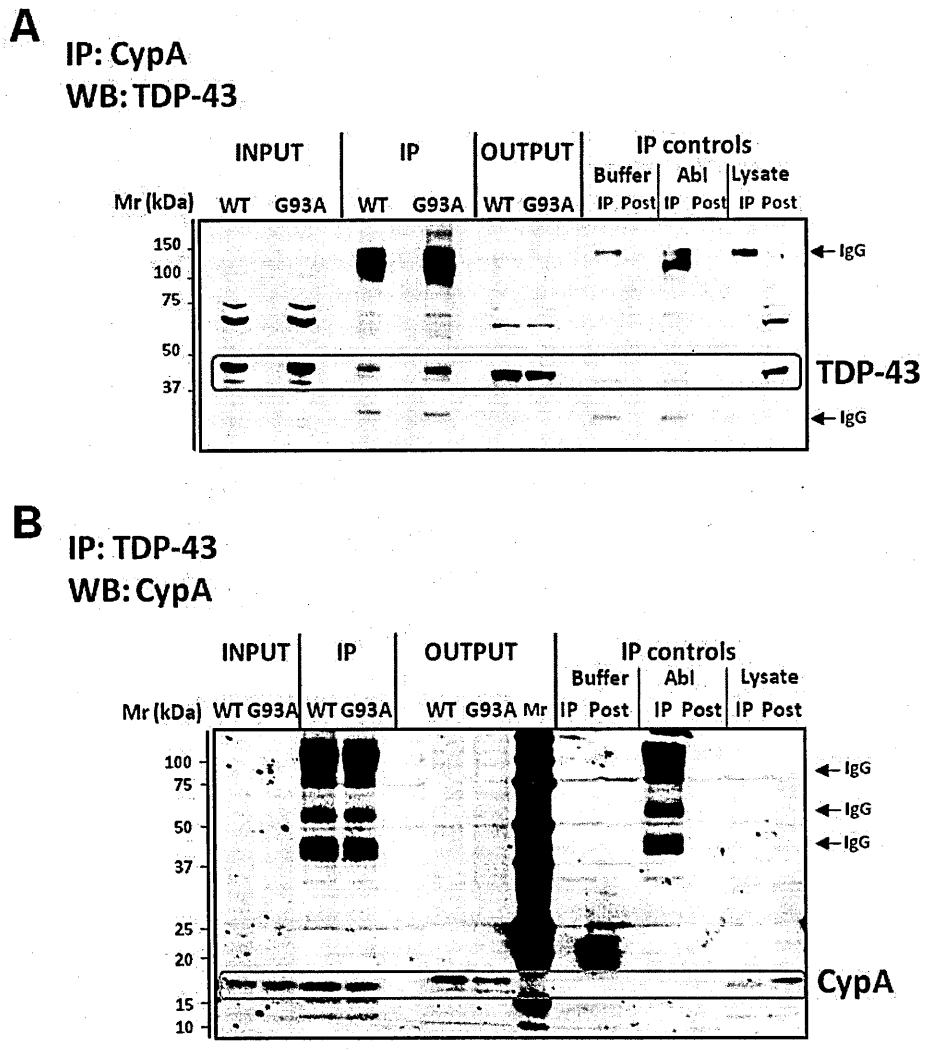

Figure 2.6 CypA and TDP-43 interact *in vitro*.

Equal amounts of proteins (500µg) were co-precipitated with the anti-CypA antibody (**A**) or with the anti-TDP-43 antibody (**B**) from HEK293 cells stably expressing WT- or G93A-SOD1. Aliquot of the cell lysates (INPUT), of the immunoprecipitates (IP) and of the proteins from the remaining fraction (OUTPUT) were loaded together with three different IP controls and their relative output fractions (POST), and subjected to SDS-PAGE. Proteins were transferred to a PVDF membrane, stained with Red Ponceau as loading control and probed with specific antibodies. TDP-43 was revealed through chemiluminescence measurements (**A**), while Qdot®800 fluorescence was used to detect CypA (**B**). Shown are representative of several independent experiments with similar results, indicating specific binding of CypA and TDP-43.

To further verify the interaction between CypA and TDP-43 the same co-IP experiment was repeated in HEK293 cells expressing WT-SOD1 or G93A-SOD1 reversing the primary antibodies previously used (**Figure 2.6B**). In particular, the immunoprecipitation by the anti-TDP-43 antibody, was followed by CypA WB, providing additional evidence that CypA interacts with TDP-43. The

same IP controls were included in the reverse analysis, obtaining analogous results. Moreover, to confirm the specificity of this binding, CypA and TDP-43 co-IP assays were performed using different commercially available polyclonal and monoclonal antibodies for both proteins. These preliminary studies revealed that a specific interaction between the two proteins occurred in mammalian cells.

2.2.1.2 CypA interacts with hnRNP A2/B1

HnRNP A2/B1 is one of a large number of hnRNPs found to interact with CypA in this proteomic analysis (**Figure 2.5B**). HnRNPA2/B1 was previously demonstrated to form a complex with CypA that undergoes nuclear export in response to chemokine stimulus (Pan 2008). HnRNP A2/B1 is one of the major components of the hnRNP core complex in mammalian cells (Kozu 1995) and participates to post-transcriptional regulation in both the nucleus and cytoplasm and also is involved in telomere biogenesis. Together with CypA and TDP-43, this protein was up-regulated in PBMC of sALS patients (Nardo 2011), suggesting an involvement for hnRNP A2/B1, and possibly also its interactions with TDP-43 and eventually with CypA, in the pathogenesis of ALS. Thus, the interaction between CypA and hnRNP A2/B1 was investigated in this *in vitro* model.

HnRNP A2/B1 immunoprecipitation followed by CypA WB confirmed the interaction between these two proteins both in WT-SOD1 and in G93A-SOD1 expressing cells (**Figure 2.7A**). A reverse co-IP approach was applied to further evaluate the association between CypA and hnRNP A2/B1 in HEK293 cells overexpressing WT or mutant SOD1 (**Figure 2.7B**). This experiment provided additional evidence that endogenous CypA forms complexes with hnRNP A2/B1 in mammal cells. The same IP controls previously described, were also analysed in these experiments and a similar band pattern was observed in all IP and Post fractions, supporting the specificity of these observations.

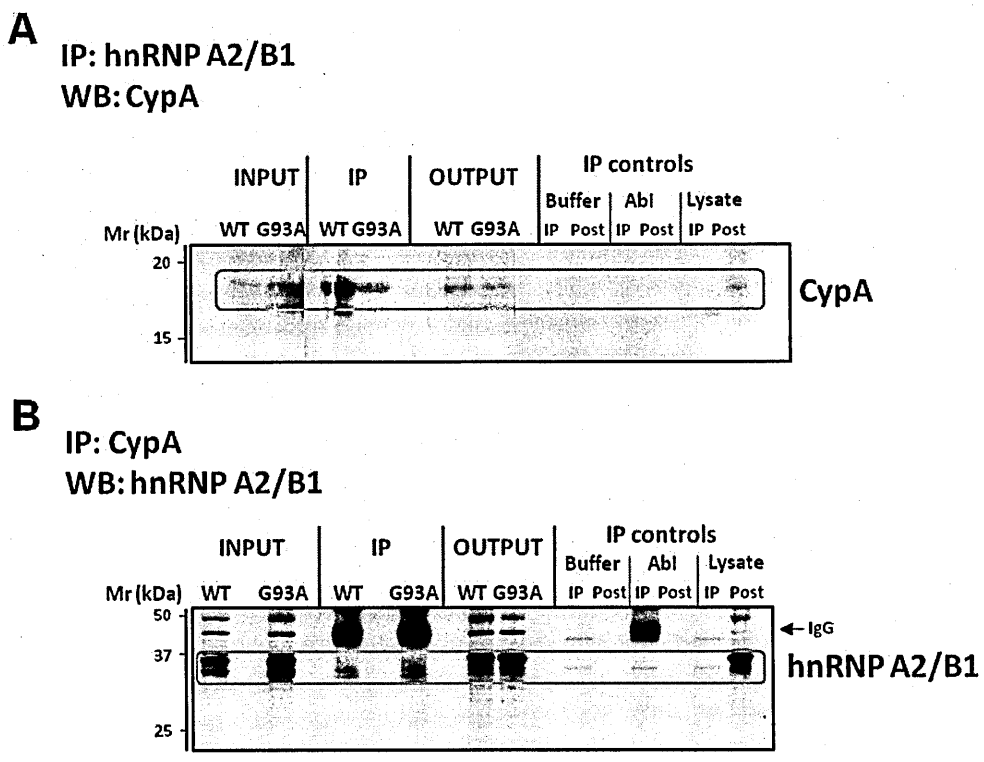

Figure 2.7 CypA and hnRNP A2/B1 interact *in vitro*.

Equal amounts of proteins (500µg) were co-precipitated with the anti-hnRNP A2/B1 antibody (**A**) or with the anti-CypA antibody (**B**) from HEK293 cells stably expressing WT- or G93A-SOD1. Aliquots of the cell lysates (INPUT), of the immunoprecipitates (IP) and of the proteins from the remaining fraction (OUTPUT) were loaded together with three different IP controls and their relative output fractions (POST), and subjected to SDS-PAGE. Proteins were transferred to PVDF membranes, stained with Red Ponceau as loading control, probed with specific antibodies and the signal was detected by chemiluminescence. IP were analysed by WB using an anti-CypA (**A**) or an anti-hnRNP A2/B1 (**B**) antibody. Representative of several independent experiments with similar results are shown, indicating specific association of CypA and hnRNP A2/B1.

2.2.1.3 TDP-43 interacts with hnRNP A2/B1

HnRNP A2/B1 is also a binding partner of TDP-43 and it seems to be crucial for at least one of its putative functions (Buratti 2005). Given the importance of TDP-43 and hnRNP A2/B1 in ALS, it was fundamental to replicate their interaction, previously described by Buratti and co-workers (Buratti 2005), also in this experimental setting. The antibodies against TDP-43 or hnRNP A2/B1 were alternatively used in co-IP and reverse co-IP experiments followed by the WB analyses of the two proteins. The association between TDP-43 and hnRNP A2/B1 was thus replicated both in wild-type and mutant HEK293 cells (**Figure 2.8**). The same IP controls were tested also in these experiments, confirming the specificity of the interactions observed.

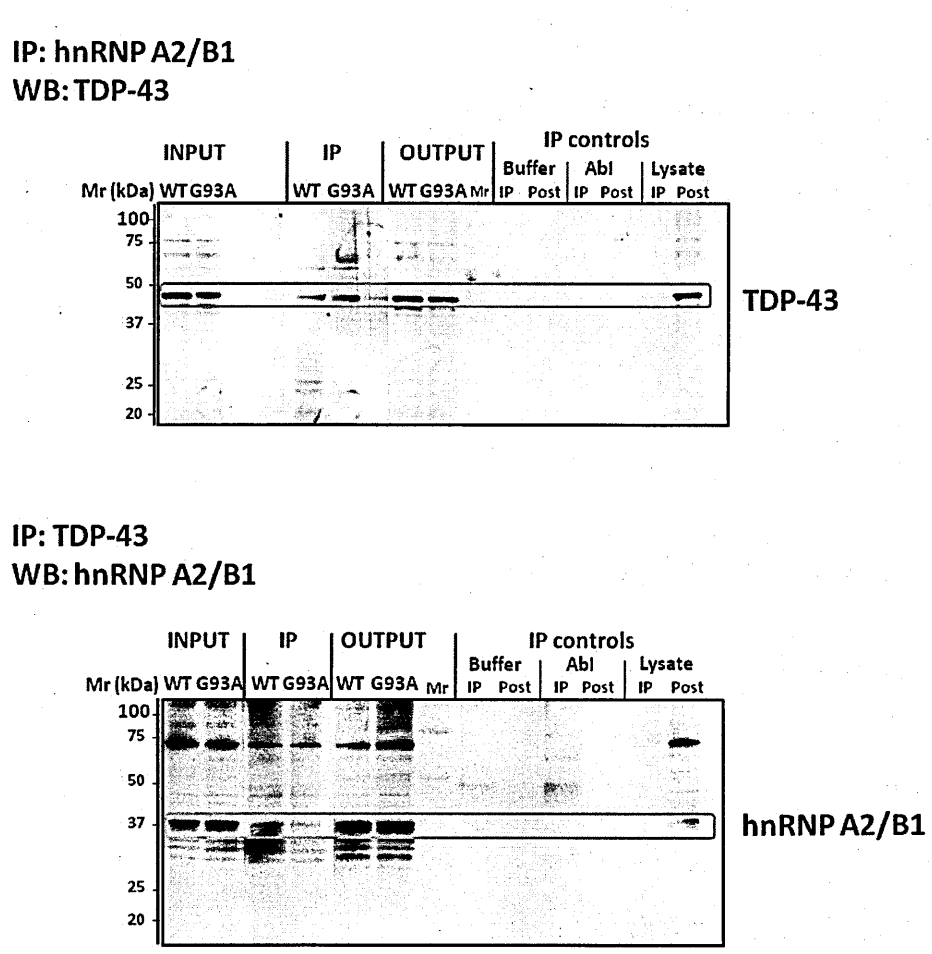

Figure 2.8 TDP-43 and hnRNP A2/B1 interact *in vitro*.

Equal amounts of proteins (500µg) were co-precipitated with the primary antibody. Aliquots of the cell lysates (INPUT), of the immunoprecipitates (IP) and of the proteins from the remaining fraction (OUTPUT) were loaded together with three different IP controls and their relative output fractions (POST), and subjected to SDS-PAGE. Proteins were transferred to PVDF membranes, and stained with Red Ponceau as loading control. (A) Lysates from HEK293 cells stably expressing WT-SOD1 or G93A-SOD1 were blotted for TDP-43 after hnRNP A2/B1 IP and protein signal was revealed through Qdot®655 fluorescence. (B) Wild-type and mutant cells were blotted for hnRNP A2/B1 after TDP-43 IP and the signal was detected by chemiluminescence. Representative of several independent experiments with similar results are shown, indicating a specific interaction of TDP-43 and hnRNP A2/B1.

2.2.2 In vitro interaction validation using exogenous tagged proteins

To confirm the interaction between CypA and TDP-43, and to further characterise it, tagged exogenous proteins were used in co-immunoprecipitation assays. In particular, a plasmid carrying

CypA cDNA with a Myc-tag epitope at its C-terminal end and a plasmid encoding TDP-43 with a short sequence codifying a Flag-tag epitope at its N-terminus (Ayala 2008) were used for these experiments. Transient co-transfection of HEK293 cells with both expression vectors allowed to specifically detect only the exogenous proteins. Moreover, a transfection protocol was optimized to obtain the highest expression levels when vectors were used individually or in combination.

2.2.2.1 Myc-CypA and Flag-TDP-43 co-transfection and co-expression

First, HEK293 cells were tested to verify if both plasmids could be co-transfected in an efficient way producing the tagged proteins together and with good expression levels. To do that, cells were simultaneously transfected with equal ratio of the two plasmids and the expression of the tagged proteins was evaluated both by WB and confocal microscopy. The WB results clearly indicated that Myc-CypA and Flag-TDP-43 proteins were expressed at good levels also when they were co-transfected together (**Figure 2.9A-B**).

Furthermore, the analysis of the immunofluorescence images showed that single cells that had been efficiently transfected with one plasmid and overexpressed one tagged protein, were preferentially transfected also with the other vector and expressed at similar levels the other tagged protein of interest too (**Figure 2.9C-D**). These experiments clearly demonstrated that transfected HEK293 cells were able to express both Myc-CypA and Flag-TDP-43 at the same time, and thus could be suitable to perform co-IP experiments with overexpressed tagged proteins.

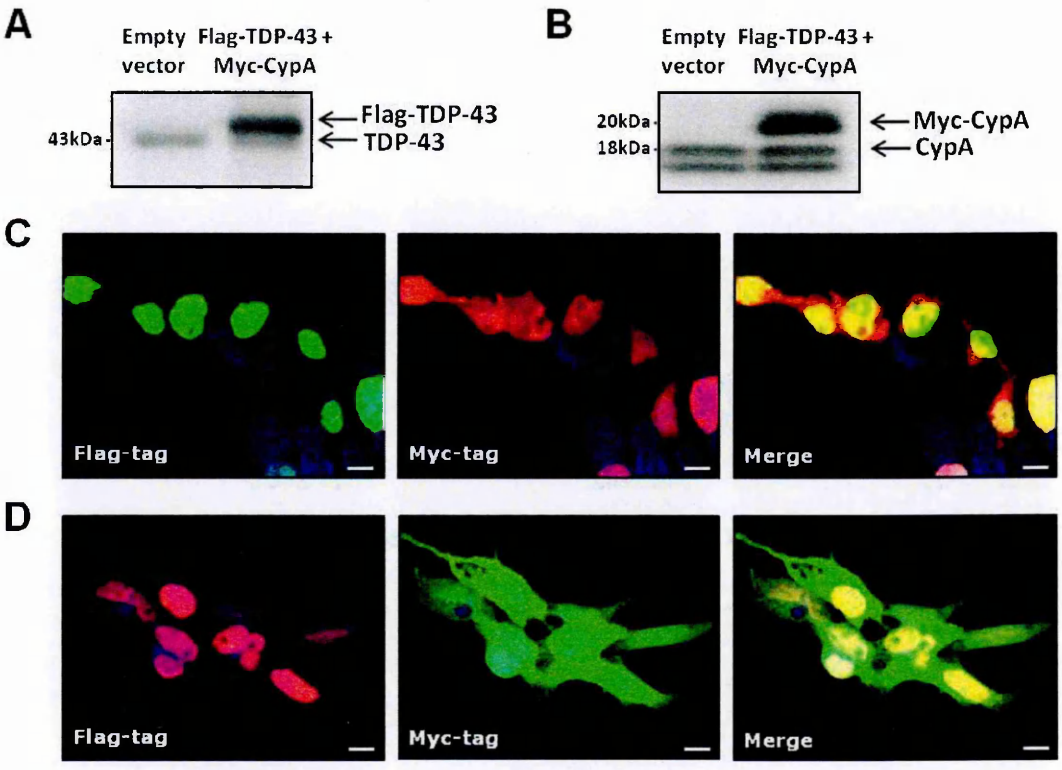

Figure 2.9 Co-transfected HEK293 cells express both tagged CypA and TDP-43.

Cells were transfected with an empty vector (negative control) or co-transfected with Flag-TDP-43 and Myc-CypA plasmids. (**A-B**) Expression of the endogenous and exogenous tagged proteins was verified after 48h by WB. The same membrane was probed with polyclonal antibodies to allow the detection of both endogenous and exogenous tagged proteins. (**A**) First WB for TDP-43 was performed to check for the presence of Flag-TDP43, and then (**B**) the membrane was incubated with anti-CypA antibody to evaluate the expression of Myc-CypA. In both cases, exogenous proteins could be distinguished from the endogenous ones, thanks to a higher molecular weight given by the tag fused to the protein sequence. (**C-D**) Exogenous protein expression was also verified in cells transiently co-transfected with both plasmids by immunofluorescence (bar: 10µm). Co-transfected cells were stained with anti-Flag-tag and anti-Myc-tag antibodies followed respectively by Alexa®488 (green)-conjugated and Alexa®647 (red)-conjugated secondary antibodies (**C**). Co-transfected cells were also reverse-stained using different anti-Flag-tag and anti-Myc-tag antibodies followed respectively by Alexa®647 (red)-conjugated and Alexa®488 (green)-conjugated secondary antibodies (**C**). Nuclei were counter-stained with DAPI (blue). Images representative of several independent experiments are shown, indicating that almost all cells transfected with one plasmid were transfected also with the other, and consequently cells expressing one tagged protein expressed also the other one.

2.2.2.2 In vitro interaction between Myc-CypA and Flag-TDP-43

Additional experiments to verify the interaction between CypA and TDP-43 were also performed using exogenous tagged proteins. The previously described approach was adapted to whole cell lysates from HEK293 cells co-transfected with Myc-CypA and Flag-TDP-43, where antibodies raised against the epitope tag were used to co-immunoprecipitate the corresponding tagged protein.

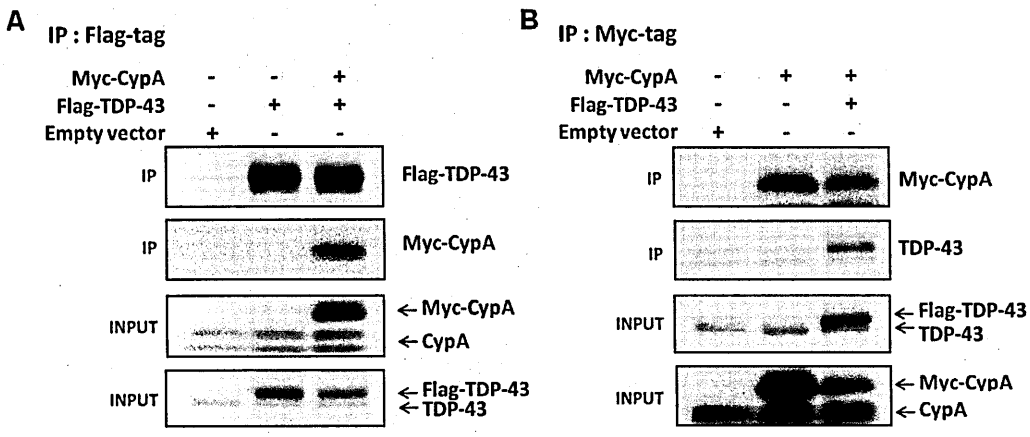

Figure 2.10 Myc-CypA and Flag-TDP-43 interact in transiently co-transfected HEK293 cells. Equal amounts of protein (500µg) were co-precipitated with the primary antibody. Aliquots of the cell lysates (INPUT) and of the immunoprecipitates (IP) were loaded, subjected to SDS-PAGE, transferred to PVDF membranes, stained with Red Ponceau as loading control, probed with different primary antibodies and the signal was detected by chemiluminescence. (**A**) Myc-CypA co-immunoprecipitated with Flag-TDP-43. HEK293 cells were transfected with an empty vector (negative control), with Flag-TDP-43, or co-transfected with Flag-TDP-43 and Myc-CypA plasmids. Cells were lysed and Flag-TDP-43 was selectively immunoprecipitated using an anti-Flag-tag antibody, as detected using an antibody against TDP-43 (upper panel IP fraction). Potentially associated CypA was detected by WB using an anti-Myc-tag antibody. (**B**) Flag-TDP-43 co-immunoprecipitated with Myc-CypA. HEK293 cells were transfected with an empty vector (negative control), with Myc-CypA, or co-transfected with Myc-CypA and Flag-TDP-43 plasmids. Cells were lysed and Myc-CypA was specifically immunoprecipitated using an anti-Myc-tag antibody. TDP-43-associated proteins were detected by WB using an anti-TDP-43 antibody, while the immunoprecipitated Myc-CypA was detected using an antibody against CypA (upper panel IP fraction). Prior to IP experiments, 15µg of the same input samples were analysed by WB to verify the expression of the endogenous and exogenous tagged proteins. Representative of several

independent experiments with consistent results are shown, indicating that overexpressed tagged Myc-CypA and Flag-TDP43 interacts *in vitro*.

First, the antibody specifically recognizing the Flag-tagged N-terminal portion of the exogenously transfected TDP-43 was used (**Figure 2.10A**). Flag-TDP-43, and not endogenous TDP-43, was selectively immunoprecipitated, as shown in the IP fraction (upper panel). WB analysis revealed the presence of Myc-CypA in the IP fraction only when cells were co-transfected with both constructs, while no signal was detected in cells transfected only with Flag-TDP-43 or with the empty vector. This experiment showed an association between the two exogenous proteins. The correct expression of these proteins was also verified analysing by WB the inputs of the same samples, as shown in the lower panels.

In the reverse approach, the antibody against the Myc-tag at the C-terminus of exogenously expressed CypA was used to selectively immunoprecipitate the Myc-CypA protein, as shown in the upper panel of **Figure 2.10B**. Co-precipitated TDP-43 was then detected by WB and the presence of Flag-TDP-43 was observed in the IP fraction of double transfected cells. In this experiment the interaction between the two proteins was further confirmed. The WB analysis of the input fractions of these samples (shown in the lower panels) revealed a correct expression of the proteins. Collectively, these data clearly demonstrate an association between Myc-CypA and Flag-TDP-43 and further support data previously obtained with the endogenous proteins.

The interaction was further confirmed with a different co-IP approach, where antibodies against endogenous proteins (anti-CypA and anti-TDP-43) were used to immunoprecipitate and the IP fractions were subsequently probed with the antibodies recognizing the tag portions of the transfected proteins. Together, these findings provide the first evidences that CypA and TDP-43 interact in mammalian cells.

2.2.3 In vivo interaction validation

Since a novel interaction was observed *in vitro*, it was really important to validate it also *in vivo*. To confirm the interaction between CypA and TDP-43, co-immunoprecipitation experiments were performed on animal tissues.

2.2.3.1 CypA interacts with TDP-43 in mouse tissues

Co-immunoprecipitation was performed from mouse lumbar spinal cord and brain homogenates to confirm that the interaction between CypA and TDP-43 occurs with the endogenous proteins in two tissues that are frequently affected in TDP-43 related diseases. Tissues from age and sex-matched mice that express (CypA+/+, n=3), have a deficient expression (CypA+/-, n=3) or do not express (CypA-/-, n=3) CypA were used to perform co-immunoprecipitation assays (**Figure 2.11**). In particular, CypA knockout mice were used as negative experimental controls, together with coated magnetic beads (Ctr). An anti-CypA antibody was used to immunoprecipitate and the following WB for TDP-43 clearly detected the protein in the IP fraction, only in mice expressing (CypA+/+) or with a reduced CypA expression (CypA+/-), and not in knockout mice (CypA-/-), thus confirming previous results. Furthermore, CypA deficiency (CypA+/-) was associated in both cases with a marked reduction of TDP-43 in the IP fraction. Collectively, these data confirm the specificity of the novel interaction described between CypA and TDP-43, demonstrating also the relevance of this association in ALS disease-related animal tissues.

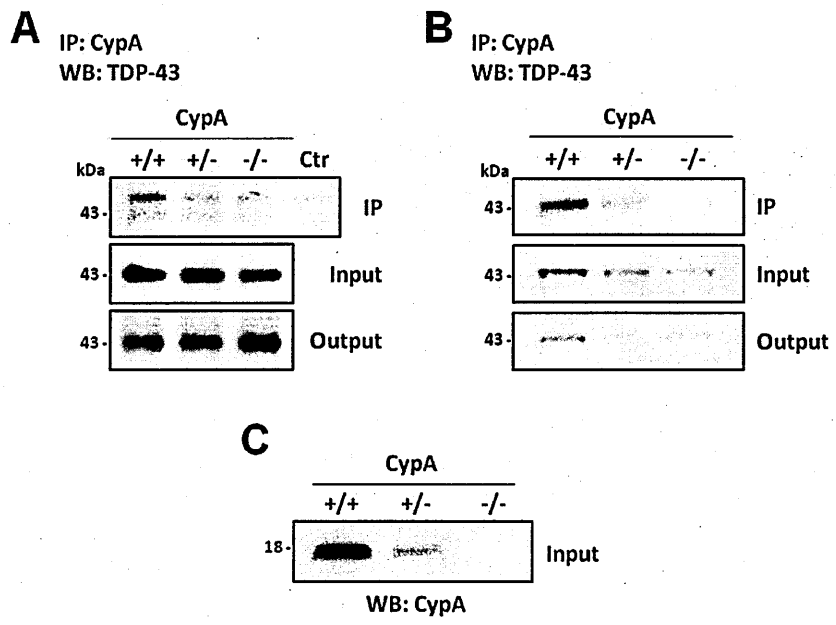

Figure 2.11 CypA and TDP-43 interact in mouse lumbar spinal cord and brain.

Representative experiments, performed on mouse lumbar spinal cord (**A**, **C**) and brain (**B**), are shown. Equal amounts of proteins (1mg) from tissue homogenates of CypA+/+ (n=3), CypA+/- (n=3) and CypA-/- (n=3) mice were co-precipitated with anti-CypA primary antibody. Aliquots of the tissue homogenates (INPUT), of the immunoprecipitates (IP) and of the remaining fraction (OUTPUT) were loaded together with coated beads as IP control, subjected to SDS-PAGE, transferred to PVDF membranes, stained with Red Ponceau as loading control, probed with anti-TDP-43 antibody and detected by chemiluminescence. Results representative of several independent experiments are shown, indicating that interaction between CypA and TDP-43 was confirmed *in vivo*.

2.3 CypA interacts with TDP-43 mainly in the nucleus

To determine the subcellular compartment in which the interaction between CypA and TDP-43 occurs, two different approaches were pursued: CypA and TDP-43 co-immunoprecipitation after biochemical fractionation and immunocytochemistry experiments were conducted in HEK293 cells.

2.3.1 CypA and TDP-43 interact in the nuclear fraction

In order to investigate where the interaction occurred, co-IP experiments were performed starting from nuclear and cytosolic-enriched fractions isolated from HEK293 cells stably

expressing WT-SOD1 or G93A-SOD1 (**Figure 2.12A**). The nuclear fraction was separated from the cytosolic fraction as described in Materials and Methods. The correct nuclei-cytosol separation was first checked by WB analyses of lamin A+C, as nuclear marker, and actin, as cytoplasmic marker. Then, each subcellular fraction was separately immunoprecipitated with an antibody against CypA, followed by TDP-43 detection by WB. In these cells TDP-43 was expressed both in the nucleus and in the cytoplasm, as shown in the input. However CypA was able to co-immunoprecipitate TDP-43 only in the nuclear fraction, both in wild-type and mutant cells.

2.3.2 Myc-CypA and Flag-TDP-43 interact in the nuclear fraction

In order to confirm this observation, subcellular fractionation and co-IP experiments were repeated in HEK293 cells transiently transfected with an empty vector (negative control) or co-transfected with Myc-CypA and Flag-TDP-43 (**Figure 2.12B**). In this case, a reverse co-IP approach is shown: each subcellular fraction was independently immunoprecipitated using the anti-Flag-tag antibody, which allowed the specific immunoprecipitation of Flag-tagged TDP-43 (upper panel). Subsequently the presence of the co-immunoprecipitated CypA in the IP fraction was verified by WB using an anti-Myc-tag antibody (lower panel). Also using this approach a preferential interaction between CypA and TDP-43 was demonstrated in the nuclear compartment; indeed the band corresponding to Myc-CypA was detected mainly in the IP lane of the nuclear fraction and not in the cytosolic one.

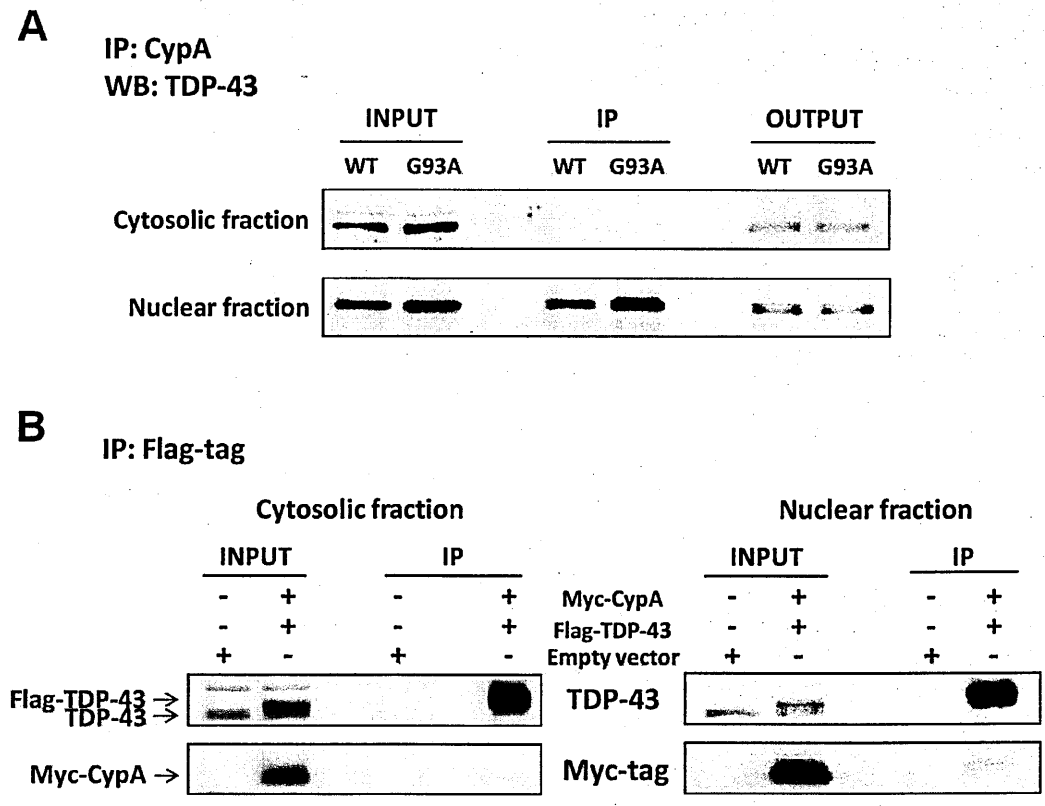

Figure 2.12 CypA and TDP-43 interact mainly in the nuclear fraction.

(**A**) Representative CypA co-immunoprecipitation in the cytosolic and corresponding nuclear fractions of HEK293 cells over-expressing WT-SOD1 or G93A-SOD1. Aliquots of the cytosolic and nuclear lysates (INPUT), of the immunoprecipitates (IP) and of the remaining fractions (OUTPUT) were loaded separately, subjected to SDS-PAGE, transferred to a PVDF membrane, stained with Red Ponceau as loading control, probed with the anti-TDP-43 antibody and detected by chemiluminescence. TDP-43 was present only in the IP fraction corresponding to the nuclear compartment (lower panel) and not in the cytosolic portion (upper panel), even if the protein was correctly expressed both in the cytosol and in the nucleus (input fraction). (**B**) The cytosolic and the nuclear fractions from HEK293 cells co-expressing Myc-CypA and Flag-TDP-43 were used to selectively immunoprecipitate Flag-TDP-43, as detected using an antibody against TDP-43 (upper panel). Cells transfected with an empty vector were used as control for the IP procedure. Potentially associated CypA was detected by anti-Myc-tag blotting (lower panel). 15μg of the corresponding input samples were loaded on the same gel and blotted with the same antibodies. The signal relative to the co-immunoprecipitated Myc-CypA was present mainly in the nuclear fraction, demonstrating that also the association between exogenous tagged CypA and TDP-43 occurs preferentially in this cellular compartment. Subcellular fractionation efficiency was verified before each co-IP experiment. Immunoprecipitation was repeated at least three times on independent sample sets with consistent results. Representative images were chosen for display.

Taken together, these data indicate that both endogenous and exogenous CypA and TDP-43 interact mainly in the nuclear fraction.

2.3.3 CypA and TDP-43 colocalize in the nuclear region

To further demonstrate CypA and TDP-43 association and to investigate the subcellular compartment in which the interaction occurred, HEK293 cells were analyzed by standard immunofluorescence microscopy and by double-label laser-scanning confocal microscopy to simultaneously visualise the two proteins.

Spatial colocalisation between fluorescently labelled CypA and TDP-43 was first performed on untransfected HEK293 cells to visualise the endogenously expressed proteins. Cells were co-immunostained with anti-CypA and anti-TDP-43 antibodies and the two-conjugated fluorochromes were simultaneously detected in the same area. As shown by single protein staining, CypA and TDP-43 both displayed the expected subcellular distribution and in the overlay were found to predominantly co-localize in the nucleus (merge) (**Figure 2.13A**).

The subcellular colocalisation of the two proteins was also visualised in HEK293 cells transiently co-transfected with both Myc-CypA and Flag-TDP-43 plasmids. This time exogenous tagged proteins were selectively immunostained, using the anti-Myc-tag and the anti-Flag-tag antibodies. As shown in **Figure 2.13B**, cells were efficiently transfected with the two constructs, and also the tagged proteins co-localized mainly in the nuclei (merge).

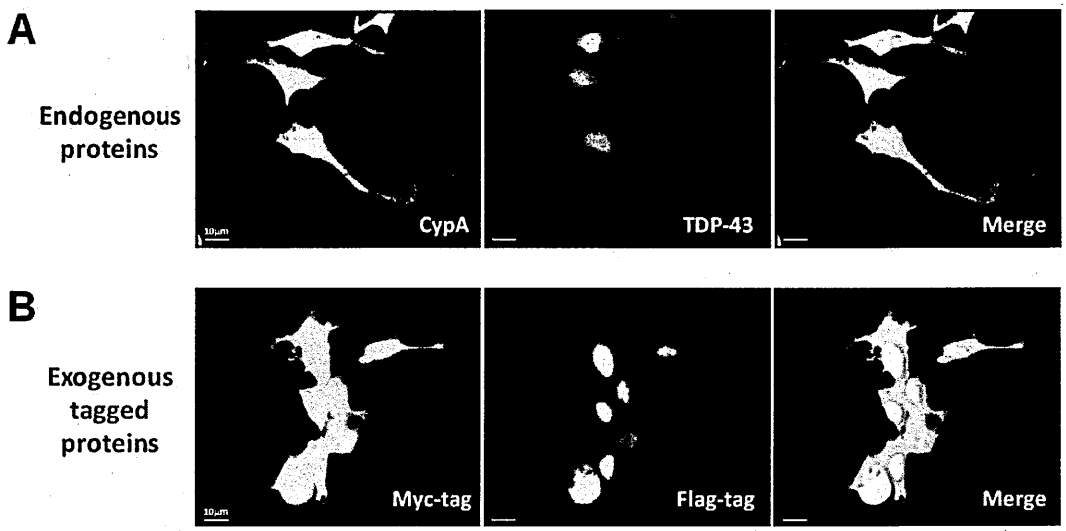

Figure 2.13 CypA and TDP-43 colocalisation analysis in HEK293 cells.

(**A**) Immunofluorescence was used to visualise the localisation of CypA and TDP-43 in HEK293 cells on endogenous proteins. Cells were co-immunostained with anti-CypA and anti-TDP-43 antibodies followed respectively by Alexa®488 (green)-conjugated and Alexa®594 (red)-conjugated secondary antibodies. (**B**) Alternatively cells were co-transfected with Flag-TDP-43 and Myc-CypA plasmids and after 48h exogenous tagged proteins were visualised by immunofluorescence. Co-transfected cells were stained with anti-Myc-tag and anti-Flag-tag antibodies followed respectively by Alexa®488 (green)-conjugated and Alexa®647 (red)-conjugated secondary antibodies. The dual channel look-up table for green and red gave rise to yellow hotspots where the two proteins of interest were present in the same pixels (merge) (bar: 10µm). CypA and TDP-43 colocalized mainly in the nuclear and peri-nuclear area. The immunofluorescence data shown represents consistent results obtained in multiple replicates using different primary and secondary antibodies.

2.4 CypA-TDP-43 colocalisation analysis in dual-colour confocal images

When visualizing protein-protein colocalisation, overlay methods help to generate visual estimates of colocalisation events in two-dimensional images. To more accurately evaluate colocalisation events three dimensional images were acquired along the z-axis. Furthermore, a statistical approach was adopted for quantification purposes to correctly interpret the colocalisation events observed (Bolte 2006).

2.4.1 CypA and TDP-43 visual colocalisation in 3D confocal microscopy in HeLa cells

Colocalisation analysis was also performed in HeLa cells, providing a second cell type in which this novel interaction was observed *in vitro*. Spatial colocalisation was generated by the z-stack projection of serial confocal section acquired by dual-confocal microscopy. Overlays of CypA (green) and TDP-43 (red) images demonstrated areas of yellow (merge) in the nuclear and mainly in the peri-nuclear area, indicating molecular association of the proteins in this region and thus demonstrating their relationship (**Figure 2.14**Figure 2.14).

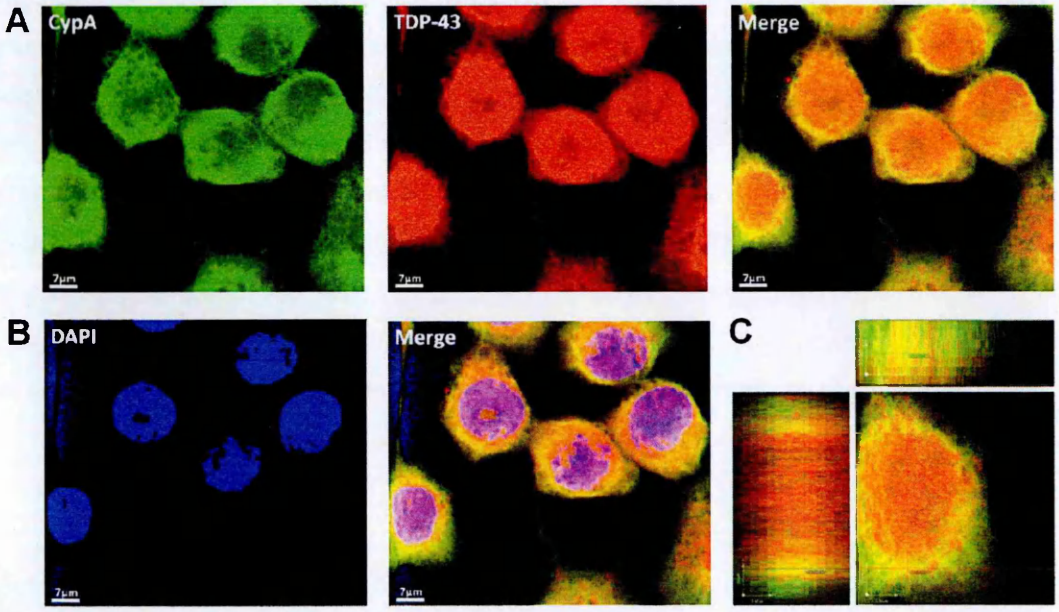

Figure 2.14 CypA and TDP-43 co-labelling in HeLa cells.

Representative immunostaining micrographs show spatial colocalisation of endogenous CypA (green) and TDP-43 (red) proteins in HeLa cells. (**A**) CypA was detected by immunofluorescence using a monoclonal mouse antibody and an Alexa®488-conjugated secondary antibody, while TDP-43 was detected by immunostaining with a polyclonal rabbit antibody followed by incubation with an Alexa®594-conjugated secondary antibody. Partial nuclear co-localisation between CypA and TDP-43 was observed in overlay of red and green images (right panel), with areas of yellow indicating colocalisation of the proteins (bar: 7.0µm). (**B**) 4'-6-Diamidino-2-phenylindole (DAPI) was used to stain the nuclei (blue). Strong perinuclear colocalisation was evidenced in overlay of red and green and blue images (right panel), with areas of yellow indicating colocalisation of the proteins (bar: 7.0µm). (**C**) Orthogonal views through one cell showed co-labelling of the proteins on XY (central

panel), XZ (upper panel) and YZ (left panel) projections, further highlighting CypA and TDP-43 colocalisation (bar: 3.5µm). The figure panels are z-stack projections of 20 to 34 confocal sections.

These data further supported the hypothesis of an interaction between TDP-43 and CypA within the nucleus of mammalian cells.

2.4.2 CypA and TDP-43 quantitative colocalisation analysis

To provide a quantitative estimate of proteins colocalisation, HEK293 cells were further analysed to obtain 3D confocal immunofluorescence microscopy images by sequential scanning for each channel (**Figure 2.15A-D**). Based on the evaluation of colour components of the selected pair of channels (Ch1=TRITC, TDP-43 and Ch2=Cy5, CypA), the degree of colocalisation was estimated using a dedicated analysis software. Colocalisation in two-colour images (CypA in red and TDP-43 in green) was visualised in a two-dimensional histogram, where the number of pixels with red and green intensities was plotted as a scatter gram with each axis representing the intensity of each colour (**Figure 2.15E**). Pearson's Correlation Coefficient (PCC) was among the variables used to analyze the entire scatter plot, which is one of the standard techniques applied in pattern recognition for matching one image to another in order to describe the degree of overlap between the two patterns. Thresholded PCC analysis (Manders 1992) was performed by Volocity® (PerkinElmer, Inc., USA) image analysis software using the Costes algorithm to automatically estimate threshold values (Costes 2004). Both Costes thresholded PCC (0.701) and global PCC (0.803) generated values close to 1, clearly demonstrating a positive correlation between the two-channel images (Barlow 2010).

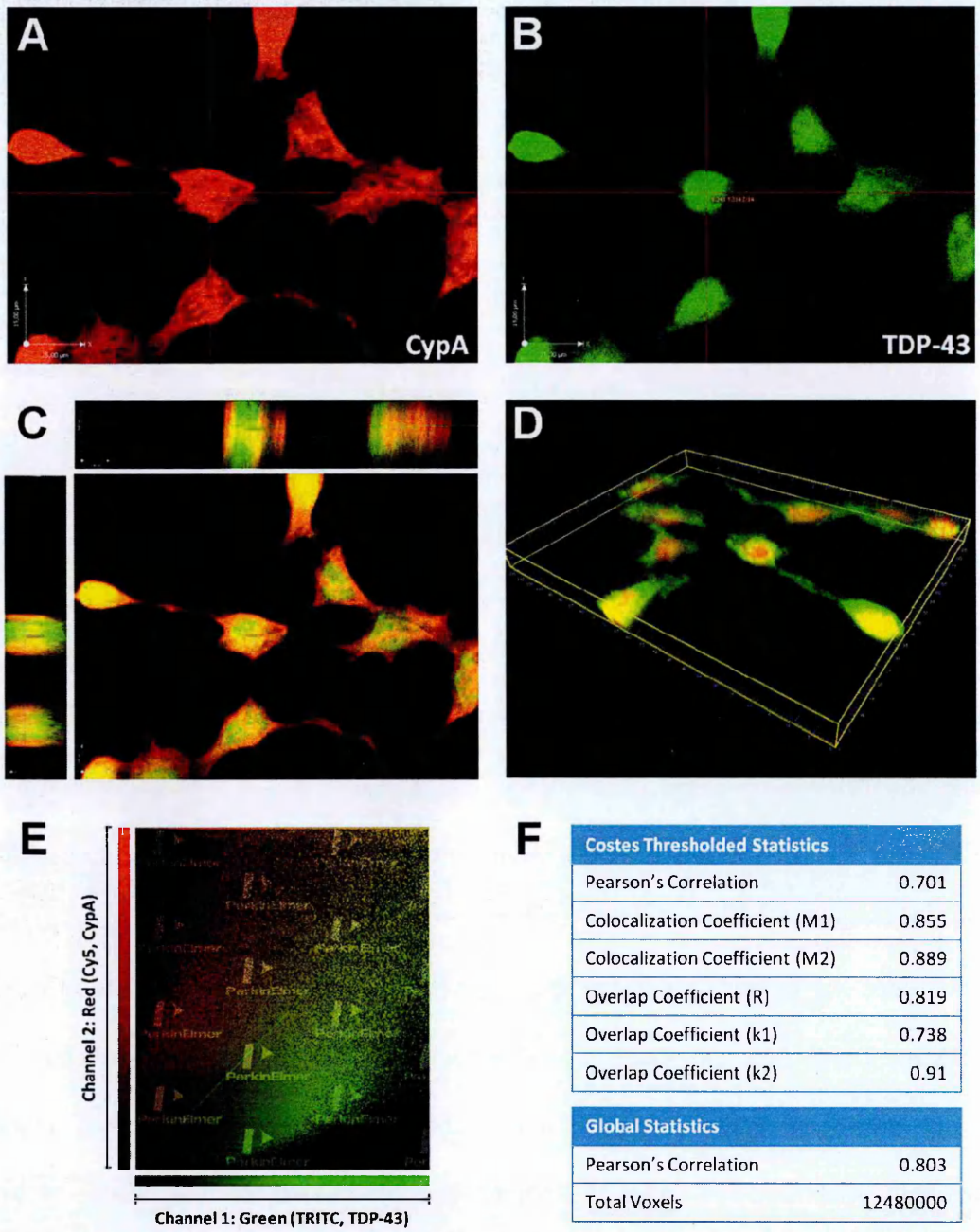

Costes Thresholded Statistics	
Pearson's Correlation	0.701
Colocalization Coefficient (M1)	0.855
Colocalization Coefficient (M2)	0.889
Overlap Coefficient (R)	0.819
Overlap Coefficient (k1)	0.738
Overlap Coefficient (k2)	0.91

Global Statistics	
Pearson's Correlation	0.803
Total Voxels	12480000

Figure 2.15 CypA and TDP-43 quantitative colocalisation analysis in HEK293 cells.

Volocity® (PerkinElmer, Inc., USA) image analysis software was used for quantitative colocalisation analysis. (**A-C**) Confocal representative slice of cultured HEK293 cells simultaneously labelled with CypA (Cy5, red) and TDP-43 (TRITC, green). Single channel and overlay of double channel fluorescence micrograph of the same field of cells for CypA and TDP-43. (**C**) The image represents the z-stack projection of 25 confocal sections: XY (central panel), YZ (left panel) and XZ (upper panel) projections are shown. The figure shows one representative experiment out of eight analysed. (**D**) Three-dimensional images were processed using Imaris® (Bitplane, Zurich, Switzerland) software and 3D rendering shows proteins colabeling further highlighting their colocalisation. (**E**) Representative 2D scatter plot of pixel intensities in the two channels: the red channel (CypA) is on the *y* axis and the green (TDP-43) is on the *x* axis. The partial colocalisation event observed resulted in a pixel distribution off the axes whose slope depended on the fluorescence ratio between the two channels

and whose spread was quantified by the Pearson' Correlation Coefficient (PCC) (F), which was close to 1, since red and green channel intensities were linked. In the tables other statistical parameters generated by quantitative colocalisation analysis are reported, including global PCC, the total overlap coefficient (R), as well as the individual k(x), and M(x) co-localisation coefficients.

Manders' Colocalisation Coefficient M(x) was calculated as a further descriptor of colocalisation (Manders 1993): M1 (0.855) was utilized to describe the contribution of the channel 1 fluorophore to the co-localized area, while M2 (0.889) was used to describe the contribution of the channel 2 fluorophore. The most important output data from Volocity® software analysis was the Overlap Coefficient (R=0.819), which indicates the actual overlap between signals and represents the true degree of overlap. This value ranges between 0 and 1 and is not sensitive to intensity variations in the image analysis. Overlap coefficients k(x) were also calculated to describe differences in intensities between the channels, with k1 (0.738) being sensitive to the differences in the intensity of channel 2 (red signal), while k2 (0.91) depends linearly on the intensity of the pixels from channel 1 (green signal). All coefficients used to estimate colocalisation under Volocity® analysis demonstrated with clarity and accuracy a relationship between CypA and TDP-43.

2.4.3 CypA and TDP-43 colocalize in primary neuronal cultures

To extend these findings from the proteomics and immunocytochemistry to a model relevant to neuronal proteinopathy, immunocytochemistry was performed on primary spinal cord cultures from non-transgenic (Ntg) mouse embryos. In particular, CypA and TDP-43 colocalisation was investigated in this biological setting by multiple-colour confocal microscopy.

Since spinal neuronal cultures contain different central nervous system populations, Smi-32 staining (blue), recognizing non-phosphorylated neurofilament H, was used to specifically label the neuronal population. Neuronal cell bodies, dendrites and some thick axons were clearly visualised, allowing to specifically identify colocalisation events in this cellular population (**Figure**

2.16). Dual staining of primary spinal neuronal cultures for TDP-43 (green) and Smi-32 (blue) revealed that TDP-43 displayed predominantly nuclear localisation, both in Smi-32 negative cells and in Smi-32 positive neurons, with some faint staining present also in soma and neurites. The combined immunostaining of CypA (red) and Smi-32 (blue) evidenced CypA expression in motor neurons as well as in other cellular populations; immunoreactivity was present both in the nuclei and in the cytoplasm of these cells. In particular, in Smi-32 positive cells, CypA labelling was clearly visualised in neuronal cell bodies, as well as in dendrites and axons. CypA (red) and TDP-43 (green) co-labelling evidenced areas of extensive overlap (yellow), particularly in association with Smi-32 staining. Interestingly, colocalisation events were clearly visualised in neuronal cell bodies, where a more intense labelling corresponded to the nuclear area. This staining profile indicated that also neuronal populations, and importantly MNs, showed CypA and TDP-43 colocalisation.

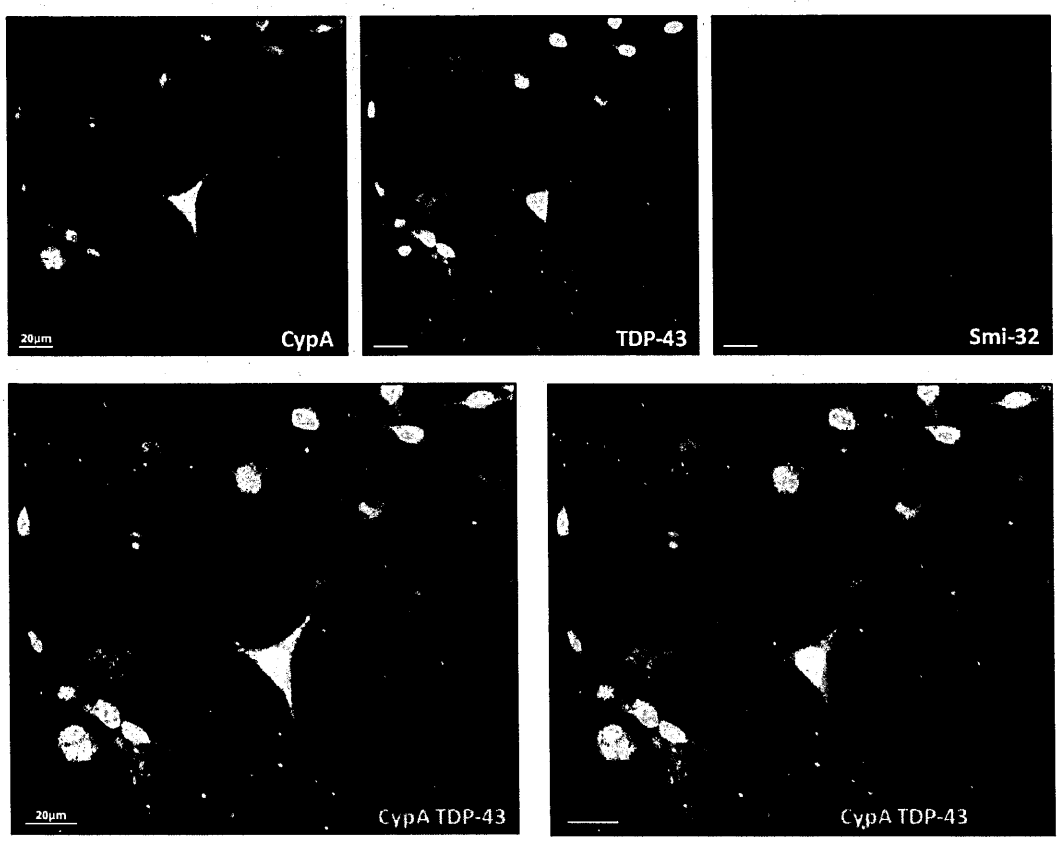

Figure 2.16 CypA and TDP-43 colocalisation in neuronal cultures.

Representative confocal micrograph of primary spinal cord cultures derived from non-transgenic embryos were co-stained for CypA (red, FITC), for TDP-43 (green, TRITC) and Smi-32 (blue, Cy5) and acquired by confocal microscopy (bar: 20µm). Insets with images at high magnifications show spatial colocalisation of endogenous CypA and TDP-43 proteins in motor neuron cells.

2.5 CypA/TDP-43 interaction is RNA-dependent

Since CypA (Montague 1994 and 1997; Krummrei 1995; Castello 2012), as well as TDP-43 (Ou 1995; Buratti 2001), and many of its interacting proteins identified in this proteomic analysis, are nucleic acid-binding proteins, we sought to determine if and how DNA or RNA binding influenced this interaction. CypA immunoprecipitation was performed in the presence of DNase I to degrade DNA or in the presence of RNase A to degrade RNA, followed by WB for TDP-43 (**Figure 2.17A**). This approach revealed that the association between CypA and TDP-43 was not abolished by DNA digestion, but was dependent upon RNA, since the interaction was almost lost after treatment with RNase A. Not treated (UNT) and coated magnetic beads (Ctr) samples were used respectively as positive and negative experimental controls.

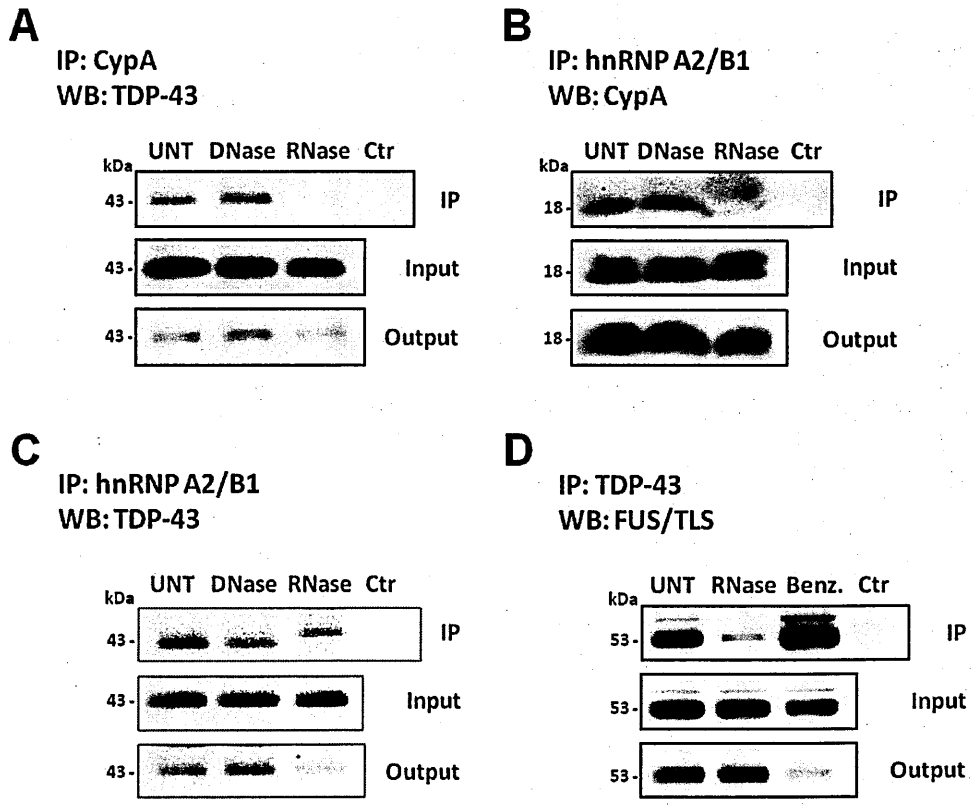

Figure 2.17 Nucleic acids impact on CypA and TDP-43 interactions.

HEK293 cells were used in co-IP experiments after pre-treatment with 5µl DNase I (Life Technologies Corporation) or 0.2mg/ml RNase A (Roche Applied Science) or 375U/ml Benzonase® Nuclease (Novagen, Inc.) for 15' at RT. Aliquot of whole cell lysates (INPUT), of the immunoprecipitates (IP) and of the remaining fractions (OUTPUT) were loaded together with coated beads as IP control, subjected to SDS-PAGE, transferred to PVDF membranes, stained with Red Ponceau as loading

control, probed with primary antibodies and detected by chemiluminescence. (**A**) TDP-43 was co-precipitated using an anti-CypA antibody. A band corresponding to TDP-43 was enriched in the IP fractions of untreated or DNase I-treated cells and was strongly reduced after RNase A treatment. (**B**) CypA co-immunoprecipitated with hnRNPA2/B1 in untreated or DNase I-treated cells. An altered staining pattern for CypA was observed in the IP fraction of RNase A-treated cells. (**C-D**) Some TDP-43 interactions are RNA-dependent. HnRNP A2/B1 co-immunoprecipitation with TDP-43 (**C**) and TDP-43 co-immunoprecipitation with FUS/TLS (**D**) were used as controls to validate this experimental approach. Immunoprecipitation was repeated at least four times with consistent results and representative images were chosen for display.

To further examine the influence of RNA on CypA interactions, hnRNP A2/B1 was immunoprecipitated in the presence of DNase I or RNase A and CypA presence was detected by WB. Also the association between CypA and hnRNP A2/B1 was dependent upon RNA, since binding was lowered by RNase A treatment and not by DNase I (**Figure 2.17B**).

To demonstrate the validity of this approach, we evaluated known interactions of TDP-43. First, RNase A treatment was demonstrated to partially mitigate the ability of TDP-43 to bind hnRNP A2/B1 (**Figure 2.17 C**). This observation was in accordance with previous data, indeed TDP-43 was reported to associate *in vitro* with hnRNP A2/B1 also in the absence of $(UG)_6$ RNA (Buratti 2005). Then TDP-43 was immunoprecipitated in the presence of RNase A or Benzonase® Nuclease, to evaluate its binding with FUS/TLS. TDP-43 and FUS/TLS interaction was strongly lowered, but not completely abolished, by RNase A and not by Benzonase® Nuclease (**Figure 2.17D**). Consistent with this finding, TDP-43 and FUS/TLS were demonstrated to associate with HDAC6 mRNA in intact cells and *in vitro*, but they were also shown to interact as purified proteins *in vitro* in an RNA-independent manner (Kim 2010).

RNase A treatment is likely to completely disassemble ribonucleoprotein complexes, thus abolishing both direct and indirect interactions between CypA and RNA binding proteins, as in the case of TDP-43 and hnRNP A2/B1 or FUS/TLS. Thus there are two possible hypothesis: the association of CypA with TDP-43 can be indirect and mediated by interaction with the same

transcript, as in the case of TDP-43 and FUS/TLS binding, or CypA can be present in a multimeric protein complex together with TDP-43 and other hnRNPs, like hnRNP A2/B1.

In conclusion, CypA and TDP-43 were demonstrated to associate in the nuclear and peri-nuclear region in the presence of RNA. These findings provide the first direct evidence that CypA and TDP-43 interact in mammalian cells.

3. Functional consequences of CypA-TDP-43 interaction

Evidence that CypA and TDP-43 are present in a biochemical complex was provided. The significance of this interaction, and the specific contribution and role of CypA in this complex needed to be further investigated. Several approaches were considered: first the construction of CypA mutants and then the protein knockdown helped to better characterise this interaction and to establish a possible functional role for this complex *in vitro*; subsequently, experiments on CypA knockout mice further evidenced putative functional effects *in vivo*.

3.1 *In vitro* evidence: Cyclophilin A mutants

The Myc-CypA construct was used to perform studies on the protein structure-function relationship: starting from site-directed mutagenesis on the protein sequence, the PPIase activity and one of its post-translational modifications (PTM) were examined to determine their requirement for CypA import and export to the nucleus or for its activity in a specific compartment of the cell, or for the interaction with other proteins.

3.1.1 PPIase-deficient mutant of CypA

To investigate the relevance and the involvement of CypA catalytic activity within this experimental setting, a mutant form of CypA that is deficient in the PPIase activity was generated. Several amino acid residues, such as His-54, Trp-121, Phe-113, His-126, Phe-60, and Arg-55, play a crucial role in the *cis-trans* isomerisation of the substrates mediated by CypA (Ansari 2002). While mutation of these individual amino acid residues differentially reduces the PPIase activity of CypA, alanine (Ala) replacement for the catalytic arginine (Arg) at position 55 has been shown to result in maximal reduction of its PPIase activity (PPIase catalysis was demonstrated to decrease by 1000 fold by Zydowsky 1992). Therefore, this substitution (Arg-55-Ala) generated a CypA lacking

its catalytic activity and thus unable to mediate the isomerisation of the peptidyl-prolyl bonds within the proteins (**Figure 3.1**).

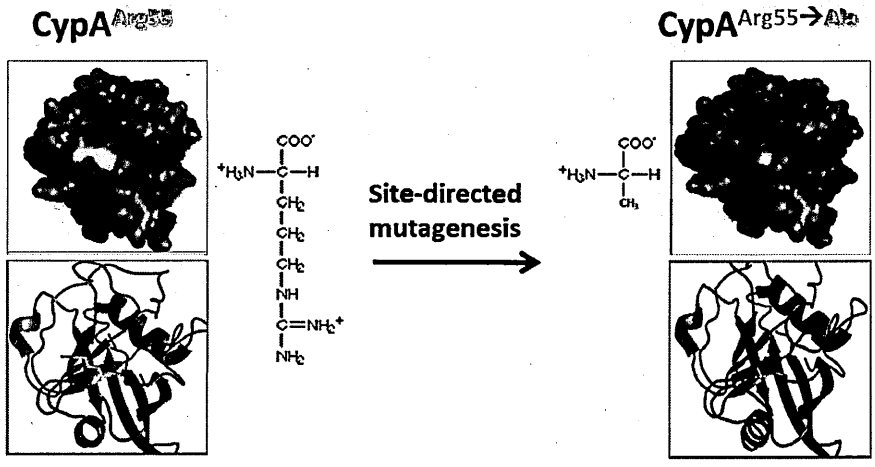

Figure 3.1 3D representations of the predicted surfaces of Arg-55-CypA and mutated Ala-55-CypA proteins.

Predicted 3D surface and cartoon representations of CypA molecular structure produced by PyMOL® Molecular Graphics System (Schrödinger). The PPIase cavity of CypA is shown in both wild type (left panel) and mutant (right panel) proteins; Arg-55, a critical residue for CypA catalytic activity, is highlighted in green, while the mutated Ala-55 is shown in red. R55A substitution within the active site of CypA causes a structural rearrangement of the PPIase pocket, thus leading to a nearly complete loss of the enzymatic activity.

3.1.2 Lysine 125 mutants of CypA

In order to deeply investigate the role of Lysine-acetylation, that is one of CypA PTMs, Lysine (Lys) in position 125 was mutagenized. In fact, CypA was demonstrated to be post-translationally modified in mammals, and in particular acetylated, on this specific residue by several studies (Kim 2006; Choudhary 2009; Chevalier 2012). Lys-125 is particularly interesting because it is located in a loop surrounding the active site of CypA and, although acetylation in this position does not seem to distort CypA conformation or rearrange its active site, it can notably alter the active site charge of the protein thus affecting/modulating the interaction with its binding partners. For example, acetylation at Lys-125 has been described to negatively affect the binding between CypA and its main ligand, cyclosporine A (CsA) (Lammers 2010). Moreover, mutations of this residue

with an anionic or neutral residue rendered the mutant protein unable to associate with calcineurin, even if both PPIase activity and high affinity for CsA were retained (Etzkorn 1994).

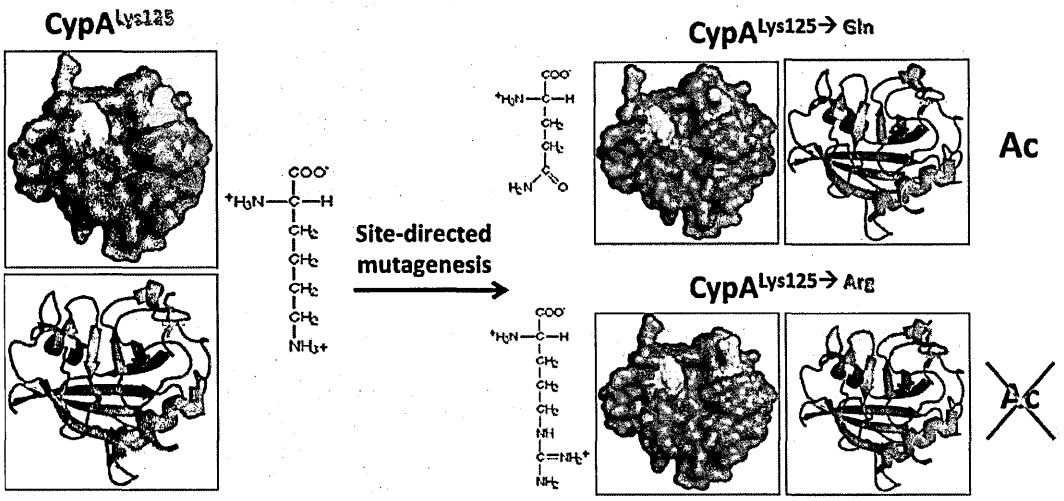

Figure 3.2 3D molecular structures of wild-type CypA and predicted representations of Gln/Arg-125-CypA mutants.

Predicted 3D surface and cartoon representations of CypA molecular structure produced by PyMOL® Molecular Graphics System (Schrödinger). Lysine (Lys) 125 (highlighted in green) is located in proximity of the PPIase cavity (active site) of CypA. In this picture the catalytic cavity is located just above this residue. The two substitutions, Lys-125-Gln (K125Q) and Lys-125-Arg (K125R) lead to the generation of mutant CypA proteins that cannot be acetylated at this position, and mimic a steadily acetylated (Ac) or non-acetylated CypA respectively (Gln and Arg in mutagenized CypA proteins are shown in red).

In this mutagenesis approach, Lys-125 was substituted with either a glutamine (Gln) or with an arginine (Arg) residue. Both mutations did not enable this position to be acetylated any more. In particular, the substitution with Gln mimicked a constitutively acetylated Lys, since Gln conserves the same structure as Lys, but abolishes its positive charge; whereas the substitution of the Lys with an Arg mimicked a constitutively non-acetylated Lys, since Arg preserves the same positive charge of the non-acetylated CypA isoform (**Figure 3.2**).

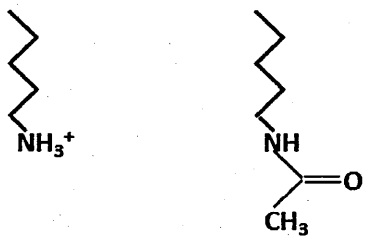

Lysine **Acetyl-Lysine**

3.1.3 CypA mutant generation

Point mutations were introduced in the CypA coding sequence by overlap-PCR (detailed procedure is explained in Materials and Methods section). Mutagenic primers were designed to alter the nucleotide sequence of CypA in a first round of PCR. The products of the first PCR were used as substrates in a second round of PCR, whose products were run on an agarose gel to verify the correct length of each fragment. Each cDNA fragment, carrying the point mutation, was digested and purified to be inserted into the original expression vector. This was used to transform competent bacteria that were plated on ampicillin-containing LB-agar plates. When ligation and transformation reactions had been achieved correctly, colonies grew only on plates where ligation products, and not digested-dephosphorylated plasmids, had been plated. To identify bacterial colonies containing the recombinant plasmid, colony screening was carried out by restriction analysis. At least four colonies for each condition were picked up and grown in liquid cultures in the presence of ampicillin. Extracted plasmid DNAs were digested and analysed on agarose gels. Correct constructs were selected when only two bands, corresponding to the linearized vector and the excised cDNA insert, were detected. Furthermore, to ensure the existence of the correct point mutations inside the generated cDNA and to exclude the presence of other unpredicted missense/non sense mutations, constructs were sequenced. Both forward and reverse sequence analyses were used to verify that the constructs carried the expected nucleotide substitutions and did not present any other mismatches (**Figure 3.3**).

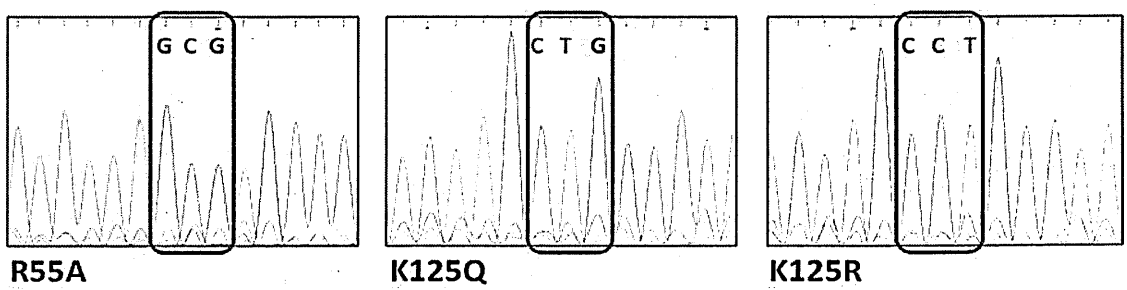

Figure 3.3 Sequencing of the cDNAs coding for Myc-CypA mutants.

Sequencing was performed on both DNA strands. The images shown highlight the codons carrying the point mutations generated and correspond to sequencing analyses performed on the reverse anti-sense DNA strand. Sequencing of the forward sense DNA strand (not shown) confirmed the same results.

Finally, selected vectors were tested for correct protein expression in HEK293 cells after transient transfection and were then amplified in bacteria to generate large amounts of plasmid DNA.

3.1.4 CypA mutant expression in HEK293 cells

First, plasmids encoding CypA mutants were tested for being efficiently transfected in HEK293 cells. To verify that, cells were transiently transfected with wild type, or R55A- or K125Q- or K125R-Myc-CypA and after 48 hours total lysates were analysed by WB. As shown in **Figure 3.4B**, the staining with the anti-CypA antibody revealed good expression levels. Myc-CypA immunoreactivity was quite similar for each mutated protein, indicating that each construct was easily received by the cells and that the corresponding protein was expressed correctly. As a negative control, cells were transfected with an empty vector.

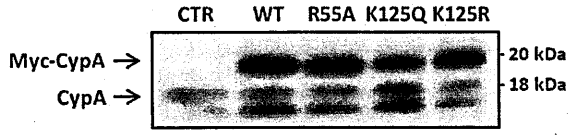

Figure 3.4 Myc-CypA mutants are expressed at similar levels in HEK293 cells.

HEK293 cells were transiently transfected with the empty vector (CTR) or the vector cloned with WT- or R55A- or K125R- or K125Q-Myc-CypA. 15 µg of total protein lysates were loaded, run on 12% SDS-PAGE gel, transferred on a PVDF membrane, stained with Red Ponceau as loading control, analysed by WB using the anti-CypA antibody and detected by chemiluminescence. Representative image was chosen for display.

3.1.5 Cell viability in cells expressing CypA mutants

In order to determine whether overexpression of mutagenized CypA proteins (R55A, K125Q or K125R) could affect cell viability, MTT assay was performed. Cells were transiently transfected

with plasmids encoding wild-type, R55A-, K125Q-, K125R- CypA or with an empty vector (CTR) as a control, and then cell viability was analysed after 48h. This experiment was repeated three times without any statistically significant alteration in cell survival among cells expressing different CypA isoforms. This result indicated that in this cell line the expression of the newly generated CypA mutated proteins (R55A, K125Q, K125R) did not have any significant effect on cell viability compared to control cells (**Figure 3.5**).

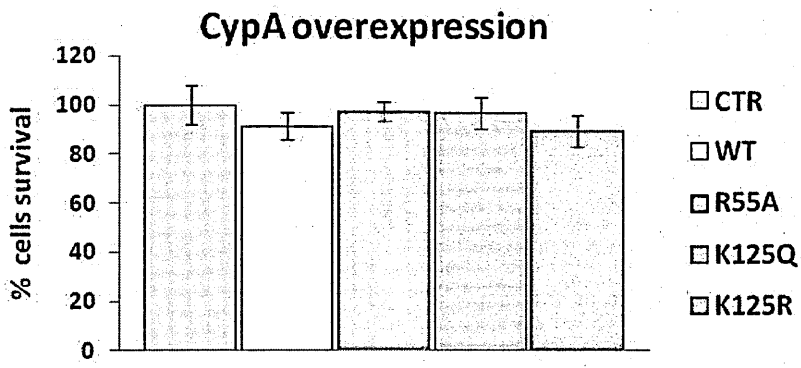

Figure 3.5 Effect of CypA mutants overexpression on cell survival.

Histograms represent the effect of wild-type and R55A-, K125Q- and K125R-Myc-CypA mutants overexpression in HEK293 on viability, compared to cells transfected with the empty vector (CTR). The conversion of MTT to formazan was used as an index of cell survival. Data (mean ± S.E., n≥5 for each sample) are expressed as percentages of control cells (CTR). Statistical analysis by Student's T-test did not evidenced any statistical significant difference in any experiment.

The same experiment was also performed in cells previously silenced for CypA and then transfected with the different constructs carrying different CypA mutations. Also in this case no differences in viability were detected among the samples analysed (data not shown). These observations were consistent with data previously obtained (Results section **1.6.4**).

3.1.6 CypA mutants isoform pattern

Once we had verified correct expression of Myc-CypA mutants in HEK293 cells, their isoform pattern was analysed by 2DE separation and WB for Myc-tag and CypA. Using the anti-Myc-tag

antibody, four protein spots were clearly detected (**Figure 3.6A**); while at least eight spots were distinguished when a polyclonal antibody against CypA was used (**Figure 3.6B**). These corresponded to four isoforms of the endogenous protein whereas four spots at higher MW were positive to both CypA and Myc-tag and corresponded to the exogenous tagged protein.

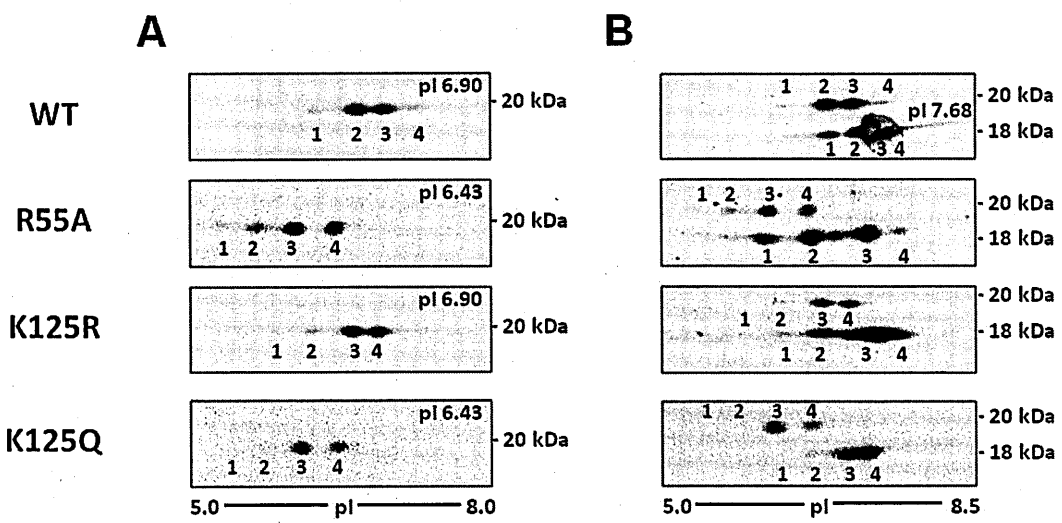

Figure 3.6 Myc-CypA mutants isoform pattern.

2DE-WB analysis of HEK293 cells transiently transfected with wild-type or R55A- or K125R- or K125Q-Myc-CypA. 50µg of total protein lysates were separated by IEF using 7cm pH 3-10NL pI range strips, run on 12% SDS-PAGE gels, transferred on PVDF membranes, stained with Sypro® Ruby Protein Blot stain as loading control, analyzed by WB using the anti-Myc-tag (**A**) or the anti-CypA (**B**) antibodies and detected by chemiluminescence. Aligned 2DE blots are shown.

The isoform pattern was different for each Myc-CypA mutant when compared both to wild-type Myc-CypA or to the endogenous protein. Furthermore, endogenous CypA behaviour by 2DE was variable, suggesting that the protein was prone to differential post-translational modification depending on the exogenous Myc-CypA mutant expressed. In addition to the difference in the molecular weight between the endogenous and the transfected proteins, due to the Myc-tag fused at the C-terminal end of the protein sequence, the isoelectric point (pI) also varied.

The expected pI values for CypA mutant proteins were computed through the proteomic server Expasy by the Swiss Institute of Bioinformatics (www.expasy.org). The PPIase-deficient mutant

and the glutamine mutant at Lys-125 of CypA had both a predicted pI of 6.43, whereas the computed pI of the Arg-125 mutant was 6.90 and thus similar to wild-type Myc-CypA. The pI values observed perfectly fitted with the predicted ones. In fact, all Myc-CypA proteins were shifted towards a more acidic pI, compared to the endogenous unmodified CypA, whose predicted pI is 7.68. In particular, the R55A and K125Q mutants were further shifted towards a more acidic pI if compared to the other Myc-tagged proteins. Indeed, in both cases a positively charged residue was substituted with a residue containing a neutral side chain.

Interestingly, Lys-125 mutants could not be acetylated at this position, and this was evidenced in the 2DE blots of both K125R and K125Q mutants by an almost complete loss of the spots corresponding to isoform one and a striking reduction of isoform two, with an overall shift towards more basic forms. This observation is in agreement with a recent work demonstrating that Lysine-acetylation is one of the PTM responsible for the shift of CypA isoforms one and two towards more acidic pI (Chevalier 2012).

3.1.7 Subcellular distribution of CypA mutants

Endogenous CypA can be found within the nucleus or the cytoplasm (Results section 1.3.3). To establish whether mutant Myc-CypA proteins retained the same distribution as the wild-type protein, two independent methods were used: biochemical fractionation of the cytoplasmic and nuclear compartments and confocal microscopy of transfected cells.

The biochemical approach consisted of the separation of the cytosolic and nuclear fractions in cells transiently transfected with wild-type or mutagenized Myc-CypA proteins or the empty vector as a negative control. To rule out nuclear and/or cytoplasmic contaminations during cellular fractionation, cytoplasmic and nuclear-specific markers, respectively actin and lamin A+C, were evaluated. Then, each subcellular fraction was independently analysed by WB using antibodies for CypA or the Myc-tag portion of the protein.

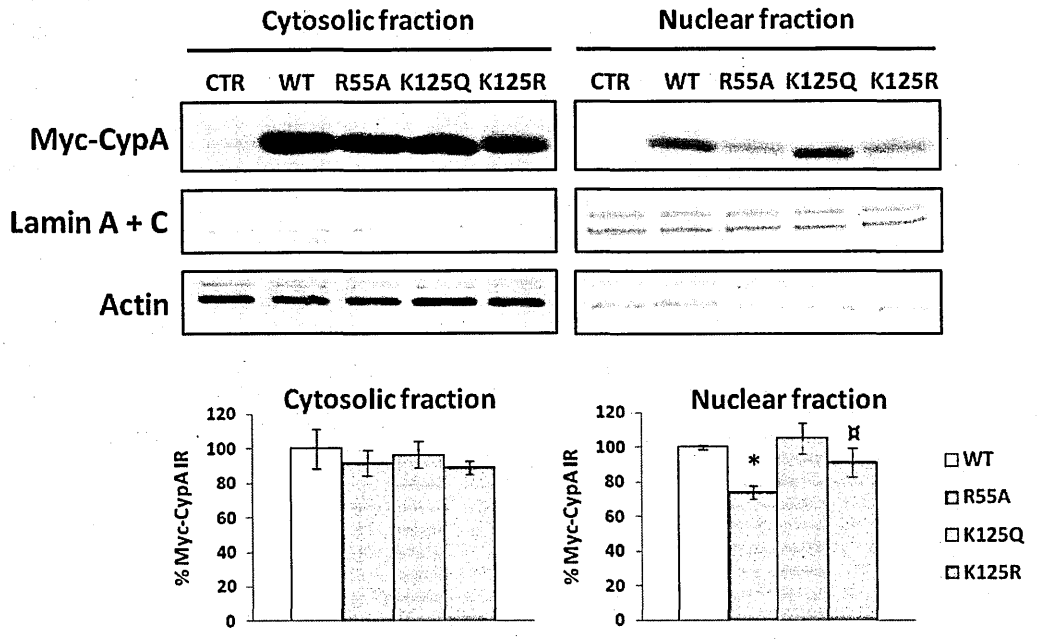

Figure 3.7 Myc-CypA mutants subcellular distribution.

HEK293 cells were transfected with the empty vector (CTR), or WT- or R55A- or K125Q- or K125R-Myc-CypA, then equal amounts of cytosolic and the corresponding nuclear fractions were independently analyzed by WB and detected by chemiluminescence. Lamin A+C and actin were evaluated as controls for nuclear and/or cytoplasmic contamination of the two fractions. Histograms represent the quantitative analysis of Myc-CypA band densities in the two subcellular compartments, normalized on the actual amount of proteins loaded, as detected by Red Ponceau staining. Data (mean ± S.E., n=3) are expressed as percentages of control cells (WT) in each subcellular fraction. Symbols indicate that samples are significantly different (*=p≤0.05 R55A vs. WT; ¤= p≤0.01 K125R vs. K125Q), as assessed by One-way Anova followed by Newman-Keuls multiple comparison test. R55A and K125R mutants displayed a lower nuclear expression.

The quantification of Myc-CypA blots clearly indicated that in the cytoplasmic fraction signals corresponding to mutagenized CypA proteins were comparable to the wild-type protein, while in the nuclear compartment Myc-CypA mutant expression changed (**Figure 3.7**). In particular, K125Q-Myc-CypA was present in the nucleus with similar levels to WT-Myc-CypA, whereas R55A- and K125R-Myc-CypA expression was significantly reduced in this cellular compartment. Indeed a substantial decrease in the intensity of the bands corresponding to R55A and K125R mutants was observed by WB in the nuclear fraction of transfected HEK293 cells. These pieces of evidence suggested that R55A and K125R substitutions within CypA sequence, resulted in a partial impaired

nuclear localisation of the protein. This could be caused by a reduction in nuclear import or, alternatively, by an increase in the rate of nuclear export of these mutated CypA proteins.

Data obtained with the PPIase-deficient mutant of CypA could be linked to a lack of enzymatic activity, that could be required for a correct localisation of this protein. Alternatively this modification, leading to a conformational structural change of the protein, could result in an anomalous folding of the polypeptide chain which likely impairs the nuclear translocation of this mutated form of CypA.

The results obtained with Lys-125 mutants, could be explained hypothesizing that CypA undergoes a covalent modification on this residue promoting its association with the nuclear transport machinery, thus resulting in an efficient nuclear translocation. Indeed the K125Q-CypA mutant, which mimics the acetylated form of CypA, was demonstrated to be more abundant in the nuclear fraction compared to the K125R mutant, which on the contrary mimics the non-acetylated CypA isoform. This evidence indicated that acetylation at Lys-125 could represent one of the factors that triggers the nuclear translocation of CypA in mammalian cells. This is in accordance with the data described in Results section 1.4, where the presence of lysine-acetylated CypA was clearly demonstrated only in the nuclear compartment and not in the cytosolic fraction.

The presence of all Myc-CypA mutants was also tested in the extracellular media of transiently transfected HEK293 cells in order to evaluate their ability to be secreted. Both Lysine-125 mutants and PPIase-deficient CypA were released from these cells, suggesting that nor acetylation at Lys-125 neither the enzymatic activity of CypA have any influence on its secretion (data not shown).

3.1.8 Localisation of CypA mutants

Additional evidence in support of the biochemical fractionation experiments was provided by confocal microscopy analysis. In particular, colocalisation of endogenous and overexpressed Myc-tagged CypA proteins was investigated to visualise whether CypA distribution could be affected by

specific point mutations in its sequence. HEK293 cells transiently transfected with WT- or R55A- or K125Q- or K125R-Myc-CypA were sequentially stained with a polyclonal anti-CypA antibody and a monoclonal anti-Myc-tag antibody (**Figure 3.8**). This double labelling allowed a fair comparison of the whole CypA (endogenous and exogenous, revealed by the CypA antibody) with the signal relative only to the exogenous one (detected with the anti-Myc-tag antibody) in the same image. The IF experiments did not show any striking variation in Myc-CypA distribution among the different mutants. However, dual staining revealed a clearer nuclear colocalisation signal in cells transfected with WT- or K125Q-Myc-CypA proteins compared to cells expressing the R55A or K125R mutants. Indeed, R55A- and K125R-Myc-CypA showed a more diffuse Myc-tag staining, thus resulting in a slight depletion from the nucleus.

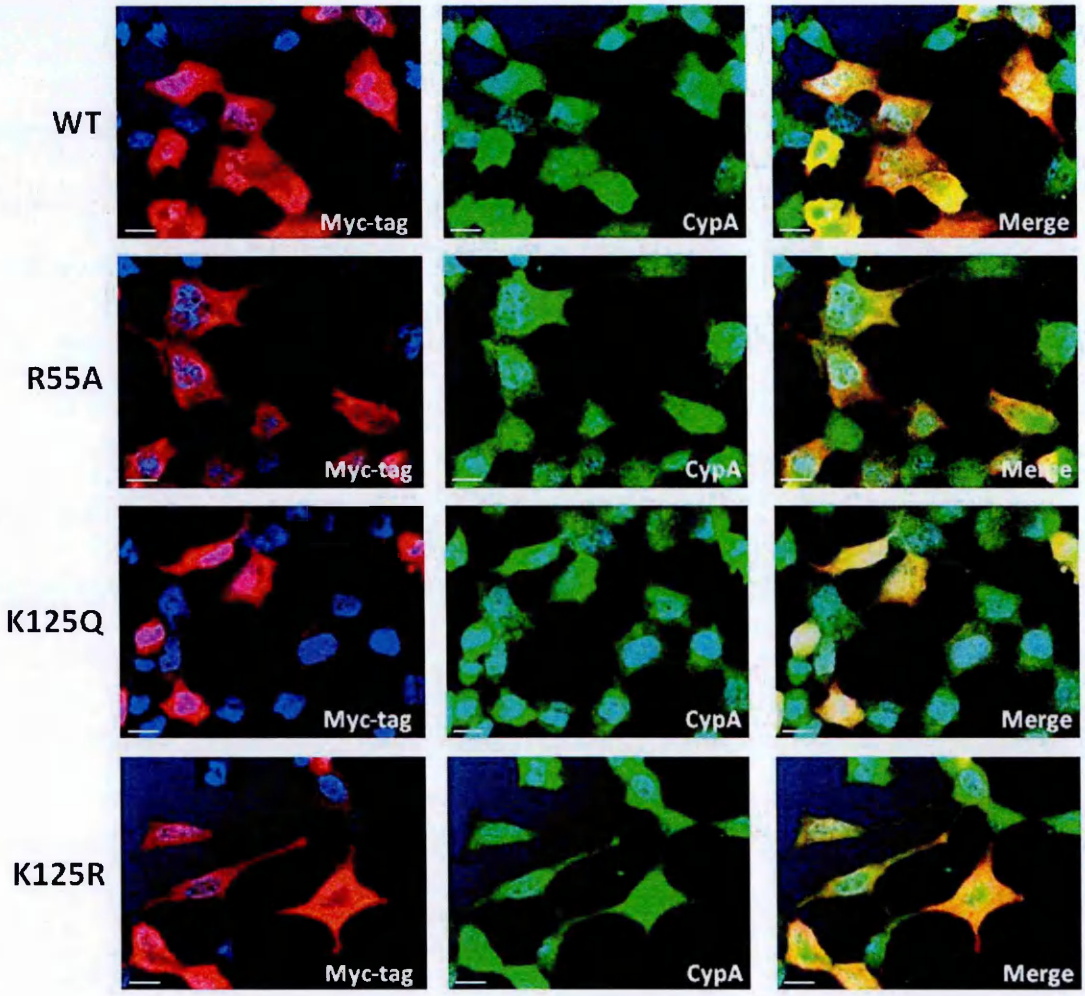

Figure 3.8 Myc-CypA mutants immunofluorescence analysis.

Representative immunostaining micrographs show spatial colocalisation of CypA (green) and Myc-tagged CypA (red) proteins in HEK293 cells 48h after transient transfection with WT- or R55A- or K125Q- or K125R-Myc-CypA (bar: 15µm). CypA was detected by a polyclonal rabbit antibody and an Alexa®488-conjugated secondary antibody, while Myc-CypA was detected by a monoclonal mouse antibody followed by incubation with an Alexa®594-conjugated secondary antibody. 4'-6-Diamidino-2-phenylindole (DAPI) was used to stain the nuclei (blue). Both the endogenous CypA and the exogenous tagged CypA were immunostained by CypA antibody (green) whereas using the anti-Myc-tag antibody only transfected Myc-CypA were recognized (red). Co-localisation between endogenous CypA and exogenous Myc-CypA was observed in overlay of red and green images (right panels), with areas of orange and yellow indicating colocalisation of the proteins. As negative experimental control, cells were transfected with an empty vector, co-immunostained with the same antibody mixture and absence of the Myc-tag signal was verified (images not shown). Experiments were repeated several times with consistent results and representative images were chosen for display. R55A- and K125R-Myc-CypA mutants showed an impaired nuclear localisation.

Immunofluorescence results supported the hypothesis, based on previous biochemical observations, that R55A and K125R substitutions in CypA sequence resulted in an impaired or less efficient translocation of these mutated proteins in the nucleus. The K125Q mutant instead was shown to maintain a correct distribution, similar to the WT protein, thus suggesting that the presence of an acetyl group on Lys125 which in this case was mimicked by an amino acid like Gln, could favour a nuclear localisation for CypA. In fact, lysine acetylation is widely reported to regulate the cellular localisation of proteins, especially for nuclear import and export. For some proteins, acetylation enhances localisation in the cytoplasm, whereas for others acetylation will preferentially favours a nuclear localisation. The mechanism by which acetylation influences cellular localisation can be either the modification of an interaction with a binding partner leading to retention in a particular compartment, or an altered interaction with nuclear import/export factors (reviewed in Sadoul 2011).

3.1.9 Interaction of CypA mutants with TDP-43

To gain a better understanding of the relationship between CypA and TDP-43, their binding was characterised using mutated CypA proteins. In particular, to understand whether the substituted

amino acids in CypA sequence could have an influence in modulating this protein-protein interaction, a co-immunoprecipitation approach was adopted. HEK293 cells were transiently co-transfected with Flag-TDP-43 along with WT-Myc-CypA or alternatively with different Myc-CypA proteins carrying the R55A, K125Q, K125R mutations. As negative control for the co-immunoprecipitation experiment, cells were transfected with an empty vector (CTR). Whole cell lysates were then subjected to immunoprecipitation with the anti-Myc-tag antibody, resolved by SDS-PAGE, and immunoblotted with a polyclonal anti-TDP-43 antibody. Subsequently, the same blots were re-probed with an anti-CypA antibody to evaluate the immunoprecipitation efficiency. This approach allowed to selectively immunoprecipitate only transfected Myc-CypA proteins (both WT and mutated ones) and to detect by WB the associated TDP-43 molecules (**Figure 3.9** and **Figure 3.10**). Indeed, only tagged Myc-CypA proteins were immunoprecipitated in a specific way, without significant contaminations, as shown in the IP fraction. This was further confirmed by the experimental negative control, whose IP fraction contained negligible amounts of proteins. Moreover, the input fractions of the same samples are shown (lower panels), indicating the presence of equal amounts of transfected and endogenous proteins.

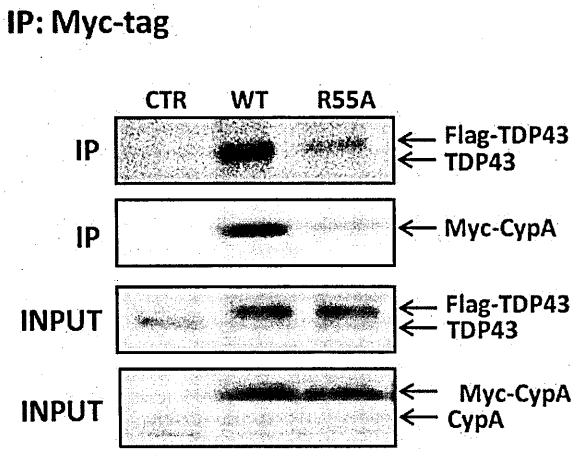

Figure 3.9 PPIase-deficient CypA interacts with TDP-43.

HEK293 cells were transfected with the empty vector (CTR), or co-transfected with Flag-TDP-43 and WT- or R55A-Myc-CypA. Myc-CypA was selectively immunoprecipitated from the cell lysate using an anti-Myc-tag antibody. Co-precipitated proteins were separated by 12% SDS-PAGE, transferred to a PVDF membrane, and reversibly stained with Red Ponceau, as a loading control. Potentially

associated TDP-43 proteins were then detected by WB using an anti-TDP-43 antibody, whereas immunoprecipitated Myc-CypA proteins were detected using an anti-CypA antibody (upper panels). 15μg of the corresponding input samples were loaded on the same gel and blotted with the same antibodies (lower panels). Representative results of three independent experiments are shown, indicating that despite the mutation in the active site, R55A-Myc-CypA maintains its capability to bind TDP-43.

PPIase-deficient CypA, like the WT protein, was able to co-immunoprecipitate TDP-43 (upper panel), thereby suggesting that the R55A mutation, which is located within CypA active site, did not affect the physical interaction with TDP-43 (**Figure 3.9**). Only a slight difference was observed between the WT condition and the R55A mutant in the IP fraction, where a lower signal for TDP-43 detected. However, it should be considered that R55A-Myc-CypA could not be efficiently immunoprecipitated, nor by the anti-Myc-tag antibody neither by the anti-CypA antibody, both monoclonal and polyclonal (not shown). For this reason, no quantification for this interaction has been reported, because it was considered not reliable, and only a qualitative evaluation was appropriate. This anomalous behaviour in IP could be explained by a decreased affinity of the primary antibody for the R55A-Myc-CypA in non-denaturing conditions. These data demonstrated that PPIase enzymatic catalysis mediated by CypA was not required for an efficient binding with TDP-43.

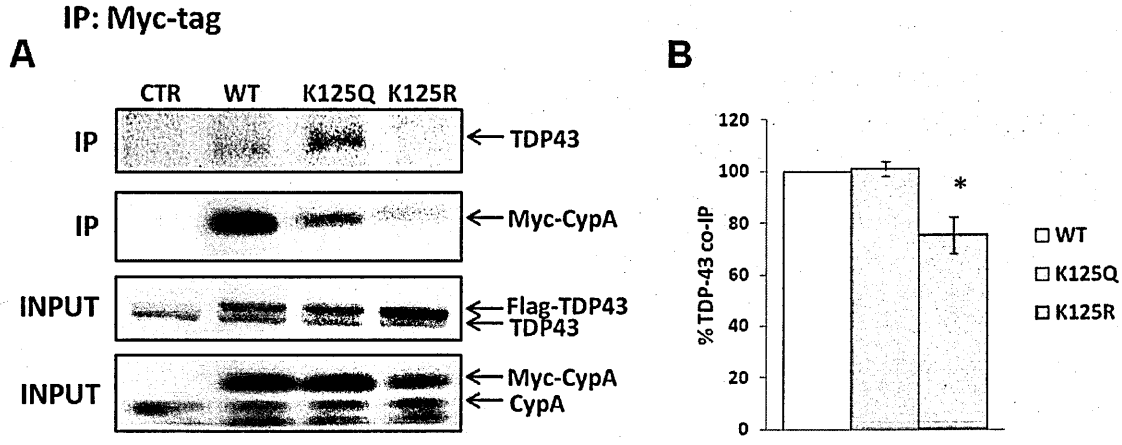

Figure 3.10 K125Q-CypA binds TDP-43, while K125R-CypA binding is impaired.

(**A**) HEK293 cells were transfected with the empty vector (CTR), or co-transfected with Flag-TDP-43 and WT- or K125Q- or K125R-Myc-CypA. Myc-CypA was selectively immunoprecipitated from whole cell lysates using an anti-Myc-tag antibody. Aliquot of the lysates (INPUT) and of the immunoprecipitates (IP) fractions were separated by 12% SDS-PAGE, transferred to a PVDF membrane, and reversibly stained with Red Ponceau, as a loading control. Potentially associated TDP-43 proteins were detected by WB using an anti-TDP-43 antibody, whereas immunoprecipitated Myc-CypA proteins were detected using an anti-CypA antibody. Representative results of three independent experiments are shown, indicating that K125Q but not K125R preserves the capability of binding TDP-43 as the WT protein. (**B**) Histograms represent the quantitative analysis of TDP-43 band densities in the IP fraction, normalized on the actual amount of Myc-CypA proteins immunoprecipitated. Data (mean ± S.E., n=3) are expressed as percentages of control cells (WT). Asterisk indicates that K125R was significantly different compared to both WT- and K125Q-Myc-CypA (*=p≤0.01), as assessed by Student's t-test.

Myc-CypA mutants at Lys-125 were both able to form complexes with TDP-43, but a sharp distinction could be made among the two proteins. In particular, K125Q-Myc-CypA co-immunoprecipitated TDP-43 like the WT protein, while there was a marked reduction in the co-immunoprecipitation rate of TDP-43 with K125R-Myc-CypA (**Figure 3.10A-B**). These experiments demonstrated that the substitution of Lys-125 with Arg was sufficient to impair the binding between TDP-43 and CypA in a statistically significant way. Interestingly, an Arg was introduced to mimic the absence of the acetyl group on a Lys residue, and Gln to mimic acetylation. These results suggested that CypA Lys-acetylation in position 125 might be one factor that promoted a correct interaction with TDP-43.

Additional experiments performed using a slightly different approach were able to replicate the observations previously described. In particular, HEK293 cells were transfected only with Myc-CypA constructs, Myc-CypA was selectively immunoprecipitated and endogenous TDP-43 was detected by WB in the co-IP fraction (images not shown).

Taken together, these data from co-immunoprecipitation experiments suggested that intrinsic PPIase activity was not essential for the binding of CypA with TDP-43, and that acetylation of a

specific lysine residue of CypA could play an essential role in regulating its affinity for its binding partner TDP-43.

3.1.10 CypA mutants expression did not alter TDP-43 or hnRNP A2/B1 subcellular distribution

CypA mutants showing an impaired interaction with TDP-43, also displayed an altered subcellular distribution with a decreased localisation in the nuclear compartment, that is where the two proteins were found associated. In order to understand if CypA mutant proteins expression was sufficient to influence also the subcellular localisation of other proteins, CypA binding partners distribution was analysed by biochemical fractionation (**Figure 3.11**). In particular, the cytosolic and the nuclear fractions were separated in HEK293 cells transiently transfected with wild-type or PPIase-deficient CypA or lysine-125 mutants or the empty vector as negative control. Each subcellular fraction was independently analysed by WB for TDP-43 and hnRNP A2/B1. No significant differences were detected in either the cytosolic or the nuclear compartment of CypA mutants transfected cells compared to both WT or CTR cells. These results clearly indicate that neither CypA Lysine-acetylation nor its catalytic activity could modify TDP-43 or hnRNP A2/B1 relative distribution in HEK293 cells.

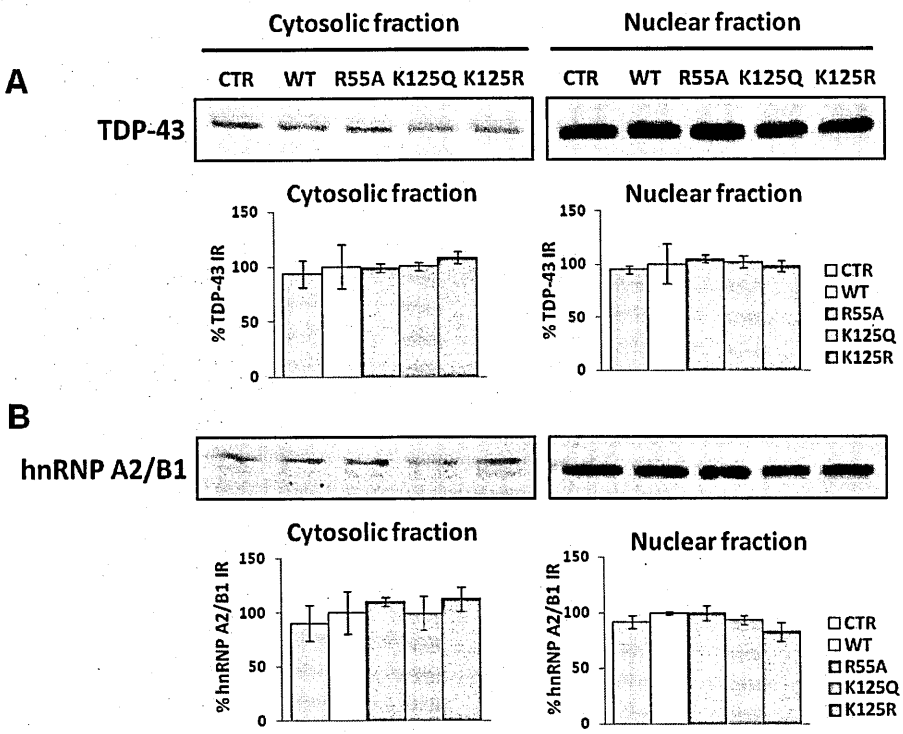

Figure 3.11 TDP-43 and hnRNP A2/B1 subcellular distribution were not altered by Myc-CypA mutants expression.

HEK293 cells were transfected with the empty vector (CTR), or WT- or R55A- or K125Q- or K125R-Myc-CypA, then equal amounts of cytosolic and the corresponding nuclear fractions were independently analysed by WB and detected by chemiluminescence. Lamin A+C and Actin were evaluated as controls for nuclear and/or cytoplasmic contamination of the two fractions (not shown). Histograms represent the quantitative analysis of (**A**) TDP-43 or (**B**) hnRNP A2/B1 band densities in the two subcellular compartments, normalized on the actual amount of proteins loaded as detected by Red Ponceau staining. Data (mean ± S.E., n=3) are expressed as percentages of control cells (WT) in each subcellular fraction. Samples were not significantly different, as assessed by One-way Anova.

3.2 *In vitro* evidence: CypA knockdown

CypA has long been known to function as a peptidyl-prolyl *cis-trans* isomerase, and it was also demonstrated to function as a chaperone (Freskgard 1992; Moparthi 2010). Nevertheless, the PPIase catalytic centre of CypA was not involved in the CypA/TDP-43 recognition event, as demonstrated by overexpression of the CypA-R55A mutant (Results section **3.1.9**). These findings raise the interesting possibility that CypA may play alternative roles in the assembly of this complex. For example, CypA could act as a chaperone molecule. Molecular chaperones, like

cyclophilins, have diverse roles to regulate protein conformation (Morimoto, 2008), and have only incremental effects on protein folding, arguing against an essential role for them in protein maturation (Dolinski 1997). Cyclophilins can bind at hydrophobic patches on their target protein without necessarily isomerising a peptidyl-prolyl bond, thereby preventing misfolding (Baker 1994; Ferreira 1996; Arié 2001) and accelerating folding (Wang 2010), assisting in assembly and disassembly of macromolecular complexes (Teigelkamp 1998), regulating translocation (Rycyzyn 2000; Ansari 2002; Pan 2008) and modulating the activity of the target protein (Braaten 1997; Streblow 1998; Shen 1998; Crenshaw 1998; Wu 2000). A particularly interesting question is whether CypA can have any influence on proper localisation of TDP-43 or can play a significant role in folding and disaggregation. A first answer came from *in vitro* experiments where CypA was specifically silenced, in order to directly observe the effects of the loss of CypA function. In particular, CypA knockdown was performed in HEK293 cells delivering a specific siRNA or a control siRNA (scramble).

3.2.1 TDP-43 expression and localisation after CypA knockdown

To start addressing this issue, 48 hours after silencing, HEK293 nuclei were separated from the cytoplasm by biochemical fractionation, and TDP-43 was detected by WB in both subcellular compartments. The quantification of TDP-43 blots clearly indicated that, in the cytoplasmic fraction, signals corresponding to CypA silenced samples were comparable to scrambled siRNA treated cells (**Figure 3.12A**). Instead, in the nuclear compartment, TDP-43 expression was significantly reduced after CypA knockdown (**Figure 3.12B**). The specific reduction in TDP-43 nuclear expression following CypA silencing could not be appreciated in whole cellular lysates, as shown in **Figure 3.12D**.

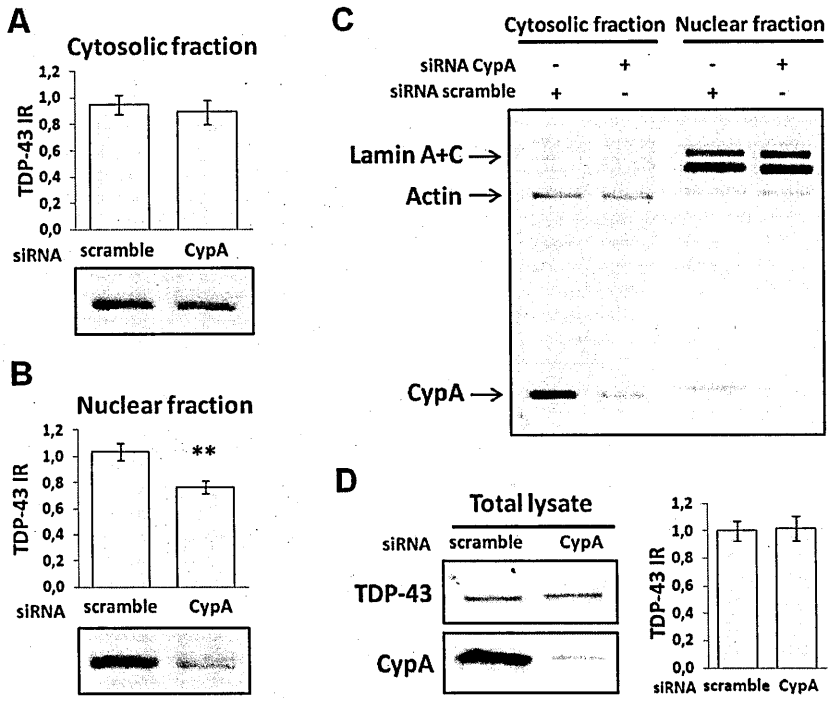

Figure 3.12 CypA silencing influenced TDP-43 nuclear distribution without significantly affecting its total expression.

HEK293 cells were transiently transfected with 10nM siRNA^{scramble} or siRNA^{CypA} for 48h. Equal amounts of whole cell lysate, and the corresponding cytosolic and nuclear fractions were independently analysed by WB and detected by chemiluminescence. Reversible Red Ponceau staining was used as loading control. (**A-B**) Representative WB for TDP-43 and relative histograms of the cytosolic (**A**) and nuclear (**B**) fractions, representing the quantitative analysis of TDP-43 band densities in the two subcellular compartments, normalized on the actual amount of proteins loaded, as detected by Red Ponceau staining. Data (mean ± S.E., n=6) are expressed as percentages of control cells (scramble) in each subcellular fraction. Symbols indicate that TDP-43 displayed a significantly lower nuclear expression after CypA knockdown (**=p≤0.01 siRNA^{CypA} vs. siRNA^{scramble}), as assessed by Student's t-test. (**C**) Lamin A+C and Actin were evaluated as controls for nuclear and/or cytoplasmic contamination of the two fractions. CypA expression was strongly reduced in each compartment after siRNA^{CypA} treatment compared to siRNA^{scramble}. (**D**) Representative WB for CypA (lower panel) or TDP-43 (upper panel) and relative histogram with its quantification are shown in whole cell lysate, where TDP-43 protein levels did not vary.

These data suggested that CypA knockdown did not substantially influence the global expression of TDP-43, but it could alter the subcellular distribution of the protein.

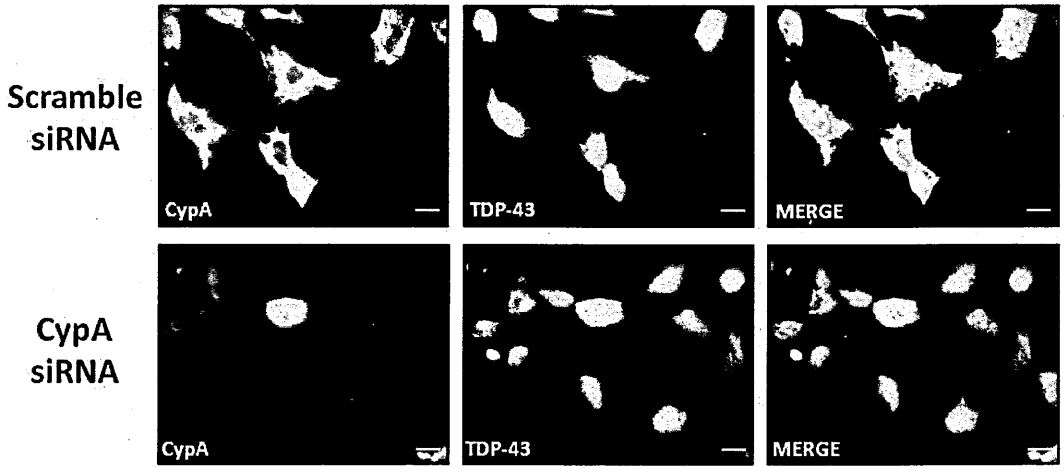

Figure 3.13 TDP-43 localisation in CypA silenced cells.

HEK293 cells were transiently transfected with 10nM $siRNA^{scramble}$ or $siRNA^{CypA}$ for 48h. Representative immunofluorescence images of HEK293 cells after silencing stained for CypA (red) using Alexa®647-conjugated secondary antibody and TDP-43 (green) using Alexa®488-conjugated secondary antibody are shown (bar: 15µm). A less intense TDP-43 nuclear staining was detected following CypA knockdown.

The effect of CypA knockdown on TDP-43 was then analysed by confocal immunofluorescence. TDP-43 (green) localisation was visualised simultaneously with CypA (red) staining in cells transfected with $siRNA^{CypA}$ or $siRNA^{scramble}$. This approach helped to distinguish cells efficiently silenced for CypA from cells still expressing the protein. In cells treated with the scrambled siRNA, TDP-43 was predominantly localized in the nucleus whereas CypA was present mainly in the cytosol but also in the nucleus (**Figure 3.14**), as previously observed (**Figure 3.13**). In cells incubated with CypA siRNA, TDP-43 seemed to preserve its localisation pattern as in control cells, although displaying a less intense nuclear staining.

Immunofluorescence results further corroborated biochemical observation, indicating that CypA could be required for TDP-43 correct localisation/redistribution inside the nucleus. However, further analyses are needed to define the real effects mediated by CypA depletion on intracellular TDP-43 trafficking and function.

3.2.2 CypA is involved in hnRNP complex formation

TDP-43 functionally associates with several hnRNP proteins and, in particular, hnRNP A2, that is the major hnRNP protein recognized by TDP-43 according to pull-down assays (Ayala 2005). This interaction leading to formation of a hnRNP-rich complex seems to be essential for the splicing inhibitory activity of TDP-43 (Buratti 2005). The results previously described clearly demonstrated that CypA, TDP-43 and hnRNP A2/B1 may form a complex with each other and these interactions are RNA-dependent. In this respect, it is possible to hypothesise that they are together part of a larger protein complex. It is therefore likely that CypA might be a component of hnRNP-rich complexes, together with TDP-43 and other hnRNP proteins, like hnRNP A2/B1, abundantly represented in CypA interactome. Indeed TDP-43 and CypA have been previously demonstrated to co-immunoprecipitate with anti-hnRNP A2/B1 antibody (Results section **2.2.1**). In order to test whether CypA is required for hnRNP complex assembly or stabilization, the same co-IP assay was replicated in cells expressing or silenced for CypA. In particular, HEK293 whole cellular lysates were co-IP 48 hours after treatment with $siRNA^{scramble}$ or $siRNA^{CypA}$. CypA knockdown was verified at the protein level, as shown in the input fraction. When the CypA expression level was decreased by a specific siRNA molecule, the presence of TDP-43 in hnRNP A2/B1 co-IP fraction was dramatically reduced in respect to scrambled siRNA treated cells, despite comparable expression levels in the starting samples (**Figure 3.14**). This experiment was repeated several times, replicating the same observation: when CypA is silenced TDP-43 and hnRNP A2/B1 interaction is severely impaired. These results suggested that CypA is fundamental for the interaction of TDP-43 with at least hnRNP A2/B1. Indeed CypA absence could disrupt the binding between these two proteins within this hnRNP complex.

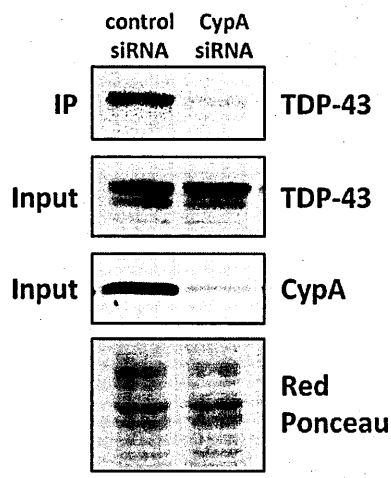

Figure 3.14 CypA interaction with TDP-43 is implicated in hnRNP complex formation.
HEK293 cells were transiently transfected with with siRNA^{scramble} or siRNA^{CypA}. TDP-43 was co-precipitated using an anti-hnRNPA2/B1 antibody. Aliquot of whole cell lysates (INPUT) and of the immunoprecipitates (IP) were loaded together, subjected to SDS-PAGE, transferred to a PVDF membrane, stained with Red Ponceau as loading control, probed with primary antibodies and detected by chemiluminescence. A band corresponding to TDP-43 was enriched in the IP fractions of cells treated with siRNA^{scramble} and was strongly reduced after siRNA^{CypA} treatment. The input fraction was first probed for TDP-43 to verify that the protein was expressed with comparable levels after silencing, and then for CypA to check knockdown efficiency. Immunoprecipitation was repeated at least three times with consistent results and representative images were chosen for display.

In this model, CypA could simply function in mediating a protein-protein interaction with TDP-43 and hnRNP A2/B1, or it could induce a conformational change in one of its target proteins. Another possibility is that the aberrant hnRNP complex formation is directly linked to the observed depletion of TDP-43 from the nucleus following CypA knockdown. In this case CypA could function in balancing TDP-43 intracellular distribution, thus contributing to the correct hnRNP complex assembly. Whatever its identity, target proteins appeared to be directly involved in this hnRNP complex formation, since CypA knockdown negatively affected the efficient binding of TDP-43 with hnRNP A2/B1.

3.2.3 CypA/ TDP-43 are involved in regulation of HDAC6 expression

To further establish the functional significance of CypA/TDP-43 association, we sought to understand how the described hnRNP complex could operate in putative TDP-43 physiological functions. Several RNA targets of TDP-43 are now known. Among them, recent microarray screens identified Histone Deacetylase 6 (HDAC6) as an altered transcript in TDP-43 silenced cells (Fiesel FC 2010) and in conditional knockout mice (Chiang 2010). Moreover, HDAC6 was consistently identified by systematic sequencing of RNA isolated by CLIP using TDP-43 antibodies *in vivo* (Tollervey 2011; Polymenidou 2011). TDP-43 was demonstrated to bind to HDAC6 mRNA and to regulate its expression (Fiesel 2010) in complex with FUS/TLS (Kim 2010). Interestingly, HDAC6 down-regulation after TDP-43 silencing was associated to impaired cellular turnover of aggregating proteins and reduced neurite outgrowth (Fiesel 2010 and 2011), a molecular mechanisms that could contribute to pathogenesis.

To gain insights on possible common biochemical pathways operated by TDP-43 and CypA, we investigated whether CypA could modulate this RNA-related TDP-43 activity. First, TDP-43 knockdown conditions were replicated treating HEK293 cells with a siRNA molecule targeting the 3'-UTR within TDP-43 locus (Results section **4.2**). TDP-43 knockdown of up to 90% was evaluated at the protein level by WB on whole cell lysates (upper panel). HEK293 cells treated with a scrambled siRNA were used as a negative experimental control. TDP-43 silencing was confirmed to reduce HDAC6 protein level relative to cells transfected with control siRNA (scramble) (**Figure 3.15**), supporting previous findings (Fiesel 2010; Kim 2010). Next, we tested whether CypA silencing could affect TDP-43-dependent regulation of HDAC6 expression. First, CypA silencing efficiency was verified by WB. Surprisingly, a downregulation of HDAC6 protein expression was detected also after CypA knockdown, relative to scrambled siRNA control cells. Furthermore, the effect observed on HDAC6 protein level was almost comparable to the one found in TDP-43 silenced cells. Equal protein expression among different samples was revealed by WB for Tubulin.

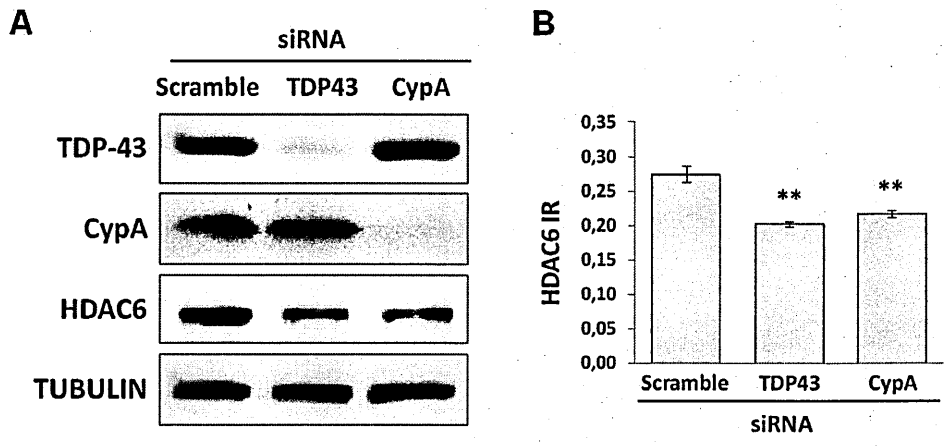

Figure 3.15 CypA has a role in TDP-43-mediated HDAC6 expression regulation.

HEK293 cells were transiently transfected with $siRNA^{scramble}$ or $siRNA^{TDP-43}$ or $siRNA^{CypA}$. (**A**) 15 µg of total protein lysates were loaded, run on SDS-PAGE gels, transferred on PVDF membranes, stained with Red Ponceau as loading control, analysed by WB and detected by chemiluminescence. TDP-43 and CypA were evaluated to check the corresponding protein knockdown (upper panels). WB for Tubulin and HDAC6 showed respectively equal protein expression and specific downregulation after silencing (lower panels). Representative images were chosen for display. (**B**) Histograms represent the quantitative analysis of HDAC6 band densities, normalized on the actual amount of proteins loaded, as detected by Red Ponceau staining. Data (mean ± S.E., n=4) are expressed as relative immunostaining values. Asterisks indicate that $siRNA^{TDP-43}$ (**=p≤0.01) or $siRNA^{CypA}$ (*=p≤0.05) were significantly different compared to $siRNA^{scramble}$, as assessed by One-way Anova followed by Bonferroni multiple comparison test.

The finding that RNA silencing of either TDP-43 or CypA reduced the expression of HDAC6 protein, indicated a co-requirement of TDP-43 and CypA for optimal HDAC6 expression, and thus established a possible biological role for the protein-protein interaction among CypA and TDP-43. Furthermore, based on previous work (Kim 2010), it is possible to speculate that the hnRNP complex described may be involved in HDAC6 mRNA processing and/or nuclear export.

3.3 *In vivo* evidence: CypA knockout mice

In vitro data consistently demonstrated the essential features of CypA/TDP-43/hnRNP A2/B1 functional association in hnRNP complex assembly/disassembly. To validate *in vivo* some of the

effects observed *in vitro* after CypA knockdown, tissues from mice expressing (CypA +/+) with a reduced (CypA +/-) or absent (CypA -/-) expression of CypA were analysed.

3.3.1 CypA is involved in TDP43/ hnRNP A2/B1 RNP complex formation

With the goal of investigating protein-protein interactions in the hnRNP complex in more detail, co-immunoprecipitation experiments were performed in a mouse tissue that is affected in TDP-43-related pathology in ALS. In particular, mouse spinal cord homogenates were analysed to further demonstrate that the interaction between TDP-43 and hnRNP A2/B1 was negatively regulated by a reduced or absent CypA expression.

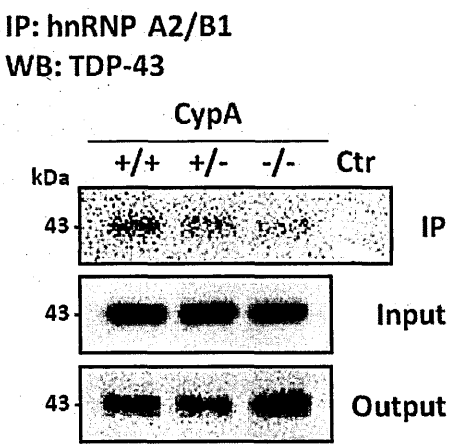

Figure 3.16 CypA interaction with TDP-43 is implicated in hnRNP complex formation in mouse lumbar SpC.

Equal amounts of proteins (1mg) from lumbar SpC homogenates of CypA+/+ (n=3), CypA+/- (n=3) and CypA-/- (n=3) mice were co-precipitated with anti-hnRNP A2/B1 primary antibody. Aliquot of the tissue homogenates (INPUT), of the immunoprecipitates (IP) and of the remaining fractions (OUTPUT) were loaded together with coated beads as IP control, subjected to SDS-PAGE, transferred to a PVDF membrane, stained with Red Ponceau as loading control, probed with anti-TDP-43 antibody and detected by chemiluminescence. Results representative of several independent experiments are shown, indicating that CypA/TDP-43 interaction is implicated in hnRNP complex formation *in vivo*.

Lumbar SpC from age and sex-matched mice that express (CypA+/+, n=3), have a reduced expression (CypA+/-, n=3) or do not express (CypA-/-, n=3) CypA were used in co-IP assays (**Figure 3.16**). Coated magnetic beads (Ctr) were used as negative experimental control. An anti-hnRNP A2/B1 antibody was used for immunoprecipitation and the WB for TDP-43 clearly detected the protein in the co-IP fraction of mice expressing CypA (CypA+/+), with a decrease and a striking reduction respectively in CypA+/- and knockout (CypA-/-) mouse samples, thus confirming previous results. This finding was further supported by the observation that TDP-43 marked reduction in the IP fraction was associated with an increased recovery of the protein in the output fraction of CypA knockout mice.

Collectively, these data suggested possible key roles of CypA in the architecture of this RNA-binding protein complex and demonstrated the relevance of this function of CypA also *in vivo*, in a disease-related tissue. However, it should be noted that TDP-43 and hnRNP A2/B1 interaction, and thus this hnRNP complex formation, was not completely inhibited in CypA knockout mice. Given the presence of multiple immunophilins in the nucleus, also identified as part of the spliceosome (reviewed in Mesa 2008), arguing for a possible functional redundancy in the splicing system, a compensatory mechanism may be hypothesised for CypA knockout mice.

3.3.2 CypA absence alters TDP-43 solubility

One of the potential consequences of TDP-43/hnRNP A2/B1 complex disruption upon CypA knock-down/out could be an impaired turnover of this hnRNP complex. Since TDP-43 is an intrinsically aggregation-prone protein (Johnson 2009), its propensity for toxic misfolding could be thus accentuated *in vivo* by CypA reduction or absence. In fact, TDP-43 depletion from the nucleus, together with its accumulation in ubiquitinated cytoplasmic inclusions are important pathological features of ALS and FTLD-U (Neumann 2006), and this could represent a possible mechanism by which CypA could contribute to TDP-43-related diseases.

To investigate whether CypA deficiency may cause protein complex instability *in vivo* we isolated and characterised the protein composition of the Triton X-100-insoluble fraction (TIF) from mouse spinal cord tissues of CypA+/+, CypA+/- and CypA-/- mice. TIF was used as our experimental model of protein aggregates because previous analyses conducted in our laboratory on Triton-insoluble fractions extracted from the spinal cord of mutant SOD1 mice demonstrated that are enriched in ubiquitinated protein aggregates and more generally in improperly folded or damaged proteins (Basso 2006 and 2009).

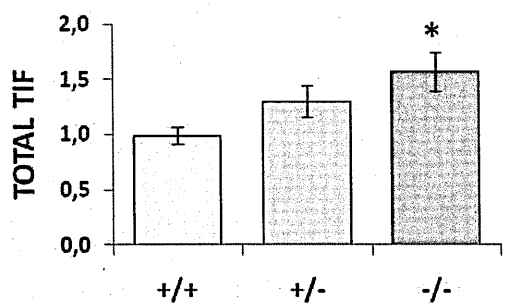

Figure 3.17 Total TIF in ventral horn mouse lumbar SpC.

Analysis of detergent-insoluble proteins from the ventral horn portion of the lumbar spinal cord of sex and age-matched CypA+/+ (n=6), CypA+/- (n=6) and CypA-/- (n=6) mice. Total TIF is the ratio of the amount of Triton-X100-insoluble proteins to the total proteins extracted in the soluble fraction. Proteins were quantified respectively by the Bradford and the BCA assays. Data (mean ± S.E., n=6) are expressed as percentages of control (CypA+/+). Asterisks indicate values significantly different from controls (**=p≤0.01 CypA-/- vs. CypA+/+; *=p≤0.05 CypA+/- vs. CypA+/+), as assessed by One-way Anova followed by Bonferroni multiple comparison test.

For this analysis, potentially aggregating proteins were enriched and separated from other contaminants, which were removed from the isolated aggregates by detergent-rich buffer extraction. The detergent-insoluble aggregates were then solubilised in an urea-based buffer and quantified. Total TIF obtained from CypA-/- mice were significantly more abundant than in CypA+/+ mice, with a higher, but not significant, amount of TIF in CypA+/- mice compared to CypA knockout mice (**Figure 3.17**).

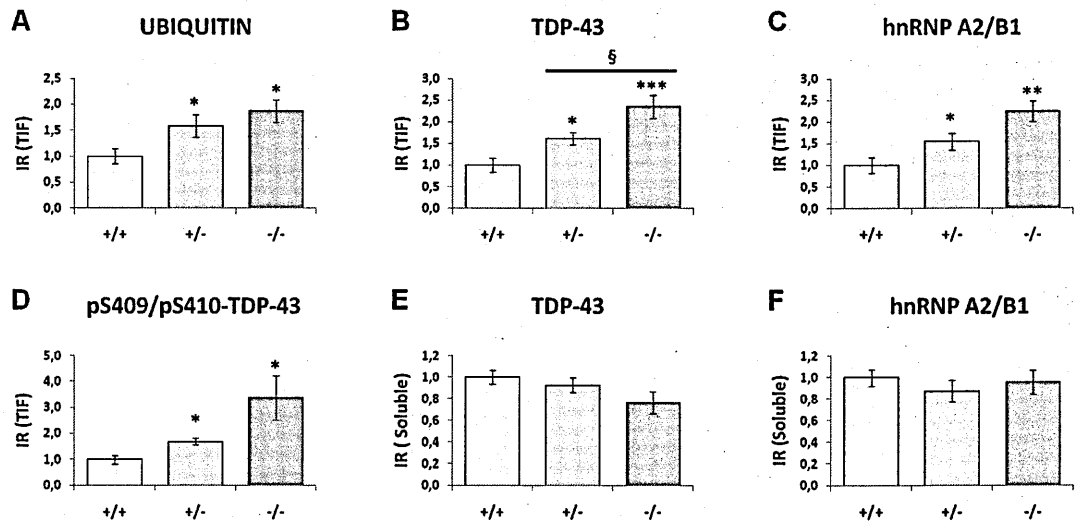

Figure 3.18 Protein composition of the insoluble and soluble fractions.

Immunoblot analysis of TIF from ventral horn lumbar spinal cord tissues of Cyp +/+ (n=6), CypA+/- (n=6) and CypA-/- (n=6) mice. The level of Ubiquitin (**A**), TDP-43 (**B**), hnRNP A2/B1 (**C**), phospho-Serine-409/410 TDP-43 (**D**) were measured in TIF. TDP-43 (**E**) and hnRNP A2/B1 (**F**) were also analysed in the Soluble fraction. Aliquot of TIF or Soluble proteins were analysed independently by WB (15µg) or dot blotting (3µg), probed with the specific antibodies and detected by chemiluminescence. Histograms represent the immunoreactivity normalised to the actual amount of protein loaded, detected after Red Ponceau or Sypro® Ruby Protein Blot staining. Values are percentages of control (CypA+/+) and are the mean ± S.E., n=6. Symbols indicate values significantly different from controls (*=p≤0.05 vs. CypA+/+; §=p≤0.05 vs. CypA+/-), as assessed by One-way Anova followed by Neuman-Keuls multiple comparison test.

A quantitative approach was employed to analyse single proteins of interest by WB, following qualitative detergent-insoluble protein enrichment. In particular, the same amounts of TIF or soluble samples were resolved on SDS-PAGE gels, blotted on PVDF membranes and probed with different primary antibodies. Alternatively, aliquots of TIF or soluble protein extracts were diluted, loaded in duplicate on nitrocellulose membranes by dot blotting, stained with Red Ponceau as loading control and blotted. We found that TIF from SpC of CypA+/- and CypA-/- mice were enriched in polyubiquitinated proteins (**Figure 3.18A**). Furthermore, TDP-43 was recovered as insoluble material, with an increasing trend, when CypA was reduced or absent (**Figure 3.18B**). Also hnRNP A2/B1 was significantly accumulated in TIF of CypA-/- and CypA+/- mice in comparison with CypA+/+ animals (**Figure 3.18C**). We then used an antibody raised against TDP-

43 phosphorylated at Serine-409/410, that allows the sensitive and specific labelling of disease-associated species (Inukai 2008). Interestingly, hyper-phosphorylated TDP-43 was also significantly enriched in tissues from CypA knock-down/out mice compared to control animals (**Figure 3.18D**). The increased amount of Triton-insoluble TDP-43 and hnRNP A2/B1 recovered when CypA protein expression was completely abrogated, was not mirrored by a significant reduction in the level of the same protein in the soluble fraction (**Figure 3.18E-F**).

These results demonstrated that in the detergent-insoluble/urea-soluble fraction from CypA knockout mice ubiquitin was co-enriched with TDP-43. Thus, TIF contained ubiquitinated and aberrantly phosphorylated TDP-43, making it possible to conclude with confidence that extracted proteins were qualitatively similar to TDP-43 aggregates and therefore had the fundamental biochemical features of protein inclusions in TDP-43-linked human pathology. Furthermore, reduction or absence of CypA augmented the amount of TDP-43 aggregates in a dose-dependent manner and, in these fractions hnRNP A2/B1 was found to co-aggregate with TDP-43. These data suggest that CypA expression at physiological levels could be protective against aggregate formation of mislocalised TDP-43.

In conclusion, *in vivo* experiments provided a framework for understanding how dysregulation of TDP-43/CypA hnRNP complex assembly could contribute to pathogenesis, in addition to HDAC6 altered expression regulation, observed *in vitro*. So, it is possible to speculate that the absence or an impaired CypA/TDP-43 binding could contribute to accelerate improper folding of this complex, leading to TDP-43 aggregation and abnormal inclusion formation, that is a highly consistent feature of TDP-43 proteinopathies (Geser 2009).

4. TDP-43-associated disease

A fraction of CypA was found to complex with TDP-43 and hnRNP A2/B1 *in vitro* and *in vivo*. These interactions are RNA-dependent and substantially enhanced by CypA lysine-acetylation. Two of the key questions for understanding the role of this protein complex are (i) what are the normal functions and (ii) what are the acquired toxicities and/or perturbed normal functions in disease conditions. To address the first question we showed that CypA is involved in the assembly and maintenance of the hnRNP complex formed by TDP43 and hnRNP A2/B1, both *in vitro* and *in vivo*. Additionally, a possible involvement of this hnRNP complex in HDAC6 expression regulation was defined *in vitro*. Furthermore, in the absence of CypA, TDP-43 was significantly enriched and aberrantly phosphorylated in proteinaceous inclusions in mouse spinal cord. Here, we tried to understand whether this hnRNP complex was involved or altered in TDP-43-related pathological conditions, when it is mutated (Kabashi 2008; Sreedharan 2008) or aberrantly phosphorylated, fragmented and ubiquitinated (Arai 2006; Neumann 2006), as in ALS or FTLD-U patients.

4.1 WT-TDP-43 over-expression in HEK293 cells

To investigate the normal functions of TDP-43, the wild-type protein was transiently expressed in the HEK293 cell line. In order to specifically detect the exogenous protein and to distinguish the transfected protein from endogenous TDP-43, an N-terminal Flag-tag was added to the TDP-43 expression construct. This time, contrary to the position of the Myc-tag fused at the C-terminal end of CypA sequence, the N-terminal end of TDP-43 was preferred, because of the peculiar structural/functional features of its C-terminal region. In fact, many works suggest that the C-terminus of TDP-43 is essential for its solubility, cellular localisation and protein-protein interactions (Buratti 2005; Ayala 2008). Thus, the introduction of an epitope at this end side of the protein could have a detrimental effect on its physiological activities.

4.1.1 Flag-tagged WT-TDP43 expression level

A transfection protocol was optimized to obtain the highest Flag-tagged TDP-43 expression level in HEK293 cells with the lowest cytotoxicity.

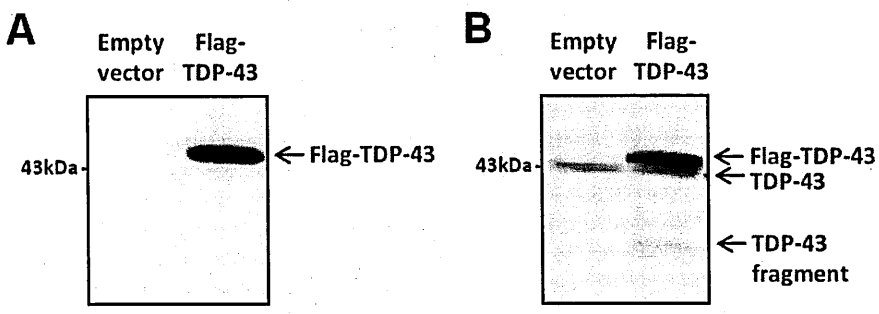

Figure 4.1 Flag-TDP-43 expression in HEK293 cells.

HEK293 cells were transiently transfected with the empty vector or the vector cloned with Flag-TDP43. 15µg of total protein lysates were loaded, run on SDS-PAGE gels, transferred onto a PVDF membrane, stained with Red Ponceau as loading control, analysed by WB using the anti-Flag-tag (**A**) or the anti-TDP-43 (**B**) antibodies and detected by chemiluminescence. The anti-Flag-tag antibody revealed only the signal corresponding to exogenous TDP-43 (computed MW ~ 45kDa), while the anti-TDP-43 antibody detected the signals relative to both the endogenous TDP-43 (43kDa) and the exogenous Flag-tagged protein. Flag-TDP-43 was expressed at high levels in HEK293 cells.

In order to verify the expression of the N-terminal Flag-tagged TDP-43 in this experimental system, HEK293 cells were transiently transfected with either an empty vector or with the vector encoding WT-Flag-TDP-43. The expression of the exogenous and the endogenous proteins was thus verified by WB analyses on whole cell lysates, using respectively an antibody for the Flag-tag or alternatively an antibody for TDP-43. The anti-Flag-tag antibody revealed only the presence of the tagged protein in the lane corresponding to cells transfected with the Flag-TDP-43 construct (**Figure 4.1A**). Using a polyclonal antibody for TDP-43, only one band at 43kDa was detected in cells transfected with the empty vector, while two bands, corresponding to the endogenous TDP-43 and the exogenous Flag-TDP-43 at a higher MW, were detected in cells transfected with Flag-TDP-43 plasmid (**Figure 4.1B**). Interestingly, another band below 37kDa was recognized by the

anti-TDP-43 antibody only in cells overexpressing TDP-43. This signal was probably due to the presence of C-terminal TDP-43 fragments, since they were not recognized by the anti-Flag-tag antibody that targets the N-terminus. C-terminal fragments were generated by the increased cleavage of TDP-43 in HEK293 cells after overexpression, as already reported in cell cultures and human disease (Zhang 2007; Neumann 2007).

4.1.2 Flag-tagged WT-TDP43 localisation

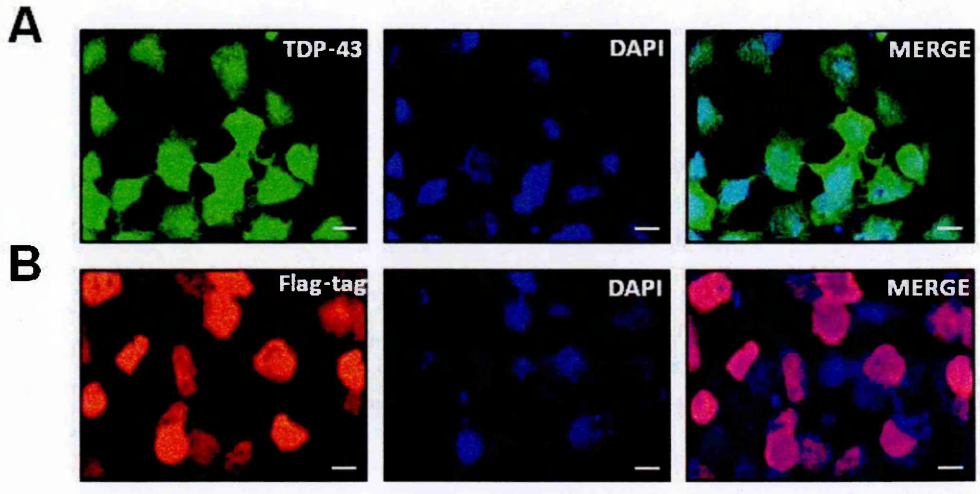

Figure 4.2 Flag-TDP-43 is expressed mainly in the nucleus of HEK293 cells.

HEK293 cells transiently transfected with the empty vector or the vector cloned with Flag-TDP-43 (bar: 15µm). Representative immunofluorescence images of HEK293 cells expressing Flag-TDP-43, immunostained with (**A**) polyclonal anti-TDP-43 antibody followed by Alexa®488 (green)-conjugated antibody or (**B**) with monoclonal anti-Flag-tag antibody followed by Alexa®647 (red)-conjugated antibody. Nuclei were detected using DAPI staining (blue). The anti-TDP-43 antibody revealed the signals of both endogenous and exogenous TDP-43, whereas with the anti-Flag-tag antibody only the signal concerning the exogenous protein was detected.

The expression of the exogenous tagged protein was also verified by immunofluorescence using confocal microscopy. Exogenous TDP-43 had to be visualised via fused Flag-tag, as HEK293 cells show robust endogenous expression of TDP-43. Cells were transfected with good efficiency and expressed Flag-TDP-43 at high levels. In particular, cells overexpressing TDP-43 were characterised by a more intense TDP-43 immunostaining (**Figure 4.2A**), while the staining for the Flag-tag was present only in transiently transfected cells correctly expressing the exogenous

tagged protein (**Figure 4.2B**). As already observed in **Figure 2.9**, the immunostaining by the anti-Flag-tag antibody further confirmed the observation that ectopic WT-Flag-TDP-43 mainly localized to the nucleus of these cells, as highlighted by magenta areas of overlay of red and blue (merge). Thus, TDP-43 immunostaining in these cells confirmed that both endogenous TDP-43 and Flag-TDP-43 had primarily nuclear localisation, nevertheless TDP-43 staining was also detected in the cytoplasm. This evidence was in accordance with data from the literature demonstrating that TDP-43 was able to shuttle continuously between the nucleus and the cytoplasm (Ayala 2008). HEK293 cells transfected with the empty vector were used as controls: Flag-tag staining was not present in these cells, whereas only basal TDP-43 signal for the endogenous protein was detected (images not shown).

4.1.3 Cell viability evaluation after Flag-tagged WT-TDP43 overexpression

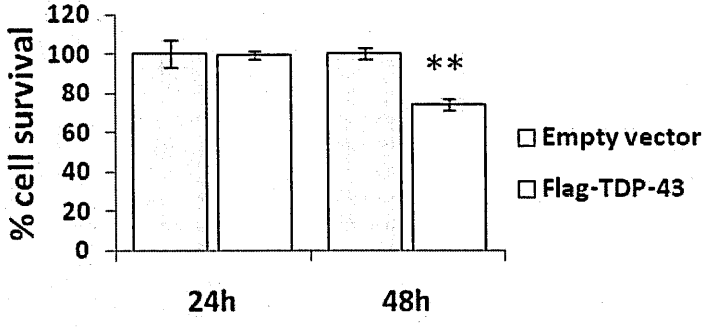

Figure 4.3 Flag-TDP-43 overexpression reduced cell survival.

HEK293 cells were transfected with the empty vector or with Flag-TDP-43. Cell viability was assessed by MTT assay 24h and 48h after transfection. Values are the mean ± S.E.M. (n≥4) and are expressed as a percentage of control cells (empty vector). Asterisk indicates values significantly different from control (*=p<0.05), as assessed by Student's t-test.

In order to determine whether an overexpression of TDP-43 in this experimental setting could have any effect on cell viability, the survival rate of transiently transfected cells was assessed by

MTT assay. A statistically significant reduction in viability was detected in cells overexpressing Flag-TDP-43 after 48h (**Figure 4.3**). These data suggested that an overexpression of wild-type TDP-43 could be toxic *per se* also *in vitro*, as previously reported by other work on yeast, mice, zebrafish, or Drosophila (Johnson 2008; Xu 2010; Wils 2010; Hanson 2010; Li 2010; Ritson 2010; Estes 2011; Miguel 2011). Furthermore, TDP-43-induced toxicity is dependent on the level of transgene expression, with intermediate expression of TDP-43 producing an attenuated phenotype, compared with models expressing higher TDP-43 levels (Johnson 2008; Stallings 2010; Wils 2010; Xu 2010; Igaz 2011). Thus, in subsequent experiments cells were analysed 24h after Flag-TDP-43 transfection, when the exogenous protein was expressed at good levels but there was no overt cytotoxicity.

4.2 TDP-43 knockdown in HEK293 cells

In order to directly observe the effects of the loss of TDP-43 function *in vitro*, RNA interference technology was used. TDP-43 silencing experiments were performed in HEK293 cells delivering a specific $siRNA^{TDP-43}$ or, as a negative control for knockdown, a scrambled siRNA that did not lead to the degradation of any specific mRNA. The $siRNA^{TDP-43}$ molecule, targeting the 3'-UTR of TDP-43 locus was transiently transfected through a cationic lipid-mediated transfection system. Once the siRNA concentration and transfection system yielding the highest efficiency of knockdown was established, the optimal time interval for *in vitro* knockdown was determined: HEK293 cells were treated with either TDP-43 or control siRNA for 24, 48, 72 and 96 hours. As shown in **Figure 4.4A**, treatment with TDP-43 siRNA markedly reduced the protein expression in a time-dependent manner, with very little detectable protein observed by WB for TDP-43 48, 72 and 96 hours after treatment compared with scramble siRNA. Thus, RNA silencing experimental conditions were optimized to obtain a constant reduction in TDP-43 protein expression up to 90% (**Figure 4.4A**). In all subsequent experiments performed, 48 hours was used as the time point to evaluate effects of TDP-43 knockdown, that was always verified analysing the protein expression level by Western or dot blotting. Targeting by siRNA the untranslated region of TDP-43 allowed to selectively silence

only the endogenous protein, and not the exogenously transfected Flag-tagged TDP-43 (**Figure 4.4B**).

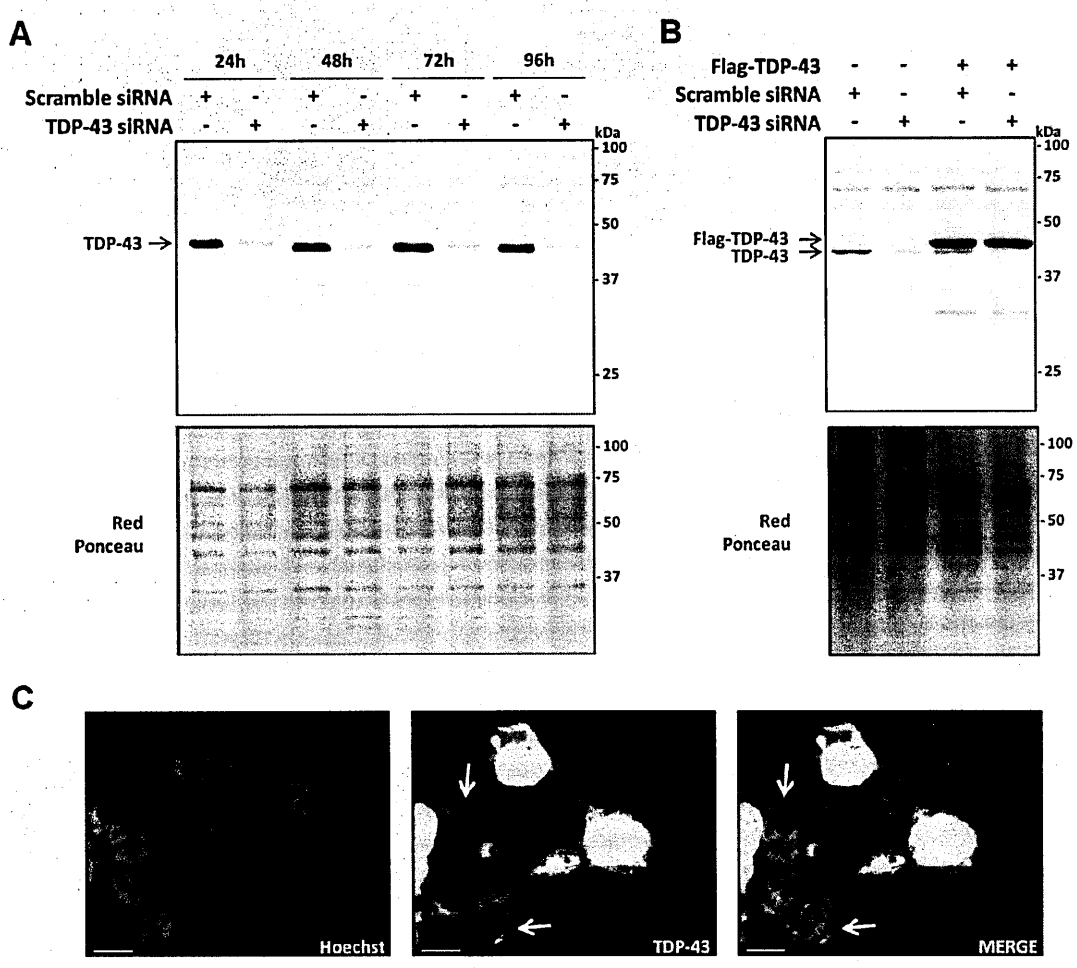

Figure 4.4 TDP-43 knockdown.

HEK293 cells were transfected with siRNA^{scramble} or siRNA^{TDP-43}. (**A-B**) 15µg of total protein lysates were loaded, run on SDS-PAGE gels, transferred on PVDF membranes, stained with Red Ponceau as loading control, analysed by WB for TDP-43 and detected by chemiluminescence. (**A**) Representative WB for TDP-43 in cells silenced at different time points. (**B**) Representative WB for TDP-43 in cells transfected with siRNA^{scramble} or siRNA^{TDP-43} or co-transfected with Flag-TDP-43 and siRNA^{scramble} or Flag-TDP-43 and siRNA^{TDP-43}. (**C**) Representative immunofluorescence images of HEK293 cells stained for TDP-43 (green) after silencing (bar: 15µm). Nuclei were stained with Hoechst (blue).

To further demonstrate the specific knockdown of TDP-43 *in vitro*, immunofluorescence (IF) staining for TDP-43 was also performed in cells that were counter-stained with Hoechst to visualise the nuclei (**Figure 4.4C**). In cells treated with siRNA^{TDP-43} the extent of TDP-43 silencing

was clear also by IF (white arrows), compared to flanking cells that were not efficiently silenced. Notably, in silenced cells TDP-43 expression was almost absent in the nucleus, while a faint staining for the protein was still noticeable in the cytosol, although it was clearly down-regulated. TDP-43 silencing did not significantly alter cell survival rate (data not shown).

4.3 ALS-mutant TDP-43

The effect of pathogenic mutations of the TDP-43 gene was then tested in this experimental system to evaluate their impact on the interaction with CypA and, on the functions of the hnRNP complex these proteins are involved in.

Mutation	ALS	Reference	Features
A315T	Familial	Kabashi 2008 Gitcho 2008	Motor phenotype when overexpressed in mice, nematode (C. elegans), zebrafish.
R361S	Sporadic	Kabashi 2008	Can't restore HDAC6 mRNA expression. Alters SG formation. Increases n. of TDP-43 aggregates.
Y374X	Sporadic	Daoud 2009	First frameshift mutation identified. Truncated protein.

Table 4.1 TDP-43 ALS-mutations analysed in this work.

The analyses in this study compared the effects of three different ALS-mutations. In particular, two missense mutations, A315T and R361S, and the frameshift mutation Y374X were considered in this work. The A315T (Gitcho 2008; Kabashi 2008) mutation causes dominantly inherited ALS, while the R361S (Kabashi 2008) and Y374X (Daoud 2009) mutations were found in sporadic ALS cases (**Table 4.1**). These three mutations are located inside the C-terminal glycine-rich domain of TDP-43, with the R361S and Y374X being respectively inside or close to the minimal hnRNP binding region (D'Ambrogio 2009; Budini 2012) (**Figure 4.5**).

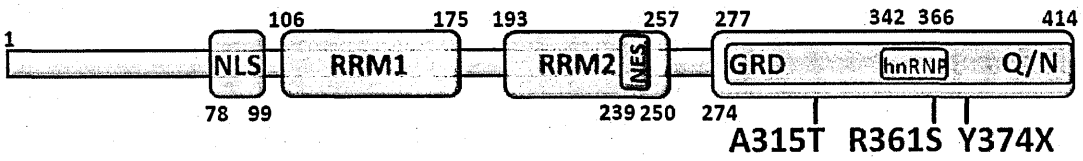

	Structural region	Residues
NLS	Nuclear Localization Signal	78-99
RRM1	RNA Recognition Motif 1	106-175
RRM2	RNA Recognition Motif 2	193-257
NES	Nuclear Export Signal	239-250
Q/N	Prion-like Q/N rich-region	277-414
GRD	Glycine Rich Domain	274-414
hnRNP	hnRNPs minimal binding region	342-366

Figure 4.5 TDP-43 structural regions.

Schematic representation of human TDP-43 protein drawn to scale. TDP-43 has five functional regions, including two RNA recognition motifs (RRM1 and RRM2) important for DNA/RNA binding, a nuclear localisation signal (NLS) and a nuclear export signal (NES) that mediate nucleo-cytoplasmic shuttling, and a glycine rich domain (GRD) that mediates protein-protein interactions. The prion-like Q/N rich region (Cushman 2010) has been highlighted, in addition to the location of the ALS-associated mutations introduced in Flag-TDP-43 sequence in this study. A structural region mediating the binding with hnRNP A2, as identified by the group of Prof. Baralle F. (D'Ambrogio 2009; Budini 2012), also spans part of the C-terminal tail of TDP-43.

Our chosen experimental approach was transient transfection of HEK293 cells with Flag-TDP-43 cDNA with or without mutations, following the specific knockdown of the endogenous protein with siRNA targeting the endogenous transcript 3'-UTR.

4.3.1 Generation of TDP-43 ALS-mutants

Point mutations were introduced in TDP-43 coding sequence by overlap-PCR (detailed procedure is explained in Materials and Methods section **12.2**), as previously described for CypA (Results section **3.1.3**). Briefly, mutagenic primers were designed to alter the nucleotide sequence of TDP-43 in a first round of PCR and the products obtained were used as substrates in a second round of PCR. The products of the second PCR were run on agarose gels to verify the correct length of each fragment. Each cDNA fragment, carrying the point mutation, was digested and purified to be inserted into the starting expression vector. This was used to transform competent bacteria that were plated on ampicillin-containing agar plates. When ligation and transformation reactions had

been achieved correctly, colonies grew only in plates where ligation products, and not digested-dephosphorylated plasmids, had been plated. To identify bacterial colonies containing the recombinant plasmid, colony screening was carried out by restriction analysis. At least four colonies for each condition were picked and grown in liquid cultures in the presence of ampicillin. Extracted plasmid DNAs were digested and analysed on agarose gel. Correct constructs were selected when only two bands, corresponding to the linearized vector and the excised cDNA insert, were detected. Furthermore, to ensure the existence of the correct point mutations inside the generated cDNA, and to exclude the presence of other unpredicted missense/nonsense mutations, constructs were sequenced. Both forward and reverse sequence analyses were used to verify that the constructs carried the expected nucleotide substitutions and did not present any other mismatches (**Figure 4.6**). Finally, selected vectors were tested for correct protein expression in HEK293 cells after transient transfection and were then amplified in bacteria to generate large amounts of plasmid DNA.

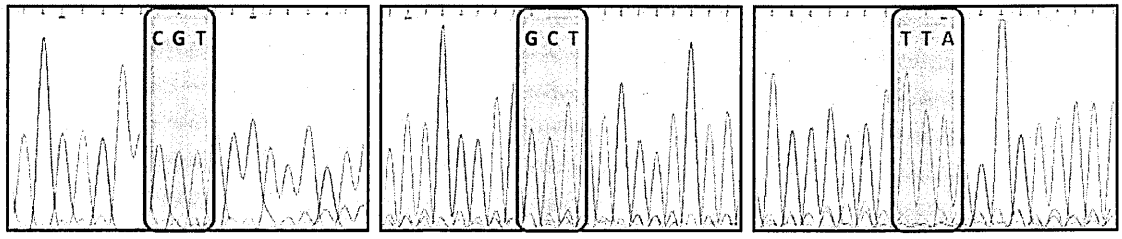

Figure 4.6 Flag-TDP-43 ALS-mutants sequencing.

Sequencing was performed on both DNA strands. The images shown highlight the codons carrying the point mutations generated and correspond to sequencing analyses performed on the reverse anti-sense DNA strand. Sequencing of the forward sense DNA strand (not shown) confirmed the same results.

4.3.2 TDP-43 ALS-mutants expression level

First, plasmids encoding TDP-43 ALS-mutants were tested for being efficiently transfected into HEK293 cells. To this extent, cells were transiently transfected with the WT- or A315T- or R361S- or Y374X-Flag-TDP-43 constructs or with the empty vector, as a negative control. Cells were

collected 24 hours after transfection, to minimize cytotoxicity after TDP-43 over-expression. WB for the Flag-tag portion of the exogenous proteins on whole cell lysates confirmed that wild-type and mutant forms of TDP-43 were expressed correctly and with comparable levels (**Figure 4.7A**). As shown in **Figure 4.7B**, also the staining with a polyclonal anti-TDP-43 antibody revealed high and similar expression levels compared to the endogenous protein and the WT-Flag-TDP-43, respectively. The Y374X-Flag-TDP-43 mutant produced a truncated form of the protein, missing the last 41 amino acids (Daoud 2009). This feature was evidenced in WB analyses for both Flag-tag and TDP-43 by a band running at a lower molecular weight. Furthermore, all three ALS-patient derived mutations produced aberrant cleavage products of TDP-43, as evidenced by the presence of 35-kDa and 25-kDa C-terminal fragments (**Figure 4.7B**). This is in accordance with the observation that mutant forms of TDP-43 form fragments more readily than wild-type TDP-43 in cell cultures (Sreedharan 2008).

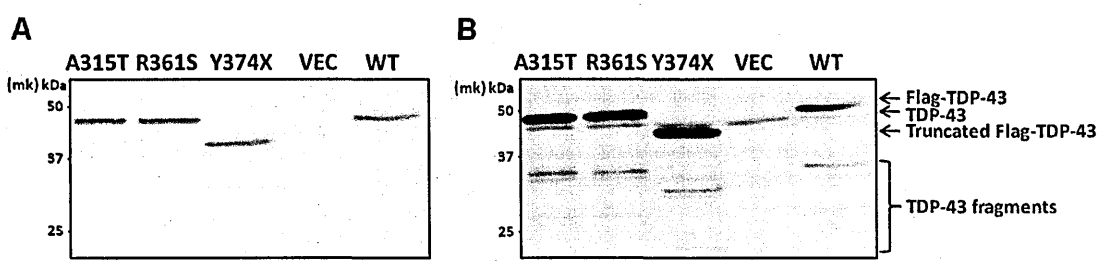

Figure 4.7 Flag-TDP-43 ALS-mutants overexpression in HEK293 cells.

HEK293 cells were transiently transfected with the empty vector (VEC) or the vector cloned with WT- or A315T- or R361S- or Y374X-Flag-TDP43. 15µg of total protein lysates were loaded, run on SDS-PAGE gel, transferred on a PVDF membrane, stained with Red Ponceau as loading control, analysed by WB using the anti-Flag-tag (**A**) or the anti-TDP-43 (**B**) antibodies and detected by chemiluminescence. All Flag-TDP-43 proteins were expressed at comparable levels in HEK293 cells.

4.3.3 Localisation of TDP-43 ALS-mutants

In physiological conditions TDP-43 is mainly localised within the nucleus. To establish whether ALS-mutant Flag-TDP-43 proteins retained the same distribution of the wild-type protein, two

independent methods were used: biochemical fractionation of the cytoplasmic and nuclear compartments and confocal microscopy of transiently transfected cells.

The biochemical approach consisted in the separation of the cytosolic from the nuclear fraction in cells expressing the wild-type or mutagenized Flag-TDP-43 proteins. Each subcellular fraction was independently analysed by WB using antibodies for TDP-43 or the Flag-tag portion of the protein.

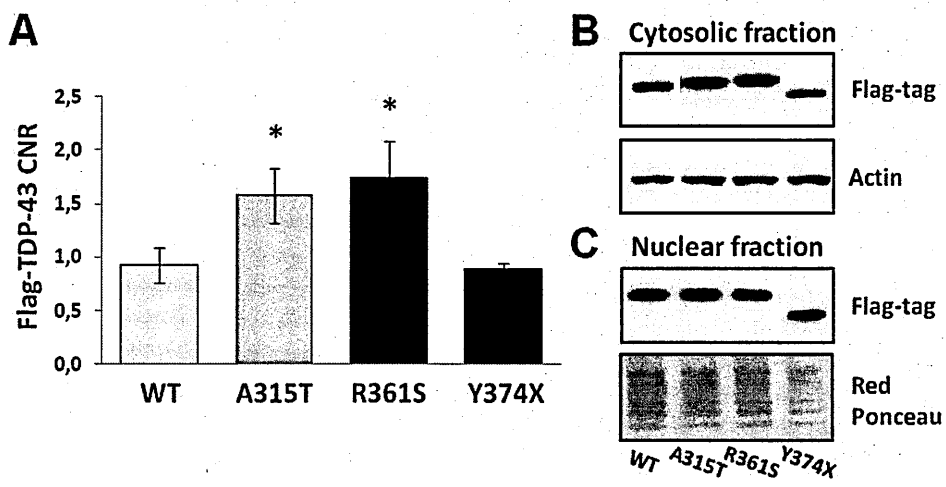

Figure 4.8 Flag-TDP-43 ALS-mutants subcellular distribution in HEK293 cells.

HEK293 cells were transiently transfected with WT- or A315T- or R361S- or Y374X-Flag-TDP-43. Equal amounts of cytosolic (**B**) and the corresponding nuclear (**C**) fractions were independently loaded, run on SDS-PAGE gels, transferred on PVDF membranes, stained with Red Ponceau as loading control, analysed by WB using the anti-Flag-tag antibody and detected by chemiluminescence. (**A**) Histograms represent the quantitative analysis of Flag-TDP-43 band densities in each compartment, normalized on the actual amount of proteins loaded, as detected by Red Ponceau staining. Data (mean ± S.E.M., n=4) in each subcellular fraction are proportioned to control cells (WT), whose value was set as one, and represented as the ratio of the values between the cytosolic and the corresponding nuclear fraction (CNR). Asterisks indicate that samples are significantly different (*=$p<0.01$) compared to control (WT), as assessed by One-way analysis of variance followed by Bonferroni's Multiple Comparison Test.

If the ALS-mutants of TDP-43 increased the proportion of cytosolic Flag-TDP-43, the ratio of cytoplasmic to nuclear protein (CNR) should be higher in cells expressing the mutant protein. To investigate this possibility, the quantification of the Flag-tag signal in the cytoplasm and in the

nucleus of independent samples, after normalization to the wild-type protein in the respective subcellular compartment, was used to calculate the CNR for each sample. Indeed, the mean CNR was significantly higher in cells expressing the A315T and R361S mutations, compared to WT-Flag-TDP-43 (**Figure 4.8**). This observation indicated that the A315T and R361S mutations enhanced protein mislocalisation and, in particular, significantly increased the protein cytoplasmic localisation, in agreement with reports by different groups (Barmada 2010; Liu-Yesucevitz 2010). In fact, in the nuclear fraction, signals corresponding to mutagenized TDP-43 proteins were comparable to the wild-type protein, while in the cytosolic compartment their levels were increased. Thus, the A315T and R361S ALS-derived mutations promoted the redistribution of the protein, increasing the proportion of cytoplasmic TDP-43 and possibly stimulating inclusions formation. In fact, increasing TDP-43 in the cytoplasm may disproportionately expose the protein to endogenous proteases, in a process generating high cytoplasmic concentrations of C-terminal TDP-43 fragments, as observed in **Figure 4.7**, which are enriched in cytoplasmic inclusions found in affected neurons (Igaz 2008). The results in this study add to previous work analysis of the frameshift mutation Y374X. In contrast to the other ALS-mutants, the cytosol/nuclei ratio for the Y374X mutant was comparable to the wild-type protein. These results suggested that enhanced cytoplasmic translocation might not be a general mechanism by which mutations in TDP-43 stimulate toxicity. These findings further corroborated the observation that mutations in TDP-43 are mechanistically divergent (McDonald 2011).

Additional evidence for biochemical fractionation experiments was provided by confocal microscopy analyses. In particular, colocalisation of endogenous and overexpressed Flag-tagged TDP-43 proteins was investigated to visualise whether TDP-43 distribution was altered by pathogenic mutations in its sequence. HEK293 cells were transiently transfected with the empty vector or WT- or A315T- or R361S- or Y374X-Flag-TDP-43 after silencing the endogenous protein. Cells were sequentially detected with a polyclonal anti-TDP-43 (left panels) and a monoclonal anti-Flag-tag (central panels) specific antibody (**Figure 4.9**), with overlays showing nuclei stained using Hoechst (right panels, merge). Under these conditions, double labelling allowed to evaluate

the knockdown of endogenous TDP-43 and to compare the localisation of the total protein (endogenous and exogenous, as revealed by the TDP-43 antibody) with the signal relative only to the exogenous one (detected with the anti-Flag-tag antibody) in the same image. All Flag-TDP-43 proteins remained largely in the nucleus of transfected cells, consistent with previous reports (Voigt 2010). However, the dual staining revealed that ALS-mutant TDP-43, and in particular the C-terminally truncated Y374X mutant protein, localised to distinct nuclear *puncta*. This is in accordance with a decreased TDP-43 mobility reported upon removal of the C-terminal region (Ayala 2008).

Thus, the IF experiments did not show any striking variation in Flag-TDP-43 distribution among the different mutants. Biochemical fractionation resulted a more sensitive method to detect differences in protein subcellular distribution, especially in the cytoplasm, where TDP-43 expression is particularly low, compared to the nucleus.

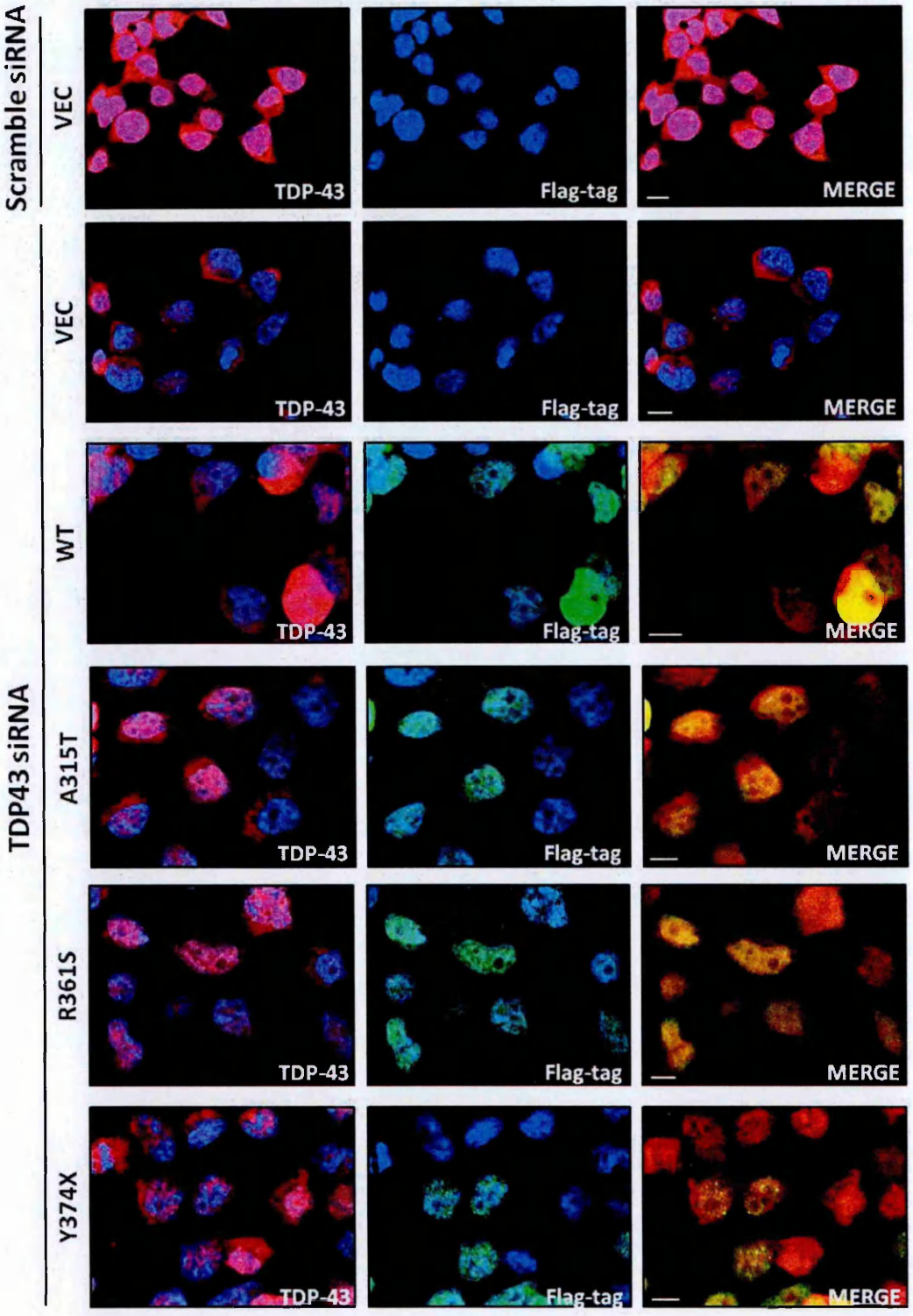

Figure 4.9 Flag-TDP-43 ALS-mutants localisation in HEK293 cells.

HEK293 cells were transiently co-transfected with siRNA^{scramble} and the empty vector (VEC) or siRNA^{TDP-43} and the empty vector or WT- or A315T- or R361S- or Y374X-Flag-TDP-43 (bar: 15µm). Cells were immunostained with polyclonal anti-TDP-43 antibody followed by Alexa®647 (red)-conjugated antibody (left panels) and with monoclonal anti-Flag-tag antibody followed by Alexa®488 (green)-conjugated antibody (central panels). Nuclei were detected using Hoechst staining (blue). Colocalisation of the proteins was evidenced with areas of yellow in overlays of red and green and blue images (right panel). Representative immunofluorescence images were chosen for display.

4.3.4 Cell viability evaluation after overexpression of TDP-43 ALS-mutants

It was then of interest to examine whether transfection with the Flag-TDP-43 ALS-mutants was associated with increased cellular toxicity, as determined by MTT assay. HEK293 cells were transiently transfected with plasmids encoding wild-type, A315T-, R361S-, Y374X-TDP-43 or with an empty vector (VEC) as a control, and then analysed after 48 hours. This experiment was repeated several times confirming that the overexpression of the wild-type protein was sufficient to induce cell death in this cellular model. This observation was consistent with data previously obtained (Results section **4.1.3**). Furthermore, under these conditions, a significant increase in cell death was induced also by the overexpression of TDP-43 ALS-mutants (**Figure 4.10**). Nevertheless, the results of this assay failed to detect any significant alteration in MTT conversion in the presence of ALS-TDP-43 constructs with respect to the wild-type protein, consistent with previous reports in primary rat cortical neurons (Barmada 2010).

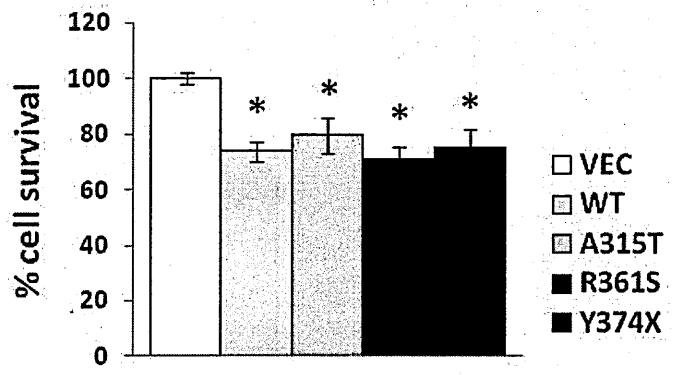

Figure 4.10 Flag-TDP-43 ALS-mutants overexpression reduced cell viability in HEK293 cells.

HEK293 cells were transiently transfected with the empty vector (VEC) or the vector cloned with WT- or A315T- or R361S- or Y374X-Flag-TDP43. Cell viability was assessed by MTT assay 48h after transfection. Values are the mean ± S.E.M. (n≥4) and are expressed as percentages of control cells (empty vector). Asterisks indicate values significantly different from control (*=p<0.001), as assessed by Student's t-test.

The same experiment was also performed in cells previously silenced for endogenous TDP-43 and then transfected with the different Flag-TDP-43 constructs. Also in this case the expression of the newly generated TDP-43 mutated proteins (A315T, R361S, Y374X) significantly altered cell survival in respect to control cells transfected with the empty vector or silenced using a scrambled siRNA. The effect observed was comparable to the toxicity induced by the overexpression of the wild-type protein.

Thus, three different mutations in TDP-43, all of which are associated with the development of ALS, caused substantial toxicity *in vitro*. These results suggest that Flag-TDP-43 overexpression, both wild-type or ALS-mutants, exhibited toxicity that led to cell death regardless of the amount of protein in the cytoplasm. Despite the simplicity of the system, the expression of Flag-TDP-43 proteins in HEK293 cells recapitulated key features of TDP-43 patho/physiology, including nuclear localisation of the wild-type protein, mislocalisation of point mutants to the cytoplasm and cytotoxicity.

4.3.5 TDP-43 ALS-mutants impaired binding with CypA and hnRNP A2/B1

Attention was then concentrated on molecular changes, such as protein-protein interactions, which may account for the toxicity of TDP-43 ALS-mutants. In fact, pathogenic mutations are located in the putative protein-protein interaction domain of TDP-43, so they could contribute to the increased proportion of cytoplasmic TDP-43 by enhancing its association with cytoplasmic binding partners, which would impair its nuclear import, and facilitate its nuclear export, or by disrupting its affinity for nuclear binding partners.

In particular, in HEK293 cells the effect of three ALS-patient derived mutations on the interaction with CypA and hnRNP A2/B1 was investigated. Co-IP experiments were performed in cells silenced for endogenous TDP-43 and transiently transfected with Flag-tagged TDP-43 constructs. TDP-43 knockdown efficiency and a comparable expression of the transfected wild-type and mutant

proteins were assessed by WB for TDP-43 on the input fraction (**Figure 4.11A**, lower panel). All Flag-TDP-43 ALS-mutants analysed showed differences in the ability of binding CypA compared to the wild-type protein (**Figure 4.11A**, upper panel). In particular, both monoclonal and polyclonal anti-CypA antibodies were not able to immunoprecipitate mutant TDP-43 as much as the wild-type protein, indicating that CypA is not able to efficiently interact with TDP-43 when it is mutated. In particular, the Y374X mutation, that leads to the expression of a C-terminally truncated form of the protein lacking the last 41 amino acids, is the one that most severely affected the interaction, while the A315T mutation seemed to have a very mild, or nearly no effect on the interaction (**Figure 4.11B**). This last result is consistent with recent reports (Freibaum 2010), where the A315T and M337V disease-causing mutations were demonstrated not to grossly alter the function of TDP-43 or its binding partners. Interestingly, the R361S mutation, that is located within the minimal hnRNP A2 interaction domain of TDP-43 (D'Ambrogio 2009; Budini 2012), decreased CypA/TDP-43 interaction, as well as CypA/hnRNP A2/B1 binding (data not shown), that it is a loss-of-function mutation with respect to this hnRNP complex formation. In these samples CypA was selectively immunoprecipitated with comparable levels (**Figure 4.11C**).

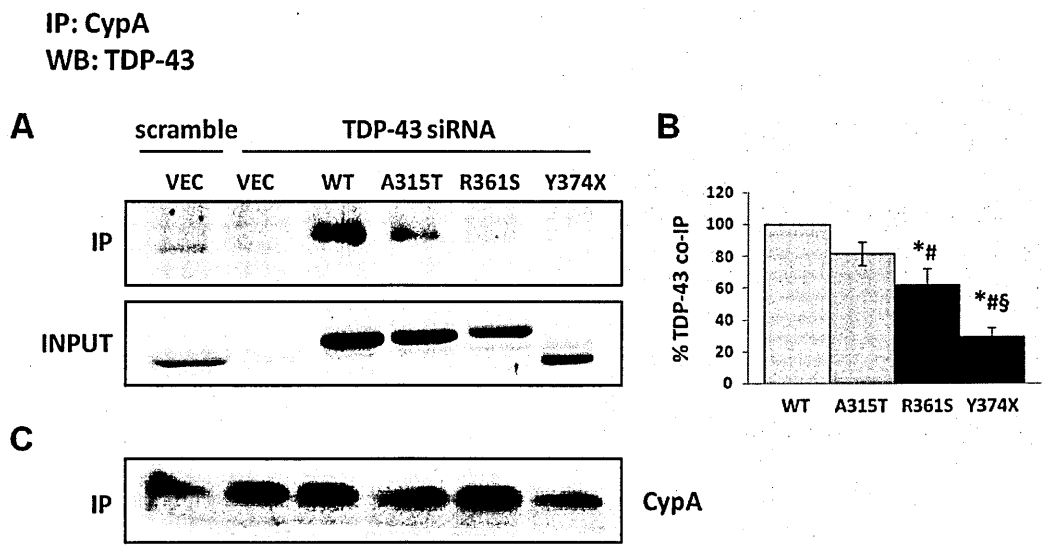

Figure 4.11 CypA binding with Flag-TDP-43 ALS-mutants is impaired.

HEK293 cells were transiently co-transfected with $siRNA^{scramble}$ and an empty vector (VEC) or with $siRNA^{TDP-43}$ and an empty vector (VEC) or WT- or A315T- or R361S- or Y374X-Flag-TDP-43. CypA was

immunoprecipitated from whole cell lysates using a monoclonal anti-CypA antibody. Aliquot of the lysates (INPUT) and of the immunoprecipitate (IP) fractions were separated by SDS-PAGE, transferred to PVDF membranes, and reversibly stained with Red Ponceau, as a loading control. (**A**) TDP-43 proteins potentially associated with CypA were detected by WB using a polyclonal anti-TDP-43 antibody (upper panel, IP fraction), while expression of the endogenous and exogenous tagged proteins was verified in the Input fraction (lower panel). Shown is a representative of several independent experiments with similar results, indicating that TDP-43 ALS-mutants display an altered capability of binding CypA compared to the WT protein. (**B**) Histograms represent the quantitative analysis of TDP-43 band densities in the IP fraction, normalized on the actual amount of Flag-TDP-43 overexpressed, detected in the Input fraction. Data (mean ± S.E.M., n=10) are expressed as percentages of control cells (WT). Symbols indicate values significantly different from controls (*=$p<0.01$ vs. WT; #= <0.05 vs. A315T; §=$p<0.01$ vs. R361S), as assessed by One-way ANOVA followed by Newman-Keuls Multiple Comparison Test. (**C**) CypA was specifically immunoprecipitated with the same yield in each experimental condition, as detected using a polyclonal antibody against CypA.

To evaluate whether TDP-43 mutations may effectively affect its binding with hnRNP A2/B1, Flag-TDP-43 ALS-mutants were tested by co-IP. In particular, HEK293 cells were transiently transfected with the empty vector or WT- or A315T- or R361S- or Y374X-Flag-TDP-43 after knockdown of the endogenous protein. TDP-43 efficient silencing and equal expression levels of the transfected Flag-tagged proteins were assessed by WB for TDP-43 on the input fraction (**Figure 4.12A**, lower panel). Whole protein lysates were co-IP with the anti-hnRNP A2/B1 antibody and hnRNP A2/B1 was specifically immunoprecipitated with comparable levels in all samples (**Figure 4.12C**). While only small differences or high variability in the interaction with TDP-43 were detected in cells expressing respectively the A315T and Y374X mutations, the association between TDP-43 and hnRNP A2/B1 was significantly decreased in R361S-TDP-43 cells (**Figure 4.12A-B**) compared to the wild-type sample. This result was similar to that observed in the same experiment with $siRNA^{TDP-43}$ and thus confirmed that the R361S is a loss-of-function mutation with regards to hnRNP A2/B1 binding. Also in these samples the R361S-TDP-43 mutant showed a decreased interaction between CypA and hnRNP A2/B1 (data not shown). These observations were in accordance with the results previously described. Therefore, the R361S mutation could contribute to toxicity

enhancing TDP-43 mislocalisation, by disrupting its affinity for nuclear binding partners, as suggested by co-IP experiments with CypA or hnRNP A2/B1.

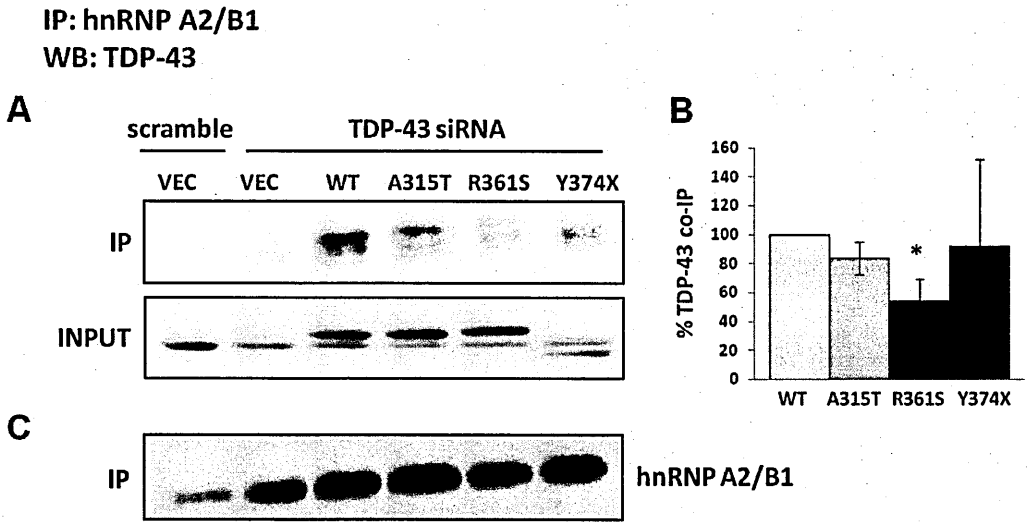

Figure 4.12 hnRNP A2/B1 binding with R361S-TDP-43 ALS-mutant is impaired.

HEK293 cells were transiently co-transfected with $siRNA^{scramble}$ and an empty vector (VEC) or with $siRNA^{TDP-43}$ and an empty vector (VEC) or WT- or A315T- or R361S- or Y374X-Flag-TDP-43. hnRNP A2/B1 was immunoprecipitated from whole cell lysates using a monoclonal anti-hnRNP A2/B1 antibody. Aliquot of the lysates (INPUT) and of the immunoprecipitate (IP) fractions were separated by SDS-PAGE, transferred to PVDF membranes, and reversibly stained with Red Ponceau, as a loading control. (**A**) TDP-43 proteins potentially associated with hnRNP A2/B1 were detected by WB using a polyclonal anti-TDP-43 antibody (upper panel, IP fraction), while expression of the endogenous and exogenous tagged proteins was verified in the Input fraction (lower panel). Shown is a representative of two independent experiments with similar results, indicating that the R361S-TDP-43 ALS-mutant shows an altered capability of binding hnRNP A2/B1 compared to the WT protein. (**B**) Histograms represent the quantitative analysis of TDP-43 band densities in the IP fraction, normalized on the actual amount of Flag-TDP-43 overexpressed, detected in the Input fraction. Data (mean ± S.E.M.) are expressed as percentages of control cells (WT). Asterisk indicates values significantly different from controls (*=$p<0.05$ vs. WT), as assessed by One-way ANOVA followed by Newman-Keuls Multiple Comparison Test. (**C**) hnRNP A2/B1 was IP with a comparable yield.

The effect of disease-associated TDP-43 mutations on the association with CypA was then analysed by confocal immunofluorescence. Endogenous CypA (red) localisation was visualised simultaneously with Flag-tagged TDP-43 (green) staining in cells transiently transfected with WT-

or A315T- or R361S- or Y374X-Flag-TDP-43 (**Figure 4.13**). Wild-type and mutant TDP-43 proteins were mainly located in the nucleus, as previously observed (**Figure 4.9**). Colocalisation of CypA and TDP-43 was clearly nuclear in wild-type cells efficiently expressing Flag-tagged TDP-43, as already described in Results section **2.3**. In accordance with co-IP experiments, CypA and Flag-TDP-43 co-labelling evidenced areas of overlap (yellow) in the nuclei of A315T-TDP-43 ALS-mutants expressing cells, while only rare co-localisation events were visualised in R361S- or Y374X-TDP-43 cells (**Figure 4.13**). Thus, also dual staining by IF revealed that some pathogenic mutations in TDP-43 sequence could impair its binding with CypA. In particular, this feature was observed when the R361S or the C-terminally truncated Y374X mutant proteins, whose staining profile did not fully correspond to endogenous TDP-43 localisation pattern, were expressed.

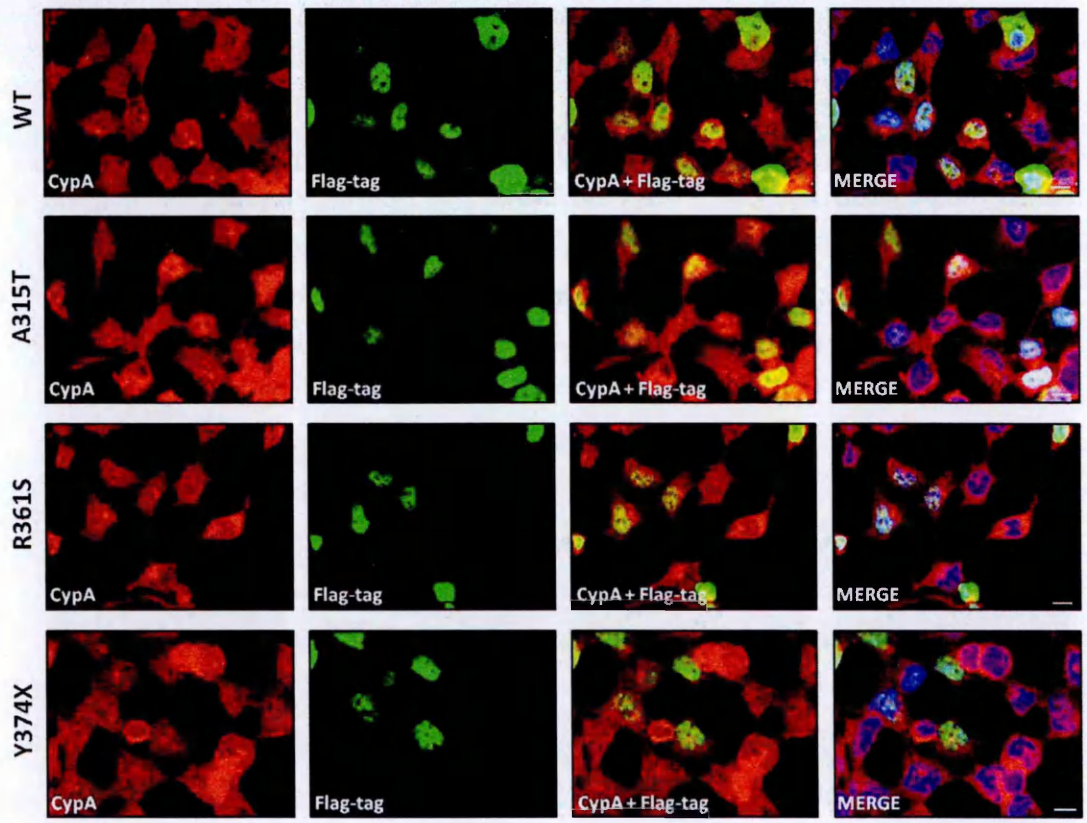

Figure 4.13 CypA co-localisation with Flag-TDP-43 ALS-mutants in HEK293 cells.

HEK293 cells were transiently transfected with WT- or A315T- or R361S- or Y374X-Flag-TDP-43 (bar:15μm). Cells were immunostained with polyclonal anti-CypA antibody followed by Alexa®647 (red)-conjugated antibody (left panels) or with monoclonal anti-Flag-tag antibody followed by Alexa®488 (green)-conjugated antibody (central panels). Nuclei were detected using Hoechst staining (blue). Colocalisation of the proteins was evidenced with areas of yellow in overlays of red

and green (central panels) and blue images (right panels, merge). Representative immunofluorescence images were chosen for display.

Summarising, TDP-43 disease-associated mutants did not efficiently bind CypA as the wild-type protein. This feature was particularly relevant in the presence of the mutation thought to impair the binding with hnRNPs (R361S), and further enhanced by the mutant missing the last forty amino acids of the C-terminal domain (Y374X). These experiments indicated that in pathological conditions an aberrant interaction may occur between TDP-43 and CypA, thus altering hnRNP complex formation, involving also hnRNP A2/B1. The results obtained with TDP-43 ALS-mutants also suggested that the C-terminal region of TDP-43 is relevant for a correct binding with CypA.

4.3.6 TDP-43 ALS-mutants influence CypA and hnRNP A2/B1 subcellular distribution

On account of a reduced binding between CypA and TDP-43 disease-associated mutants, together with altered complex formation with hnRNP A2/B1, the effect of the three ALS-patient derived mutations was further investigated on the subcellular distribution and expression of CypA and hnRNP A2/B1. To address this issue, HEK293 nuclei were separated from the cytoplasm of cells transiently transfected with the empty vector or WT- or A315T- or R361S- or Y374X-Flag-TDP-43 and silenced for the endogenous protein, by biochemical fractionation. Each subcellular fraction was independently analysed by WB for CypA (**Figure 4.14A**) and hnRNP A2/B1 (**Figure 4.14B**).

No significant differences were detected for cytosolic or nuclear CypA in TDP-43 silenced samples transfected with VEC or WT-TDP-43 compared to scrambled siRNA treated cells. Interestingly, the quantification of CypA blots clearly indicated that, in the cytosolic fraction, signals corresponding to TDP-43 disease-associated mutants were comparable to wild-type cells, except for the R361S mutation, that caused a statistically significant up-regulation in CypA levels (**Figure 4.14A**, blue graph). Instead, in the nuclear compartment, CypA was significantly increased after the expression of all TDP-43 ALS-mutants (**Figure 4.14A**, red graph). These variation in CypA nuclear

and cytosolic expression, following TDP-43 pathologic mutants transfection, were not observed in whole cellular lysates (data not shown). Nevertheless the trend described for CypA after biochemical observations could be also appreciated by confocal immunofluorescence in cells efficiently expressing TDP-43 Flag-tagged proteins (**Figure 4.13**). These data suggested that TDP-43 ALS-mutants did not substantially influence the global expression of CypA, but they could differentially alter the subcellular distribution of the protein.

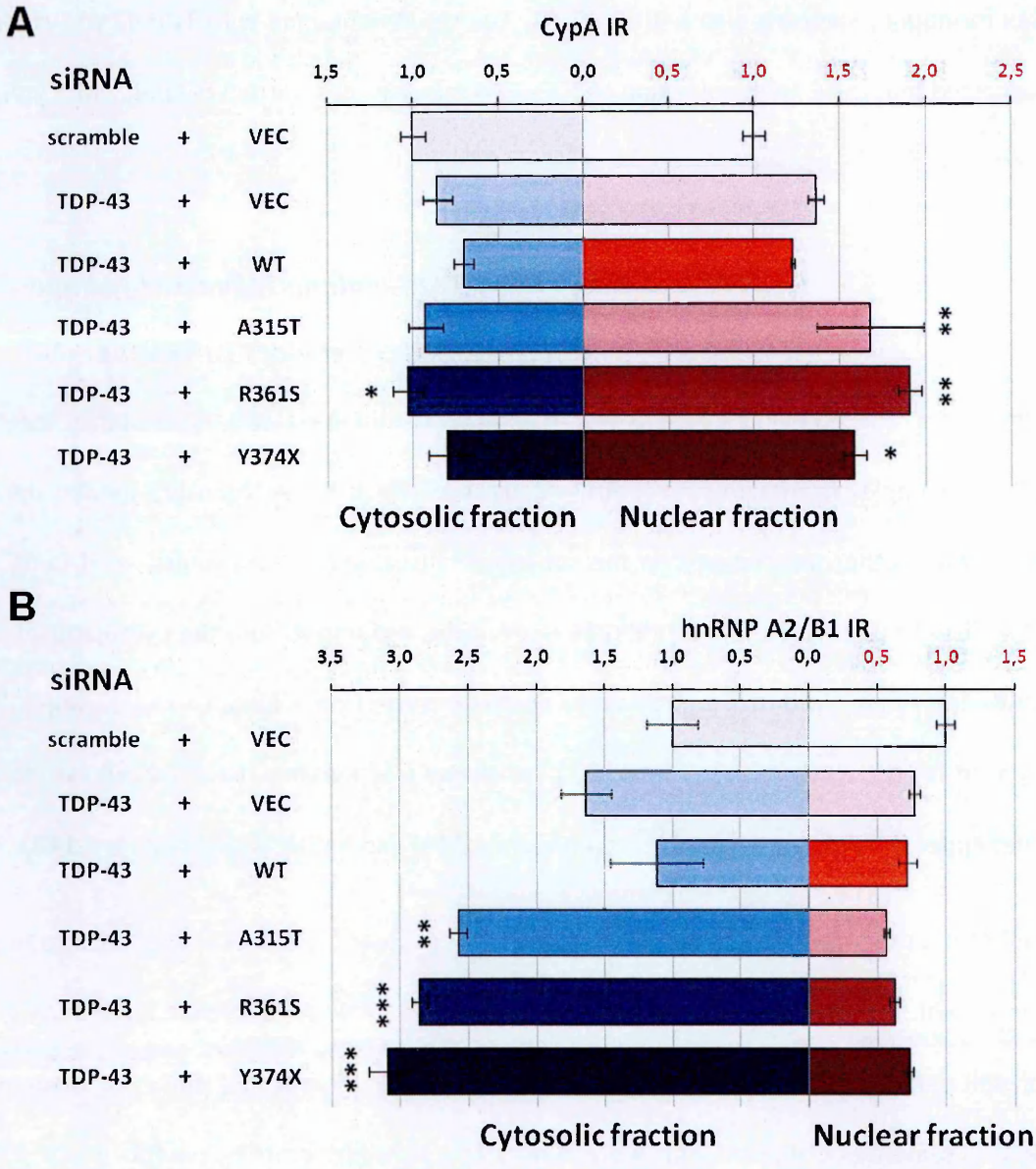

Figure 4.14 CypA and hnRNP A2/B1 subcellular distribution in cells expressing TDP-43 ALS-mutants.

HEK293 cells were transiently co-transfected with siRNA^{scramble} and an empty vector (VEC) or siRNA^{TDP-43} and an empty vector (VEC) or WT- or A315T- or R361S- or Y374X-Flag-TDP-43. Equal

amounts of cytosolic and the corresponding nuclear fractions were independently loaded, run on SDS-PAGE gels, transferred on PVDF membranes, stained with Red Ponceau as loading control, analysed by WB using the anti-CypA (**A**) or the anti-hnRNP A2/B1 (**B**) antibodies and detected by chemiluminescence. Histograms represent the quantitative analysis of CypA (**A**) or hnRNP A2/B1 (**B**) band densities in each compartment, normalized on the actual amount of proteins loaded, as detected by Red Ponceau staining. Data (mean ± S.E.M., n=4) in each subcellular fraction are proportioned to control cells ($siRNA^{scramble}$ + VEC), whose immunoreactivity (IR) value was set as one. The cytosolic and the corresponding nuclear fractions are represented in blue and red, respectively. Asterisks indicate that samples are significantly different (*=$p<0.05$) compared to WT, as assessed by One-way analysis of variance followed by Bonferroni's Multiple Comparison Test.

In cells incubated with $siRNA^{TDP-43}$ together with VEC or WT-TDP-43 constructs, hnRNP A2/B1 preserved its localisation pattern as in control cells, treated with a scrambled siRNA. However, in the cytosolic fraction, the level of hnRNP A2/B1 was significantly higher in ALS-mutant cells than in WT-TDP-43 cells (**Figure 4.14B**, blue graph). This increase could also be appreciated in whole cellular lysates of R361S- and Y374X-TDP-43 expressing cells (data not shown). In the nuclear fraction no differences were detectable between wild-type and TDP-43 mutant cells (**Figure 4.14B**, red graph). Together these results indicated that TDP-43 associated mutations could modify hnRNP A2/B1 relative expression and distribution in the cytoplasm of HEK293 cells.

Under basal condition CypA is predominantly localised in the cytoplasm, whereas hnRNP A2/B1 is almost exclusively localised in the nucleus. TDP-43 down-regulation did not significantly influence the stoichiometry of the other hnRNP complex protein components analysed, CypA and hnRNP A2/B1. Instead, a shift in the subcellular localisation of both CypA and hnRNP A2/B1, whose levels were increased respectively in the nuclear and in the cytosolic fractions, was detected in all TDP-43 ALS-mutants analysed. Furthermore, TDP-43 disease-causing mutations could alter the binding with CypA and hnRNP A2/B1. In particular, at least one TDP-43 ALS-causing mutation severely impacted on this hnRNP complex formation and on both CypA and hnRNP A2/B1 levels. In fact, in cells expressing the R361S-TDP-43 mutant CypA was increased not only in the nucleus, but, together with hnRNP A2/B1, an up-regulation of the cytosolic protein was also observed. Notably, these cells not only showed a decreased ability of interaction between CypA and TDP-43, but also

among TDP-43 and hnRNP A2/B1, and CypA and hnRNP A2/B1. Thus, in this case a correct hnRNP complex assembly and trafficking was impaired not only by CypA/TDP-43 altered binding, but also by TDP-43/hnRNP A2/B1 loss of interaction due to the presence of the R361S mutation within the minimal hnRNP A2 binding domain of TDP-43 (D'Ambrogio 2009; Budini 2012).

Taking these experiments together, it is possible to hypothesise that the effects of the three ALS-patient derived mutations on the interaction with CypA and hnRNP A2/B1 and their subcellular localisation in HEK293 cells are linked. In fact, alterations of the CypA/TDP-43 interaction, detected when TDP-43 is mutated, could have important implications for hnRNP complex formation and maintenance, and in TDP-43 cytoplasmic mislocalisation, which is considered a hallmark of TDP-43 proteinopathies. Thus, the changes observed in CypA and hnRNP A2/B1 subcellular distribution could represent a compensatory mechanism to restore the hnRNP complex.

Interestingly, CypA was reported to play an important regulatory role in the trafficking of hnRNP A2, since they formed a complex, which underwent nuclear export in response to chemokine stimuli (Pan 2008). In association with a reduced binding between CypA and TDP-43 mutants, we detected a shift in the subcellular localisation of both TDP-43 mutants and hnRNP A2/B1, that increased in the cytosolic fractions. These results indicated that CypA could be required for the correct localisation or redistribution of the members of this hnRNP complex. However, further analyses are needed to define the effects mediated by CypA on intracellular wild-type and ALS-mutant TDP-43 trafficking and function.

4.3.7 TDP-43 ALS-mutants cannot rescue HDAC6 protein expression level in HEK293 cells

Given these observations, the functional effect of TDP-43 clinical mutations were assessed on one well characterised mRNA target of TDP-43: HDAC6. In fact, in this study, the CypA/TDP-43 hnRNP complex involvement was already established in HDAC6 expression regulation (Results section

3.2.3). To further address this issue, HEK293 cells were silenced for endogenous TDP-43 targeting its 3'-UTR, thus allowing the efficient retransfection with Flag-TDP-43 cDNA. HDAC6 protein level was detected by WB analysis. As previously observed, HDAC6 protein expression was significantly downregulated on TDP-43 knockdown (**Figure 4.15**). Decreased HDAC6 protein levels could be restored to normal levels after retransfection of silenced cells with WT-TDP-43 cDNA, replicating the work by Fiesel and coworkers. The A315T- and R361S-TDP-43 pathogenic point mutants were able to restore HDAC6 protein levels with a slightly reduced capacity compared to the wild-type protein, similar to as described for HDAC6 mRNA levels (Fiesel 2009). In contrast, the Y374X-TDP-43 mutant failed to restore HDAC6 levels, consistent with a previous report on a truncated form of TDP-43 lacking the C-terminal glycin-rich domain (Fiesel 2009).

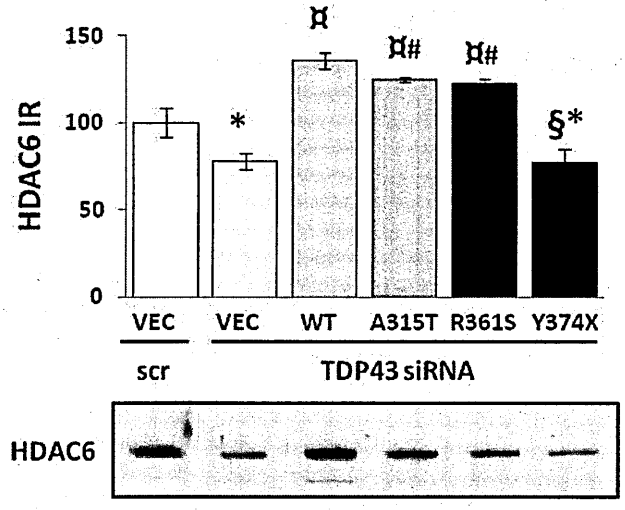

Figure 4.15 ALS-TDP-43 mutants-mediated HDAC6 expression regulation.

HEK293 cells were transiently co-transfected with $siRNA^{scramble}$ (scr) and an empty vector (VEC) or $siRNA^{TDP-43}$ and an empty vector (VEC) or WT- or A315T- or R361S- or Y374X-Flag-TDP-43. 15 µg of total protein lysates were loaded, run on SDS-PAGE gels, transferred on PVDF membranes, stained with Red Ponceau as loading control, analysed by WB for HDAC6 and detected by chemiluminescence. Histograms represent the quantitative analysis of HDAC6 band densities, normalized to the actual amount of proteins loaded, as detected by Red Ponceau staining. Data (mean ± S.E., n=4) are expressed as percentage of the immunoreactivity (IR) values. Symbols indicate values significantly different from controls (*=$p<0.05$ vs. $siRNA^{scramble}$; ¤= <0.05 vs. $siRNA^{TDP-43}$ + VEC; §=$p<0.05$ vs. WT), as assessed by One-way ANOVA followed by Bonferroni's Multiple Comparison Test, or (#=$p<0.05$ vs. WT) as assessed by Student's t-test.

Nuclear localisation of TDP-43 as well as its nucleic acid and protein-binding capacities are important determinants of HDAC6 regulation (Fiesel 2009). These features were severely impaired by the ALS-mutations described in this work, and significantly impacted on a well established function of TDP-43. Correct protein-protein interaction between hnRNPs, such as TDP-43 and hnRNP A2/B1, as well as their efficient association with molecular chaperones, like CypA, may thus contribute to RNA-protein complex formation along with direct RNA-protein interaction between hnRNPs and mRNAs (Kim 2000).

5. SOD1-associated disease

A novel protein interaction between CypA and TDP-43 was described, demonstrating the importance of CypA for TDP-43/hnRNP A2/B1 complex formation, maintenance and function in normal or TDP-43-related disease conditions. These findings opened up interesting new avenues for investigating CypA functions in other biological processes and contexts. Indeed, previous studies in our laboratory have demonstrated that CypA was altered both in sporadic ALS patients and in *in vivo* animal models carrying SOD1 mutation (Basso 2009; Nardo 2011), already at a pre-symptomatic stage of the disease (Massignan 2007). This left open the possibility that CypA could have a relevant role in ALS pathogenesis and that this hnRNP complex could be also directly or indirectly involved in TDP-43-independent cases of ALS pathology. To investigate this option, CypA functions were explored in pathological conditions associated with SOD1.

5.1 CypA interacts with ALS-mutant SOD1

Recently, the proteomic study of the Triton-insoluble proteins extracted from the spinal cord of fALS mice demonstrated that CypA is recovered, together with G93A-SOD1, as insoluble material in protein aggregates. This feature was not observed in wild-type mice, thus CypA co-aggregated specifically with ALS-mutant SOD1. Interestingly, CypA was present also in the aggregates from post-mortem spinal cord tissues of sporadic ALS patients (Basso 2009). Therefore, the hypothesis that CypA and SOD1 could specifically interact was tested. Indeed, mutant SOD1 is known to cause motor neuron degeneration by toxic gain-of-function(s). Thus, the toxic properties of mutant SOD1 may be exerted, at least in part, through aberrant interactions with other proteins.

5.1.1 In vitro interaction using endogenous proteins

To determine whether CypA could interact with SOD1 and if this association could have any functional role, a co-immunoprecipitation approach was adopted. First this interaction was

studied *in vitro*, analysing HEK293 cell lines stably expressing WT-SOD1 or G93A-SOD1. CypA was immunoprecipitated in whole cellular lysates and the antibody anti-SOD1 was used to evaluate its presence in CypA co-IP fraction. Interestingly, SOD1 was recovered mainly in the IP fraction from mutant SOD1 cells (**Figure 5.1A**), suggesting that CypA has a preferential affinity for G93A-SOD1. The association of CypA with ALS-mutant SOD1 was specific, as determined by several positive and negative controls. In particular, different starting IP solutions were used as experimental controls, as previously described in Results section **2.2.1.1**, obtaining analogous results.

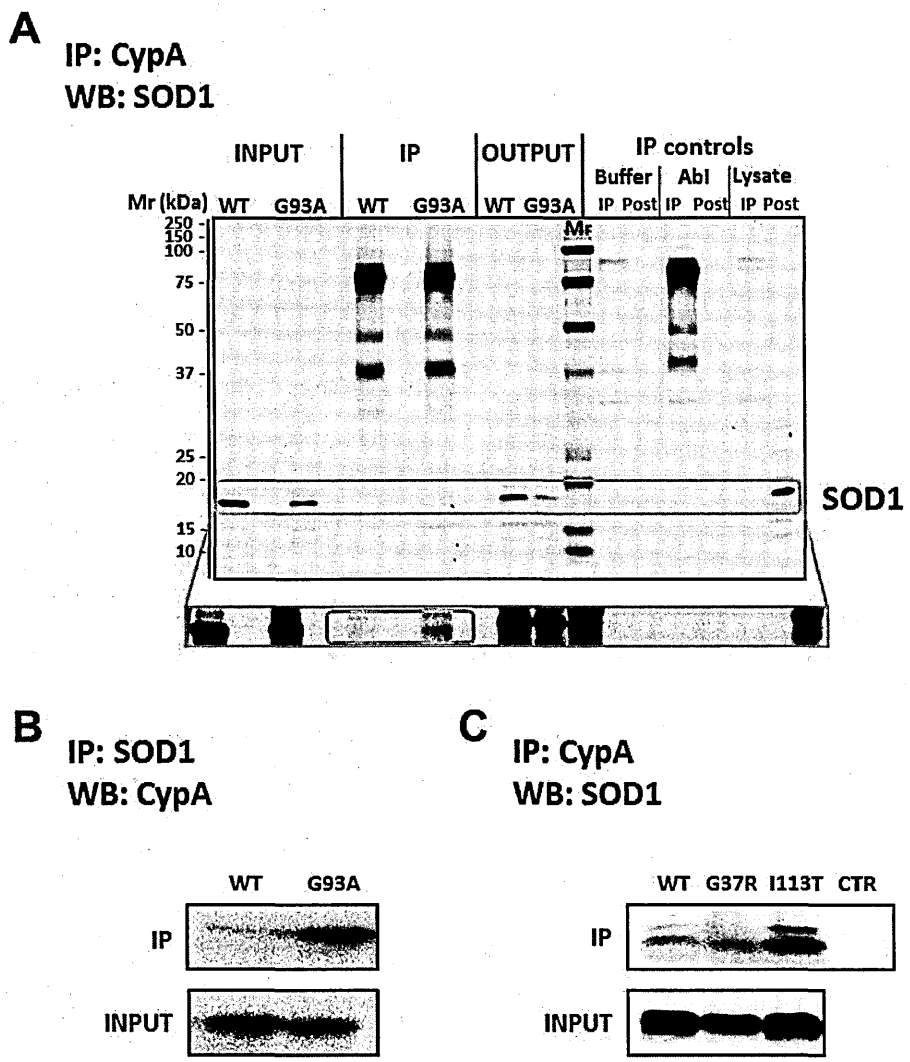

Figure 5.1 CypA preferentially interacts with mutant SOD1 *in vitro*.

Equal amounts of proteins (500µg) were co-precipitated with the primary antibody. Aliquots of the cell lysates (INPUT), of the immunoprecipitates (IP) and of the proteins from the remaining fraction (OUTPUT) were loaded together with three different IP controls and their relative output fractions (POST), and subjected to SDS-PAGE. Proteins were transferred to PVDF membranes, reversibly

stained with Red Ponceau as loading control, probed with specific antibodies and the signal was detected by chemiluminescence. (**A**) Lysates from HEK293 cells stably expressing WT-SOD1 or G93A-SOD1 were blotted for SOD1 after CypA immunoprecipitation. (**B**) Wild-type and mutant cells were blotted for CypA after SOD1 immunoprecipitation. (**C**) HEK293 cells were transiently transfected with WT- or G37R- or I113T-SOD1 plasmids. Cellular lysates, together with coated beads as IP control, were immunoprecipitated using an anti-CypA antibody and potentially associated SOD1 was detected by WB. Representative of several independent experiments with similar results are shown, indicating CypA preferential interaction for ALS-mutant SOD1.

Moreover, to confirm the specificity of this binding, CypA co-IP assay was performed using different commercially available polyclonal and monoclonal antibodies. These preliminary experiments revealed that CypA interacted preferentially with G93A-SOD1 in mammalian cells.

To further verify the interaction between CypA and G93A-SOD1 the same co-IP experiment was repeated in HEK293 cells expressing WT-SOD1 or G93A-SOD1 reversing the primary antibodies previously used (**Figure 5.1B**). In particular, the immunoprecipitation by the anti-SOD1 antibody, was followed by the WB for CypA, providing additional evidence that the two proteins interacted preferentially in mutant cells.

5.1.2 In vitro interaction using transiently-transfected SOD1 ALS-mutants

In order to evaluate if mutSOD1/CypA gain-of-interaction was specific for the G93A mutation or it was a common feature of ALS-associated mutant SOD1, the co-IP analysis of two more hSOD1 ALS-mutants was performed. In particular, plasmids carrying hSOD1 cDNA wild-type or with the G37R or I113T mutations (kindly provided by Dr. Grierson, University of Sheffield, UK), both of which give rise to an ALS phenotype *in vivo*, were used for these experiments. HEK293 cells were transiently transfected with the three constructs. First, an efficient transfection method was optimized to produce the exogenous proteins with good and similar levels, as shown by the WB for SOD1 in the input fraction (**Figure 5.1C**). Then, the antibody anti-CypA was used to co-IP and co-precipitated SOD1 was detected by WB. Coated magnetic beads (CTR) were used as negative

experimental control. This experiment was repeated several times with the common effect of both mutant proteins to preferentially interact with CypA. Thus, the interaction of mutant SOD1 with CypA was not limited to the G93A ALS-mutant. Indeed, both G37R- and, to a greater extent, I113T-SOD1 mutants were co-IP by anti-CypA antibodies when overexpressed in HEK293 cells. These mutations, like the G93A, can accelerate SOD1 unfolding kinetics compared to the wild-type protein (Ip 2011), suggesting a prominent role for protein misfolding in this protein-protein interaction.

5.1.3 In vivo interaction validation

To confirm the novel interaction observed *in vitro* between ALS-mutant SOD1 and CypA, validation experiments were performed *in vivo*. Indeed, the tissue mostly affected in ALS was analysed in mouse models of the disease. Protein extracts of lumbar spinal cord (containing the motor neurons innervating the lower limbs) from symptomatic double transgenic mice over-expressing ALS-mutant hSOD1 and expressing (G93A-SOD1/CypA+/+) or knock-out (G93A-SOD1/CypA-/-) for CypA, and age and sex-matched control mice over-expressing wild-type hSOD1 (WT-SOD1/CypA+/+) were used in co-IP assays. In particular, CypA knockout mice were used as negative experimental controls. An anti-CypA antibody was used to immunoprecipitate and the following WB for SOD1 clearly detected the protein in the co-IP fraction, only in mutant SOD1 mice expressing CypA (G93A-SOD1/CypA+/+), and neither in wild-type SOD1 mice nor in CypA knockout mice (**Figure 5.2A**). As in *in vitro* experiments, failure to detect complexes of CypA and wild-type SOD1, was not due to lack of protein expression (Input fraction). Thus, CypA was confirmed as a novel mutant-SOD1 interacting protein, validating previous results *in vivo* and demonstrating the specificity of these findings.

To further evaluate if this gain of interaction was specifically linked to ALS, the previous experiment was repeated splitting the lumbar spinal cord tract into the dorsal (DH) and the ventral (VH) horn, that is the motor neuron-enriched portion. CypA preferential interaction for

G93A-SOD1, in respect to WT-SOD1, was confirmed and it was clearly detected mainly in the ventral horn, where motor neurons are located (**Figure 5.2B**).

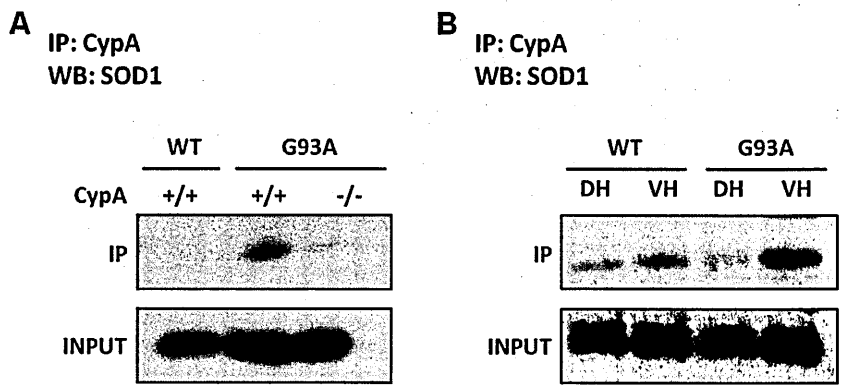

Figure 5.2 CypA preferentially interacts with mSOD1 *in vivo*.

(**A**) Lumbar SpC of WT-SOD1/CypA+/+ (n=3), G93A-SOD1/CypA+/+ (n=3) and G93A-SOD1/CypA-/- (n=3) mice were analysed. (**B**) Lumbar SpC of WT-SOD1 (n=3) and G93A-SOD1 (n=3) mice split into dorsal (DH) and ventral (VH) horn sections were analysed. Equal amounts of proteins (1mg) from tissue homogenates were co-precipitated with anti-CypA primary antibody. Aliquots of the tissue homogenates (INPUT) and of the immunoprecipitates (IP) were loaded together, subjected to SDS-PAGE, transferred to PVDF membranes, reversibly stained with Red Ponceau as loading control, probed with anti-SOD1 antibody and detected by chemiluminescence. Representative experiments with consistent results are shown, indicating that interaction between CypA and ALS-mutant G93A-SOD1 was confirmed *in vivo*.

Collectively, these data demonstrated that ALS-mutant SOD1 co-immunoprecipitated with CypA, confirmed the specificity of the novel interaction described, and also its relevance in ALS disease-related animal tissues.

5.2 CypA absence alters G93A-SOD1 solubility

In order to understand if this gain of interaction could have a role in ALS pathogenesis, detergent-insoluble proteins were analyzed as a model of protein aggregates. In fact, proteinaceous inclusions rich in mutant SOD1 have been found in tissues from fALS patients, mutant SOD1

animals and cellular models (Wood 2003; Basso 2006 and 2009). The propensity of mutant SOD1 to aggregate is one of the most sustained hypotheses to explain the toxicity of this enzyme.

In particular, Triton X-100-insoluble proteins (TIF) were extracted from ventral horn lumbar spinal cords of G93A-SOD1 mice, expressing (G93A-SOD1/CypA+/+), with a deficient expression (G93A-SOD1/CypA+/-) or not expressing (G93A-SOD1/CypA-/-) CypA, just prior to the expected onset of clinical symptoms. Potentially aggregating proteins were indeed enriched in detergent-insoluble fractions and separated from soluble proteins. The same amount of TIF and the corresponding soluble samples were independently analysed by WB for SOD1. The relative quantification of SOD1 blots revealed that an increasing amount of insoluble mutant SOD1 was recovered when CypA was reduced or totally deficient (**Figure 5.3A**), while no differences were observed in the soluble fraction (**Figure 5.3B**).

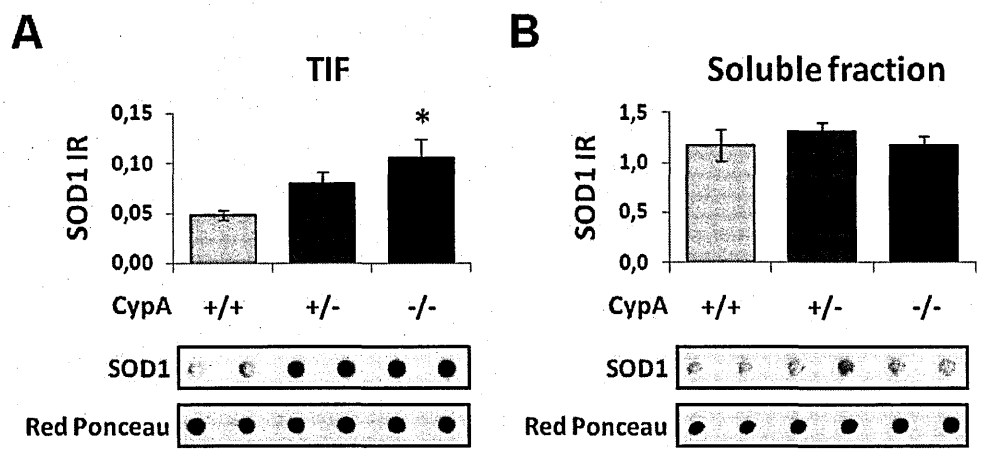

Figure 5.3 CypA absence increases mutant SOD1 in the insoluble but not in the soluble fractions.

Immunoblot analysis of TIF from ventral horn lumbar spinal cord tissues of G93A-SOD1/CypA+/+ (n=3), G93A-SOD1/CypA+/- (n=3) and G93A-SOD1/CypA-/- (n=3) mice. Aliquots of TIF (**A**) or Soluble (**B**) proteins were analysed independently by dot (3µg) blotting for SOD1 and detected by chemiluminescence. Histograms represent the immunoreactivity normalised to the actual amount of protein loaded, detected after Red Ponceau staining. Data (mean ± S.E.M., n=3) are expressed as relative immunoreactivity values. Asterisks indicate values significantly different from controls (*=p≤0.05 vs. G93A-SOD1/CypA+/+), as assessed by One-way Anova followed by Neuman-Keuls multiple comparison test.

These results demonstrated that depletion of CypA resulted in more mutant SOD1 aggregates formation. Thus, it is possible to speculate that in ALS-mutant SOD1 motor neurons, where the interaction between CypA and mutant SOD1, as well as their presence in the detergent-insoluble fraction have been described, CypA could act as a chaperone.

In order to describe which are the most relevant features of the TX-insoluble fraction when CypA is depleted in fALS mice, in addition to SOD1, some insoluble/aggregate components previously characterised (Basso 2009) in TIF spinal cord of G93A-SOD1 mice were analysed. WB analysis for Ubiquitin confirmed that insoluble ubiquitinated proteins were isolated from the spinal cords of fALS mice (**Figure 5.4A**). Also CypA was significantly enriched in TIF of G93A-SOD1 mice, replicating a previous study performed in our laboratory (Basso 2009) on the G93A-SOD1 mouse model and on ALS patients (**Figure 5.4B**). Therefore TIF was confirmed to have the biochemical features of ALS protein inclusions. Furthermore, TIFs recovered from CypA+/- mice were significantly enriched in ubiquitinated proteins and the same trend was observed in knockout mice (**Figure 5.4A**). Moreover, protein carbonyl content, a marker of protein oxidation (Castegna 2002), was significantly enriched in TIFs from CypA depleted mice (**Figure 5.4C**). In addition to oxidative damage to proteins, nitration of actin, but not total protein 3-nitro-tyrosine levels, was increased in spinal cords of CypA depleted G93A-SOD1 mice (**Figure 5.4D-E**). The expression of individual chaperone proteins in the soluble fraction of mutant SOD1 mice, both HSC70 (**Figure 5.4G**) and HSP90 (**Figure 5.4I**), was not modified by CypA depletion. Nevertheless, HSC70 (**Figure 5.4F**), but not HSP90 (**Figure 5.4H**), was specifically increased in the detergent-insoluble fraction in association with CypA absence.

Summarizing, knockout animals being deficient in CypA chaperoning activity, formed more aggregates of mutant SOD1 and irreversibly damaged proteins (ubiquitinated and aberrantly oxidized), possibly sequestering other protein components essential for motor neuronal function, such as HSC70. In fALS mice CypA, together with other chaperones, could form complexes with mutant misfolded SOD1 and thus could contribute to protect cells from mutant SOD1 toxicity by direct interaction, preventing aggregation and facilitating degradation of damaged protein.

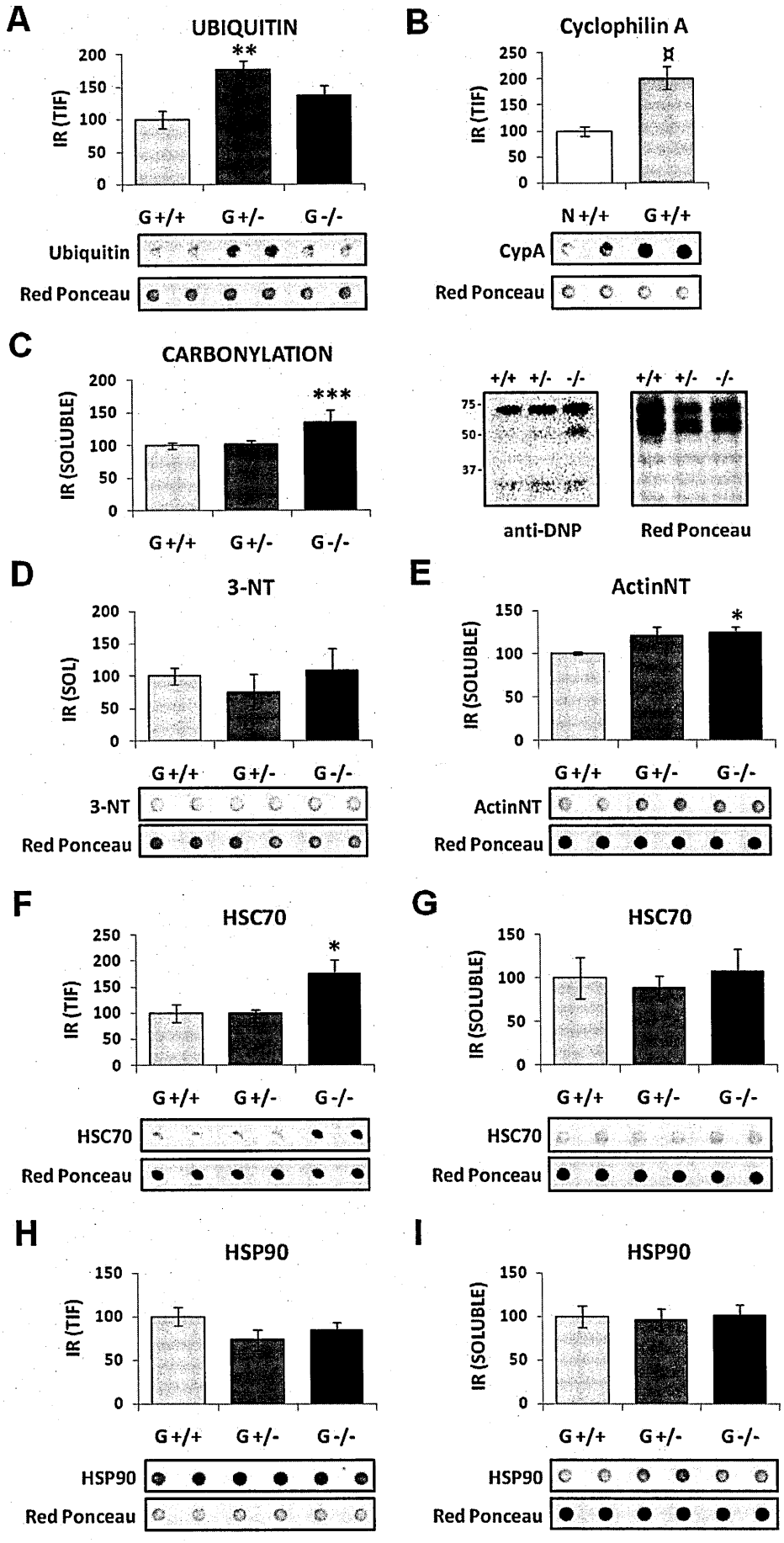

Figure 5.4 Protein composition of TIF in G93A-SOD1/CypA double transgenic mice samples.

Immunoblot analyses of TIF from ventral horn lumbar spinal cord tissues of age-matched non-transgenic/CypA+/+ (N+/+), G93A-SOD1/CypA+/+ (G+/+), G93A-SOD1/CypA+/- (G+/-) and G93A-SOD1/CypA-/- (G-/-) mice at disease onset. The level of Ubiquitin (**A**), CypA (**B**), HSC70 (**F**) and HSP90 (**H**) were measured in TIF. Carbonylated proteins (**C**), 3-Nitro-tyrosine (**D**), nitrated Actin (**E**), HSC70 (**G**) and HSP90 (**I**) were analysed in the Soluble (SOL) fraction. Aliquot of TIF or Soluble proteins were analysed independently by Western (15µg) or dot blotting (3µg), probed with the specific antibodies and detected by chemiluminescence. Histograms represent the immunoreactivity normalised to the actual amount of protein loaded, detected after Red Ponceau staining. Data (mean ± S.E.M., n=3) are expressed as percentages of control samples. Symbols indicate values significantly different from controls (*=p≤0.05 vs. G93A-SOD1/CypA+/+) as assessed by One-way ANOVA followed by Neuman-Keuls multiple comparison test, or (¤=p≤0.05 vs. Ntg/CypA+/+) as assessed by t test.

5.3 Mutant SOD1 alters CypA/ TDP-43 interaction

At the same time, mutant SOD1 interaction with CypA could exert a negative effect. In fact, the binding of CypA to mutant forms of a protein abundant in motor neurons, such as SOD1, could make it unavailable for other intracellular functions. For example, mutant SOD1 association with CypA could have the effect of decreasing its availability for interactions with other proteins, like TDP-43.

5.3.1 In vitro evidence: G93A-SOD1 HEK293 cells

To investigate this possibility, CypA/TDP-43 interaction was evaluated in HEK293 cells stably expressing WT-SOD1 or G93A-SOD1. WB for TDP-43, and its relative quantification, showed that the anti-CypA antibody was not able to co-immunoprecipitate TDP-43 in G93A-SOD1 cells as much as in wild-type cells (**Figure 5.5A-B**). In association with a reduced binding, we detected an abnormal subcellular localisation of both CypA (**Figure 1.6**) and TDP-43 (**Figure 5.5C**), that increased in the cytosolic fractions.

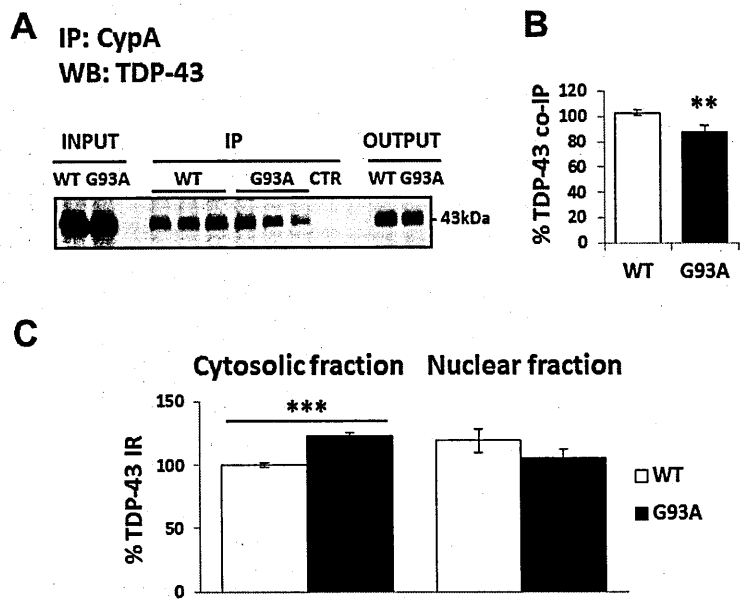

Figure 5.5 CypA/TDP-43 binding is altered in HEK293 stably expressing mutant SOD1.

(**A**) Equal amounts of proteins (500µg) from HEK293 cells stably expressing WT-SOD1 or G93A-SOD1, together with coated beads as IP control (CTR), were immunoprecipitated using an anti-CypA antibody. Aliquots of the cell lysates (INPUT), of the immunoprecipitates (IP) and of the proteins from the remaining fraction (OUTPUT) were loaded, subjected to SDS-PAGE, transferred to PVDF membranes, reversibly stained with Red Ponceau as loading control, probed for TDP-43 and detected by chemiluminescence. (**B**) Histograms represent the quantitative analysis of TDP-43 band densities in the IP fraction, normalized on the actual amount of proteins immunoprecipitated, as detected by Red Ponceau staining. (**C**) Equal amounts of cytosolic and the corresponding nuclear fractions from HEK293 cells stably expressing WT-SOD1 or G93A-SOD1 were independently analysed for TDP-43 by WB. Histograms represent the quantitative analysis of TDP-43 band densities in each compartment, normalized on the actual amount of proteins loaded, as detected by Red Ponceau staining. Data (mean ± S.E.M., n=3) are expressed as percentages of control cells (WT). Asterisk indicates values significantly different from controls (*=$p<0.05$ vs. WT), as assessed by Student's t-test.

These results suggested that alterations of the CypA/TDP-43 interaction, as well as their cytoplasmic mislocalisation, could be detected in presence of mutant SOD1. These events could have important implications in hnRNP complex formation and stability, as well as in TDP-43-related functions. In particular, these effects could be particularly detrimental in the context of a diseased tissue, like lumbar spinal cord in ALS.

5.3.2 In vivo evidence: G93A-SOD1/CypA knockout double transgenic mice

The impaired binding between CypA and TDP-43 significantly increased TDP-43 insolubility in NTg mice knockout for CypA (Results section **3.3**). To explore if their altered association could be detrimental in SOD1-related pathological conditions, TDP-43 was analysed in TIFs from ventral horn spinal cord of G93A-SOD1/CypA double transgenic mice at disease onset. Interestingly, TDP-43 was recovered in the detergent-insoluble fraction of mutant SOD1 mice, and higher amount of insoluble TDP-43 was accumulated when CypA was completely absent (**Figure 5.6A**), thus confirming previous results. While, no statistically significant differences were detected in the soluble fractions (**Figure 5.6D**). No differences were observed for hnRNP A2/B1 both in TIFs (**Figure 5.6B**) and in the soluble fractions (**Figure 5.6E**) of G93A-SOD1 animals. In the absence of CypA also in mutant SOD1 mice spinal cord there was a huge increase of aberrantly phosphorylated TDP-43 in the aggregates, compared to G93A-SOD1/CypA+/+ animals (**Figure 5.6C**).

TDP-43 deficiency, as it may occur in SOD1-related fALS in association with CypA depletion, by cytosolic sequestration of this nuclear protein in insoluble complexes, may contribute to motor neuron disease through impaired TDP-43 functions. To rule out this possibility, HDAC6 protein levels were analysed by WB in the soluble fractions of double transgenic mice. Interestingly, ventral horn spinal cords from G93A-SOD1/CypA knockout mice showed a significant reduction of HDAC6 protein expression (**Figure 5.6F**). Even though only indirectly disturbed in SOD1-associated disease, early alterations in this pathway, that is decisive for neurite outgrowth (Fiesel 2011), may thus contribute to neurodegenerative events in ALS.

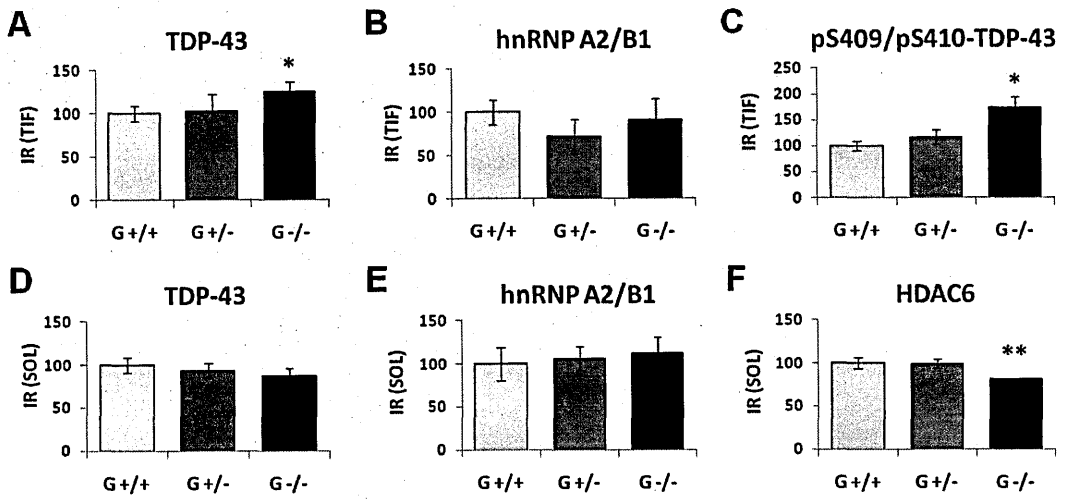

Figure 5.6 Protein composition of TIF in G93A-SOD1/CypA double transgenic mice samples.

Immunoblot analyses of TIF from ventral horn lumbar spinal cord tissues of age and sex-matched G93A-SOD1/CypA+/+ (n=3), G93A-SOD1/CypA+/- (n=3) and G93A-SOD1/CypA-/- (n=3) mice at disease onset. The level of TDP-43 (**A**), hnRNP A2/B1 (**B**) and pS409/pS410-TDP-43 (**C**) were measured in TIF. TDP-43 (**D**), hnRNP A2/B1 (**E**), and HDAC6 (**F**) were also analysed in the Soluble fraction. Aliquot of TIF or soluble proteins were analysed independently by Western (15µg) or dot blotting (3µg), probed with the specific antibodies and detected by chemiluminescence. Histograms represent the immunoreactivity normalised to the actual amount of protein loaded, detected after Red Ponceau or Sypro® Ruby Protein Blot staining. Data (mean ± S.E.M., n=3) are expressed as percentages of control samples (G93A-SOD1/CypA+/+). Symbols indicate values significantly different from controls (*=p≤0.05 vs. G93A-SOD1/CypA+/+), as assessed by One-way Anova followed by Neuman-Keuls multiple comparison test.

Finally, in order to determine whether the results described at disease onset could represent a relevant mechanism for ALS pathogenesis and disease progression, TDP-43 was quantified in TIFs of G93A-SOD1/CypA double transgenic mice at different stages of the disease. In particular, samples from ventral horn spinal cords were analysed just prior to the expected onset of clinical symptoms (14 weeks of age) and at a late symptomatic stage of the disease (20 weeks of age), and compared to sex and age-matched NTg mice expressing, with a reduced expression or knockout for CypA.

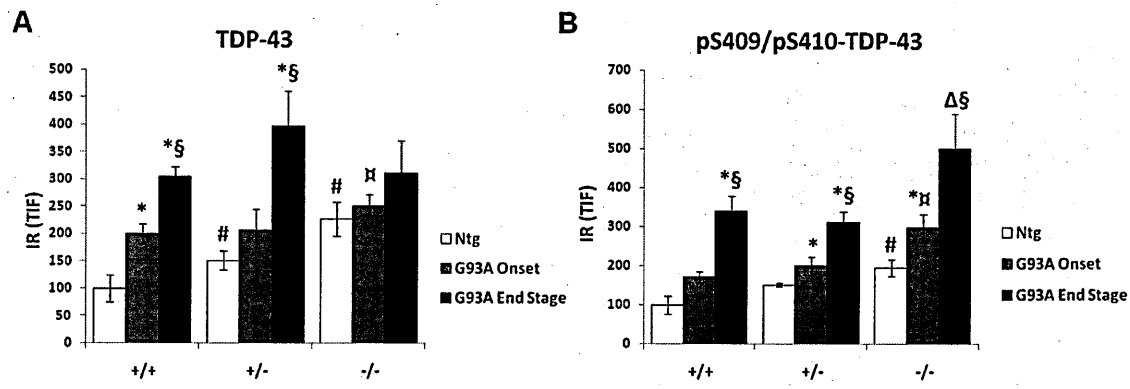

Figure 5.7 CypA absence or reduction increase TDP-43 in TIF of ALS-mutant SOD1 mice samples and enhance its aberrant phosphorylation.

Immunoblot analyses of TIF from ventral horn lumbar spinal cord tissues of age and sex-matched G93A-SOD1 and NTg mice for three different CypA genotypes at disease onset and end stage. Histograms represent the immunoreactivity of TDP-43 (**A**) and pS409/pS410-TDP-43 (**B**) normalised to the actual amount of protein loaded, detected after Red Ponceau or Sypro® Ruby Protein Blot staining. Data (mean ± S.E.M., n=3) are expressed as percentages of control samples (NTg/CypA+/+) at the respective age. Symbols indicate values significantly different from controls (*=p≤0.05 NTg vs. G93A-SOD1; #=p≤0.05 vs. NTg/CypA+/+; ¤=p≤0.05 vs. G93A-SOD1/CypA+/+ onset; Δ=p≤0.05 vs. G93A-SOD1/CypA+/+ end stage; §=p≤0.05 onset vs. end stage), as assessed by One-way Anova followed by Neuman-Keuls multiple comparison test.

The expression of mutant SOD1 was sufficient to enhance TDP-43 aggregation into pathological inclusions at disease onset compared to NTg mice, with a statistically significant increase at the end stage (**Figure 5.7A**). Nevertheless, both in NTg and in mutant SOD1 mice, TDP-43 was increasingly recovered in the insoluble fraction when CypA expression was reduced or completely absent. These results suggested that CypA protein level was inversely proportional to the amount of insoluble TDP-43 recovered. Furthermore, the accumulation of TDP-43 in TIFs of NTg/CypA knockout mice was comparable with mutant SOD1/CypA+/+ mice at both disease stages, indicating that respectively CypA direct or indirect depletion could contribute to TDP-43 detergent-insolubility.

A pattern similar to TDP-43 was observed with the antibody raised against aberrantly phosphorylated TDP-43 species, with CypA knockout mice expressing mSOD1 displaying greater differences. Furthermore, aberrantly phosphorylated TDP-43 could clearly differentiate the two

stages of the disease. In these animals, both mutant SOD1 expression and CypA depletion contributed to enhance sequestration of hyper-phosphorylated TDP-43 into pathological inclusions, that accumulated with disease progression (**Figure 5.7B**). In particular, this analysis suggested that CypA absence could have an influence on disease progression. In fact, the early presence of TDP-43 alterations in the detergent-insoluble fraction of G93A-SOD1/CypA-/- mice was comparable with G93A-SOD1/CypA+/+ animals at the end stage of the disease, indicating that CypA should influence both initiation and progression of the pathology.

Summarizing, CypA was confirmed to interact specifically with mutant SOD1, possibly acting as a chaperone. As a consequence of chaperones preferential binding for misfolded proteins, mutant SOD1/CypA complex may recruit also other proteins to form aggregates. Indeed, mutant SOD1 could sequester CypA in the cytosol impeding CypA functions in the nucleus, including its association with TDP-43. Dysregulation of TDP-43/CypA hnRNP complex could contribute to alter TDP-43 subcellular distribution, thus further favouring aggregation and impairing TDP-43 nuclear functions, such as HDAC6 mRNA processing.

In conclusion, alterations of the CypA/TDP-43 interaction, detected both when TDP-43 or SOD1 were mutated, could have important implications in hnRNP complex formation and stability, and in TDP-43 mislocalisation and functions. Given these observations, CypA should be considered an aggregation modifier in ALS.

V. DISCUSSION

The purpose of this thesis work was to investigate the overall contribution of CypA to ALS and possibly its involvement in the patho-mechanisms of the disease. In particular, this study was carried out to test whether an early systemic translational biomarker for ALS could shed light on disease-causing mechanisms. Indeed, CypA revealed to be an interesting molecule that is worthwhile to deeply study and characterise for its relevance as a possible molecular link between two pathogenic mechanisms in sporadic and familial ALS.

CypA was previously identified in our lab as a hallmark of the disease in the G93A-SOD1 mouse model of fALS (Massignan 2007; Basso 2009) and in sALS patients (Nardo 2011). In particular, an altered expression pattern of CypA isoforms was observed already at a milder stage of the pathology in PBMC from sALS patients, and at a pre-symptomatic stage of the disease in the SpC of mSOD1 mice (Massignan 2007; unpublished data from the lab). Moreover, elevated levels of CypA were detected in PBMC from sALS and G93A-SOD1 rats, already at the pre-symptomatic stage (Nardo 2011). Furthermore, CypA was recovered as insoluble material together with mSOD1 in SpC extracts of fALS mice, and was significantly enriched also in the insoluble fraction of SpC of ALS patients (Basso 2009).

CypA best characterised properties are the peptidyl-prolyl *cis-trans* isomerase and chaperone activities, which are linked to its intracellular beneficial functions in protein folding and in protecting from oxidative stress. In addition, CypA has been recently suggested to play important roles in diverse cellular processes including intracellular trafficking (Uittenbogaard 1998), signal transduction (Brazin 2002), cell cycle regulation (Zander 2003), transcription regulation (Krummerei 1995), neuronal differentiation (Hovland 1999; Nahreini 2001; Chiu 2003; Song 2004; Urano 2006), ribonucleoprotein trafficking (Pan 2008), viral replication (Foster 2011). Here we show that CypA has a protective role in ALS, not only as an antioxidant (Lee 1999), but also as a chaperone and in maintenance of multi-protein complex stability.

1. Establishment of a cell model of ALS disease

To provide further insights into CypA functions and to unravel if this protein is involved in ALS pathogenesis, HEK293 cells overexpressing mutant SOD1 or TDP-43 were used as *in vitro* model of ALS. Since CypA is an ubiquitous protein, we used the HEK293 cell line as a versatile cellular model to investigate molecular mechanisms that can take place in different cell types. Interestingly, although the HEK293 cell line was derived by transformation of primary cultures of human embryonic kidney (HEK) cells (Graham 1977), they resemble developing neurons and neuronal stem cells. In fact, they express the neurofilament (NF) subunits NF-L, NF-M, NF-H, and α-internexin, as well as many other proteins typically found in neurons. Moreover, HEK293 cells reveal little spontaneous electrical activity and electrophysiological studies have shown expression of several endogenous voltage-activated ion currents, thus further arguing that transformed HEK lines belong to neuronal lineage (Shaw 2002).

HEK293 cell lines stably expressing human WT-SOD1 and the fALS mutant G93A-SOD1, were generated. Although this is a simple system that cannot accurately model more complex pathological features associated with mammalian nervous system dynamics, it allowed us to model some cellular and molecular changes already reported in fALS models of the disease and in patients. Indeed, the overexpression of mSOD1 was sufficient to increase the cell death rate in respect to WT cells, demonstrating that mSOD1 stably expressed in HEK293 cells is toxic. Further analyses revealed also increased levels of free and protein-bound 3-nitrotyrosine, nitrated actin and protein-disulfide isomerase, that are important characteristic features of nitrative, oxidative and ER-stress, respectively. These protein profile changes are in line with similar findings in ALS patients, as well as in *in vivo* and *in vitro* models (Abe 1997; Beal 1997; Bruijn 1997; Ferrante 1997; Casoni 2005; Atkin 2006 and 2008; Massignan 2007; Basso 2009; Nardo 2009 and 2011), and with the observation that mSOD1 has an increased ability to catalyse aberrant oxidative reactions, including protein nitration (Beckman 1993; Estévez 1999). So, we can consider these cells a valid *in vitro* model to dissect mSOD1-related disease mechanisms at a molecular level. Nevertheless, the selective neuronal vulnerability or the focal onset, progression, and spreading

of ALS require a model with the complexity of the mammalian CNS architecture. Thus, the most interesting results were also investigated in relevant animal models.

1.1 Cyclophilin A in HEK293 cells stably expressing mutant SOD1

Starting from the observation that CypA is up-regulated early in the disease in fALS animal models and in patients (Nardo 2011), we investigated the biochemical properties of CypA in our *in vitro* system. CypA alterations previously found in sALS patients and fALS animal models were mirrored in our experimental model, suggesting that it is a relevant system to dissect the determinants of CypA impairment. In particular, mSOD1 overexpression was sufficient to alter CypA pattern of isoforms, with a pattern change, a shift toward acidic pI, similar to sALS patients and fALS mice (Massignan 2007; unpublished data from the laboratory). Moreover, CypA was significantly up-regulated in mSOD1 cells compared to WT cells following serum withdrawal, but not under basal conditions. The change detected in CypA pattern of isoforms in mSOD1-overexpressing cells points out a variation in its post-translational modification (PTM) profile in a pathological condition, that could interfere, directly or indirectly, with its functions or subcellular distribution. Indeed, CypA has been implicated in multiple extracellular and intracellular functions, both within the nucleus or the cytoplasm, and possibly its multifaceted nature is linked to its high propensity to undergo PTMs. In mSOD1 cells, the modified PTMs profile observed directly affected nuclear CypA, with a concomitant increase in the cytosolic protein levels. Impairment of CypA subcellular localisation may thus reflect disturbancies in its nuclear activities, that are still poorly characterised. A recent work demonstrates that acetylation is one of the PTM responsible for the shift of CypA isoforms towards a more acidic pI (Chevalier 2012). Possibly, this indicates that CypA impairment in ALS is likely linked to an altered acetylation pattern.

CypA is extensively lysine-acetylated (Kim 2006; Choudhary 2009; Chevalier 2012), nevertheless this still represents a poorly examined aspect of CypA biology. Lysine-acetylation is a very

important PTM and it can exert its impact via alteration of protein-protein interactions, subcellular localisation, enzymatic activity. Here, we demonstrated for the first time that lysine-acetylated CypA was present exclusively in the nucleus and not in the cytoplasm, suggesting that lysine acetylation influences CypA nuclear translocation. Since CypA nuclear levels as well as lysine-acetylation displayed an altered pattern in mSOD1 cells and as well in stress conditions, our findings suggest that the fine regulation of CypA lysine-acetylation and de-acetylation could play a role in disease and stress response.

Lysine-acetylation occurs on several nuclear substrates (Glozak 2005), such as histones, DNA-binding transcription factors, acetylases, but also non-nuclear proteins, such as α-tubulin, and proteins that shuttle from the nucleus to the cytoplasm, such as the nuclear import factor importin-α. In many cases lysine-acetylation occurs in known or putative nuclear localisation signal (NLS) sequences, therefore a change of subcellular localisation may be one of the effects of this modification (Kim 2006). The results obtained, prompt us to suppose that also CypA acetylation is likely to have a marked effect on its subcellular distribution, in a similar way that acetylation regulates the nuclear-cytoplasm trafficking of importin-α (Bannister 2000). Indeed, importin-α acetylation on a specific residue (Lys-22) promotes the binding with a second nuclear import factor (importin-β), thus allowing the correct translocation of the protein into the nucleus. CypA does not possess a classical NLS (Rycyzyn 2000) and the mechanism of CypA nuclear translocation has long been elusive. Nevertheless, roles for CypA in nuclear trafficking of cellular factors have been proposed in several studies (Ansari 2002; Zhu 2007; Pan 2008). Recently, the comparison of CypA and hnRNP A1 protein sequences revealed a M9-like motif embedded in the glycine-rich domain (aa 41-125) of CypA, that directs its nuclear translocation through transportin 1 (Pan 2008). Interestingly, CypA-Lys125, that has been recently shown to be acetylated in mammal cells, is located within this motif (Kim 2006; Choudhary 2009). These observations possibly suggest that lysine acetylation within CypA M9-like motif may be a PTM promoting CypA nuclear localisation. Lys125 is located in a loop in proximity of the PPIase cavity of CypA and provides the greatest positive charge within the active site region, and this charge is largely

neutralized when an acetyl-group is introduced (Lammers 2010). Although Lys125 acetylation does not seem to substantially rearrange CypA active site, it markedly affects CypA surface electrostatics (Lammers 2010). To deeply explore this PTM, Lys125 was substituted either with a Gln (K125Q), in order to mimic a constitutively acetylated-Lys, or with an Arg (K125R) which mimics a constitutively non-acetylated-Lys. When transfected in HEK293 cells, the K125Q-CypA mutant displayed a normal subcellular distribution, while K125R-CypA showed a reduced nuclear localisation, thus confirming acetylation as the PTM promoting CypA efficient nuclear localisation. Nevertheless, CypA nuclear import was not completely abolished in the absence of the acetyl-group on Lys125, but only decreased. This possibly suggests that additional PTM are required to enable the bidirectional trafficking of CypA across the nuclear envelope, or alternatively that, in addition to Lys125, acetylation is also needed on the other lysines within the M9-like motif of CypA, to efficiently regulate its nuclear trafficking in mammalian cells. Thus, the possible additive effect of acetylation on multiple lysines should be further investigated on the nucleo-cytoplasm shuttling of CypA.

Collectively, our data demonstrated that in this *in vitro* model the overexpression of G93A-hSOD1, even though not evidently altering CypA total level, was sufficient to alter CypA isoform pattern, mirroring the trend observed in sALS patients and fALS murine models, and this directly correlated to the shift observed in its subcellular localisation and possibly PTMs profile. Thus, this experimental model of fALS is relevant to investigate the role of CypA and the molecular events induced by SOD1 mutation in ALS.

2. Identification of Cyclophilin A interacting proteins

CypA is present as a relatively abundant protein in the cytoplasm and in the nucleus of all mammalian cells. In particular, brain tissue constitutively expresses CypA in high amount (Goldner 1996) and several works reported CypA involvement in neuronal differentiation (Hovland 1999; Nahreini 2001; Chiu 2003; Song 2004; Urano 2006). Nevertheless the specific functions CypA plays in neurons and MNs, beyond its PPIase and chaperone activities, have not been defined yet. On the basis of these observations, of our *in vitro* findings and previous data from the lab describing CypA as a hallmark of ALS in patients and *in vivo* models, also additional evidences support a possible involvement of CypA in ALS pathogenesis. In particular, three independent studies conducted on the G93A-SOD1 fALS animal model have shown that treatment with the immunosuppressive drug CsA extends mice survival (Keep 2001; Kirkinezos 2004; Karlsson 2004). CsA binds and inhibits CypA with more efficiency in respect to other Cyps (Mikol 1994), thus suggesting that CypA could represent an attracting pharmacological target for ALS and that CsA could exert an effect on CypA functions in the CNS. In addition, CypA is required for the efficient nuclear translocation of AIF in degenerating MNs of G93A-SOD1 mice (Tanaka 2010), suggesting that CypA and AIF may cooperate to mediate the late stage of MN death in diseased fALS mice. On the contrary, a protective role for CypA PPIase activity has been hypothesised in mSOD1 *in vitro* model of fALS, independently from its CsA-dependent function (Lee 1999). These evidences provided sufficient basis to hypothesise that CypA is mechanistically linked to ALS, although the fundamental question of whether CypA participates to neurodegeneration through gain of toxic function or a loss of protective function remains controversial.

Several reports have noted that CypA associates with specific proteins, nevertheless these findings have not led to a general model for CypA function in mammalian cells or possible aberrant function in disease conditions. Thus, we employed a global proteomic approach to investigate CypA interactome network, in order to provide insights into the (patho)physiologically relevant molecular functions of this protein.

We identified twenty-eight proteins in association with CypA by mass spectrometry in HEK293 cells stably expressing WT- or G93A-SOD1. Most of these were unknown CypA-binding partners and all need to be deeply investigated to establish a functional link among them. Some proteins showed common biological denominator, and were divided into seven main functional categories: DNA/RNA binding proteins (TDP-43, hnRNP A1, A2/B1, C1/C2, G, K ,M, IF4A1/2/3, DDX3X, PRP19, SFPQ, HKR1, NR1I2, NPM), cytoskeleton-associated proteins (actin, tubulin, vimentin, tropomodulin-2), energy metabolism (ENOA, KCRU, G3P), protein biosynthesis (EF2), protein folding and degradation (TCPA, HSP71), trafficking (RAN), and other functions (PHB). Therefore, we found that CypA is able to interact with different groups of proteins, thus providing an important perspective about how CypA could be involved in different biological pathways, likely suggesting a possible functional role in these processes too. Moreover, CypA was largely associated with nuclear proteins, cytoplasmic proteins, and proteins known to undergo nucleo-cytoplasmic shuttling. Our results are consistent with the observation that CypA is a cellular component of both the nucleus and the cytoplasm, and possibly indicate that CypA could have important unknown functions in the nucleus. Possibly, we can hypothesise that mSOD1-mediated decrese of nuclear CypA, as described in our *in vitro* model, could contribute or be caused by the impaired interaction with one of these proteins, and further perturb the processes listed, through a loss of nuclear function of CypA.

2.1 DNA/RNA binding proteins

The main result presented in this thesis is the novel observation that CypA is strongly associated with RNA processing, whose misregulation is emerging as a common patho-mechanism in ALS. In particular, we revealed extensive interaction of CypA with proteins that regulate multiple steps of RNA metabolism, and these include proteins involved in mRNA splicing, transport and stability, RNA helicases, as well as several hnRNPs, and interestingly also TDP-43, that is a major disease protein in ALS, thus adding evidence to a mechanistic involvement of CypA in ALS pathogenesis.

Notably, CypA has been already associated with RNA in a wide proteomic study of HeLa mRNA interactome (Castello 2012). In particular, CypA was among the PPIases identified as RNA-binding proteins. Indeed, PPIases have been previously demonstrated to play diverse regulatory roles in spliceosome and ribonucleoprotein dynamics, and possibly their role in RNA biology is broader than previously suggested (Mesa 2008). Thus, our findings provide added evidence to support a role for CypA in RNA processing and this is likely to be the the most relevant feature of CypA to investigate in association with neurodegeneration in ALS.

Among the identified CypA interacting proteins, there are several members of the hnRNP family, specifically hnRNPs A1, A2/B1, C1/C2, G, K, M and TDP-43. HnRNPs are abundant nuclear proteins that rapidly shuttle between the nucleus and the cytosol and, organized in large complexes, have key roles in RNA processing, transport, localisation, translation and stability (Dreyfuss 2002). CypA involvement in ALS results a particularly interesting possibility since here it has been shown to interact with **TDP-43**. Indeed, TDP-43 has been identified as the major component of neuronal ubiquitinated inclusions (Neumann 2006), the most striking pathological hallmark of ALS, in sALS and SOD1-negative fALS patients. Furthermore, both sALS and fALS patients present mutations in the TARDBP gene (Kabashi 2008; Sreedharan 2008), mainly in the C-terminal region that is the site of interaction with other proteins, and among them also members of the hnRNP family (Buratti 2005). It is a RNA/DNA binding protein that structurally resembles a typical hnRNP and is involved in multiple steps of RNA lifecycle including transcription, splicing, transport, translation, stability, degradation and miRNA processing (see Introduction section **1.5.6**). Nevertheless, its precise role in ALS pathogenesis has not been deciphered yet. Notably, CypA was previously identified in a global proteomic analysis of TDP-43 interacting proteins, although it was not considered a specific interactor since it was enriched in the control sample relative to the TDP-43 co-immunoprecipitate (Freibaum 2011). Instead, here we demonstrated the specificity of this interaction and established a functional connection.

Interestingly, hnRNP A2 had already been demonstrated to form a complex with CypA which undergoes nuclear export in response to chemokine stimulus, thus suggesting a regulatory role of

CypA in the trafficking of hnRNP A2 (Pan 2008). In this analysis both **hnRNP A2** and **B1**, that are alternative splicing isoforms differing from each other by only a 12-aa insertion in the N-terminal region of A2 (Kozu 1995), have been identified. The interaction between CypA and hnRNP A2/B1 is particularly interesting for its possible significance in ALS pathogenesis. Indeed, (i) hnRNP A2/B1 is one of the best characterised interactor of TDP-43 (Buratti 2005), (ii) it was identified as a potential biomarker in sALS patients together with CypA and TDP-43 (Nardo 2011), (iii) it is known to interact with the C/G-rich repeats that form RNA foci in another neurodegenerative condition (FXTAS) (Sofola 2007) and possibly it is dysregulated in a similar way in *C9ORF72* $(G_4C_2)_n$ repeats carrier (Dejesus-Hernandez 2011). Thus, the involvement of CypA and hnRNP A2/B1 in ALS was further investigated in this study.

CypA interaction with **hnRNP K** could be of interest to investigate whether CypA plays a role in chemotaxis. Indeed, CypA was demonstrated to bind N-WASP and stabilise its complex formation with Arp2/3 for nucleation/initiation of actin polymerisation (Calhoun 2009). Interestingly, also hnRNP K is involved in cytoskeletal organisation, cell spreading and migration through direct association with N-WASP (Yoo 2006). Thus, CypA could be involved in chemotaxis and cytoskeletal organisation, regulating hnRNP K nuclear-cytoplasm transport, as demonstrated for hnRNP A2 (Pan 2008).

CypA was found to interact with a large number of **RNA helicases**, specifically with the ATP-dependent RNA helicase DDX2A (eIF4A1), DDX2B (eIF4A2), DDX48 (eIF4A3) and DDX3X. These proteins are members of the DEAD/DEXH-box protein family, characterised by the conserved motif Asp-Glu-Ala-Asp (DEAD). RNA helicases are implicated in a number of cellular processes involving alteration of RNA secondary structure, such as translation initiation, splicing, nonsense-mediated decay, and ribosome and spliceosome assembly. Possibly CypA/RNA helicases complex within RNP particles, which undergo many conformational rearrangements at the RNA and protein level, and it is likely that proteins of the DEAD/DEXH-box RNA helicase family and CypA mediate some of these conformational changes through a direct interaction with RNA or proteins, respectively. Moreover, the interaction between CypA and DDX3X could be of interest in

association with their roles in HIV-1 and HCV viral replication (Braaten 2001; Foster 2011; Yedavalli 2004; Owsianka 1999).

PRP19 (Pre-mRNA-processing factor 19) is essential for spliceosome assembly, and may also be important for its stability and activity. It also plays a role in DNA repair and pre-mRNA splicing. Interestingly, PRP19 was demonstrated to function as a neuron-astroglial switch during retinoic acid (RA)-induced neuronal differentiation *in vitro*, and CypA was identified as a specific binding partner of the PRP19β-variant (Urano 2006). In particular, CypA participates in the early stages of neuronal differentiation (Song 2004) acting as a transcriptional activator, and its activity is suppressed by PRP19β binding (Urano 2006). It would be interesting to deeply investigate this mechanism in association with ALS, where astrogliosis is emerging as a prominent feature of disease (Vargas 2010).

PSF/SFPQ (Splicing factor, proline- and glutamine-rich) is a nuclear splicing factor and transcriptional regulator, and it also functions in DNA repair (Ha 2011). SFPQ is a core protein of paraspeckles, that are dynamic ribonucleoprotein bodies found in the interchromatin space of mammalian nuclei formed around long noncoding RNA (Bond 2009). Moreover, it is a host factor essential for HCV and influenza virus infection (Landeras-Bueno 2011; Harris 2006). Interestingly, it was recently found depleted in the nucleus and accumulated in the cytoplasm in tau-mediated pathological conditions in Alzheimer's and Pick's disease (Ke 2012), similar to what has been reported for TDP-43 and FUS in ALS and FTLD. This possibly suggests that an altered nucleo-cytoplasm redistribution of proteins implicated in mRNA processing might be a prominent patho-mechanism under neurodegenerative conditions. Moreover, in this context the interaction between SFPQ and CypA should be further investigated, since CypA has a role in the nuclear transport of cellular factors, such as hnRNP A2 (Pan 2008), AIF (Candé 2004) and Zpr1p (Ansari 2002).

2.2 Trafficking and cytoskeleton-associated proteins

CypA was found to interact with a small number of trafficking and cytoskeleton-associated proteins, particularly **actin**, **tubulin**, **vimentin**, **tropomodulin-2** and the GTP-binding nuclear protein **RAN** (Ras-related nuclear protein or GTPase Ran). This finding is consistent with previously described roles for CypA (see Introduction section **2.4**), in maintaining the native folding of actin and associated proteins during transit in axons, and assembly and disassembly in growth cones (Yuan 1997), and in linking client proteins, bound to hsp90, to the dynamitin component of the movement machinery for retrograde movement, including dynein and tubulin, along microtubules (Galignana 2004). Moreover, in hippocampal neurons from developing brain CypA was found among the adaptor proteins in RNA-transporting granules which translocate to dendritic spines (Elvira 2006). The presence of CypA, together with ribosomal proteins, RNA-binding proteins already implicated in transport (hnRNP A1 and hnRNP A2), the transport motor complex dynein/dynactin and TDP-43, is in line with our findings, possibly suggesting that it is involved in RNA trafficking within neuronal processes. In addition, the identification of **RAN** is particularly interesting given its involvement in the nucleo-cytoplasmic transport pathway mediated by M9-NLS (Moroianu 1996; Chook 1999): it is required for the bidirectional transport of several mRNA processing proteins, including hnRNPs A1 and A2/B1 through transportin, also known as karyopherinβ2 (Kapβ2) (Lee 2006), and thus possibly for RNA export. The binding with this protein should be further investigated, especially in a pathologic context, consistent with the observation that CypA is in the cytoplasm and in the nucleus, and likely reflecting a functional role for CypA in nucleo-cytoplasmic trafficking of other proteins (see Introduction section **2.4.5**).

2.3 Protein folding

The association of CypA with other molecular chaperones, in this case TCPA and HSP71, is in accordance with previous reports describing CypA cooperating with (i) Hsc70 in maintaining the native folding of actin and associated proteins during transit in axons (Yuan 1997), or with (ii)

HSP56 and Cyp40 as part of a cytosolic caveolin-chaperone complex involved in cholesterol intracellular trafficking (Uittenbogaard 1998). **TCPA** (TCP1 or T-complex protein 1 subunit alpha) is a molecular chaperone known to play a role in the folding of actin and tubulin *in vitro* (Seo 2010). **HSP71** (HSPA1 or Heat shock 70 kDa protein 1A/1B) is a chaperone belonging to the heat shock protein 70 family. It is localized in cytoplasmic mRNP granules containing several hnRNPs and untranslated mRNAs (Jønson 2007). These observations further strengthen CypA functional involvement in other aspects correlated with protein folding, such as the formation of heterocomplexes mediating trafficking dynamics.

2.4 Energy metabolism

Several enzymes important in energy metabolism were also identified in our proteomic analysis of CypA interactors. In particular, **KCRU** (ubiquitous mitochondrial creatine kinase or CKMT), **G3P** (glyceraldehyde-3-phosphate dehydrogenase or GAPDH), and **ENOA** (alpha-enolase or MBP-1, NNE or non-neural enolase).

Creatine kinase (CK) reversibly catalyzes the transfer of phosphate between ATP and various phosphogens (e.g. phosphocreatine). CK is a key enzyme of cellular energy metabolism and plays a central role in tissues with large, fluctuating energy demands, such as skeletal muscle, heart, brain and spermatozoa. The identification of this protein is in line with previous reports demonstrating the ability of CypA to accelerate CK refolding and improve the reactivation yields *in vitro,* independently of its PPIase activity (Yang 1997; OU 2001). Our finding results particularly interesting, since it likely suggests a chaperone-like activity of CypA on CK also in living cells. Indeed CypA chaperone activity in living cells was demonstrated only on procollagen I triple-helix (Steinmann 1991). Furthermore, *in vitro* CypA is able to accelerate folding of other metabolic enzymes, namely carbonic anhydrase (Freskgård 1992) and citrate synthase (Moparthi 2010), possibly indicating a chaperoning activity of CypA also on analogous protein substrates.

Also **G3P** represents an interesting protein interactor of CypA, since in addition to playing a role in glycolysis through its glyceraldehyde-3-phosphate dehydrogenase activity, it also functions within signal transduction cascades as a nuclear S-nitrosylase (Kornberg 2010). Indeed, regulated protein-protein transnitrosylation represents a mechanism of signal transduction with implications for nitric oxide biology and redox signalling. CypA has been found to be S-nitrosylated (Wu 2011; Camerini 2007) and this possibly indicates a common transnitrosylation-mediated mechanism of signaling regulation.

2.5 Other interactors

EF2 (EEF2 or elongation factor2) belongs to the GTP-binding elongation factor family and catalyzes the GTP-dependent ribosomal translocation step during translation elongation. CsA/CypA complex was found to alter EF2 by affecting transcriptional regulation or enzymatic activity, thus causing widespread disturbances that may underlie the wide spectrum of toxicities observed during CsA therapy (Buss 1994) and possibly when CypA intracellular functions are impaired.

PHB (prohibitin) has been connected to diverse cellular functions including inhibition of cell proliferation, stabilization of imported proteins in mitochondria, cell cycle control, senescence, and apoptosis. PHB interacts with all members of the Retinoblastoma (RB) tumor suppressor family, thereby preventing the transcriptional activity of E2F members (Rajalingam 2005). Also CypA binds RB, and their interaction interferes with CsA/CypA complex, negatively affecting CsA-inhibited NFAT signaling (Cui 2002). In addition, in a model of neuronal differentiation, the nuclear translocation of CypA, the appearance of hypophosphorylated RB and the enhancement of RB/CypA complex formation correlates with retinoic acid induced neuronal differentiation (Chiu 2003). Possibly, PHB and CypA converge on RB pathway, with relevant functions in tumors.

Overall, our proteomic analysis of CypA interactors is in accordance with previous reports, and further contributes to underscore the pleiotropic nature of this protein, that likely carries out its

diverse functions by varying its binding partners, as well as PTMs and subcellular localisation, and possibly sharpens underrated roles of this protein in ribonucleoprotein dynamics. Indeed, CypA emerged as a relatively new player in a growing list of proteins, especially RNA binding proteins. Moreover, linking CypA interactome with a pathologic condition, in which CypA is altered in its levels, PTMs and subcellular localisation, as it is in sALS patients and mSOD1 fALS models, contributes to explain the broad spectrum of impaired pathways observed to converge in a common phenotype. This latter aspect is particularly relevant in the pathogenesis of sALS and mSOD1-linked fALS, since we show that CypA and TDP-43 interact, thus providing the first connection between two patho-mechanism almost established as independent.

3. CypA/TDP-43 interaction

Among all CypA interactors, we have shown here that TDP-43, the major constituent of the proteinaceous inclusions that are characteristic of most forms of ALS and FTLD (Neumann 2006) and are associated with other neurodegenerative diseases (Geser 2009), is in complex with CypA. Despite the progresses toward revealing the full spectrum of TDP-43 pathology in human neurodegenerative diseases (Geser 2009), it remains to be determined which particular aspect of TDP-43 biology is perturbed in common amongst these diseases. There is a growing consensus that misfolding and abnormal protein aggregation are a common underlying mechanism of neurotoxicity in neurodegeneration. It has been shown previously that the toxicity of protein aggregation is due to soluble intermediate forms rather than the insoluble end product inclusions that accumulate in tissues. Species formed early in the aggregation process of disease-associated proteins are inherently highly cytotoxic rather than simply non-functional, thus providing evidence that avoidance of protein aggregation is crucial for the preservation of biological functions (Bucciantini 2002). Hence, either a loss or a gain of neurotoxic interactions may precede the formation of inclusions, and the control of protein misfolding and aggregation is of fundamental importance to preserve cell viability. Notably, molecular chaperones, ubiquitination enzymes and proteasome are evolutionary conserved means to increase the efficiency of folding and rescuing misfolded proteins after biosynthesis.

Cyclophilins form a structurally well characterised family of closely related proteins that exhibit PPIase activity and thereby accelerate the folding of proteins requiring the isomerisation of a peptidyl-prolyl bond. However, there is a growing evidence that their main function may be to act as chaperones (Baker 1994; Zhao 1997). In particular, CypA can interact with proteins to guide their proper folding and assembly. Therefore, we have hypothesised a function for CypA as a chaperone in directing proper folding and stabilization of TDP-43.

3.1 Verification and characterization of CypA/TDP-43 interaction

We tested the reliability of CypA/TDP-43 interaction by different approaches and in different systems. We showed that CypA and TDP-43 interact *in vitro* at endogenous expression levels and when transiently overexpressed. Their interaction occurred in the nuclear region, in an RNA-dependent manner. Moreover, CypA and TDP-43 specifically associated in mouse spinal cord and brain extracts. The combined colocalisation analyses in HEK293 cells, HeLa cells and primary neuronal cultures, and the binding studies provided definitive evidence that CypA and TDP-43 exist in complex in mammalian cells *in vitro* and *in vivo*. These results further strengthened our hypothesis that the two proteins are part of a common intracellular pathway, which might result impaired in ALS. Moreover, the finding that these proteins interact in the nucleus and that their interaction depends on RNA, further suggest a novel important role for CypA in the nuclear compartment in RNA-related biological processes.

Our data indicate that CypA lysine-acetylation occurs only in the nucleus. Besides affecting CypA nuclear import (see Discussion section **1.1**) and stability (see Introduction section **2.6.6**), acetylation could also impact on protein-protein or protein-nucleic acid interactions. Indeed, lysine acetylation not only neutralizes a positive charge, but also increases the hydrophobicity and the size of lysine's side chain, thus it is likely to induce significant conformational changes of substrate proteins. For example, acetylation induced the formation of a docking site within α-tubulin, that resulted into a major affinity with other motor proteins (Reed 2006; Dompierre 2007). In a similar way, CypA lysine-acetylation, modifying the external surface of the protein, can possibly lead to changes in its function and affect its binding with protein partners, such as TDP-43. We used CypA mutants at Lys-125 to evaluate this possibility, and observed that acetylation on this residue is required for a more efficient binding with TDP-43. Moreover, it should also be considered that acetylation frequently occurs in a position directly adjacent to the DNA/RNA binding domain of a protein, and results in the consequent stimulation of nucleic acid binding (Gu 1997; Boyes 1998; Zhang 1998; Martínez-Balbás 2000). Possibly, also in this case, CypA acetylation

could influence recognition of RNA and thus enhance the binding with TDP-43. Our findings indicate that lysine-acetylation, besides regulating the nuclear import of CypA, could also favour, either directly or indirectly, the interaction with TDP-43. However one note of caution should be considered: we cannot exclude that the lack of acetylation on Lys-125, affecting the import of CypA into the nucleus, also reduced the binding with TDP-43, or alternatively, that both nuclear import and effective TDP-43 binding were impaired, possibly with a synergistic effect. Notably, we observed an altered pattern of CypA acetylation in stress conditions and in mSOD1 fALS cells, and this could possibly modify its interaction with TDP-43 or other RNA-binding proteins, such as members of the hnRNP family.

Complexes of RNA-binding proteins often contain interactions dependent on both protein-protein and protein-RNA interactions. The interaction between CypA and TDP-43 likely reflects a mixed mechanism involving protein-protein as well as protein-RNA interactions. Notably, a previous work demonstrated that CypA enahances HCV RNA replication stimulating the RNA binding ability of the NS5A protein, modulating the conformation of the RNA binding motif by *cis-trans* isomerisation (Foster 2011). Possibly, CypA could impact on the RNA binding activities of TDP-43 with a similar mechanism. We investigated this possibility using the PPIase-deficient CypA carrying the Arg55Ala substitution which is predicted to completely inhibit CypA isomerase activity (Zydowsky 1992). Indeed, Arg55 is located within the active site and it plays a crucial role during the transition state of the isomerisation reaction. Despite the mutation in its active site, and in contrast with other known CypA-protein interactions, PPIase-deficient CypA was still able to bind TDP-43, although a slight decrease was observed in respect to the WT protein. However, it should be considered that PPIase-deficient CypA could not be efficiently immunoprecipitated, possibly because Arg55Ala replacement significantly disturbed the overall folding of the protein, with a reduced affinity for the primary antibody in non-denaturing conditions. Similar results were obtained using CsA, which is as well reported to bind CypA catalytic site (unpublished data from the lab). Therefore, our data only demonstrate that CypA PPIase activity is not essential for CypA/TDP43 interaction, but do not completely exclude the possibility that CypA rotamase

activity may be required for the *cis-trans* isomerisation of a prolyl-bond within TDP-43 sequence. Further experiments for addressing this question are under way in our laboratory. In addition, PPIase-deficient CypA displayed an altered nuclear import/export ratio, suggesting that the protein was not efficiently translocated in the nuclear compartment, possibly because the enzymatic activity is required for a correct localisation of this protein, or more likely because the Arg55Ala point mutation induces conformational changes impairing the binding with proteins important for its nuclear translocation, such as transportin.

Overall, although CypA consists only of the CLD, with no other distinguishable domains, still the catalytic pocket, and as a result the isomerase activity, are not essential for TDP-43 binding, while acetylation of a specific lysine residue of CypA could play an essential role in regulating its affinity for its binding partner TDP-43. It will be of considerable interest to investigate in more detail which domains of the two proteins participate in complex formation and, in particular, whether other PTMs are involved in this recognition event.

3.2 CypA/TDP-43 interaction: implications in hnRNP complex formation and stability

TDP-43 is a 414 aa protein with two RNA-recognition motifs (RRM1 and RRM2) that enable the interaction with nucleic acids, and a C-terminal glycine-rich domain that mediates protein-protein interactions. TDP-43 functionally associates with the majority of the hnRNP proteins and is an integral component of hnRNP-rich complexes (D'Ambrogio 2009; Freibaum 2010; Ling 2010). Previous studies have shown that TDP-43 binds hnRNPs, and in particular hnRNP A2/B1, through its C-terminal tail (Buratti 2005). Indeed, hnRNP A2/B1 is the major hnRNP protein recognized by TDP-43 (Ayala 2005), and it is one of the major components of the hnRNP core complex in mammalian cells (Kozu 1995). hnRNP A2/B1 and TDP-43 are, in association with other RNA binding proteins, components of larger protein complexes required for the stabilization, transport, and metabolism of mRNA. Moreover, hnRNP A2/B1 is also one of a large number of

hnRNPs found to interact with CypA in our proteomic analysis, and it was previously demonstrated to form a complex with CypA (Pan 2008). We confirmed the association of hnRNP A2/B1 with either CypA and TDP-43 *in vitro*. Thus, CypA, TDP-43 and hnRNP A2/B1 may form a complex with each other and these interactions are RNA-dependent. In this respect, it is possible to hypothesise that they are together part of a larger protein complex. It is therefore likely that CypA might be a component of hnRNP-rich particles, in complex with TDP-43 and other hnRNP proteins, such as hnRNP A2/B1, abundantly present in the interactome (**Table 2.1**). This is in line with a previous work where CypA was identified in RNA-transporting granules from developing brain, together with hnRNPs, TDP-43, RNA helicases and the transport motor complex dynein/dynactin (Elvira 2006).

In order to deeply elucidate CypA functions within such complexes, we adopted a siRNA interference technology approach to selectively knock-down CypA. When CypA was silenced, TDP-43 and hnRNP A2/B1 interaction was severely impaired, suggesting that CypA absence could disrupt the binding between these two proteins within this hnRNP complex. Similar results were obtained in SpC extracts from mice with a reduced (CypA+/-) or absent (CypA-/-) expression of CypA, in respect to non-transgenic animals (CypA+/+). Thus *in vivo* experiments provided added evidence to *in vitro* data evidencing a fundamental role of CypA in the interaction of TDP-43 with at least hnRNP A2/B1. In this paradigm, CypA could simply function in mediating a protein-protein interaction with TDP-43 and hnRNP A2/B1, or more likely it could induce a conformational change in one of its target proteins, overall suggesting an important role in the assembly of TDP-43 and hnRNP A2/B1 into a complex. For example, CypA could act as a chaperone-like molecule and, due to its interaction with TDP-43, impart it a protein conformation necessary for complex formation with the hnRNP proteins or with RNA target molecules. In this way, CypA could resemble somewhat the function of Drosophila NinaA cyclophilin, which stably binds and thus prevents misfolding of rhodopsin (Baker 1994). Another possibility is that the aberrant hnRNP complex formation is directly linked to the observed depletion of TDP-43 from the nucleus following CypA knockdown. In this case CypA could function in TDP-43 trafficking, as in the case of hnRNP A2 (Pan

2008), and thus contribute to the correct hnRNP complex assembly. Unexpectedly, it was not possible to reconstitute a stable CypA/TDP-43/hnRNPA2B1 protein heteromer with recombinant proteins on a chip in Surface Plasmonic Resonance experiments (data not shown), suggesting that this assembly process has more complex requirements that were not met by our *in vitro* conditions. A simple explanation for the lack of complex formation could be that one or more PTMs, such as lysine-acetylation, that were missing from the *in vitro*-synthesized proteins, are required for a stable interaction. Alternatively, it may be possible that one or more factors facilitating the stable association of TDP-43 with hnRNP A2/B1 and CypA *in vivo*, such as RNA, were lacking from our reconstitution system.

Our findings raise the interesting possibility that CypA may play a key role in the architecture of the RNA binding protein complements. One of the potential consequences of TDP-43/hnRNP A2/B1 complex disruption upon CypA knock-down/out could be protein complex instability *in vivo* caused by an impaired turnover of this hnRNP complex. We isolated Triton-insoluble fractions (TIF), that are enriched in ubiquitinated protein aggregates and more generally in improperly folded or damaged proteins (Basso 2006 and 2009), from SpC of CypA+/+, CypA+/- and CypA-/- mice. The total amount of insoluble proteins in CypA knockout mice was higher than in non-transgenic animals, providing direct and added evidence to CypA chaperone activity *in vivo*. Moreover, triton-insoluble fractions extracted from the SpC of CypA knockout mice were enriched in poly-ubiquitinated proteins. TDP-43 and hnRNP A2/B1 were significantly accumulated in TIF of CypA knock-down/out mice, in comparison with CypA+/+ mice, without any significant variation in the soluble fraction. Since TDP-43 is an intrinsically aggregation-prone protein (Johnson 2009), its propensity for toxic misfolding was accentuated *in vivo* by CypA reduction or absence. Moreover, insoluble TDP-43 was also hyper-phosphorylated in tissues from CypA knock-down/out mice compared to control animals, with a dose-dependent effect. Our data suggest that CypA expression at physiological levels is protective against aggregates formation of ubiquitinated and aberrantly phosphorylated TDP-43, that are a highly consistent feature of TDP-43 proteinopathies (Geser 2009). Indeed, in CypA knockout mice insoluble TDP-43 displayed the fundamental

biochemical features of protein inclusions in TDP-43-linked human pathology, suggesting that this could represent a possible mechanism by which CypA contributes to TDP-43-related diseases and this could eventually be considered a model to study TDP-43 aggregation process.

Overall, CypA has a key role in the interaction of TDP-43 with hnRNP A2/B1, possibly promoting a correct architecture and stability of the complex. The absence or an impaired CypA/TDP-43/hnRNPs binding could accelerate improper folding of this complex and dysregulate complex assembly, leading to TDP-43 aggregation and associated pathology. These findings further strengthens the hypothesis that normal interactions of TDP-43 with other hnRNPs might keep TDP-43 soluble, that protein-protein contact rather than RNA binding may modulate the aggregation process, and that the trigger may be a defect in the TDP-43 normal interactions (Budini 2012).

We speculate that these events represent a more relevant (patho)mechanism in MNs, where such proteins may be transported as a multiprotein complex in axons. This hypothesis is supported by previous findings demonstrating a prominent role for CypA in maintaining the native folding of actin and associated proteins during transit in axons and assembly in growth cones (Yuan 1997). Thus, these evidences, together with the high concentrations of CypA in brain, as well as its role in neuronal growth, underlie the importance of its chaperone activity in neuronal processes.

3.3 CypA has a role in TDP-43-mediated HDAC6 expression regulation

To further establish the functional significance of CypA/TDP-43 association, we sought to understand how the described hnRNP complex could operate in putative TDP-43 physiological functions. TDP-43 is a RNA binding protein and several RNA targets of TDP-43 are now known. Among them, HDAC6 has been consistently identified in a number of works, including in mouse brain (Polymenidou 2011; Tollervey 2011). TDP-43, by binding to HDAC6 mRNA, regulates its expression (Fiesel 2010; Kim 2010). HDAC6 down-regulation after TDP-43 knock-down/out is

associated to impaired cellular turnover of aggregating proteins and reduced neurite outgrowth (Chiang 2010; Fiesel 2010 and 2011), molecular mechanisms that could be relevant in TDP-43 diseases. We therefore investigated whether CypA could modulate this TDP-43 activity. TDP-43 silencing was confirmed to reduce HDAC6 protein level, which supports previous findings (Fiesel 2010; Kim 2010). We found a comparable downregulation of HDAC6 also after CypA knockdown and the effect observed was almost comparable to the one detected in TDP-43 silenced cells. Our data suggest that a reduction of CypA levels can affect TDP-43-dependent HDAC6 expression regulation, thus revealing a co-requirement of TDP-43 and CypA for optimal HDAC6 expression. Our findings established a biological role for CypA/TDP-43 complex, and we speculate that the hnRNP complex described may be involved in HDAC6 mRNA processing and/or nuclear export. Indeed, these complexes are likely involved in one or multiple steps of RNA lifecycle, processes that involve extremes rearrangements of the RNA components, that imply also significant rearrangements and conformational changes of a number of proteins. CypA was found associated with proteins of the DEAD/DEXH-box RNA helicase family, that play an important role in mediating some of these conformational changes through a direct interaction with RNA. In this context, due to its PPIase and chaperone activities, it is conceivable that CypA may also function as a molecular switch by directly triggering conformational changes in one or more proteins, and these changes could in turn influence the RNA binding ability of its target interactors, as in the case of CypA/NS5A complex (Foster 2011). Therefore CypA, being a small and versatile protein could be a good candidate to catalyze such conformational changes in large multiprotein complexes.

Moreover, HDAC6 is a common RNA target of the RNA-binding proteins TDP-43 and FUS, both identified as causative factors of fALS and sALS (see Introduction section **1.4.1**). Since the mutation or the cytoplasmic aggregation of either TDP-43 or FUS cause similar phenotypes in humans, and both proteins are involved in the same RNA-processing steps, a plausible hypothesis is that the RNA-targets affected by both proteins may be the most relevant for disease (Polymenidou 2012). Therefore, disregulation of HDAC6 RNA metabolism following TDP-43

deficiency, as it may occur in human disease by cytosolic sequestration of this nuclear protein, and possibly upon CypA loss-of-interaction, as it may occur when CypA is depleted or aberrantly post-translationally modified, may contribute to MN disease in ALS, and if occurring in the frontal and temporal cortex also to FTLD-TDP, through deregulation of aggregating toxic protein turnover (Fiesel 2010), and impaired neurite outgrowth (Fiesel 2011).

3.4 Alterations of CypA/TDP-43 interaction in association with ALS-linked mutations

We evaluated whether the effect of pathogenic mutations in (i) TDP-43 or (ii) SOD1 sequence impacted on CypA/TDP-43 interaction. (i) We considered three different mutations previously found in fALS and sALS patients (Gitcho 2008; Kabashi 2008; Daoud 2009): the missense mutations A315T and R361S, and the frameshift mutation Y374X. All ALS-mutants, as well as WT-TDP-43, displayed substantial cytotoxicity when overexpressed in HEK293 cells. Moreover, the A315T and R361S ALS-derived mutations enhanced TDP-43 mislocalisation to the cytoplasm, while the frameshift mutation Y374X did not. Our findings suggest that enhanced cytoplasmic translocation might not be a general mechanism by which mutations in TDP-43 stimulate toxicity, further corroborating the observation that mislocalisation alone is not responsible for TDP-43 driven neurodegeneration (Liachko 2010) and that mutations in TDP-43 are mechanistically divergent (McDonald 2011). Therefore, other molecular changes, such as protein-protein interactions, may account for the toxicity of TDP-43 ALS-mutants. In fact, TDP-43 mutations are located inside the C-terminal glycine-rich domain, which is the putative protein-protein interaction domain of TDP-43, with the R361S and Y374X being respectively inside or close to the minimal hnRNP binding region (D'Ambrogio 2009; Budini 2012). TDP-43 disease-associated mutants did not efficiently bind CypA as the wild-type protein. In particular, the A315T mutation had very mild or nearly no effect on the interaction with either CypA and hnRNP A2/B1, consistent with previous reports (Freibaum 2010) where the A315T and M337V disease-causing mutations were demonstrated not to grossly alter the function of TDP-43 or its binding partners. The

association between TDP-43, CypA and hnRNP A2/B1 was significantly decreased in R361S-TDP-43 cells, suggesting that the R361S is a loss-of-function mutation with respect to this hnRNP complex formation. This was consistent with the observation that the R361S mutation is located within the minimal hnRNP A2 interaction domain of TDP-43 (D'Ambrogio 2009; Budini 2012). The Y374X mutation, that led to the expression of a C-terminally truncated form of the protein lacking the last 41 aa, is the one that mostly affected the interaction between CypA and TDP-43. Combining these data, it seems likely that the C-terminal region of TDP-43 is relevant for a correct binding with CypA, and in particular, the minimal hnRNP A2 binding region of TDP-43 could serve as an anchor site for CypA, which may act as a chaperone or PPIase, possibly facilitating rearrangements of protein interactions during RNA processing/complex formation. In addition, our data indicate that in pathological conditions associated with ALS-TDP-43, it may occur an aberrant interaction between TDP-43 and CypA, that could have negative implications for hnRNP complex formation and stability.

In association with a reduced binding between CypA and TDP-43, we detected a shift in the subcellular localisation of both CypA and hnRNP A2/B1, whose levels were increased in the nucleus and in the cytoplasm, respectively. Under basal condition CypA is predominantly localised in the cytoplasm, whereas hnRNP A2/B1 is almost exclusively localised in the nucleus. Moreover, in association with an altered CypA/TDP-43/hnRNP A2/B1 complex formation in cells expressing the R361S-TDP-43 mutant, CypA was also up-regulated in the cytosol. Thus, the changes observed in CypA and hnRNP A2/B1 subcellular distribution could represent a compensatory mechanism to restore a correct hnRNP complex. It has been recently shown that CypA plays an important regulatory role in the trafficking of hnRNP A2, since they form a complex that undergo nuclear export in response to chemokine stimuli (Pan 2008). Either TDP-43 mutants and hnRNP A2/B1 displayed a shift in their subcellular localisation concomitantly with a reduced binding between CypA and TDP-43. Our results possibly subtend an important role for CypA for the correct localisation or subcellular redistribution of the members of this hnRNP complex, that could

represent an early impairement in desease conditions. However, this remains to be demonstrated.

TDP-43 ALS-mutations were also analysed for their impact on a well established function of TDP-43: HDAC6 expression regulation. In TDP-43-silenced cells, decreased HDAC6 protein levels were restored to normal levels after retransfection with the WT protein, whereas the A315T and R361S mutants were able to restore HDAC6 protein levels, but with a reduced capacity compared to the wild-type protein, replicating a previous work on HDAC6 mRNA levels (Fiesel 2009). In contrast, the Y374X mutant failed to restore HDAC6 levels, consistent with previous findings on a truncated form of TDP-43 lacking the C-terminal glycin-rich domain (Fiesel 2009). In particular, the latter result was similar to what observed after TDP-43 knockdown, suggesting that the Y374X is a loss-of-function mutation with regards to HDAC6 regulation, as well as CypA/TDP-43 hnRNP complex formation. Therefore, our findings indicate that a correct protein-binding capacity could represent a more important determinant of HDAC6 regulation than TDP-43 nuclear localisation, since TDP-43/CypA interaction was necessary to maintain physiological levels of HDAC6. We speculate that the efficient association with CypA could contribute to RNA-protein complex formation along with direct interaction between TDP-43 and other hnRNPs. Thus, in the pathology, it is plausible that TDP-43/CypA/hnRNPs impaired binding may lead to defective RNA metabolism, contributing to pathogenesis and disease progression. In particular, HDAC6 is a key player in autophagy-mediated degradation of misfolded proteins (Boyault 2006) and HDAC6 downregulation upon a severely damaged hnRNP complex may lead to subsequent impairment in toxic protein turnover, further enhancing proteotoxicity. These results are in line with previous works suggesting that the mutations in TDP-43 found in patients do not contribute to a drastic protein loss-of-function, whereas they may more likely contribute to a predisposition to deveop the disease (i.e. more readily form aggregates) (D'Ambrogio 2009), possibly through an impaired interaction with CypA.

(ii) In addition, we detected a reduced CypA/TDP-43 binding, as well as their cytoplasmic mislocalisation in presence of mSOD1. Our findings likely suggest that the consequences of an impaired hnRNP complex formation and stability could be particularly detrimental in a disease

context already associated with mSOD1, as they could have negative implications for TDP-43-related functions, further contributing to the pathology. An interesting possibility is that the altered pattern of CypA lysine-acetylation observed in mSOD1 cells could represent a primary causative event that affects CypA import into the nucleus and impairs its binding with TDP-43, and possibly also its trafficking. Therefore, the fine regulation of CypA lysine-acetylation and de-acetylation could be an important element in pathological conditions. A future challenge for basic research, but also for the putative implications in disease treatment, is the identification of the acetyltransferases (HATs) and deacetylases (HDACs) able to modulate CypA acetylation. Moreover, it would be of particular interest to test whether these enzymes could also modulate CypA subcellular distribution or the binding with other proteins, and overall confer CypA specificity for its substrates. Indeed, acetylation may inhibit binding to some substrates but allow CypA to bind (and to isomerise) new ones, and an imbalance between the activities of HATs and HDACs could lead to a disease state. HDAC inhibitors, that have recently emerged as potential neuroprotective drugs for the treatment of neurodegenerative diseases such ALS, could be tested and used in order to modulate CypA acetylation.

Overall, alterations of the CypA/TDP-43 interaction, detected when TDP-43 is mutated or in presence of mSOD1, could have important implications for hnRNP complex formation and stability; the slight disruption of its activity perpetuated over a long time might be the cause for TDP-43 mislocalisation and possibly the trigger for pathological inclusions formation, hallmarks of TDP-43 proteinopathies. This mechanism of neurodegeneration is in accordance with the recently proposed "two-hit" model of pathology (Dormann 2010).

4. CypA/mSOD1 interaction

Protein aggregation is strongly implicated in the pathogenesis of MN degeneration due to mSOD1. The propensity of mSOD1 to aggregate is one of the most sustained hypotheses to explain the toxicity of this enzyme. SOD1 has been recognized as a primary component of protein aggregates in patients carrying SOD1 mutations and in mSOD1 rodent disease models (Wood 2003). Antibodies specific for misfolded forms of SOD1 have shown that granular SOD1 inclusions can be found in autopsy tissues from sALS patients, providing a possible mechanistic link between the sporadic and familial forms of disease (Bosco 2010; Forsberg 2010 and 2011). However, not very much is known about the role of SOD1 aggregation in the pathogenesis of ALS. Insoluble SOD1 complexes can start to be detected prior to disease onset (Basso 2006; Johnston 2000). Several, contributing factors have been proposed for the formation of SOD1-rich protein inclusions: structure instability and aggregation propensity of mSOD1 (Lindberg 2002; Stathopulos 2003; Tiwari 2003), inhibition of chaperone activity (Tummala 2005), and alteration of the UPS (Kabashi 2004; Cheroni 2005). Ubiquitinated protein aggregates are TX-insoluble (Ouyang 2001) and mSOD1 has an altered solubility in TX with the progression of the disease (Cheroni 2005).

4.1 CypA interacts specifically with mutant, but not with wild-type SOD1

The aggregate protein constituents of TX-insoluble fractions enriched in ubiquitinated protein aggregates and mSOD1, have been studied in our laboratory. CypA was recovered in protein aggregates isolated from the SpC of the G93A-SOD1 mouse model together with mSOD1, and in the aggregates from post-mortem SpC tissues of sALS patients (Basso 2009). Inclusions present in disease commonly contain many different types of proteins, and some of the associated proteins are Hsps and chaperones that might reflect the cellular response to limit protein aggregation (Morimoto 2008). Nevertheless, a possible mechanism of toxicity of SOD1-rich aggregates is that they may sequester other protein components essential for MN function, such as chaperones and anti-apoptotic molecules (Pasinelli 2004), inhibit the ubiquitin-proteasome system (Bence 2001)

and, by associating with motor proteins, impair axonal transport (Ligon 2005). mSOD1 is known to cause MN degeneration by toxic gain-of-function(s) that could be exerted, at least in part, through aberrant interactions with other proteins, unless prevented from doing so by association with chaperone proteins. Studies in our laboratory have shown that CypA is up-regulated in ALS, suggesting that it could play a role in protecting cells from the toxicity of mSOD1. This hypothesis was supported by the finding that CypA has a preferential affinity for G93A-SOD1 in our *in vitro* model. Similar results were obtained with other SOD1 ALS-mutants transiently expressed in HEK293 cells, providing added evidence that the two proteins associate preferentially in mutant cells, and suggesting that mSOD1/CypA gain-of-interaction was a common feature of the ALS-associated SOD1-mutants analysed. Furthermore, we confirmed CypA as a novel mutant-SOD1 interacting protein also in mouse lumbar SpC ventral horn, that is where the two proteins have been found to co-aggregate. Therefore, this gain-of-interaction between mSOD1 and CypA was observed *in vitro* and *in vivo*, and may be particularly critical for fALS-associated mSOD1. Since SOD1 mutations destabilize SOD1 or the dimer (Borchelt 1994; Deng 1993), leading to misfolding and aggregation of the protein (Durham 1997), our data support the hypothesis that CypA, by direct association with the mutant protein, could help stabilize and refold misfolded SOD1. Moreover, the binding of CypA, as a molecular chaperone, could be protective by preventing abnormal protein-protein interactions and/or facilitating degradation.

4.2 CypA is an aggregation modifier

The involvement of CypA in the development of the disease was further investigated through the generation of double transgenic animals G93A-SOD1 expressing (G93A-SOD1/CypA+/+), with a reduced expression (G93A-SOD1/CypA+/-) or knockout (G93A-SOD1/CypA-/-) for CypA (Pozzi, manuscript in preparation). CypA reduced or absent expression worsened motor performances and disease progression in G93A-SOD1 mice. Moreover, CypA deficiency anticipated the disease and reduced the survival time of G93A-SOD1 mice. From these analyses CypA emerged as a disease modifier gene. In addition, we evaluated the detergent-insoluble proteins extracted from

ventral horn SpC of G93A-SOD1/CypA double transgenic mice, as a model of protein aggregates, just prior to the expected onset of clinical symptoms. We recovered an increasing amount of insoluble mSOD1 in mice with a reduced or a totally deficient expression of CypA, while no differences were observed in the soluble fractions. These results indicate that depletion of CypA resulted in more mSOD1 aggregates formation. Therefore, we speculate that in mSOD1 MNs, where the interaction between CypA and mSOD1, as well as their presence in the detergent-insoluble fraction have been described, CypA could act as a chaperone, promoting protein folding and refolding. Our findings are consistent with a previous report suggesting a protective role for CypA in mSOD1-induced cell death, in association with its rotamase activity (Lee 1999). This is also in line with other works demonstrating that mSOD1 toxicity could be ameliorated upregulating heat-shock protein chaperones in order to refold the soluble misfolded protein (Brotherton 2012). Moreover, previous co-IP studies already reported mSOD1 interaction with chaperones, such as Hsp25, Hsp70, Hsp40 and αB-crystallin, with mSOD1/HSP70 forming complexes predominantly in the detergent-insoluble fraction (Shinder 2001; Okado-Matsumoto 2002). Therefore, as suggested for heat shock proteins, CypA could protect cells from mSOD1 toxicity by direct interaction, thus preventing aggregation and facilitating degradation, or indirectly by protecting cells from downstream consequences of some other toxic properties. In diseased tissues CypA may also be needed to refold other proteins that are partly denatured by oxidative damage. CypA has been proposed to be a protective agent against oxidative stress by reducing ROS production (Choi 2007; Hong 2004), inducing anti-oxidant protein (Lee 2001; Jaschke 1998; Reddy 1999) or pro-survival factors (Boulos 2007). MNs may be especially sensitive to the free radical damage induced by mSOD1, because of their high oxidative activity, at least partly resulting from their large surface area and dependence on intracellular transport of proteins (Collard 1995) and muscle-derived trophic factor signaling. G93A-SOD1/CypA knockout animals, being deficient in CypA chaperoning activity, not only formed more aggregates of mSOD1, but also irreversibly damaged proteins (ubiquitinated and aberrantly oxidized) were significantly enriched, possibly further enhancing the co-sequestration of other protein components essential for MN function,

including HSC70. Interestingly, specifically nitrated actin, but not general protein nitration, was increased in association with CypA absence in mSOD1 mice. Possibly this finding is consistent with previous reports demonstrating a role for CypA in the maintenance of a normal actin structure (Calhoun 2009; Hasková 1994; Kołcz 1999), also in association with slow axonal transport in MNs (Yuan 1997). Overall our data suggest that in mSOD1 fALS mice CypA, together with other chaperones, could form complexes with misfolded mSOD1, and thus could contribute to protect cells from mSOD1 toxicity by direct interaction, preventing aggregation, or indirectly by protecting cells from down-stream consequences of some other toxic event, such as facilitating degradation of damaged proteins and maintaining the native folding of actin.

On the other side, the binding of CypA to mutant forms of a protein abundant in MNs, such as SOD1, makes it unavailable for other physiological functions. Indeed, we showed that CypA is a highly interactive protein, with potential relevant activities in multiple neuronal pathways; thus, mSOD1 association with CypA could have the effect of decreasing its availability for interactions with other protein partners. In particular, the involvement of CypA in mSOD1 aggregation in MN degeneration may be interesting in view of its interaction with other RNA-binding proteins, especially TDP-43, given its causative role in ALS. Indeed, we observed the presence of detergent-insoluble TDP-43 in mSOD1 mice, and the highest levels of insoluble TDP-43 were observed in CypA knockout mice, although no differences were detected in the soluble fraction. Moreover, we observed robust phosphorylation of TDP-43 at Ser-409/410, that are major sites of pathological phosphorylation and indicate the presence of toxic misfolded species (Liatchko 2010). hnRNP A2/B1 was recovered in the detergent-insoluble fraction of mSOD1 animals, but no differences were observed in the absence of CypA, either in TIFs and in the soluble fractions. We speculate that TDP-43 pathology, commonly associated with sporadic and non-SOD1 fALS (Mackenzie 2007), could also contribute to mSOD1-associated disease, through impaired TDP-43 functions in association with CypA depletion and sequestration of this nuclear protein in insoluble complexes. In fact, HDAC6 protein levels, whose control is mediated by TDP-43, were reduced in ventral horn SpC from G93A-SOD1/CypA knockout mice. Hence, early alterations in this pathway that is

decisive for neurite outgrowth and clearance of misfolded proteins through the autophagy pathway (Boyault 2007; Fiesel 2010 and 2011), even though only indirectly disturbed in SOD1-associated disease, may contribute to neurodegenerative events in ALS. Therefore, there are likely multiple effects mediated by CypA that could be relevant to explain several pathogenic features of ALS, some of which converge on TDP-43, and others that do not.

Finally, we demonstrated the relevance of the mechanisms described for disease progression, analysing ventral horn SpC of mSOD1/CypA double transgenic mice at different stages of the pathology: just prior to the expected onset of clinical symptoms and at a late symptomatic stage of the disease. In these animals we recovered detergent-insoluble and hyper-phosphorylated TDP-43 independent of ALS causing TDP-43 mutations. Therefore, the overexpression of mSOD1 can enhance wild-type TDP-43 aggregation. In particular, the increasing amount of insoluble and aberrantly phosphorylated TDP-43 correlated with disease progression and with CypA depletion, either in non-transgenic and in mSOD1 mice. Our findings indicate that CypA direct or indirect depletion, following CypA knockout or mSOD1/CypA interaction respectively, could contribute to TDP-43 detergent-insolubility. Moreover, in the absence of CypA, the progressive misfolding or aggregation of wild-type TDP-43 could contribute to neurotoxicity, as a cellular consequence of TDP-43 dysfunction, thus accelerating mSOD1 pathology. These findings indicate that CypA could influence both initiation and progression of the pathology. However, the presence of pathological lesions containing detergent insoluble, phosphorylated, and aggregated TDP-43, that are a key feature of TDP-43 proteinopathies, should be deeply investigated by immunohistochemistry in these animals. Furthermore, since TDP-43 misfolding contributes to neurodegenerative diseases very broadly, its association with CypA should be analysed also in other systems.

In summary, as a consequence of chaperones preferential binding for misfolded proteins, CypA interacts with mSOD1. Possibly, mSOD1 sequesters CypA to insoluble aggregates in the cytosol, thus depleting CypA in the nucleus and impeding its physiologic functions, including its association with TDP-43. In fact, interactions of multi-component complexes, such as CypA/TDP-43/hnRNPs complex, could be influenced by specific neuronal microenvironment, as demonstrated in the

case of aggregating mSOD1. Dysregulation of TDP-43/CypA hnRNP complex could contribute to alter TDP-43 solubility and subcellular distribution, or possibly RNA-binding properties, thus favouring aggregation and impairing TDP-43 nuclear functions. Moreover, the multi-component complex containing CypA that interacts with TDP-43 and hnRNP A2/B1 could be important for maintaining homeostasis of several mRNA transcripts, including HDAC6, and alterations of this complex can contribute to give rise to a pathological state. Therefore, alterations of CypA/TDP-43 interaction, detected both when TDP-43 or SOD1 were mutated, could have important implications for hnRNP complex formation, stability, and function.

Overall, our work reveals a novel role for CypA as a molecular chaperone of mSOD1 and TDP-43. Hence, accumulations of TDP-43 and mSOD1 insoluble species in degenerating MNs resulted from an alteration in an interaction intended to maintain protein functional solubility. Given these observations, CypA should be considered an aggregation modifier in ALS. Therefore, regardless of the point at which mutations in either SOD1 or TDP-43 introduce an aberrant gain- or loss-of-function, the net effect may be an impairment of the same multi-component complex, thereby causing a vicious cycle of pathological aggregates formation and compromised RNA metabolism at multiple levels. These events represent a severe damage for cells, particularly for MNs, that progressively degenerate. Thus, since the upstream triggering event could arise from alteration of individual components within the complex or from their altered interactions in the complex or with components in other pathways in the cell, it is likely that different perturbations could arise in diverse neurodegenerative settings, possibly synergizing to contribute to a clinically and genetically heterogeneous disease phenotype, as ALS is.

We conclude that CypA, being an interacting partner of both SOD1 and TDP-43, represents the "missing link" of two pathogenic mechanisms of ALS, that converge on CypA functional network.

VI. CONCLUSION

As most neurodegenerative diseases, clinically indistinguishable ALS phenotypes can be caused by genetic mutations in different genes, including SOD1 and TDP-43, that destabilize the encoded proteins and predispose them to aggregation, or can occur in the absence of known mutation as sporadic disease. The mechanistic relationship between SOD1- and TDP-43-associated familial or sporadic forms of the disease is not well understood. In fact, concomitantly with protein misfolding, there is a series of poorly understood events that lead to degeneration of a selective subset of cells, resulting in loss of function. Several aberrant regulatory processes have been reported, such as mitochondrial dysfunction, impaired RNA processing, glutamate cytotoxicity, impaired axonal transport and oxidative stress. Some of these pathways have been linked to one another in a sequential manner, while there are many that are not obviously connected. In spite of these complexities, there are common features of disease pathogenesis between sporadic and familial, SOD1-dependent ALS suggesting that common (Ferrante 1997; Beal 1997; Atkin 2008; Pokrishevsky 2012), but unknown molecular mechanisms are at work. Identifying and deciphering these connections is thus crucial to understanding the disease and for effectively developing therapies. In the present work, this issue has been approached investigating an early systemic translational biomarker for sporadic and SOD1-linked fALS.

The study of CypA revealed an unexpected relationship between TDP-43 and SOD1, with relevant implications for disease pathogenesis and progression. In fact, we demonstrate that two ALS-causing proteins, SOD1 and TDP-43, share CypA as interacting partner, suggesting a direct molecular link between two pathogenic mechanisms in sporadic and familial ALS. In particular, this thesis work indicates that when SOD1 is mutated, it can bind and sequester CypA in proteinaceous aggregates, altering CypA physiological activities including the interaction with TDP-43, which is in fact recovered in the aggregates. When TDP-43 is mutated or altered, the interaction with CypA is impaired, leading to the disruption of hnRNP-associated complexes and downregulation of HDAC6. Thus, regardless the cause of the disease, mutations in SOD1 or alterations in TDP-43, the net effect is the formation of pathological aggregates and a compromised RNA metabolism. Therefore, impaired association with a common chaperone

protein, CypA, could cause misfolding, that is a critical molecular event in the unified pathogenesis of sALS and fALS, likely further triggering misfolding and propagating the disease.

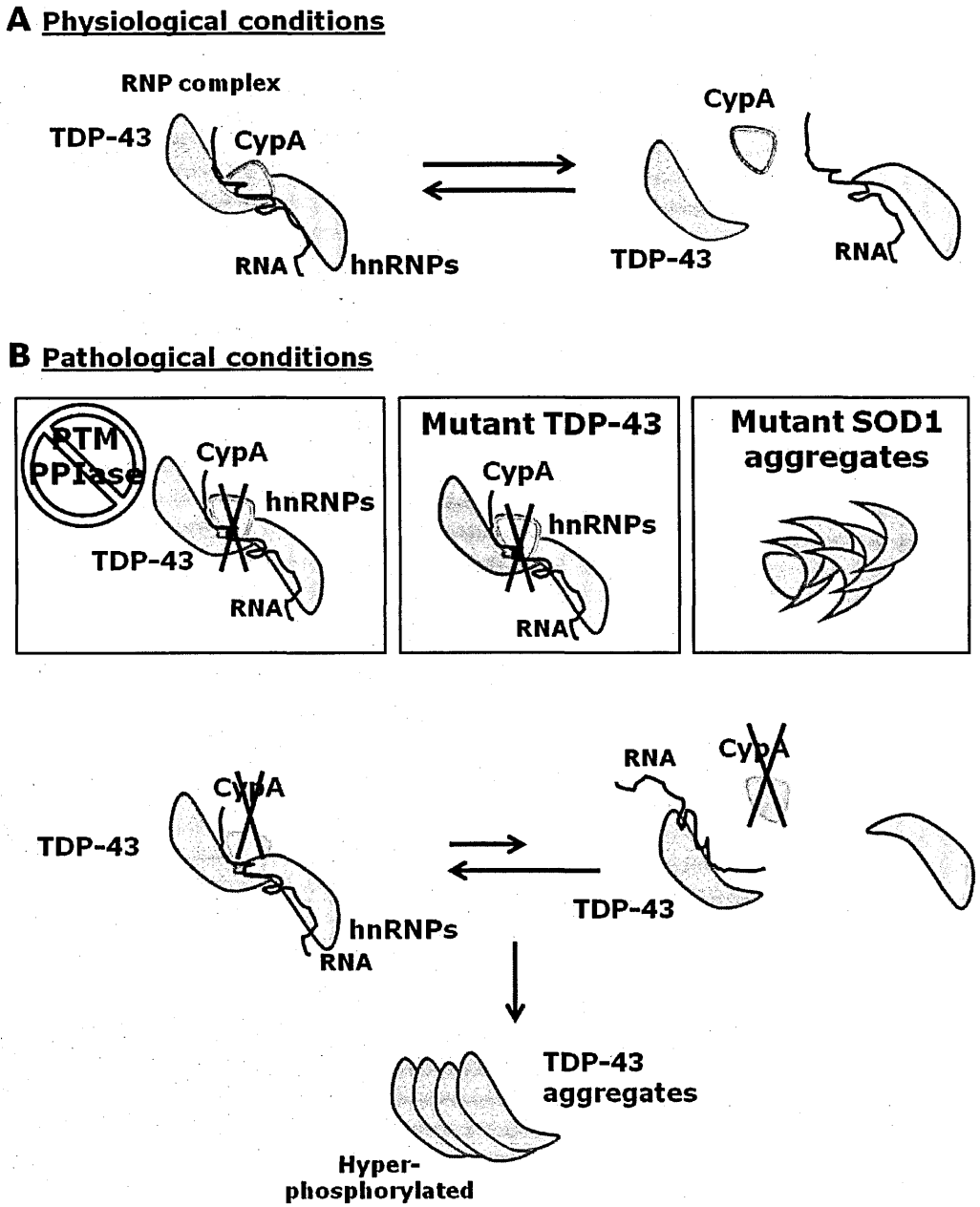

Figure 1. Schematic representation of the working hypothesis.

(A) This thesis work shows that CypA functionally associates with proteins regulating RNA metabolism, including several hnRNPs and TDP-43, forming a highly dynamic multi-component RNP complex. **(B)** In pathological conditions, (i) CypA altered PPIase activity or PTM (e.g. lysine-acetylation), (ii) aberrant TDP-43 or (iii) SOD1 mutation, the interaction between CypA and TDP-43 is impaired. The equilibrium of the complex is shifted toward a more static structure, the complex looses its dynamic modulation and possibly function, leading to the disruption of the complex. The net effect is the formation of TDP-43 rich aggregates that may lead to a compromised RNA metabolism.

The identification of CypA interactome thus provides a tool for understanding pathogenic mechanisms common for this neurodegenerative disorder (see **Figure 1**). In fact, CypA associates with distinct protein interaction networks, one implicated in RNA processing and others involving protein folding, trafficking and cytoskeleton-associated proteins, suggesting that CypA could couple protein folded state to the trafficking pathway. Furthermore, CypA specifically binds hnRNP A2/B1. Since TDP-43 and hnRNP A2/B1 are both structurally typical hnRNP proteins, CypA presumably binds both proteins in a similar mode, and they participate in a multi-component complex that modulates HDAC6 expression. In this model, CypA functions as a molecular chaperone, binding the functional state of a protein (e.g. TDP-43/RNA) and stabilizing it or inducing a conformational change, and it can prevent its denaturation and misassembly into cytotoxic aggregates. These are important features for proteins that form heterocomplexes involved in multiple steps of RNA processing. Knowledge about protein-protein interactions between hnRNPs is limited and further analyses of hnRNP complexes with different components may shed light on the functions of hnRNPs in the many different RNA-related biological processes. Whatever its identity, CypA is directly implicated in hnRNP-rich complexes formation and maintenance, since its downregulation significantly reduces the interaction between TDP-43 and hnRNP A2/B1, affecting also HDAC6 expression. Therefore, CypA can be considered a novel modifier of TDP-43 activity. Notably, other two disease-relevant proteins have been associated with HDAC6: FUS modulates HDAC6 expression in complex with TDP-43 (Kim 2010), while a finely tuned balance between VCP and HDAC6 directs ubiquitinated aggregates either to the UPS or to the autophagic pathway (Boyault 2006). Thereby, a disturbance in the expression or in the equilibrium between the different functions of HDAC6 could play an important role in neurodegeneration (d'Ydewalle 2012). We also provide preliminary evidence that CypA/TDP-43 binding may be involved in TDP-43 mislocalisation and that CypA acetylation at lysine-125 is specifically required for the interaction. The role of CypA PTMs in modulating its various functions has yet to be investigated, as well as the function of the extracellular and circulating CypA. Clearly we are still at a very early stage in understanding the biology of CypA in ALS. Additional

exploration in this area may provide further insight into the very early observation that CypA is required for the correct hnRNP complex assembly and maintenance, and HDAC6 expression regulation. Moreover, experiments in CypA knockout animals, where very specific questions are addressed, will be important in determining the significance of the various interactions of CypA that have been demonstrated *in vitro*. This study further highlights the importance of aberrant RNA metabolism as a cause of disease and supports the idea that accumulation of insoluble TDP-43 plays an important role in ALS pathogenesis. In fact, considering the sheer number of potentially misregulated targets/pathways after changes in cellular distribution and solubility of TDP-43, it is likely that even small alterations in a member of the multi-component complex described might cause neurodegeneration over a long period of time, especially if we consider that the ability of cells to compensate for even small changes from normality gradually diminishes with age.

Finally, the identification of a common molecular pathway in ALS has important implications for the effective treatment of this devastating disease. Our observations have implications regarding the potential use of chaperone proteins or agents that modulate their activity or PTMs to correct the deficits. In particular, CypA could be a potential therapeutic target to delay ALS progression.

VII. BIBLIOGRAPHY

Abe K, Pan LH, Watanabe M, et al. (1997) Upregulation of protein-tyrosine nitration in the anterior horn cells of amyotrophic lateral sclerosis. Neurol Res, 19 (2):124-8.

Abhyankar MM, Urekar C, Reddi PP. (2007) A novel CpG-free vertebrate insulator silences the testis-specific SP-10 gene in somatic tissues: role for TDP-43 in insulator function. J Biol Chem. 282(50):36143-54.

Abramzon Y, Johnson JO, Scholz SW, et al. (2012) Valosin-containing protein (VCP) mutations in sporadic amyotrophic lateral sclerosis. Neurobiol Aging. 33(9):2231.e1-2231.e6.

Adams B, Musiyenko A, Kumar R, Barik S. (2005) A novel class of dual-family immunophilins. Journal of Biological Chemistry, 280:24308-14.

Aizawa H, Kimura T, Hashimoto K, et al. (2000) Basophilic cytoplasmic inclusions in a case of sporadic juvenile amyotrophic lateral sclerosis. J Neurol Sci. 176(2):109-13.

Al-Chalabi A, Andersen PM, Nilsson P, et al. (1999) Deletions of the heavy neurofilament subunit tail in amyotrophic lateral sclerosis. Hum Mol Genet. 8(2):157-64.

Al-Chalabi A, Jones A, Troakes C, et al. (2012) The genetics and neuropathology of amyotrophic lateral sclerosis. Acta Neuropathol. 124(3):339-52.

Alexander GM, Erwin KL, Byers N, et al. (2004) Effect of transgene copy number on survival in the G93A-SOD1 transgenic mouse model of ALS. Brain Res Mol Brain Res 130:7-15.

Alexianu ME, Ho BK, Mohamed AH, et al. (1994) The role of calcium-binding proteins in selective motoneuron vulnerability in amyotrophic lateral sclerosis. Ann Neurol. 36(6):846-58.

Almer G, Guégan C, Teismann P, et al. (2001) Increased expression of the pro-inflammatory enzyme cyclooxygenase-2 in amyotrophic lateral sclerosis. Ann Neurol. 49(2):176-85.

Alonso A, Logroscino G, Hernán MA. (2010) Smoking and the risk of amyotrophic lateral sclerosis: a systematic review and meta-analysis. J Neurol Neurosurg Psychiatry. 81(11):1249-52.

Alonso A, Logroscino G, Jick SS, Hernán MA. (2009) Incidence and lifetime risk of motor neuron disease in the United Kingdom: a population-based study. Eur J Neurol.16(6):745-51.

Al-Saif A, Al-Mohanna F, Bohlega S. (2011) A mutation in sigma-1 receptor causes juvenile amyotrophic lateral sclerosis. Ann Neurol. 70(6):913-9.

Al-Sarraj S, King A, Troakes C, et al. (2011) p62 positive, TDP-43 negative, neuronal cytoplasmic and intranuclear inclusions in the cerebellum and hippocampus define the pathology of C9orf72-linked FTLD and MND/ALS. Acta Neuropathol. 122(6):691-702.

Al-Sarraj S, Maekawa S, Kibble M, et al. (2002) Ubiquitin-only intraneuronal inclusion in the substantia nigra is a characteristic feature of motor neurone disease with dementia. Neuropathol Appl Neurobiol. 28:120-128.

Anand P, Parrett A, Martin J, et al. (1995) Regional changes of ciliary neurotrophic factor and nerve growth factor levels in post mortem spinal cord and cerebral cortex from patients with motor disease. Nat Med. 1(2):168-72.

Andersen PM, Al-Chalabi A. (2011) Clinical genetics of amyotrophic lateral sclerosis: what do we really know? Nat Rev Neurol. 7(11):603-15.

Andersen PM, Forsgren L, Binzer M, et al. (1996) Autosomal recessive adult-onset amyotrophic lateral sclerosis associated with homozygosity for Asp90Ala CuZn-superoxide dismutase mutation. A clinical and genealogical study of 36 patients. Brain. 119 (Pt 4):1153-72.

Andersen PM, Nilsson P, Ala-Hurula V, et al. (1995) Amyotrophic lateral sclerosis associated with homozygosity for an Asp90Ala mutation in CuZn-superoxide dismutase. Nat Genet. 10(1):61-6.

Andersson MK, Ståhlberg A, Arvidsson Y, et al. (2008) The multifunctional FUS, EWS and TAF15 proto-oncoproteins show cell type-specific expression patterns and involvement in cell spreading and stress response. BMC Cell Biol. 9:37.

Andreeva L, Heads R, Green CJ. (1999) Cyclophilins and their possible role in the stress response. Int J Exp Pathol. 80(6):305-15.

Andreotti AH. (2003) Native state proline isomerization: an intrinsic molecular switch. Biochemistry. 42(32):9515-24.

Andrus PK, Fleck TJ, Gurney ME, Hall ED. (1998) Protein oxidative damage in a transgenic mouse model of familial amyotrophic lateral sclerosis. J Neurochem. 71(5):2041-8.

Ansari H, Greco G, Luban J. (2002) Cyclophilin A peptidyl-prolyl isomerase activity promotes ZPR1 nuclear export. Mol Cell Biol, 22(20):6993-7003.

Appel SH, Beers DR, Henkel JS. (2010) T cell-microglial dialogue in Parkinson's disease and amyotrophic lateral sclerosis: are we listening? Trends Immunol.31(1):7-17.

Appel SH, Rowland LP. (2012) Amyotrophic lateral sclerosis, frontotemporal lobar dementia, and p62: A functional convergence? Neurology.

Appel SH, Smith RG, Alexianu MF, et al. (1995) Autoimmunity as an etiological factor in sporadic amyotrophic lateral sclerosis. Adv Neurol. 68:47-57.

Arai T, Hasegawa M, Akiyama H, et al. (2006) TDP-43 is a component of ubiquitin-positive tau-negative inclusions in frontotemporal lobar degeneration and amyotrophic lateral sclerosis. Biochem Biophys Res Commun. 22;351(3):602-11.

Arai T, Hasegawa M, Nonoka T, et al. (2010) Phosphorylated and cleaved TDP-43 in ALS, FTLD and other neurodegenerative disorders and in cellular models of TDP-43 proteinopathy. Neuropathology. 30(2):170-81.

Aran FA. (1850) Recherches sur une maladie non encore décrite du systemé musculaire (atrophie musculaire progressive). Arch Gen Med 14:5-35. 172–214

Arckens L, Van der Gucht E, Van den Bergh G, et al. (2003) Differential display implicates cyclophilin A in adult cortical plasticity. Eur J Neurosci. 18(1):61-75.

Arévalo-Rodríguez M, Cardenas ME, Wu X, et al. (2000) Cyclophilin A and Ess1 interact with and regulate silencing by the Sin3-Rpd3 histone deacetylase. EMBO J. 19(14):3739-49.

Arévalo-Rodríguez M, Heitman J. (2005) Cyclophilin A is localized to the nucleus and controls meiosis in Saccharomyces cerevisiae. Eukaryot Cell. 4(1):17-29.

Arevalo-Rodriguez M, Wu X, Hanes SD, Heitman J. (2004) Prolyl isomerases in yeast. Front Biosci. 9:2420-46.

Arié JP, Sassoon N, Betton JM. (2001) Chaperone function of FkpA, a heat shock prolyl isomerase, in the periplasm of Escherichia coli. Mol Microbiol, 39:199-210.

Armon C. (2003) An evidence-based medicine approach to the evaluation of the role of exogenous risk factors in sporadic amyotrophic lateral sclerosis. Neuroepidemiology, 22:217-228.

Armon C. (2009) Smoking may be considered an established risk factor for sporadic ALS. Neurology. Nov 17;73(20):1693-8.

Arnesano F, Banci L, Bertini I, et al. (2004) The unusually stable quaternary structure of human Cu,Zn-superoxide dismutase 1 is controlled by both metal occupancy and disulfide status. J Biol Chem. 279(46):47998-8003.

Arora K, Gwinn WM, Bower MA, et al. (2005) Extracellular cyclophilins contribute to the regulation of inflammatory responses. J Immunol. 175(1):517-22.

Atkin JD, Farg MA, Turner BJ, et al. (2006) Induction of the unfolded protein response in familial amyotrophic lateral sclerosis and association of protein-disulfide isomerase with superoxide dismutase 1. J Biol Chem, 281(40):30152-65.

Atkin JD, Farg MA, Walker AK, et al. (2008) Endoplasmic reticulum stress and induction of the unfolded protein response in human sporadic amyotrophic lateral sclerosis. Neurobiol Dis, 30(3):400-7.

Ayala YM, Pantano S, D'Ambrogio A, et al. (2005) Human, Drosophila, and C.elegans TDP43: nucleic acid binding properties and splicing regulatory function. J Mol Biol. 348(3):575-88.

Ayala YM, Zago P, D'Ambrogio A, et al. (2008) Structural determinants of the cellular localization and shuttling of TDP-43. J Cell Sci, 121:3778-85.

Azzouz M, Ralph GS, Storkebaum E, et al. (2004) VEGF delivery with retrogradely transported lentivector prolongs survival in a mouse ALS model. Nature. 429(6990):413-7.

Babetto E, Mangolini A, Rizzardini M, et al. (2005) Tetracycline-regulated gene expression in the NSC-34-tTA cell line for investigation of motor neuron diseases. Brain Res Mol Brain Res. 140(1-2):63-72

Babu JR, Geetha T, Wooten MW. (2005) Sequestosome 1/p62 shuttles polyubiquitinated tau for proteasomal degradation. J Neurochem. 94(1):192-203.

Baker EK, Colley NJ, Zuker CS. (1994) The cyclophilin homolog NinaA functions as a chaperone, forming a stable complex in vivo with its protein target rhodopsin. EMBO J, 13:4886-95.

Baneyx F. (2004) Keeping up with protein folding. Microbial Cell Factories, 3:6.

Baneyx F, Mujacic M. (2004) Recombinant protein folding and misfolding in Escherichia coli. Nat Biotechnol. 22(11):1399-408.

Barik S. (2006) Immunophilins: for the love of proteins.Cell Mol Life Sci. 63(24):2889-900.

Barlow AL, Macleod A, Noppen S, et al. (2010) Colocalization analysis in fluorescence micrographs: verification of a more accurate calculation of pearson's correlation coefficient. Microsc Microanal, 16(6):710-24.

Barmada SJ, Skibinski G, Korb E, et al. (2010) Cytoplasmic mislocalization of TDP-43 is toxic to neurons and enhanced by a mutation associated with familial amyotrophic lateral sclerosis. J Neurosci. 30(2):639-49.

Baron P, Bussini S, Cardin V, et al. (2005) Production of monocyte chemoattractant protein-1 in amyotrophic lateral sclerosis. Muscle Nerve. 32(4):541-4.

Basso M, Massignan T, Samengo G, et al. (2006) Insoluble mutant SOD1 is partly oligoubiquitinated in amyotrophic lateral sclerosis mice. J Biol Chem. 281(44):33325-35.

Basso M, Samengo G, Nardo G, et al. (2009) Characterization of detergent-insoluble proteins in ALS indicates a causal link between nitrative stress and aggregation in pathogenesis. PLoS One 4(12):e8130.

Beal MF, Ferrante RJ, Browne SE, et al. (1997) Increased 3-nitrotyrosine in both sporadic and familial amyotrophic lateral sclerosis. Ann Neurol. 42(4):644-54.

Beaulieu JM, Nguyen MD, Julien JP. (1999) Late onset of motor neurons in mice overexpressing wild-type peripherin. J Cell Biol. 147(3):531-44.

Beckman JS, Carson M, Smith CD, Koppenol WH. (1993) ALS, SOD and peroxynitrite. Nature. 364(6438):584.

Beers DR, Henkel JS, Zhao W, et al. (2011) Endogenous regulatory T lymphocytes ameliorate amyotrophic lateral sclerosis in mice and correlate with disease progression in patients with amyotrophic lateral sclerosis. Brain.134(Pt 5):1293-314.

Beghi E, Chiò A, Couratier P, et al. (2011) The epidemiology and treatment of ALS: focus on the heterogeneity of the disease and critical appraisal of therapeutic trials. Amyotroph Lateral Scler. 12(1):1-10.

Beleza-Meireles A, Al-Chalabi A. (2009) Genetic studies of amyotrophic lateral sclerosis: controversies and perspectives. Amyotroph Lateral Scler. Feb;10(1):1-14.

Bell RD, Winkler EA, Singh I, et al. (2012) Apolipoprotein E controls cerebrovascular integrity via cyclophilin A. Nature. 485(7399):512-6.

Belly A, Moreau-Gachelin F, Sadoul R, Goldberg Y. (2005) Delocalization of the multifunctional RNA splicing factor TLS/FUS in hippocampal neurones: exclusion from the nucleus and accumulation in dendritic granules and spine heads. Neurosci Lett. 379(3):152-7.

Belzil VV, Daoud H, Desjarlais A, et al. (2011) Analysis of OPTN as a causative gene for amyotrophic lateral sclerosis. Neurobiol Aging. 32(3):555.e13-4.

Benatar M. (2007) Lost in translation: treatment trials in the SOD1 mouse and in human ALS. Neurobiol Dis. 26(1):1-13.

Bendotti C, Calvaresi N, Chiveri L, et al. (2001) Early vacuolization and mitochondrial damage in motor neurons of FALS mice are not associated with apoptosis or with changes in cytochrome oxidase histochemical reactivity. J Neurol Sci. 191(1-2):25-33.

Bendotti C, Carri MT. (2004) Lessons from models of SOD1-linked familial ALS. Trends Mol Med 10:393-400.

Berlett BS, Stadtman ER. (1997) Protein oxidation in aging, disease, and oxidative stress. J Biol Chem. 272(33):20313-6.

Bertolotti A, Lutz Y, Heard DJ, et al. (1996) hTAF(II)68, a novel RNA/ssDNA-binding protein with homology to the pro-oncoproteins TLS/FUS and EWS is associated with both TFIID and RNA polymerase II. EMBO J. 15(18):5022-31.

Billich A, Winkler G, Aschauer H, et al. (1997) Presence of cyclophilin A in synovial fluids of patients with rheumatoid arthritis. J Exp Med. 185(5):975-80.

Bilsland LG, Nirmalananthan N, Yip J, et al. (2008) Expression of mutant SOD1 in astrocytes induces functional deficits in motoneuron mitochondria. J Neurochem 107:1271-1283.

Biomarkers Definitions Working Group. (2001) Biomarkers and surrogate endpoints: preferred definitions and conceptual framework. Clin Pharmacol Ther. 69(3):89-95.

Bjørkøy G, Lamark T, Johansen T. (2006) p62/SQSTM1: a missing link between protein aggregates and the autophagy machinery. Autophagy. 2(2):138-9.

Blackburn D, Sargsyan S, Monk PN, Shaw PJ. (2009) Astrocyte function and role in motor neuron disease: a future therapeutic target? Glia. 57(12):1251-64.

Blander G, Guarente L. (2004) The Sir2 family of protein deacetylases. Annu Rev Biochem. 73:417-35.

Boillée S, Vande Velde C, Cleveland DW. (2006) ALS: a disease of motor neurons and their nonneuronal neighbors. Neuron. 52(1):39-59.

Bolte S, Cordelières FP. (2006) A guided tour into subcellular colocalization analysis in light microscopy. J Microsc, 224:213-32.

Bond CS, Fox AH. (2009) Paraspeckles: nuclear bodies built on long noncoding RNA. J Cell Biol. 186(5):637-44.

Bonfils C, Bec N, Larroque C, et al. (2010) Cyclophilin A as negative regulator of apoptosis by sequestering cytochrome c. Biochem Biophys Res Commun. 393(2):325-30.

Borasio GD, Robberecht W, Leigh PN, et al. (1998) A placebo-controlled trial of insulin-like growth factor-I in amyotrophic lateral sclerosis. European ALS/IGF-I Study Group. Neurology. 51(2):583-6.

Borchelt DR, Lee MK, Slunt HS, et al. (1994) Superoxide dismutase 1 with mutations linked to familial amyotrophic lateral sclerosis possesses significant activity. Proc Natl Acad Sci U S A. 91(17):8292-6.

Borchelt DR, Wong PC, Becher MW, et al. (1998) Axonal transport of mutant superoxide dismutase 1 and focal axonal abnormalities in the proximal axons of transgenic mice. Neurobiol Dis. 5(1):27-35.

Borel JF. (1989) The cyclosporins. Transplant Proc. 21(1 Pt 1):810-5.

Bosco DA, Eisenmesser EZ, Pochapsky S, et al. (2002) Catalysis of cis/trans isomerization in native HIV-1 capsid by human cyclophilin A. Proc Natl Acad Sci U S A. 99(8):5247-52.

Bose JK, Wang IF, Hung L, et al. (2008) TDP-43 overexpression enhances exon 7 inclusion during the survival of motor neuron pre-mRNA splicing. J Biol Chem. 283(43):28852-9.

Boulos S, Meloni BP, Arthur PG, et al. (2007) Evidence that intracellular cyclophilin A and cyclophilin A/CD147 receptor-mediated ERK1/2 signalling can protect neurons against in vitro oxidative and ischemic injury. Neurobiol Dis. 25(1):54-64.

Bourquin JP, Stagljar I, Meier P, et al. (1997) A serine/arginine-rich nuclear matrix cyclophilin interacts with the C-terminal domain of RNA polymerase II. Nucleic Acids Research, 25:2055–61.

Bowling AC, Schulz JB, Brown RH Jr, Beal MF. (1993) Superoxide dismutase activity, oxidative damage, and mitochondrial energy metabolism in familial and sporadic amyotrophic lateral sclerosis. J Neurochem. 61(6):2322-5.

Boxer AL, Mackenzie IR, Boeve BF, et al. (2011) Clinical, neuroimaging and neuropathological features of a new chromosome 9p-linked FTD-ALS family. J Neurol Neurosurg Psychiatry. 82(2):196-203.

Boyault C, Zhang Y, Fritah S, et al. (2007) HDAC6 controls major cell response pathways to cytotoxic accumulation of protein aggregates. Genes Dev. 21(17):2172-81.

Boyes J, Byfield P, Nakatani Y, Ogryzko V. (1998) Regulation of activity of the transcription factor GATA-1 by acetylation. Nature. 396(6711):594-8.

Braaten D, Ansari H, Luban J. (1997) The hydrophobic pocket of cyclophilin is the binding site for the human immunodeficiency virus type 1 Gag polyprotein. J. Virol., 71:2107-13.

Braaten D, Franke EK, Luban J. (1996) Cyclophilin A is required for an early step in the life cycle of human immunodeficiency virus type 1 before the initiation of reverse transcription. J Virol. 70(6):3551-60.

Braaten D, Luban J. (2001) Cyclophilin A regulates HIV-1 infectivity, as demonstrated by gene targeting in human T cells. EMBO J. 20(6):1300-9.

Bradley WG, Good P, Rasool CG, Adelman LS. (1983) Morphometric and biochemical studies of peripheral nerves in amyotrophic lateral sclerosis. Ann Neurol, 14:267-277.

Brazin KN, Mallis RJ, Fulton DB, Andreotti AH. (2002) Regulation of the tyrosine kinase Itk by the peptidyl-prolyl isomerase cyclophilin A. Proc Natl Acad Sci U S A, 99(4):1899-904.

Brelstaff J, Lashley T, Holton JL, et al. (2011) Transportin1: a marker of FTLD-FUS. Acta Neuropathol. 122(5):591-600.

Brettschneider J, Lehmensiek V, Mogel H, et al. (2010) Proteome analysis reveals candidate markers of disease progression in amyotrophic lateral sclerosis (ALS). Neurosci Lett. 468(1):23-7. Epub 2009 Oct 22.

Brown J, Ashworth A, Gydesen S, et al. (1995) Familial non-specific dementia maps to chromosome 3. Hum Mol Genet. 4(9):1625-8.

Brownell B, Oppenheimer DR, Hughes JT. (1970) The central nervous system in motor neurone disease. J Neurol Neurosurg Psychiatry, 33:338-357.

Bruening W, Roy J, Giasson B, Figlewicz DA, et al. (1999) Up-regulation of protein chaperones preserves viability of cells expressing toxic Cu/Zn-superoxide dismutase mutants associated with amyotrophic lateral sclerosis. J Neurochem. 72(2):693-9.

Bruijn, LI, Beal MF, Becher MW, Schulz JB, et al. (1997) Elevated free nitrotyrosine levels, but not protein-bound nitrotyrosine or hydroxyl radicals, throughout amyotrophic lateral sclerosis (ALS)-like disease implicate tyrosine nitration as an aberrant in vivo property of one familial ALS-linked superoxide dismutase 1 mutant. Proc Natl Acad Sci U S A, 94 (14):7606-11.

Bucciantini M, Giannoni E, Chiti F, Baroni F, et al. (2002) Inherent toxicity of aggregates implies a common mechanism for protein misfolding diseases. Nature. 416(6880):507-11.

Budini M, Buratti E, Stuani C, Guarnaccia C, et al. (2012) Cellular model of TAR DNA-binding protein 43 (TDP-43) aggregation based on its C-terminal Gln/Asn-rich region. J Biol Chem. 287(10):7512-25. Epub 2012 Jan 10.

Bunina TL. (1962) On intracellular inclusions in familial amyotrophic lateral sclerosis. Zh Nevropatol Psikhiatr Im S S Korsakova 62:1293-9.

Buratti E, Baralle FE. (2001) Characterization and functional implications of the RNA binding properties of nuclear factor TDP-43, a novel splicing regulator of CFTR exon 9. J Biol Chem. 276(39):36337-43.

Buratti E, Baralle FE. (2008) Multiple roles of TDP-43 in gene expression, splicing regulation, and human disease. Front Biosci. 13:867-78.

Buratti E, Baralle FE. (2012) TDP-43: gumming up neurons through protein-protein and protein-RNA interactions. Trends Biochem Sci. 37(6):237-47.

Buratti E, Brindisi A, Giombi M, Tisminetzky S, et al. (2005) TDP-43 binds heterogeneous nuclear ribonucleoprotein A/B through its C-terminal tail: an important region for the inhibition of cystic fibrosis transmembrane conductance regulator exon 9 splicing. J Biol Chem, 280(45):37572-84.

Buratti E, De Conti L, Stuani C, Romano M, et al. (2010) Nuclear factor TDP-43 can affect selected microRNA levels. FEBS J. 277(10):2268-81.

Buratti E, Dörk T, Zuccato E, Pagani F, et al. (2001) Nuclear factor TDP-43 and SR proteins promote in vitro and in vivo CFTR exon 9 skipping. EMBO J. 20(7):1774-84.

Buss WC, Stepanek J, Queen SA. (1994) Association of tissue-specific changes in translation elongation after cyclosporin with changes in elongation factor 2 phosphorylation. Biochem Pharmacol. 48(7):1459-69.

Butterfield DA, Stadtman ER. (1997) Protein oxidation processes in aging brain. Adv. Cell Aging Gerontol. 2:161–191.

Byrne S, Walsh C, Lynch C, Bede P, et al. (2011) Rate of familial amyotrophic lateral sclerosis: a systematic review and meta-analysis. J Neurol Neurosurg Psychiatry. 82(6):623-7.

Cai H, Lin X, Xie C, Laird FM, et al. (2005) Loss of ALS2 function is insufficient to trigger motor neuron degeneration in knock-out mice but predisposes neurons to oxidative stress. J Neurosci. 25(33):7567-74.

Calhoun CC, Lu YC, Song J, Chiu R. (2009) Knockdown endogenous CypA with siRNA in U2OS cells results in disruption of F-actin structure and alters tumor phenotype. Mol Cell Biochem. 320(1-2):35-43.

Camerini S, Polci ML, Restuccia U, Usuelli V, et al. (2007) A novel approach to identify proteins modified by nitric oxide: the HIS-TAG switch method. J Proteome Res. 6(8):3224-31.

Campos-Olivas R, Summers MF. (1999) Backbone dynamics of the N-terminal domain of the HIV-1 capsid protein and comparison with the G94D mutant conferring cyclosporin resistance/dependence. Biochemistry. 38(32):10262-71.

Camu W, Billiard M, Baldy-Moulinier M. (1993) Fasting plasma and CSF amino acid levels in amyotrophic lateral sclerosis: a subtype analysis. Acta Neurol Scand.88(1):51-5.

Candé C, Vahsen N, Kouranti I, Schmitt E, et al. (2004) AIF and cyclophilin A cooperate in apoptosis-associated chromatinolysis. Oncogene.23(8):1514-21.

Capano M, Virji S, Crompton M. (2002) Cyclophilin-A is involved in excitotoxin-induced caspase activation in rat neuronal B50 cells. Biochem J. 363(Pt 1):29-36.

Carpenter S. (1968) Proximal axonal enlargement in motor neuron disease. Neurology. 18(9):841-51.

Carriedo SG, Yin HZ, Weiss JH. (1996) Motor neurons are selectively vulnerable to AMPA/kainate receptor-mediated injury in vitro. J Neurosci. 16(13):4069-79.

Carrozza MJ, Utley RT, Workman JL, Côté J. (2003) The diverse functions of histone acetyltransferase complexes. Trends Genet. 19(6):321-9.

Casagrande S, Bonetto V, Fratelli M, Gianazza E, et al. (2002) Glutathionylation of human thioredoxin: a possible crosstalk between the glutathione and thioredoxin systems. Proc Natl Acad Sci U S A. 99(15):9745-9.

Casoni F, Basso M, Massignan T, Gianazza E, et al. (2005) Protein nitration in a mouse model of familial amyotrophic lateral sclerosis: possible multifunctional role in the pathogenesis. J Biol Chem, 280:16295-304.

Castegna A, Aksenov M, Thongboonkerd V, Klein JB, et al. (2002) Proteomic identification of oxidatively modified proteins in Alzheimer's disease brain. Part II: dihydropyrimidinase-related protein 2, alpha-enolase and heat shock cognate 71. J Neurochem. 82(6):1524-32.

Castello A, Fischer B, Eichelbaum K, Horos R, et al. (2012) Insights into RNA biology from an atlas of mammalian mRNA-binding proteins. Cell. 149(6):1393-406.

Chan N, Le C, Shieh P, Mozaffar T, et al. (2012) Valosin-containing protein mutation and Parkinson's disease. Parkinsonism Relat Disord. 18(1):107-9.

Chang Y, Kong Q, Shan X, Tian G, et al. (2008) Messenger RNA oxidation occurs early in disease pathogenesis and promotes motor neuron degeneration in ALS. PLoS One. 3(8):e2849.

Charcot JM. (1874) De la sclérose latérale amyotrophique. Prog Med, 23; 24; 29:235-237. 341–232; 453–235

Charcot JM, Joffroy A. (1869) Deux cas d'atrophie musculaire progressive avec lésions de la substance grise et de faisceaux antérolatérauxde la moelle épinière. Arch Physiol Norm Pathol. 1:354-357. 352:628–649; 353:744–757

Chen H, Kubo Y, Hoshi T, Heinemann SH. (1998) Cyclosporin A selectively reduces the functional expression of Kir2.1 potassium channels in Xenopus oocytes. FEBS Lett. 422(3):307-10.

Chen R, Grand'Maison F, Strong MJ, Ramsay DA, Bolton CF. (1996) Motor neuron disease presenting as acute respiratory failure: a clinical and pathological study. J Neurol Neurosurg Psychiatry, 60:455-458.

Chen S, Zhang X, Song L, Le W. (2012) Autophagy dysregulation in amyotrophic lateral sclerosis. Brain Pathol. 22(1):110-6.

Chen W, Saeed M, Mao H, Siddique N, et al. (2006) Lack of association of VEGF promoter polymorphisms with sporadic ALS. Neurology. 67(3):508-10.

Chen Y, Huang R, Chen K, Song W, et al. (2012) Association analysis of PON polymorphisms in sporadic ALS in a Chinese population. Neurobiol Aging.

Chen Y, Huang R, Yang Y, Chen K, et al. (2011) Ataxin-2 intermediate-length polyglutamine: a possible risk factor for Chinese patients with amyotrophic lateral sclerosis. Neurobiol Aging. 32(10):1925.e1-5.

Chen YI, Moore RE, Ge HY, Young MK, et al. (2007) Proteomic analysis of in vivo assembled pre-mRNA splicing complexes expands the catalog of participating factors. Nucleic Acids Research, 35:3928–44.

Chen YZ, Bennett CL, Huynh HM, Blair IP, et al. (2004) DNA/RNA helicase gene mutations in a form of juvenile amyotrophic lateral sclerosis (ALS4). Am J Hum Genet. 74(6):1128-35.

Chen-Plotkin AS, Lee VM, Trojanowski JQ. (2010) TAR DNA-binding protein 43 in neurodegenerative disease. Nat Rev Neurol. 6(4):211-20.

Cheroni C, Marino M, Tortarolo M, Veglianese P, et al. (2009) Functional alterations of the ubiquitin-proteasome system in motor neurons of a mouse model of familial amyotrophic lateral sclerosis. Hum Mol Genet. 18(1):82-96.

Cheroni C, Peviani M, Cascio P, Debiasi S, et al. (2005) Accumulation of human SOD1 and ubiquitinated deposits in the spinal cord of SOD1G93A mice during motor neuron disease progression correlates with a decrease of proteasome. Neurobiol Dis. 18(3):509-22.

Chevalier F, Depagne J, Hem S, Chevillard S, et al. (2012) Accumulation of Cyclophilin A isoforms in conditioned medium of irradiated breast cancer cells. Proteomics.

Chiang PM, Ling J, Jeong YH, Price DL, et al. (2010) Deletion of TDP-43 down-regulates Tbc1d1, a gene linked to obesity, and alters body fat metabolism. Proc Natl Acad Sci U S A. 107(37):16320-4.

Chiò A, Benzi G, Dossena M, Mutani R, Mora G. (2005) Severely increased risk of amyotrophic lateral sclerosis among Italian professional football players. Brain. 128(Pt 3):472-6. Epub 2005 Jan 5.

Chiò A, Borghero G, Pugliatti M, Ticca A, et al.; Italian Amyotrophic Lateral Sclerosis Genetic (ITALSGEN) Consortium. (2011) Large proportion of amyotrophic lateral sclerosis cases in Sardinia due to a single founder mutation of the TARDBP gene. Arch Neurol. 68(5):594-8.

Chiò A, Calvo A, Dossena M, Ghiglione P, et al. (2009) ALS in Italian professional soccer players: the risk is still present and could be soccer-specific. Amyotroph Lateral Scler. 10(4):205-9.

Chiò A, Calvo A, Moglia C, Mazzini L, Mora G; PARALS study group. (2011) Phenotypic heterogeneity of amyotrophic lateral sclerosis: a population based study. J Neurol Neurosurg Psychiatry. 82(7):740-6.

Chiò A, Mora G, Calvo A, Mazzini L, et al.; PARALS (2009) Epidemiology of ALS in Italy: a 10-year prospective population-based study. Neurology. 72(8):725-31.

Chiò A, Mora G, Restagno G, Brunetti M, et al. (2012) UNC13A influences survival in Italian amyotrophic lateral sclerosis patients: a population-based study. Neurobiol Aging.

Chiò A, Schymick JC, Restagno G, Scholz SW, et al. (2009) A two-stage genome-wide association study of sporadic amyotrophic lateral sclerosis. Hum Mol Genet. 18(8):1524-32.

Chiu R, Rey O, Zheng JQ, Twiss JL, et al. (2003) Effects of altered expression and localization of cyclophilin A on differentiation of p19 embryonic carcinoma cells. Cell Mol Neurobiol. 23(6):929-43.

Choi KJ, Piao YJ, Lim MJ, Kim JH, et al. (2007) Overexpressed cyclophilin A in cancer cells renders resistance to hypoxia- and cisplatin-induced cell death. Cancer Res. 67(8):3654-62.

Chook YM, Blobel G. (1999) Structure of the nuclear transport complex karyopherin-beta2-Ran x GppNHp. Nature.399(6733):230-7.

Choudhary C, Kumar C, Gnad F, Nielsen ML, et al. (2009) Lysine acetylation targets protein complexes and co-regulates major cellular functions. Science, 325(5942):834-40.

Chow CY, Landers JE, Bergren SK, Sapp PC, et al. (2009) Deleterious variants of FIG4, a phosphoinositide phosphatase, in patients with ALS. Am J Hum Genet. 84(1):85-8.

Chow CY, Zhang Y, Dowling JJ, Jin N, et al. (2007) Mutation of FIG4 causes neurodegeneration in the pale tremor mouse and patients with CMT4J. Nature. 448(7149):68-72.

Christofferson DE, Yuan J. (2010) Cyclophilin A release as a biomarker of necrotic cell death. Cell Death Differ. 17(12):1942-3.

Cleveland DW, Rothstein JD. (2001) From Charcot to Lou Gehrig: deciphering selective motor neuron death in ALS. Nat Rev Neurosci. 2(11):806-19.

Cleveland DW. (1999) From Charcot to SOD1: mechanisms of selective motor neuron death in ALS. Neuron. 24(3):515-20.

Clevenger CV, Gadd SL, Zheng J. (2009) New mechanisms for PRLr action in breast cancer. Trends Endocrinol Metab. 20(5):223-9.

Colgan J, Asmal M, Luban J (2000) Isolation, characterization and targeted disruption of mouse ppia: cyclophilin A is not essential for mammalian cell viability. Genomics, 68(2):167-78.

Colgan J, Asmal M, Neagu M, Yu B, et al. (2004) Cyclophilin A regulates TCR signal strength in CD4+ T cells via a proline-directed conformational switch in Itk. Immunity, 21(2):189-201.

Collard JF, Côté F, Julien JP. (1995) Defective axonal transport in a transgenic mouse model of amyotrophic lateral sclerosis. Nature. 375(6526):61-4.

Colombrita C, Zennaro E, Fallini C, Weber M, et al. (2009) TDP-43 is recruited to stress granules in conditions of oxidative insult. J Neurochem. 111(4):1051-61.

Conforti FL, Sprovieri T, Mazzei R, Ungaro C, et al. (2008) A novel Angiogenin gene mutation in a sporadic patient with amyotrophic lateral sclerosis from southern Italy. Neuromuscul Disord. 18(1):68-70.

Coppedè F, Lo Gerfo A, Carlesi C, Piazza S, et al. (2010) Lack of association between the APEX1 Asp148Glu polymorphism and sporadic amyotrophic lateral sclerosis. Neurobiol Aging. 31(2):353-5.

Coppinger JA, Cagney G, Toomey S, Kislinger T, et al. (2004) Characterization of the proteins released from activated platelets leads to localization of novel platelet proteins in human atherosclerotic lesions. Blood. 103(6):2096-104.

Corbo M, Hays AP. (1992) Peripherin and neurofilament protein coexist in spinal spheroids of motor neuron disease. J Neuropathol Exp Neurol. 51(5):531-7.

Corcia P, Camu W, Halimi JM, Vourc'h P, et al.; French ALS Study Group. (2006) SMN1 gene, but not SMN2, is a risk factor for sporadic ALS. Neurology. 67(7):1147-50.

Corcia P, Khoris J, Couratier P, Mayeux-Portas V, et al. (2002) SMN1 gene study in three families in which ALS and spinal muscular atrophy co-exist. Neurology. 59(9):1464-6.

Corcia P, Mayeux-Portas V, Khoris J, de Toffol B, et al.; French ALS Research Group. (2002) Amyotrophic Lateral Sclerosis. Abnormal SMN1 gene copy number is a susceptibility factor for amyotrophic lateral sclerosis. Ann Neurol. 51(2):243-6.

Costes SV, Daelemans D, Cho EH, Dobbin Z, et al. (2004) Automatic and quantitative measurement of protein-protein colocalization in live cells. Biophys J, 86(6):3993-4003.

Côté F, Collard JF, Julien JP. (1993) Progressive neuronopathy in transgenic mice expressing the human neurofilament heavy gene: a mouse model of amyotrophic lateral sclerosis. Cell. 9;73(1):35-46.

Couthouis J, Hart MP, Erion R, King OD, et al. (2012) Evaluating the role of the FUS/TLS-related gene EWSR1 in amyotrophic lateral sclerosis. Hum Mol Genet. 21(13):2899-911.

Couthouis J, Hart MP, Shorter J, DeJesus-Hernandez M, et al. (2011) A yeast functional screen predicts new candidate ALS disease genes. Proc Natl Acad Sci U S A. 108(52):20881-90.

Cox LE, Ferraiuolo L, Goodall EF, Heath PR, et al. (2010) Mutations in CHMP2B in lower motor neuron predominant amyotrophic lateral sclerosis (ALS). PLoS One. 5(3):e9872.

Creighton TE, Darby NJ, Kemmink J. (1996) The roles of partly folded intermediates in protein folding. FASEB J. 10(1):110-8.

Crenshaw DG, Yang J, Means AR and Kornbluth S. (1998) The mitotic peptidyl±prolyl isomerase, Pin1, interacts with Cdc25 and Plx1. EMBO J, 17:1315-27.

Cronin S, Berger S, Ding J, Schymick JC, et al. (2008) A genome-wide association study of sporadic ALS in a homogenous Irish population. Hum Mol Genet. 17(5):768-74.

Cronin S, Greenway MJ, Ennis S, Kieran D, et al. (2006) Elevated serum angiogenin levels in ALS. Neurology.67(10):1833-6.

Cronin S, Greenway MJ, Prehn JH, Hardiman O. (2007) Paraoxonase promoter and intronic variants modify risk of sporadic amyotrophic lateral sclerosis. J Neurol Neurosurg Psychiatry. 78(9):984-6.

Cronin S, Hardiman O, Traynor BJ (2007) Ethnic variation in the incidence of ALS: a systematic review. Neurology. 68(13):1002-7.

Cruveilhier J. (1853) Sur le paralysie musculaire, progressive, atrophique. Bull Acad Med, 18:490-501. 546–583

Cushman M, Johnson BS, King OD, Gitler AD, Shorter J. (2010) Prion-like disorders: blurring the divide between transmissibility and infectivity. J Cell Sci. 123(Pt 8):1191-201.

Da Cruz S, Cleveland DW. (2011) Understanding the role of TDP-43 and FUS/TLS in ALS and beyond. Curr Opin Neurobiol. 21(6):904-19.

Dai RM, Li CC. (2001) Valosin-containing protein is a multi-ubiquitin chain-targeting factor required in ubiquitin-proteasome degradation. Nat Cell Biol. 3(8):740-4.

Damiano M, Starkov AA, Petri S, Kipiani K, et al. (2006) Neural mitochondrial Ca2+ capacity impairment precedes the onset of motor symptoms in G93A Cu/Zn-superoxide dismutase mutant mice. J Neurochem. 96(5):1349-61.

Daoud H, Belzil V, Martins S, Sabbagh M, et al. (2011) Association of long ATXN2 CAG repeat sizes with increased risk of amyotrophic lateral sclerosis. Arch Neurol. 68(6):739-42.

Daoud H, Valdmanis PN, Dion PA, Rouleau GA. (2010) Analysis of DPP6 and FGGY as candidate genes for amyotrophic lateral sclerosis. Amyotroph Lateral Scler. 11(4):389-91.

Daoud H, Valdmanis PN, Kabashi E, Dion P, et al. (2009) Contribution of TARDBP mutations to sporadic amyotrophic lateral sclerosis. J Med Genet. 46(2):112-4.

Daugas E, Susin SA, Zamzami N, Ferri KF, et al. (2000) Mitochondrio-nuclear translocation of AIF in apoptosis and necrosis. FASEB J. 14(5):729-39.

Daum S, Schumann M, Mathea S, Aumüller T, et al. (2009) Isoform-specific inhibition of cyclophilins. Biochemistry. 48(26):6268-77.

Davidson YS, Robinson AC, Hu Q, Mishra M, et al. (2012) Nuclear Carrier and RNA Binding Proteins in Frontotemporal Lobar Degeneration associated with Fused in Sarcoma (FUS) pathological changes. Neuropathol Appl Neurobiol.

De Carvalho M, Matias T, Coelho F, Evangelista T, et al. (1996) Motor neuron disease presenting with respiratory failure. J Neurol Sci, 139(Suppl):117-122.

De Felice B, Guida M, Guida M, Coppola C, et al. (2012) A miRNA signature in leukocytes from sporadic amyotrophic lateral sclerosis. Gene. 508(1):35-40.

De Marco G, Lupino E, Calvo A, Moglia C, et al. (2011) Cytoplasmic accumulation of TDP-43 in circulating lymphomonocytes of ALS patients with and without TARDBP mutations. Acta Neuropathol.121(5):611-22.

De Vos KJ, Chapman AL, Tennant ME, Manser C, et al. (2007) Familial amyotrophic lateral sclerosis-linked SOD1 mutants perturb fast axonal transport to reduce axonal mitochondria content. Hum Mol Genet. 16(22):2720-8.

De Vos KJ, Grierson AJ, Ackerley S, Miller CC. (2008) Role of axonal transport in neurodegenerative diseases. Annu Rev Neurosci. 31:151-73.

Dean RT, Fu S, Stocker R, Davies MJ (1997) Biochemistry and pathology of radical-mediated protein oxidation. Biochem J. 324 (Pt 1):1-18.

DeJesus-Hernandez M, Desaro P, Johnston A, Ross OA, et al. (2011) Novel p.Ile151Val mutation in VCP in a patient of African American descent with sporadic ALS. Neurology. 77(11):1102-3.

DeJesus-Hernandez M, Mackenzie IR, Boeve BF, Boxer AL, et al. (2011) Expanded GGGGCC hexanucleotide repeat in noncoding region of C9ORF72 causes chromosome 9p-linked FTD and ALS. Neuron. 72(2):245-56.

Deng HX, Chen W, Hong ST, Boycott KM, et al. (2011) Mutations in UBQLN2 cause dominant X-linked juvenile and adult-onset ALS and ALS/dementia. Nature. 477(7363):211-5.

Deng HX, Hentati A, Tainer JA, Iqbal Z, et al. (1993) Amyotrophic lateral sclerosis and structural defects in Cu,Zn superoxide dismutase. Science. 261(5124):1047-51.

Deng HX, Shi Y, Furukawa Y, Zhai H, et al. (2006) Conversion to the amyotrophic lateral sclerosis phenotype is associated with intermolecular linked insoluble aggregates of SOD1 in mitochondria. Proc Natl Acad Sci U S A. 103(18):7142-7.

Deng HX, Zhai H, Bigio EH, Yan J, et al. (2010) FUS-immunoreactive inclusions are a common feature in sporadic and non-SOD1 familial amyotrophic lateral sclerosis. Ann Neurol. 67(6):739-48.

Derakhshan B, Hao G, Gross SS. (2007) Balancing reactivity against selectivity: the evolution of protein S-nitrosylation as an effector of cell signaling by nitric oxide. Cardiovasc Res. 75(2):210-9.

Devon RS, Helm JR, Rouleau GA, Leitner Y, et al. (2003) The first nonsense mutation in alsin results in a homogeneous phenotype of infantile-onset ascending spastic paralysis with bulbar involvement in two siblings. Clin Genet. 64(3):210-5.

Dhaliwal GK, Grewal RP. (2000) Mitochondrial DNA deletion mutation levels are elevated in ALS brains. Neuroreport. 11(11):2507-9.

Diekstra FP, van Vught PW, van Rheenen W, Koppers M, et al. (2012) UNC13A is a modifier of survival in amyotrophic lateral sclerosis. Neurobiol Aging. 33(3):630.e3-8.

DiNovo AA, Schey KL, Vachon WS, McGuffie EM, et al. (2006) ADP-ribosylation of cyclophilin A by Pseudomonas aeruginosa exoenzyme S. Biochemistry. 45(14):4664-73.

Doi H, Koyano S, Suzuki Y, Nukina N, Kuroiwa Y. (2010) The RNA-binding protein FUS/TLS is a common aggregate-interacting protein in polyglutamine diseases. Neurosci Res. 66(1):131-3.

Dolinski K, Muir S, Cardenas M and Heitman J. (1997) All cyclophilins and FK506 binding proteins are, individually and collectively, dispensable for viability in Saccharomyces cerevisiae. Proc. Natl Acad. Sci. USA, 94:13093-8.

Dompierre JP, Godin JD, Charrin BC, Cordelières FP, et al. (2007) Histone deacetylase 6 inhibition compensates for the transport deficit in Huntington's disease by increasing tubulin acetylation. J Neurosci. 27(13):3571-83.

Dormann D, Capell A, Carlson AM, Shankaran SS, et al. (2009) Proteolytic processing of TAR DNA binding protein-43 by caspases produces C-terminal fragments with disease defining properties independent of progranulin. J Neurochem. 110(3):1082-94.

Dormann D, Haass C. (2011) TDP-43 and FUS: a nuclear affair. Trends Neurosci.

Dormann D, Rodde R, Edbauer D, Bentmann E, Fischer I, et al. (2010) ALS-associated fused in sarcoma (FUS) mutations disrupt Transportin-mediated nuclear import. EMBO J. 29(16):2841-57.

Doyle V, Virji S, Crompton M. (1999) Evidence that cyclophilin-A protects cells against oxidative stress. Biochem. J. 341: 127–132.

Drachman DB, Rothstein JD. (2000) Inhibition of cyclooxygenase-2 protects motor neurons in an organotypic model of amyotrophic lateral sclerosis. Ann Neurol. 48(5):792-5.

Dreyfuss G, Kim VN, Kataoka N (2002) Messenger-RNA-binding proteins and the messages they carry. Nat Rev Mol Cell Biol, 3(3):195-205.

Duan W, Li X, Shi J, Guo Y, et al. (2010) Mutant TAR DNA-binding protein-43 induces oxidative injury in motor neuron-like cell. Neuroscience. 169(4):1621-9.

Duchenne de Boulogne GB (1851) Recherches électro-physiologiques et thérapeutiques. Comp Rend Seances Acad Sci, 32:506.

Duffy LM, Chapman AL, Shaw PJ, Grierson AJ. (2011) Review: The role of mitochondria in the pathogenesis of amyotrophic lateral sclerosis. Neuropathol Appl Neurobiol. 37(4):336-52.

Durham HD, Roy J, Dong L, Figlewicz DA. (1997) Aggregation of mutant Cu/Zn superoxide dismutase proteins in a culture model of ALS. J Neuropathol Exp Neurol. 56(5):523-30.

Dyck PJ, Stevens JC, Mulder DW, Espinosa RE. (1975) Frequency of nerve fiber degeneration of peripheral motor and sensory neurons in amyotrophic lateral sclerosis. Morphometry of deep and superficial peroneal nerves. Neurology, 25:781-785.

d'Ydewalle C, Bogaert E, Van Den Bosch L. (2012) HDAC6 at the Intersection of Neuroprotection and Neurodegeneration. Traffic. 13(6):771-9.

Ebneth A, Godemann R, Stamer K, Illenberger S, et al. (1998) Overexpression of tau protein inhibits kinesin-dependent trafficking of vesicles, mitochondria, and endoplasmic reticulum: implications for Alzheimer's disease. J Cell Biol. 143(3):777-94.

Elamin M, Phukan J, Bede P, Jordan N, et al. Executive dysfunction is a negative prognostic indicator in patients with ALS without dementia. Neurology. 2011 Apr 5;76(14):1263-9.

Elbaz B, Valitsky M, Davidov G, Rahamimoff H. (2010) Cyclophilin A is involved in functional expression of the Na(+)-Ca(2+) exchanger NCX1. Biochemistry. 49(35):7634-42.

Elden AC, Kim HJ, Hart MP, Chen-Plotkin AS, et al. (2010) Ataxin-2 intermediate-length polyglutamine expansions are associated with increased risk for ALS. Nature. 466(7310):1069-75.

Elliott JL, Snider WD. (1996) Motor neuron growth factors. Neurology. 47(4 Suppl 2):S47-53.

Elvira G, Wasiak S, Blandford V, Tong XK, et al. (2006) Characterization of an RNA granule from developing brain. Mol Cell Proteomics. Apr;5(4):635-51.

Emmel EA, Verweij CL, Durand DB, Higgins KM, et al. (1989) Cyclosporin A specifically inhibits function of nuclear proteins involved in T cell activation. Science. 246(4937):1617-20.

Endrich MM, Gehring H. (1998) The V3 loop of human immunodeficiency virus type-1 envelope protein is a high-affinity ligand for immunophilins present in human blood. Eur J Biochem. 252(3):441-6.

Estes PS, Boehringer A, Zwick R, Tang JE, et al. (2011) Wild-type and A315T mutant TDP-43 exert differential neurotoxicity in a Drosophila model of ALS. Hum Mol Genet. 20(12):2308-21. Epub 2011 Mar 26.

Estévez AG, Crow JP, Sampson JB, Reiter C, et al. (1999) Induction of nitric oxide-dependent apoptosis in motor neurons by zinc-deficient superoxide dismutase. Science, 286 (5449):2498-500.

Etzkorn FA, Chang ZY, Stolz LA, Walsh CT. (1994) Cyclophilin residues that affect noncompetitive inhibition of the protein serine phosphatase activity of calcineurin by the cyclophilin.cyclosporin A complex. Biochemistry, 33(9):2380-8.

Eymard-Pierre E, Lesca G, Dollet S, Santorelli FM, et al. (2002) Infantile-onset ascending hereditary spastic paralysis is associated with mutations in the alsin gene. Am J Hum Genet. 71(3):518-27.

Fallini C, Bassell GJ, Rossoll W. (2012) The ALS disease protein TDP-43 is actively transported in motor neuron axons and regulates axon outgrowth. Hum Mol Genet.

Fang L, Huber-Abel F, Teuchert M, Hendrich C, et al. (2009) Linking neuron and skin: matrix metalloproteinases in amyotrophic lateral sclerosis (ALS). J Neurol Sci. 285(1-2):62-6.

Fang L, Teuchert M, Huber-Abel F, Schattauer D, et al. (2010) MMP-2 and MMP-9 are elevated in spinal cord and skin in a mouse model of ALS. J Neurol Sci. 294(1-2):51-6.

Farrer MJ, Hulihan MM, Kachergus JM, Dächsel JC, et al. (2009) DCTN1 mutations in Perry syndrome. Nat Genet. 41(2):163-5.

Fauré J, Lachenal G, Court M, Hirrlinger J, et al. (2006) Exosomes are released by cultured cortical neurones. Mol Cell Neurosci. 31(4):642-8.

Fecto F, Yan J, Vemula SP, Liu E, et al. (2011) SQSTM1 mutations in familial and sporadic amyotrophic lateral sclerosis. Arch Neurol.68(11):1440-6.

Feiguin F, Godena VK, Romano G, D'Ambrogio A, et al. (2009) Depletion of TDP-43 affects Drosophila motoneurons terminal synapsis and locomotive behavior. FEBS Lett. 583(10):1586-92.

Fernández-Santiago R, Hoenig S, Lichtner P, Sperfeld AD, et al. (2009) Identification of novel Angiogenin (ANG) gene missense variants in German patients with amyotrophic lateral sclerosis. J Neurol. 256(8):1337-42.

Ferrante RJ, Browne SE, Shinobu LA, Bowling AC, et al. (1997) Evidence of increased oxidative damage in both sporadic and familial amyotrophic lateral sclerosis. J Neurochem. 69(5):2064-74.

Ferrante RJ, Shinobu LA, Schulz JB, Matthews RT, et al. (1997) Increased 3-nitrotyrosine and oxidative damage in mice with a human copper/zinc superoxide dismutase mutation. Ann Neurol, 42 (3):326-34.

Ferreira PA, Nakayama TA, Pak WL, Travis GH. (1996) Cyclophilin-related protein RanBP2 acts as chaperone for red/green opsin. Nature, 383:637-40.

Ferri A, Cozzolino M, Crosio C, Nencini M, et al. (2006) Familial ALS-superoxide dismutases associate with mitochondria and shift their redox potentials. Proc Natl Acad Sci U S A. 103(37):13860-5.

Ferri A, Nencini M, Casciati A, Cozzolino M, et al. (2004) Cell death in amyotrophic lateral sclerosis: interplay between neuronal and glial cells. Faseb J 18:1261-1263.

Fiesel FC, Kahle PJ. (2011) TDP-43 and FUS/TLS: cellular functions and implications for neurodegeneration. FEBS Journal, 278:3550-68.

Fiesel FC, Schurr C, Weber SS, Kahle PJ. (2011) TDP-43 knockdown impairs neurite outgrowth dependent on its target histone deacetylase 6. Mol Neurodegener. 6:64.

Fiesel FC, Voigt A, Weber SS, Van den Haute C, et al. (2010) Knockdown of transactive response DNA-binding protein (TDP-43) downregulates histone deacetylase 6. EMBO J. 29(1):209-21.

Figlewicz DA, Krizus A, Martinoli MG, Meininger V, et al. (1994) Variants of the heavy neurofilament subunit are associated with the development of amyotrophic lateral sclerosis. Hum Mol Genet. 3(10):1757-61.

Fischer G (1994) Peptydil-prolyl *cis/trans* isomerases and their effectors. Angew Chem Int Ed, 33:1415-36.

Fischer G, Bang H, Mech C. (1984) Determination of enzymatic catalysis for the cis-trans-isomerization of peptide binding in proline-containing peptides. *Biomed Biochim Acta.* 43(10):1101-11.

Fischer G, Liebold BW, Lang K, Kiefhaber T, Schmid FX (1989) Cyclophilin and peptidyl-prolyl *cistrans* isomerase are probably identical proteins. Nature, 337:476-8.

Fischer LR, Culver DG, Tennant P, Davis AA, et al. (2004) Amyotrophic lateral sclerosis is a distal axonopathy: evidence in mice and man. Exp Neurol. 185(2):232-40.

Fitzmaurice PS, Shaw IC, Kleiner HE, Miller RT, et al. (1996) Evidence for DNA damage in amyotrophic lateral sclerosis. Muscle Nerve. 19(6):797-8

Flanagan WM, Corthésy B, Bram RJ, Crabtree GR. (1991) Nuclear association of a T-cell transcription factor blocked by FK-506 and cyclosporin A. Nature. 352(6338):803-7.

Fogh I, D'Alfonso S, Gellera C, Ratti A, et al. (2011) No association of DPP6 with amyotrophic lateral sclerosis in an Italian population. Neurobiol Aging. 32(5):966-7.

Foran E, Trotti D. (2009) Glutamate transporters and the excitotoxic path to motor neuron degeneration in amyotrophic lateral sclerosis. Antioxid Redox Signal. 11(7):1587-602.

Foster TL, Gallay P, Stonehouse NJ, Harris M. (2011) Cyclophilin A interacts with domain II of hepatitis C virus NS5A and stimulates RNA binding in an isomerase-dependent manner. J Virol.85(14):7460-4.

Foulds P, McAuley E, Gibbons L, Davidson Y, et al. (2008) TDP-43 protein in plasma may index TDP-43 brain pathology in Alzheimer's disease and frontotemporal lobar degeneration. Acta Neuropathol. 116(2):141-6.

Frantz B, Nordby EC, Bren G, Steffan N, et al. (1994) Calcineurin acts in synergy with PMA to inactivate I kappa B/MAD3, an inhibitor of NF-kappa B. EMBO J. 13(4):861-70.

Fratelli M, Demol H, Puype M, Casagrande S, et al. (2002) Identification by redox proteomics of glutathionylated proteins in oxidatively stressed human T lymphocytes. Proc Natl Acad Sci U S A.99(6):3505-10.

Fratelli M, Demol H, Puype M, Casagrande S, et al. (2003) Identification of proteins undergoing glutathionylation in oxidatively stressed hepatocytes and hepatoma cells. Proteomics. 3(7):1154-61.

Freibaum BD, Chitta RK, High AA, Taylor JP. (2010) Global analysis of TDP-43 interacting proteins reveals strong association with RNA splicing and translation machinery. J Proteome Res. 9(2):1104-20.

Freskgård PO, Bergenhem N, Jonsson BH, Svensson M, Carlsson U. (1992) Isomerase and chaperone activity of prolyl isomerase in the folding of carbonic anhydrase. Science. 258(5081):466-8.

Fruman DA, Mather PE, Burakoff SJ, Bierer BE. (1992) Correlation of calcineurin phosphatase activity and programmed cell death in murine T cell hybridomas. Eur J Immunol. 22(10):2513-7.

Fujii R, Okabe S, Urushido T, Inoue K, et al. (2005) The RNA binding protein TLS is translocated to dendritic spines by mGluR5 activation and regulates spine morphology. Curr Biol. 15(6):587-93.

Fujii R, Takumi T. (2005a) TLS facilitates transport of mRNA encoding an actin-stabilizing protein to dendritic spines. J Cell Sci. 118(Pt 24):5755-65.

Fujita Y, Okamoto K (2005) Golgi apparatus of the motor neurons in patients with amyotrophic lateral sclerosis and in mice models of amyotrophic lateral sclerosis. Neuropathology. 25(4):388-94.

Fujiyama S, Yanagida M, Hayano T, Miura Y, et al. (2002) Isolation and proteomic characterization of human Parvulin-associating preribosomal ribonucleoprotein complexes. J Biol Chem, 277:23773-80.

Funke AD, Esser M, Krüttgen A, Weis J, et al. (2010) The p.P56S mutation in the VAPB gene is not due to a single founder: the first European case. Clin Genet. 77(3):302-3.

Gaido ML, Cidlowski JA. (1991) Identification, purification, and characterization of a calcium-dependent endonuclease (NUC18) from apoptotic rat thymocytes. NUC18 is not histone H2B. J Biol Chem. 266(28):18580-5.

Gal J, Ström AL, Kilty R, Zhang F, Zhu H. (2007) p62 accumulates and enhances aggregate formation in model systems of familial amyotrophic lateral sclerosis. J Biol Chem. 282(15):11068-77.

Galat A. (2003) Peptidylprolyl *cis/trans* isomerases (immunophilins): biological diversity-targets-functions. Curr Top Med Chem, 3:1315-47.

Galat A, Metcalfe SM (1995) Peptydilprolyl *cis/trans* isomerases. Prog Biophys Mol Biol, 63:67-118.

Galigniana MD, Harrell JM, O'Hagen HM, Ljungman M, Pratt WB. (2004b) Hsp90-binding immunophilins link p53 to dynein during p53 transport to the nucleus. J Biol Chem. 279(21):22483-9.

Galigniana MD, Morishima Y, Gallay PA, Pratt WB. (2004a) Cyclophilin-A is bound through its peptidylprolyl isomerase domain to the cytoplasmic dynein motor protein complex. J Biol Chem. 279(53):55754-9.

Gamble TR, Vajdos FF, Yoo S, Worthylake DK, et al. (1996) Crystal structure of human cyclophilin A bound to the amino-terminal domain of HIV-1 capsid. Cell. 87(7):1285-94.

Gellera C, Colombrita C, Ticozzi N, Castellotti B, et al. (2008) Identification of new ANG gene mutations in a large cohort of Italian patients with amyotrophic lateral sclerosis. Neurogenetics. 9(1):33-40.

Geser F, Martinez-Lage M, Robinson J, Uryu K, et al. (2009a) Clinical and pathological continuum of multisystem TDP-43 proteinopathies. Arch Neurol, 66(2):180-9.

Geser F, Martinez-Lage M, Kwong LK, Lee VM, Trojanowski JQ. (2009b) Amyotrophic lateral sclerosis, frontotemporal dementia and beyond: the TDP-43 diseases. J Neurol, 256(8):1205-14.

Gevaert K, Staes A, Van Damme J, De Groot S, et al. (2005) Global phosphoproteome analysis on human HepG2 hepatocytes using reversed-phase diagonal LC. Proteomics. Sep;5(14):3589-99.

Ghezzi P, Casagrande S, Massignan T, Basso M, et al. (2006) Redox regulation of cyclophilin A by glutathionylation. Proteomics, 6(3):817-25.

Gijselinck I, Van Langenhove T, van der Zee J, Sleegers K, et al. (2012) A C9orf72 promoter repeat expansion in a Flanders-Belgian cohort with disorders of the frontotemporal lobar degeneration-amyotrophic lateral sclerosis spectrum: a gene identification study. Lancet Neurol. 11(1):54-65.

Gingras M, Gagnon V, Minotti S, Durham HD, Berthod F. (2007) Optimized protocols for isolation of primary motor neurons, astrocytes and microglia from embryonic mouse spinal cord. J Neurosci Methods. 163(1):111-8.

Gispert S, Kurz A, Waibel S, Bauer P, et al. (2012) The modulation of Amyotrophic Lateral Sclerosis risk by ataxin-2 intermediate polyglutamine expansions is a specific effect. Neurobiol Dis. 45(1):356-61.

Gitcho MA, Baloh RH, Chakraverty S, Mayo K, et al. (2008) TDP-43 A315T mutation in familial motor neuron disease. Ann Neurol. 63(4):535-8.

Goetz CG. (2000) Amyotrophic lateral sclerosis: Early contributions of Jean-Martin Charcot. Muscle & Nerve, 23:336-343.

Göldner FM, Patrick JW. (1996) Neuronal localization of the cyclophilin A protein in the adult rat brain. J Comp Neurol. 372(2):283-93.

Gomes C, Palma AS, Almeida R, Regalla M, et al. (2008) Establishment of a cell model of ALS disease: Golgi apparatus disruption occurs independently from apoptosis. Biotechnol Lett. 30(4):603-10.

Gong YH, Parsadanian AS, Andreeva A, Snider WD, Elliott JL. (2000) Restricted expression of G86R Cu/Zn superoxide dismutase in astrocytes results in astrocytosis but does not cause motoneuron degeneration. J Neurosci. 20(2):660-5.

Goodall EF, Greenway MJ, van Marion I, Carroll CB, et al. (2005) Association of the H63D polymorphism in the hemochromatosis gene with sporadic ALS. Neurology. 65(6):934-7.

Göthel SF, Marahiel MA. (1999) Peptidyl-prolyl cis-trans isomerases, a superfamily of ubiquitous folding catalysts. Cell Mol Life Sci. 55(3):423-36.

Graham FL, Smiley J, Russell WC, Nairn R. (1977) Characteristics of a human cell line transformed by DNA from human adenovirus type 5. J Gen Virol. 36(1):59-74.

Greenway MJ, Alexander MD, Ennis S, Traynor BJ, et al. (2004) A novel candidate region for ALS on chromosome 14q11.2. Neurology. 63(10):1936-8.

Greenway MJ, Andersen PM, Russ C, Ennis S, et al. (2006) ANG mutations segregate with familial and 'sporadic' amyotrophic lateral sclerosis. Nat Genet.38(4):411-3.

Gros-Louis F, Larivière R, Gowing G, Laurent S, et al. (2004) A frameshift deletion in peripherin gene associated with amyotrophic lateral sclerosis. J Biol Chem. 279(44):45951-6.

Gros-Louis F, Laurent S, Lopes AA, Khoris J, et al. (2003) Absence of mutations in the hypoxia response element of VEGF in ALS. Muscle Nerve. 28(6):774-5

Grosskreutz J, Van Den Bosch L, Keller BU. (2010) Calcium dysregulation in amyotrophic lateral sclerosis. Cell Calcium. 47(2):165-74.

Grundström E, Lindholm D, Johansson A, Blennow K, Askmark H. (2000) GDNF but not BDNF is increased in cerebrospinal fluid in amyotrophic lateral sclerosis. Neuroreport. 11(8):1781-3.

Gu W, Roeder RG. (1997) Activation of p53 sequence-specific DNA binding by acetylation of the p53 C-terminal domain. Cell. 90(4):595-606.

Gunnarsson LG, Dahlbom K, Strandman E. (1991) Motor neuron disease and dementia reported among 13 members of a single family. Acta Neurol Scand. 84(5):429-33.

Guo W, Chen Y, Zhou X, Kar A, et al. (2011) An ALS-associated mutation affecting TDP-43 enhances protein aggregation, fibril formation and neurotoxicity. Nat Struct Mol Biol. 18(7):822-30.

Gurney ME, Pu H, Chiu AY, Dal Canto MC, et al. (1994) Motor neuron degeneration in mice that express a human Cu,Zn superoxide dismutase mutation. Science. 264(5166):1772-5.

Gydesen S, Brown JM, Brun A, Chakrabarti L, et al. (2002) Chromosome 3 linked frontotemporal dementia (FTD-3). Neurology. 59(10):1585-94.

Ha K, Takeda Y, Dynan WS. (2011) Sequences in PSF/SFPQ mediate radioresistance and recruitment of PSF/SFPQ-containing complexes to DNA damage sites in human cells. DNA Repair (Amst). 10(3):252-9.

Hadano S, Benn SC, Kakuta S, Otomo A, et al. (2006) Mice deficient in the Rab5 guanine nucleotide exchange factor ALS2/alsin exhibit age-dependent neurological deficits and altered endosome trafficking. Hum Mol Genet. 15(2):233-50.

Hadano S, Hand CK, Osuga H, Yanagisawa Y, et al. (2001) A gene encoding a putative GTPase regulator is mutated in familial amyotrophic lateral sclerosis 2. Nat Genet. 29(2):166-73.

Hafezparast M, Ahmad-Annuar A, Hummerich H, Shah P, et al. (2003) Paradigms for the identification of new genes in motor neuron degeneration. Amyotroph Lateral Scler Other Motor Neuron Disord. 4(4):249-57.

Haidet-Phillips AM, Hester ME, Miranda CJ, Meyer K, et al. (2011) Astrocytes from familial and sporadic ALS patients are toxic to motor neurons. Nat Biotechnol. 29(9):824-8.

Halawani D, Latterich M. (2006) p97: The cell's molecular purgatory? Mol Cell. 22(6):713-7.

Hall ED, Oostveen JA, Gurney ME. (1998) Relationship of microglial and astrocytic activation to disease onset and progression in a transgenic model of familial ALS. Glia. 23(3):249-56.

Hand CK, Khoris J, Salachas F, Gros-Louis F, et al. (2002) A novel locus for familial amyotrophic lateral sclerosis, on chromosome 18q. Am J Hum Genet. 70(1):251-6.

Handschumacher RE, Harding MW, Rice J, Drugge RJ, Speicher DW. (1984) Cyclophilin: a specific cytosolic binding protein for cyclosporin A. Science, 226:544-7.

Hanson KA, Kim SH, Wassarman DA, Tibbetts RS. (2010) Ubiquilin modifies TDP-43 toxicity in a Drosophila model of amyotrophic lateral sclerosis (ALS). J Biol Chem. 285(15):11068-72.

Harraz MM, Marden JJ, Zhou W, Zhang Y, et al. (2008) SOD1 mutations disrupt redox-sensitive Rac regulation of NADPH oxidase in a familial ALS model. J Clin Invest. 118(2):659-70.

Harris D, Zhang Z, Chaubey B, Pandey VN. (2006) Identification of cellular factors associated with the 3'-nontranslated region of the hepatitis C virus genome. Mol Cell Proteomics. 5(6):1006-18.

Hasegawa M, Arai T, Nonaka T, Kametani F, et al. (2008) Phosphorylated TDP-43 in frontotemporal lobar degeneration and amyotrophic lateral sclerosis. Ann Neurol. 64(1):60-70.

Hasková V, Rozprimová L, Hasek J, Jelínková M. (1994) Immunolocalization of cyclophilin in normal and cyclosporin A-treated human lymphocytes. Immunol Lett. 41(2-3):267-72.

Hayashi H, Kato S (1989) Total manifestations of amyotrophic lateral sclerosis: ALS in the totally locked-in state. Journal of the Neurological Sciences, 93:19-35.

Hayward C, Colville S, Swingler RJ, Brock DJ. (1999) Molecular genetic analysis of the APEX nuclease gene in amyotrophic lateral sclerosis. Neurology. 52(9):1899-901.

He CZ, Hays AP. (2004) Expression of peripherin in ubiquinated inclusions of amyotrophic lateral sclerosis. J Neurol Sci. 217(1):47-54.

Heiman-Patterson TD, Deitch JS, Blankenhorn EP, Erwin KL, et al. (2005) Background and gender effects on survival in the TgN(SOD1-G93A)1Gur mouse model of ALS. J Neurol Sci 236:1-7.

Helekar SA, Char D, Neff S, Patrick J. (1994) Prolyl isomerase requirement for the expression of functional homo-oligomeric ligand-gated ion channels. Neuron. 12(1):179-89.

Helekar SA, Patrick J. (1997) Peptidyl prolyl cis-trans isomerase activity of cyclophilin A in functional homo-oligomeric receptor expression. Proc Natl Acad Sci U S A. 94(10):5432-7.

Henkel JS, Engelhardt JI, Siklós L, Simpson EP, et al. (2004) Presence of dendritic cells, MCP-1, and activated microglia/macrophages in amyotrophic lateral sclerosis spinal cord tissue. Ann Neurol. 55(2):221-35.

Hervias I, Beal MF, Manfredi G. (2006) Mitochondrial dysfunction and amyotrophic lateral sclerosis. Muscle Nerve. 33(5):598-608.

Higgins CM, Jung C, Ding H, Xu Z. (2002) Mutant Cu, Zn superoxide dismutase that causes motoneuron degeneration is present in mitochondria in the CNS. J Neurosci. 22(6):RC215.

Higgins CM, Jung C, Xu Z. (2003) ALS-associated mutant SOD1G93A causes mitochondrial vacuolation by expansion of the intermembrane space and by involvement of SOD1 aggregation and peroxisomes. BMC Neurosci. 4:16.

Hirabayashi M, Inoue K, Tanaka K, Nakadate K, et al. (2001) VCP/p97 in abnormal protein aggregates, cytoplasmic vacuoles, and cell death, phenotypes relevant to neurodegeneration. Cell Death Differ. 8(10):977-84.

Hirano A, Donnenfeld H, Sasaki S, Nakano I. (1984) Fine structural observations of neurofilamentous changes in amyotrophic lateral sclerosis. J Neuropathol Exp Neurol. 43(5):461-70.

Hirano A, Nakano I, Kurland LT, Mulder DW, et al. (1984) Fine structural study of neurofibrillary changes in a family with amyotrophic lateral sclerosis. J Neuropathol Exp Neurol. 43(5):471-80.

Hirano M, Quinzii CM, Mitsumoto H, Hays AP, et al. (2011) Senataxin mutations and amyotrophic lateral sclerosis. Amyotroph Lateral Scler. 12(3):223-7.

Ho S, Clipstone N, Timmermann L, Northrop J, et al. (1996) The mechanism of action of cyclosporine A and FK506. Clinical Immunology and Immunopathology, 80:S40–5.

Hong F, Lee J, Piao YJ, Jae YK, et al. (2004) Transgenic mice overexpressing cyclophilin A are resistant to cyclosporin A-induced nephrotoxicity via peptidyl-prolyl cis-trans isomerase activity. Biochem Biophys Res Commun. 316(4):1073-80.

Hong F, Lee J, Song JW, Lee SJ, et al. (2002) Cyclosporin A blocks muscle differentiation by inducing oxidative stress and inhibiting the peptidyl-prolyl-cis-trans isomerase activity of cyclophilin A: cyclophilin A protects myoblasts from cyclosporin A-induced cytotoxicity. FASEB J. 16(12):1633-5.

Honjo Y, Kaneko S, Ito H, Horibe T, et al. (2011) Protein disulfide isomerase-immunopositive inclusions in patients with amyotrophic lateral sclerosis. Amyotroph Lateral Scler. 12(6):444-50.

Hornbogen T, Pieper R, Hoffmann K, Kleinkauf H, Zocher R. (1992) Two new cyclophilins from Fusarium sambucinum and Aspergillus niger: resistance of cyclophilin/cyclosporin A complexes against proteolysis. Biochem Biophys Res Commun. 187(2):791-6.

Horner RD, Grambow SC, Coffman CJ, Lindquist JH, et al. (2008) Amyotrophic lateral sclerosis among 1991 Gulf War veterans: evidence for a time-limited outbreak. Neuroepidemiology. 31(1):28-32.

Horowitz DS, Lee EJ, Mabon SA, Misteli T. (2002) A cyclophilin functions in pre-mRNA splicing. EMBO J. 21(3):470-80.

Hortobágyi T, Troakes C, Nishimura AL, Vance C, et al. (2011) Optineurin inclusions occur in a minority of TDP-43 positive ALS and FTLD-TDP cases and are rarely observed in other neurodegenerative disorders. Acta Neuropathol. 121(4):519-27.

Hosback S, Hardiman O, Nolan CM, Doyle MA, et al. (2007) Circulating insulin-like growth factors and related binding proteins are selectively altered in amyotrophic lateral sclerosis and multiple sclerosis. Growth Horm IGF Res.17(6):472-9.

Hosler BA, Siddique T, Sapp PC, Sailor W, et al. (2000) Linkage of familial amyotrophic lateral sclerosis with frontotemporal dementia to chromosome 9q21-q22. JAMA. 284(13):1664-9.

Hovland AR, La Rosa FG, Hovland PG, Cole WC, et al. (1999) Cyclosporin A regulates the levels of cyclophilin A in neuroblastoma cells in culture. Neurochem Int.35(3):229-35.

Howard BR, Vajdos FF, Li S, Sundquist WI, Hill CP. (2003) Structural insights into the catalytic mechanism of cyclophilin A. Nat Struct Biol. 10(6):475-81.

Howland DS, Liu J, She Y, Goad B, et al. (2002) Focal loss of the glutamate transporter EAAT2 in a transgenic rat model of SOD1 mutant-mediated amyotrophic lateral sclerosis (ALS). Proc Natl Acad Sci U S A. 99(3):1604-9.

Hu BR, Martone ME, Jones YZ, Liu CL. (2000) Protein aggregation after transient cerebral ischemia. J Neurosci. 20(9):3191-9.

Huang CM, Ananthaswamy HN, Barnes S, Ma Y, et al. (2006) Mass spectrometric proteomics profiles of in vivo tumor secretomes: capillary ultrafiltration sampling of regressive tumor masses. Proteomics. 6(22):6107-16.

Huang Q, Figueiredo-Pereira ME. (2010) Ubiquitin/proteasome pathway impairment in neurodegeneration: therapeutic implications. Apoptosis. 15(11):1292-311.

Igaz LM, Kwong LK, Chen-Plotkin A, Winton MJ, et al. (2009) Expression of TDP-43 C-terminal Fragments in Vitro Recapitulates Pathological Features of TDP-43 Proteinopathies. J Biol Chem. 284(13):8516-24.

Igaz LM, Kwong LK, Lee EB, Chen-Plotkin A, et al. (2011) Dysregulation of the ALS-associated gene TDP-43 leads to neuronal death and degeneration in mice. J Clin Invest. 121(2):726-38.

Igaz LM, Kwong LK, Xu Y, Truax AC, et al. (2008) Enrichment of C-terminal fragments in TAR DNA-binding protein-43 cytoplasmic inclusions in brain but not in spinal cord of frontotemporal lobar degeneration and amyotrophic lateral sclerosis. Am J Pathol. 173(1):182-94.

Ihara Y, Nobukuni K, Takata H, Hayabara T. (2005) Oxidative stress and metal content in blood and cerebrospinal fluid of amyotrophic lateral sclerosis patients with and without a Cu, Zn-superoxide dismutase mutation. Neurol Res. 27(1):105-8.

Iłzecka J, Stelmasiak Z, Dobosz B. (2002) Transforming growth factor-Beta 1 (tgf-Beta 1) in patients with amyotrophic lateral sclerosis. Cytokine. 20(5):239-43.

Iłzecka J, Stelmasiak Z, Solski J, Wawrzycki S, Szpetnar M. (2003) Plasma amino acids percentages in amyotrophic lateral sclerosis patients.Neurol Sci. 24(4):293-5.

Iłzecka J. (2011) EMMPRIN levels in serum of patients with amyotrophic lateral sclerosis. Acta Neurol Scand. 124(6):424-8.

Ince PG (2000) Neuropathology. In Amyotrophic lateral sclerosis Edited by: Brown RJ, Meininger V, Swash M. London: Martin Dunitz;:83-112.

Ince PG, Evans J, Knopp M, Forster G, et al. (2003) Corticospinal tract degeneration in the progressive muscular atrophy variant of ALS. Neurology 60:1252-1258.

Ince PG, Lowe J, Shaw PJ (1998) Amyotrophic lateral sclerosis: current issues in classification, pathogenesis and molecular pathology. Neuropathol Appl Neurobiol. 24(2):104-17.

Ince PG, Wharton SB (2007) Cytopathology of the motor neuron. In Motor neurone disorders and related diseases Edited by: Eisen AA, Shaw PJ. Amsterdam: Elsevier;:89-110. [Aminoff MJ, Boller F, Swaab DF (Series Editor): Handbook of clinical neurology]

Inukai Y, Nonaka T, Arai T, Yoshida M, et al. (2008) Abnormal phosphorylation of Ser409/410 of TDP-43 in FTLD-U and ALS. FEBS Lett. 582(19):2899-904.

Ip P, Mulligan VK, Chakrabartty A. (2011) ALS-causing SOD1 mutations promote production of copper-deficient misfolded species. J Mol Biol. 409(5):839-52.

Ishigaki S, Hishikawa N, Niwa J, Iemura S, et al. (2004) Physical and functional interaction between Dorfin and Valosin-containing protein that are colocalized in ubiquitylated inclusions in neurodegenerative disorders. J Biol Chem. 279(49):51376-85.

Ito A, Kawaguchi Y, Lai CH, Kovacs JJ, et al. (2002) MDM2-HDAC1-mediated deacetylation of p53 is required for its degradation. EMBO J. 21(22):6236-45.

Iwata M, Hirano A (1978) Sparing of the Onufrowicz nucleus in sacral anterior horn lesions. Ann Neurol 4:245-249.

Jaarsma D, Haasdijk ED, Grashorn JA, Hawkins R, et al. (2000) Human Cu/Zn superoxide dismutase (SOD1) overexpression in mice causes mitochondrial vacuolization, axonal degeneration, and premature motoneuron death and accelerates motoneuron disease in mice expressing a familial amyotrophic lateral sclerosis mutant SOD1. Neurobiol Dis. 7(6 Pt B):623-43.

Jain J, McCaffrey PG, Miner Z, Kerppola TK, et al. (1993) The T-cell transcription factor NFATp is a substrate for calcineurin and interacts with Fos and Jun. Nature. 365(6444):352-5.

Janknecht R. (2005) EWS-ETS oncoproteins: the linchpins of Ewing tumors. Gene. 363:1-14.

Jäschke A, Mi H, Tropschug M. (1998) Human T cell cyclophilin18 binds to thiol-specific antioxidant protein Aop1 and stimulates its activity. J Mol Biol. 277(4):763-9.

Jellinger KA (2008) Neuropathological aspects of Alzheimer disease, Parkinson disease and frontotemporal dementia. Neurodegener Dis. 5(3-4):118-21.

Jesse S, Brettschneider J, Süssmuth SD, Landwehrmeyer BG, et al. (2011) Summary of cerebrospinal fluid routine parameters in neurodegenerative diseases. J Neurol. 258(6):1034-41.

Jin L, Harrison SC. (2002) Crystal structure of human calcineurin complexed with cyclosporin A and human cyclophilin. Proc Natl Acad Sci U S A. 99(21):13522-6.

Jin ZG, Lungu AO, Xie L, Wang M, Wong C, Berk BC. (2004) Cyclophilin A is a proinflammatory cytokine that activates endothelial cells. Arterioscler Thromb Vasc Biol. 24(7):1186-91.

Jin ZG, Melaragno MG, Liao DF, Yan C, Haendeler J, et al. (2000) Cyclophilin A is a secreted growth factor induced by oxidative stress. Circ Res. 87(9):789-96.

Johnson BS, McCaffery JM, Lindquist S, Gitler AD. (2008) A yeast TDP-43 proteinopathy model: Exploring the molecular determinants of TDP-43 aggregation and cellular toxicity. Proc Natl Acad Sci U S A. 105(17):6439-44. Epub 2008 Apr 23.

Johnson BS, Snead D, Lee JJ, McCaffery JM, et al. (2009) TDP-43 is intrinsically aggregation-prone, and amyotrophic lateral sclerosis-linked mutations accelerate aggregation and increase toxicity. J Biol Chem, 284(30):20329-39.

Johnson JO, Mandrioli J, Benatar M, Abramzon Y, et al. (2010) Exome sequencing reveals VCP mutations as a cause of familial ALS. Neuron. 68(5):857-64.

Johnston CA, Stanton BR, Turner MR, Gray R, et al. (2006) Amyotrophic lateral sclerosis in an urban setting: a population based study of inner city London. J Neurol. 253(12):1642-3.

Johnston JA, Dalton MJ, Gurney ME, Kopito RR. (2000) Formation of high molecular weight complexes of mutant Cu, Zn-superoxide dismutase in a mouse model for familial amyotrophic lateral sclerosis. Proc Natl Acad Sci U S A. 97(23):12571-6.

Jønson L, Vikesaa J, Krogh A, Nielsen LK, et al. (2007) Molecular composition of IMP1 ribonucleoprotein granules. Mol Cell Proteomics.6(5):798-811.

Jung C, Higgins CM, Xu Z. (2002) Mitochondrial electron transport chain complex dysfunction in a transgenic mouse model for amyotrophic lateral sclerosis. J Neurochem. 83(3):535-45.

Jurica MS, Moore MJ. (2003) Pre-mRNA splicing: awash in a sea of proteins. Molecular Cell, 12:5–14.

Kabashi E, Agar JN, Hong Y, Taylor DM, et al. (2008) Proteasomes remain intact, but show early focal alteration in their composition in a mouse model of amyotrophic lateral sclerosis. J Neurochem. 105(6):2353-66.

Kabashi E, Lin L, Tradewell ML, Dion PA, Bercier V, et al. (2010) Gain and loss of function of ALS-related mutations of TARDBP (TDP-43) cause motor deficits in vivo. Hum Mol Genet. 19(4):671-83.

Kabashi E, Valdmanis PN, Dion P, Spiegelman D, et al. (2008) TARDBP mutations in individuals with sporadic and familial amyotrophic lateral sclerosis. Nat Genet, 40(5):572-4.

Kaleem M, Zhao A, Hamshere M, Myers AJ. (2007) Identification of a novel valosin-containing protein polymorphism in late-onset Alzheimer's disease. Neurodegener Dis. 4(5):376-81

Kallen J, Spitzfaden C, Zurini MG, Wider G, et al. (1991) Structure of human cyclophilin and its binding site for cyclosporin A determined by X-ray crystallography and NMR spectroscopy. Nature. 353(6341):276-9.

Kaminska B, Figiel I, Pyrzynska B, Czajkowski R, Mosieniak G. (2001) Treatment of hippocampal neurons with cyclosporin A results in calcium overload and apoptosis which are independent on NMDA receptor activation. Br J Pharmacol. 133(7):997-1004.

Kanekura K, Nishimoto I, Aiso S, Matsuoka M. (2006) Characterization of amyotrophic lateral sclerosis-linked P56S mutation of vesicle-associated membrane protein-associated protein B (VAPB/ALS8). J Biol Chem. 281(40):30223-33.

Kanekura K, Suzuki H, Aiso S, Matsuoka M. (2009) ER stress and unfolded protein response in amyotrophic lateral sclerosis. Mol Neurobiol. 39(2):81-9.

Kano O, Beers DR, Henkel JS, Appel SH. (2012) Peripheral nerve inflammation in ALS mice: cause or consequence. Neurology. 78(11):833-5.

Kasai T, Tokuda T, Ishigami N, Sasayama H, et al. (2009) Increased TDP-43 protein in cerebrospinal fluid of patients with amyotrophic lateral sclerosis. Acta Neuropathol. 117(1):55-62.

Kasarskis EJ, Lindquist JH, Coffman CJ, Grambow SC, et al; Als Gulf War Clinical Review Team (2009) Clinical aspects of ALS in Gulf War veterans. Amyotroph Lateral Scler. 10(1):35-41.

Kaspar BK, Lladó J, Shérkat N, Rothstein JD, Gage FH. (2003) Retrograde viral delivery of IGF-1 prolongs survival in a mouse ALS model. Science. 301(5634):839-42.

Kato S, Funakoshi H, Nakamura T, Kato M, et al. (2003) Expression of hepatocyte growth factor and c-Met in the anterior horn cells of the spinal cord in the patients with amyotrophic lateral sclerosis (ALS): immunohistochemical studies on sporadic ALS and familial ALS with superoxide dismutase 1 gene mutation. Acta Neuropathol. 106(2):112-20.

Kato S, Horiuchi S, Nakashima K, Hirano A, et al. (1999) Astrocytic hyaline inclusions contain advanced glycation endproducts in familial amyotrophic lateral sclerosis with superoxide dismutase 1 gene mutation: immunohistochemical and immunoelectron microscopical analyses. Acta Neuropathol. 97(3):260-6.

Kato S, Shaw P, Wood-Allum C, Leigh PN, Shaw CE. (2003) Amyotrophic lateral sclerosis. In Neurodegeneration: The molecular pathology of dementia and movement disorders Edited by: Dickson DW. ISN Neuropath press: 350-371.

Kawahara Y, Ito K, Sun H, Aizawa H, et al. (2004) Glutamate receptors: RNA editing and death of motor neurons. Nature. 427(6977):801.

Kawamata T, Akiyama H, Yamada T, McGeer PL. (1992) Immunologic reactions in amyotrophic lateral sclerosis brain and spinal cord tissue. Am J Pathol. 140(3):691-707.

Ke H, Huai Q. (2004) Crystal structures of cyclophilin and its partners. Front Biosci. 9:2285-96.

Ke H, Mayrose D, Belshaw PJ, Alberg DG, et al. (1994) Crystal structures of cyclophilin A complexed with cyclosporin A and N-methyl-4-[(E)-2-butenyl]-4,4-dimethylthreonine cyclosporin A. Structure. 2(1):33-44.

Ke H, Zhao Y, Luo F, Weissman I, Friedman J. (1993) Crystal structure of murine cyclophilin C complexed with immunosuppressive drug cyclosporin A. Proc Natl Acad Sci U S A. 90(24):11850-4.

Ke HM, Zydowsky LD, Liu J, Walsh CT. (1991) Crystal structure of recombinant human T-cell cyclophilin A at 2.5 A resolution. Proc Natl Acad Sci U S A. 88(21):9483-7.

Ke Y, Dramiga J, Schütz U, Kril JJ, et al. (2012) Tau-mediated nuclear depletion and cytoplasmic accumulation of SFPQ in Alzheimer's and Pick's disease. PLoS One.7(4):e35678.

Keller BA, Volkening K, Droppelmann CA, Ang LC, et al. (2012) Co-aggregation of RNA binding proteins in ALS spinal motor neurons: evidence of a common pathogenic mechanism. Acta Neuropathol.

Kennel PF, Fonteneau P, Martin E, Schmidt JM, et al. (1996) Electromyographical and motor performance studies in the pmn mouse model of neurodegenerative disease. Neurobiol Dis. 3(2):137-47.

Kern G, Kern D, Schmid FX, Fischer G. (1995) A kinetic analysis of the folding of human carbonic anhydrase II and its catalysis by cyclophilin. J Biol Chem. 270(2):740-5.

Kern MA, Friese M, Grundstrom E, Korhonen L, Wallin A, et al. (2001) Amyotrophic lateral sclerosis: evidence for intact hepatocyte growth factor/met signalling axis. Cytokine. 15(6):315-9.

Kiaei M, Kipiani K, Calingasan NY, Wille E, et al. (2007) Matrix metalloproteinase-9 regulates TNF-alpha and FasL expression in neuronal, glial cells and its absence extends life in a transgenic mouse model of amyotrophic lateral sclerosis. Exp Neurol. 205(1):74-81.

Kieran D, Kalmar B, Dick JR, Riddoch-Contreras J, et al. (2004) Treatment with arimoclomol, a coinducer of heat shock proteins, delays disease progression in ALS mice. Nat Med. 10(4):402-5.

Kim H, Kim WJ, Jeon ST, Koh EM, et al. (2005) Cyclophilin A may contribute to the inflammatory processes in rheumatoid arthritis through induction of matrix degrading enzymes and inflammatory cytokines from macrophages. Clin Immunol.116(3):217-24.

Kim HJ, Chong KH, Kang SW, Lee JR, et al. (2004) Identification of cyclophilin A as a CD99-binding protein by yeast two-hybrid screening. Immunol Lett. 95(2):155-9.

Kim I, Xu W, Reed JC (2008) Cell death and endoplasmic reticulum stress: disease relevance and therapeutic opportunities. Nat Rev Drug Discov, 7(12):1013-30.

Kim IS, Shin SY, Kim YS, Kim HY, et al. (2010a) Expression of yeast cyclophilin A (Cpr1) provides improved stress tolerance in Escherichia coli. *J Microbiol Biotechnol.* 20(6):974-7.

Kim IS, Kim HY, Shin SY, Kim YS, et al. (2010b) A cyclophilin A CPR1 overexpression enhances stress acquisition in Saccharomyces cerevisiae. *Mol Cells.* 29(6):567-74.

Kim JH, Hahm B, Kim YK, Choi M, Jang SK. (2000) Protein-protein interaction among hnRNPs shuttling between nucleus and cytoplasm. J Mol Biol. 298(3):395-405.

Kim PK, Hailey DW, Mullen RT, Lippincott-Schwartz J. (2008) Ubiquitin signals autophagic degradation of cytosolic proteins and peroxisomes. Proc Natl Acad Sci U S A. 105(52):20567-74.

Kim SC, Sprung R, Chen Y, Xu Y, et al. (2006) Substrate and functional diversity of lysine acetylation revealed by a proteomics survey. Mol Cell. 23(4):607-18.

Kim SH, Lessner SM, Sakurai Y, Galis ZS. (2004) Cyclophilin A as a novel biphasic mediator of endothelial activation and dysfunction. Am J Pathol. 164(5):1567-74.

Kim SH, Shanware NP, Bowler MJ, Tibbetts RS. (2010) Amyotrophic lateral sclerosis-associated proteins TDP-43 and FUS/TLS function in a common biochemical complex to co-regulate HDAC6 mRNA. J Biol Chem. 285(44):34097-105.

Kimonis VE, Mehta SG, Fulchiero EC, Thomasova D, et al. (2008) Clinical studies in familial VCP myopathy associated with Paget disease of bone and frontotemporal dementia. Am J Med Genet A. 146A(6):745-57.

Kobayashi M, Ikeda K, Kinoshita M, Iwasaki Y. (1999) Amyotrophic lateral sclerosis with supranuclear ophthalmoplegia and rigidity. Neurol Res, 21:661-664.

Kołcz J, Drukała J, Jurkiewicz A, Pfitzner R, et al. (1999) Effects of cyclosporin A on contractile activity and cytoskeleton in chick embryo cardiomyocytes. Biochem Cell Biol. 77(2):133-40.

Koletsky AJ, Harding MW, Handschumacher RE. (1986) Cyclophilin: distribution and variant properties in normal and neoplastic tissues. J Immunol. 137(3):1054-9.

Kong J, Xu Z. (1998) Massive mitochondrial degeneration in motor neurons triggers the onset of amyotrophic lateral sclerosis in mice expressing a mutant SOD1. J Neurosci. 18(9):3241-50.

Kornberg MD, Sen N, Hara MR, Juluri KR, et al. (2010) GAPDH mediates nitrosylation of nuclear proteins. Nat Cell Biol. 12(11):1094-100.

Kozu T, Henrich B, Schäfer KP. (1995) Structure and expression of the gene (HNRPA2B1) encoding the human hnRNP protein A2/B1. Genomics, 25(2):365-71.

Krishnan J, Vannuvel K, Andries M, Waelkens E, et al. (2008) Over-expression of Hsp27 does not influence disease in the mutant SOD1(G93A) mouse model of amyotrophic lateral sclerosis. J Neurochem. 106(5):2170-83.

Krummrei U, Bang R, Schmidtchen R, Brune K, Bang H. (1995) Cyclophilin-A is a zinc-dependent DNA binding protein in macrophages. FEBS Lett, 28;371(1):47-51.

Kruse M, Brunke M, Escher A, Szalay AA, et al. (1995) Enzyme assembly after de novo synthesis in rabbit reticulocyte lysate involves molecular chaperones and immunophilins. J Biol Chem. 270(6):2588-94.

Kuhle J, Lindberg RL, Regeniter A, Mehling M, et al. (2009) Increased levels of inflammatory chemokines in amyotrophic lateral sclerosis. Eur J Neurol.16(6):771-4.

Kuiperij HB, Abdo WF, van Engelen BG, Schelhaas HJ, Verbeek MM. (2010) TDP-43 plasma levels do not differentiate sporadic inclusion body myositis from other inflammatory myopathies. Acta Neuropathol.120(6):825-6.

Kuncl RW, Bilak MM, Bilak SR, Corse AM, et al. (2002) Pigment epithelium-derived factor is elevated in CSF of patients with amyotrophic lateral sclerosis. J Neurochem. 81(1):178-84.

Kuusisto E, Salminen A, Alafuzoff I. (2001) Ubiquitin-binding protein p62 is present in neuronal and glial inclusions in human tauopathies and synucleinopathies. Neuroreport. 12(10):2085-90.

Kuzuhara S (2011) Muro disease: amyotrophic lateral sclerosis/parkinsonism-dementia complex in Kii peninsula of Japan. Brain Nerve. 63(2):119-29.

Kuzuhara S, Kokubo Y (2005) Atypical parkinsonism of Japan: amyotrophic lateral sclerosis-parkinsonism-dementia complex of the Kii peninsula of Japan (Muro disease): an update. Mov Disord. 20 Suppl 12:S108-13.

Kwiatkowski TJ Jr, Bosco DA, Leclerc AL, Tamrazian E, et al. (2009) Mutations in the FUS/TLS gene on chromosome 16 cause familial amyotrophic lateral sclerosis. Science. 323(5918):1205-8.

Kwong LK, Uryu K, Trojanowski JQ, Lee VM. (2008) TDP-43 proteinopathies: neurodegenerative protein misfolding diseases without amyloidosis. Neurosignals. 16(1):41-51.

Laaksovirta H, Peuralinna T, Schymick JC, Scholz SW, et al. (2010) Chromosome 9p21 in amyotrophic lateral sclerosis in Finland: a genome-wide association study. Lancet Neurol. 9(10):978-85.

Lafon-Cazal M, Adjali O, Galéotti N, Poncet J, et al. (2003) Proteomic analysis of astrocytic secretion in the mouse. Comparison with the cerebrospinal fluid proteome. J Biol Chem. 278(27):24438-48.

Lagier-Tourenne C, Cleveland DW. (2009) Rethinking ALS: the FUS about TDP-43. Cell. 136(6):1001-4.

Lagier-Tourenne C, Polymenidou M, Cleveland DW. (2010) TDP-43 and FUS/TLS: emerging roles in RNA processing and neurodegeneration. Hum Mol Genet. 19(R1):R46-64.

Lai EC, Felice KJ, Festoff BW, Gawel MJ, Gelinas DF, et al. (1997) Effect of recombinant human insulin-like growth factor-I on progression of ALS. A placebo-controlled study. The North America ALS/IGF-I Study Group. Neurology. 49(6):1621-30.

Lambrechts D, Poesen K, Fernández-Santiago R, Al-Chalabi A, et al. (2009) Meta-analysis of vascular endothelial growth factor variations in amyotrophic lateral sclerosis: increased susceptibility in male carriers of the -2578AA genotype. J Med Genet. 46(12):840-6.

Lambrechts D, Storkebaum E, Morimoto M, Del-Favero J, et al. (2003) VEGF is a modifier of amyotrophic lateral sclerosis in mice and humans and protects motoneurons against ischemic death. Nat Genet. 34(4):383-94.

Lammers M, Neumann H, Chin JW, James LC. (2010) Acetylation regulates cyclophilin A catalysis, immunosuppression and HIV isomerization. Nat Chem Biol, 6(5):331-7.

LaMonte BH, Wallace KE, Holloway BA, Shelly SS, et al. (2002) Disruption of dynein/dynactin inhibits axonal transport in motor neurons causing late-onset progressive degeneration. Neuron. 34(5):715-27.

Landeras-Bueno S, Jorba N, Pérez-Cidoncha M, Ortín J. (2011) The splicing factor proline-glutamine rich (SFPQ/PSF) is involved in influenza virus transcription. PLoS Pathog.7(11):e1002397.

Landers JE, Leclerc AL, Shi L, Virkud A, et al. (2008) New VAPB deletion variant and exclusion of VAPB mutations in familial ALS. Neurology. 70(14):1179-85.

Landers JE, Melki J, Meininger V, Glass JD, et al. (2009) Reduced expression of the Kinesin-Associated Protein 3 (KIFAP3) gene increases survival in sporadic amyotrophic lateral sclerosis. Proc Natl Acad Sci U S A. 106(22):9004-9.

Landers JE, Shi L, Cho TJ, Glass JD, et al. (2008) A common haplotype within the PON1 promoter region is associated with sporadic ALS. Amyotroph Lateral Scler. 9(5):306-14.

Lawyer T Jr, Netsky MG. (1953) Amyotrophic lateral sclerosis. AMA Arch Neurol Psychiatry 69:171-192.

Lee BJ, Cansizoglu AE, Süel KE, Louis TH, et al. (2006) Rules for nuclear localization sequence recognition by karyopherin beta 2. Cell. 126(3):543-58.

Lee JP, Palfrey HC, Bindokas VP, Ghadge GD, et al. (1999) The role of immunophilins in mutant superoxide dismutase-1linked familial amyotrophic lateral sclerosis. Proc Natl Acad Sci U S A. 96(6):3251-6.

Lee JY, Koga H, Kawaguchi Y, Tang W, et al. (2010) HDAC6 controls autophagosome maturation essential for ubiquitin-selective quality-control autophagy. EMBO J. 29(5):969-80.

Lee SP, Hwang YS, Kim YJ, Kwon KS, et al. (2001). Cyclophilin a binds to peroxiredoxins and activates its peroxidase activity. J. Biol. Chem. 276: 29826–29832.

Lee T, Li YR, Ingre C, Weber M, et al. (2011) Ataxin-2 intermediate-length polyglutamine expansions in European ALS patients. Hum Mol Genet. 20(9):1697-700.

Leigh PN, Abrahams S, Al-Chalabi A, Ampong MA, et al; King's MND Care and Research Team. (2003) The management of motor neurone disease. J Neurol Neurosurg Psychiatry. 74 Suppl 4:iv32-iv47.

Leigh PN, Anderton BH, Dodson A, Gallo JM, et al. (1988) Ubiquitin deposits in anterior horn cells in motor neurone disease. Neurosci Lett, 93:197-203.

Leigh PN, Whitwell H, Garofalo O, Buller J, et al. (1991) Ubiquitin-immunoreactive intraneuronal inclusions in amyotrophic lateral sclerosis. Morphology, distribution, and specificity. Brain 114(Pt 2):775-788.

Lesca G, Eymard-Pierre E, Santorelli FM, Cusmai R, et al. (2003) Infantile ascending hereditary spastic paralysis (IAHSP): clinical features in 11 families. Neurology. 60(4):674-82.

Leung CL, He CZ, Kaufmann P, Chin SS, et al. (2004) A pathogenic peripherin gene mutation in a patient with amyotrophic lateral sclerosis. Brain Pathol. 14(3):290-6.

Li XG, Zhang JH, Xie MQ, Liu MS, et al. (2009) Association between DPP6 polymorphism and the risk of sporadic amyotrophic lateral sclerosis in Chinese patients. Chin Med J (Engl). Dec 20;122(24):2989-92.

Li Y, Ray P, Rao EJ, Shi C, et al. (2010) A Drosophila model for TDP-43 proteinopathy. Proc Natl Acad Sci U S A.107(7):3169-74.

Li YJ, Pericak-Vance MA, Haines JL, Siddique N, et al. (2004) Apolipoprotein E is associated with age at onset of amyotrophic lateral sclerosis. Neurogenetics. 5(4):209-13.

Liachko NF, Guthrie CR, Kraemer BC. (2010) Phosphorylation promotes neurotoxicity in a Caenorhabditis elegans model of TDP-43 proteinopathy. J Neurosci. 30(48):16208-19.

Licatalosi DD, Mele A, Fak JJ, Ule J, Kayikci M, et al. (2008) HITS-CLIP yields genome-wide insights into brain alternative RNA processing. Nature. 456(7221):464-9.

Lill CM, Abel O, Bertram L, Al-Chalabi A. (2011) Keeping up with genetic discoveries in amyotrophic lateral sclerosis: the ALSoD and ALSGene databases. Amyotroph Lateral Scler. 12(4):238-49.

Lim GP, Backstrom JR, Cullen MJ, Miller CA, et al. (1996) Matrix metalloproteinases in the neocortex and spinal cord of amyotrophic lateral sclerosis patients. J Neurochem. 67(1):251-9.

Lin CL, Bristol LA, Jin L, Dykes-Hoberg M, et al. (1998) Aberrant RNA processing in a neurodegenerative disease: the cause for absent EAAT2, a glutamate transporter, in amyotrophic lateral sclerosis. Neuron. 20(3):589-602.

Ling SC, Albuquerque CP, Han JS, Lagier-Tourenne C, et al. (2010) ALS-associated mutations in TDP-43 increase its stability and promote TDP-43 complexes with FUS/TLS. Proc Natl Acad Sci U S A. 107(30):13318-23.

Liu J, Farmer JD Jr, Lane WS, Friedman J, et al. (1991) Calcineurin is a common target of cyclophilin-cyclosporin A and FKBP-FK506 complexes. Cell. 23;66(4):807-15.

Liu J, Lillo C, Jonsson PA, Vande Velde C, et al. (2004) Toxicity of familial ALS-linked SOD1 mutants from selective recruitment to spinal mitochondria. Neuron. 43(1):5-17.

Liu J, Narasimhan P, Yu F, Chan PH. (2005) Neuroprotection by hypoxic preconditioning involves oxidative stress-mediated expression of hypoxia-inducible factor and erythropoietin. Stroke. 36, 1264–1269.

Liu Y, Hao W, Dawson A, Liu S, Fassbender K. (2009) Expression of amyotrophic lateral sclerosis-linked SOD1 mutant increases the neurotoxic potential of microglia via TLR2. J Biol Chem 284:3691-3699.

Liu-Yesucevitz L, Bilgutay A, Zhang YJ, Vanderweyde T, et al. (2010) Tar DNA binding protein-43 (TDP-43) associates with stress granules: analysis of cultured cells and pathological brain tissue. PLoS One. 5(10):e13250.

Logroscino G, Traynor BJ, Hardiman O, Chiò A, et al; EURALS. (2010) Incidence of amyotrophic lateral sclerosis in Europe. J Neurol Neurosurg Psychiatry. 81(4):385-90.

Lowe J, Lennox G, Jefferson D, Morrell K, et al. (1988) A filamentous inclusion body within anterior horn neurones in motor neurone disease defined by immunocytochemical localisation of ubiquitin. Neurosci Lett. 94:203-210.

Lu Y, Ferris J, Gao FB. (2009) Frontotemporal dementia and amyotrophic lateral sclerosis-associated disease protein TDP-43 promotes dendritic branching. Mol Brain. 2(1):30.

Lu YC, Song J, Cho HY, Fan G, Yokoyama KK, Chiu R. (2006) Cyclophilin a protects Peg3 from hypermethylation and inactive histone modification. J Biol Chem. Dec 22;281(51):39081-7.

Luban J, Bossolt KL, Franke EK, Kalpana GV, Goff SP. (1993) Human immunodeficiency virus type 1 Gag protein binds to cyclophilins A and B. Cell. 73(6):1067-78.

Luty AA, Kwok JB, Dobson-Stone C, Loy CT, et al. (2010) Sigma nonopioid intracellular receptor 1 mutations cause frontotemporal lobar degeneration-motor neuron disease. Ann Neurol. 68(5):639-49.

Mackenzie IR, Bigio EH, Ince PG, Geser F, et al. (2007) Pathological TDP-43 distinguishes sporadic amyotrophic lateral sclerosis from amyotrophic lateral sclerosis with SOD1 mutations. Ann Neurol. 61(5):427-34.

Mackenzie IR, Neumann M, Bigio EH, Cairns NJ, et al. (2010) Nomenclature and nosology for neuropathologic subtypes of frontotemporal lobar degeneration: an update. Acta Neuropathol. 119(1):1-4.

Mackenzie IR, Rademakers R, Neumann M. (2010) TDP-43 and FUS in amyotrophic lateral sclerosis and frontotemporal dementia. Lancet Neurol. 9(10):995-1007.

Magrané J, Manfredi G (2009) Mitochondrial function, morphology, and axonal transport in amyotrophic lateral sclerosis. Antioxid Redox Signal. 11(7):1615-26.

Majounie E, Abramzon Y, Renton AE, Perry R, et al. (2012) Repeat expansion in C9ORF72 in Alzheimer's disease. N Engl J Med. 366(3):283-4.

Manders EM, Stap J, Brakenhoff GJ, van Driel R, Aten JA. (1992) Dynamics of three-dimensional replication patterns during the S-phase, analysed by double labelling of DNA and confocal microscopy. J Cell Sci, 103:857-62.

Manders EMM, Verbeek FJ, Aten JA. (1993) Measurement of co-localization of objects in dual-colour confocal images. J Microscopy, 169(3):375-382.

Marchetto MC, Winner B, Gage FH. (2010) Pluripotent stem cells in neurodegenerative and neurodevelopmental diseases. Hum Mol Genet. 19(R1):R71-6.

Marks AR. (1996) Cellular functions of immunophilins. Physiol Rev. 76(3):631-49.

Martin E, Yanicostas C, Rastetter A, Naini SM, et al. (2012) Spatacsin and spastizin act in the same pathway required for proper spinal motor neuron axon outgrowth in zebrafish. Neurobiol Dis. 48(3):299-308.

Martin N, Jaubert J, Gounon P, Salido E, et al. (2002) A missense mutation in Tbce causes progressive motor neuronopathy in mice. Nat Genet 32:443-447.

Martínez-Balbás MA, Bauer UM, Nielsen SJ, Brehm A, Kouzarides T. (2000) Regulation of E2F1 activity by acetylation. EMBO J. 19(4):662-71.

Maruyama H, Morino H, Ito H, Izumi Y, et al. (2010). Mutations of optineurin in amyotrophic lateral sclerosis. Nature. 465(7295):223-6.

Massignan T, Casoni F, Basso M, Stefanazzi P, Biasini E, et al. (2007) Proteomic analysis of spinal cord of presymptomatic amyotrophic lateral sclerosis G93A SOD1 mouse. Biochem Biophys Res Commun 353:719-25.

Matsumoto G, Kim S, Morimoto RI. (2006) Huntingtin and mutant SOD1 form aggregate structures with distinct molecular properties in human cells. J Biol Chem. 281(7):4477-85.

Matsumoto G, Stojanovic A, Holmberg CI, Kim S, Morimoto RI. (2005) Structural properties and neuronal toxicity of amyotrophic lateral sclerosis-associated Cu/Zn superoxide dismutase 1 aggregates. J Cell Biol. 171(1):75-85.

McCaffrey PG, Luo C, Kerppola TK, Jain J, et al. (1993) Isolation of the cyclosporin-sensitive T cell transcription factor NFATp. Science. 262(5134):750-4.

McCord JM, Fridovich I. (1969) Superoxide dismutase. An enzymic function for erythrocuprein (hemocuprein). J Biol Chem. 244(22):6049-55.

McDonald JW, Goldberg MP, Gwag BJ, Chi SI, Choi DW. (1996) Cyclosporine induces neuronal apoptosis and selective oligodendrocyte death in cortical cultures. Ann Neurol. 40(5):750-8.

McDonald KK, Aulas A, Destroismaisons L, Pickles S, et al. (2011) TAR DNA-binding protein 43 (TDP-43) regulates stress granule dynamics via differential regulation of G3BP and TIA-1. Hum Mol Genet. 20(7):1400-10.

McKinsey TA, Olson EN. (2004) Dual roles of histone deacetylases in the control of cardiac growth. Novartis Found Symp. 259:132-41.

Mehta SG, Khare M, Ramani R, Watts GD, Simon M, et al. (2012) Genotype-Phenotype studies of VCP-associated Inclusion Body Myopathy with Paget Disease of Bone and/or Frontotemporal Dementia. Clin Genet.

Meierhofer D, Wang X, Huang L, Kaiser P. (2008) Quantitative analysis of global ubiquitination in HeLa cells by mass spectrometry. J Proteome Res. 7(10):4566-76.

Meloni BP, Tilbrook PA, Boulos S, Arthu PG, Knuckey NW. (2006) Erythropoietin preconditioning in neuronal cultures: signaling, protection from in vitro ischemia, and proteomic analysis. J Neurosci Res. 83(4):584-93.

Meloni BP, Van Dyk D, Cole R, Knuckey NW. (2005) Proteome analysis of cortical neuronal cultures following cycloheximide, heat stress and MK801 preconditioning. Proteomics. 5(18):4743-53.

Menzies FM, Ince PG, Shaw PJ. (2002) Mitochondrial involvement in amyotrophic lateral sclerosis. Neurochem Int. 40(6):543-51.

Mesa A, Somarelli JA, Herrera RJ (2008) Spliceosomal immunophilins. FEBS Lett. 582(16):2345-51.

Mi H, Kops O, Zimmermann E, Jäschke A, Tropschug M. (1996) A nuclear RNA-binding cyclophilin in human T cells. FEBS Letters, 398:201–5.

Miguel L, Frébourg T, Campion D, Lecourtois M. (2011) Both cytoplasmic and nuclear accumulations of the protein are neurotoxic in Drosophila models of TDP-43 proteinopathies. Neurobiol Dis. 41(2):398-406. Epub 2010 Oct 14.

Mikol V, Kallen J, Walkinshaw MD. (1994) X-ray structure of a cyclophilin B/cyclosporin complex: comparison with cyclophilin A and delineation of its calcineurin-binding domain. Proc Natl Acad Sci U S A. 91(11):5183-6.

Miller JW, Urbinati CR, Teng-Umnuay P, Stenberg MG, et al. (2000) Recruitment of human muscleblind proteins to (CUG)(n) expansions associated with myotonic dystrophy. EMBO J. 19(17):4439-48.

Mitchell J, Paul P, Chen HJ, Morris A, et al. (2010) Familial amyotrophic lateral sclerosis is associated with a mutation in D-amino acid oxidase. Proc Natl Acad Sci U S A. 107(16):7556-61.

Mitchell RM, Freeman WM, Randazzo WT, Stephens HE, et al. (2009) A CSF biomarker panel for identification of patients with amyotrophic lateral sclerosis. Neurology. 72(1):14-9.

Mitchell RM, Simmons Z, Beard JL, Stephens HE, Connor JR. (2010) Plasma biomarkers associated with ALS and their relationship to iron homeostasis. Muscle Nerve.42(1):95-103.

Mitne-Neto M, Machado-Costa M, Marchetto MC, Bengtson MH, et al. (2011) Downregulation of VAPB expression in motor neurons derived from induced pluripotent stem cells of ALS8 patients. Hum Mol Genet. 20(18):3642-52.

Mizuno Y, Amari M, Takatama M, Aizawa H, et al. (2006) Immunoreactivities of p62, an ubiqutin-binding protein, in the spinal anterior horn cells of patients with amyotrophic lateral sclerosis. J Neurol Sci. 249(1):13-8.

Mizuno Y, Hori S, Kakizuka A, Okamoto K. (2003) Vacuole-creating protein in neurodegenerative diseases in humans. Neurosci Lett. 343(2):77-80.

Moisse K, Mepham J, Volkening K, Welch I, et al. (2009) Cytosolic TDP-43 expression following axotomy is associated with caspase 3 activation in NFL-/- mice: support for a role for TDP-43 in the physiological response to neuronal injury. Brain Res. 1296:176-86.

Mok K, Traynor BJ, Schymick J, Tienari PJ, et al. (2012) Chromosome 9 ALS and FTD locus is probably derived from a single founder. Neurobiol Aging. 33(1):209.e3-8.

Momeni P, Bell J, Duckworth J, Hutton M, et al. (2006) Sequence analysis of all identified open reading frames on the frontal temporal dementia haplotype on chromosome 3 fails to identify unique coding variants except in CHMP2B. Neurosci Lett. 410(2):77-9.

Montague JW, Gaido ML, Frye C, Cidlowski JA. (1994) A calcium-dependent nuclease from apoptotic rat thymocytes is homologous with cyclophilin. Recombinant cyclophilins A, B, and C have nuclease activity. J Biol Chem. 22;269(29):18877-80.

Montague JW, Hughes FM Jr, Cidlowski JA. (1997) Native recombinant cyclophilins A, B, and C degrade DNA independently of peptidylprolyl cis-trans-isomerase activity. Potential roles of cyclophilins in apoptosis. J Biol Chem. 272(10):6677-84.

Moparthi SB, Fristedt R, Mishra R, Almstedt K, et al. (2010) Chaperone activity of Cyp18 through hydrophobic condensation that enables rescue of transient misfolded molten globule intermediates. Biochemistry.49(6):1137-45.

Morahan JM, Yu B, Trent RJ, Pamphlett R. (2007) A gene-environment study of the paraoxonase 1 gene and pesticides in amyotrophic lateral sclerosis. Neurotoxicology. 28(3):532-40.

Moreau C, Devos D, Brunaud-Danel V, Defebvre L, et al. (2006) Paradoxical response of VEGF expression to hypoxia in CSF of patients with ALS. J Neurol Neurosurg Psychiatry. 77(2):255-7.

Moreira MC, Klur S, Watanabe M, Németh AH, et al. (2004) Senataxin, the ortholog of a yeast RNA helicase, is mutant in ataxia-ocular apraxia 2. Nat Genet. 36(3):225-7.

Morimoto RI (2008) Proteotoxic stress and inducible chaperone networks in neurodegenerative disease and aging. Genes Dev.22(11):1427-38.

Morita M, Al-Chalabi A, Andersen PM, Hosler B, et al. (2006) A locus on chromosome 9p confers susceptibility to ALS and frontotemporal dementia. Neurology. 66(6):839-44.

Moroianu J, Blobel G, Radu A. (1996) Nuclear protein import: Ran-GTP dissociates the karyopherin alphabeta heterodimer by displacing alpha from an overlapping binding site on beta. Proc Natl Acad Sci U S A. 93(14):7059-62.

Moroianu J, Riordan JF. (1994) Nuclear translocation of angiogenin in proliferating endothelial cells is essential to its angiogenic activity. Proc Natl Acad Sci U S A. 91(5):1677-81.

Mórotz GM, De Vos KJ, Vagnoni A, Ackerley S, et al. (2012) Amyotrophic lateral sclerosis-associated mutant VAPBP56S perturbs calcium homeostasis to disrupt axonal transport of mitochondria. Hum Mol Genet. 21(9):1979-88.

Moumen A, Virard I, Raoul C. (2011) Accumulation of wildtype and ALS-linked mutated VAPB impairs activity of the proteasome. PLoS One. 6(10):e26066.

Mourelatos Z, Hirano A, Rosenquist AC, Gonatas NK. (1994) Fragmentation of the Golgi apparatus of motor neurons in amyotrophic lateral sclerosis (ALS). Clinical studies in ALS of Guam and experimental studies in deafferented neurons and in beta,beta'-iminodipropionitrile axonopathy. Am J Pathol. 144(6):1288-300.

Münch C, Sedlmeier R, Meyer T, Homberg V, et al. (2004) Point mutations of the p150 subunit of dynactin (DCTN1) gene in ALS. Neurology. 63(4):724-6.

Murakami T, Nagano I, Hayashi T, Manabe Y, et al. (2001) Impaired retrograde axonal transport of adenovirus-mediated E. coli LacZ gene in the mice carrying mutant SOD1 gene. Neurosci Lett. 308(3):149-52.

Nadeau K, Das A, Walsh CT. (1993) Hsp90 chaperonins possess ATPase activity and bind heat shock transcription factors and peptidyl prolyl isomerases. J Biol Chem. 268(2):1479-87.

Nagai M, Aoki M, Miyoshi I, Kato M, et al. (2001) Rats expressing human cytosolic copper-zinc superoxide dismutase transgenes with amyotrophic lateral sclerosis: associated mutations develop motor neuron disease. J Neurosci. 21(23):9246-54.

Nahreini P, Hovland AR, Kumar B, Andreatta C, et al. (2001) Effects of altered cyclophilin A expression on growth and differentiation of human and mouse neuronal cells. Cell Mol Neurobiol. 21(1):65-79.

Nakano T, Nakaso K, Nakashima K, Ohama E. (2004) Expression of ubiquitin-binding protein p62 in ubiquitin-immunoreactive intraneuronal inclusions in amyotrophic lateral sclerosis with

dementia: analysis of five autopsy cases with broad clinicopathological spectrum. Acta Neuropathol. 107(4):359-64.

Nakaso K, Yoshimoto Y, Nakano T, Takeshima T, et al. (2004) Transcriptional activation of p62/A170/ZIP during the formation of the aggregates: possible mechanisms and the role in Lewy body formation in Parkinson's disease. Brain Res. 1012(1-2):42-51.

Nardo G, Pozzi S, Mantovani S, Garbelli S, et al. (2009) Nitroproteomics of peripheral blood mononuclear cells from patients and a rat model of ALS. Antioxid Redox Signal, 11 (7): 1559-67.

Nardo G, Pozzi S, Pignataro M, Lauranzano E, et al. (2011) Amyotrophic lateral sclerosis multiprotein biomarkers in peripheral blood mononuclear cells. PloS One, 6(10):e25545.

Nelson LM, McGuire V, Longstreth WT Jr, Matkin C. (2000) Population based case-control study of amyotrophic lateral sclerosis in western Washington State. I. Cigarette smoking and alcohol consumption. Am J Epidemiol. 151:156-163.

Neumann M, Bentmann E, Dormann D, Jawaid A, et al. (2011) FET proteins TAF15 and EWS are selective markers that distinguish FTLD with FUS pathology from amyotrophic lateral sclerosis with FUS mutations. Brain. 134(Pt 9):2595-609

Neumann M, Igaz LM, Kwong LK, Nakashima-Yasuda H, et al. (2007) Absence of heterogeneous nuclear ribonucleoproteins and survival motor neuron protein in TDP-43 positive inclusions in frontotemporal lobar degeneration. Acta Neuropathol. 113(5):543-8.

Neumann M, Kwong LK, Truax AC, Vanmassenhove B, et al. (2007) TDP-43-positive white matter pathology in frontotemporal lobar degeneration with ubiquitin-positive inclusions. J Neuropathol Exp Neurol. 66(3):177-83.

Neumann M, Rademakers R, Roeber S, Baker M, et al. (2009) A new subtype of frontotemporal lobar degeneration with FUS pathology. Brain. 132(Pt 11):2922-31.

Neumann M, Roeber S, Kretzschmar HA, Rademakers R, et al. (2009) Abundant FUS-immunoreactive pathology in neuronal intermediate filament inclusion disease. Acta Neuropathol. 118(5):605-16.

Neumann M, Sampathu DM, Kwong LK, Truax AC, et al. (2006) Ubiquitinated TDP-43 in frontotemporal lobar degeneration and amyotrophic lateral sclerosis. Science, 314(5796):130-3.

Newbery HJ, Gillingwater TH, Dharmasaroja P, Peters J, et al. (2005) Progressive loss of motor neuron function in wasted mice: effects of a spontaneous null mutation in the gene for the eEF1 A2 translation factor. J Neuropathol Exp Neurol 64:295-303.

Niebroj-Dobosz I, Janik P, Sokołowska B, Kwiecinski H. (2010) Matrix metalloproteinases and their tissue inhibitors in serum and cerebrospinal fluid of patients with amyotrophic lateral sclerosis. Eur J Neurol. 17(2):226-31.

Nigro P, Satoh K, O'Dell MR, Soe NN, et al. (2011) Cyclophilin A is an inflammatory mediator that promotes atherosclerosis in apolipoprotein E-deficient mice. J Exp Med. 17;208(1):53-66.

Nishihara JC, Champion KM. (2002) Quantitative evaluation of proteins in one- and two-dimensional polyacrylamide gels using a fluorescent stain. Electrophoresis. 23(14):2203-15.

Nishimoto Y, Ito D, Yagi T, Nihei Y, Tsunoda Y, Suzuki N. (2010) Characterization of alternative isoforms and inclusion body of the TAR DNA-binding protein-43. J Biol Chem. 285(1):608-19.

Nishimura AL, Al-Chalabi A, Zatz M. (2005) A common founder for amyotrophic lateral sclerosis type 8 (ALS8) in the Brazilian population. Hum Genet. 118(3-4):499-500.

Nishimura AL, Mitne-Neto M, Silva HC, Richieri-Costa A, et al. (2004) A mutation in the vesicle-trafficking protein VAPB causes late-onset spinal muscular atrophy and amyotrophic lateral sclerosis. Am J Hum Genet. 75(5):822-31.

Niwa J, Ishigaki S, Hishikawa N, Yamamoto M, et al. (2002) Dorfin ubiquitylates mutant SOD1 and prevents mutant SOD1-mediated neurotoxicity. J Biol Chem. 277(39):36793-8.

Nonaka T, Kametani F, Arai T, Akiyama H, Hasegawa M. (2009) Truncation and pathogenic mutations facilitate the formation of intracellular aggregates of TDP-43. Hum Mol Genet. 18(18):3353-64.

Noto Y, Shibuya K, Sato Y, Kanai K, et al. (2011) Elevated CSF TDP-43 levels in amyotrophic lateral sclerosis: specificity, sensitivity, and a possible prognostic value. Amyotroph Lateral Scler. 12(2):140-3.

Nygren I, Larsson A, Johansson A, Askmark H. (2002) VEGF is increased in serum but not in spinal cord from patients with amyotrophic lateral sclerosis. Neuroreport. 13(17):2199-201.

Ogaki K, Li Y, Takanashi M, Ishikawa KI, et al. (2012) Analyses of the MAPT, PGRN, and C9orf72 mutations in Japanese patients with FTLD, PSP, and CBS. Parkinsonism Relat Disord.

Ogura T, Wilkinson AJ. (2001) AAA+ superfamily ATPases: common structure--diverse function. Genes Cells. 6(7):575-97.

Oh YK, Shin KS, Kang SJ. (2006) AIF translocates to the nucleus in the spinal motor neurons in a mouse model of ALS. Neurosci Lett. 406(3):205-10.

Okado-Matsumoto A, Fridovich I. (2002) Amyotrophic lateral sclerosis: a proposed mechanism. Proc Natl Acad Sci U S A. 99(13):9010-4.

Okado-Matsumoto A, Fridovich I. (2001) Subcellular distribution of superoxide dismutases (SOD) in rat liver: Cu,Zn-SOD in mitochondria. J Biol Chem. 276(42):38388-93.

Okamoto K, Fujita Y, Mizuno Y. (2010) Pathology of protein synthesis and degradation systems in ALS. Neuropathology. 30(2):189-93.

Okamoto K, Mizuno Y, Fujita Y. (2008) Bunina bodies in amyotrophic lateral sclerosis. Neuropathology. 28(2):109-15.

Okamoto Y, Ihara M, Urushitani M, Yamashita H, Kondo T, et al. (2011) An autopsy case of SOD1-related ALS with TDP-43 positive inclusions. Neurology. 77(22):1993-5.

O'Keefe SJ, Tamura J, Kincaid RL, Tocci MJ, O'Neill EA. (1992) FK-506- and CsA-sensitive activation of the interleukin-2 promoter by calcineurin. Nature. 357(6380):692-4.

Okuda B, Yamamoto T, Yamasaki M, Maya K, Imai T. (1992) Motor neuron disease with slow eye movements and vertical gaze palsy. Acta Neurol Scand, 85:71-76.

Oosthuyse B, Moons L, Storkebaum E, Beck H, et al. (2001) Deletion of the hypoxia-response element in the vascular endothelial growth factor promoter causes motor neuron degeneration. Nat Genet. 28(2):131-8.

Oppenheim RW. (1996) Neurotrophic survival molecules for motoneurons: an embarrassment of riches. Neuron. 17(2):195-7.

Orlacchio A, Babalini C, Borreca A, Patrono C, et al. (2010) SPATACSIN mutations cause autosomal recessive juvenile amyotrophic lateral sclerosis. Brain. 133(Pt 2):591-8.

Orrell RW. (2000) Amyotrophic lateral sclerosis: copper/zinc superoxide dismutase (SOD1) gene mutations. Neuromuscul Disord. 10(1):63-8. Review.

Orrell RW, Lane RJ, Ross M. (2007) Antioxidant treatment for amyotrophic lateral sclerosis / motor neuron disease. Cochrane Database Syst Rev. (1):CD002829.

Osawa T, Mizuno Y, Fujita Y, Takatama M, et al. (2011) Optineurin in neurodegenerative diseases. Neuropathology. 31(6):569-74.

Otomo A, Hadano S, Okada T, Mizumura H, et al. (2003) ALS2, a novel guanine nucleotide exchange factor for the small GTPase Rab5, is implicated in endosomal dynamics. Hum Mol Genet. 12(14):1671-87.

O'Toole O, Traynor BJ, Brennan P, Sheehan C, et al. (2008) Epidemiology and clinical features of amyotrophic lateral sclerosis in Ireland between 1995 and 2004. J Neurol Neurosurg Psychiatry. 79(1):30-2.

Ou SH, Wu F, Harrich D, García-Martínez LF, Gaynor RB. (1995) Cloning and characterization of a novel cellular protein, TDP-43, that binds to human immunodeficiency virus type 1 TAR DNA sequence motifs. J Virol. 69(6):3584-96.

Ou WB, Luo W, Park YD, Zhou HM. (2001) Chaperone-like activity of peptidyl-prolyl cis-trans isomerase during creatine kinase refolding. Protein Sci. 10(11):2346-53.

Owsianka AM, Patel AH. (1999) Hepatitis C virus core protein interacts with a human DEAD box protein DDX3. Virology. 257(2):330-40.

Pacher P, Beckman JS, Liaudet L (2007) Nitric oxide and peroxynitrite in health and disease. Physiol Rev, 87 (1):315-424.

Paisán-Ruiz C, Guevara R, Federoff M, Hanagasi H, et al. (2010) Early-onset L-dopa-responsive parkinsonism with pyramidal signs due to ATP13A2, PLA2G6, FBXO7 and spatacsin mutations. Mov Disord. 25(12):1791-800.

Pan H, Luo C, Li R, Qiao A, Zhang L, et al. (2008) Cyclophilin A is required for CXCR4-mediated nuclear export of heterogeneous nuclear ribonucleoprotein A2, activation and nuclear translocation of ERK1/2, and chemotactic cell migration. J Biol Chem, 283(1):623-37.

Pandey UB, Nie Z, Batlevi Y, McCray BA, Ritson GP, et al. (2007) HDAC6 rescues neurodegeneration and provides an essential link between autophagy and the UPS. Nature. 447(7146):859-63.

Pankiv S, Clausen TH, Lamark T, Brech A, et al. (2007) p62/SQSTM1 binds directly to Atg8/LC3 to facilitate degradation of ubiquitinated protein aggregates by autophagy. J Biol Chem. 282(33):24131-45.

Pappin DJ, Hojrup P, Bleasby AJ. (1993) Rapid identification of proteins by peptide-mass fingerprinting. Curr Biol, 3(6):327-32.

Parkinson N, Ince PG, Smith MO, Highley R, et al; MRC Proteomics in ALS Study; FReJA Consortium. (2006) ALS phenotypes with mutations in CHMP2B (charged multivesicular body protein 2B). Neurology. 67(6):1074-7.

Parsell DA, Lindquist S. (1993) The function of heat-shock proteins in stress tolerance: degradation and reactivation of damaged proteins. Annu Rev Genet. 27:437-96.

Pasinelli P, Belford ME, Lennon N, Bacskai BJ, Hyman BT, et al. (2004) Amyotrophic lateral sclerosis-associated SOD1 mutant proteins bind and aggregate with Bcl-2 in spinal cord mitochondria. Neuron. 43(1):19-30.

Pasinelli P, Borchelt DR, Houseweart MK, Cleveland DW, Brown RH Jr. (1998) Caspase-1 is activated in neural cells and tissue with amyotrophic lateral sclerosis-associated mutations in copper-zinc superoxide dismutase. Proc Natl Acad Sci U S A. 95(26):15763-8.

Pasinelli P, Brown RH. (2006) Molecular biology of amyotrophic lateral sclerosis: insights from genetics. Nat Rev Neurosci. 7(9):710-23.

Pasinetti GM, Ungar LH, Lange DJ, Yemul S, Deng H, Yu et al. (2006) Identification of potential CSF biomarkers in ALS. Neurology. 66(8):1218-22.

Patel YJ, Payne Smith MD, de Belleroche J, Latchman DS. (2005) Hsp27 and Hsp70 administered in combination have a potent protective effect against FALS-associated SOD1-mutant-induced cell death in mammalian neuronal cells. Brain Res Mol Brain Res. 134(2):256-74.

Patten BM, Harati Y, Acosta L, Jung SS, Felmus MT. (1978) Free amino acid levels in amyotrophic lateral sclerosis. Ann Neurol.3(4):305-9.

Pearson JP, Williams NM, Majounie E, Waite A, Stott J, et al. (2011) Familial frontotemporal dementia with amyotrophic lateral sclerosis and a shared haplotype on chromosome 9p. J Neurol. 258(4):647-55.

Pemberton TJ. (2006) Identification and comparative analysis of sixteen fungal peptidyl-prolyl cis/trans isomerase repertoires. BMC Genomics,7:244.

Peviani M, Caron I, Pizzasegola C, Gensano F, Tortarolo M, Bendotti C. (2010) Unraveling the complexity of amyotrophic lateral sclerosis: recent advances from the transgenic mutant SOD1 mice. CNS Neurol Disord Drug Targets. 9(4):491-503.

Phukan J, Elamin M, Bede P, Jordan N, Gallagher L, et al. (2012) The syndrome of cognitive impairment in amyotrophic lateral sclerosis: a population-based study. J Neurol Neurosurg Psychiatry. 83(1):102-8.

Phukan J, Pender NP, Hardiman O. (2007) Cognitive impairment in amyotrophic lateral sclerosis. Lancet Neurol. 6(11):994-1003.

Piao YS, Wakabayashi K, Kakita A, Yamada M, Hayashi S, et al. (2003) Neuropathology with clinical correlations of sporadic amyotrophic lateral sclerosis: 102 autopsy cases examined between 1962 and 2000. Brain Pathol. 13(1):10-22.

Piotukh K, Gu W, Kofler M, Labudde D, Helms V, Freund C. (2005) Cyclophilin A binds to linear peptide motifs containing a consensus that is present in many human proteins. J Biol Chem. (25):23668-74.

Pisitkun T, Shen RF, Knepper MA. (2004) Identification and proteomic profiling of exosomes in human urine. Proc Natl Acad Sci U S A. 101(36):13368-73.

Pokrishevsky E, Grad LI, Yousefi M, Wang J, et al. (2012) Aberrant localization of FUS and TDP43 is associated with misfolding of SOD1 in amyotrophic lateral sclerosis. PLoS One. 7(4):e35050.

Polkey MI, Lyall RA, Moxham J, Leigh PN. (1999) Respiratory aspects of neurological disease. J Neurol Neurosurg Psychiatry, 66:5-15.

Polymenidou M, Lagier-Tourenne C, Hutt KR, Bennett CF, Cleveland DW, Yeo GW. (2012) Misregulated RNA processing in amyotrophic lateral sclerosis. Brain Res. 1462:3-15.

Polymenidou M, Lagier-Tourenne C, Hutt KR, Huelga SC, Moran J, et al. (2011) Long pre-mRNA depletion and RNA missplicing contribute to neuronal vulnerability from loss of TDP-43. Nat Neurosci. 14(4):459-68.

Praline J, Blasco H, Vourc'h P, Garrigue MA, Gordon PH, et al; French ALS Study Group. (2011) APOE ε4 allele is associated with an increased risk of bulbar-onset amyotrophic lateral sclerosis in men. Eur J Neurol. 18(8):1046-52.

Praline J, Blasco H, Vourc'h P, Rat V, Gendrot C, et al; French ALS Study Group. (2012) Study of the HFE gene common polymorphisms in French patients with sporadic amyotrophic lateral sclerosis. J Neurol Sci. 317(1-2):58-61.

Pramatarova A, Laganière J, Roussel J, Brisebois K, Rouleau GA. (2001) Neuron-specific expression of mutant superoxide dismutase 1 in transgenic mice does not lead to motor impairment. J Neurosci. 21(10):3369-74.

Pullen AH, Humphreys P. (2000) Ultrastructural analysis of spinal motoneurones from mice treated with IgG from ALS patients, healthy individuals, or disease controls. J Neurol Sci. 180(1-2):35-45.

Puls I, Jonnakuty C, LaMonte BH, Holzbaur EL, Tokito M, M et al. (2003) Mutant dynactin in motor neuron disease. Nat Genet. 33(4):455-6.

Pushkarsky T, Zybarth G, Dubrovsky Ll, Yurchenko V, Tang H, et al. (2001) CD147 facilitates HIV-1 infection by interacting with virus-associated cyclophilin A. Proceedings of the National Academy of Sciences U S A, 98:6360–65.

Raaphorst J, de Visser M, Linssen WH, de Haan RJ, Schmand B. (2010) The cognitive profile of amyotrophic lateral sclerosis: A meta-analysis. Amyotroph Lateral Scler. 11(1-2):27-37.

Rabin SJ, Kim JM, Baughn M, Libby RT, Kim YJ, et al. (2010) Sporadic ALS has compartment-specific aberrant exon splicing and altered cell-matrix adhesion biology. Hum Mol Genet. 19(2):313-28.

Rademakers R, Stewart H, Dejesus-Hernandez M, Krieger C, Graff-Radford N, et al. (2010) Fus gene mutations in familial and sporadic amyotrophic lateral sclerosis. Muscle Nerve. 42(2):170-6.

Raimondi A, Mangolini A, Rizzardini M, Tartari S, Massari S, et al. (2006) Cell culture models to investigate the selective vulnerability of motoneuronal mitochondria to familial ALS-linked G93ASOD1. Eur J Neurosci 24:387-399

Rajalingam K, Rudel T. (2005) Ras-Raf signaling needs prohibitin. Cell Cycle. 4(11):1503-5.

Ranganathan S, Williams E, Ganchev P, Gopalakrishnan V, Lacomis D, et al. (2005) Proteomic profiling of cerebrospinal fluid identifies biomarkers for amyotrophic lateral sclerosis. J Neurochem. 95(5):1461-71.

Rao SD, Weiss JH. (2004) Excitotoxic and oxidative cross-talk between motor neurons and glia in ALS pathogenesis. Trends Neurosci. 27(1):17-23.

Rappsilber J, Ryder U, Lamond AI, Mann M. (2002) Large-scale proteomic analysis of the human spliceosome. Genome Res, 12:1231-45.

Ratajczak T, Ward BK, Minchin RF. (2003) Immunophilin chaperones in steroid receptor signalling. Curr Top Med Chem. 3(12):1348-57.

Rautajoki K, Nyman TA, Lahesmaa R. (2004) Proteome characterization of human T helper 1 and 2 cells. Proteomics. 4(1):84-92.

Ray SS, Nowak RJ, Strokovich K, Brown RH Jr, et al. (2004) An intersubunit disulfide bond prevents in vitro aggregation of a superoxide dismutase-1 mutant linked to familial amytrophic lateral sclerosis. Biochemistry. 43(17):4899-905.

Reaume AG, Elliott JL, Hoffman EK, Kowall NW, Ferra et al. (1996) Motor neurons in Cu/Zn superoxide dismutase-deficient mice develop normally but exhibit enhanced cell death after axonal injury. Nat Genet. 13(1):43-7.

Reddy PA, Atreya CD. (1999) Identification of simian cyclophilin A as a calreticulin-binding protein in yeast two-hybrid screen and demonstration of cyclophilin A interaction with calreticulin. Int J Biol Macromol. 25(4):345-51.

Redell JB, Zhao J, Dash PK. (2007) Acutely increased cyclophilin A expression after brain injury: a role in blood-brain barrier function and tissue preservation. J Neurosci Res.85(9):1980-8.

Reed NA, Cai D, Blasius TL, Jih GT, Meyhofer E, et al. (2006) Microtubule acetylation promotes kinesin-1 binding and transport. Curr Biol. 16(21):2166-72.

Reid E, Kloos M, Ashley-Koch A, Hughes L, Bevan S, et al. (2002) A kinesin heavy chain (KIF5A) mutation in hereditary spastic paraplegia (SPG10). Am J Hum Genet. 71(5):1189-94.

Renton AE, Majounie E, Waite A, Simón-Sánchez J, Rollinson S, et al. (2011) A hexanucleotide repeat expansion in C9ORF72 is the cause of chromosome 9p21-linked ALS-FTD. Neuron. 72(2):257-68.

Ricci C, Battistini S, Cozzi L, Benigni M, Origone P, et al. (2011) Lack of association of PON polymorphisms with sporadic ALS in an Italian population. Neurobiol Aging. 32(3):552.e7-13.

Richardson J.S. (1981) The anatomy and taxonomy of protein structure. Adv Protein Chem. 34: 167-339.

Ritson GP, Custer SK, Freibaum BD, Guinto JB, Geffel D, et al. (2010) TDP-43 mediates degeneration in a novel Drosophila model of disease caused by mutations in VCP/p97. J Neurosci. 30(22):7729-39.

Rizzardini M, Lupi M, Mangolini A, Babetto E, Ubezio P, Cantoni L. (2006) Neurodegeneration induced by complex I inhibition in a cellular model of familial amyotrophic lateral sclerosis. Brain Res Bull. 69(4):465-74.

Ro LS, Lai SL, Chen CM, Chen ST. (2003) Deleted 4977-bp mitochondrial DNA mutation is associated with sporadic amyotrophic lateral sclerosis: a hospital-based case-control study. Muscle Nerve. 28(6):737-43.

Robberecht W, Aguirre T, Van den Bosch L, Tilkin P, et al. (1996) D90A heterozygosity in the SOD1 gene is associated with familial and apparently sporadic amyotrophic lateral sclerosis. Neurology. 47(5):1336-9.

Robertson J, Beaulieu JM, Doroudchi MM, Durham HD, et al. (2001) Apoptotic death of neurons exhibiting peripherin aggregates is mediated by the proinflammatory cytokine tumor necrosis factor-alpha. J Cell Biol. 155(2):217-26.

Robertson J, Kriz J, Nguyen MD, Julien JP. (2002) Pathways to motor neuron degeneration in transgenic mouse models. Biochimie. 84(11):1151-60.

Robertson J, Sanelli T, Xiao S, Yang W, Horne P, et al. (2007) Lack of TDP-43 abnormalities in mutant SOD1 transgenic mice shows disparity with ALS. Neurosci Lett. 420(2):128-32.

Rollinson S, Mead S, Snowden J, Richardson A, Rohrer J, et al. (2011) Frontotemporal lobar degeneration genome wide association study replication confirms a risk locus shared with amyotrophic lateral sclerosis. Neurobiol Aging. 32(4):758.e1-7.

Rooke K, Figlewicz DA, Han FY, Rouleau GA. (1996) Analysis of the KSP repeat of the neurofilament heavy subunit in familiar amyotrophic lateral sclerosis. Neurology. 46(3):789-90.

Rosen DR, Siddique T, Patterson D, Figlewicz DA, Sapp P, et al. (1993) Mutations in Cu/Zn superoxide dismutase gene are associated with familial amyotrophic lateral sclerosis. Nature. 364(6435):362

Rosengren LE, Karlsson JE, Karlsson JO, Persson LI, Wikkelsø C. (1996) Patients with amyotrophic lateral sclerosis and other neurodegenerative diseases have increased levels of neurofilament protein in CSF. J Neurochem. 67(5):2013-8.

Ross OA, Rutherford NJ, Baker M, Soto-Ortolaza AI, Carrasquillo MM, et al. (2011) Ataxin-2 repeat-length variation and neurodegeneration. Hum Mol Genet. 20(16):3207-12.

Rossner S, Fuchsbrunner K, Lange-Dohna C, Hartlage-Rübsamen M, Bigl V, et al. (2004) Munc13-1-mediated vesicle priming contributes to secretory amyloid precursor protein processing. J Biol Chem. 279(27):27841-4.

Rothstein JD, Tsai G, Kuncl RW, Clawson L, Cornblath DR, et al. (1990) Abnormal excitatory amino acid metabolism in amyotrophic lateral sclerosis. Ann Neurol. 28(1):18-25.

Rothstein JD, Van Kammen M, Levey AI, Martin LJ, Kuncl RW. (1995) Selective loss of glial glutamate transporter GLT-1 in amyotrophic lateral sclerosis. Ann Neurol. 38(1):73-84.

Rowland LP. (2001) How Amyotrophic Lateral Sclerosis Got Its Name: The Clinical-Pathologic Genius of Jean-Martin Charcot. Arch Neurol, 58:512-515.

Rowland LP, Shneider NA. (2001) Amyotrophic lateral sclerosis. N Engl J Med. 344(22):1688-700.

Rubino E, Rainero I, Chiò A, Rogaeva E, Galimberti D, et al; For the TODEM Study Group. (2012) SQSTM1 mutations in frontotemporal lobar degeneration and amyotrophic lateral sclerosis. Neurology.

Russell AP, Wada S, Vergani L, Hock MB, Lamon S, et al. (2012) Disruption of skeletal muscle mitochondrial network genes and miRNAs in amyotrophic lateral sclerosis. Neurobiol Dis.

Rutherford AC, Traer C, Wassmer T, Pattni K, et al. (2006) The mammalian phosphatidylinositol 3-phosphate 5-kinase (PIKfyve) regulates endosome-to-TGN retrograde transport. J Cell Sci. 119(Pt 19):3944-57.

Ryberg H, An J, Darko S, Lustgarten JL, Jaffa M, et al. (2010) Discovery and verification of amyotrophic lateral sclerosis biomarkers by proteomics. Muscle Nerve. 42(1):104-11.

Rycyzyn MA, Reilly SC, O'Malley K, Clevenger CV. (2000) Role of cyclophilin B in prolactin signal transduction and nuclear retrotranslocation. Mol Endocrinol, 14(8):1175-86.

Sadoul K, Wang J, Diagouraga B, Khochbin S. (2011) The tale of protein lysine acetylation in the cytoplasm. J Biomed Biotechnol. 2011:970382.

Saeed M, Siddique N, Hung WY, Usacheva E, et al. (2006) Paraoxonase cluster polymorphisms are associated with sporadic ALS. Neurology. 67(5):771-6.

Salinas S, Proukakis C, Crosby A, Warner TT. (2008) Hereditary spastic paraplegia: clinical features and pathogenetic mechanisms. Lancet Neurol. 7(12):1127-38.

Sapp PC, Hosler BA, McKenna-Yasek D, Chin W, et al. (2003) Identification of two novel loci for dominantly inherited familial amyotrophic lateral sclerosis. Am J Hum Genet. 73(2):397-403.

Sargsyan SA, Monk PN, Shaw PJ. (2005) Microglia as potential contributors to motor neuron injury in amyotrophic lateral sclerosis. Glia. 51(4):241-53.

Sarkar P, Reichman C, Saleh T, Birge RB, Kalodimos CG. (2007) Proline cis-trans isomerization controls autoinhibition of a signaling protein. Mol Cell. 25(3):413-26.

Sasabe J, Chiba T, Yamada M, Okamoto K, et al. (2007) D-serine is a key determinant of glutamate toxicity in amyotrophic lateral sclerosis. EMBO J. 26(18):4149-59.

Sasaki S, Iwata M. (1996) Impairment of fast axonal transport in the proximal axons of anterior horn neurons in amyotrophic lateral sclerosis. Neurology. 47(2):535-40.

Sasaki S, Maruyama S (1991) Immunocytochemical and ultrastructural studies of hyaline inclusions in sporadic motor neuron disease. Acta Neuropathol. 82(4):295-301.

Sasaki S, Tsutsumi Y, Yamane K, Sakuma H, Maruyama S (1992) Sporadic amyotrophic lateral sclerosis with extensive neurological involvement. Acta Neuropathol, 84:211-215.

Sasaki S, Warita H, Murakami T, Abe K, Iwata M. (2004) Ultrastructural study of mitochondria in the spinal cord of transgenic mice with a G93A mutant SOD1 gene. Acta Neuropathol. 107(5):461-74.

Sato T, Takeuchi S, Saito A, Ding W, et al. (2009) Axonal ligation induces transient redistribution of TDP-43 in brainstem motor neurons. Neuroscience. 164(4):1565-78.

Satoh K, Nigro P, Matoba T, O'Dell MR, et al. (2009) Cyclophilin A enhances vascular oxidative stress and the development of angiotensin II-induced aortic aneurysms. Nat Med. 15(6):649-56.

Sato-Harada R, Okabe S, Umeyama T, Kanai Y, Hirokawa N. (1996) Microtubule-associated proteins regulate microtubule function as the track for intracellular membrane organelle transports. Cell Struct Funct. 21(5):283-95.

Sau D, De Biasi S, Vitellaro-Zuccarello L, Riso P, et al. (2007) Mutation of SOD1 in ALS: a gain of a loss of function. Hum Mol Genet. 16(13):1604-18.

Sawyer L. (1987) Protein structure. One fold among many. Nature. 327(6124): 659.

Schiene C and Fischer G. (2000) Enzymes that catalyse the restructuring of proteins. Curr Opin Struct Biol, 10:40-5.

Schlegel J, Redzic JS, Porter CC, Yurchenko V, Bukrinsky M, Labeikovsky W, Armstrong GS, Zhang F, Isern NG, DeGregori J, Hodges R, Eisenmesser EZ. (2009) Solution characterization of the extracellular region of CD147 and its interaction with its enzyme ligand cyclophilin A. J Mol Biol. 391(3):518-35.

Schmid FX. (1995) Protein folding. Prolyl isomerases join the fold. Curr Biol, 5:993-4.

Schmitt-John T, Drepper C, Mussmann A, Hahn P, et al. (2005) Mutation of Vps54 causes motor neuron disease and defective spermiogenesis in the wobbler mouse. Nat Genet 37:1213-1215.

Schochet SS Jr, Hardman JM, Ladewig PP, Earle KM. (1969) Intraneuronal conglomerates in sporadic motor neuron disease. A light and electron microscopic study. Arch Neurol. 20(5):548-53.

Sebastià J, Kieran D, Breen B, King MA, et al. (2009) Angiogenin protects motoneurons against hypoxic injury. Cell Death Differ. 16(9):1238-47.

Seibenhener ML, Babu JR, Geetha T, Wong HC, et al. (2004) Sequestosome 1/p62 is a polyubiquitin chain binding protein involved in ubiquitin proteasome degradation. Mol Cell Biol. 24(18):8055-68.

Seizer P, Schönberger T, Schött M, Lang MR, et al. (2010) EMMPRIN and its ligand cyclophilin A regulate MT1-MMP, MMP-9 and M-CSF during foam cell formation. Atherosclerosis. 209(1):51-7.

Sekizawa T, Openshaw H, Ohbo K, Sugamura K, et al. (1998) Cerebrospinal fluid interleukin 6 in amyotrophic lateral sclerosis: immunological parameter and comparison with inflammatory and non-inflammatory central nervous system diseases. J Neurol Sci. 154(2):194-9.

Seko Y, Fujimura T, Taka H, Mineki R, et al. (2004) Hypoxia followed by reoxygenation induces secretion of cyclophilin A from cultured rat cardiac myocytes. Biochem Biophys Res Commun. 317(1):162-8.

Seo S, Baye LM, Schulz NP, Beck JS, et al. (2010) BBS6, BBS10, and BBS12 form a complex with CCT/TRiC family chaperonins and mediate BBSome assembly. Proc Natl Acad Sci U S A. 107(4):1488-93.

Sephton CF, Cenik C, Kucukural A, Dammer EB, et al. (2011) Identification of neuronal RNA targets of TDP-43-containing ribonucleoprotein complexes. J Biol Chem. 286(2):1204-15.

Shan X, Vocadlo D, Krieger C. (2009) Mislocalization of TDP-43 in the G93A mutant SOD1 transgenic mouse model of ALS. Neurosci Lett. 458(2):70-4.

Shaw BF, Valentine JS. (2007) How do ALS-associated mutations in superoxide dismutase 1 promote aggregation of the protein? Trends Biochem Sci. 32(2):78-85.

Shaw G, Morse S, Ararat M, Graham FL. (2002) Preferential transformation of human neuronal cells by human adenoviruses and the origin of HEK 293 cells. FASEB J.16(8):869-71.

Shaw PJ, Forrest V, Ince PG, Richardson JP, Wastell HJ. (1995) CSF and plasma amino acid levels in motor neuron disease: elevation of CSF glutamate in a subset of patients. Neurodegeneration. 4(2):209-16.

Shen M, Stukenberg PT, Kirschner MW, Lu KP (1998) The essential mitotic peptidyl±prolyl isomerase Pin1 binds and regulates mitosis-specific phosphoproteins. Genes Dev, 12:706-20.

Sherry B, Yarlett N, Strupp A, Cerami A. (1992) Identification of cyclophilin as a proinflammatory secretory product of lipopolysaccharide-activated macrophages. Proc Natl Acad Sci U S A. 89(8):3511-5.

Shibata N, Hirano A, Kobayashi M, Siddique T, et al. (1996) Intense superoxide dismutase-1 immunoreactivity in intracytoplasmic hyaline inclusions of familial amyotrophic lateral sclerosis with posterior column involvement. J Neuropathol Exp Neurol. 55(4):481-90.

Shibata N, Kakita A, Takahashi H, Ihara Y, et al. (2009) Persistent cleavage and nuclear translocation of apoptosis-inducing factor in motor neurons in the spinal cord of sporadic amyotrophic lateral sclerosis patients. Acta Neuropathol. 118(6):755-62.

Shibata N, Nagai R, Uchida K, Horiuchi S, et al. (2001) Morphological evidence for lipid peroxidation and protein glycoxidation in spinal cords from sporadic amyotrophic lateral sclerosis patients. Brain Res. 917(1):97-104.

Shinder GA, Lacourse MC, Minotti S, Durham HD. (2001) Mutant Cu/Zn-superoxide dismutase proteins have altered solubility and interact with heat shock/stress proteins in models of amyotrophic lateral sclerosis. J Biol Chem. 276(16):12791-6.

Shiraishi S, Yokoo H, Kobayashi H, Yanagita T, et al. (2000) Post-translational reduction of cell surface expression of insulin receptors by cyclosporin A, FK506 and rapamycin in bovine adrenal chromaffin cells. Neurosci Lett. 293(3):211-5.

Siciliano G, Piazza S, Carlesi C, Del Corona A, Franzini M, Pompella A, Malvaldi G, Mancuso M, Paolicchi A, Murri L. (2007) Antioxidant capacity and protein oxidation in cerebrospinal fluid of amyotrophic lateral sclerosis. J Neurol. 254(5):575-80.

Siddique T, Deng HX. (1996) Genetics of amyotrophic lateral sclerosis Hum Mol Genet, 5 Spec No:1465-70.

Siddique T, Hentati A. (1995) Familial amyotrophic lateral sclerosis. Clin Neurosci. 3(6):338-47.

Siklós L, Engelhardt J, Harati Y, Smith RG, et al. (1996) Ultrastructural evidence for altered calcium in motor nerve terminals in amyotropic lateral sclerosis. Ann Neurol. 39(2):203-16.

Siklós L, Engelhardt JI, Alexianu ME, Gurney ME, et al. (1998) Intracellular calcium parallels motoneuron degeneration in SOD-1 mutant mice. J Neuropathol Exp Neurol. 57(6):571-87.

Silani V, Messina S, Poletti B, Morelli C, et al. (2011) The diagnosis of Amyotrophic lateral sclerosis in 2010. Arch Ital Biol. 149(1):5-27.

Simpson CL, Lemmens R, Miskiewicz K, Broom WJ, et al. (2009) Variants of the elongator protein 3 (ELP3) gene are associated with motor neuron degeneration. Hum Mol Genet. 18(3):472-81.

Simpson EP, Henry YK, Henkel JS, Smith RG, Appel SH. (2004) Increased lipid peroxidation in sera of ALS patients: a potential biomarker of disease burden. Neurology. 62(10):1758-65.

Skibinski G, Parkinson NJ, Brown JM, Chakrabarti L, et al. (2005) Mutations in the endosomal ESCRTIII-complex subunit CHMP2B in frontotemporal dementia. Nat Genet. 37(8):806-8

Slowik A, Tomik B, Wolkow PP, Partyka D, et al. (2006) Paraoxonase gene polymorphisms and sporadic ALS. Neurology. 67(5):766-70.

Smajlović A, Berbić S, Schiene-Fischer C, Tusek-Znidaric M, et al. (2009) Essential role of Pro 74 in stefin B amyloid-fibril formation: dual action of cyclophilin A on the process. FEBS Lett. 583(7):1114-20.

Smith BD, Raines RT. (2006) Genetic selection for critical residues in ribonucleases. J Mol Biol. 362(3):459-78.

Smith RG, Henry YK, Mattson MP, Appel SH. (1998) Presence of 4-hydroxynonenal in cerebrospinal fluid of patients with sporadic amyotrophic lateral sclerosis. Ann Neurol. 44(4):696-9.

Sofola OA, Jin P, Qin Y, Duan R, et al. (2007) RNA-binding proteins hnRNP A2/B1 and CUGBP1 suppress fragile X CGG premutation repeat-induced neurodegeneration in a Drosophila model of FXTAS. Neuron. 55(4):565-71.

Sokolskaja E, Sayah DM, Luban J. (2004) Target cell cyclophilin A modulates human immunodeficiency virus type 1 infectivity. J Virol. 78(23):12800-8.

Song J, Lu YC, Yokoyama K, Rossi J, Chiu R. (2004) Cyclophilin A is required for retinoic acid-induced neuronal differentiation in p19 cells. J Biol Chem. 279(23):24414-9.

Sorarú G, Orsetti V, Buratti E, Baralle F, et al. (2010) TDP-43 in skeletal muscle of patients affected with amyotrophic lateral sclerosis. Amyotroph Lateral Scler.11(1-2):240-3.

Spalloni A, Pascucci T, Albo F, Ferrari F, et al. (2004) Altered vulnerability to kainate excitotoxicity of transgenic-Cu/Zn SOD1 neurones. Neuroreport 15:2477-2480.

Spina S, Van Laar AD, Murrell JR, Hamilton RL, Kof et al. (2012) Phenotypic variability in three families with valosin-containing protein mutation. Eur J Neurol.

Sreedharan J, Blair IP, Tripathi VB, Hu X, Van et al. (2008) TDP-43 mutations in familial and sporadic amyotrophic lateral sclerosis. Science, 319(5870):1668-72.

Stallings NR, Puttaparthi K, Luther CM, Burns DK, Elliott JL (2010) Progressive motor weakness in transgenic mice expressing human TDP-43. Neurobiol Dis. 40(2):404-14.

Steele JC. (2005) Parkinsonism-dementia complex of Guam. Mov Disord. 20 Suppl 12:S99-S107.

Steele JC, McGeer PL. (2008) The ALS/PDC syndrome of Guam and the cycad hypothesis. Neurology. 70(21):1984-90.

Steinacker P, Hendrich C, Sperfeld AD, Jesse S, et al. (2008) TDP-43 in cerebrospinal fluid of patients with frontotemporal lobar degeneration and amyotrophic lateral sclerosis. Arch Neurol.65(11):1481-7.

Steinmann B, Bruckner P, Superti-Furga A. (1991) Cyclosporin A slows collagen triple-helix formation in vivo: indirect evidence for a physiologic role of peptidyl-prolyl cis-trans-isomerase. J Biol Chem. 266(2):1299-303.

Stevanin G, Santorelli FM, Azzedine H, Coutinho P, et al. (2007) Mutations in SPG11, encoding spatacsin, are a major cause of spastic paraplegia with thin corpus callosum. Nat Genet. 39(3):366-72.

Stewart H, Rutherford NJ, Briemberg H, Krieger C, et al. (2012) Clinical and pathological features of amyotrophic lateral sclerosis caused by mutation in the C9ORF72 gene on chromosome 9p. Acta Neuropathol. 123(3):409-17

Stieber A, Gonatas JO, Gonatas NK. (2000) Aggregation of ubiquitin and a mutant ALS-linked SOD1 protein correlate with disease progression and fragmentation of the Golgi apparatus. J.Neurol Sci. 173(1):53-62.

Stokin GB, Lillo C, Falzone TL, Brusch RG, et al. (2005) Axonopathy and transport deficits early in the pathogenesis of Alzheimer's disease. Science. 307(5713):1282-8.

Storkebaum E, Lambrechts D, Dewerchin M, Moreno-Murciano MP, et al. (2005) Treatment of motoneuron degeneration by intracerebroventricular delivery of VEGF in a rat model of ALS. Nat Neurosci. 8(1):85-92.

Streblow DN, Kitabwalla M, Malkovsky M, Pauza CD. (1998) Cyclophilin A modulates processing of human immunodeficiency virus type 1 p55Gag: mechanism for antiviral effects of cyclosporin A. Virology, 245:197-202.

Ström AL, Gal J, Shi P, Kasarskis EJ, et al. (2008) Retrograde axonal transport and motor neuron disease. J Neurochem. 106(2):495-505.

Strong MJ. (2008) The syndromes of frontotemporal dysfunction in amyotrophic lateral sclerosis. Amyotroph Lateral Scler. 9(6):323-38.

Strong MJ, Grace GM, Freedman M, Lomen-Hoerth C, et al. (2009) Consensus criteria for the diagnosis of frontotemporal cognitive and behavioural syndromes in amyotrophic lateral sclerosis. Amyotroph Lateral Scler. 10(3):131-46.

Strong MJ, Kesavapany S, Pant HC. (2005) The pathobiology of amyotrophic lateral sclerosis: a proteinopathy? J Neuropathol Exp Neurol. 64(8):649-64.

Strong MJ, Volkening K, Hammond R, Yang W, et al. (2007) TDP43 is a human low molecular weight neurofilament (hNFL) mRNA-binding protein. Mol Cell Neurosci. 35(2):320-7.

Strong MJ. (2010) The evidence for altered RNA metabolism in amyotrophic lateral sclerosis (ALS). J Neurol Sci. 288(1-2):1-12.

Subramanian V, Crabtree B, Acharya KR. (2008) Human angiogenin is a neuroprotective factor and amyotrophic lateral sclerosis associated angiogenin variants affect neurite extension/pathfinding and survival of motor neurons. Hum Mol Genet. 17(1):130-49.

Subramanian V, Feng Y. (2007) A new role for angiogenin in neurite growth and pathfinding: implications for amyotrophic lateral sclerosis. Hum Mol Genet. 16(12):1445-53.

Suetsugu S, Miki H, Takenawa T. (2001) Identification of another actin-related protein (Arp) 2/3 complex binding site in neural Wiskott-Aldrich syndrome protein (N-WASP) that complements actin polymerization induced by the Arp2/3 complex activating (VCA) domain of N-WASP. J Biol Chem. 276(35):33175-80.

Sumi H, Kato S, Mochimaru Y, Fujimura H, et al. (2009) Nuclear TAR DNA binding protein 43 expression in spinal cord neurons correlates with the clinical course in amyotrophic lateral sclerosis. J Neuropathol Exp Neurol. 68(1):37-47.

Sumi H, Nagano S, Fujimura H, Kato S, Sakoda S. (2006) Inverse correlation between the formation of mitochondria-derived vacuoles and Lewy-body-like hyaline inclusions in G93A superoxide-dismutase-transgenic mice. Acta Neuropathol. 112(1):52-63.

Sun Z, Diaz Z, Fang X, Hart MP, et al. (2011) Molecular determinants and genetic modifiers of aggregation and toxicity for the ALS disease protein FUS/TLS. PLoS Biol. 9(4):e1000614.

Suraweera A, Becherel OJ, Chen P, Rundle N, et al. (2007) Senataxin, defective in ataxia oculomotor apraxia type 2, is involved in the defense against oxidative DNA damage. J Cell Biol. 177(6):969-79.

Susin SA, Lorenzo HK, Zamzami N, Marzo I, et al. (1999) Molecular characterization of mitochondrial apoptosis-inducing factor. Nature. 397(6718):441-6.

Sutedja NA, Fischer K, Veldink JH, van der Heijden GJ, et al. (2009) What we truly know about occupation as a risk factor for ALS: a critical and systematic review. Amyotroph Lateral Scler. 10(5-6):295-301.

Sutedja NA, Sinke RJ, Van Vught PW, Van der Linden MW, et al. (2007) The association between H63D mutations in HFE and amyotrophic lateral sclerosis in a Dutch population. Arch Neurol. 64(1):63-7.

Sutedja NA, Veldink JH, Fischer K, Kromhout H, et al. (2009) Exposure to chemicals and metals and risk of amyotrophic lateral sclerosis: a systematic review. Amyotroph Lateral Scler. 10(5-6):302-9.

Suzuki J, Jin ZG, Meoli DF, Matoba T, Berk BC. (2006) Cyclophilin A is secreted by a vesicular pathway in vascular smooth muscle cells. Circ Res. 98(6):811-7.

Suzuki M, Mikami H, Watanabe T, Yamano T, et al. (2010) Increased expression of TDP-43 in the skin of amyotrophic lateral sclerosis. Acta Neurol Scand.122(5):367-72.

Swash M, Desai J. (2000) Motor neuron disease: classification and nomenclature. Amyotroph Lateral Scler Other Motor Neuron Disord. 1(2):105-12.

Swash M, Leader M, Brown A, Swettenham KW. (1986) Focal loss of anterior horn cells in the cervical cord in motor neuron disease. Brain 109(Pt 5):939-952.

Swerdlow RH, Parks JK, Cassarino DS, Trimmer PA, et al. (1998) Mitochondria in sporadic amyotrophic lateral sclerosis. Exp Neurol. 153(1):135-42.

Syed F, Rycyzyn MA, Westgate L, Clevenger CV. (2003) A novel and functional interaction between cyclophilin A and prolactin receptor. Endocrine. 20(1-2):83-90.

Takeuchi H, Kobayashi Y, Ishigaki S, Doyu M, Sobue G. (2002) Mitochondrial localization of mutant superoxide dismutase 1 triggers caspase-dependent cell death in a cellular model of familial amyotrophic lateral sclerosis. J Biol Chem. 277(52):50966-72.

Tan CF, Eguchi H, Tagawa A, Onodera O, et al. (2007) TDP-43 immunoreactivity in neuronal inclusions in familial amyotrophic lateral sclerosis with or without SOD1 gene mutation. Acta Neuropathol. 113(5):535-42.

Tanaka H, Shimazaki H, Kimura M, Izuta H, et al. (2011) Apoptosis-inducing factor and cyclophilin A cotranslocate to the motor neuronal nuclei in amyotrophic lateral sclerosis model mice. CNS Neurosci Ther.17(5):294-304.

Tang Y, Zhao W, Chen Y, Zhao Y, Gu W. (2008) Acetylation is indispensable for p53 activation. Cell. 133(4):612-26.

Tateishi T, Hokonohara T, Yamasaki R, Miura S, et al. (2010) Multiple system degeneration with basophilic inclusions in Japanese ALS patients with FUS mutation. Acta Neuropathol. 119(3):355-64.

Tatom JB, Wang DB, Dayton RD, et al. (2009) Mimicking aspects of frontotemporal lobar degeneration and Lou Gehrig's disease in rats via TDP-43 overexpression. Mol Ther. 17(4):607-13

Tegeder I, Schumacher A, John S, Geiger H, et al. (1997) Elevated serum cyclophilin levels in patients with severe sepsis. J Clin Immunol. 17(5):380-6.

Teigelkamp S, Achsel T, Mundt C, Göthel SF, et al. (1998) The 20kD protein of human [U4/U6.U5] tri-snRNPs is a novel cyclophilin that forms a complex with the U4/U6-specific 60kD and 90kD proteins. RNA. 4(2):127-41.

Ticozzi N, LeClerc AL, Keagle PJ, Glass JD, et al. (2010) Paraoxonase gene mutations in amyotrophic lateral sclerosis. Ann Neurol. 68(1):102-7.

Ticozzi N, Ratti A, Silani V. (2010) Protein aggregation and defective RNA metabolism as mechanisms for motor neuron damage. CNS Neurol Disord Drug Targets. 9(3):285-96.

Ticozzi N, Vance C, Leclerc AL, Keagle P, Glass et al. (2011) Mutational analysis reveals the FUS homolog TAF15 as a candidate gene for familial amyotrophic lateral sclerosis. Am J Med Genet B Neuropsychiatr Genet. 156B(3):285-90.

Timchenko LT, Miller JW, Timchenko NA, DeVore DR, et al. (1996) Identification of a (CUG)n triplet repeat RNA-binding protein and its expression in myotonic dystrophy. Nucleic Acids Res. 24(22):4407-14.

Tobisawa S, Hozumi Y, Arawaka S, Koyama S, et al. (2003) Mutant SOD1 linked to familial amyotrophic lateral sclerosis, but not wild-type SOD1, induces ER stress in COS7 cells and transgenic mice. Biochem Biophys Res Commun. 303(2):496-503.

Todd PK, Paulson HL. (2010) RNA-mediated neurodegeneration in repeat expansion disorders. Ann Neurol. 67(3):291-300.

Tollervey JR, Curk T, Rogelj B, Briese M, et al. (2011) Characterizing the RNA targets and position-dependent splicing regulation by TDP-43. Nat Neurosci. 14(4):452-8.

Tomik B, Adamek D, Pierzchalski P, Banares S, et al. (2005) Does apoptosis occur in amyotrophic lateral sclerosis? TUNEL experience from human amyotrophic lateral sclerosis (ALS) tissues. Folia Neuropathol. 43(2):75-80.

Tomkins J, Usher P, Slade JY, Ince PG, et al. (1998) Novel insertion in the KSP region of the neurofilament heavy gene in amyotrophic lateral sclerosis (ALS). Neuroreport. 9(17):3967-70

Topp JD, Gray NW, Gerard RD, Horazdovsky BF. (2004) Alsin is a Rab5 and Rac1 guanine nucleotide exchange factor. J Biol Chem. 279(23):24612-23. Epub 2004 Mar 19.

Tortarolo M, Crossthwaite AJ, Conforti L, Spencer JP, et al. (2004) Expression of SOD1 G93A or wild-type SOD1 in primary cultures of astrocytes down-regulates the glutamate transporter GLT-1: lack of involvement of oxidative stress. J Neurochem 88:481-493.

Tortarolo M, Grignaschi G, Calvaresi N, Zennaro E, et al. (2006) Glutamate AMPA receptors change in motor neurons of SOD1G93A transgenic mice and their inhibition by a noncompetitive antagonist ameliorates the progression of amytrophic lateral sclerosis-like disease. J Neurosci Res. 83(1):134-46.

Towers GJ, Hatziioannou T, Cowan S, Goff SP, et al. (2003) Cyclophilin A modulates the sensitivity of HIV-1 to host restriction factors. Nat Med. 9(9):1138-43.

Tran D, Chalhoub A, Schooley A, Zhang W, Ngsee JK. (2012) A mutation in VAPB that causes amyotrophic lateral sclerosis also causes a nuclear envelope defect. J Cell Sci. 125(Pt 12):2831-6.

Tran PB, Miller RJ. (1999) Aggregates in neurodegenerative disease: crowds and power? Trends Neurosci. 22(5):194-7.

Tran TT, Dai W, Sarkar HK. (2000) Cyclosporin A inhibits creatine uptake by altering surface expression of the creatine transporter. J Biol Chem. 275(46):35708-14.

Traynor BJ, Nalls M, Lai SL, Gibbs RJ, et al. (2010) Kinesin-associated protein 3 (KIFAP3) has no effect on survival in a population-based cohort of ALS patients. Proc Natl Acad Sci U S A. 107(27):12335-8.

Troakes C, Hortobágyi T, Vance C, Al-Sarraj S, et al. (2012) Transportin 1 co-localisation with FUS inclusions is not characteristic for ALS-FUS confirming disrupted nuclear import of mutant FUS and distinguishing it from FTLD-FUS. Neuropathol Appl Neurobiol.

Troost D, van den Oord JJ, de Jong JM, Swaab DF. (1989) Lymphocytic infiltration in the spinal cord of patients with amyotrophic lateral sclerosis. Clin Neuropathol. 8(6):289-94.

Troost D, Van den Oord JJ, Vianney de Jong JM. (1990) Immunohistochemical characterization of the inflammatory infiltrate in amyotrophic lateral sclerosis. Neuropathol Appl Neurobiol. 16(5):401-10.

Trotti D, Rolfs A, Danbolt NC, Brown RH Jr, Hediger MA. (1999) SOD1 mutants linked to amyotrophic lateral sclerosis selectively inactivate a glial glutamate transporter. Nat Neurosci. 2(9):848.

Tudor EL, Perkinton MS, Schmidt A, Ackerley S, et al. (2005) ALS2/Alsin regulates Rac-PAK signaling and neurite outgrowth. J Biol Chem. 280(41):34735-40.

Turner BJ, Talbot K. (2008) Transgenics, toxicity and therapeutics in rodent models of mutant SOD1-mediated familial ALS. Prog Neurobiol. 85(1):94-134.

Turner MR, Grosskreutz J, Kassubek J, Abrahams S, et al; first Neuroimaging Symosium in ALS (NISALS). (2011) Towards a neuroimaging biomarker for amyotrophic lateral sclerosis. Lancet Neurol. 10(5):400-3.

Tyler HR, Shefner J. (1991) Amyotrophic lateral sclerosis. Handb Clin Neurol:169-215.

Uchino H, Elmér E, Uchino K, Lindvall O, Siesjö BK. (1995) Cyclosporin A dramatically ameliorates CA1 hippocampal damage following transient forebrain ischaemia in the rat. Acta Physiol Scand. 155(4):469-71.

Uittenbogaard A, Ying Y, Smart EJ. (1998) Characterization of a cytosolic heat-shock protein-caveolin chaperone complex. Involvement in cholesterol trafficking. J Biol Chem. 273(11):6525-32.

Unrath A, Ludolph AC, Kassubek J. (2011) Alterations of the corpus callosum as an MR imaging-based hallmark of motor neuron diseases. AJNR Am J Neuroradiol. 32(5):E90.

Urano Y, Iiduka M, Sugiyama A, Akiyama H, et al. (2006) Involvement of the mouse Prp19 gene in neuronal/astroglial cell fate decisions. J Biol Chem. 281(11):7498-514.

Valdmanis PN, Kabashi E, Dyck A, Hince P, et al. (2008) Association of paraoxonase gene cluster polymorphisms with ALS in France, Quebec, and Sweden. Neurology. 71(7):514-20.

Valentine JS. (2002) Do oxidatively modified proteins cause ALS? Free Radic Biol Med. 33(10):1314-20.

van Blitterswijk M, Blokhuis A, van Es MA, van Vught PW, et al. (2012) Rare and common paraoxonase gene variants in amyotrophic lateral sclerosis patients. Neurobiol Aging. 33(8):1845.e1-3.

van Blitterswijk M, Landers JE. (2010) RNA processing pathways in amyotrophic lateral sclerosis. Neurogenetics. 11(3):275-90.

van Blitterswijk M, van Es MA, Hennekam EA, Dooijes D, et al. (2012) Evidence for an oligogenic basis of amyotrophic lateral sclerosis. Hum Mol Genet. 21(17):3776-84.

van Blitterswijk M, van Es MA, Koppers M, van Rheenen W, et al. (2012) VAPB and C9orf72 mutations in 1 familial amyotrophic lateral sclerosis patient. Neurobiol Aging.

van Blitterswijk M, van Vught PW, van Es MA, Schelhaas HJ, et al. (2012) Novel optineurin mutations in sporadic amyotrophic lateral sclerosis patients. Neurobiol Aging. 33(5):1016.e1-7.

Van Damme P, Leyssen M, Callewaert G, Robberecht W, Van Den Bosch L. (2003) The AMPA receptor antagonist NBQX prolongs survival in a transgenic mouse model of amyotrophic lateral sclerosis. Neurosci Lett. 343(2):81-4.

Van Damme P, Veldink JH, van Blitterswijk M, Corveleyn A, et al. (2011) Expanded ATXN2 CAG repeat size in ALS identifies genetic overlap between ALS and SCA2. Neurology. 76(24):2066-72.

Van Deerlin VM, Leverenz JB, Bekris LM, Bird TD, et al. (2008) TARDBP mutations in amyotrophic lateral sclerosis with TDP-43 neuropathology: a genetic and histopathological analysis. Lancet Neurol. 7(5):409-16.

van der Zee J, Urwin H, Engelborghs S, Bruyland M, et al. (2008) CHMP2B C-truncating mutations in frontotemporal lobar degeneration are associated with an aberrant endosomal phenotype in vitro. Hum Mol Genet. 17(2):313-22.

van Es MA, Diekstra FP, Veldink JH, Baas F, et al. (2009) A case of ALS-FTD in a large FALS pedigree with a K17I ANG mutation. Neurology. 72(3):287-8.

van Es MA, Schelhaas HJ, van Vught PW, Ticozzi N, et al. (2011) Angiogenin variants in Parkinson disease and amyotrophic lateral sclerosis. Ann Neurol. 70(6):964-73

van Es MA, van Vught PW, Blauw HM, Franke L, et al. (2008) Genetic variation in DPP6 is associated with susceptibility to amyotrophic lateral sclerosis. Nat Genet. 40(1):29-31.

van Es MA, Veldink JH, Saris CG, Blauw HM, et al. (2009) Genome-wide association study identifies 19p13.3 (UNC13A) and 9p21.2 as susceptibility loci for sporadic amyotrophic lateral sclerosis. Nat Genet.41(10):1083-7

Van Hoecke A, Schoonaert L, Lemmens R, Timmers M, et al. (2012) EPHA4 is a disease modifier of amyotrophic lateral sclerosis in animal models and in humans. Nat Med.

Van Langenhove T, van der Zee J, Engelborghs S, Vandenberghe R, et al. (2012) Ataxin-2 polyQ expansions in FTLD-ALS spectrum disorders in Flanders-Belgian cohorts. Neurobiol Aging. 33(5):1004.e17-20.

Vance C, Al-Chalabi A, Ruddy D, Smith BN, et al. (2006) Familial amyotrophic lateral sclerosis with frontotemporal dementia is linked to a locus on chromosome 9p13.2-21.3. Brain. 129(Pt 4):868-76.

Vance C, Rogelj B, Hortobágyi T, De Vos KJ, et al. (2009) Mutations in FUS, an RNA processing protein, cause familial amyotrophic lateral sclerosis type 6. Science. 323(5918):1208-11.

Vargas MR, Johnson JA. (2010) Astrogliosis in amyotrophic lateral sclerosis: role and therapeutic potential of astrocytes. Neurotherapeutics. 7(4):471-81.

Veldink JH, Kalmijn S, Van der Hout AH, Lemmink HH, et al. (2005) SMN genotypes producing less SMN protein increase susceptibility to and severity of sporadic ALS. Neurology. 65(6):820-5.

Veldink JH, van den Berg LH, Cobben JM, Stulp RP, et al. (2001) Homozygous deletion of the survival motor neuron 2 gene is a prognostic factor in sporadic ALS. Neurology. 56(6):749-52.

Vidali G, Gershey EL, Allfrey VG. (1968) Chemical studies of histone acetylation. The distribution of epsilon-N-acetyllysine in calf thymus histones. J Biol Chem. 243(24):6361-6.

Vielhaber S, Kunz D, Winkler K, Wiedemann FR, et al. (2000) Mitochondrial DNA abnormalities in skeletal muscle of patients with sporadic amyotrophic lateral sclerosis. Brain. 123 (Pt 7):1339-48.

Vijayvergiya C, Beal MF, Buck J, Manfredi G. (2005) Mutant superoxide dismutase 1 forms aggregates in the brain mitochondrial matrix of amyotrophic lateral sclerosis mice. J Neurosci. 25(10):2463-70.

Voigt A, Herholz D, Fiesel FC, Kaur K, et al. (2010) TDP-43-mediated neuron loss in vivo requires RNA-binding activity. PLoS One. 5(8):e12247.

Vosseller K, Hansen KC, Chalkley RJ, Trinidad JC, et al. (2005) Quantitative analysis of both protein expression and serine / threonine post-translational modifications through stable isotope labeling with dithiothreitol. Proteomics. 5(2):388-98.

Wang J, Xu G, Borchelt DR. (2002) High molecular weight complexes of mutant superoxide dismutase 1: age-dependent and tissue-specific accumulation. Neurobiol Dis. 9(2):139-48.

Wang L, Wang CH, Jia JF, Ma XK, et al. (2010) Contribution of cyclophilin A to the regulation of inflammatory processes in rheumatoid arthritis. J Clin Immunol. 30(1):24-33.

Wang P, Heitman J. (2005) The cyclophilin. Genome Biology, 6:226.

Wang X, Arai S, Song X, Reichart D, et al. (2008) Induced ncRNAs allosterically modify RNA-binding proteins in cis to inhibit transcription. Nature. 454(7200):126-30.

Wang X, Zhang S, Zhang J, Huang X, et al. (2010) A large intrinsically disordered region in SKIP and its disorder-order transition induced by PPIL1 binding revealed by NMR. J Biol Chem. 285(7):4951-63.

Wang XS, Lee S, Simmons Z, Boyer P, et al. (2004) Increased incidence of the Hfe mutation in amyotrophic lateral sclerosis and related cellular consequences. J Neurol Sci. 227(1):27-33.

Wang Y, Mao XO, Xie L, Banwait S, et al. (2007) Vascular endothelial growth factor overexpression delays neurodegeneration and prolongs survival in amyotrophic lateral sclerosis mice. J Neurosci. 27(2):304-7.

Watanabe M, Dykes-Hoberg M, Culotta VC, Price DL, et al. (2001) Histological evidence of protein aggregation in mutant SOD1 transgenic mice and in amyotrophic lateral sclerosis neural tissues. Neurobiol Dis. 8(6):933-41.

Watts GD, Wymer J, Kovach MJ, Mehta SG, et al. (2004) Inclusion body myopathy associated with Paget disease of bone and frontotemporal dementia is caused by mutant valosin-containing protein. Nat Genet. 36(4):377-81.

Wegorzewska I, Bell S, Cairns NJ, Miller TM, Baloh RH. (2009) TDP-43 mutant transgenic mice develop features of ALS and frontotemporal lobar degeneration. Proc Natl Acad Sci U S A. 106(44):18809-14.

Weis J, Katona I, Müller-Newen G, Sommer C, et al. (2011) Small-fiber neuropathy in patients with ALS. Neurology. 76(23):2024-9.

Wharton S, Ince PG. (2003) Pathology of Motor Neurone Disorders. In Motor Neuron Disorders Volume 28. Edited by: Shaw PJ, Strong MJ. Philadelphia: Butterworth Heinemann: 17-41.

White MC, Gao R, Xu W, Mandal SM, et al. (2010) Inactivation of hnRNP K by expanded intronic AUUCU repeat induces apoptosis via translocation of PKCdelta to mitochondria in spinocerebellar ataxia 10. PLoS Genet. 6(6):e1000984.

Wicks P, Abrahams S, Papps B, Al-Chalabi A, et al. (2009) SOD1 and cognitive dysfunction in familial amyotrophic lateral sclerosis. J Neurol. 256(2):234-41.

Wiedau-Pazos M, Goto JJ, Rabizadeh S, Gralla EB, et al. (1996) Altered reactivity of superoxide dismutase in familial amyotrophic lateral sclerosis. Science. 271(5248):515-8.

Wiedemann FR, Winkler K, Kuznetsov AV, Bartels C, et al. (1998) Impairment of mitochondrial function in skeletal muscle of patients with amyotrophic lateral sclerosis. J Neurol Sci. 156(1):65-72.

Wilhelmsen KC, Forman MS, Rosen HJ, Alving LI, et al. (2004) 17q-linked frontotemporal dementia-amyotrophic lateral sclerosis without tau mutations with tau and alpha-synuclein inclusions. Arch Neurol. 61(3):398-406.

Williams AH, Valdez G, Moresi V, Qi X, et al. (2009) MicroRNA-206 delays ALS progression and promotes regeneration of neuromuscular synapses in mice. Science. 326(5959):1549-54.

Williamson TL, Cleveland DW. (1999) Slowing of axonal transport is a very early event in the toxicity of ALS-linked SOD1 mutants to motor neurons. Nat Neurosci. 2(1):50-6.

Wills AM, Cronin S, Slowik A, Kasperaviciute D, et al. (2009) A large-scale international meta-analysis of paraoxonase gene polymorphisms in sporadic ALS. Neurology. 73(1):16-24.

Wilms H, Sievers J, Dengler R, Bufler J, et al. (2003) Intrathecal synthesis of monocyte chemoattractant protein-1 (MCP-1) in amyotrophic lateral sclerosis: further evidence for microglial activation in neurodegeneration. J Neuroimmunol. 144(1-2):139-42.

Wils H, Kleinberger G, Janssens J, Pereson S, et al. (2010) TDP-43 transgenic mice develop spastic paralysis and neuronal inclusions characteristic of ALS and frontotemporal lobar degeneration. Proc Natl Acad Sci U S A. 107(8):3858-63.

Wilson ME, Boumaza I, Lacomis D, Bowser R. (2010) Cystatin C: a candidate biomarker for amyotrophic lateral sclerosis. PLoS One. 5(12):e15133.

Wissing S, Ludovico P, Herker E, Büttner S, et al. (2004) An AIF orthologue regulates apoptosis in yeast. J Cell Biol. 166(7):969-74.

Wood JD, Beaujeux TP, Shaw PJ. (2003) Protein aggregation in motor neurone disorders. Neuropathol Appl Neurobiol. 29(6):529-45.

Worms PM (2001) The epidemiology of motor neuron diseases: a review of recent studies. J Neurol Sci. 191(1-2):3-9.

Woulfe J, Gray DA, Mackenzie IR. (2010) FUS-immunoreactive intranuclear inclusions in neurodegenerative disease. Brain Pathol. 20(3):589-97.

Wu C, Parrott AM, Liu T, Jain MR, et al. (2011) Distinction of thioredoxin transnitrosylation and denitrosylation target proteins by the ICAT quantitative approach. J Proteomics. 74(11):2498-509.

Wu CH, Fallini C, Ticozzi N, Keagle PJ, et al. (2012) Mutations in the profilin 1 gene cause familial amyotrophic lateral sclerosis. Nature. 488(7412):499-503.

Wu D, Yu W, Kishikawa H, Folkerth RD, et al. (2007) Angiogenin loss-of-function mutations in amyotrophic lateral sclerosis. Ann Neurol. 62(6):609-17.

Wu X, Wilcox CB, Devasahayam G, Hackett RL, et al. (2000) The Ess1 prolyl isomerase is linked to chromatin remodeling complexes and the general transcription machinery. EMBO J, 19:3727-38.

Xiao S, Sanelli T, Dib S, Sheps D, et al. (2011) RNA targets of TDP-43 identified by UV-CLIP are deregulated in ALS. Mol Cell Neurosci. 47(3):167-80.

Xu Q, Leiva MC, Fischkoff SA, Handschumacher RE, Lyttle CR. (1992) Leukocyte chemotactic activity of cyclophilin. J Biol Chem. 267(17):11968-71.

Xu YF, Gendron TF, Zhang YJ, Lin WL, et al. (2010) Wild-type human TDP-43 expression causes TDP-43 phosphorylation, mitochondrial aggregation, motor deficits, and early mortality in transgenic mice. J Neurosci. 30(32):10851-9.

Yamanaka K, Miller TM, McAlonis-Downes M, Chun SJ, Cleveland DW. (2006) Progressive spinal axonal degeneration and slowness in ALS2-deficient mice. Ann Neurol. 60(1):95-104.

Yamanaka K, Vande Velde C, Eymard-Pierre E, Bertini E, et al. (2003) Unstable mutants in the peripheral endosomal membrane component ALS2 cause early-onset motor neuron disease. Proc Natl Acad Sci U S A. 100(26):16041-6.

Yang H, Chen J, Yang J, Qiao S, et al. (2007) Cyclophilin A is upregulated in small cell lung cancer and activates ERK1/2 signal. Biochem Biophys Res Commun. 361(3):763-7.

Yang HP, Zhong HN, Zhou HM. (1997) Catalysis of the refolding of urea denatured creatine kinase by peptidyl-prolyl cis-trans isomerase. Biochim Biophys Acta. 1338(2):147-50.

Yang L, Embree LJ, Hickstein DD. (2000) TLS-ERG leukemia fusion protein inhibits RNA splicing mediated by serine-arginine proteins. Mol Cell Biol. 20(10):3345-54.

Yang WM, Inouye CJ, Seto E. (1995) Cyclophilin A and FKBP12 interact with YY1 and alter its transcriptional activity. J Biol Chem. 270(25):15187-93.

Yang Y, Hentati A, Deng HX, Dabbagh O, et al. (2001) The gene encoding alsin, a protein with three guanine-nucleotide exchange factor domains, is mutated in a form of recessive amyotrophic lateral sclerosis. Nat Genet. 29(2):160-5.

Yang Y, Lu N, Zhou J, Chen ZN, Zhu P. (2008) Cyclophilin A up-regulates MMP-9 expression and adhesion of monocytes/macrophages via CD147 signalling pathway in rheumatoid arthritis. Rheumatology (Oxford). 47(9):1299-310.

Yasser S, Fecto F, Siddique T, Sheikh KA, Athar P. (2010) An unusual case of familial ALS and cerebellar ataxia. Amyotroph Lateral Scler. 11(6):568-70.

Ye H, Cande C, Stephanou NC, Jiang S, et al. (2002) DNA binding is required for the apoptogenic action of apoptosis inducing factor. Nat Struct Biol. 9(9):680-4.

Yedavalli VS, Neuveut C, Chi YH, Kleiman L, Jeang KT. (2004) Requirement of DDX3 DEAD box RNA helicase for HIV-1 Rev-RRE export function. Cell. 119(3):381-92.

Yen AA, Simpson EP, Henkel JS, Beers DR, Appel SH. (2004) HFE mutations are not strongly associated with sporadic ALS. Neurology. 62(9):1611-2.

Yokoseki A, Shiga A, Tan CF, Tagawa A, et al. (2008) TDP-43 mutation in familial amyotrophic lateral sclerosis. Ann Neurol. 63(4):538-42.

Yoo Y, Wu X, Egile C, Li R, Guan JL. (2006) Interaction of N-WASP with hnRNPK and its role in filopodia formation and cell spreading. J Biol Chem. 281(22):15352-60.

Yoshihara T, Ishigaki S, Yamamoto M, Liang Y, et al. (2002) Differential expression of inflammation- and apoptosis-related genes in spinal cords of a mutant SOD1 transgenic mouse model of familial amyotrophic lateral sclerosis. J Neurochem. 80(1):158-67.

Yuan A, Mills RG, Bamburg JR, Bray JJ. (1997) Axonal transport and distribution of cyclophilin A in chicken neurones. Brain Res. 771(2):203-12.

Yuan W, Ge H, He B. (2010) Pro-inflammatory activities induced by CyPA-EMMPRIN interaction in monocytes. Atherosclerosis. 213(2):415-21.

Yurchenko V, Constant S, Eisenmesser E, Bukrinsky M. (2010) Cyclophilin-CD147 interactions: a new target for anti-inflammatory therapeutics. Clin Exp Immunol. 160(3):305-17.

Yurchenko V, Zybarth G, O'Connor M, Dai WW, et al. (2002) Active site residues of cyclophilin A are crucial for its signaling activity via CD147. J Biol Chem. 277(25):22959-65.

Zaldivar T, Gutierrez J, Lara G, Carbonara M, et al. (2009) Reduced frequency of ALS in an ethnically mixed population: a population-based mortality study. Neurology. 72(19):1640-5.

Zander K, Sherman MP, Tessmer U, Bruns K, et al. (2003) Cyclophilin A interacts with HIV-1 Vpr and is required for its functional expression. J Biol Chem.278(44):43202-13.

Zatloukal K, Stumptner C, Fuchsbichler A, Heid H, et al. (2002) p62 Is a common component of cytoplasmic inclusions in protein aggregation diseases. Am J Pathol. 160(1):255-63.

Zetterberg H, Jacobsson J, Rosengren L, Blennow K, Andersen PM. (2008) Association of APOE with age at onset of sporadic amyotrophic lateral sclerosis. J Neurol Sci. 273(1-2):67-9.

Zetterström P, Graffmo KS, Andersen PM, Brännström T, Marklund SL. (2011) Proteins that bind to misfolded mutant superoxide dismutase-1 in spinal cords from transgenic amyotrophic lateral sclerosis (ALS) model mice. J Biol Chem. Jun 10;286(23):20130-6.

Zhang B, Tu P, Abtahian F, Trojanowski JQ, Lee VM. (1997) Neurofilaments and orthograde transport are reduced in ventral root axons of transgenic mice that express human SOD1 with a G93A mutation. J Cell Biol. 139(5):1307-15.

Zhang F, Ström AL, Fukada K, Lee S, et al. (2007) Interaction between familial amyotrophic lateral sclerosis (ALS)-linked SOD1 mutants and the dynein complex. J Biol Chem. 282(22):16691-9.

Zhang W, Bieker JJ. (1998) Acetylation and modulation of erythroid Krüppel-like factor (EKLF) activity by interaction with histone acetyltransferases. Proc Natl Acad Sci U S A. 95(17):9855-60.

Zhang YJ, Xu YF, Cook C, Gendron TF, et al. (2009) Aberrant cleavage of TDP-43 enhances aggregation and cellular toxicity. Proc Natl Acad Sci U S A. 106(18):7607-12.

Zhang YJ, Xu YF, Dickey CA, Buratti E, et al. (2007) Progranulin mediates caspase-dependent cleavage of TAR DNA binding protein-43. J Neurosci. 27(39):10530-4.

Zhao C, Takita J, Tanaka Y, Setou M, et al. (2001) Charcot-Marie-Tooth disease type 2A caused by mutation in a microtubule motor KIF1Bbeta. Cell. 105(5):587-97.

Zhao Y, Chen Y, Schutkowski M, Fischer G, Ke H. (1997) Cyclophilin A complexed with a fragment of HIV-1 gag protein: insights into HIV-1 infectious activity. Structure. 5(1):139-46.

Zhou JY, Afjehi-Sadat L, Asress S, Duong DM, et al. (2010) Galectin-3 is a candidate biomarker for amyotrophic lateral sclerosis: discovery by a proteomics approach. J Proteome Res. 9(10):5133-41.

Zhou Z, Licklider LJ, Gygi SP, Reed R. (2002) Comprehensive proteomic analysis of the human spliceosome, Nature, 419:182-5.

Zhu C, Wang X, Deinum J, Huang Z, et al. (2007) Cyclophilin A participates in the nuclear translocation of apoptosis-inducing factor in neurons after cerebral hypoxia-ischemia. J Exp Med, 204(8):1741-8.

Zinszner H, Sok J, Immanuel D, Yin Y, Ron D. (1997) TLS (FUS) binds RNA in vivo and engages in nucleo-cytoplasmic shuttling. J Cell Sci. 110 (Pt 15):1741-50.

Zydowsky LD, Etzkorn FA, Chang HY, Ferguson SB, et al. (1992) Active site mutants of human cyclophilin A separate peptidyl-prolyl isomerase activity from cyclosporin A binding and calcineurin inhibition. Protein Sci, 1(9):1092-9.